CENTRAL WATER AND POWER RESEARCH STATION POONA

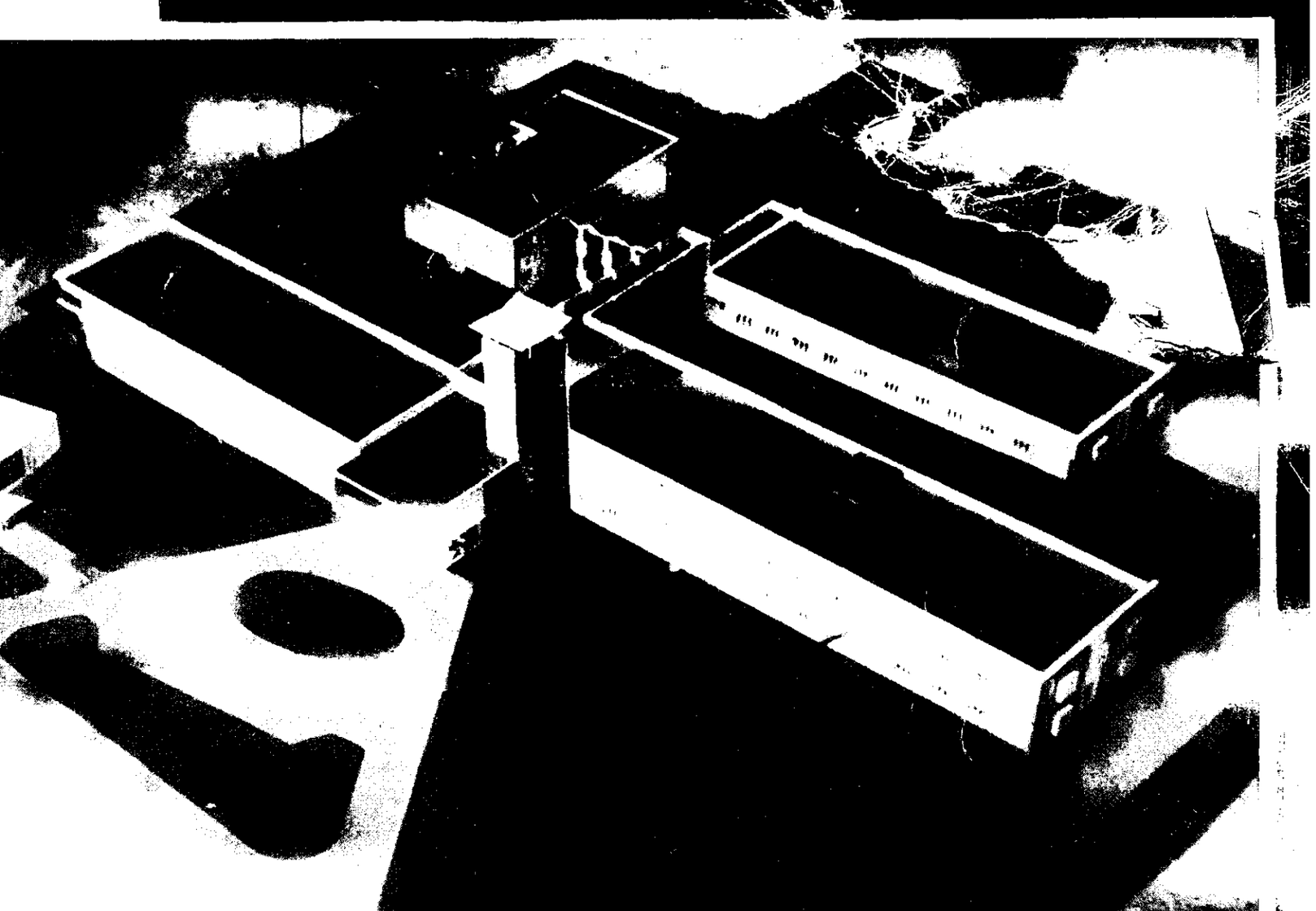

ANNUAL RESEARCH MEMOIRS 1960

DIRECTOR M G HIRANANDANI

GOVERNMENT OF IN

MINISTRY OF IRRIGATI

CENTRAL WATER AND POWER RESEARCH STATION POONA

ANNUAL RESEARCH MEMOIRS 1960

Government of India
Ministry of Irrigation and Power

1961

FOREWORD

The launching of a new project for a fully-equipped Cavitation Laboratory in the Central Water and Power Research Station, Poona came as a significant landmark of the year 1960. The United Nations Special Fund allocated a grant of $ 364,000 for technical and financial assistance in the supply and installation of a multi-test water tunnel in cavitation research on hydraulic structures, gates and valves, turbines, pumps and marine propellers. The project is included for full development in the Third Plan period.

On the successful completion of the application of the Radioactive Tracer method for detecting sediment movement around Bombay Harbour waters, applications of the method are being examined for other areas for similar investigations. A separate component unit has been added to the *CWPRS* for specializing in the applications of Radioactive Tracer techniques. In certain instances when the use of Radioisotopes may not be advisable on account of its deleterious effects or other natural limitations, fluorescent materials have been found an effective substitute for facilitating the studies. Preliminary investigations made in collaboration with the National Chemical Laboratory have shown that fluorescent materials can be manufactured indigenously at low cost.

In their third meeting the Advisory Committee for Ship Model Testing Tank decided to add a 36 *ft* wide and 250 *ft* long extension to the existing tank. The work will be undertaken during the 3rd Five Year Plan. Considerable work has been done on resistance measurement and turbulence stimulation devices. A new type of turbulence stimulator for Ship Models has been successfully tested.

The second session of the Refresher Course in Hydraulics was held in June. A two-week refresher course in Waterways Engineering for the benefit of rail and road engineers was also inaugurated at the same time, with the concurrence of the Ministry of Railways and the Ministry of Transport and Communications.

Following the experiments on Surge Tank of Koyna Hydroelectric Project, similar model tests for Sharavati Hydroelectric Project have been taken up. The design of spillway and energy dissipation devices downstream of Kohira Dam, Meshwa Dam, Banas Dam and Badua Spillway Chute were tested. Experiments were conducted also for training the river Jhelum and evolving protective measures at Mohora Power House near Srinagar. Various proposals for stabilising the entrance channel of Cuddalore Port and maintaining adequate depths therein were tested. Foundation investigations and geophysical exploration were carried out at the sites of Tawa Dam, Linganamakki Dam, Mettur Tunnel scheme *etc.* Experimental stress analysis by photoelastic method were conducted for Gandhisagar Dam Spillway piers and Nagarjunasagar trestle bridge *etc.*

Development of precision instruments such as automatic tide generator, electronic counter for miniature currentmeter, bed profile recorder *etc* required for model experimentation continued. Suitable adjustments have been made for improving their performance.

A new series of Technical Memorandums were started during 1960. The first two memorandums published were on the

1. Use of Radioactive Tracer for the study of Sediment Movement of Bombay Harbour and 2. Effect of Temperature and Boundary on Currentmeter Ratings.

Consequent on a proposal sponsored at the December 1958 meeting of the Central India Rivers Commission at Bhuvaneswar, the *CWPRS* issued an up-to-date manual on 'Stream Gauging'.

CONVERSIONS INTO METRIC UNITS

1 *in*	=	2·54 *cm*	1 *sq ml*	=	2·590 *sq km*
1 *ft*	=	30·48 *cm*	1 *acre*	=	$4·047 \times 10^{-3}$ *sq km*
1 *ml*	=	1·609 *km*	1 *cft* or ft^3	=	$2·832 \times 10^{-2}$ m^3
1 nautical *ml*	=	1·853 *km*	1 *gm*	=	$1·205 \times 10^{-3}$ *lbs*
1 *sq ft*	=	$9·290 \times 10^{-2}$ *sq m*	1 *psi*	=	703·1 *kg/sq m*

NOTATIONS

A	Catchment area
°*C*	Degree centigrade
cc	Cubic centimeter
cfs	Cubit feet per second
cft or ft^3	Cubic feet
cm	Centimeter
m^3	Cubic meter
CS	Cross-section
D/S	Downstream
El	Elevation
°*F*	Degree Fareinheit
fig	Figure
FRL	Full Reservoir Level
FSL	Full Suply Level
ft	Foot, feet
gm	Gram
hr	Hour
HFL	High Flood Level
HW	High water
in	Inch
km	Kilometer
kw	Kilowatt
KRL	Koyna Reduced Level
LW	Low water
LWOST	Low water ordinary spring tide
LWL	Low water level
Lat	Latitude
Long	Longitude
lbs	Pounds
m	Meter
ml	Mile
mw	Mega-watts
min	Minute
m a ft	Million acre feet
m c ft	Million cubic feet
m^3/s	Cubic meters per second
ppm	Parts per million
psi	Pounds per square inch
Q	Discharge
RD	Reduced distance
RL	Reduced Level
sq	Square
SE	Slope exaggeration
sec or *s*	Second
TWL	Tail Water Level
U/S	Upstream
VE	Vertical exaggeration
WL	Water level
wt	Weight

CONTENTS

RIVER TRAINING AND FLOOD CONTROL

1. Training Yamuna at Delhi
   - I. Near rail-*cum*-road bridge 1
   - II. Near Wazirabad Pump House 3

*2. Training Jhelum at Mohora Power House, Kashmir 10

3. Breach in Katjuri embankment at Simuldaghai 14

4. Protection of Sabarmati left bank near Rinza bridge 17

5. Protection of Ichapur from erosion by Ambika 20

6. Protection of abutment of Kalol bridge on Goma 21

7. Behaviour of coffer dam of Kosi barrage
   1959 Post-flood conditions 23

8. West afflux bund of Kosi barrage
   Testing of alternative alignments 25

DESIGN OF HYDRAULIC STRUCTURES

9. Road and railway bridges across Yamuna at Delhi 27

10. Mundali weir across Mahanadi and undersluices
    - I. Weir 30
    - II. Protection works for undersluices 32

11. Canal syphons across two branches of Mahanadi 34

12. Design of spillway and energy dissipation devices
    - I. Vir Dam Project 36
    - II. Kohira Dam Project 40
    - III. Meshwa Dam Project 46
    - *IV. Banas Dam, Dantiwada Project 51
    - *V. Badua Dam Project 56
    - VI. Yeldari Spillway, Purna Project 62
    - VII. Sone Barrage, Amarkantak Thermal Scheme 67

13. Discharging capacity and design of toe protective works
    - I. Yeldari spillway; Purna Project 73
    - II. Kadana spillway, Kadana Project 78
    - III. Bhadar spillway 80
    - IV. Koyna sluice, Koyna *HE* Project 83

*14. Hydraulic Model studies of surge tanks
    Sharavathi *HE* Project 90

---

* Proposed for discussion by *CBIP* Research Committee.

15. Supplementary tests on Kota Barrage Model 98
16. Misalignments in excluder walls of Kosi barrage 102
*17. Silting in relation to Hirakud Lake Model 107

STRUCTURAL DESIGNS

18. Two dimensional photoelastic analysis
I. Gandhisagar spillway piers 111
II. Stresses in the vicinity of "No stress meters" in dams 114
*19. Three dimensional photoelastic analysis
Gandhisagar spillway piers 120
20. Experimental Stress Analysis
I. A 40 ft steel tower 123
*II. Nagarjunasagar-construction trestle bridge 128

WATER STUDIES AND HYDROLOGY

A. RAINFALL AND RUNOFF

21. Optimum number of years for computing mean annual precipitation 135

C. QUANTITY OF WATER

22. Effect of temperature and boundary on currentmeter ratings 142
23. Number of constant velocity runs for rating currentmeters 157

IRRIGATION, DRAINAGE AND RECLAMATION

A. SURFACE AND SUB-SURFACE IRRIGATION

24. Quality of irrigation waters
I. Indian Rivers 160
II. Wells and tube-wells 164

NAVIGATION

A. PORTS, HARBOURS AND ESTUARIES

*25. Development of Cuddalore port 167
26. Development of Kelva-Mahim Fishing port
Protection of coast against erosion 179
27. Resonance tests for coastal harbour at Paradip... 188
28. Distributions of wave heights
Bay of Bengal (1949-59) 191

C. COASTAL EROSION

29. Coastal erosion near naval battery at Cochin 195

SOIL MECHANICS AND FOUNDATION ENGINEERING

A. INVESTIGATIONS

30. Pore Pressure in Triaxial Shear Test 199

31. Compaction and shear strength of soils 202

C. FOUNDATION STUDIES INCLUDING GEOPHYSICAL

32. Foundation Investigation

I. Tawa Dam site 204

II. Thanneermukkom Regulator 210

III. Right Flank, Liganamakki Dam 216

33. Earth Tremors at Mangalam Dam site
January-March 1960 221

34. Mettur Tunnel Scheme

I. Seismic refraction on bed-rock 224

*II. Maximum allowable charge during blasting 225

35. Electrical Analogy for stratified foundations 227

36. Geophysical Investigations

I. Hathmati Reservoir Project 230

II. Alternative weir sites on Koyna 234

III. Spillway site, Badua Project... 236

IV. Navagam Dam Site, Narmada Project 240

CONSTRUCTION MATERIALS AND PRACTICES

A. CONCRETE TECHNOLOGY

37. Base exchange reactions
Sodium and Calcium 248

38. "One shot" Chemical Grout 251

39. Physico-chemical properties of Indian bentonites 257

B. BUILDING AND OTHER MATERIALS

40. Swelling pressure of black cotton soil
Effect of various chemical treatments 259

41. Bentonite as a grouting material 261

42. Modulus of elasticity of rock cores 264

43. Typical sand from Deccan trap 266

44. Studies on Puzzolona 267

45. Admixtures in mortars and concrete 269

INSTRUMENTATION

46. Activities in Instrumentation
I. Automatic tide generator 273
II. Miniature Currentmeter 274
III. Bed profile recorder for model... 276
IV. Wave height recorder for prototype 277
V. Capacitive wave height recorder 278
VI. Velocity tables and temperature corrections for liquids in manometers ... 280
47. Activities in Ship Model Testing Tank 285

OTHER MISCELLANEOUS

48. Bed material for Hydraulic models
I. Physical properties 287
II. Biological studies 291
*49. Fluorescent material as sediment transport tracer 294
50. Studies on aquatic weed Ceratophyllum Demersum 295
51. Khadakwasla weather summary : 1960 297

Divisionwise Distribution of Chapters

Division	*Chapter numbers*
Chemistry	24(I, II), 37, 38, 39, 48(I, II), 50
Floods	5, 6, 7, 8, 12 (VII), 16
Geophysics	36 (I to IV)
High Head Structures	12 (I to V), 51
Mathematics	12 (VI), 13 (I to IV), 14, 15, 17
Photoelasticity	18 (I & II), 19, 20 (I & II)
Physics	33, 34 (I & II), 35
Ports and Harbours	25, 26, 27, 29, 49
Rivers and Canals	1 (I & II), 2, 3, 4, 9, 10 (I & II), 11
Ship Testing and Instrumentation	46 (I to VI), 47
Soils and Concrete	30, 31, 32 (I to III), 40, 41, 42, 43, 44, 45
Statistics	21, 22, 23, 28, 46 (VI), 51

1. Training Yamuna at Delhi

I. Near rail-*cum*-road bridge

EXPERIMENTS were conducted for (*ibid* 1957) improving the flow conditions at the existing rail-*cum*-road bridge across the river Yamuna at Delhi. From the results of these experiments, it was concluded that diverting more flow to the left spans of the bridge was not possible with the help of cut off channels as then proposed. A proposal of (*fig 1*) constructing a pitched island with a cunnette prepared by the Director, Irrigation and Power Research Institute, Amritsar, Punjab, was forwarded to the *CWPRS* by the Northern Railway authorities. Experiments were therefore, conducted to test the above proposal for improving the flow conditions at the bridge.

2. Model and experiments

The existing 1/150 and 1/30 scale model of the river Yamuna from Wazirabad Pumping Station to Culvert *No* 14 was utilised and laid according to the following river survey data:

(i) 1955 post flood survey for the river upstream of the Railway bridge.
(ii) 1958 survey for the river below the Railway bridge.
(iii) A plan showing the 1956 post flood channel configuration for some distance upstream of the bridge laid according to 1955 cross-sections suitably modified, as the proposal of the pitched island was made with reference to this channel configuration.

It was expected by the author of this proposal that the pitched island with cunnette would divide the 75 *percent* of the river flow towards the right bank and 25 *percent* towards the left. The stage of the river at which this diversion was expected to occur was not mentioned. Unfortunately no prototype data giving the discharge distribution at the bridge at different flood stages was available. For determining the discharge taken by each span individually, all the spans of the bridge were reproduced in the model. This reproduction of all the spans individually, coupled with the vertical exaggeration of 5 imposed a model limitation, the individual span width being small did not allow sufficient width for reproducing the side slopes in a scoured bed. This restricted the depth of scour shown by the model. The model results could therefore, only be comparative, under different conditions.

(*a*) *Experiment under existing conditions*: With the model laid according to the survey data mentioned above, five flood cycles representing the average flood hydrograph rising from 325.634 m^3/sec (11,500 *cfs*) to 2548.54 m^3/sec (90,000 *cfs*) and back were run. Observations about flow lines, velocities and discharge distribution at the railway bridge for 1274.26 m^3/sec (45,000 *cfs*), 2548.54 m^3/sec (90,000 *cfs*) and 3681.19 m^3/sec (1,30,000 *cfs*) were made (*table 1*).

Table 1: Percentage discharge distribution at the existing road-*cum*-rail bridge under various conditions

Span *No*	1274.26 m^3/sec (45,000 *cfs*)			2548.52 m^3/sec (90,000 *cfs*)			3681.19 m^3/sec (1.3 lakh *cfs*)		
	A	*B*	*C*	*A*	*B*	*C*	*A*	*B*	*C*
1	3.64	3.50	...	5.20	4.53	5.46	6.15	4.11	5.25
2	2.17	3.30	2.10	7.47	9.00	8.46	11.70	11.10	10.90
3	3.08	2.20	5.51	6.57	6.62	6.58	6.00	6.91	7.35
4	3.00	2.89	6.92	5.79	5.55	7.65	5.43	6.33	7.00
5	6.58	8.70	8.18	5.62	8.27	8.16	5.63	7.41	7.15
6	9.01	11.50	7.17	8.48	10.38	7.82	9.18	9.98	8.20
7	8.55	11.20	9.18	8.46	10.18	7.94	7.93	8.94	8.70
8	12.44	10.80	9.79	9.89	9.92	8.84	10.10	8.89	9.80
9	17.39	14.00	15.27	11.04	8.70	10.14	10.50	10.92	10.30
10	21.86	20.81	24.48	17.24	15.30	16.89	15.25	14.28	13.35
11	12.31	11.10	11.40	14.04	12.55	11.87	12.13	11.13	12.00

Note: *A* = Existing conditions; *B* = With pitched island and cunnette joined to span *No* 6; *C* = With pitched island and cunnette joined to span *No* 4.

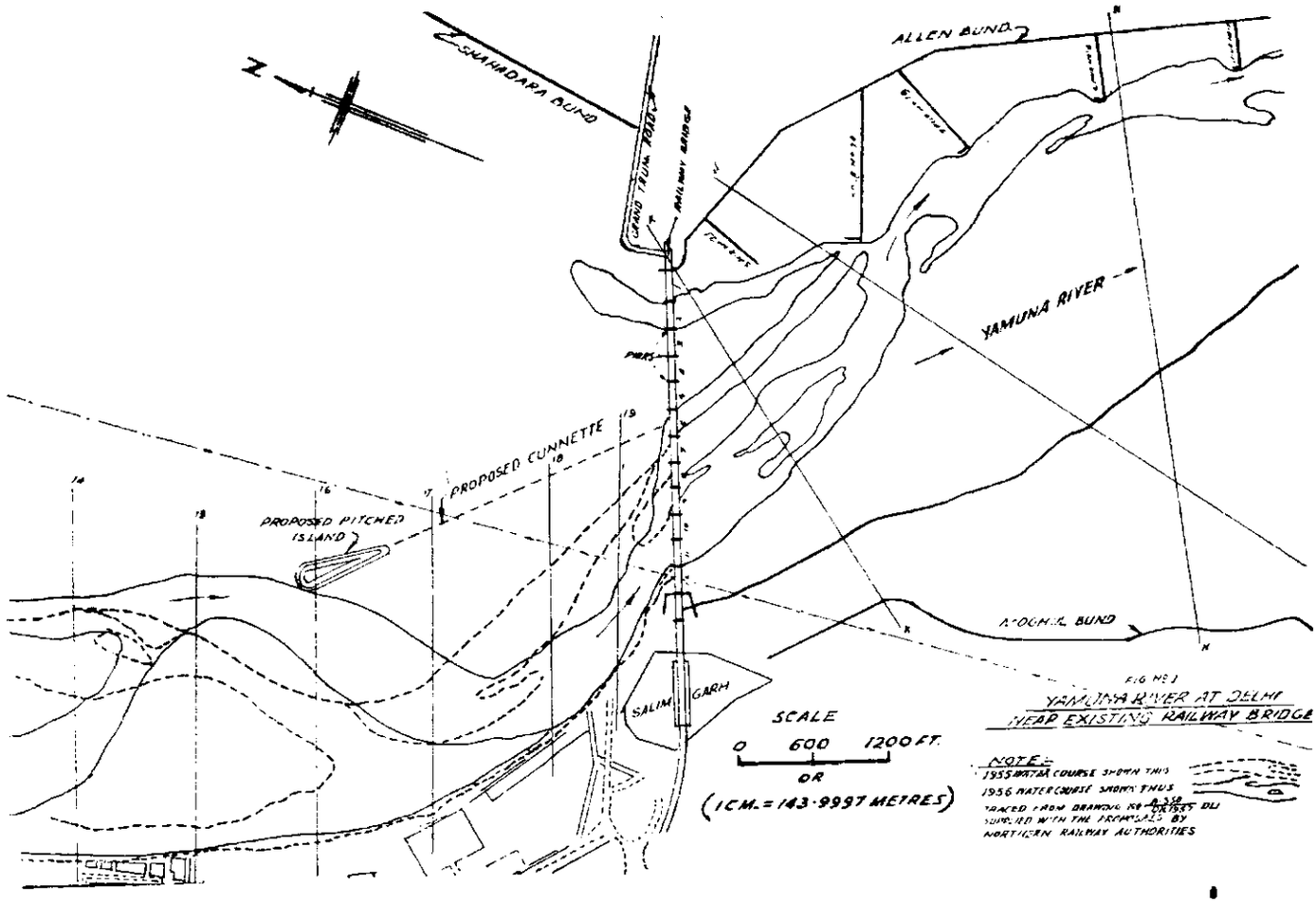

FIG. No 1

YAMUNA RIVER AT DELHI
NEAR EXISTING RAILWAY BRIDGE

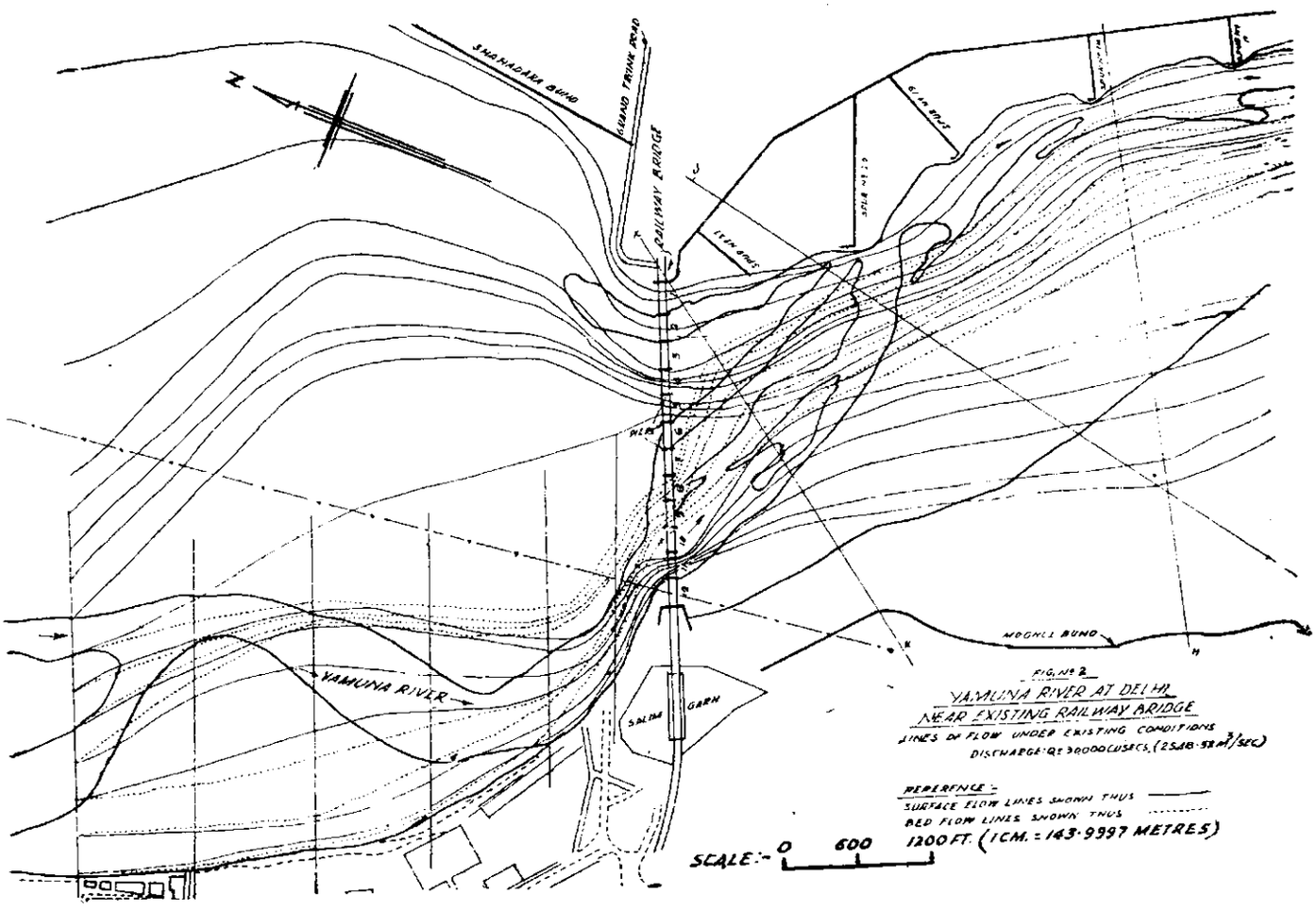

FIG. No 2

YAMUNA RIVER AT DELHI
NEAR EXISTING RAILWAY BRIDGE
LINES OF FLOW UNDER EXISTING CONDITIONS
DISCHARGE: Q = 300000 CUSECS. (25418·58 m^3/SEC)

(*b*) *Experiment with pitched island and cunnette laid in position as proposed* (*fig 1*): Pitched island was constructed as proposed with side slopes 2:1 on the right side and 1½:1 on the other side. This steeper slope was given on the left side of the island to give it a better chance to develop the cut off channel on this side. Top of the island was kept at *RL* 682 *ie* above *HFL* and the cunnette was made 30.48 *m* (100 *ft*) wide at bottom with side slopes 2:1 in the model and excavated to *RL* 665. Two experiments were carried out—one with the cunnette joined to span *No* 6 of the bridge and the other to span *No* 4.

As usual five flood cycles were run and observations about flow lines velocities and discharge distribution for 1274.26 m^3/sec (45,000 *cfs*); 2548.54 m^3/sec (90,000 *cfs*) and 3681.19 m^3/sec (1,30,000 *cfs*) were made at the bridge and recorded in *table 1*.

3. Discussion of results

It was observed during the experiments that the cunnette in both the positions had silted up, thus serving no useful purpose. This was also supported by the flow line observations as shown in *figs 2* and *3* (p4), for 2548.54 m^3/sec (90,000 *cfs*) which was slightly higher than average discharge. There was no improvement of flow with the pitched island. The discharge distribution at the bridge (*table 1*) also showed no appreciable change at different stages under different conditions.

4. Conclusion

The construction of a pitched island with a cunnette as proposed was not likely to be effective in improving the flow conditions at the existing rail-*cum*-road bridge, nor could the pitched island be expected to effect the flow conditions permanently, when it was located in an unstable reach of the river. This will be clear from perusal of *fig 1* which shows the river channels of 1955 and 1956. The position of the pitched island selected in the present case is the apex of one of the sub-meanders which was different in 1955 and might change in future. Naturally under such a condition the direction of the currents approaching the island would change and the effects of such an island could not be predicted.

II. Near Wazirabad Pump House

THE WAZIRABAD Barrage across the river Yamuna with its protective works as given below was completed before the 1959 floods:

Main barrage overall length 334.67 *m* (1098 *ft*) with crest at *RL* 665.

Undersluices, overall length 117.348 *m* (385 *ft*) with sill at *RL* 661.

A Pitched embankment 914.40 *m* (3000 *ft*) long including a curved head on the right bank.

A short guide bank 68.58 *m* (225 *ft*) long upstream of the barrage and 53.34 *m* (175 *ft*) long downstream, including the curved heads, on the left bank.

Two old spurs and the spur bund on the left bank were maintained.

It was apprehended by the authorities that the maintenance of the spurs on the left bank might be difficult. The Research Station, was therefore, requested to investigate whether the present left bank protective works consisting of a small guide bank and spurs could be replaced by a single guide bank. Experiments were therefore, conducted to determine the optimum length and alignment of the left guide bank.

2. Model and experiments

Experiments were conducted on the existing 1/150, 1/30 scale model of the river Yamuna extending from about 3 *miles* upstream of the barrage down to the existing railway bridge.

The protective works on the left flank of the barrage in this particular case were required to serve two-fold purpose.

(i) To give sufficient protection to the left approach embankment of the barrage against a high velocity current even in case of worst embayment.

(ii) To keep the main current of the river upstream of the barrage towards the right side without exerting any attracting influence on the left.

A study of the past river courses (*fig 1*) showed that a river course similar to that of 1916 was likely to cause a worst embayment behind the left guide bank and thus attack the approach

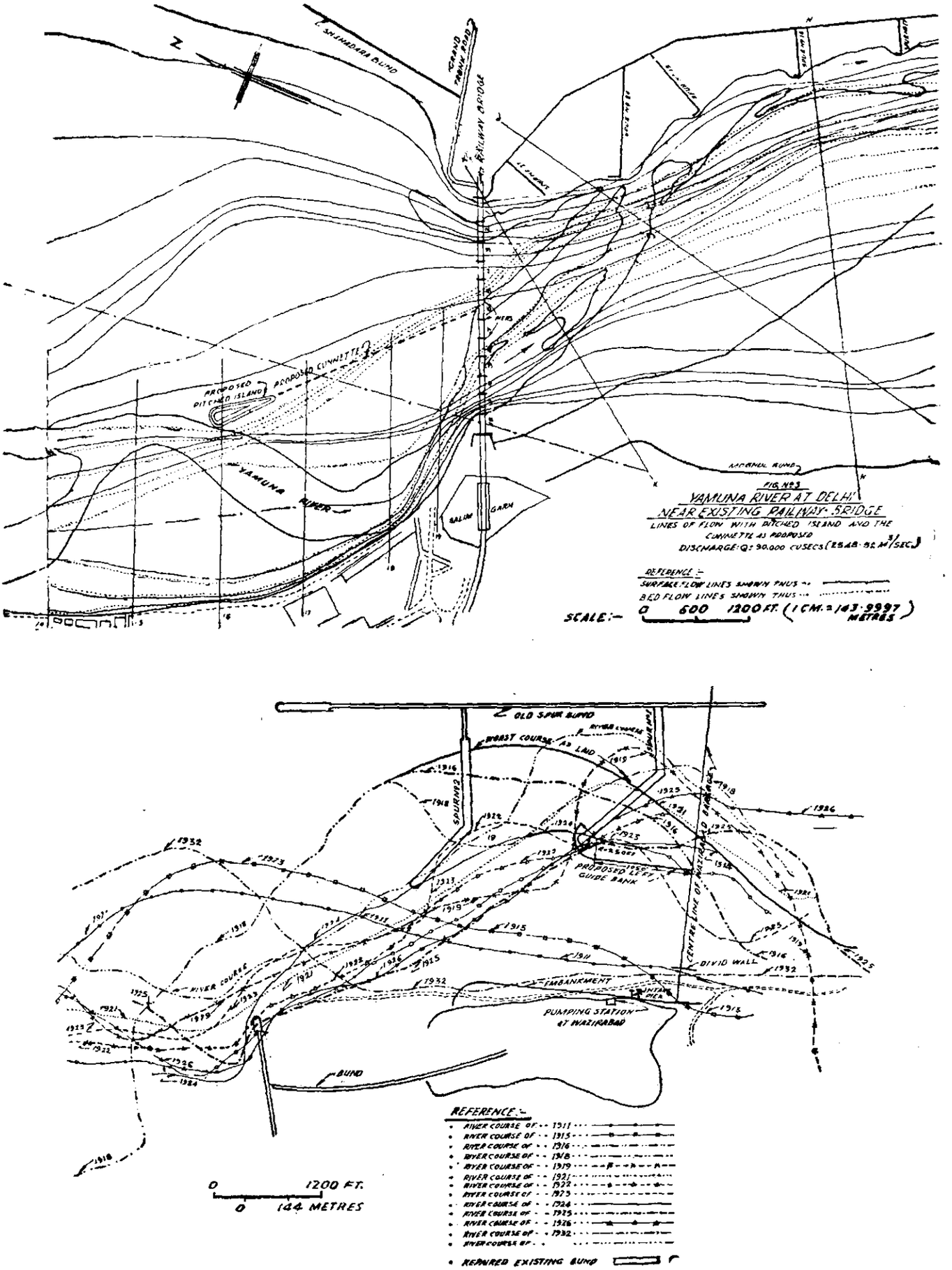

Fig 1 : Plan showing river courses for different years.

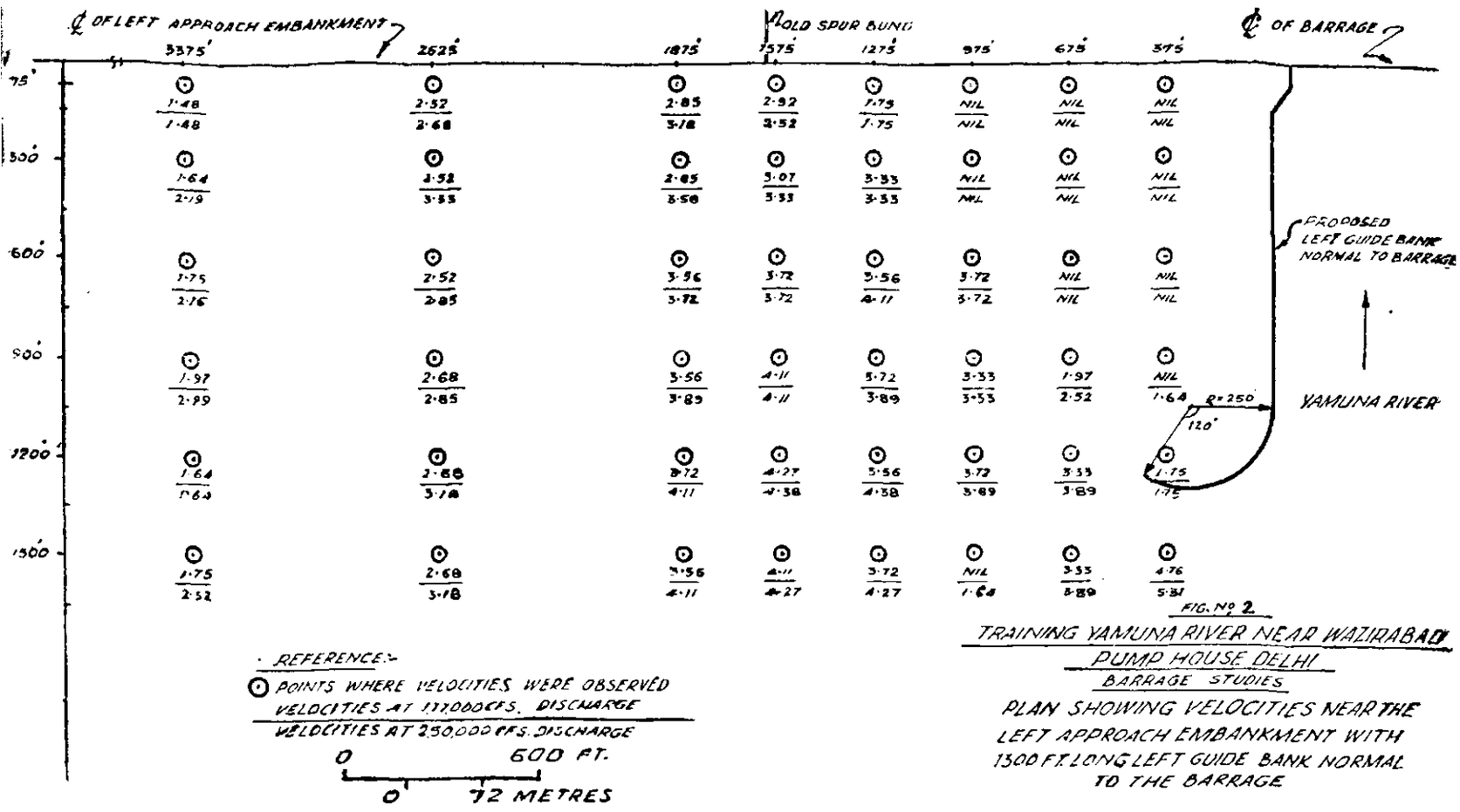

FIG. No 2.

TRAINING YAMUNA RIVER NEAR WAZIRABAD PUMP HOUSE DELHI BARRAGE STUDIES

PLAN SHOWING VELOCITIES NEAR THE LEFT APPROACH EMBANKMENT WITH 1300 FT. LONG LEFT GUIDE BANK NORMAL TO THE BARRAGE

embankment. This river course was, therefore, chosen for investigating a suitable length of the left guide bank. In absence of any specific information about the scouring velocities of the material used for the approach embankment, it was decided to permit a maximum velocity of .9144 *m/sec* (3 *ft/sec*) near the approach embankment. With proper turfing *etc*, the embankment was expected to be safe against such a velocity.

In the initial experiments, various lengths from 68.58 *m* (225 *ft*) to 487.68 *m* (1600 *ft*) upstream of the barrage were tried in the model under the unfavourable river course mentioned above. It was found that a 396.24 *m* (1300 *ft*) long guide bank (*fig 2*) was the optimum required.

With a view to make the construction more economical, the alignment of the guide bank was inclined so as to locate it on high ground on the left bank.

The following experiments were conducted:

I Experiments with the two existing spurs and the short left guide bank, under the existing river course of pre-1959 floods.

II Experiments with 396.24 *m* (1300 *ft*) long left guide bank.

(*a*) Under existing river course of pre-1959 floods.

(*b*) With the most unfavourable river course.

(*c*) With different inclinations of 5°, 13°, 21°, 24° and normal to the barrage. Results of alignments normal and inclined at 5° to the normal to the barrage as well as those inclined at 21° and 24° were found to be about the same. Results of alignments normal and inclined at 13° and 21° have only been considered for discussions.

3. Discussion of results

With the model laid to pre-1959 floods and with the two existing spurs and the short left guide bank in position more surface flow was diverted to the centre whereas the bed flow was deflected to the left bank (*fig 4*). Velocity observations for 1274.26 m^3/ *sec* (45,000 *cfs*) which is the bankful stage when major changes take place in the river bed, also showed that the concentration was more central. This scoured the central island to *RL* 670. Velocities along the right bank channel were higher than 1.0668 *m/sec* (3.5 *ft/sec*) and those along the left bank channel were much lower. This indicated that the left bank channel was likely to silt up and main channel might tend to be central with a fairly deep channel developing along the right bank.

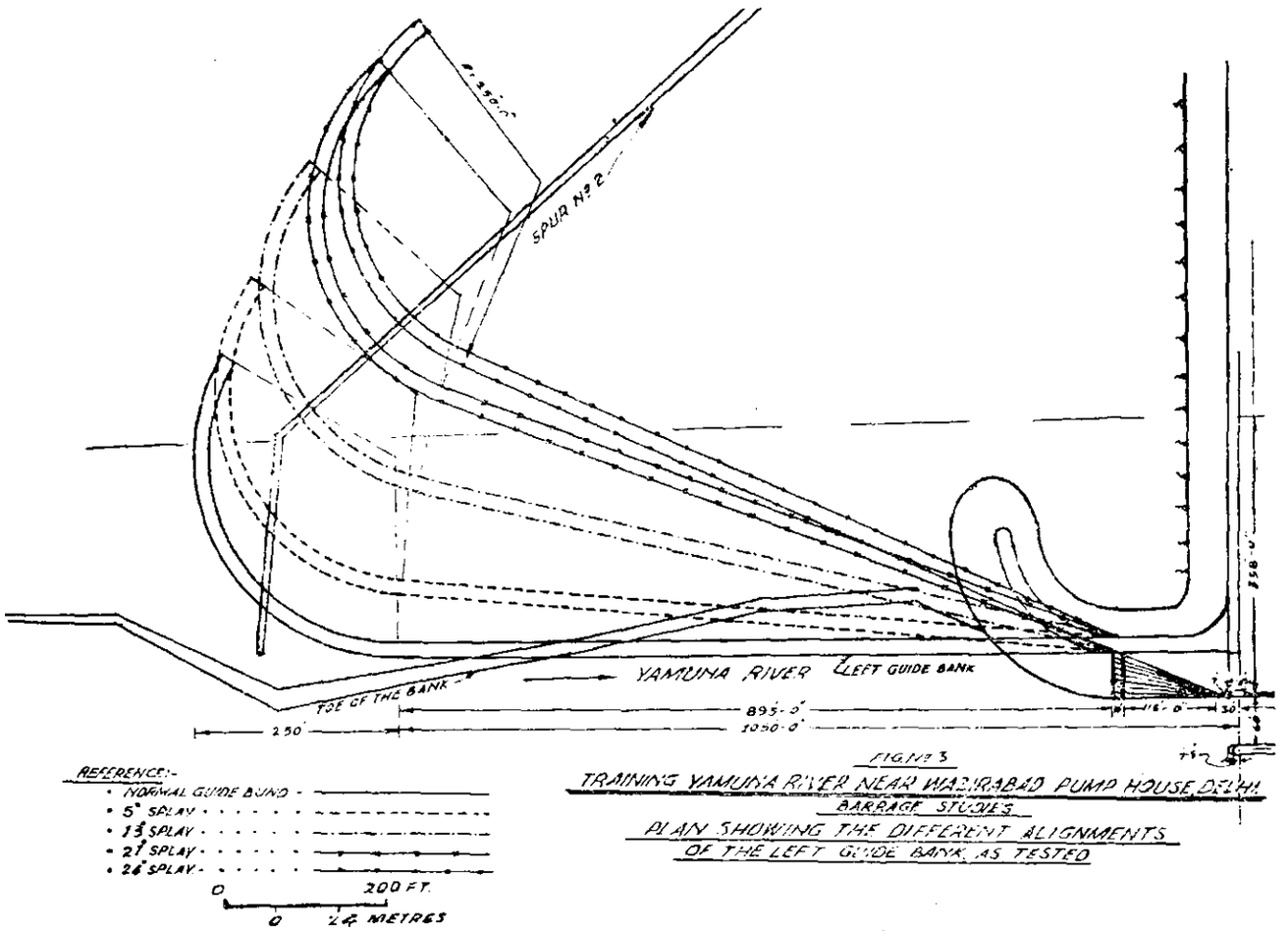

FIG No 3

TRAINING YAMUNA RIVER NEAR WAZIRABAD PUMP HOUSE DELHI

BARRAGE STUDIES

PLAN SHOWING THE DIFFERENT ALIGNMENTS OF THE LEFT GUIDE BANK AS TESTED

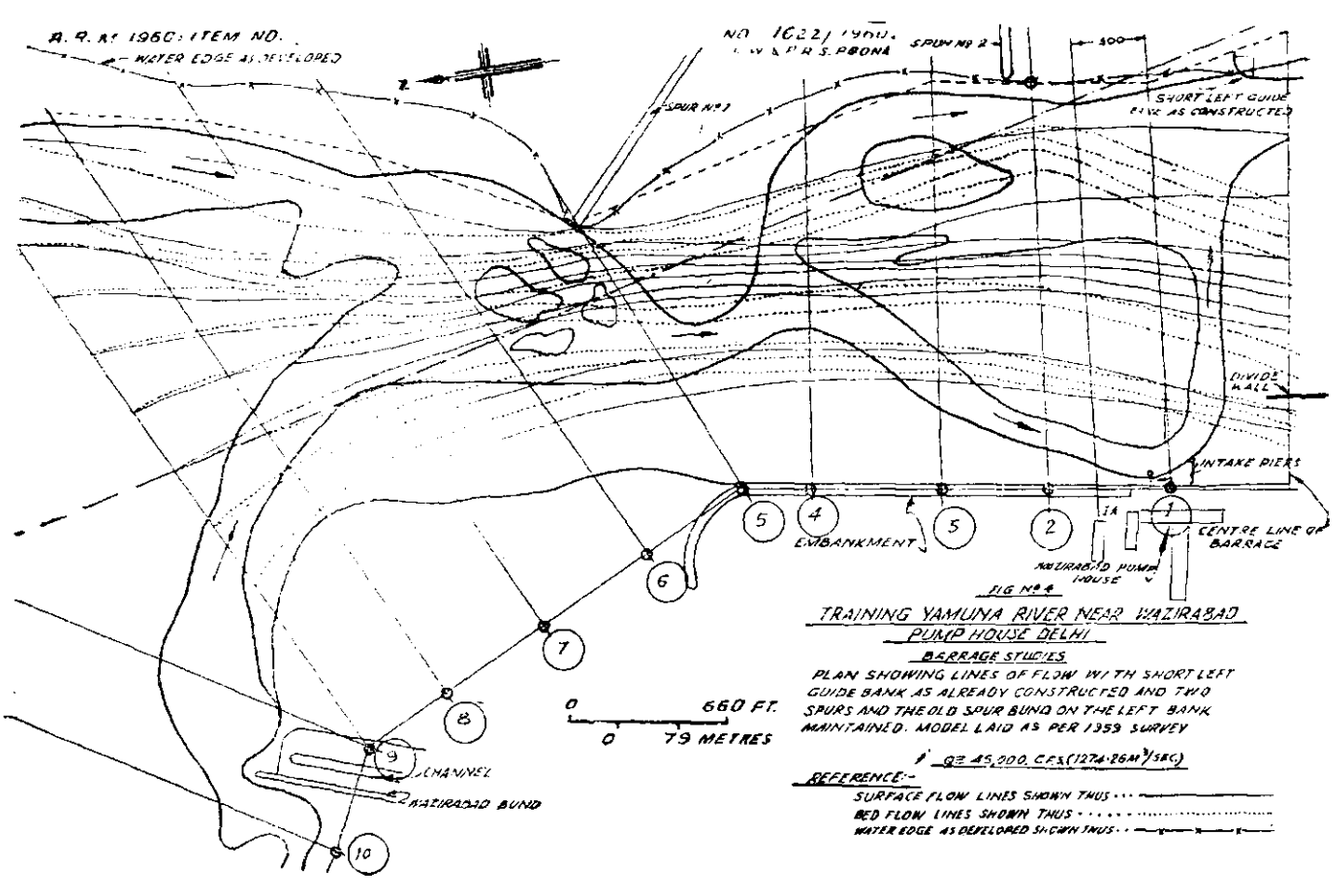

FIG No 4

TRAINING YAMUNA RIVER NEAR WAZIRABAD PUMP HOUSE DELHI

BARRAGE STUDIES

PLAN SHOWING LINES OF FLOW WITH SHORT LEFT GUIDE BANK AS ALREADY CONSTRUCTED AND TWO SPURS AND THE OLD SPUR BUND ON THE LEFT BANK MAINTAINED. MODEL LAID AS PER 1959 SURVEY

@ 45,200 CFS (1274·26 M³/SEC)

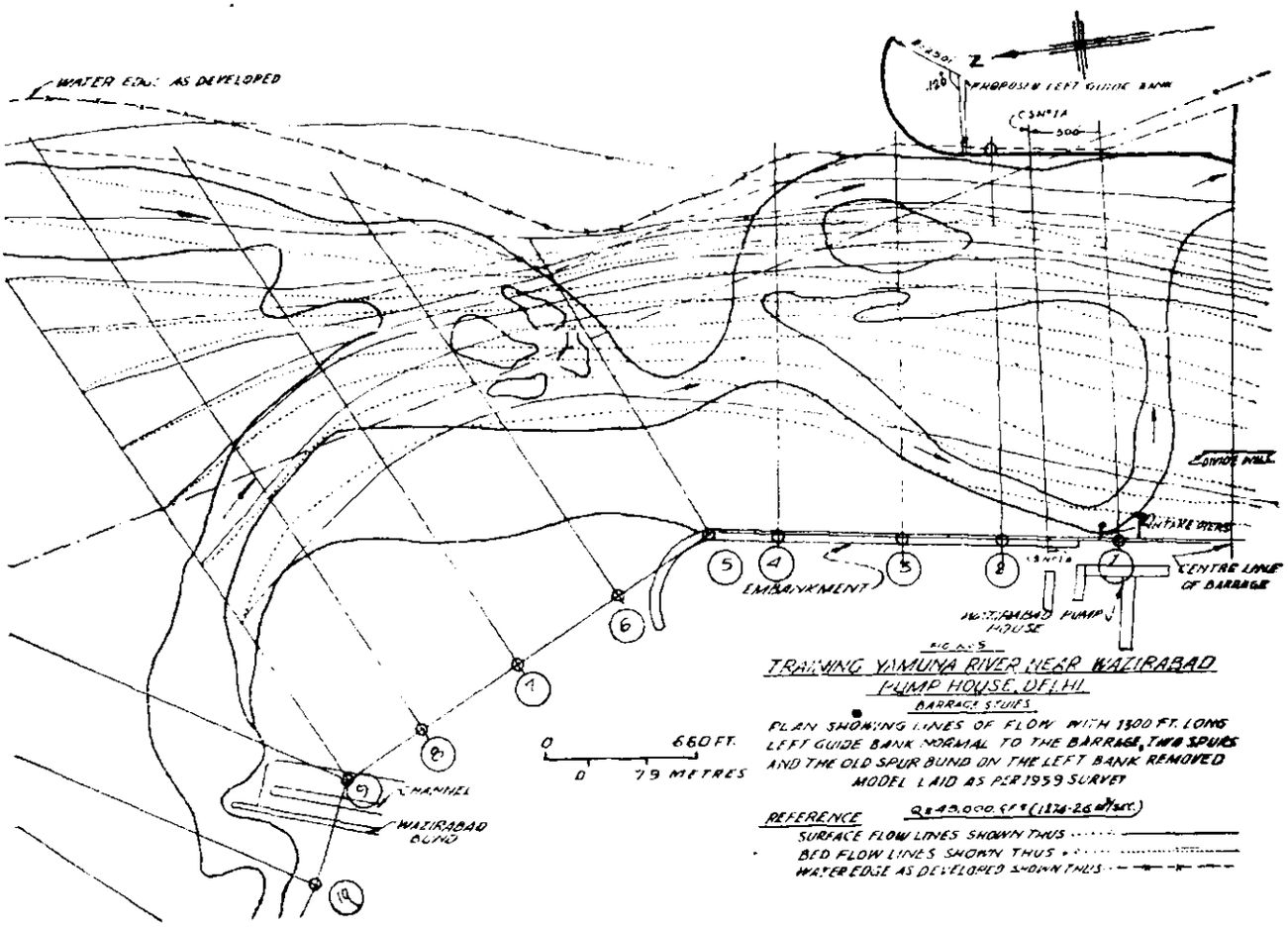

FIG. N°5

TRAINING YAMUNA RIVER NEAR WAZIRABAD PUMP HOUSE, DELHI

BARRAGE STUDIES

PLAN SHOWING LINES OF FLOW WITH 1300 FT. LONG LEFT GUIDE BANK NORMAL TO THE BARRAGE, TWO SPURS AND THE OLD SPUR BUND ON THE LEFT BANK REMOVED MODEL LAID AS PER 1959 SURVEY

REFERENCE Q = 43,000 CFS (1176·26 m³/sec.)

SURFACE FLOW LINES SHOWN THUS .....

BED FLOW LINES SHOWN THUS .....

WATER EDGE AS DEVELOPED SHOWN THUS

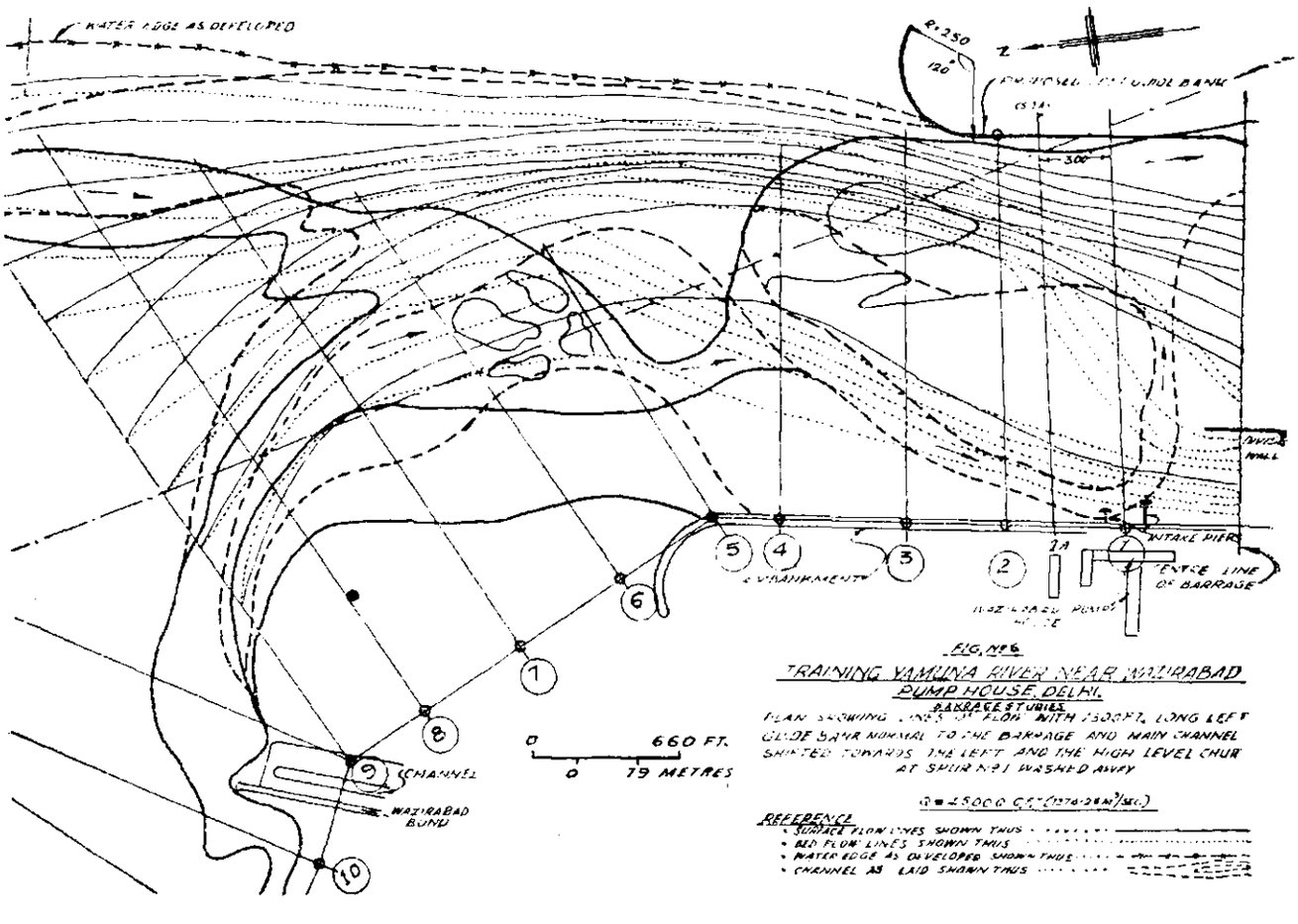

FIG. N°6

TRAINING YAMUNA RIVER NEAR WAZIRABAD PUMP HOUSE, DELHI.

BARRAGE STUDIES

PLAN SHOWING LINES OF FLOW WITH 1300 FT. LONG LEFT GUIDE BANK NORMAL TO THE BARRAGE AND MAIN CHANNEL SHIFTED TOWARDS THE LEFT AND THE HIGH LEVEL CHUR AT SPUR N°1 WASHED AWAY

Q = 43000 CFS (1176·26 m³/sec.)

REFERENCE

SURFACE FLOW LINES SHOWN THUS

BED FLOW LINES SHOWN THUS

WATER EDGE AS DEVELOPED SHOWN THUS

CHANNEL AS LAID SHOWN THUS

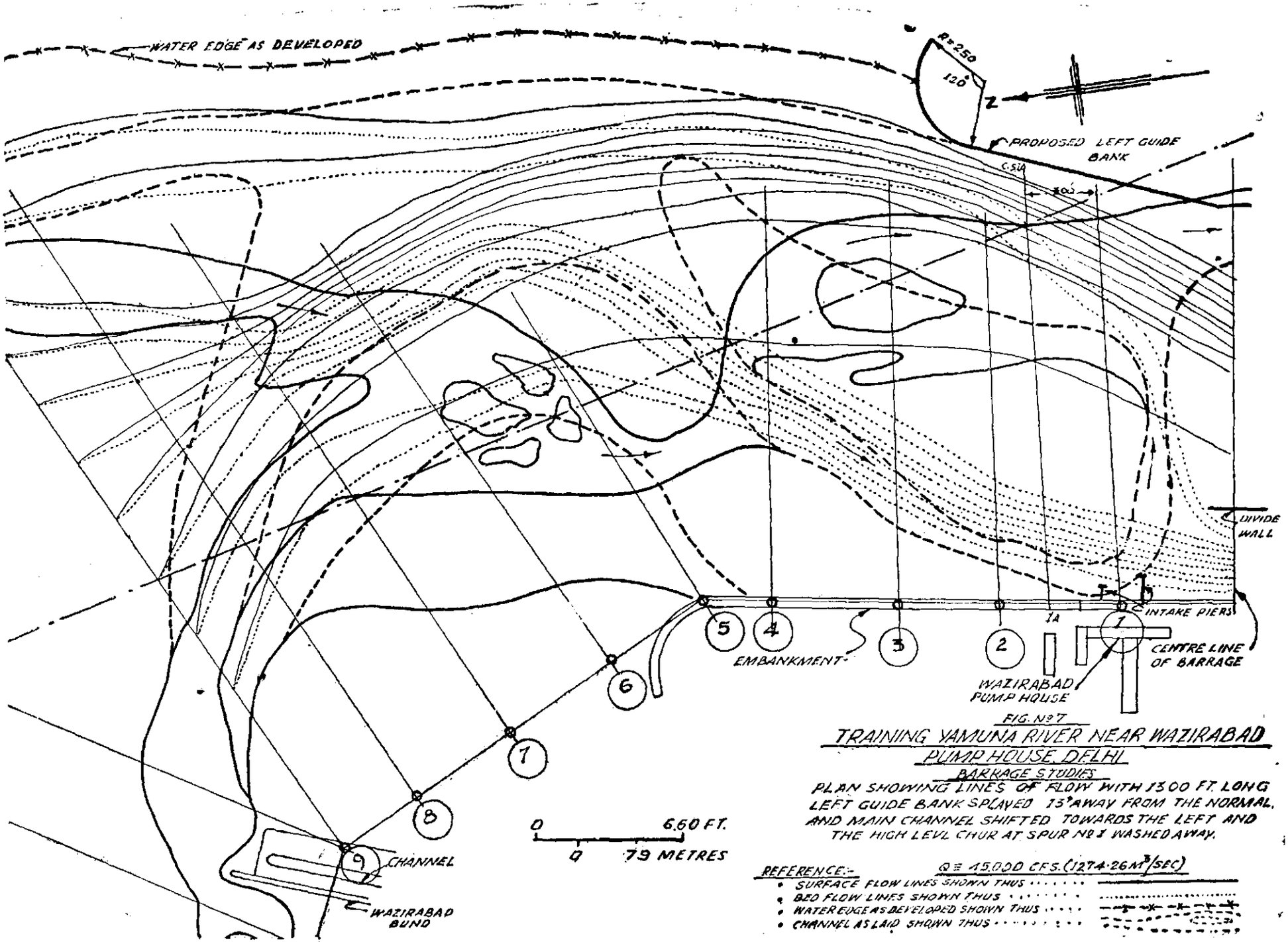

FIG. No 7

TRAINING YAMUNA RIVER NEAR WAZIRABAD PUMP HOUSE DELHI

BARRAGE STUDIES

PLAN SHOWING LINES OF FLOW WITH 1300 FT LONG LEFT GUIDE BANK SPLAYED 13° AWAY FROM THE NORMAL, AND MAIN CHANNEL SHIFTED TOWARDS THE LEFT AND THE HIGH LEVL CHUR AT SPUR No 1 WASHED AWAY.

REFERENCE:- Q = 45,000 CFS. (1274·26 M³/SEC)

- SURFACE FLOW LINES SHOWN THUS
- BED FLOW LINES SHOWN THUS
- WATER EDGE AS DEVELOPED SHOWN THUS
- CHANNEL AS LAID SHOWN THUS

Flow line observations with 396.24 *m* (1300 *ft*) long left guide bank normal to the barrage under the pre-1959 floods river course (*fig* 5) showed that the surface flow shifted to the left whereas the bed flow was diverted to the centre, indicating possibility of development of the channel on the left. This tendency was not reflected by the velocity observations, which showed low velocities along the left bank and high velocities along the right. This was attributed to the existence of a high shoal at the site of spur *No* 1 which acted as a submerged spur and deflected the water to the right. This projection showed a tendency to wash away. The next experiment was conducted with the following changes:

(*a*) Removal of shoal at the site of spur *No* 1 and

(*b*) Slight shifting of the channel position to the left.

With these changes bed flow was diverted to the right bank and the surface flow concentrated near the left bank (*fig 6*). This was confirmed by the velocity observations, but velocities near the right bank were of the order of about 1.2192 *m/sec* (4 *ft/sec*) as compared to about 1.524 *m/sec* (5 *ft/sec*) near the left bank, thereby indicating availability of some water near the intake piers.

The 396.24 *m* (1300 *ft*) long left guide bank normal to the barrage under the worst river course of 1916 deflected the current towards the centre (*photo 1*) indicating possibility of getting the supplies near the intake piers.

It was found in an experiment with 396.24 *m* (1300 *ft*) long left guide bank splayed at 13° to the normal that surface flow was mainly concentrated near the left bank, while bed flow was deflected to the right bank (*fig* 7). This was also supported by the velocity observations, which showed high velocity of the order of 1.6764 *m/sec* (5.50 *ft/sec*) near the left bank and comparatively low velocities near the right bank. The central island was also fairly high. These observations, therefore, indicated the difficulty of obtaining the supplies near the intake piers.

This set up under the most unfavourable river course of 1916 indicated pinning of the channel along the splayed left guide bank (*photo 2*).

A study of *figs 4. 6* and 7 showing flow lines under different conditions supported by velocity observations indicated that the set up with short guide bank with the two old spurs maintained gave the best results for maintaining the channel near the right bank. The next in order of preference was the 396.24 *m* (1300 *ft*) long left guide bank normal to the barrage, when the channel may maintain itself near the right bank with little dredging. With left guide bank at an inclination of 13° and 21° to the normal the right bank may silt up and defeat very purpose of the barrage.

It was felt that construction of an inclined guide bank would not effect any appreciable economy in cost, as the likely reduction in height of the embankment was about 2.74 *m* (9 *ft*) only, but increased quantity of stone would be required in flexible apron to allow for greater dispersion.

4. Conclusions

(*i*) A short guide bank which had already been constructed with the two old spurs and the connecting spur bund on the left bank maintained would develop the channel along the right bank. This was likely to cause greater submergence in the areas upstream.

(*ii*) If for any reasons the old spurs and the spur bund on the left cannot be maintained properly, then a 396.24 *m* (1300 *ft*) long left guide bank normal to the barrage appeared to be the next best, though this might require some maintenance dredging. The guide bank on the left may however, exert an attracting influence and keep the channel on the left bank, if the river channel were to swing back to the right bank near Jagatpur, as after the 1957 floods.

The length of 396.24 *m* (1300 *ft*) of the left guide bank to be made up as follows as shown in *fig 3*.

Straight length:	320.04 *m* (1050 *ft*) including 47.244 *m* (155 *ft*) of the short guide bank as already constructed.
Curved head:	76.2 *m* (250 *ft*) radius with sweep 120°.

Left approach embankment of the barrage should be protected by proper turfing *etc.*

(*iii*) The 396.24 *m* (1300 *ft*) long left guide bank inclined to the normal could not be recommended as it would silt up the channel on the right bank and also pin down the channel to the left guide bank under the unfavourable river course.

2. Training Jhelum at Mohora Power House, Kashmir

DURING the high floods in July 1959, the river Jhelum attacked its left bank near the Mohora Power House, situated about 48 *km* (30 *miles*) downstream of Wular lake in Kashmir and eroded the bank over a depth of about 60 *m* (200 *ft*). The probable causes of this erosion were changes in the upstream portion of the river which resulted in eroding the right bank about 330 *m* (1000 *ft*) upstream of the power house. Huge quantities of boulders, eroded from the right bank, travelled a little downstream and deposited on the right bank itself opposite the power house. This naturally resulted in the channel being shifted towards the left bank, causing heavy erosion near the power house. Due to this erosion, a third of the power house building and other ancillary structures were washed away. Model studies were undertaken for—

(i) devising temporary protective measures for the existing power house until such time a new power house was constructed.

(ii) training the river in this reach.

2. Model and hydraulic data

The model covered a reach of about 3 *km* (2 *miles*) in the vicinity of the Mohora Power House. It was laid according to the plan and 11 cross-sections which were the only sections giving the bed levels of the channel in this reach.

The scales of the model were as below:—

Length scale	...	1/150
Depth scale	...	1/30
Discharge scale	...	1/24,640

The only hydraulic data available consisted of daily water levels at 6 gauge stations for a period of 3 to 4 months collected after August 1959. No water levels had actually been observed during the high floods. High flood levels were, however, supplied at a few points in the model reach from local enquiries. No information about the river discharge corresponding to any of the stages was available.

The data available for proving the model was very meagre. The conditions observed in the river on 1st October 1959 (when the site was inspected) were seen to have been reproduced in the model at a discharge equivalent to 318.56 m^3/sec (11,250 *cfs*). The water levels at the washed away bridge (*fig 1*) and the gauge station immediately upstream were reproduced at a discharge equivalent to 2661.8 m^3/sec (94,000 *cfs*). It was, however, found that the gauge at Mohora Power House was reading 1.524 *m* (5 *ft*) higher than required (*RL* 4390.5). This higher level at the power house gauge was probably due to the formation of a high island a little below the power house. This was confirmed in the model as by artificial lowering of the island the lower gauge could be obtained at Mohora Power house. In absence of any further data, the model was taken to be proved.

3. Temporary protective measures for existing Power House

As mentioned above, the water level at Mohora Power House could be lowered by artificial lowering of the island below the power house. This lowering of water level naturally increased the velocities near the Power House. With the island lowered, the maximum velocity for a discharge equivalent to 2661.8 m^3/sec (94,000 *cfs*) on cross-section 40 about 9.144 *m* (30 *ft*) inside from the Power House (*fig 1*) was 8.84 *m/sec* (29 *ft/sec*), whereas velocity near the power house on the same cross-section was 7.315 *m/sec* (24 *ft* per *sec*). The velocity on cross-section 36 *ie* at the site of the proposed power house was 9.65 *m/sec* (31.7 *ft/sec*). As the river in this reach was narrow, only local bank protection measures were possible. Also, the velocities being of the order of 9.14 *m/sec* (30 *ft/sec*) the required bank protection could be only with stone crates.

4. Geometrically similar model

For determining the size of the crates for this purpose, tests were carried out in a flume on a 1/30 scale geometrically similar model. Crates of sizes equivalent to 3.05, 5.08, 7.6 *m tons* (3, 5, 7½ tons) were tested on bank slopes of 1:1 and 1½:1. It was seen that 3.05 *m tons* (3 *tons*) crates were washed away at velocities less than 9.144 *m/sec* (30 *ft/sec*). Similarly 5.08 *m tons* (5 *tons*) crates, could hardly stand upto a velocity of 10.06 *m/sec* (33 *ft/sec*). During these tests it was observed that the crates in the apron were washed away first. It was therefore, decided to provide more stable crates in this portion. Sizes of the crates were, accordingly increased to 7.62 *m tons* (7½ *tons*) and were tested with slopes of 1:1 and 1½:1. In combination with the 7.62 *m tons* (7½ *tons*)

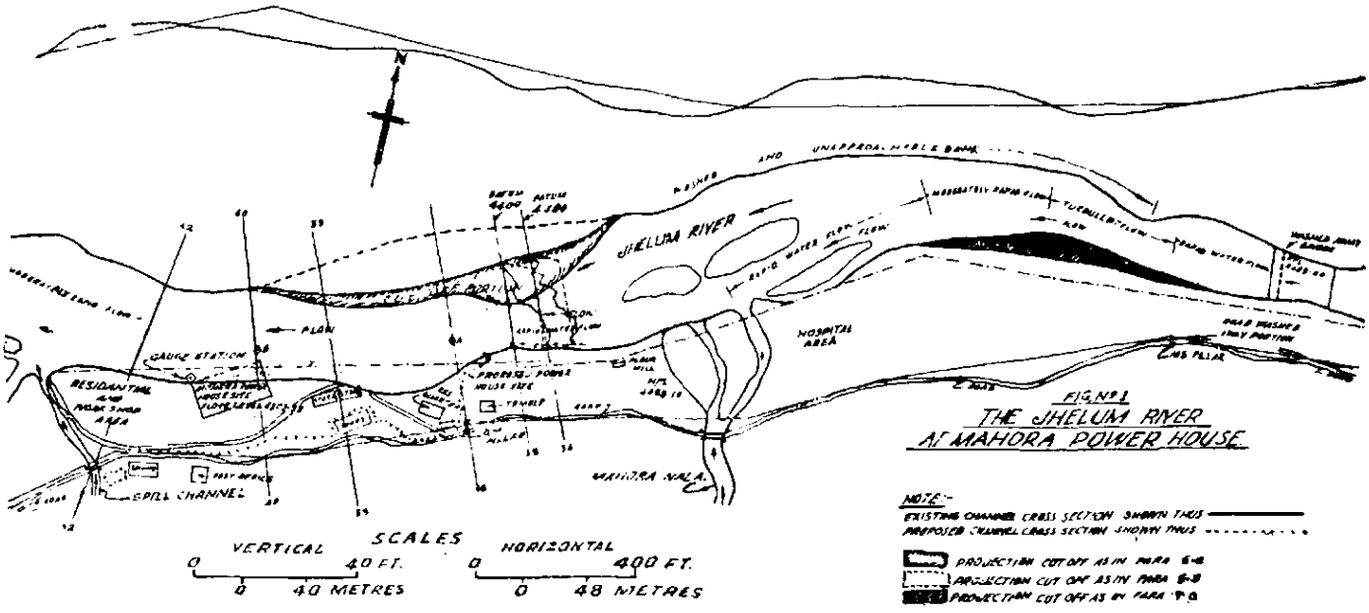

FIG. No 1
THE JHELUM RIVER AT MAHORA POWER HOUSE

crates on the slopes, three rows of 10.16 *m tons* (10 *tons*) crates were put in the apron on the bed. Tests carried out showed that the above crates laid at 1 : 1 slope were not stable. The crates laid at slope of $1\frac{1}{2}$: 1 were however, found to stand a velocity of 12.19 *m/sec* (40 *ft/sec*). This result was confirmed in a bigger flume where the bank line of the river between cross-sections 38 to 42 was reproduced.

The protection measures suggested were to extend from slightly upstream of cross-section 38 to cross-section 42 a length of 228.6 *m* (750 *ft*) because in addition to protecting the most important reach, it had fairly convenient points for anchoring the same (*fig 2*).

5. Training river near Mohora Power House

(*i*) The experiments under existing conditions in the distorted model had showed that water from upstream of cross-section 36 impinged on the left bank due to projection of the right bank into the channel (*photo 3*) at cross-sections 34 and 35 (*fig 1*). The velocity at point *A* on cross-section 36 was found to be 9.144 *m/sec* (30 *ft/sec*) while at point *B* on cross-section 40, it was of the order of 7.62 *m/sec* (25 *ft/sec*) for a discharge equivalent to 2661.8 m^3/sec (94,000 *cfs*).

(*ii*) As the river width in the reach near the power house was very narrow varying from 45.72 *m* to 91.44 *m* (150 *ft* to 300 *ft*) and velocities very high, the training measure like spurs *etc* were not possible. These could only consist of widening of the channel and removal of any obstructions which projected into the channel. Accordingly the projection at cross-sections 34 and 35, which was the cause of severe attack of water on the left bank was removed (*fig 1*) and its bed level kept the same as the existing average bed level of the channel (*ie* about 4370.0). The velocity observations after the removal of the projection showed that the velocity had reduced from 9.14 *m/sec* (30 *ft/sec*) to 6.096 *m/sec* (20 *ft/sec*) on cross-section 36, and from 7.62 *m/sec* (25 *ft/sec*) to 4.572 *m/sec* (15 *ft/sec*) on cross-section 40 (*fig 3*). It was further observed that on cross-sections 36 and 39, high velocity flow shifted towards right and on cross-section 40, the velocity was evenly distributed over the entire section. The attack on the left bank had been reduced (*photo 4*).

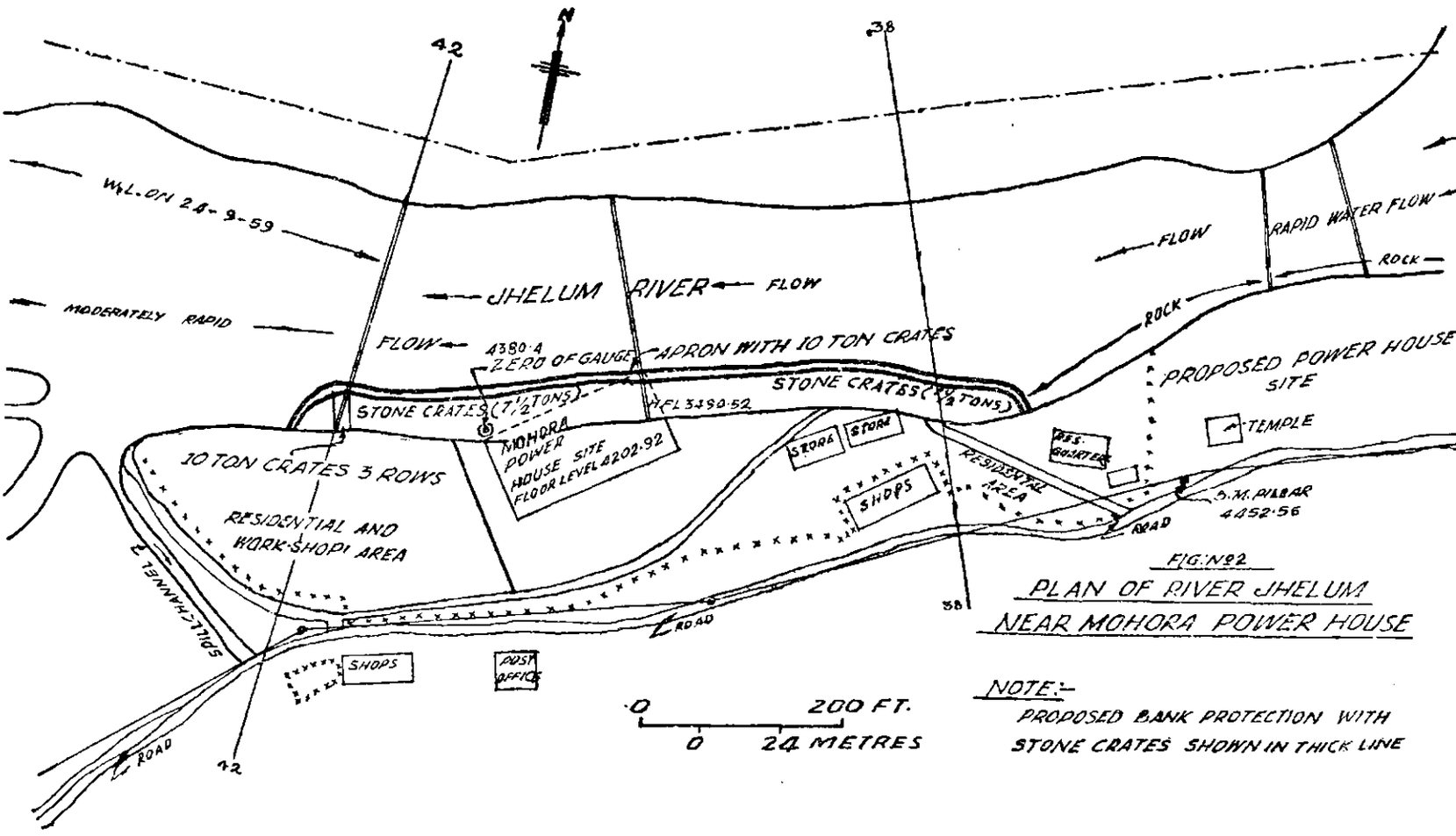

FIG. NO 2
PLAN OF RIVER JHELUM NEAR MOHORA POWER HOUSE

(*iii*) An experiment was conducted in order to see if further widening of the channel at cross-sections 34 and 35 (shown in dotted lines in *fig 1*) would further reduce the attack on the left bank. The level of the excavated channel at cross-section 34 was kept at *RL* 4375 as against *RL* 4370 in the previous experiment. The observations, however, showed that there was a rise in the bed level of channel both at cross-section 39 and cross-section 40 due to the incoming debris and consequently the velocities on these sections increased appreciably (*fig* 3). Hence it became apparent that the extra cutting did not improve the conditions further.

Observations were also made to see if widening the channel shown fully shaded in *fig 1* just below the washed away bridge 823 *m* (2700 *ft*) upstream of the existing power house in addition to the proposed in 5 (*ii*) would help in straightening the flow, thus further reducing the velocities on the left bank near the power house. The observations, however showed that the effect of widening of the channel near the washed away bridge was nullified by the time cross-section 36 was reached.

3. Recommendations

Temporary protective measures for the existing power house:—

(*i*) Length of the reach to be protected should start from cross-section 42 at downstream end and should extend a little upstream of cross-section 38.

(*ii*) Crates weighing 7.62 *m tons* (7½ *tons*) each should be laid on a slope of 1½:1.

(*iii*) Three rows of 10.16 *metric tonne* (10 *ton*) crates should be laid as apron to the 7.62 *metric tonne* (7½ *ton*) crates on the slope. Three rows of 10.16 *metric tonne* (10 *ton*) crates should be laid on the slope at the tail end at the point where the end curve started.

(*iv*) Crates should be laid longitudinally.

Training of the river in the vicinity of the Power house:—

(*i*) The projection opposite the proposed power house site should be removed to the extent

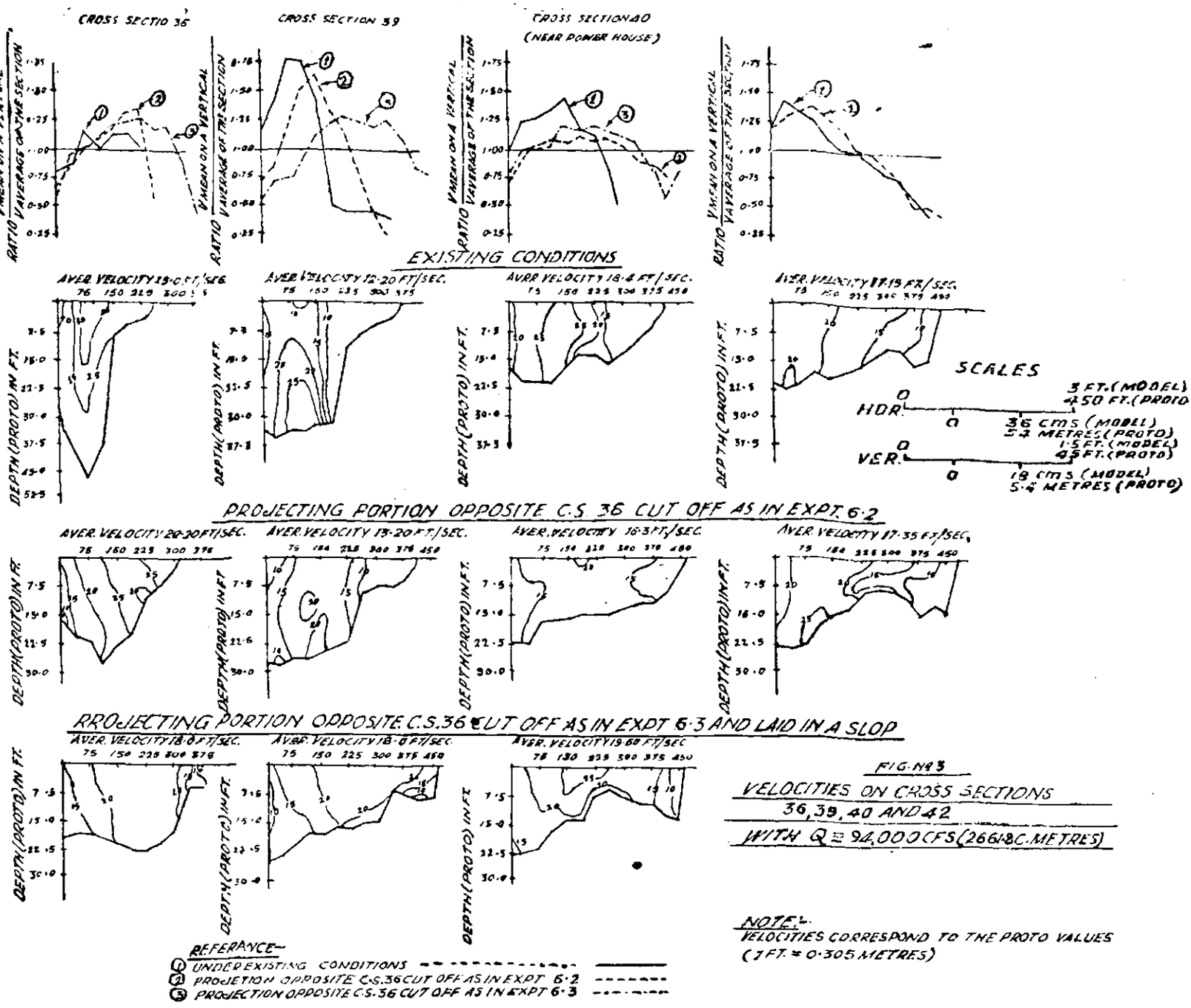

FIG. NO 3

VELOCITIES ON CROSS SECTIONS 36, 39, 40 AND 42 WITH Q = 94,000 CFS (2661·8 C. METRES)

NOTE:—
VELOCITIES CORRESPOND TO THE PROTO VALUES (1 FT. = 0·305 METRES)

partially shaded as shown in *fig 1* and described in 5 (*ii*).

(*ii*) It is also desirable that the right bank immediately upstream of the projection, should be protected from further erosion as it is the main cause of the deposition of boulders opposite the proposed power house site. This bank is, however, inaccessible and is a steep cliff 30.5 *m* to 45.75 *m* (100 *ft* to 150 *ft*) high. It may not, therefore, be possible to undertake any protective measures in this reach. Under the circumstances, it is suggested that debris brought down and deposited opposite the proposed power house site from time to time, should be removed so that sufficient channel width is maintained.

3. Breach in Katjuri embankment at Simuldaghai

THE RIVER Katjuri, a branch of the Mahanadi, attacked its left bank at a place called Dalaighai 14.40 *km* (9 *miles*) from Cuttack in 1953 (*fig 1*). After a series of experiments in the *CWPRS* the following spurs were recommended and constructed to the lengths as below (*fig 1*).

Spur *No* 2	— 42.5 *m* (130 *ft*)
Spur *No* 2A	— 49.1 *m* (150 *ft*)
Spur *No* 3	— 36.4 *m* (112 *ft*)
Spur *No* 4	— 41.0 *m* (125 *ft*)
One permeable spur between spurs *Nos* 2A and 3	29.5 *m* (90 *ft*)

During September 1959 the right bank about 3.2 *km* (2 *miles*) downstream of Dalaighai breached to a length of 360 *m* (1100 *ft*) near a village called Simuldaghai inundating an area roughly 12,950 *hectares* (50 *sq miles*).

Experiments were conducted in a model to find out if the existing Dalaighai spurs had any adverse effect in the Simuldaghai reach.

2. Model and experiments

A model to scales 1/250 horizontal and 1/40 vertical ($V\ E = 6.25$) had been constructed and a reach of 11.2 *km* (7 *miles*) upstream and 3.2 *km* (2 *miles*) downstream of Simuldaghai had been reproduced. The model was laid to post-1958 survey data to reproduce pre-breach conditions. 1959 hydrograph was run on the model for experiments. To obtain the correct gauges, the model was titled to $S\ E = 5$ and additional roughness was introduced in the bed near Dalaighai.

(*a*) *With spurs at Dalaighai as existing*: Surface flow lines and velocity observations were made for various flood stages *viz*, 2260 to 11,000 m^3/sec (.8 to 3.9 lakh *cfs*). *Figs 2* and *3* show the flow lines for discharges 4250 m^3/sec (1.5 lakh *cfs*) and 11,000 m^3/sec (3.9 lakh *cfs*). It will be seen from the figures that the flow which was near Simuldaghai bank at low stages straightened out with higher discharges and at high flood of 11,000 m^3/sec (3.9 lakh *cfs*) was well inside the river.

Photos 5 and *6* clearly indicate how the flow shifted from the bank as the discharge increased.

(*b*) *Without Dalaighai spurs*: The above set of experiments was repeated to study the flow conditions near Simuldaghai bank with removal of

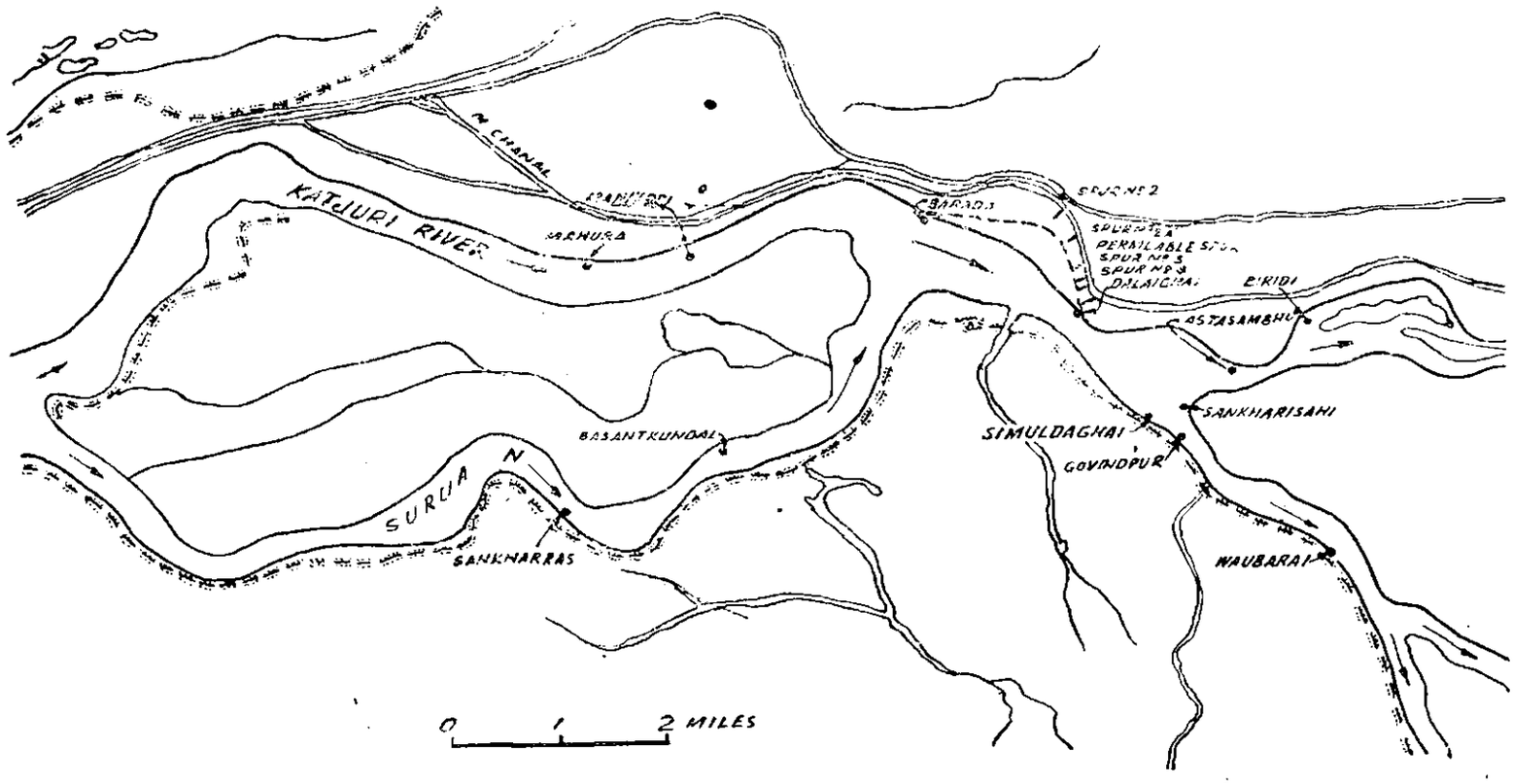

Fig 1: Index Plan showing the river reach with gauge stations.

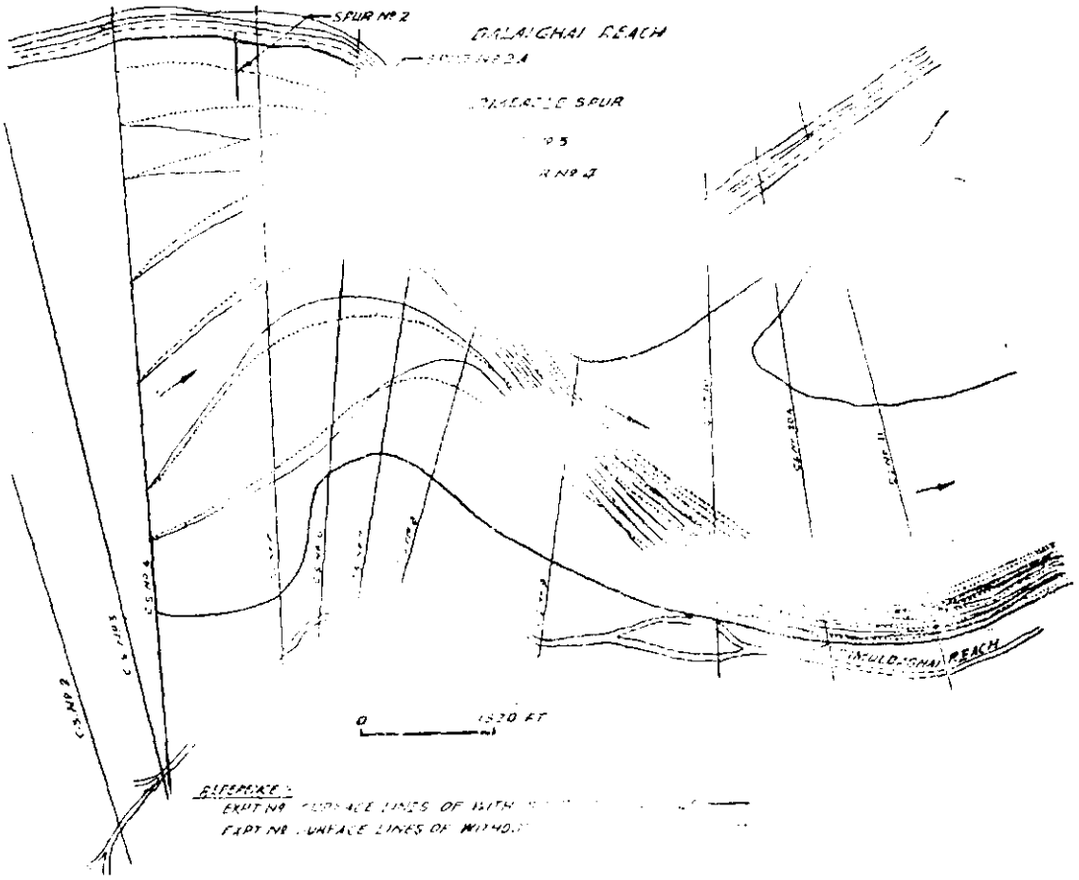

Fig 2: Surface lines of flow, conditions:—(1) With the existing 4 spurs at Dalaighai. (2) With the above spurs removed. $Q = 1{,}50{,}000$ *cfs*.

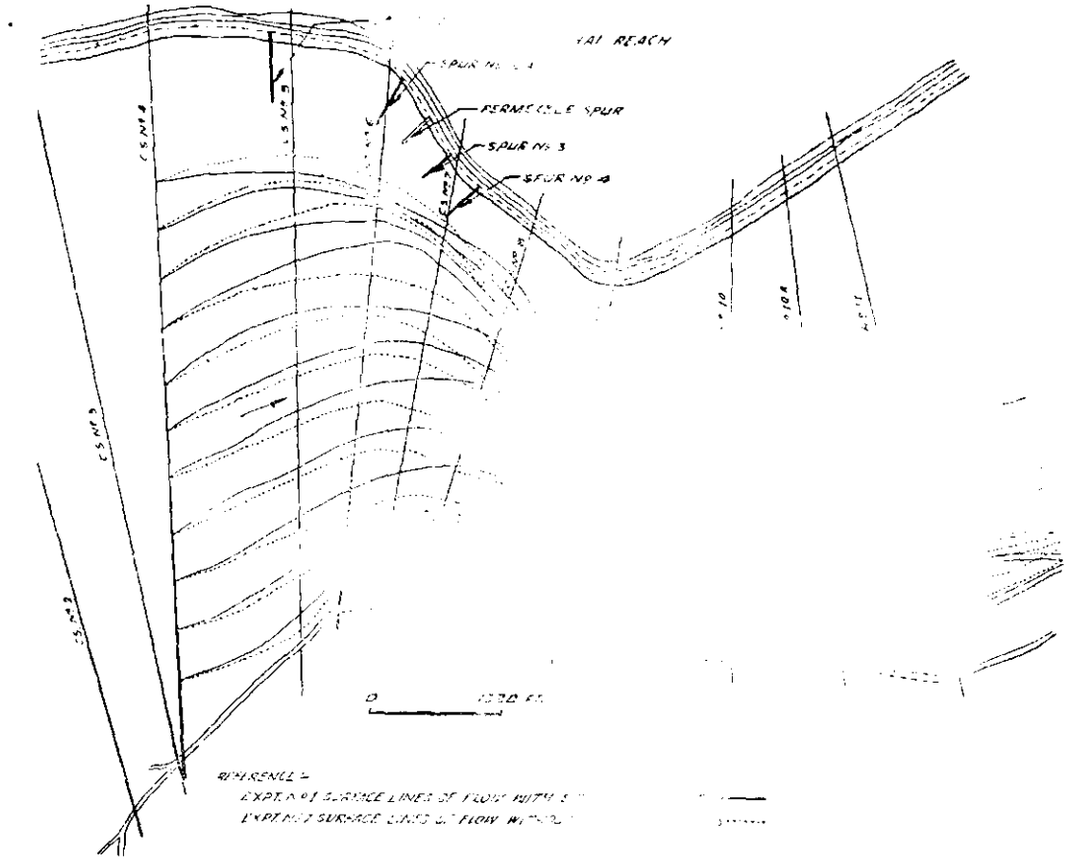

Fig 3: Surface lines of flow, condition:—(1) With the existing 4 spurs at Dalaighai. (2) With the above spurs removed. $Q = 3{,}90{,}000$ *cfs*.

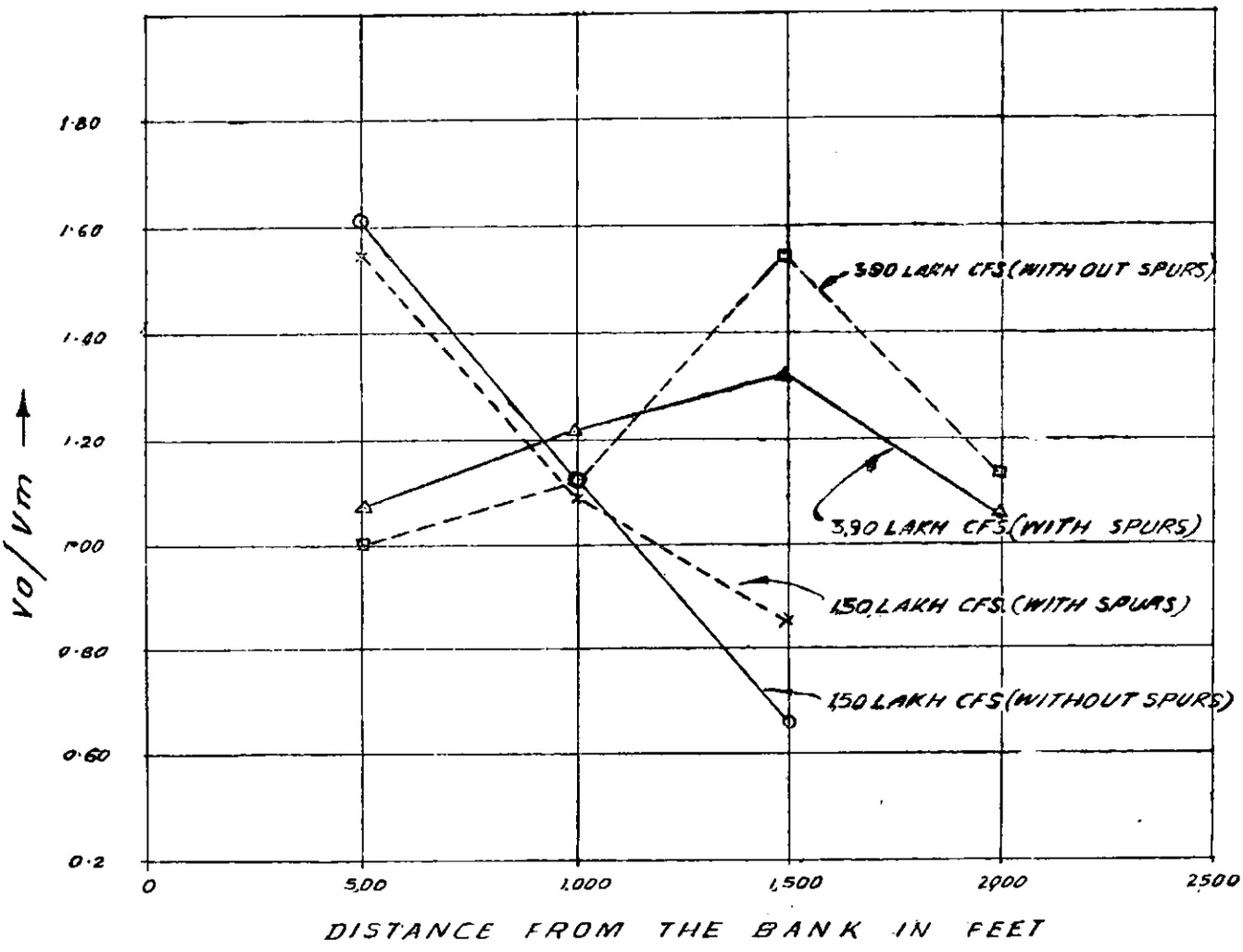

Fig 4: Diposition of velocity concentration in experiment *No* 1 and experiment *No* 2 in the Simuldaghai reach at C. S. *No* 10A.

Dalaighai spurs. The surface flow lines observations were superimposed in *figs 2* and *3* showing corresponding flow lines with spurs. It was found that the flow pattern was unaffected and the current moved away from the bank with the increase in discharge.

Velocity observations were taken at cross-sections 10, 10A and 11 near Simuldaghai reach for discharges Q = 4250 and 11,000 m^3/sec (1.5 and 3.9 lakh *cfs*) with and without spurs at Dalaighai. The concentration of velocities for these discharges at cross-sections 10A near Simuldaghai were plotted in *fig 4*. This figure indicates that the velocity concentration moved away from the bank with increase in discharge under both the conditions *viz*, with spurs and without spurs. Thus the Dalaighai spurs had not adversely affected the flow conditions near Simuldaghai bank.

3. Conclusions

(*a*) With or without spurs at Dalaighai, the flow below Dalaighai restriction straightens out as the discharge increased and for high flood stages it is well within the river and is far away from the Simuldaghai bank.

(*b*) Construction of Dalaighai spurs had not adversely affected the flow conditions in the Simuldaghai reach.

4. Protection of Sabarmati left bank near Rinza bridge

SABARMATI, one of the principal rivers of Gujerat State, rises in the Aravalli Hills of Rajasthan. The river meets the gulf of Cambay after passing through the city of Ahmedabad. Since 1956, the river has been eroding the left bank opposite the village Ganol and within 3.22 *km* (2 *miles*) upstream of the road bridge near Rinza village on the Tarapur-Rinza road about 80.47 *km* (50 *miles*) south of Ahmedabad (*fig 1*). During the 1959 floods, it eroded the left bank to a width of 365.76 *m* (1200 *ft*) completely engulfing the road embankment. The problem had become very acute and cut off was imminent if erosion on the Rinza side was not immediately controlled (*fig 2*).

2. Model and data

A model covering a reach of about 3.0467 *km* (5 *miles*) upstream and about 4.83 *km* (3 *miles*) downstream of the Rinza bridge was constructed to the following scales:—

L scale	=	1/200
D scale	=	1/36
VE = *SE*	=	5.56
Discharge scale	=	1/40,000

The following data was available—

(i) Catchment area 18906.9 *sq km* (7300 *sq miles*)

(ii) Designed *HFL* at the bridge site=*RL* 52.5

(iii) Maximum discharge for which the bridge has been designed: 2208.71 m^3/sec (78,000 *cfs*).

(iv) 1959 post-flood river cross-sections at every 304.8 *m* (1000 *ft*).

(v) Slopes corresponding to the highest flood discharge in 1958 and 1959 based on water marks and local inquiry. This data gave local high flood slopes over a very short reach of 853.44 *m* (2800 *ft*) upstream and 548.64 *m* (1800 *ft*) downstream of the bridge.

(vi) High flood discharge of 1959 through the bridge as calculated from the observed high flood cross-section at the bridge site and one surface velocity in the last span on the right bank, and discharge over the left bank spill area as calculated and supplied by the Deputy Engineer, Kaira. According to these calculations, a discharge of 8211.9 m^3/sec (2.9 lakh *cfs*) was obtained by summing up the calculated discharge through the bridge and the spill areas on the left bank upto chainage 7315.2 *m* (24,000 *ft*) along the base line (see *fig 2* and *col* 3 of *table 1*). Discharge over the right bank spill was not available.

No data about the total discharge in the river and gauges at different stages was available, thus imposing a serious restriction on the model experiments and ultimately on the interpretation of the results.

Table 1: Showing discharge distribution on left bank spills

Q=2·9 lakh *cfs*

Sl No	Chainage along base line (*ft*)	Discharge as calculated and supplied by Dy. Engineer, Kaira (*cfs*)	Discharge as on model under existing conditions (*cfs*)	Discharge as on model with the extended waterway and spills closed upto 7000 *ft* chainage (*cfs*)
1	2	3	4	5
1	Bridge	1,01,944	1,03,800	2,39,400
2	from 0 to 2,000 (left abutment)	Nil	23,300	Nil
3	2,000—2,700	6,460	11,000	Nil
4	2,700—3,100	6,780	12,200	Nil
5	3,100—4,150	13,450	17,150	Nil.
6	4,150—4,600	18,550	15,600	Nil
7	4,600—5,100	12,800	9,100	Nil
8	5,100—6,000	25,900	29,700	Nil
9	6,000—7,000	1,285	1,500	Nil
10	Total	1,87,169	2,23,350	2,39,400
11	7,000—8,000	9,840	6,450	3,940
12	8,000—9,000	18,350	8,000	11,500
13	9,000—10,000	17,600	10,400	9,600
14	10,000—14,500	18,200*	...	...
15	14,500—24,000	37,800	38,200	50,000
16	Total	2,88,959	2,91,400	3,14,440

*This spill does not flow as assumed in the calculations as there is a high ground behind.

L—S 3401—3

3. Experiment with existing condition

The model was proved only for the high flood stage of 8211.9 m^3/sec (2.9 lakh *cfs*) in absence of data at various stages. For want of information from prototype, the right bank spill area was restricted in the model. At the high flood stage, the water level at the bridge site was controlled in the model. At this stage the discharge through the bridge and over the left bank spills was fairly well reproduced in the model according to prototype calculated values. The discharge distribution as calculated for the prototype and as obtained in the model is shown *vide cols* 3 and 4 of *table 1*. Water levels observed at various points on the prototype were also fairly reproduced. A guage was installed in the model 2133.6 *m* (7000 *ft*) downstream of the bridge to read the water level under this condition.

It was observed that out of a total discharge of 8211.9 m^3/sec (2.9 lakh *cfs*) a discharge equivalent to 2944.4 m^3/sec (1.04 lakh *cfs*) passed through the bridge. The remaining, 5266.9248 m^3/sec (1.86 lakh *cfs*) flowed over the left spill area upto chainage 7315.2 *m* (24,000 *ft*) with concentration of 3511.28 m^3/sec (1.24 lakh *cfs*) upto chainage 2133.6 *m* (7000 *ft*) from the bridge. This indicated a development of a cut off from the left bank spill area, if the concentration of discharge flowing over it was not controlled.

4. Experiment with water way 570.588 *m* (1872 *ft*) and spills on left bank closed up to chainage 2133.6 *m* (7000 *ft*)

It was evident from the results of the above experiment that in order to save the bridge from an imminent cut off, the spill discharge at least upto chainage 2133.6 *m* (7000 *ft*) should be controlled. This would result in an increase in the discharge through the bridge which would have to be catered for by extending the waterway. The Authorities concerned had intimated that a discharge of 6088.112 m^3/sec (2.15 lakh *cfs*) would pass through the bridge if the spills upto chainage 2133.6 *m* (7000 *ft*) were closed. Besides 6088.112 m^3/sec (2.15 lakh *cfs*) there would be a spill discharge from the right bank which would flow through the bridge and would have to be accounted for also.

It, therefore, appeared desirable that the waterway at the bridge be designed for a discharge of at least 7079.2 m^3/sec (2.5 lakh *cfs*). This did not take full cognisance of the spill discharge on the right bank, which was restricted in the model. It was therefore, reported that the Authorities may consider this and provide somewhat higher waterway if required. The width of the waterway for Q = 7079.2 m^3/sec (2.5 lakh *cfs*) was therefore, increased from 262.13 *m* (860 *ft*) to 570.588 *m* (1872 *ft*). Experiment was conducted under the following conditions:

(*a*) Waterway 570.588 *m* (1872 *ft*).

(*b*) The proposed Tarapur Rinza road realigned as shown in *fig 3* with formation level of the road raised above the *HFL* upto chainage 2133.6 *m* (7000 *ft*) so as to divert all the discharge flowing over the spills, through the bridge. The road embankment beyond chainage 2133.6 *m* (7000 *ft*) was raised .9144 *m* (3 *ft*) above the ground to allow only partial spills.

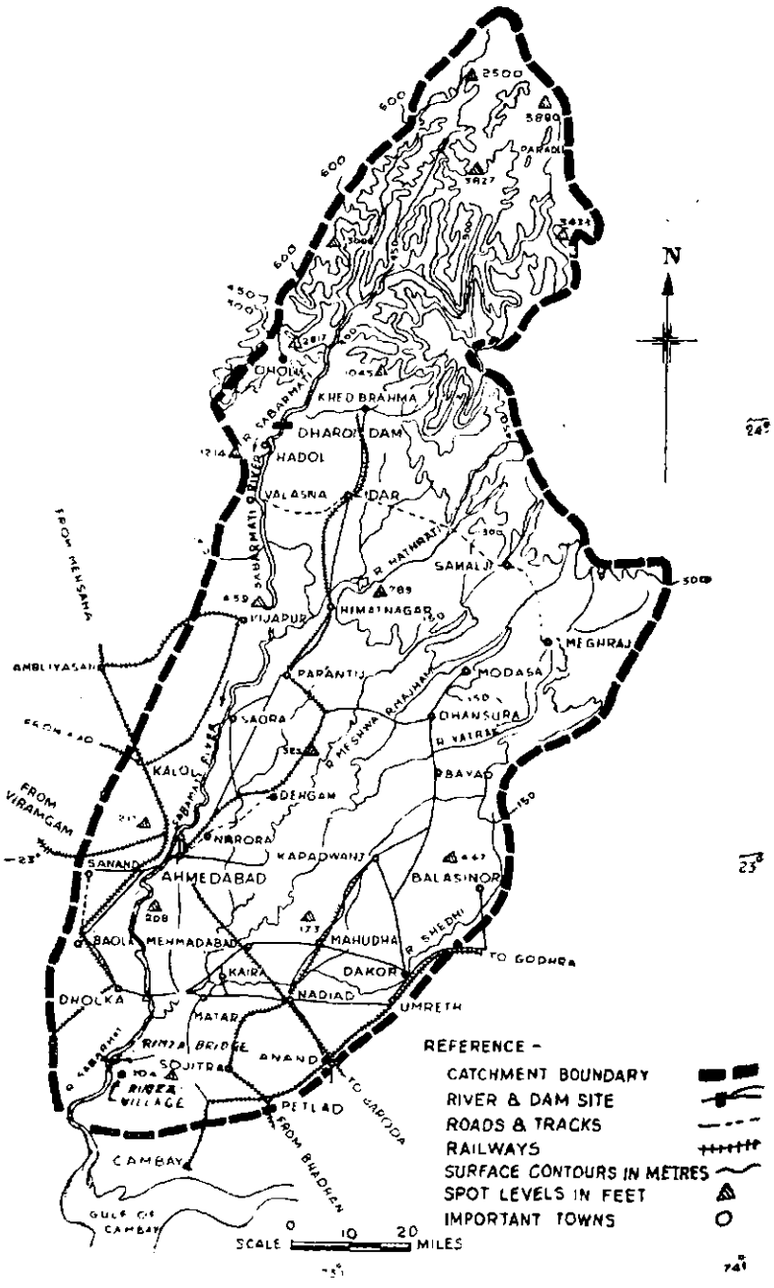

Fig 1: Sabarmati Basin Map *No* 1.

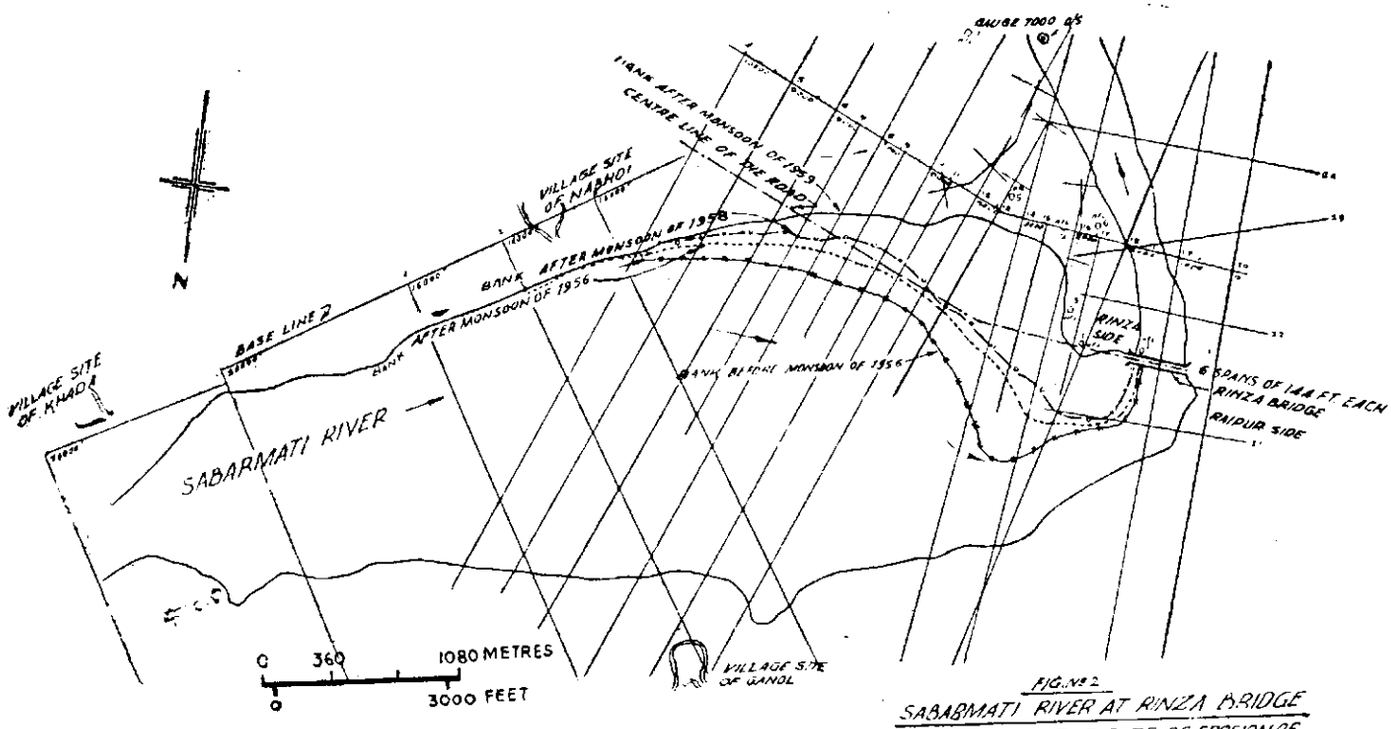

REFERENCE
BANK BEFORE MONSOON OF 1956 SHOWN THUS
BANK AFTER MONSOON OF 1956 SHOWN THUS
BANK AFTER MONSOON OF 1958 SHOWN THUS
BANK AFTER MONSOON OF 1959 SHOWN THUS

FIG. No 2
SABARMATI RIVER AT RINZA BRIDGE
PLAN SHOWING THE RATE OF EROSION OF THE LEFT BANK OF RIVER SABARMATI UPSTREAM OF THE RINZA BRIDGE
SCALE:- 1" = 3000 FT.
1CM. = 360 METRES

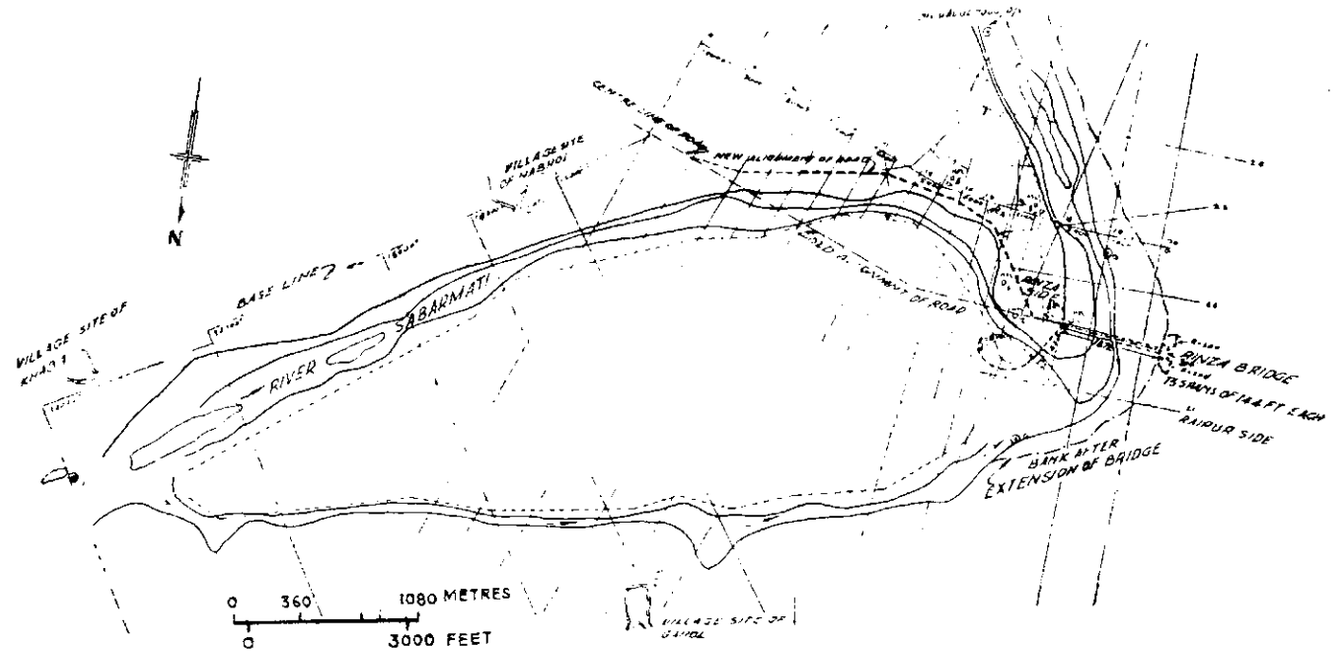

DETAILS OF GUIDE BANKS

S.No	DETAILS	LEFT GUIDE BANK		RIGHT GUIDE BANK	
		U/S	D/S	U/S	D/S
1	STRAIGHT LENGTH	800 FT.	100 FT	100 FT.	100 FT.
2	SPLAY	30°	NORMAL	NORMAL	NORMAL
3	CURVE RADIUS	600 FT	200 FT	200 FT.	200 FT.
4	SWEEP	120°	90°	90°	90°

FIG. No 3
SABARMATI RIVER AT RINZA BRIDGE
PLAN SHOWING THE PROPOSED WORKS
SCALE:- 1" = 3000 FT.
1CM. = 360 METRES

(c) Guide banks on both the sides of the bridge having dimensions and alignment as shown in *fig 3* to guide the flow. These were arrived at by trials.

(d) Approach embankment on the right side raised above the *HFL* for a length of two furlongs beyond the bridge.

It was found that with a total discharge equivalent to 8211.9 m^3/sec (2.9 lakh *cfs*) in the river, a discharge equivalent to 6978.24 m^3/sec (2,39,400 *cfs*) (see *table 1*) passed through the bridge with the water level of *RL* 54.46 which is about .6096 *m* (2 *ft*) higher than the designed *HFL* of 52.5 for the bridge. The water levels in the model under this experiment were controlled by the gauge installed at 2133.6 *m* (7000 *ft*) downstream of the bridge to the value as obtained during the previous experiment. Discharge intensities were observed through the existing as well as the extended portion of the bridge. Maximum intensity was found to be 29.563 $m^3/sec/metre$ (318 *cfs/ft*). It will be necessary to consider this intensity while designing the new foundations.

During the course of this experiment attack was noticed at some points along the left bank along the raised road embankment. These points were proposed to be protected by suitable permeable spurs and screens.

5. Recommendations

(a) The road embankment according to the new alignment on the left, between the bridge and chainage 2133.6 *m* (7000 *ft*) of base line be raised above *HFL* . Beyond chainage 2133.6 *m* (7000 *ft*) the road embankment be raised by .9144 *m* (3 *ft*) above the existing ground level so as to partially close the spills.

(b) The waterway for the bridge should be increased from 262.12 *m* (860 *ft*) to 570.588 *m* (1872 *ft*) [*ie* 13 spans of 43.8912 *m* (144 *ft*) each] corresponding to a design discharge of 7079.2 m^3/sec (2.5 lakh *cfs*) through the bridge. This waterway may have to be suitably increased taking cognisance of the full discharge from the right bank spills.

(c) The bridge foundations should be designed taking into consideration maximum discharge intensities through the bridge, as observed on the model.

(d) The bridge should be provided with guide banks on both sides as shown in *fig 3*.

(e) The approach embankment on the right bank should be raised above the *HFL* at least for a distance of 402.33 *m* (2 *furlongs*) beyond the bridge.

(f) Protection to be provided to all points of attack along the left bank along the raised road embankment by suitable permeable spurs and screens.

---

5. Protection of Ichapur from erosion by Ambika

ICHAPUR village in Gandevi Taluka of Surat District (Gujerat) is situated on the right bank of Ambika river about 12.87 *km* (8 *miles*) upstream of the railway bridge on Bombay-Baroda line of Western Railway. The river was reported to be eroding its bank at the village by as much as 45.7 *m* (150 *ft*) in the last 30 to 40 years. As a result, some of the houses are standing almost on the edge of river bank which is quite steep, with a height of about 10.67 *m* (35 *ft*) and at places consists even of a vertical bluff. Advice of the *CWPRS* was sought on measures to arrest further bank erosion on the village side.

Fig 1 shows location of the eroding reach. It is apparent that the erosion is due to curved flow in the river bend. In absence of hydrographic data, the flood discharge and velocities had to be estimated by empirical methods. The river catchment of 1372.7 *sq km* (530 *sq miles*) would give according to Inglis formula, $Q = \frac{7000\ A}{\sqrt{A}+4}$, a maximum flood of 4587.3 m^3/sec (1.62 lakh *cfs*) and a mean velocity of 2.27 *m/sec* (7.45 *ft/sec*) near the village. Assuming water surface slope equal to bed slope in the reach of 1/1260 and Manning's '*n*' = 0.03, the maximum flood discharge under *HFL* of 97.5 would be 5663.36 m^3/sec (2 lakh *cfs*) and the mean velocity 2.8 *m/sec* (9.2 *ft/sec*). Mean diameter of samples of bed sand varied from 1.69 *mm* to 5.32 *mm* and indicated high velocities prevalent in the river.

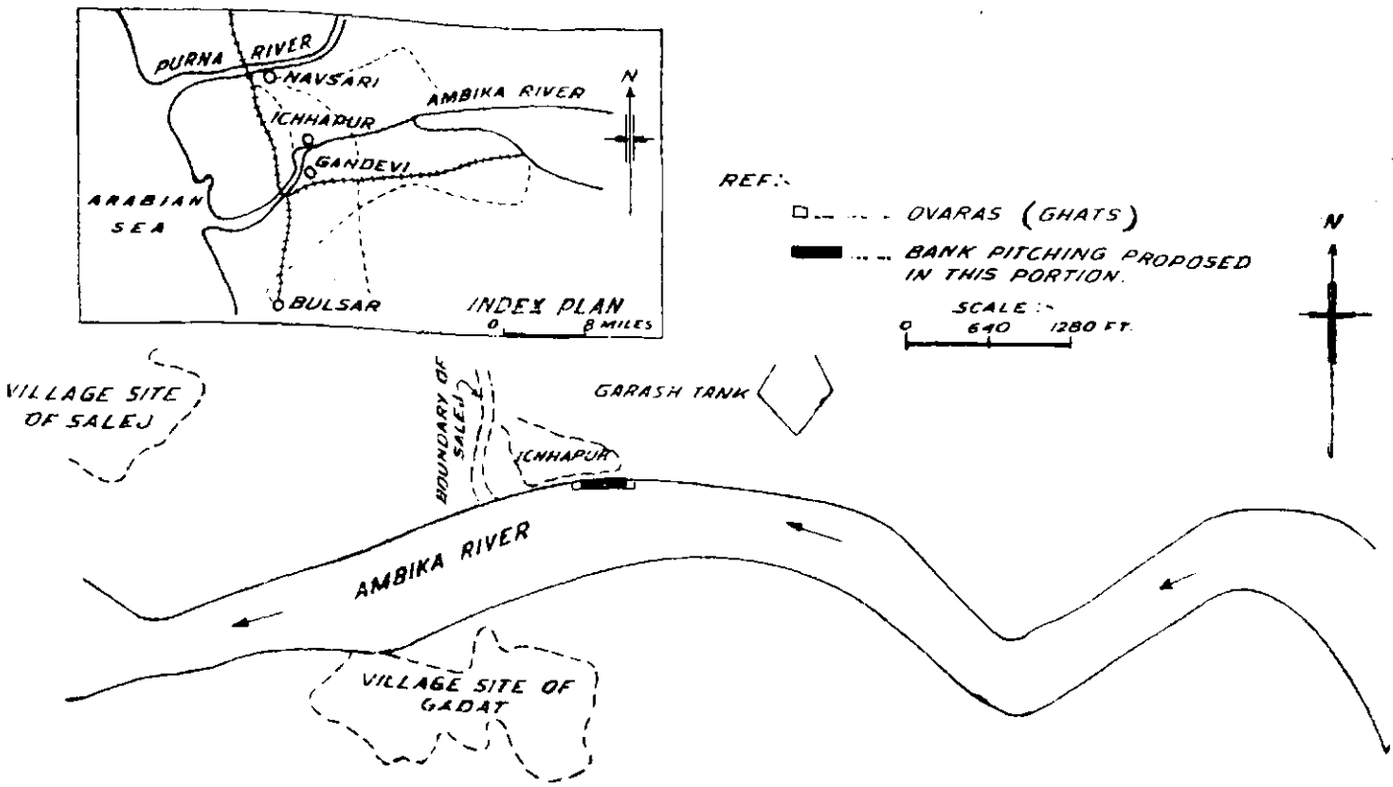

Fig 1: Plan of Ambika river at Ichapur village—Gujerat.

Site inspection revealed that the portion of the bank requiring immediate protection was about 91.44 *m* (300 *ft*) in length extending between the two ovaras *ie* ghats. In between the ovaras and at about the same level as the top of the ovaras is a horizontal clay ledge (*photo 7*) which apparently has been formed and probably maintained by the ovaras. Considering the high cost of providing spurs for protection of the 10.67 *m* (35 *ft*) high bank and incident high velocities, .61 *m* (2 *ft*) thick bank pitching of hand-packed stones with 0.15 *m* (6 *in*) quarry spall backing and with a toe wall 1.2 to 1.5 *m* (4 to 5 *ft*) high, constructed into the clay ledge was recommended. To conform more or less to the existing bank, the side slope of the pitched bank recommended was 1:1. In case the clay ledge erodes in future, provision of additional low spurs in the reach similar to the existing ovaras was proposed.

---

6. Protection of abutment of Kalol bridge on Goma

River Goma is a tributary of the Mahi, one of the major rivers flowing through North Gujerat. The Godhra-Halol road crosses the Goma over a bridge of 7 spans of 16.92 *m* (55 *ft* 6 *in*) about 1.61 *km* (a *mile*) below Kalol town in Panchmahals District. The bridge is located just below a right angled bend in the river and as such the left abutment of the bridge was subject to river attack. After site inspection in December, 1954, construction of a 30.48 *m* (100 *ft*) long deflecting spur located 60.96 *m* (200 *ft*) upstream of the bridge at an angle of 70° to the left bank was recommended, (*fig 1*). This spur was constructed before the monsoons of 1955 and had helped to induce shoaling in the two left end spans of the bridge, (*photo 8*). In the heavy floods of

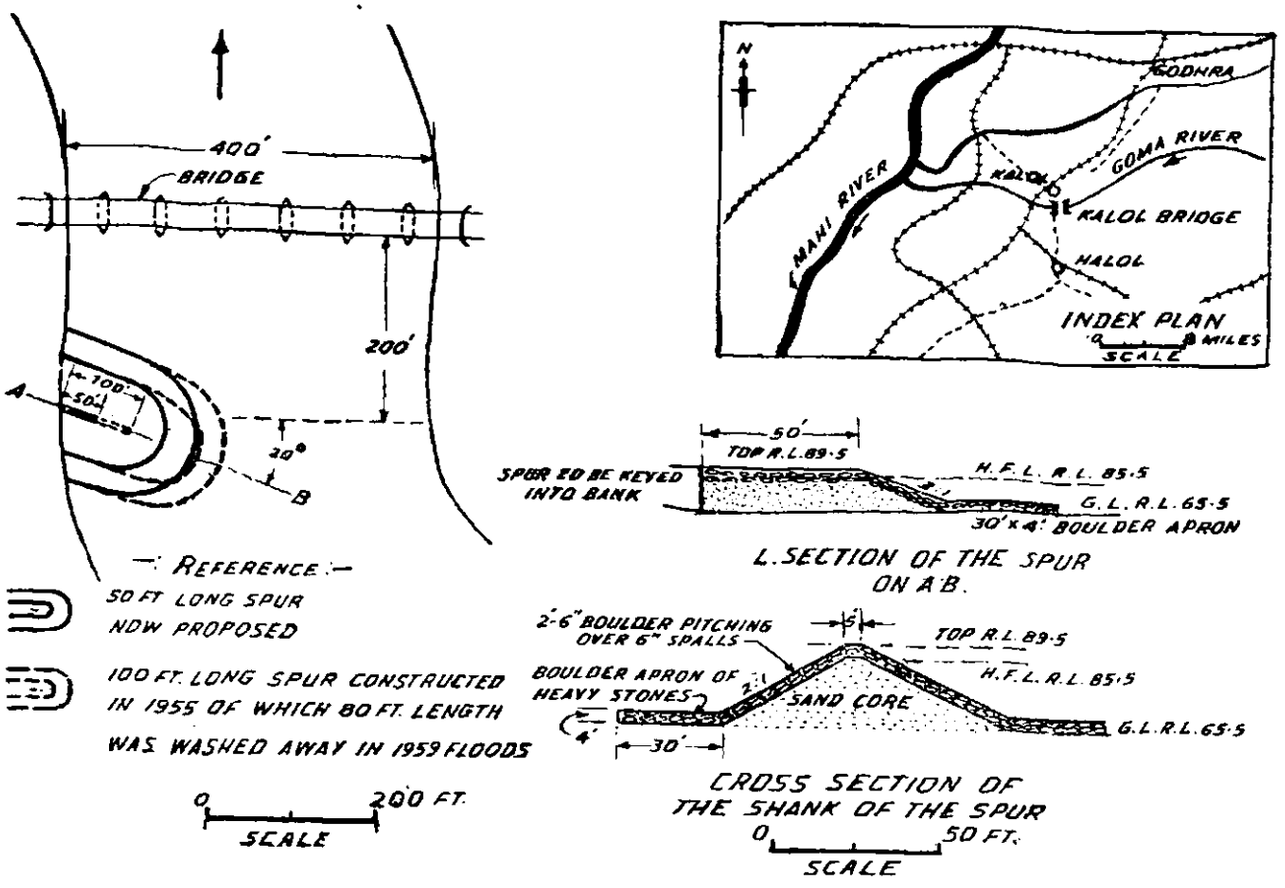

Fig 1: Details of the proposed 50 *ft* long spur.

1959, however, the spur gave way and was washed out except for a length of 6.1 *m* (20 *ft*) from the bank.

The river catchment at the bridge is 233.1 *sq km* (90 *sq miles*) which gives a maximum flood discharge of 1840.59 m^3/sec (65,000 *cfs*) according to Inglis formula, $Q = \frac{7000A.}{\sqrt{A+4}}$. As against this, the discharge adopted for the design of the bridge is stated to be 2058.63 m^3/sec (72,700 *cfs*) worked out from Kutter's formula with $n = .025$, surface slope of 1/1000 and natural waterway 716.56 m^2 (7713 *sq ft*) under *HFL* of 85.5. This gives a mean velocity of 2.87 *m/sec* (9.4 *ft/sec*) in the river and approximately 4.42 *m/sec* (14.5 *ft/sec*) under the bridge. The maximum flood level recorded in 1959 was 1.52 *m* (5 *ft*) below the *HFL* and if velocity is assumed to be proportional to the square root of depth of flow, maximum flood discharge of 1959 could be estimated at 1415.84 m^3/sec (50,000 *cfs*) and mean velocity of 3.17 *m/sec* (10.4 *ft/sec*) under the bridge. Actually on account of the constriction of natural river width from 121.92 *m* (400 *ft*) to 86.87 *m* (285 *ft*) at the spur, velocities at the nose of the spur would have been as high as 4.88 *m/sec* (16 *ft/sec*). This high velocity at the spur was probably the cause of the failure of the spur.

While providing the protection required for the left abutment of the bridge, reconstruction of the spur to a length of only 15.24 *m* (50 *ft*) was recommended so as to reduce constriction caused by it (*fig 1*). Since velocity at the nose under design flood would even then be as high as 4.21 *m/sec* (13.8 *ft/sec*) use of heavy stones or crates weighing upto 90.72 *kg* (200 *lbs*) was recommended for the facing of the nose. In addition, as a precautionary measure, extension of the bank pitching for a length of 15.24 *m* (50 *ft*) downstream of the left abutment was also suggested.

7. Behaviour of cofferdam of Kosi barrage

1959 Post-flood conditions

EXPERIMENTS were conducted during the last two years in connection with flood protection required for the cofferdam and appurtenant works of the barrage and were reported in previous *Annual Research Memoirs*. The protective works so designed well withstood the 1958 and 1959 floods. It was reported that during 1959 floods marked changes had taken place in the channel configuration near Chapri island (upstream of the Chapri ring bund) and slight damage to the spurs in the vicinity was experienced. A flood report describing the behaviour of the cofferdam during 1959 floods was also furnished by the Chief Engineer, Kosi Project. Experiments were subsequently taken up to see if as a consequence, any modifications were necessary in the protective scheme of the cofferdam. The model was laid to 1959 post flood cross-sections supplied by the Kosi Project. Barrage works were reproduced (*fig 1*).

2. Experiments and results

(*i*) Maximum flood recorded during 1959 was of the order of 5097.02 m^3/sec (1.8 lakh *cfs*). It was reported that the downstream head of the right guide bank was under attack throughout the flood season. At low flood stages, spur *No* 4 (*fig 1*) at the barrage axis was effective. The deep channel was stated to be away from the spur *Nos* 3 and 4 at peak flood. Spur *No* 2 was stated to have come under attack only during the falling flood stages, when the river configuration upstream of Chapri island nose had changed adversely.

Verification tests were conducted with the discharge varying from 339.80 m^3/sec (12,000 *cfs*) to 5663.36 m^3/sec (2 lakh *cfs*).

It was seen that the downstream right guide bank nose was under constant attack at all discharge stages upto 5663.36 m^3/sec (2 lakh *cfs*). Maximum velocity recorded here was 1.43 m/s (4.7 ft/sec) at 4247.52 m^3/s (1.5 lakh *cfs*) river stage. Maximum velocity of 1.28 m/sec (4.2 ft/sec) was recorded at the river stage of 4247.52 m^3/s (1.5 lakh *cfs*) at the nose of spur *No* 4. It dropped to 1.04 m/sec (3.4 ft/sec) at 5663.36 m^3/s (2 lakh *cfs*) flood stage thus confirming the prototype behaviour. High velocity of the order of 1.71 m/sec (5.6 ft/sec) was observed at the nose of spur *No* 2 on the Chapri island at 5663.36 m^3/s (2 lakh *cfs*).

Water levels were also observed at the barrage axis. These are given below.

Water levels on the barrage axis at point *No* *G—1* (*fig 1*) up to 5663.36 m^3/s (2 lakh *cfs*).

River discharge in 10^5 *cfs*	Water levels (*RL*) observed in model	Prototype
1	2	3
0.5	241.83	241.6
1.0	242.85	242.6
1.5	243.16	242.9
1.8	...	244.2
2.0	243.44	...

100.0 *cfs* = 28.32 m^3/sec

Observations showed agreement between model and prototype water levels.

(*ii*) The behaviour of the various portions of the cofferdam starting from the upstream end is described below.

Between eastern connecting bund and spur No 2: Eastern connecting bund was found to experience river attack beyond a flood stage of 5663.36 m^3/s (2 lakh *cfs*) and velocities of the order of 1.77 m/sec (5.8 ft/sec) and 2.13 m/sec (7.0 ft/sec) at 14158.4 m^3/sec (5 lakh *cfs*) and 25485.12 m^3/s (9 lakh *cfs*) were recorded at point *No* 13. High velocity parallel flow along this bund would be obtained only when a sustained flood in the river was experienced, causing river reach upstream of the connecting bund to collect spill waters.

Velocities of the order of 1.74 m/sec (5.7 ft/sec), 2.53 m/sec (8.3 ft/sec) and 2.83 m/sec (9.3 ft/sec) at river discharges of 8495.04, 14158.40 and 25485.12 m^3/s (3, 5 and 9 lakh *cfs*) respectively were recorded at the nose of spur *No* 1 (Point *No* 2). These were more or less same as those obtained in model experiments conducted last year with post 1958 survey.

Spur *No* 2 was observed to be under increased river attack this time. Velocities recorded at the nose (point *No* 3) were 2.13 m/sec (7 ft/sec) and 2.68 m/sec (8.8 ft/sec) at 14158.4 and 25485.12 m^3/s (5 and 9 lakh *cfs*) as against 1.40

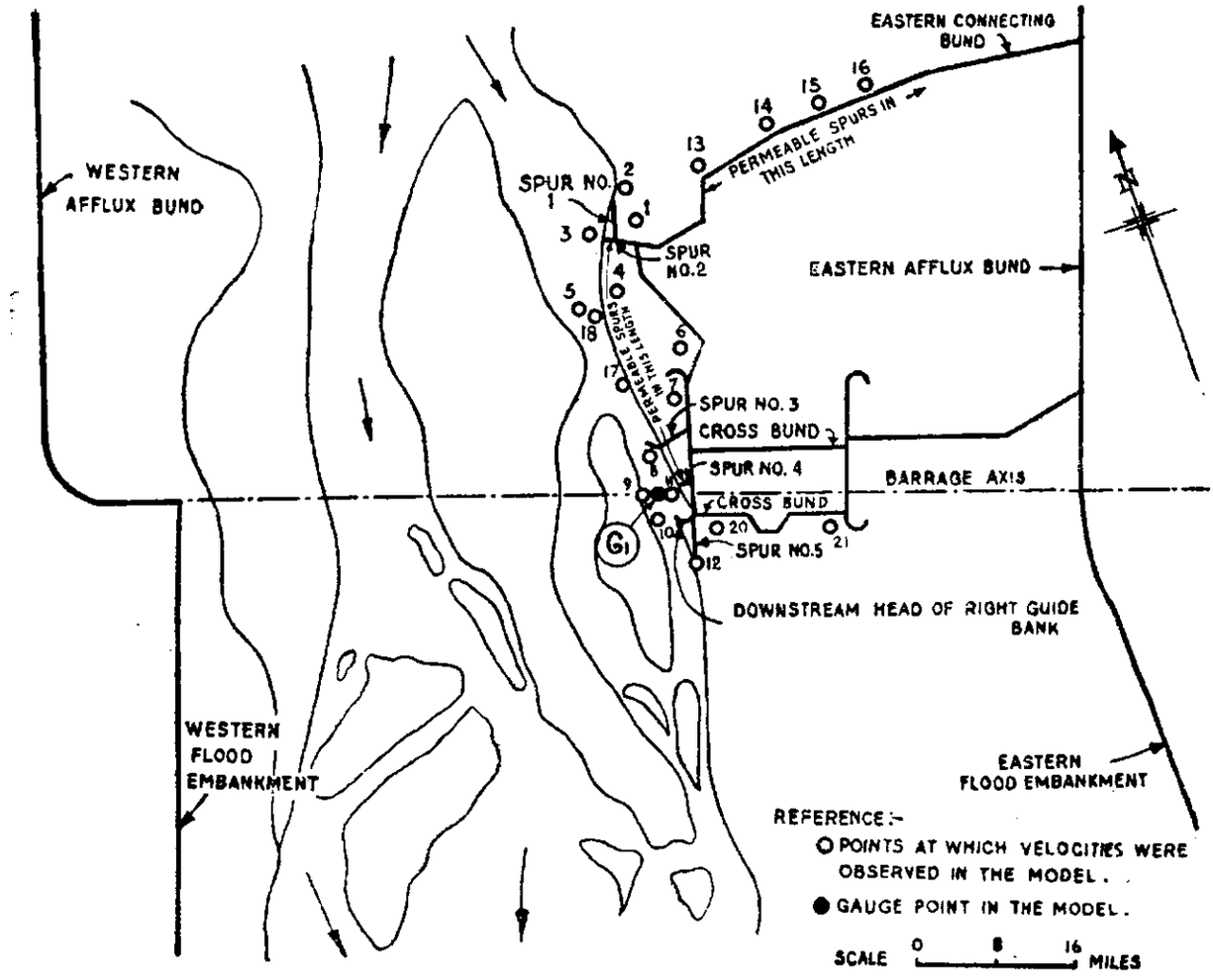

Fig 1: Plan of Kosi river in the vicinity of cofferdam for Hanumannagar barrage.

and 1.80 *m/sec* (4.6 and 5.9 *ft/sec*) noted last year.

Between spur No 2 and spur No 3: Model indicated that Chapri bank between these spurs would be under river attack. High velocities of the order of 1.64 and 1.49 *m/sec* (5.4 and 4.9 *ft/sec*) at 14158.40 m^3/s (5 lakh *cfs*) were observed at velocity point *Nos* 17 and 18.

Conditions at the nose of spur *No* 3 were found to be less severe this year. Velocities at the nose (point *No* 8) were 1.71, 2.04, 2.32 *m/sec* (5.6, 6.7, 7.6 *ft/sec*) against 2.65, 2.83, 3.11 *m/sec* (8.7, 9.3, 10.2 *ft/sec*) recorded last year at 8495.04, 14158.40 and 25485.12 m^3/s (3, 5 and 9 lakh *cfs*) respectively.

Below spur No 3: It was seen that both the downstream head of the right guide bank and spur *No* 5 would be vulnerable to the river attack during 1960 floods. Velocities recorded at the nose of the guide bank were 1.58, 2.22 and 2.56 *m/sec* (5.2, 7.3 and 8.4 *ft/sec*) as against 1.98, 2.50 and 2.80 *m/sec* (6.5, 8.2 and 9.2 *ft/sec*) obtained last year for 8495.04, 14158.40 and 25485.12 m^3/sec (3, 5 and 9 lakh *cfs*).

Effect of washing away of the existing 30.48 *m* (100 *ft*) long extension at 25° of spur *No* 3, and spur *No* 5 was observed in the model, on the portions of the cofferdam, below spur *No* 3. It was seen that the downstream head of the guide bank would be more prone to river attack if the above works could not be maintained to their original lengths.

3. Conclusions

(*a*) Protection by way of permeable spurs was suggested for the eastern connecting bund.

Special vigilance at spur *Nos* 1 and 2 due to adverse approach conditions created during 1959 floods was indicated.

(*b*) Construction of permeable spurs was advocated for the safety of Chapri bank between spur *Nos* 2 and 3.

(*c*) Maintenance of spur *No* 3 with its extension of 30.48 *m* (100 *ft*) at 25° and spur *No* 5 was stressed, for protection of the downstream head of the right guide bank.

(*d*) Stocking of reserve stone at all spurs for emergencies was suggested.

8. West afflux bund of Kosi barrage

Testing of alternative alignments

ALIGNMENT of west afflux bund of Kosi barrage suggested originally by *CWPC* was proposed to be shifted towards the river over a length of 6.44 *km* (4 *miles*), just upstream of the barrage. Purpose of this shift was to avoid submergence of rich paddy lands on the river side of the *CWPC* alignment. Two alternative alignments of the proposed recessed bund were tested in this connection, under both-pre-barrage (*ie* with coffer dam) and post-barrage conditions.

2. Model experiments and results

(*i*) *CWPC alignment*: Under pre-barrage conditions, the river hugged the bund only in the portion between sections 24 and 25 and that also at the flood stage of 26901 m^3/sec (9.5 lakh *cfs*). Maximum velocity of 1.04 *m/sec* (3.4 *ft/sec*) was recorded at velocity point *No* 13 located at about 1.61 *km* (1 *mile*) upstream of the barrage (*fig 1*).

Under post-barrage conditions, (lower pond stage of *RL* 245) water touched the bund between section 20 and barrage axis at only 26901 m^3/sec (9.5 lakh *cfs*). Velocities were, however, very low along the bund.

No protective measures were thus indicated for the bund under any condition.

(*ii*) *Alignment along ABCDEF* (*fig 1*): Under pre-barrage conditions, the flow hugged the bund between *C* and *F*, and velocities in excess of 1.22 *m/sec* (4 *ft/sec*) were observed to exist for equivalent flood stages of 8495, 14158 and 26901 m^3/sec (3, 5 and 9.5 lakh *cfs*). Maximum velocity of 2.56 *m/sec* (8.4 *ft/sec*) at 14158 m^3/sec (5 lakh *cfs*) was recorded at point *No* 8, while at 26901 m^3/sec (9.5 lakh *cfs*) the highest velocity was 2.41 *m/sec* (7.9 *ft/sec*) at point *No* 7. A spur scheme (*fig 1*) was evolved to safeguard the bund at these high velocities encountered at 14158 and 26901 m^3/sec (5 and 9.5 lakh *cfs*) flood stages. It comprised of one stone spur and 3 permeable spurs for a design flood of 14158 m^3/sec (5 lakh *cfs*) and 5 additional permeable spurs for design discharge of 28901 m^3/sec (9.5 lakh *cfs*). All the permeable spurs were 60.96 *m* (200 *ft*) long. The stone spur was 91.44 (300 *ft*) long.

Under post-barrage conditions, velocities along the bund at all flood stages were lower, indicating no necessity of any protective measures.

(*iii*) *Alignment along ABDX* (*fig 2*): It was seen that costly protective measures would be necessitated under pre-barrage conditions if the alignment *ABCDEF* was adopted. An alignment along *ABDX* recessed by about .4 *km* ($\frac{1}{4}$ *mile*) towards west and running along higher spot levels was, therefore, tested. At 14158 m^3/sec (5 lakh *cfs*) velocities of 1.46 *m/sec* (4.8 *ft/sec*) and 1.10 *m/sec* (3.6 *ft/sec*) were recorded at velocity point *Nos* 7 and 8 as against 1.86 and 2.56 *m/sec* (6.1 and 8.4 *ft/sec*) on the alignment along *ABCDEF*. Three permeable spurs each 60.96 *m* (200 *ft*) long and spaced at 457.20 *m* (1500 *ft*) were found necessary to bring down the velocities below 1.22 *m/sec* (4 *ft/sec*). At the flood stage of 26901 m^3/sec (9.5 lakh *cfs*), maximum velocity equal to 2.56 *m/sec* (8.4 *ft/sec*) was recorded at point *D*. Three more permeable spurs were indicated to safeguard against erosion at this river stage.

Under post-barrage conditions, this alignment was free from river attack along its entire length at all flood stages.

3. Recommendations

(*a*) In view of lower velocities along the alignment *ABDX*, and consequent lesser vulnerability to river attack, its adoption on site was recommended. It would not be necessary at all to put up a spur scheme for the bund as the velocities against the embankment recorded in the model for a discharge of 14158 m^3/sec (5 lakh *cfs*) were lower than 1.52 *m/sec* (5 *ft/sec*). Diversion of the river is also expected to be completed by 1962. This would leave a very short time interval between construction of the bund and river diversion, and the bund would be safe once river diversion is complete. It was learnt subsequently from the Project authorities that the land discarded by a recession of .4 *km* ($\frac{1}{4}$ *mile*) from the alignment along *ABCDEF* was also not suited to cultivation.

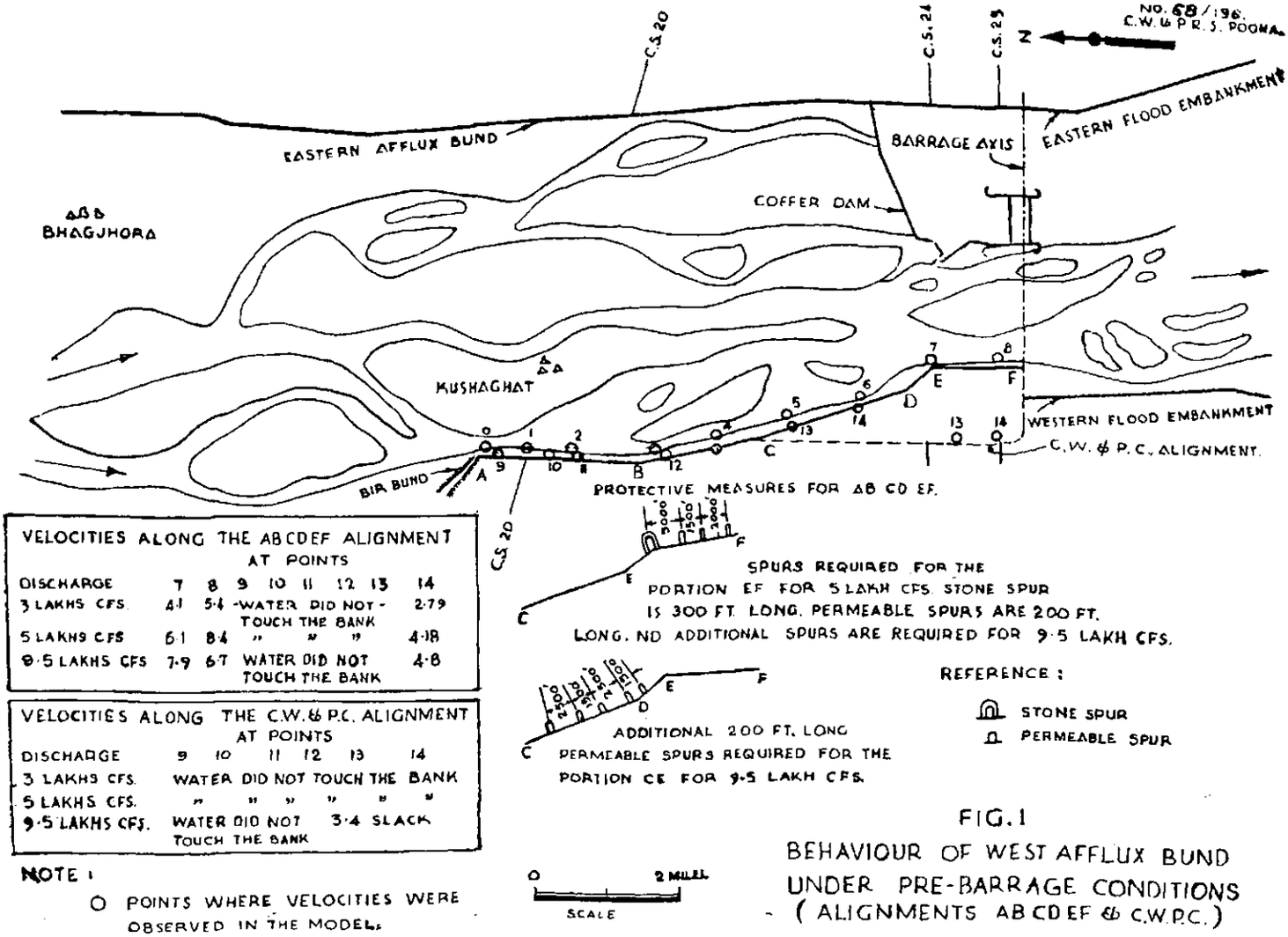

VELOCITIES ALONG THE ABCDEF ALIGNMENT AT POINTS

DISCHARGE	7	8	9	10	11	12	13	14
3 LAKHS CFS.	4·1	5·4	-WATER DID NOT- TOUCH THE BANK					2·79
5 LAKHS CFS	6·1	8·4	"	"	"			4·18
9·5 LAKHS CFS	7·9	6·7	WATER DID NOT TOUCH THE BANK					4·8

VELOCITIES ALONG THE C.W.& P.C. ALIGNMENT AT POINTS

DISCHARGE	9	10	11	12	13	14
3 LAKHS CFS.	WATER DID NOT TOUCH THE BANK					
5 LAKHS CFS.	"	"	"	"	"	"
9·5 LAKHS CFS.	WATER DID NOT TOUCH THE BANK			3·4 SLACK		

NOTE :
O POINTS WHERE VELOCITIES WERE OBSERVED IN THE MODEL.

FIG. 1
BEHAVIOUR OF WEST AFFLUX BUND UNDER PRE-BARRAGE CONDITIONS (ALIGNMENTS AB CD EF & C.W.P.C.)

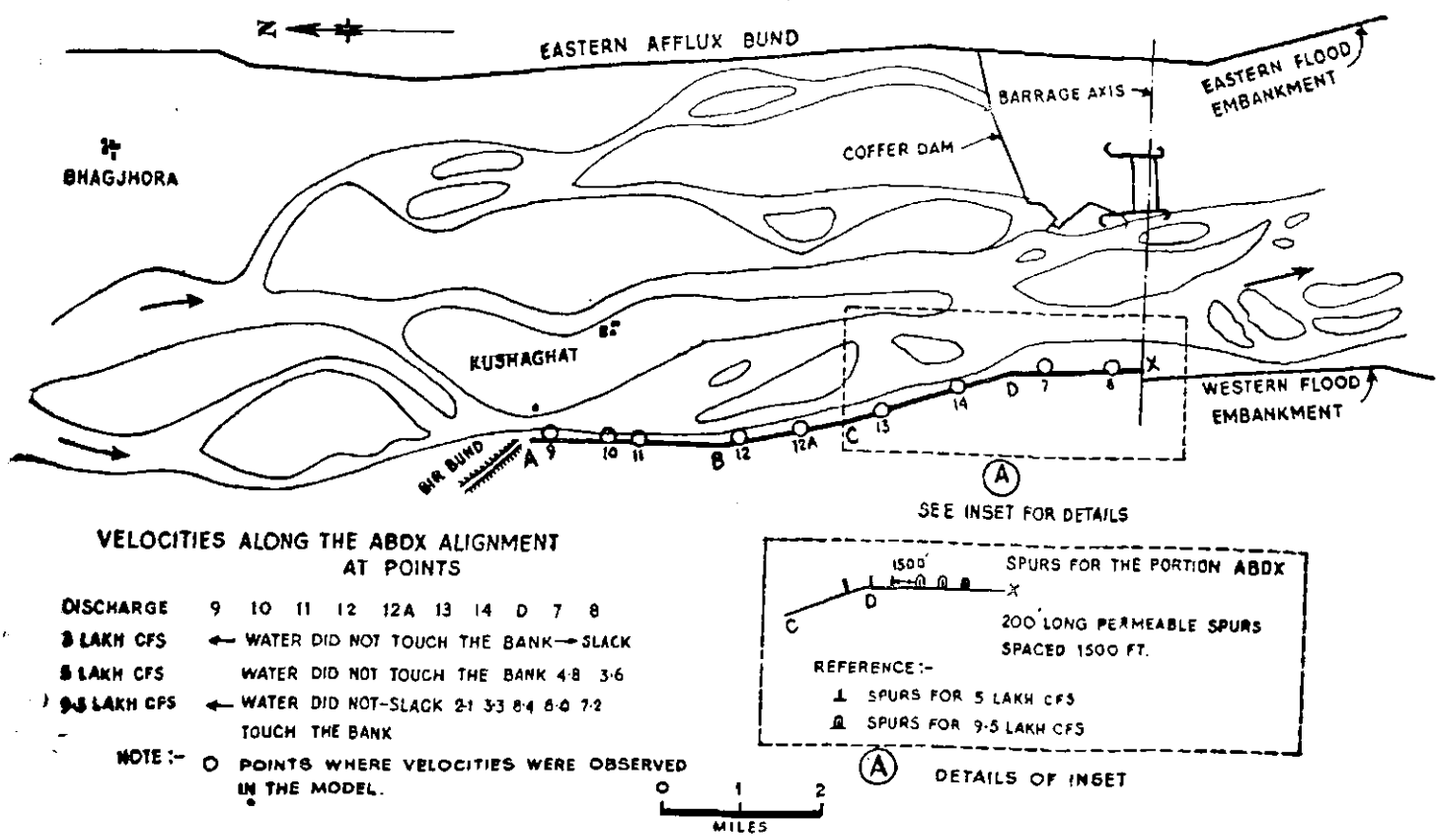

VELOCITIES ALONG THE ABDX ALIGNMENT AT POINTS

DISCHARGE	9	10	11	12	12A	13	14	D	7	8
3 LAKH CFS	← WATER DID NOT TOUCH THE BANK → SLACK									
5 LAKH CFS	WATER DID NOT TOUCH THE BANK							4·8		3·6
9·5 LAKH CFS	← WATER DID NOT TOUCH THE BANK → SLACK							2·1	3·3	8·4 6·0 7·2

NOTE :- O POINTS WHERE VELOCITIES WERE OBSERVED IN THE MODEL.

Fig 2: Behaviour of west afflux bund under pre-barrage conditions; alignment *ABDX*.

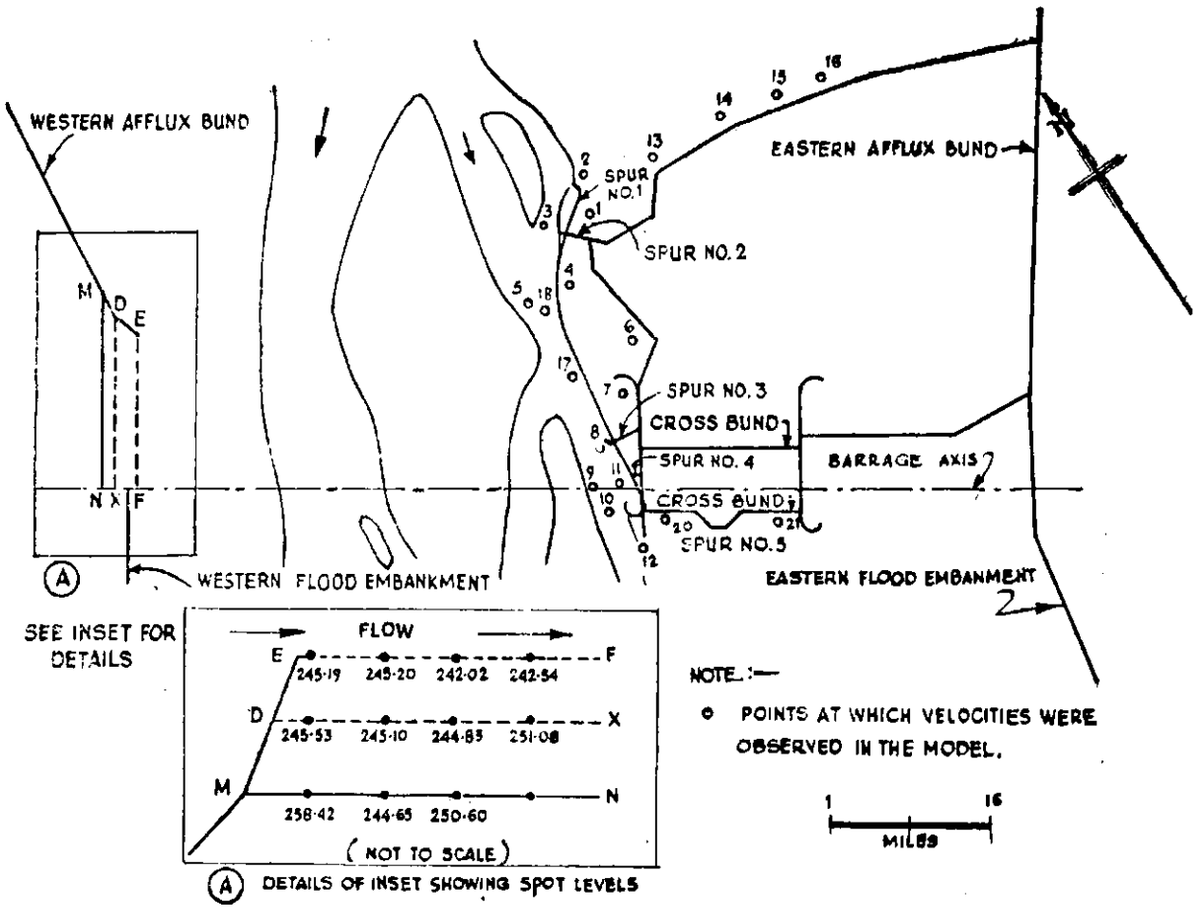

Fig 3: Plan of Kosi river in the vicinity of the cofferdam for Hanumannagar barrage.

(*b*) A study of the spot levels on cross-sections of 1959 post-flood survey in the vicinity of the barrage indicated that the alignment if located along still higher spot levels by a further shift of 60.96—91.44 *m* (200—300 *ft*) (roughly along *MN* see *fig 3*) would involve lesser earthwork. Depth of water against the bund would also be reduced, thus obviating the necessity of any spurs.

4. Effect of shifting west afflux bund

In order to assess whether the conditions would be aggravated at the cofferdam by the proposed shifting of the afflux bund from *CWPC* alignment, velocities were observed at various points along the cofferdam and water levels were recorded on the barrage axis, with both *CWPC* and shifted alignments respectively. No change was indicated by model observations under both conditions, suggesting that situation may not worsen at the cofferdam due to the riverward shift in the alignment.

---

9. Road and railway bridges across Yamuna at Delhi

EXPERIMENTS to find afflux at various points between the proposed road and railway bridges and the existing railway bridge for discharges upto 7079.2 m^3/sec (2.5 lakh *cfs*) were conducted during 1958 with the model laid to 1956 survey (*ibid* 1958). It was, however, decided in a meeting held in Delhi on 20th Nov 1958 that the afflux caused at a discharge of 8495 m^3/sec (3 lakh *cfs*) may be found out on the model so that this value could be taken into account by the Railway authorities for raising the girders of the existing bridge. This would also enable to determine the rise in water level near the marginal embankments, so that the same could be raised and strengthened wherever necessary.

3. Model

The model extends from above the existing Railway bridge down to Okhla weir—a length of about 12.8 *km* (8 *miles*). The model scales are as below

Length scale	...	1/150
Depth scale	...	1/30
Discharge Scale	...	1/24640
$VE = SE$	...	5

After the experiments with the model laid according to 1956 survey were completed, a closed traverse survey of the river from the existing bridge to Okhla weir conducted in 1958 was received. Comparative study of 1956 and 1958 surveys revealed that in the former survey several physical features like embankments, Okhla weir *etc* were differing markedly from the survey of 1958, which was considered to be more accurate. It was, therefore, decided to adopt 1958 survey for the present tests.

An examination of the cross-sections of the two surveys showed that while the channel levels compared fairly well, the spill levels between the left embankment and the channel below the Delhigate pump house had considerably altered during the period 1956 to 1958 (*fig 1*). The spill levels for 1958 survey were 1.5 *m* to 1.8 *m* (5 *ft* to 6 *ft*) lower than those of 1956 (post-monsoon)

Table 1

Discharge in m^3/sec (Gauge Nos in *fig 1*)		Existing road-*cum*-railway bridge	Delhi gate pump house	Nala *No* 12	Proposed Railway bridge		Along Rly bridge near Allen bund.	*C S L L*	Proposed road bridge		Along Road bridge near Allen bund	Okhla Weir
					Curved head *R B*	Centre line *R B*			Curved head *R B*	Centre line *R B*		
		1	2	3	5	7	8	9	11	13	14	
	A.	676·89	672·79	670·50	670·59	670·28	670·35	669·75	669·54	669·33	669·06	665·9
5012·07 (1·77 lakh *cfs*)	*B.*	677·16	673·53	672·21	671·94	671·30	673·47	670·68	670·32	669·33	670·92	,,
	C.	·27	·74	1·71	1·35	1·02	3·12	·93	·78	...	1·86	
	A.	677·76	673·44	671·10	671·19	670·88	670·83	670·43	670·14	670·02	669·66	666·3
5663·36 (2 lakh *cfs*)	*B.*	678·12	674·46	673·23	672·99	671·97	674·34	671·37	671·04	670·02	671·97	,,
	C.	·36	1·02	2·13	1·80	1·09	3·51	·94	·90	...	2·31	
	A.	678·79	674·30	672·32	672·24	671·90	671·64	671 65	671·30	671·10	670·74	666·5
7079·2 (2·5 lakh *cfs*)	*B.*	679·54	675·72	674·55	674·45	673·41	675·96	672·70	672·39	671·10	673·24	,,
	C.	·75	1·42	2·23	2·21	1·51	4·32	1·05	1·09	...	2·50	
	A.	680·26	675·02	673·59	673·59	672·81	672·26	672·72	672·54	672·27	672·13	666·8
8495·0 (3 lakh *cfs*)	*B.*	681·33	677·22	676·05	675·99	674·64	677·04	674·07	673·83	672·27	674·82	,,
	C.	1·07	2·20	2·46	2·40	1·83	4·78	1·35	1·29	...	2·69	

Note: *A* = *HFL* under existing conditions ; *B* = *HFL* with both the bridges constructed ; *C* = Afflux in *ft* due to the proposed two bridges.

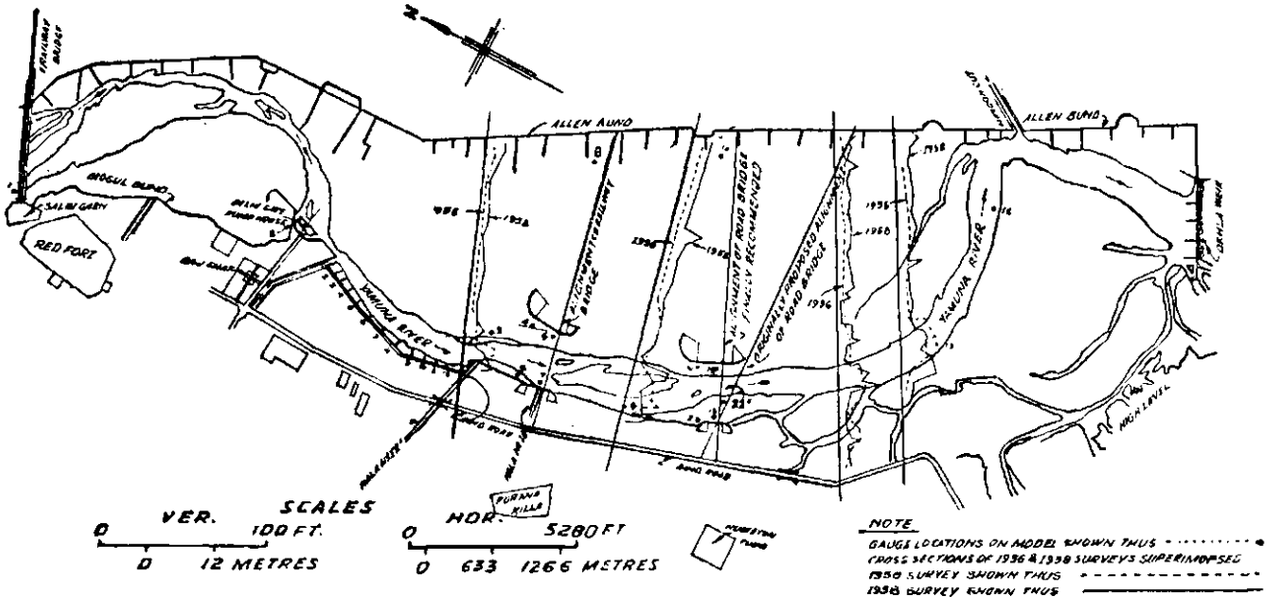

Fig 1: Plan showing the two proposed bridges as constructed.

BRIDGE DETAILS

	Railway Bridge-Water way 1800 *ft*		Road Bridge-Water way 1800 *ft*	
	Left Guide Bund	Right Guide Bund	Left Guide Bund	Right Guide Bund
Downstream Straight Length	800 *ft* Splayed 15° out wards	620 *ft* Normal	800 *ft* Normal	300 *ft* Normal
Mole Head Radius	600 *ft*	300 *ft*	600 *ft*	300 *ft*
Mole Head Sweep	120°	90°	120°	90°
Downstream Straight Length	100 *ft* Normal	100 *ft* Normal	200 *ft* Normal	100 *ft* Normal
Mole Head Radius	300 *ft*	300 *ft*	600 *ft*	300 *ft*
Mole Head Sweep	90°	90°	45°	90°

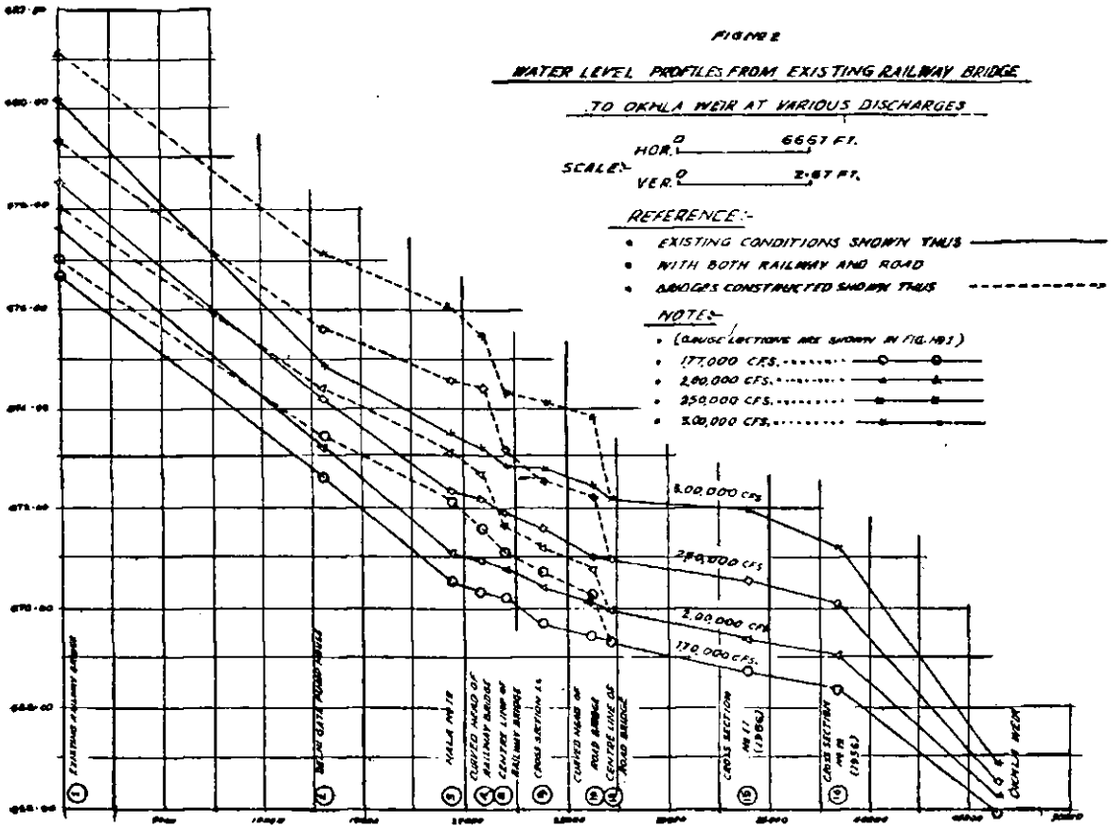

survey. A study of the water levels in the Yamuna in the past had shown that after the high floods there was a general lowering of the stages, which gradually rose till the old values were nearly re-established. With a view to get the afflux values corresponding to these higher stages in the river, the spill levels referred to above, were laid to 1956 survey.

The model was thus laid as follows:—

(i) Upstream of the railway bridge to 1955 survey.
(ii) Between the railway bridge and the Okhla weir.
  (a) the channel portion to 1958 survey and
  (b) the spill levels between the left embankment and the channel to 1956 survey.

3. Experiments and discussion of results

Water levels for various discharges upto the maximum flood stage of 8495 m^3/sec (3 lakh *cfs*) at different gauge stations shown in *fig 1*, were recorded under existing conditions and with the proposed road and railway bridges constructed as recommended in the *Annual Research Memoirs 1959*.

The afflux observed at 8495 m^3/sec (3 lakh *cfs*) near the curved head of the right guide bund of the proposed road bridge *ie* at point 11 was .41 *m* (1.29 *ft*) corresponding to *HFL* 673.83; at the Allen Bund in between the two bridges *ie* at point 14, .82 *m* (2.69 *ft*) corresponding to *HFL* 674.82; at the curved head of the right guide bund of the proposed railway bridge *ie* at point 5, .74 *m* (2.4 *ft*) corresponding to *HFL* 675.99 and along the Allen Bund upstream of the railway bridge *ie* at point 8, 1.46 *m* (4.78 *ft*) corresponding to *HFL* 677.04. It will be seen that the afflux at point *Nos* 8 and 14 was higher than that at point *Nos* 5 and 11 respectively, the reason for this being that point *Nos* 8 and 14 are situated in locations where there was no flow and all the kinetic energy was converted to potential head. The back water caused by this afflux was found to be progressively reducing on the upstream and at the existing bridge, it was observed to be .33 *m* (1.07 *ft*). The water levels and afflux figures at various points for discharges upto 8495 m^3/sec (3 lakh *cfs*) are recorded in *table 1* and *fig 2*.

During the course of the experiment, it was observed that the affluxes observed upto flood stage of 7079.2 m^3/sec (2.5 lakh *cfs*) in the present experiments were only slightly higher than those obtained in the previous experiments (*ibid* 1958) and may probably be due to changes in river cross-sections.

4. Conclusions

(*i*) Afflux at the existing bridge on account of construction of the proposed two bridges with the flood discharge equivalent to 8495 m^3/sec (3 lakh *cfs*) is expected to be .33 *m* (1.07 *ft*).

(*ii*) Afflux at Allen bund (left embankment) in the reach between the two proposed bridges may be of the order of .82 *m* (2.69 *ft*) with discharge of 8495 m^3/sec (3 lakh *cfs*) while upstream of the proposed railway bridge, the rise is expected to be of the order of 1.46 *m* (4.78 *ft*).

---

10. Mundali weir across Mahanadi and undersluices

I. Weir

EXPERIMENTS in connection with the proposed weir across Mahanadi river at Mundali (Orissa State) have been reported (*ibid* 1958 and 1959). During the current year, experiments to test two more design features *viz*, the third divide wall for the Mundali weir and the shape of the wing wall between the regulator and the weir were conducted.

2. Third divide wall

The Mundali weir across the Mahanadi is tentatively proposed to be 1332 *m* (4370 *ft*) long with its right abutment at the right bank. The deep river portion is along the right bank in this reach and its width is about 353.6 *m* (1160 *ft*). The pocket sluices and the undersluices covering a length of 213.4 *m* (700 *ft*) are located on the deep

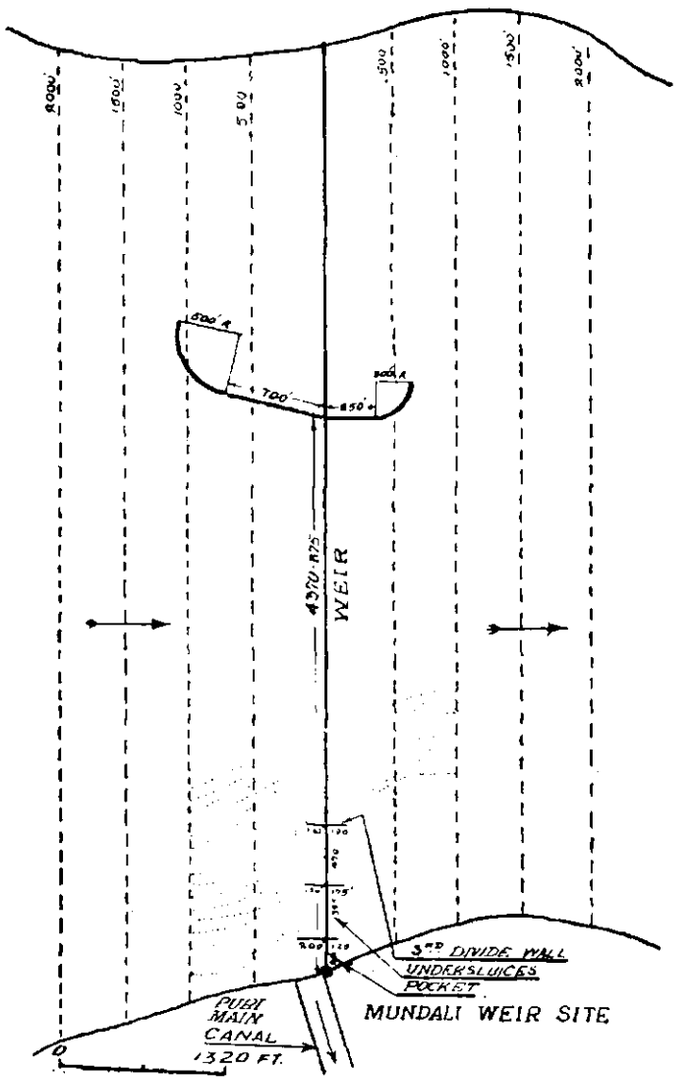

Fig 1: Bed lines of flow with the divide wall *No* 3 according to *CDO* design [top of downstream divide wall 67.0] $Q = 6.0$ lakh *cfs*.

river portion and the remaining 140.2 *m* (460 *ft*) length of the deep river will be covered by the portion of the main weir. The pocket and undersluices are founded on rock whereas the main weir is designed as a weir on permeable foundations. As rock is available in the deep river portion the 140.2 *m* (460 *ft*) length of the main weir in the deep river portion can also be designed as on rock foundations. To separate this deep river weir portion from the rest of the weir on permeable foundations, a third divide wall is proposed at a distance of 140.2 *m* (460 *ft*) from the undersluices divide wall. The proposed third divide wall is 42.7 *m* (140 *ft*) long on the upstream side with top at *RL* 70.0 (*ie* same as upstream pavement level of the main weir) whereas on the downstream side the divide wall extends to 57.9 *m* (190 *ft*) (*fig 1*). Two alternative heights were proposed for the downstream divide wall *viz*, at *RL* 67 (same as downstream pavement level) and at *RL* 90.

It was desired that the proposal of the third divide wall should be tested in the 1/400: 1/60 model of the Mahanadi river.

3. Experiments

Model experiments were conducted for various flood stages upto 42450 m^3/sec (15 lakh *cfs*) with downstream divide wall at *RL* 67. As the proposed divide wall on the upstream side is at the pavement level only, there was no marked change in flow conditions except diversion of bed flow further away from the pocket and undersluices which is a favourable feature. This can be seen from *fig 1* showing the bed flow lines at 16980 m^3/sec (6 lakh *cfs*) stage (Canal closure stage).

The flow conditions were almost the same under all stages even when the downstream divide wall top was raised from *RL* 67 to *RL* 90 and there was no specific improvement with the higher divide wall.

It was recommended that the third divide wall with top *RL* 70 on the upstream and top at *RL* 67 on the downstream side with lengths as proposed should be adopted.

4. Shape of the wing wall

The Puri main canal head regulator is located on the right bank near the pocket sluices. The wing wall joining the regulator to the pocket was tested in the model. It was found that a circular wing wall of radius 9.14 *m* (30 *ft*) was satisfactory as the flow round the wing wall was smooth without any undesirable turbulence under all flood stages upto 42450 m^3/sec (15 lakh *cfs*).

II. Protection works for undersluices

SINCE THE construction of the Hirakud Dam and the operation of the hydroelectric plant, adequate supply of water is available in the Mahanadi Delta. In order to improve the existing system of irrigation and to bring more land in the Puri district (Orissa State) into cultivation, a weir at Mundali, about 320 *km* (200 *miles*) downstream of the Hirakud and about 4 *km* (2½ *miles*) upstream of Naraj weir, has been proposed. Originally the undersluices were designed on permeable foundations. Later on, however, it was found that foundation rock was available at the undersluice site at *RL* 31 and it was reported that it was possible to dewater upto the rock level. Hence it was decided to construct the undersluices on the open rock foundations. Accordingly Central Designs Organisation of the *CWPC* prepared three alternative designs for scour protection for the undersluices. All the alternatives had the same profile and were provided with masonry cut-off walls, the difference among them being only in respect of scour protection works (*fig 1*). The detailed information on the experiments for estimation of scour under various conditions has already been published (*ibid* 1959, *p.* 106).

2. Experiments for coefficient of discharge

This note describes the results of experiments conducted to determine the coefficient of discharge under the different alternatives as given in *fig 1*. These tests were carried out on a 1/46 *GS* model in a rectangular flume .91 *m* (3 *ft*) wide. *Fig 1* (*a, b, c, d*) gives the original and three alternative designs tested in the model. *Table 1* below shows the coefficient of discharge obtained for these alternatives.

Table 1

		% submergence	C
Original design	(*fig 1a*)	90.2	2.20
Alternative: I	(*fig 1b*)	91.2	2.24
II	(*fig 1c*)	90.7	2.22
III	(*fig 1d*)	90.7	2.22

Note:—(1) River discharge 34,000 m^3/sec (12 lakh *cfs*)

(2) Intensity in undersluices 41 m^3/sec per *meter* (436 *cfs* per *ft*)

(3) Formula: $Q = CD^{1.5}$ where
Q = discharge.
C = Coeff. of discharge
D = upstream total head.

It will be seen that there is very little difference in the coefficients of discharge for the various alternatives, and the choice will have to be made on the comparative economics for the various designs. In the *Annual Research Memoirs of 1959*, it was explained that in respect of scour, alternative I was the best. It may, however, be noted that the depth and the extent of scour are not the guiding criteria in selecting the design in the present case, in view of the natural rock being available at *RL* 9.45 *m* (31 *ft*).

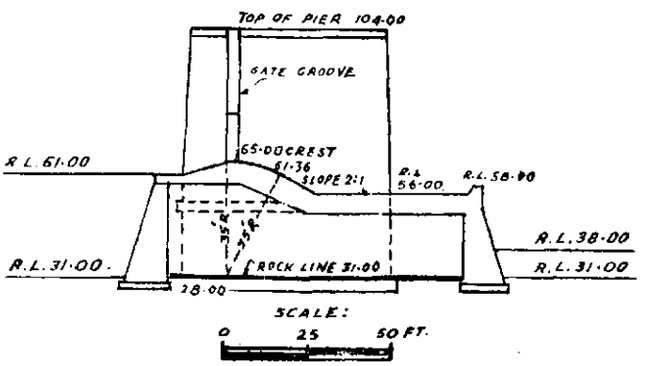

Fig 2: The profile without upstream and downstream pitching and aprons.

In view of this, the design *vide fig 1* (*b*) was modified as shown in *fig 2* in which the upstream and downstream protection works were omitted. With upstream bed assumed at *RL* 18.6 *m* 61 *ft ie* upstream pavement level, the value of the coefficient obtained for a discharge of 34,000 m^3/sec (12 lakh *cfs*) was 2.18 with submergence of 90 *percent*, as against 2.22 for the four alternatives tested.

3. Conclusion

In view of rock being available at shallow depths and the coefficient of discharge not being much different, it was suggested that the flexible protection works may be omitted and the design shown in *fig 2* may be considered for adoption.

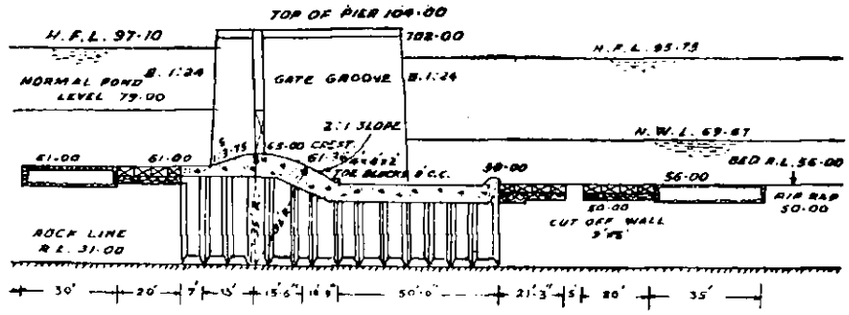

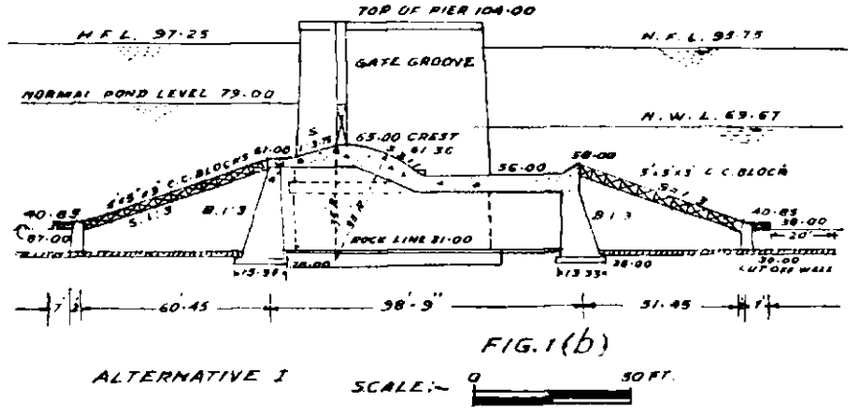

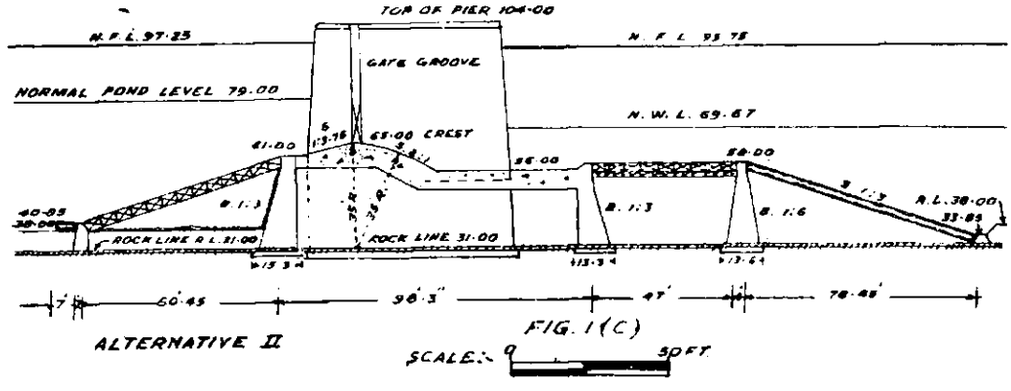

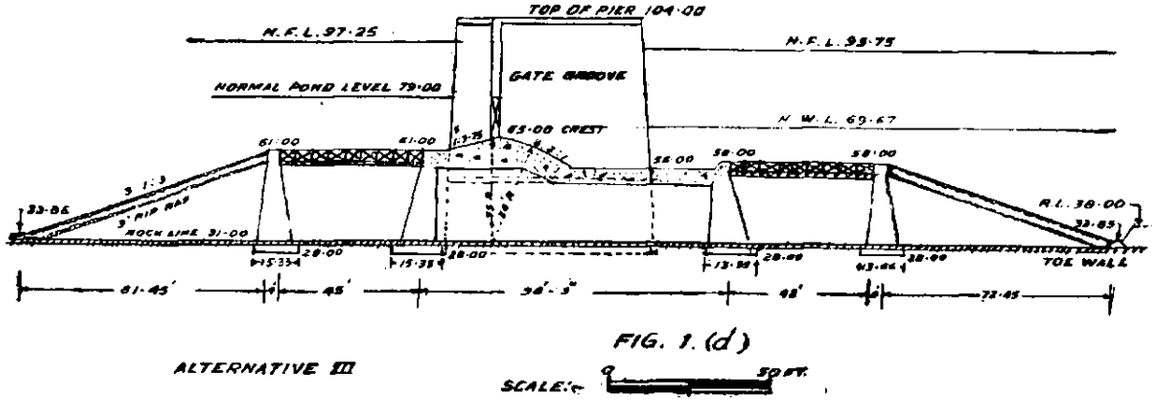

Fig 1: Mundali undersluices showing original and alternative designs.

11. Canal syphons across two branches of Mahanadi

THE PURI main canal taking off from right flank of the Mundali weir across the Mahanadi in Orissa is designed to irrigate the lands in Puri and Cuttack districts. This canal during its course has to cross the Kuakhai and the Kushabhadra branches of the Mahanadi in these two districts. The crossings are proposed to be canal syphons.

A proposal is under consideration for using these syphon crossings as foundations of bridges which may be constructed at a later date.

The problem was referred to the *CWPRS* for determining the scour conditions that may be obtained due to the introduction of bridge piers over the syphon barrels. As the designs for the syphons as well as the road bridges were similar for both the Kuakhai and Kushabhadra crossings experiments were conducted with the Kuakhai syphon only.

2. Hydraulic data

The canal is syphoned below the Kuakhai river.

River:

High flood discharge	= 4662 m^3/sec (1,93,000 *cfs*)
HFL	= *RL* 74.6
Deepest bed level	= *RL* 49.99

Canal:

Full supply discharge	= 150.0 m^3/sec (5303 *cfs*)
FS level upstream	= *RL* 71
FS level downstream	= *RL* 68
Bed level upstream	= *RL* 60.7
Bed level downstream	= *RL* 57.7
FS depth	= 3.14 *m* (10.3 *ft*)
Bed Width	= 54 *m* (165 *ft*)
Waterway	= 9 barrels of 2.67 *m* ×2.67 *m* (8.75 *ft* ×8.75 *ft*)

The syphon barrels are of *RCC* and founded on wells.

Bottom level of foundation *RL* = 10.41

Top level of syphon barrel *RL* = 42.5

Over the barrel top pitching upto *RL* 45.5 is laid extending 15.24 *m* (50 *ft*) on either side of the barrels. The pitching thickness over the erodible bed beyond the syphon barrels is 1.22 *m* (4 *ft*).

Length of the syphon = 328 *m* (1000 *ft*)

Bridge: The proposed road bridge consists of combined piers spaced 8.53 *m* (28 *ft*) centre to

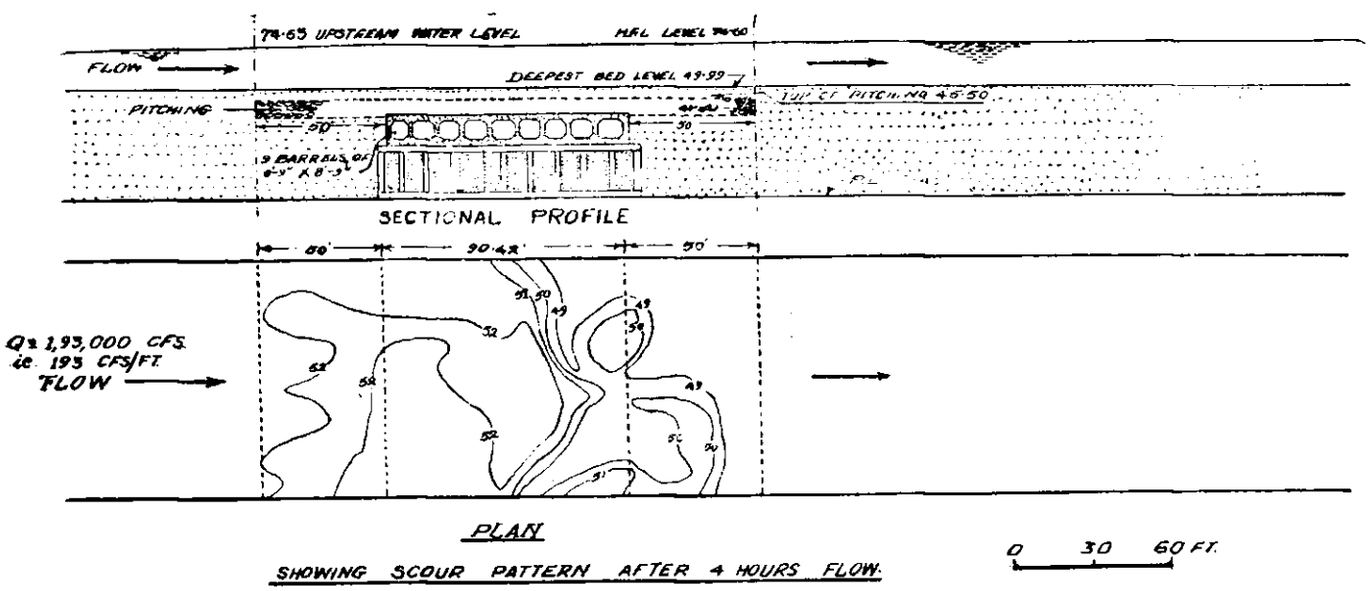

Fig 1: Design, without the proposed road bridge.

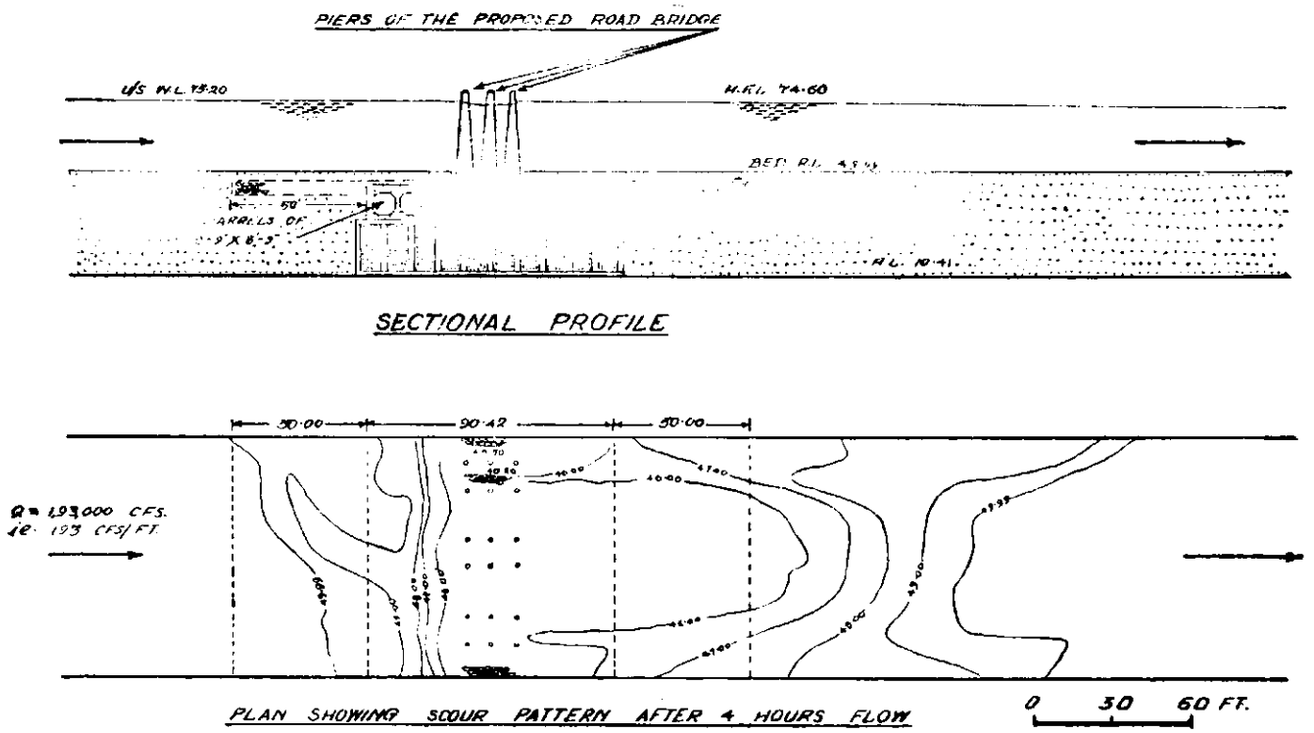

Fig 2. CDO design with the proposed road bridge.

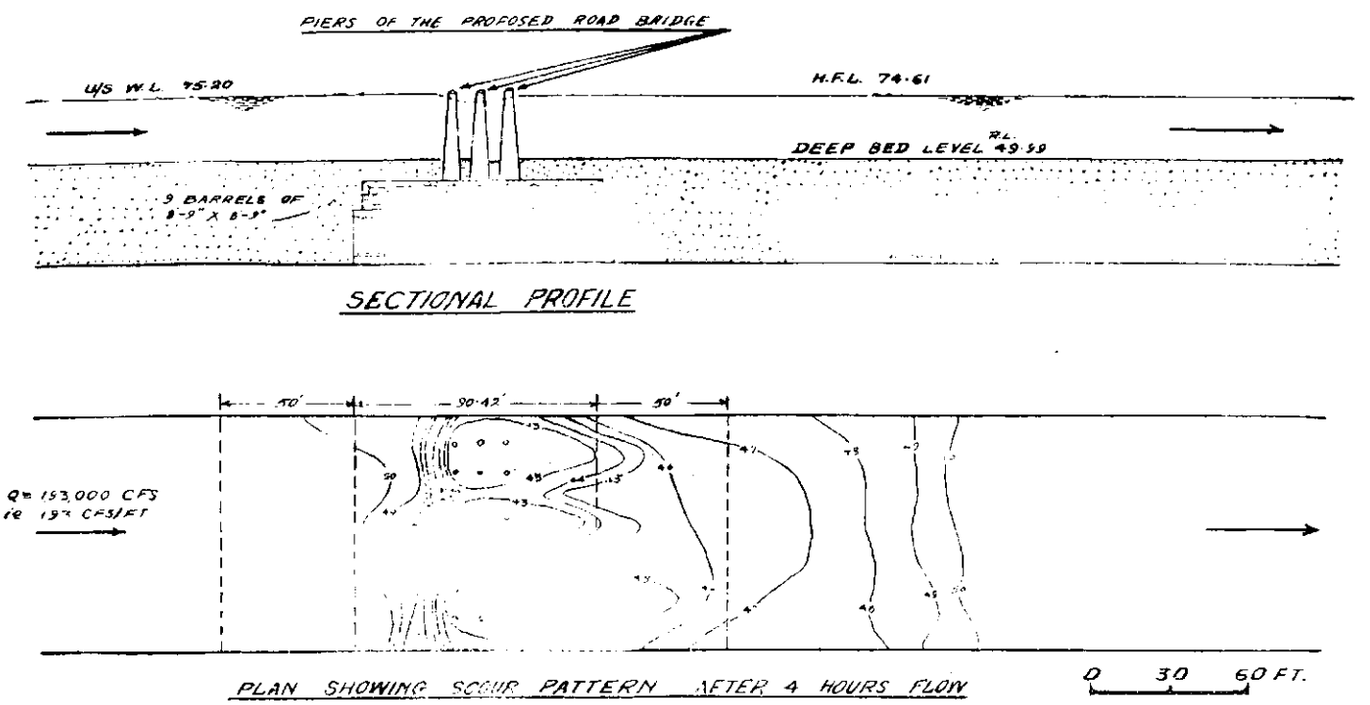

Fig 3: CDO Design with the road bridge and with erodible bed only

centre spanning the entire 328 *m* (1000 *ft*) wide river. Each combined pier consists of six *RCC* piers of .91 *m* (3 *ft*) top and 1.37 *m* (4.5 *ft*) bottom diameters joined by *RCC* bracings.

3. Model

Studies were carried out in a 1/30 *GS* sectional model reproducing length of the syphon equivalent to 3 spans of the proposed bridge. The syphon was reproduced in section, the over burden of the river bed material being of 20 mesh Koregaon sand. The pitching over the syphon barrels was also reproduced using about 1.27 *cm* (½ *inch*) size metal corresponding roughly to one-man stone in the prototype.

4. Experiments

Model tests were conducted under the high flood conditions. An equivalent discharge intensity corresponding to 18.4 m^3/sec per *m* (193 *cfs/rft*) high flood of 5466 m^3/sec (1,93,000 *cfs*) was run for four hours in each experiment and the scour pattern developed was studied.

Experiment 1: *Original syphon design (without bridge)*: The flow conditions were found to be quite normal as there was no obstruction to the flow. The deepest scour contour obtained was at *RL* 48, whereas the bed was laid at *RL* 49.99 (see *fig 1*). *Photo 9* shows this scour condition.

Experiment 3: *With proposed road bridge over the syphon and with the stone pitching as designed*: The road bridge piers were constructed above the barrel tops reproducing 2 full and 2 half spans. Flow conditions showed that the introduction of the bridge piers had created turbulence in their vicinity. This can be seen from *photo 10*. Due to this, erodible bed round the piers started scouring out and after four hours of flow even the pitching over the barrel top laid at *RL* 45.5 was exposed as can be seen from *photo 11* and *fig 2*. The stone pitching was disturbed but the top of the barrel was not exposed.

Experiment 2: *With proposed road bridge over the syphon and with the over-burden of only erodible bed material*: As the pitching will be laid over the smooth syphon barrels in proto it is likely that the pitching may get washed out under high flood conditions. So, as a worst case, a test was conducted by having the entire over-burden on the barrel top laid of only erodible sand. The bed around the piers got scoured out right down to the barrel top during the experiments. Beyond the barrels, no scour developed below the top of the barrels. The bed, however, gradually built up back to *RL* 49.99 at a distance of about 54.86 *m* (180 *ft*) from end of the barrel. *Photo 12* and *fig 3* show the scour conditions.

5. Conclusions

(*i*) The road bridge piers induced local scour over the syphon top and model indicated that some pitching might get disturbed but the barrel top was not likely to be exposed.

(*ii*) The scour beyond the syphon barrels developed to *RL* 46 in experiment 2 and to *RL* 44 in experiment 3, the top of the syphon being at *RL* 42.5. This indicated that there appeared no likelihood of any serious scour developing beyond the syphon barrels in the prototype.

(*iii*) Experiment 3 showed that in the absence of stone pitching the whole of sand cover was likely to be washed away exposing the barrel tops; but the scour did not extend to levels lower than the top of the barrels.

---

12. Design of spillway and energy dissipation devices

I. Vir Dam Project

MODEL TESTS were conducted last year for observing floor pressures round friction blocks and chute blocks and lateral pressures on the piers (*ibid* 1959). Tests were also done on the design of the guide walls and mode of operation of the crest gates for flood disposal. Subsequently, the Central Designs Organisation, Bombay, expressed doubts on the safety of the friction blocks against damage by large floating trees as also by probable cavitation. Further tests were made for evolving stilling basin design without friction blocks.

2. Tests on 1/36 sectional model

In the first instance the length of the apron was kept at 30.48 *m* (100 *ft*), the slope being retained at 1 in 16 ending in a dentated sill 3.504 *m*

(11.5 *ft*) high as shown in *fig 1 (a)*. For various discharges the results of the experiments in regard to water profiles, scour pressures on the apron and end sill are shown in *figs 1 (a)*, *1 (b)*, *1 (c)* and *1 (d)*. The hydraulic jump was not well defined and extended beyond the apron with an active secondary wave occurring further downstream. At the highest discharge stage the maximum depth of scour reached 3.504 *m* (11.5 *ft*) at a distance of 24.38 *m* (80 *ft*) from the end sill. The pressures on the end sill were, however, positive for all stages of overflow.

In order to achieve better dissipation of energy, the length of the sloping apron was increased in stages to 33.53 *m* (110 *ft*) and subsequently to 36.58 *m* (120 *ft*) as in the former case the results did not show appreciable improvement. This design was tested with both dentated end sill and plain end baffle 3.05 *m* (10 *ft*) high. The observations indicated that the effects of the two types of end sill were more or less similar. The maximum scour reached was 3.05 *m* (10 *ft*) at a distance of 19.81 *m* (65 *ft*) from the end sill in the case of the former whereas it was 3.05 *m* (10 *ft*) at a distance of 18.29 *m* (60 *ft*) from the end sill in the case of the latter. *Figs 2 (a)*, *2 (b)* and photos *13* and *14* show the characteristics for the apron with plain end sill for design depth of 4.57 *m*

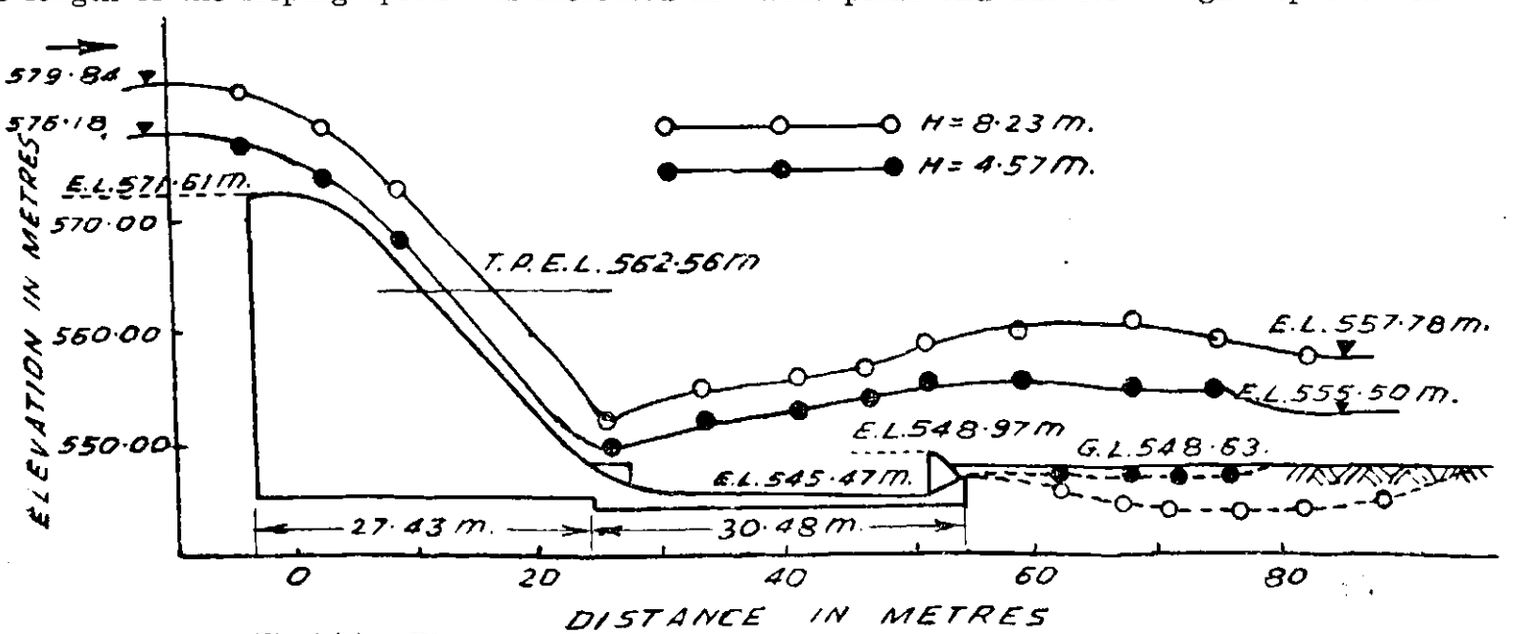

Fig 1 (a): Water profiles and scour profiles for different overflow depths.

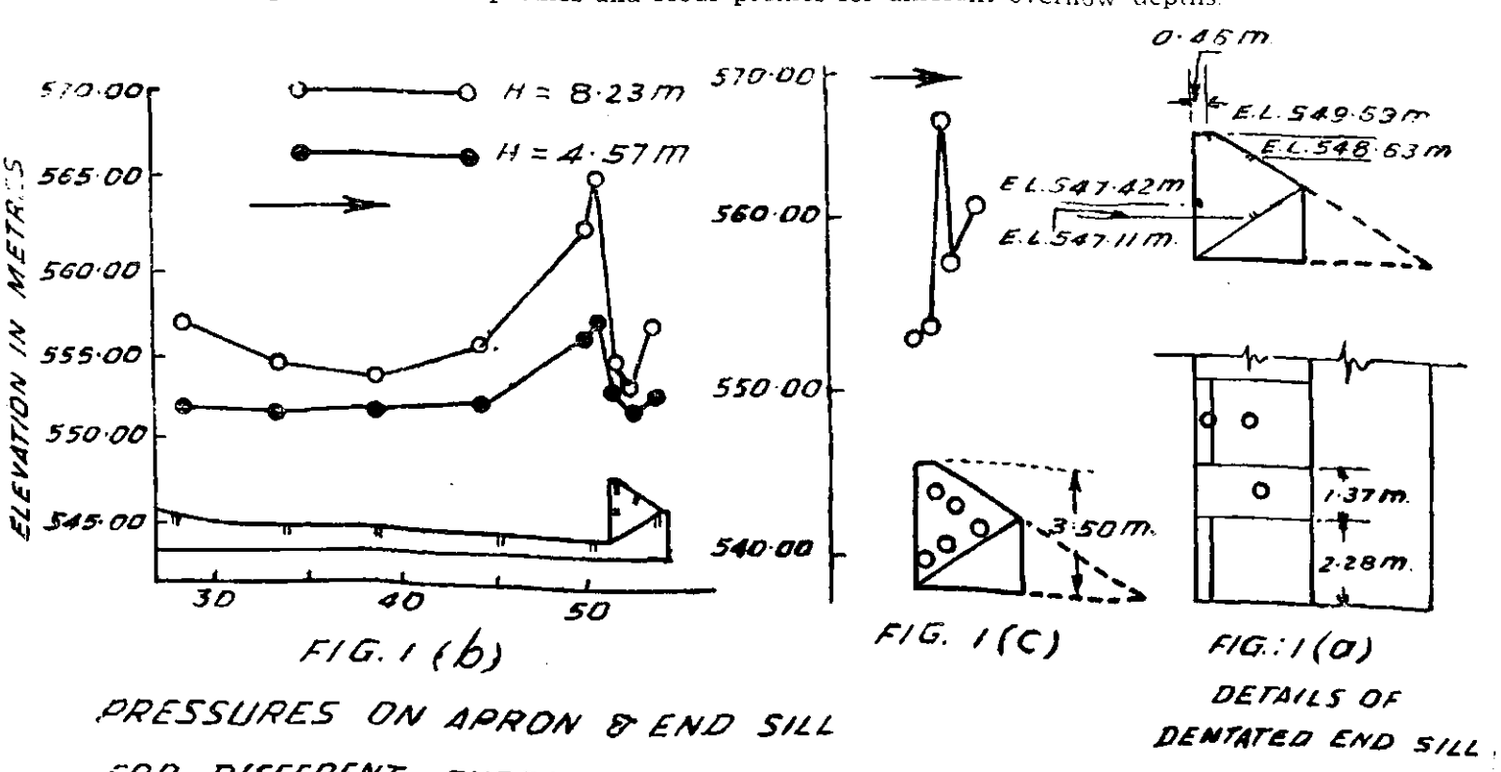

Fig 1: Vir dam project.

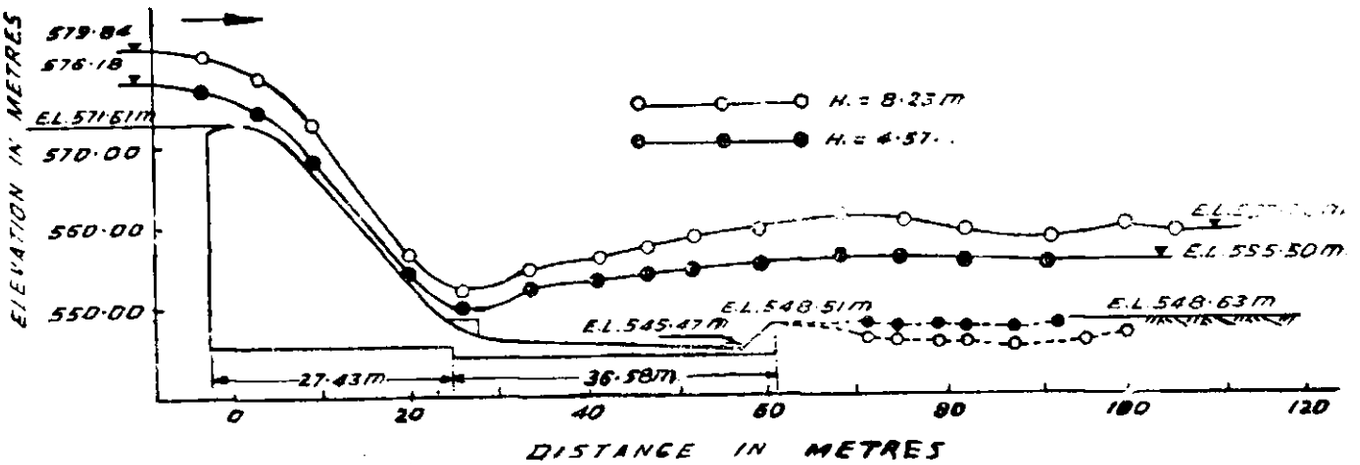

Fig 2 (a): Water and scour profiles for different overflow depths.

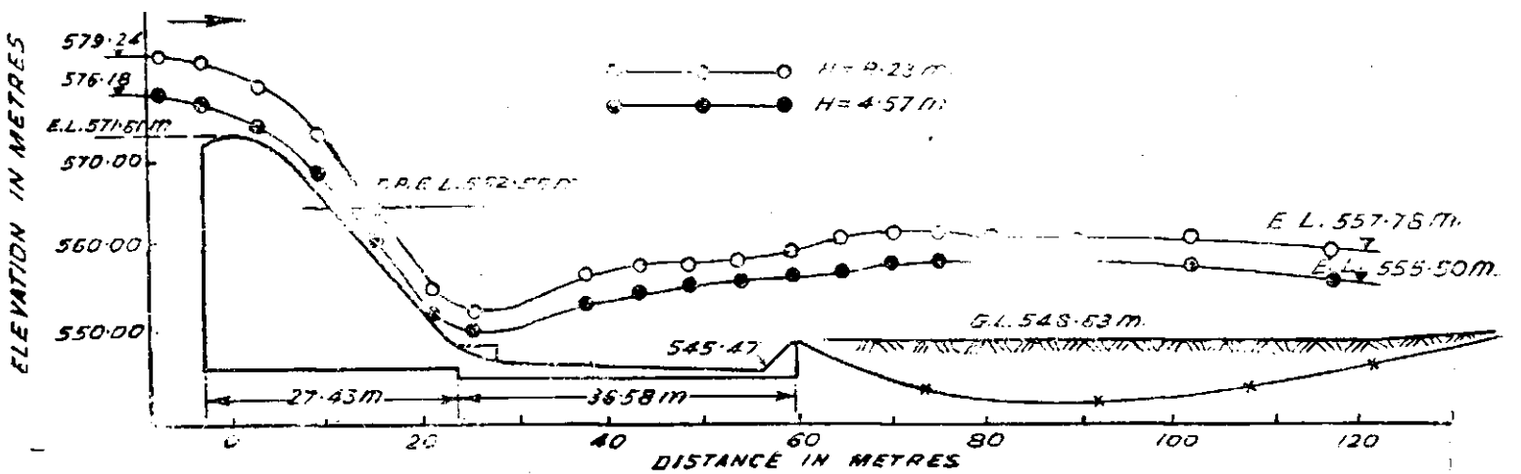

Fig 3 (a): Water profile for different depths of overflow and scour for design depth of overflow.

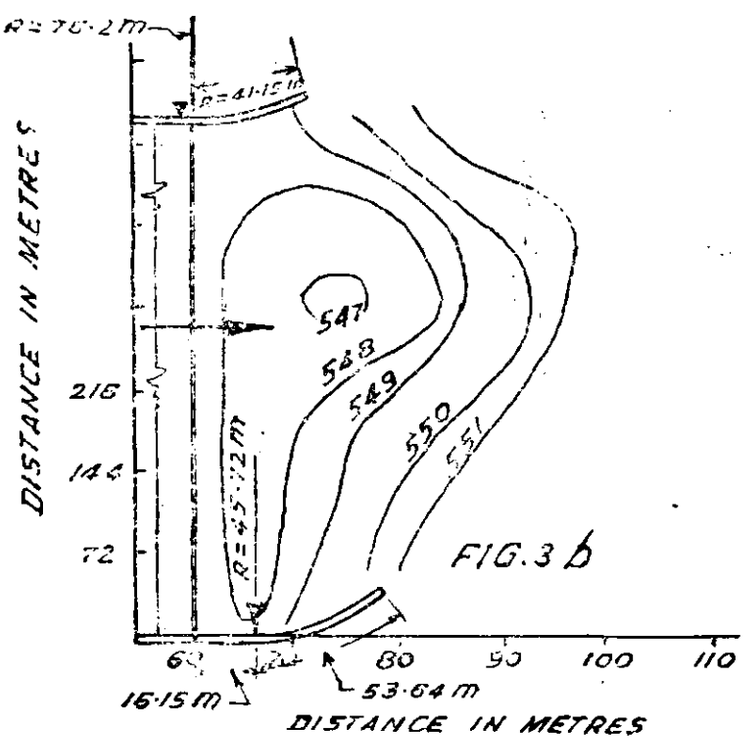

(15 *ft*) of overflow and 8.23 m (27 *ft*) of overflow respectively. Though there was no marked difference in the action of these end sills, the plain end sill was preferred in view of the simplicity of construction and immunity from clogging with debris.

3. Tests on 1/72 three dimensional composite model

(*a*) *Performance of the sloping apron, length 36.58 m (120 ft), slope 1 in 16, chute blocks and end sill 3.05 m (10 ft) high*: The water surface profiles given in *fig 3* (*a*) confirmed the corresponding results in the sectional model. The maximum scour reached 3·05 *m* (10 *ft*) at a distance of 27.43 *m* (90 *ft*) during maximum discharge stage as shown in *fig 3* (*b*). The results of these tests indicated and confirmed satisfactory performance of the design.

(*b*) *Guide walls*: The increased length of sloping apron *viz* 36.58 *m* (120 *ft*) called for repeating tests on the design of guide walls. The model

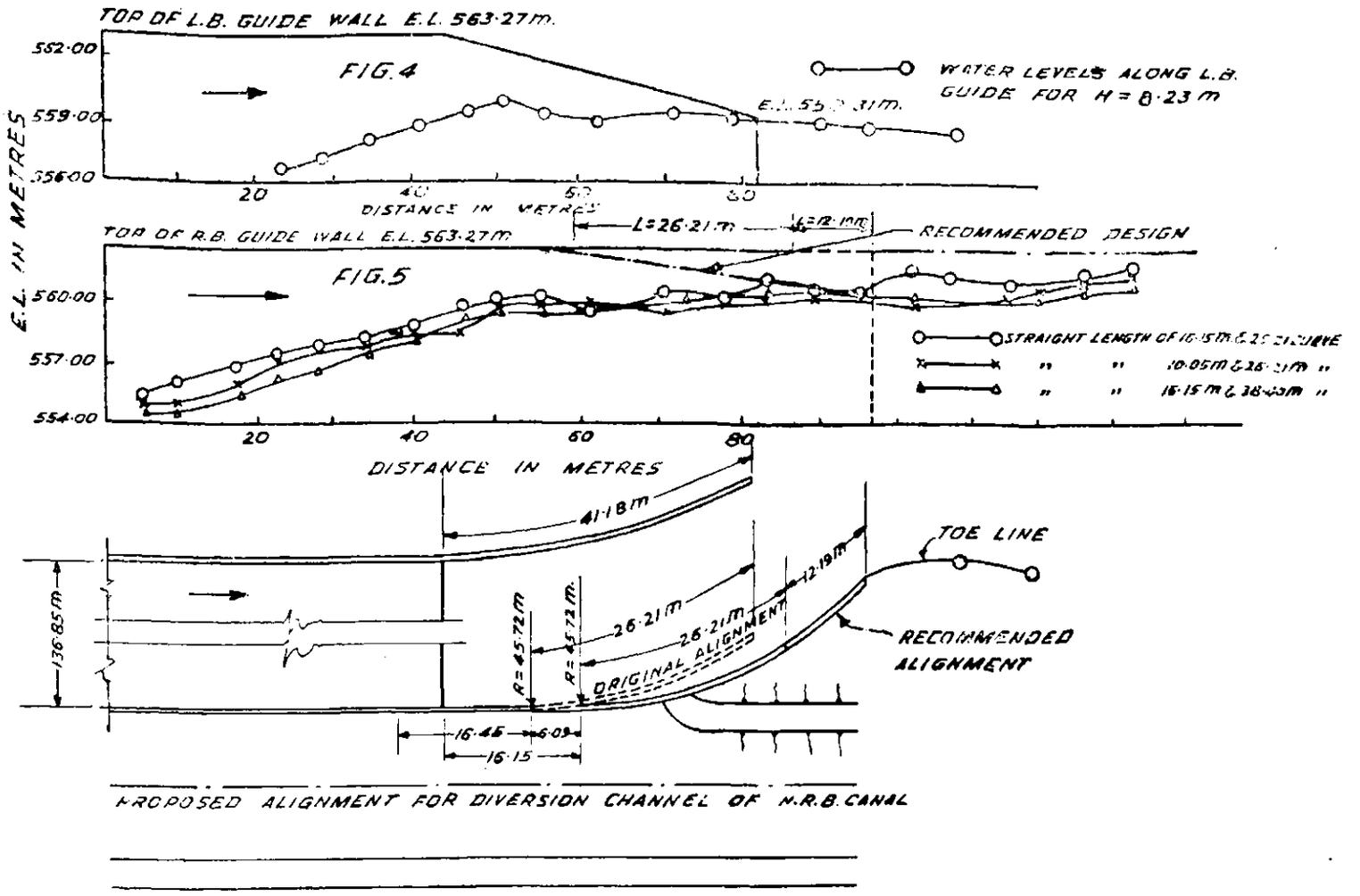

FIG. 6

was run for the design head of 8.23 *m* (27 *ft*) and conditions of water profile observed at the sides of both the guide walls. The observations of water profile along the left guide wall are plotted in *fig 4*. The results showed that the left guide wall was satisfactorily designed.

Conditions on the right bank however necessitated modifications. The guide wall was found to be insufficient to cover the hydraulic jump height. Due to heavy wave splash water was overflowing the Nira Right Bank canal embankments periodically. Further the splashes continued for a considerable distance downstream along the canal bank as shown in *photo 15*.

In the first instance the original right guide wall (project design) was amended by raising it to *RL* 1848.5 as shown in *fig 5* without altering the total length of the guide wall. The results of water profile along the guide wall for design head of 8.23 *m* (27 *ft*), shown in *fig 5* indicated the persistance of the ruffled flow conditions but to a lesser degree. The wave travel downstream was reduced. The general conditions however indicated modifications of curved head of the guide wall to suppress the waves affecting the canal bank.

The satisfactory design of the right guide wall finally arrived at and recommended conformed to the dimensions indicated in *fig 6*. The observation of water profile for the design head of 8.23 *m* (27 *ft*) showed that the wave splash was considerably reduced as shown in *photo 16*. The maximum level reached was *El* 561.4 *m* (1842 *ft*) along the canal bank. The eddy downstream of the curved head of the guide wall was very weak to be of any consequence.

4. Conclusions

Tests with sloping apron 36.58 *m* (120 *ft*) long sloping at 1 in 16, with chute blocks and end sill showed that,

(*i*) The general performance of the stilling basin was satisfactory. The maximum scour obtained was equivalent to 3.05 *m* (10 *ft*) at a distance of 25.9 *m* (85 *ft*) from the apron (*figs 3 a* and *3 b*).

(*ii*) There was no change in the design of the left guide wall (*fig* 4).

(*iii*) The right guide wall however required modifications. In the design recommended, the dimensions were

52.73 *m* (173 *ft*) straight.
38.40 *m* (126 *ft*) curved, $R = 45.72$ *m* (150 *ft*)
91.13 *m* (299 *ft*) Total length

The guide wall needed to be raised to *El* 563.3 *m* (1848 *ft*) with the top level lowered gradually as shown in *fig* 5.

II. Kohira Dam Project

THE KOHIRA dam project envisages construction of a masonry dam with earthen dikes across river Kohira near village Jagdishpur (Bihar State). The flow from the reservoir would be diverted through a pick-up weir 4.02 *km* (2.5 *miles*) downstream of the dam which is under construction. *Fig 1* shows the index plan of the project.

The *salient features* of the project are given below:

(i) Catchment area ...	88.98 *sq km* (34.29 *sq miles*).
(ii) Average rainfall for 20 years.	1082.04 *mm* (42.6 *inches*).
(iii) Mean annual run-off (by observation).	4464 million m^3 (36,194 *ac ft*).
(iv) Gross capacity ...	2832 million m^3 (22.960 *ac ft*).
(v) Maximum flood discharge.	736.24 m^3/sec (26,000 *cfs*).
(vi) Dead storage ...	284.0 million m^3 (2296 *ac ft*).
(vii) Total storage ...	2548 million m^3 (20,664 *ac ft*).
(viii) Length of the dam—	
(*a*) Masonry spillway section.	85.65 *m* (281 *ft*).
(*b*) Masonry non-overflow section.	48.16 *m* (158 *ft*).
(*c*) Earthen section...	131.37 *m* (431 *ft*).

2. Spillway design

In the original design the spillway consisted of 10 spans of 7.47 *m* (24.5 *ft*) each with the depth of flow of 3.05 *m* (10 *ft*) over the spillway crest. The crest level of the spillway was at *El* 101.65 *m* (333.5 *ft*). The equation to the spillway profile below the gate was $X^2 = 7.62\,y$. The stilling arrangement consisted of a 30.48 *m* (100 *ft*) long horizontal apron at *El* 88.70 *m* (291 *ft*) with an end sill 609 *m* (2 *ft*) high. Four sluices were also provided each 1.219 *m* × 0.914 *m* (4 *ft* × 3 *ft*) in cross-section as shown in *fig 2* (*a*).

Subsequently several modifications of design were made both to the spillway and the apron by the design organisation and the project authorities. The latest design of spillway consisted of 8 spans each 7.47 *m* (24.5 *ft*) wide with depth of overflow on the spillway increased to 3.66 *m* (12 *ft*). The crest level was lowered by .609 *m* (2 *ft*) *ie* to *El* 101.04 *m* (331.5 *ft*). The equation of the spillway profile downstream of the gate was modified to $X^2 = 9.39\,y$. The tainter gates were substituted by vertical lift gates. *Fig 2* (*b*) shows the details of the spillway design with the undersluices.

3. Estimate of maximum flood discharge

The maximum flood discharge of 736.24 m^3/sec (26,000 *cfs*) was reported to have been observed in the year 1956 with the corresponding tailwater *El* 93.72 *m* (*HFL* 307.48). The gauge discharge curve extrapolated to the design flood of 736.24 m^3/sec (26,000 *cfs*) is shown in *fig 3*. It was noticed that the tailwater level for design flood of 736.24 m^3/sec (26,000 *cfs*) corresponded to *El* 91.90 *m* (301.5 *ft*) as against *El* 93.72 *m* (307.48 *ft*) mentioned in the project report. Later on it was confirmed that the stage corresponding to 736.24 m^3/sec (26,000 *cfs*) discharge was *El* 93.73 *m* (307.5 *ft*).

4. Terms of reference

The following terms of reference were stipulated for the model tests.

(*a*) Determination of discharging capacity of the spillway.

(*b*) Pressure distribution on the spillway profile.

(*c*) Design of energy dissipation arrangements.

5. Tests in 1/24 geometrically similar model

Tests were conducted on the following designs in the sectional model as and when the designs underwent successive modifications.

(*a*) Tests with design in *fig 2* (*a*) with length of apron 30.48 *m* (100 *ft*), apron level *El* 88.7 *m* (291 *ft*), *TWL*=*El* 93.73 *m* (307.5 *ft*)

(*b*) Tests with design in *fig 2* (*a*) with horizontal apron at *El* 87.17 *m* (286 *ft*), $L = 30.48$ *m* (100 *ft*), *TWL El* 93.73 *m* (307.5 *ft*).

(*c*) Tests with horizontal apron at *El* 87.17 *m* (286 *ft*), $L = 24.38$ *m* (80 *ft*), $L = 4D$, *TWL* = *El* 93.73 *m* (307.5 *ft*).

(*d*) **Tests with design in** *fig 2* (*a*) **with horizontal apron at** *El* 87.17 *m* (286 *ft*), $L = 18.29$ *m* (60 *ft*), with chute blocks, $TWL = El$ 93.73 *m* (307.5 *ft*).

(*e*) Tests with design in *fig* 2 (*a*) with horizontal apron 18.29 *m* (60 *ft*) long at *El* 87.17 *m* (286 *ft*), with chute blocks (as already constructed) at *El* 89.38 *m* (293.25 *ft*), no curvature for toe of spillway, $TWL = 93.73$ *m* (307.5 *ft*).

6. Further tests

At this stage the project site was inspected and it was observed that construction had reached upto *El* 94.79 *m* (311 *ft*) which included the sluices and chute blocks at *El* 89.38 *m* (293.25 *ft*). The apron at the flanks had been concreted upto *El* 87.93 *m* (288.5 *ft*) and *El* 88.14 *m* (289.5 *ft*) respectively and the central apron upto *El* 86.87 *m* (285 *ft*). The guide walls between the aprons were also under construction and were proposed to be raised upto *El* 94.49 *m* (310 *ft*). The width of the spillway was 13.11 *m* (43 *ft*) at *El* 88.39 *m* (290 *ft*) and 8.84 *m* (29 *ft*) at *El* 94.79 *m* (311 *ft*) giving a slope of .667 to 1. *Fig 4* shows the stage of spillway construction.

The following points required further attention in the model studies.

(*a*) The design of the crest of the spillway to suit the present dimensions of construction

(*b*) Performance of higher apron at *El* 88.39 *m* (290 *ft*), for design discharge of 736.24 m^3/sec (26,000 *cfs*) and corresponding tailwater level *El* 93.73 *m* (307.5 *ft*)

(*c*) Differential pressures on the divide wall between the higher and lower aprons.

(*d*) Performance of uniform level apron at *El* 88.39 *m* (290 *ft*) without divide wall.

(*e*) Performance of sluices already constructed.

(*a*) *Design of crest of spillway*: The dimensions governing the design of the spillway crest were the elevation of the crest, actual spillway slope of .667 to 1 and the width of the spillway of 13.11 *m* (43 *ft*) at *El* 94.79 *m* (311 *ft*). The equation of the curve conforming to the above conditions was found to be $X^2 = 9.71\ Y$. The profile upstream of the crest consisted of circular arcs of radii 1.83 *m* (6 *ft*) and .73 *m* (2.4 *ft*) as shown in *fig* 5. The coefficient of discharge and discharging capacity for the profile are shown in *figs 6* (*a*) and *6* (*b*). The pressure distribution is shown in *fig 7*.

(*b*) *Performance of stilling basin : (i) Tests on 16.46 m (54 ft) long apron (lower) at El 87.17 m (286 ft) with 1.22 m (4 ft) end sill.*—The water surface, scour profiles and pressures are represented in *fig 8*. The maximum scour obtained below the original ground level *El* 89.306 *m* (293 *ft*) was 1.22 *m* (4 *ft*) at 7.315 *m* (24 *ft*) downstream of the end sill for design discharge of 736.24 m^3/sec (26,000 *cfs*). The pressures were all positive throughout. Energy dissipation was quite efficient for maximum discharge even under

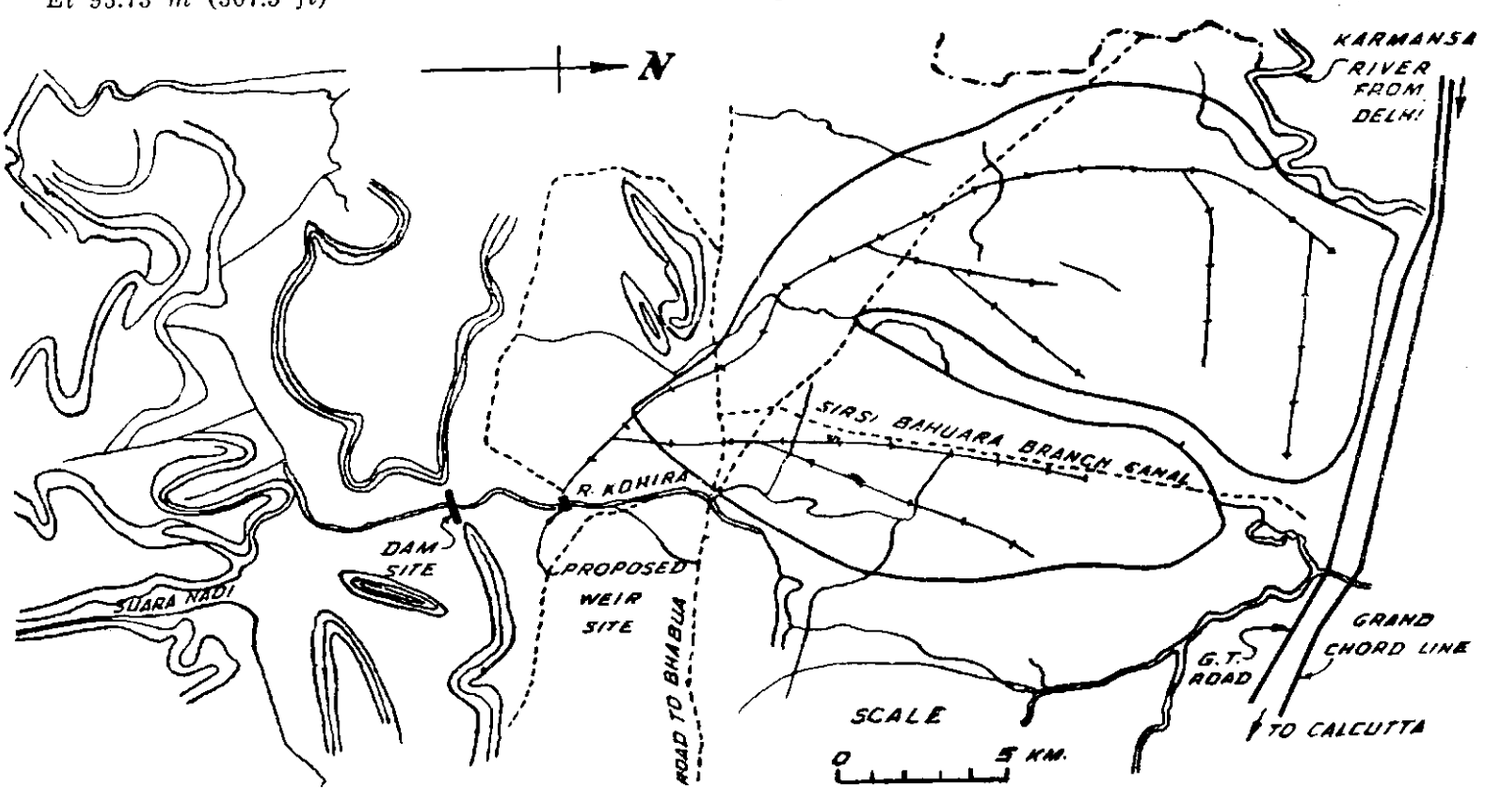

Fig 1: Index Plan Kohira Dam Project.

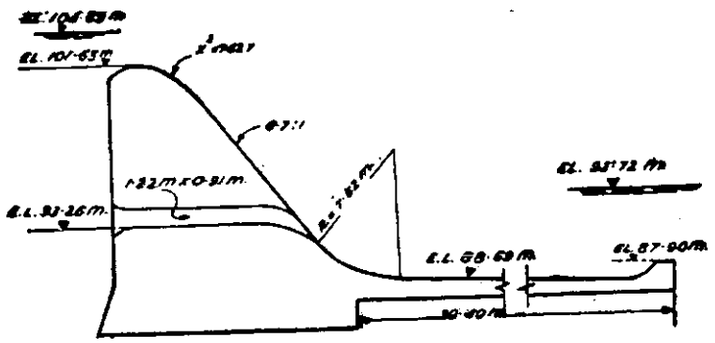

Fig 2a: Original design.

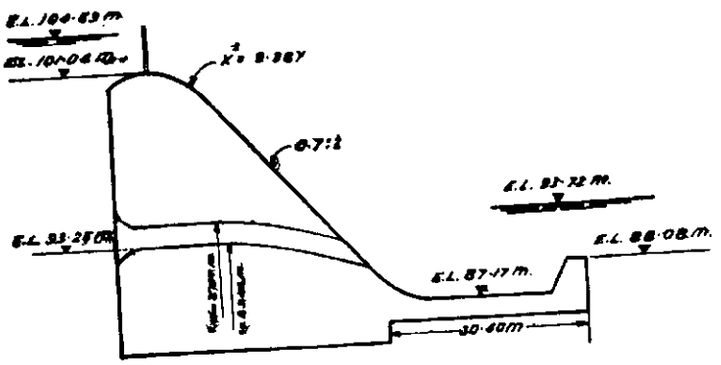

Fig 2b: Modified Design.

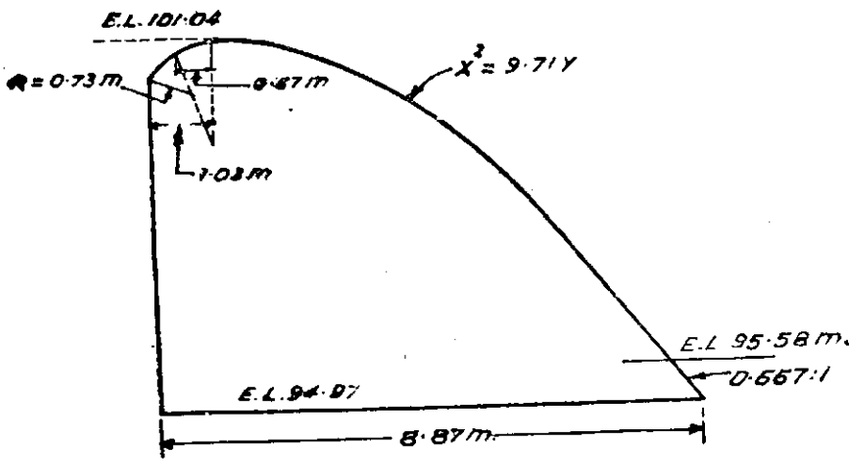

Fig 5: Details of the crest of spillway.

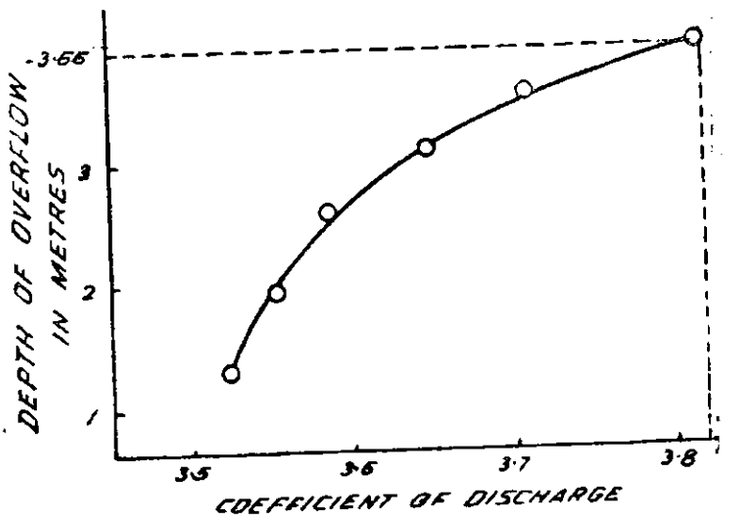

Fig 6a.

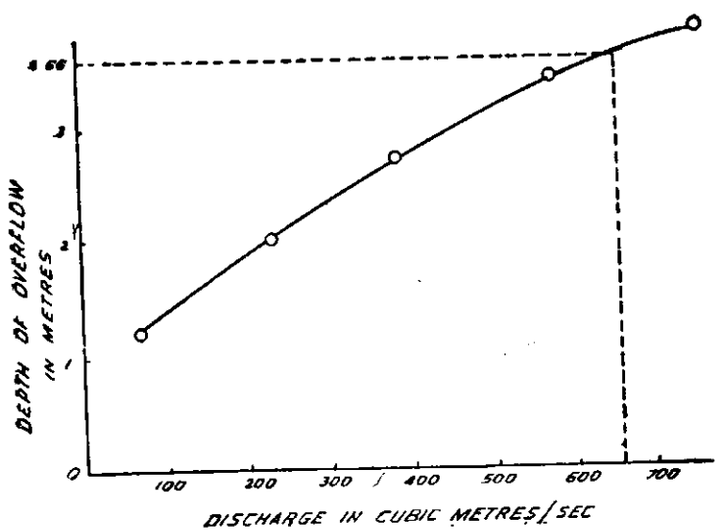

Fig 6b.

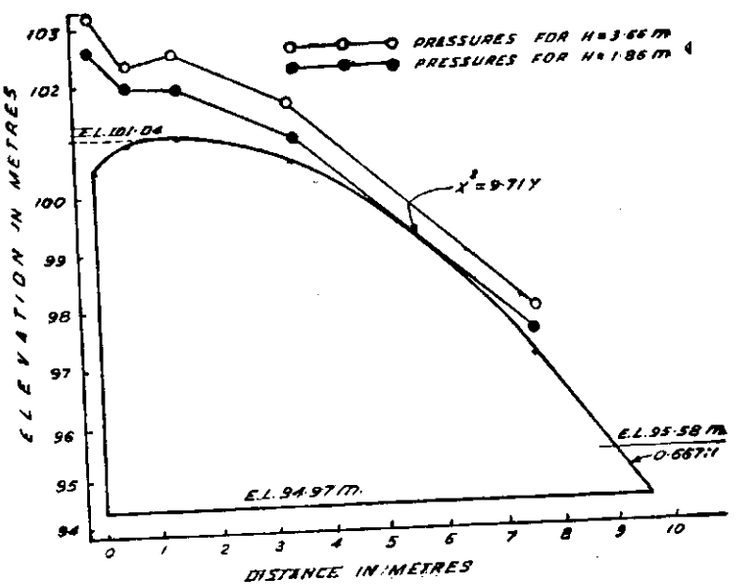

Fig 7: Pressure distribution on the crest region.

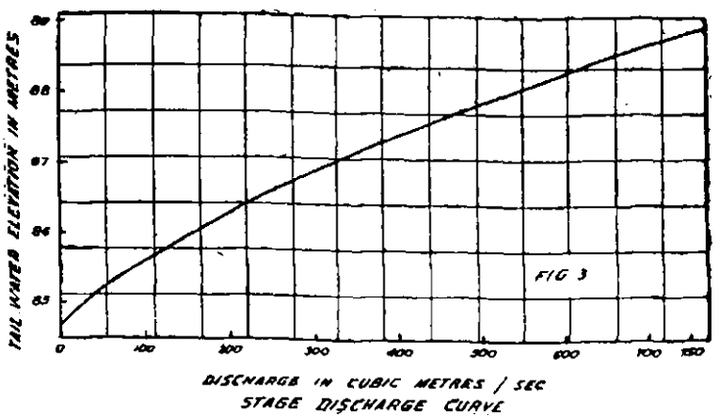

Fig 3:

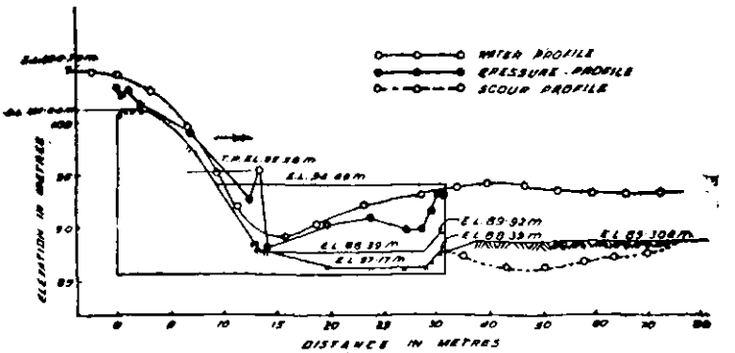

Fig 8: Water profiles and pressures on lower apron for design discharge of 736.24 m^3/sec and tail water *EL*, 93.77 *m*.

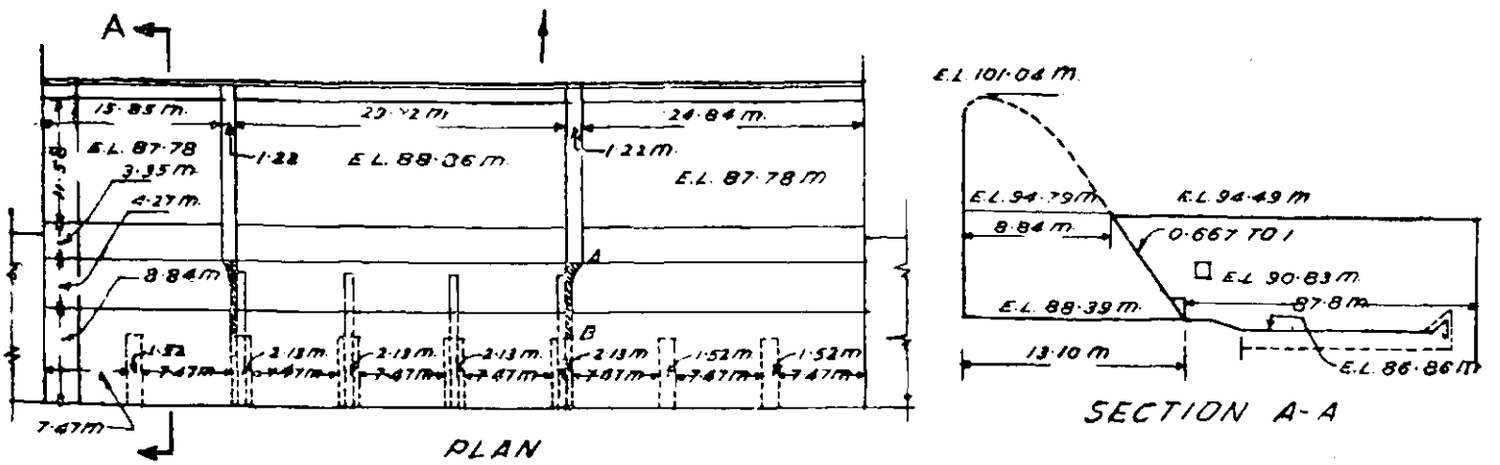

Fig 4: Details of spillway as constructed.

retrograded levels at *El* 92.96 *m* (305 *ft*). The scour was 2.44 *m* (8 *ft*) at 7.32 *m* (24 *ft*) below ground level downstream of the end sill.

(*ii*) *Tests on higher apron at El 88.39 m (290 ft) and end sill raised by 1.52 m (5 ft) to El 89.92 m (295 ft).*—The profiles of water surface, scour and pressures are shown in *fig 9*. The formation of hydraulic jump was efficient but slightly marred by a secondary wave. The secondary wave about .45 *m* (1.50 *ft*) high was noticed beyond the apron but it occurred at the surface bearing no influence on scour, which reached a maximum of 2.44 *m* (8 *ft*) below ground level at 10.67 *m* (35 *ft*) downstream of the end sill.

(c) *Differential pressures on the divide wall.*—As mentioned earlier the divide wall between the higher and lower aprons was tested in the model keeping the top at *El* 94.49 *m* (310 *ft*). The maximum pressures were observed for design discharge of 736.24 m^3/*sec* (26,000 *cfs*) and tailwater level of *El* 93.73 *m* (307.5 *ft*) at various points shown in the *fig 10*. The maximum differential pressure recorded was 6.1 *m* (20 *ft*) of water which should be taken into account in the design. The divide wall with top at *El* 94.49 *m* (310 *ft*) had to be raised in the hatched portion *AB* and linked up with the pier as shown in *figs 4* and *10* to prevent the flow coming down the spillway crossing into the adjacent spans.

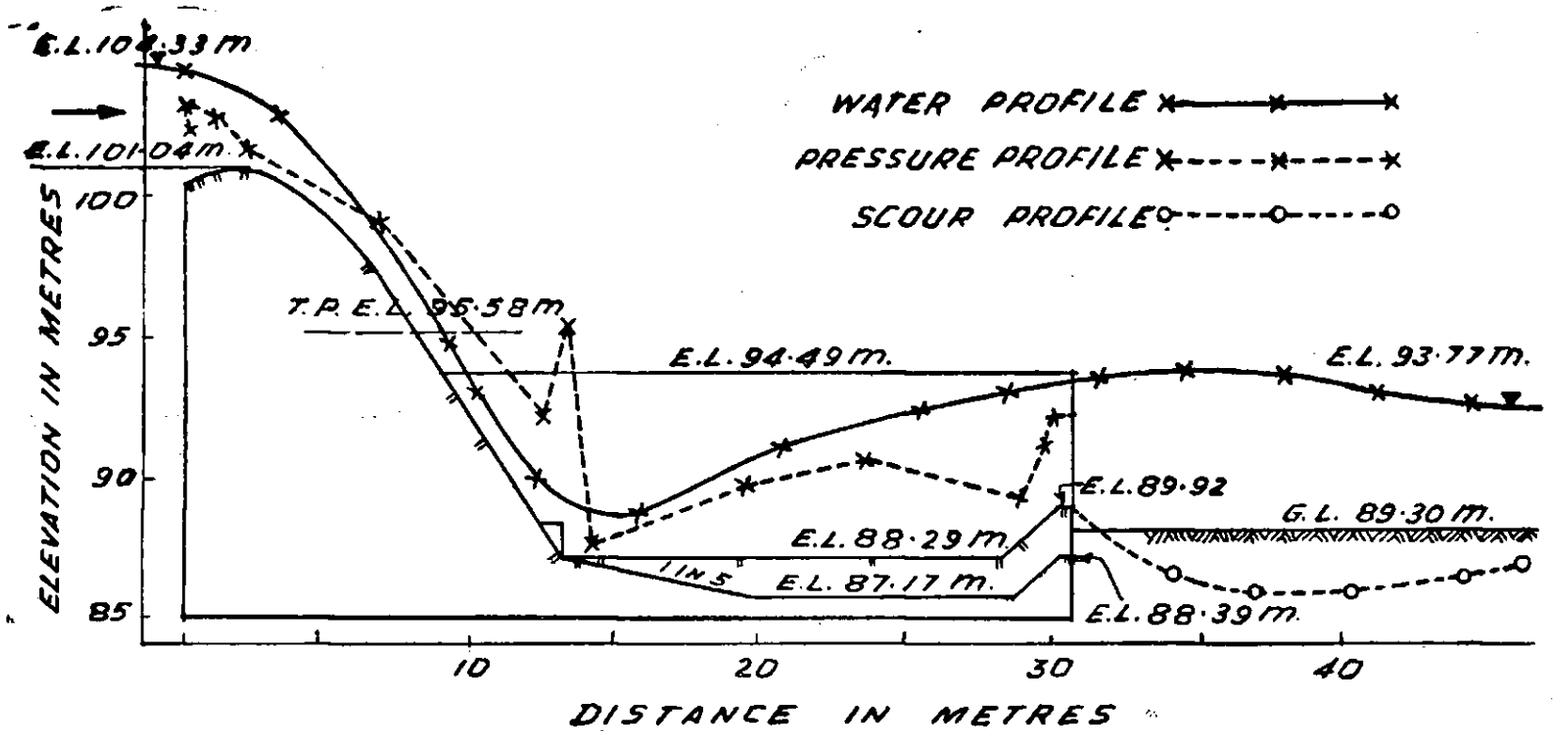

Fig 9: Water profile scour pressures on higher apron for design discharge of 736.24 m^3/s and tail water *EL* 93.77 *m*.

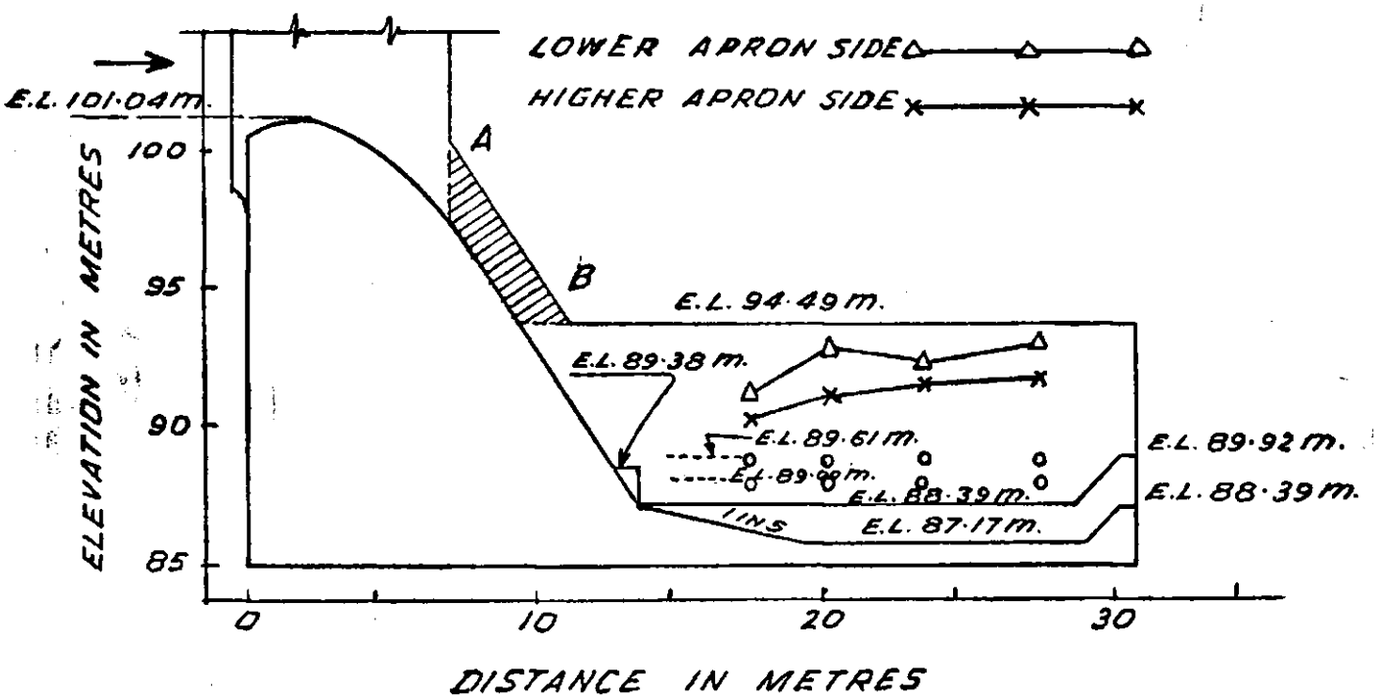

Fig 10: Pressures on divide wall.

(*d*) *Tests with entire apron at El 88.39 m (290 ft) without divide wall.*—The differential pressure on the divide wall was 6.1 *m* (20 *ft*) of water, which was too high to be sustained by masonry wall of 1.22 *m* (4 *ft*) thickness as designed and constructed by the project authorities. It would be economical to maintain the aprons at the same elevation which would result in the elimination of the divide wall. Hence the central apron was raised from *El* 87.17 *m* (286 *ft*) to *El* 88.39 *m* (290 *ft*). Rigid bed was reproduced at *El* 89.3 *m* (293 *ft*) to conform to existing rock levels. The performance of the stilling basin, in spite of the secondary wave occurring at the surface downstream of the apron was satisfactory even for a retrogression of .45 *m* (1.5 *ft*) in water level and could be accepted in view of the exposed rock downstream.

(*e*) *Test on the sluices in the body of the spillway*: (*i*) *Tests on the sluice designed and*

constructed by the project authorities.—The section of the sluice designed and constructed by the project authorities is shown in *fig 11*. Under the condition of maximum head of 10.67 *m* (35 *ft*) corresponding to *MWL* 104.7 *m* (343.5 *ft*) upstream, the jet impinged at 4.88 *m* (16 *ft*) from the vertical downstream face of the chute block on the pool of water in the apron without following the profile of the spillway. Though the jet impact was partly absorbed by the pool of water in the apron it would be necessary to provide extra reinforcement and a rich concrete mix in the region of impact of the jet. There was no sub-atmospheric pressures anywhere on the sluice. The maximum pressure on the sluice was 7.32 *m* (24 *ft*) of water. The condition of flow is shown in *photo 17*.

(*ii*) *Tests on the modified sluice design.*—The design of the sluice is shown in *fig 12*. The sluice was tested for the maximum head. The profiles of the jet and pressures are indicated in *fig 12*. The jet issuing from the sluice followed the profile in this case. The pressures on the sluice were positive as shown in *fig 12* and *photo 18*.

7. Conclusions

(*i*) The equation of the crest of the spillway should conform to $X^2 = 9.71\ Y$ to suit the maximum head of 3.66 *m* (12 *ft*) and present dimensions of construction *viz* .667 to 1 spillway slope

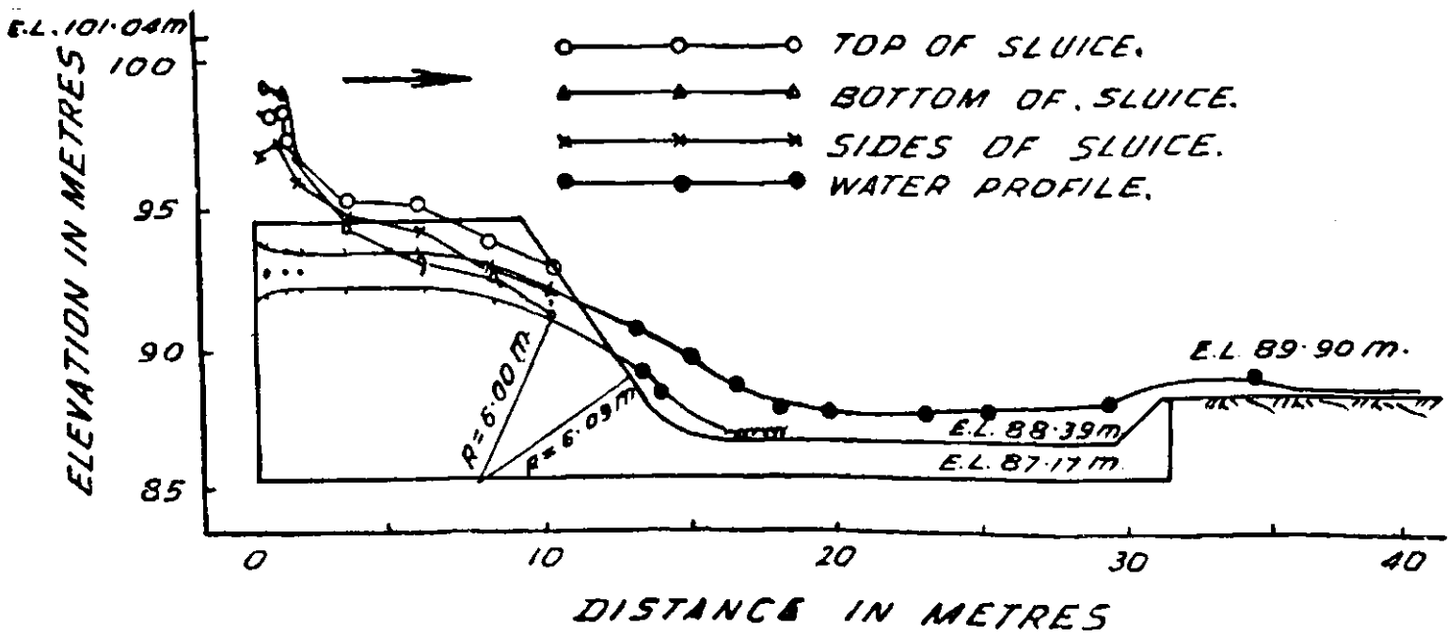

Fig 11: Water profile of jet and pressures on the sluice already constructed.

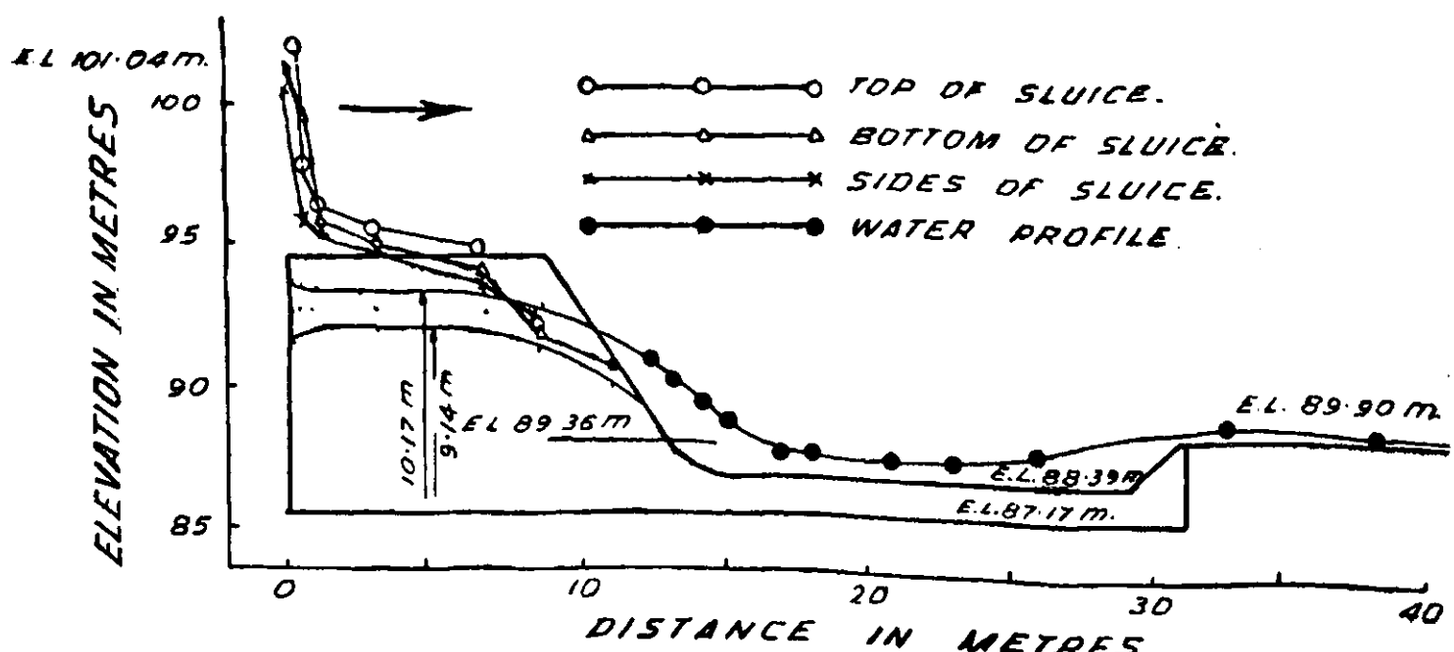

Fig 12: Water profile of jet and pressures on the sluice (original design).

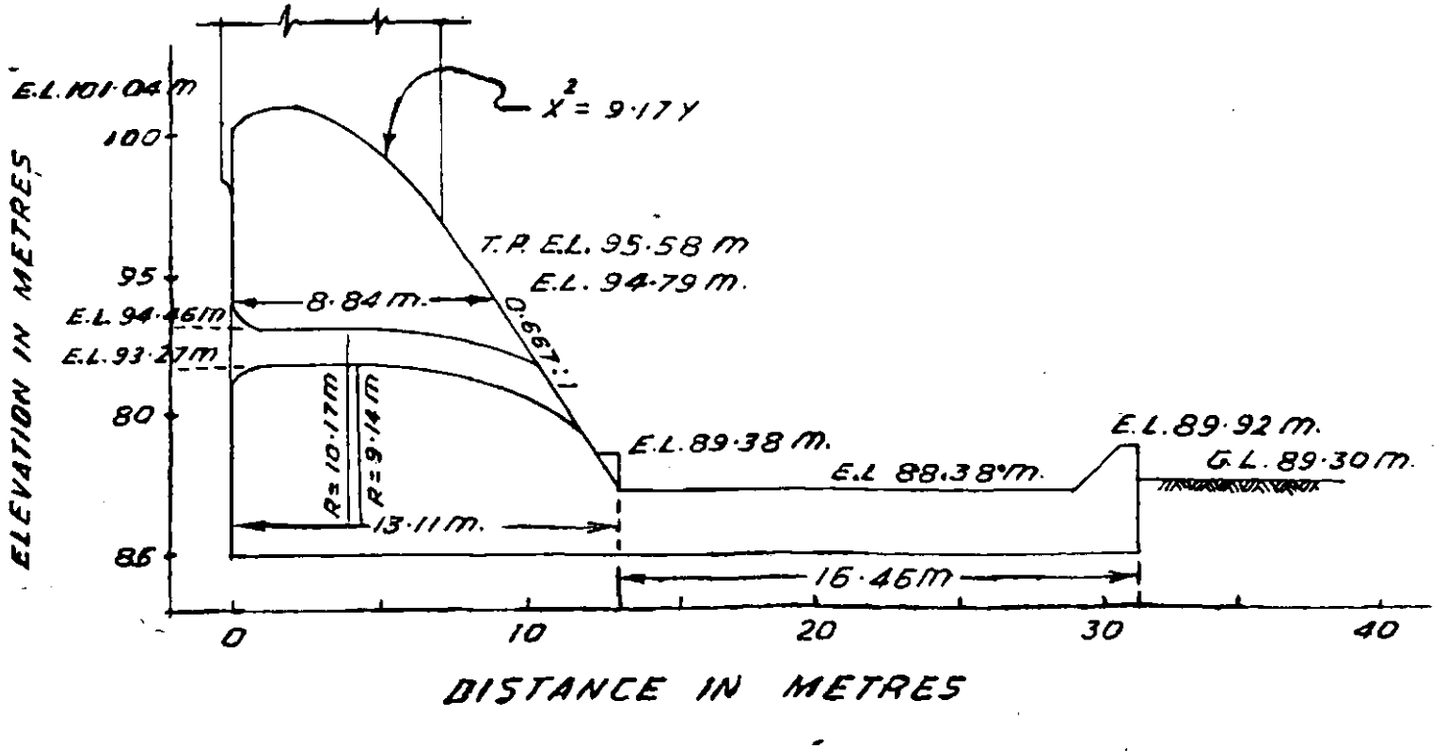

Fig 13: Recommended design.

and basal widths of 8.84 *m* (29 *ft*) at *El* 94.79 *m* (311 *ft*) and 13.11 *m* (43 *ft*) at *El* 88.39 *m* (290 *ft*) (*fig 13*).

(*ii*) The design of the crest assured adequacy of discharging capacity and freedom from sub-atmospheric pressures (*figs 6a, b* and *7*).

(*iii*) The maximum differential pressure on the divide wall between the aprons at *El* 87.17 *m* (*RL* 286) and *El* 88.39 *m* (290 *ft*) was of the order of 6.09 *m* (20 *ft*) which was excessive for the 1.22 *m* (4 *ft*) masonry section. In case the downstream aprons were decided to be laid at two different levels *viz El* 86.86 *m* (285 *ft*) and *El* 88.39 *m* (290 *ft*) it would be necessary to raise the divide wall to *El* 94.49 *m* (310 ft) and extended it upstream to link up with the pier (*figs 4* and *10*).

(*iv*) It would achieve greater economy if a single uniform level apron at El 88.39 *m* (290 *ft*) is provided which would not only achieve energy dissipation but also obviate expensive divide walls in between the stepped aprons (*fig 13*).

(*v*) The sluice designed originally gave satisfactory performance both from the point of view of the flow conditions of the jet as well as pressure distribution. However, the jet emerging from the sluice already constructed sprang clear of the spillway profile and impinged directly on the pool below. This condition was not satisfactory. Sub-atmospheric pressure did not exist in the sluice barrel. Additional reinforcement with rich mix of concrete should be provided on the apron where the jet impinged directly (*figs 11* and *12*).

III. Meshwa Dam Project

THE PROJECT envisages the construction of a storage reservoir across the river Meshwa near the village of Shamlaji in Sabarkantha District. The present proposals provide for a masonry dam with a central ungated overflow spillway and earthen banks to block low saddles. The left bank canal 64.37 *km* (40 *miles*) long with a discharging capacity of 5.66 m^3/sec (200 *cfs*) will irrigate an additional area of 5625 *hectares* (13,906 *acres*) besides assuring supplies to 8093.7 *hectares* (20,000 *acres*) under the existing Meshwa pick up weir and canal scheme. *Fig 1* shows the index plan of the project.

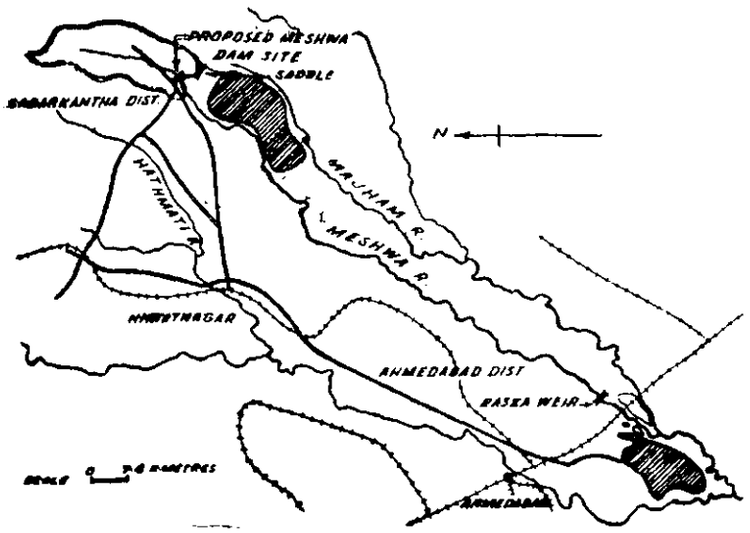

Fig 1: **Index plan.**

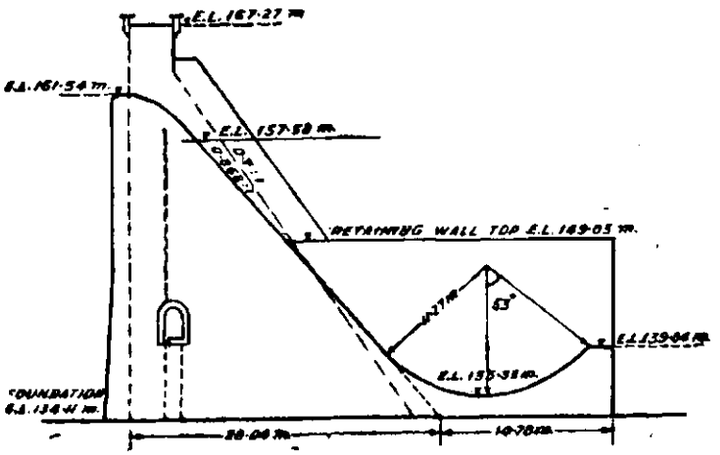

Fig 2: Details of original design.

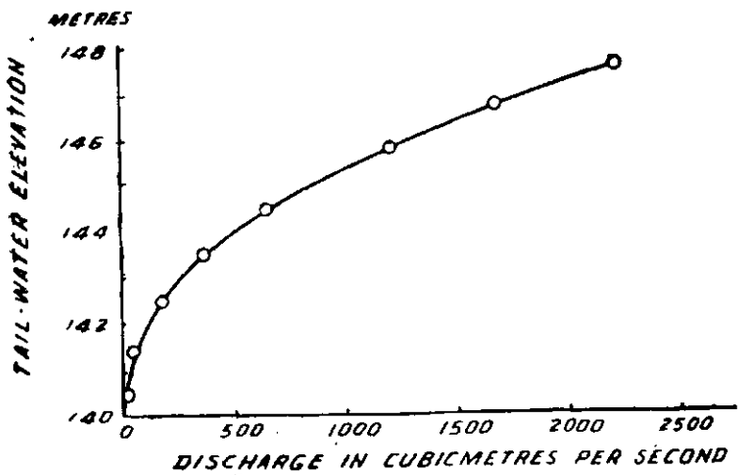

Fig 3: Stage-discharge curve.

The *salient features* of the project are given below.

(i)	Catchment area at dam site.	253.81 *sq km* (98.04 sq *miles*)
(ii)	Average annual rainfall in catchment area at dam site.	849.50 *mm* (33.45 *inches*)
(iii)	Gross capacity of the reservoir ...	54.33 million m^3 (2330 *m* ft^3)
(iv)	Dead storage ...	2.26 million m^3 (80 *m* ft^3)
(v)	Full reservoir level ...	*El* 161.54 *m* (530 *ft*)
(vi)	High flood level ...	*El* 166.52 *m* (546 *ft*)
(vii)	Sill level of head sluice.	*El* 146.30 *m* (480 *ft*)
(viii)	maximum design flood.	2066 m^3/sec (73,000 *cfs*)
(ix)	Length of dam	
	Masonry ...	169.16 *m* (555 *ft*)
	Earthen ...	2727.96 *m* (8950 *ft*)
(x)	Irrigated area ...	14932.9 *hectares* (36,900 *acres*)
(xi)	Estimated cost of the scheme.	*Rs* 156 lakh

2. Details of spillway design

Flood disposal was proposed to be effected by a 85.34 *m* (280 *ft*) long ungated spillway. In the design the crest of the spillway was kept at *El* 161.54 *m* (530 *ft*). The spillway had been designed for a flood lift of 5.02 *m* (16.50 *ft*) over the crest, thereby assuming the full reservoir level at *El* 166.52 *m* (546 *ft*). For dissipation of energy a roller bucket of radius 11.27 *m* (37 *ft*) lip angle 53° and invert at *El* 135.33 *m* (444.25 *ft*) had been designed. The maximum flood stage in the river downstream has been recorded as *El* 147.82 *m* (485 *ft*). The details of the original design are shown in *fig 2*.

3. Estimate of design flood discharge

The maximum flood discharge had been estimated at 2066 m^3/sec (73,000 *cfs*) by comparison with the adjacent Hathmathi catchment. For working out the absorption of flood, the duration of storms actually observed were studied and the outgoing flood was worked out by step method to 1794 m^3/sec (60,400 *cfs*) which conforms to a flood lift of 4.5 *m* (14.8 *ft*) assuming a coefficient of 3.9. However paucity of data on storm characteristic dictated the adoption of higher design flood of 2066 m^3/sec (73,000 *cfs*) which is also proximate to the Inglis flood. It appears that discharge observations have not been conducted by velocity area method. For the purposes of design, the discharges have been worked out on

slope area method for different stages. The stage discharge relationship worked out on this basis is shown in *fig 3.*

4. Terms of reference

Advice was sought on the following points of reference.

(i) Discharging capacity of spillway
(ii) Pressure distribution on the spillway profile
(iii) Radius, invert level and lip angle of the bucket
(iv) Effective energy dissipation downstream of the spillway and length of the training walls on the sides of the bucket.

Two models of the spillway were constructed for the purpose.

(i) 1/30 scale geometrically similar sectional model.
(ii) 1/60 scale three dimensional composite model.

5. Experiments on sectional model

(*a*) *Discharging capacity of the spillway*: The coefficient of discharge computed from discharge observations for different depths of overflow is plotted in *fig* 4(*a*) and 4(*b*). The highest coefficient was 4.20 for the maximum depth of overflow *viz* 5.02 *m* (16.5 *ft*) when slight negative pressures were observed in the spillway crest region. The highest discharging capacity worked out to 2264.8 m^3/sec (80,000 *cfs*) which was quite adequate.

(*b*) *Pressure distribution on the spillway profile*: When the model was run for various depths of overflow ranging from 5.02 *m* (16.50 *ft*) to 1.82 *m* (6 *ft*), the pressures were positive throughout upto a depth of overflow of 3.64 *m* (12 *ft*). However, there were indications of negative pressures upstream of the crest when the head exceeded 3.64 *m* (12 *ft*). This was obvious since the original spillway profile conformed to Creager curve for 3.64 *m* (12 *ft*) head. The maximum negative pressure recorded was of the order of 1.82 *m* (6 *ft*) for the design depth of overflow of 5.02 *m* (16.5 *ft*). The pressures on the crest of the spillway are shown in *fig* 5. No change in the profile was necessary since the negative pressure of 1.82 *m* (6 *ft*) was considered admissible on account of its very low frequency of occurrence.

(*c*) *Design of the energy dissipation device downstream of the spillway*: (*i*) *Experiments on the original roller bucket, radius 11.27 m (37 ft), lip angle of 53°, invert El 135.33 m (444.25 ft).*—As the tailwater curve was persistently higher than the jump height curve for all discharges, a roller bucket was designed for dissipation of energy.

During the tests with depths of overflow varying from 5.02 *m* (16.50 *ft*) to 1.82 *m* (6 *ft*), the performance of the bucket was found to be entirely unsatisfactory. The dissipating roller was

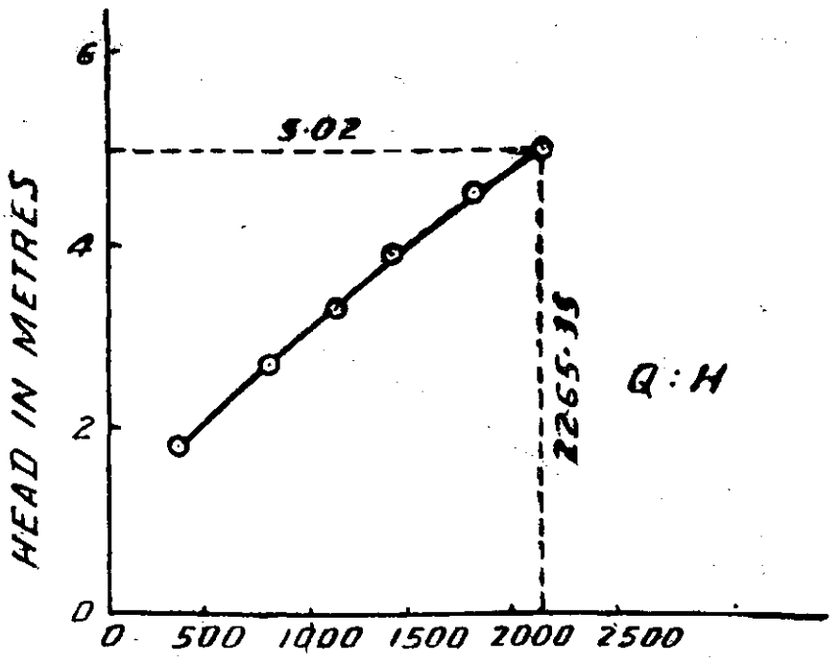

FIG.-4a
DISCHARGE IN CUBIC METRES PER SECOND.

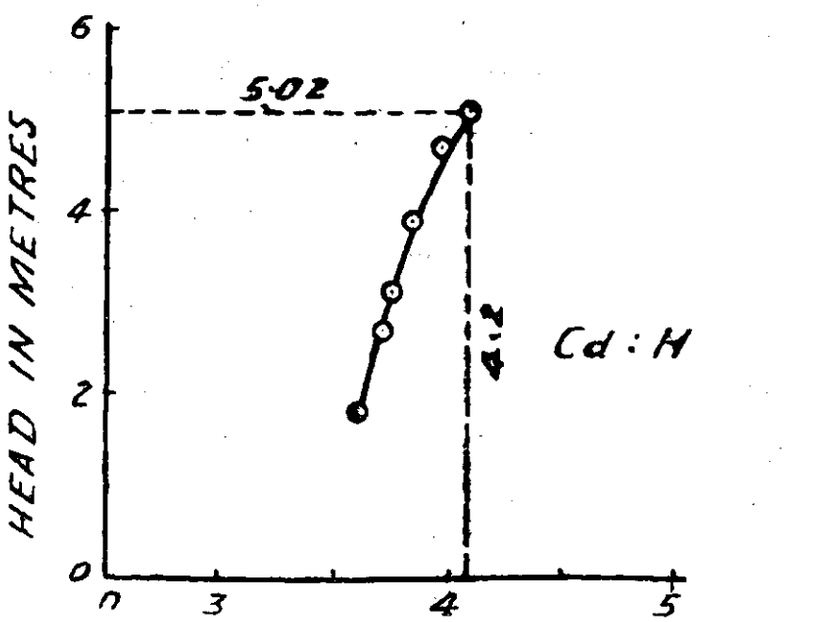

FIG.-4b
COEFFICIENT OF DISCHARGE

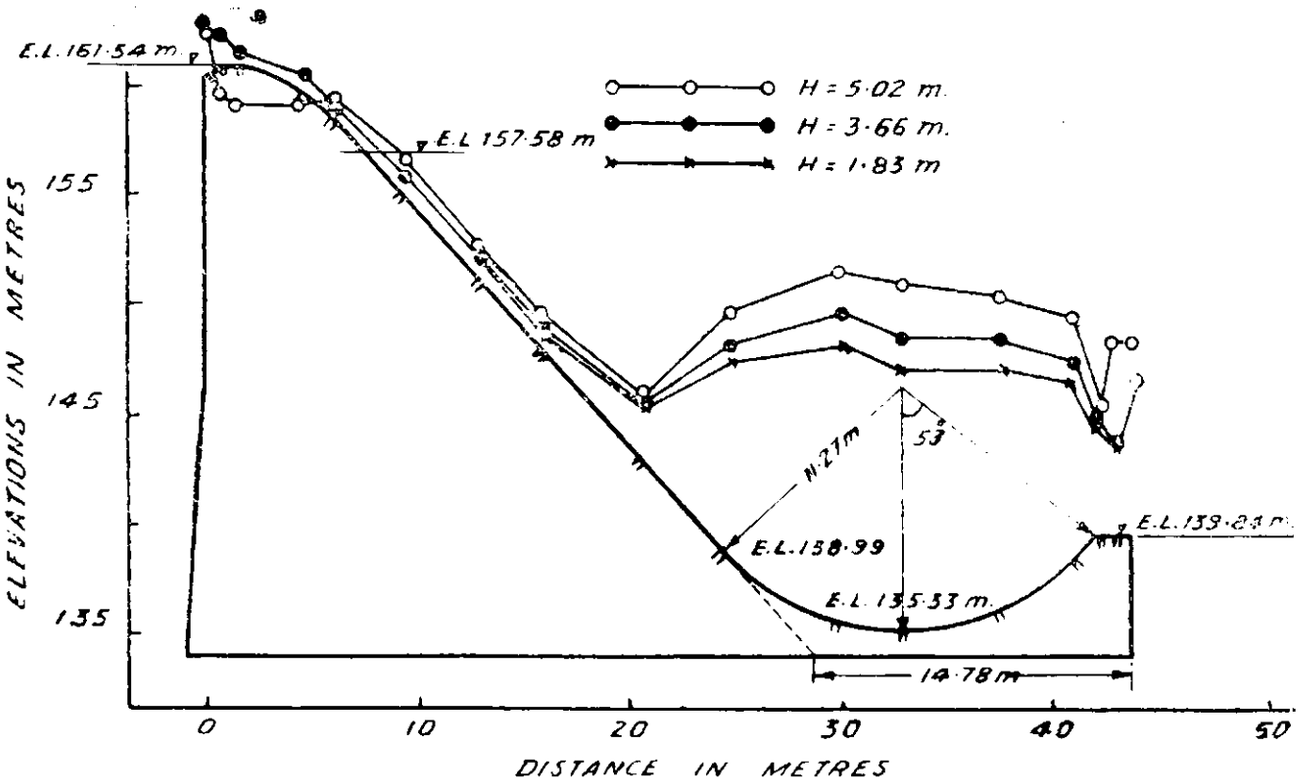

Fig 5: Pressure distribution on the spillway.

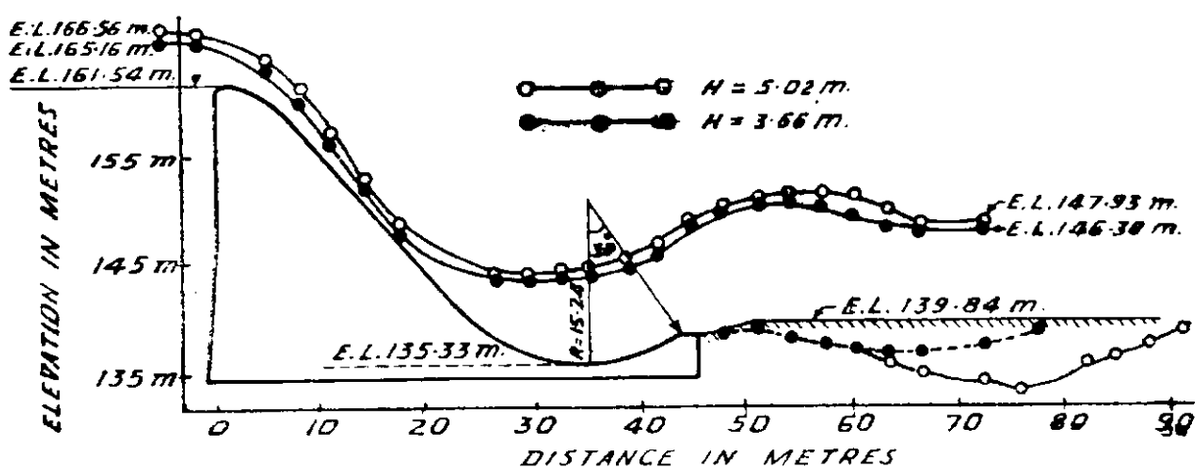

Fig 6a: Profile of water surface and scour.

vigorous and well defined but the stabilizing roller was imperfect and weak. A hump could be noticed on the water surface downstream of the bucket lip from where the flow dived down to cause considerable scour downstream. The maximum scour reached 9.45 *m* (31 *ft*) below groundlevel at a distance of 27.43 *m* (90 *ft*) downstream of the end sill. The performance of the bucket for the design depth of flow is seen in *photo 19*.

(*ii*) *Experiments on roller bucket radius 11.28 m (37 ft), lip angle 35°, invert El 135.33 m (444.25 ft)* : In order to minimise the throw-off of the jet directed towards the surface, the lip angle was decreased to 35° keeping the same radius and invert as before. Except reduction in the water

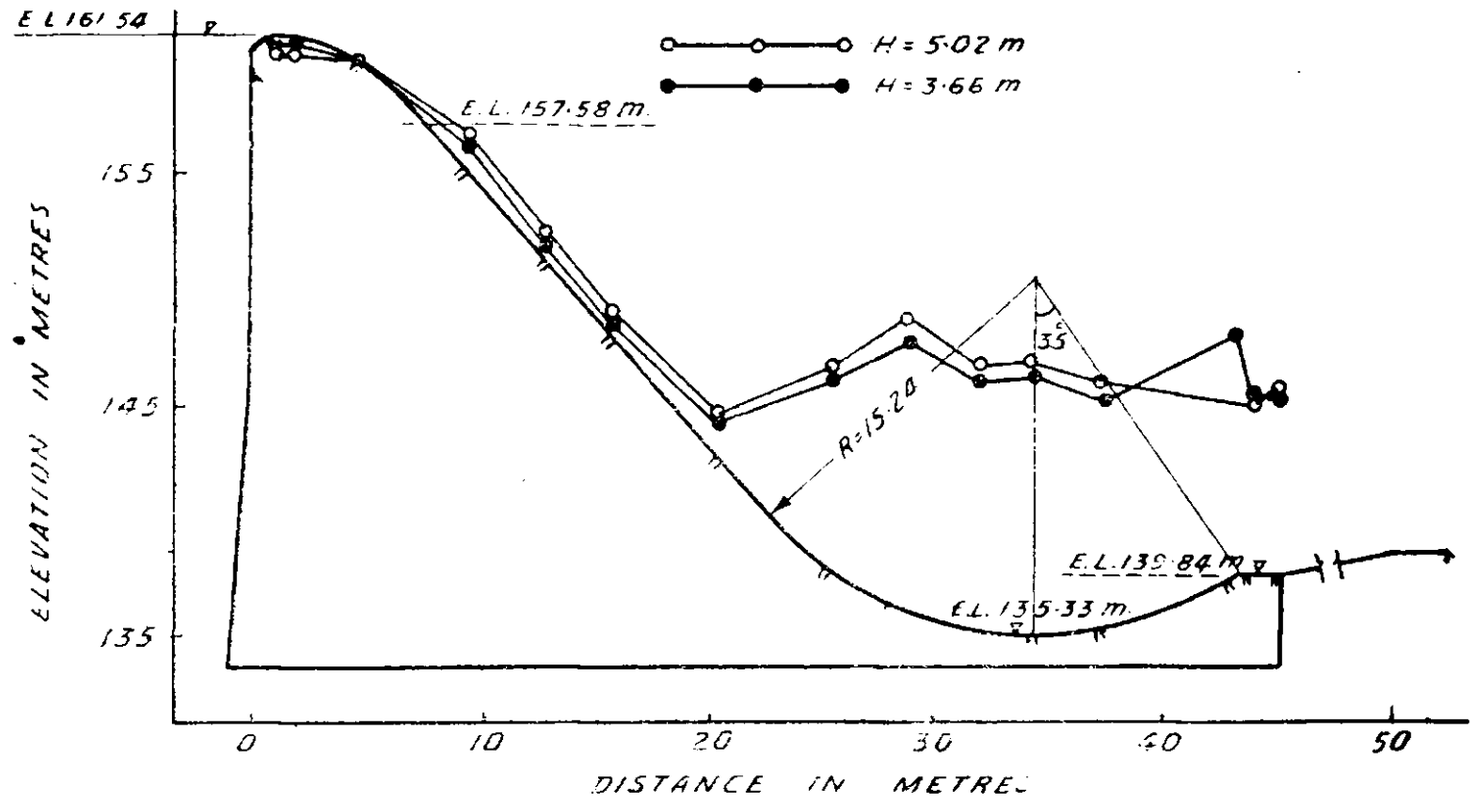

Fig 6b: Pressure distribution on the spillway.

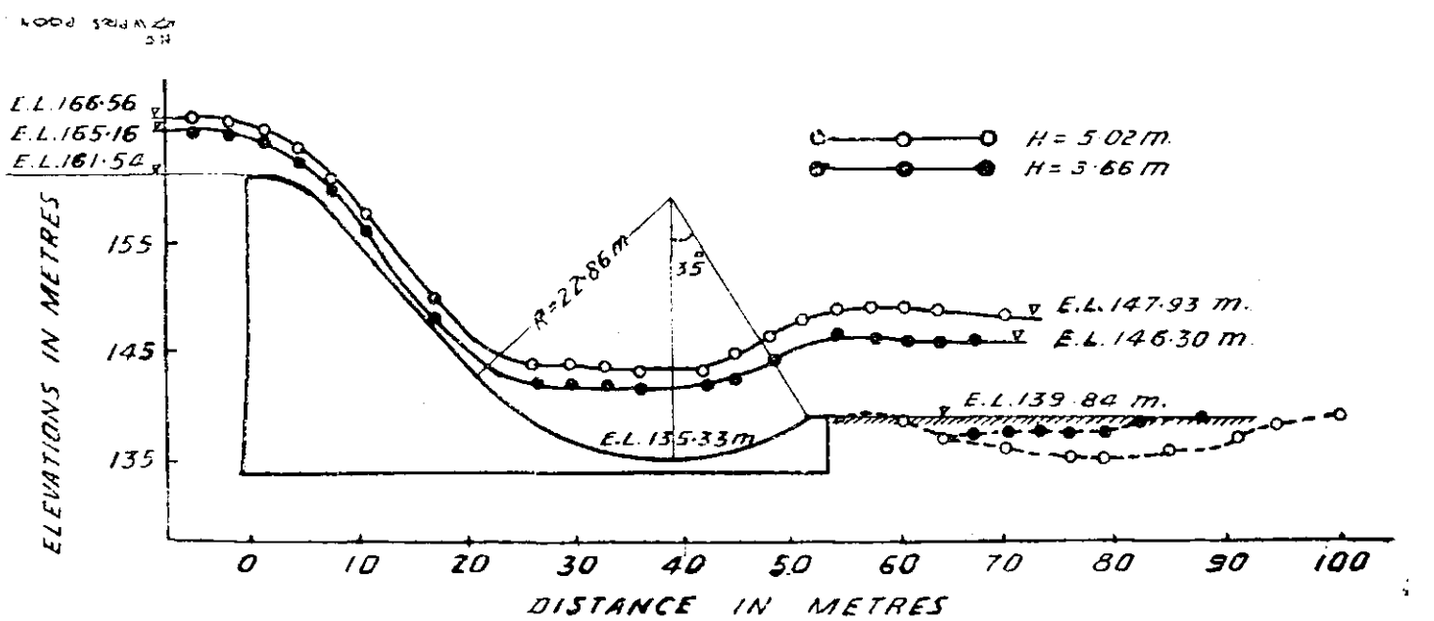

Fig 7a: Water and scour profile for various depths of over-flow.

surface hump the performance of the bucket did not show any improvement. The maximum scour in this case was 8.84 *m* (29 *ft*) below ground level.

(*iii*) *Experiments on the roller bucket radius 15.24 m (50 ft), lip angle 35°, invert El 135.33 m (444.25 ft)*: As a change in the lip angle alone was ineffective the radius was increased to 15.24 *m* (50 *ft*) keeping the same invert. In this design the performance of the bucket showed some improvement in the action of both the dissipating roller and the stabilizing roller. The maximum scour for design depth of 5.02 *m* (16.50 *ft*) of overflow reduced by 2.13 *m* (7 *ft*) than in the original design. *Figs 6a* and *b* show the profiles of

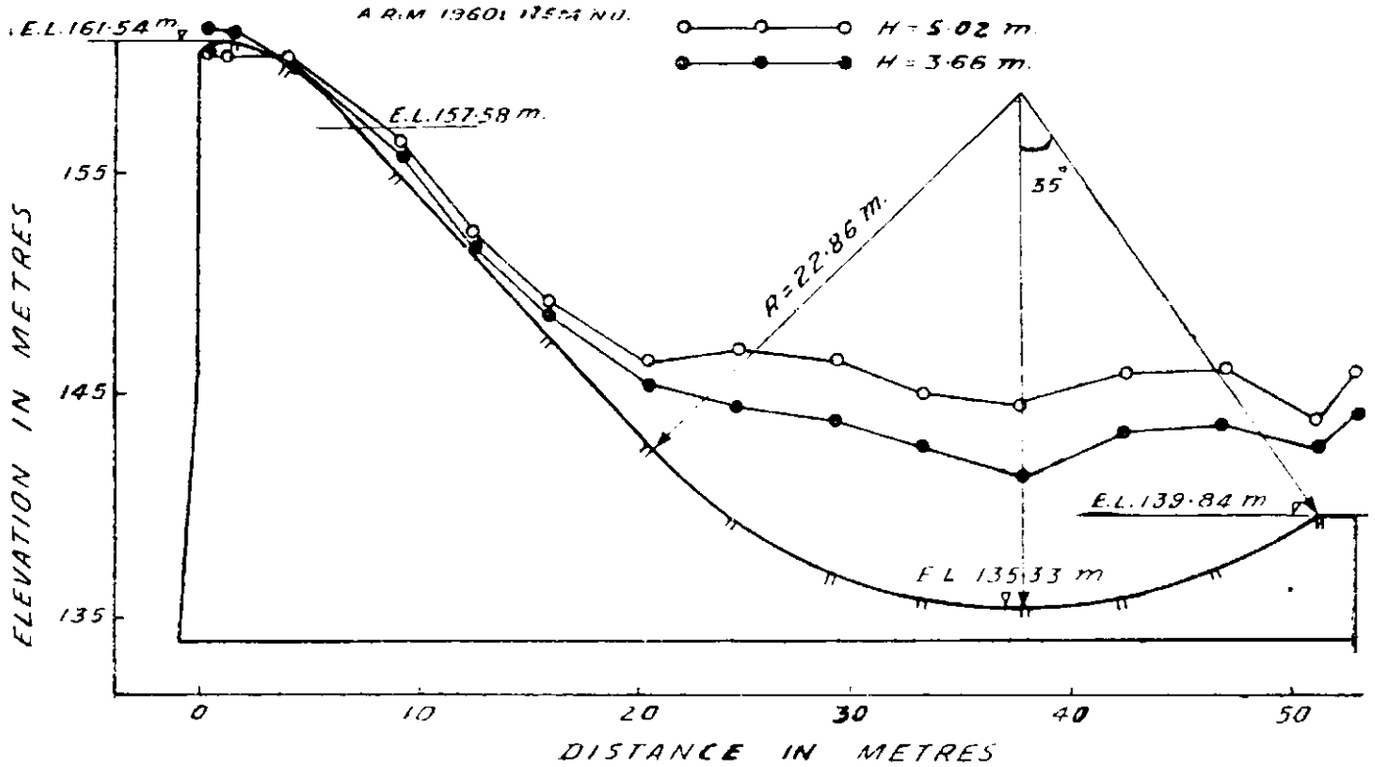

Fig 7b: Pressure profile for various depths of over-flow.

water surface, scour and pressures for various depths of overflow. However, it was necessary to improve the design to limit the scour to rock level. Lowering of the bucket invert could perhaps help. But already the invert was three feet below rock level. It was, therefore, thought fit to increase the radius to its limiting value of 22.86 *m* (75 *ft*) so that roller action would prevail.

(*iv*) *Experiments on the roller bucket, radius 22.86 m (75 ft), lip angle 35°, invert El 135.33 (444.25 ft)*: The radius of the bucket was increased to 22.86 *m* (75 *ft*) without altering the invert level and the lip angle. There was very substantial improvement both in roller action and scour. *Figs 7a* and *b* show the profiles of water surface, scour and pressure profile for various depths of overflow. The maximum depth of scour was reduced to 4.05 *m* (13.3 *ft*) below ground level. Water surface disturbances downstream of the bucket minimized appreciably. A check on the scour levels with downstream rock contours reproduced in the model confirmed that scour would reach rock level only at the maximum discharge.

Note.—When the design finalized from the sectional model tests was under investigation in the three dimensional composite model, the project authorities informed that the spillway site had now been shifted to the Venpur saddle as foundations opened at the dam site were found to be poor. It is now proposed to replace the design of masonry dam by an earth dam with the spillway located in a saddle. Further tests will be resumed on receipt of data on the new saddle spillway design.

IV. Banas Dam, Dantiwada Project

IN THE *Annual Research Memoirs 1959* an interim report on the model experiments for the design of Banas dam spillway was published. As stated therein the original stilling basin design with a horizontal apron was found to be uneconomical though hydraulically sound. From the plots of tailwater rating curve and jump height curve it was observed that the available depth of water at different stages of discharge was much in excess of the sequent depth for hydraulic jump formation. This fact and the rock foundations at *El* 141.732 *m* (465 *ft*) indicated the possibility of substituting the horizontal apron by a roller bucket. Accordingly tests were continued for evolving a

suitable design of a roller bucket for the spillway which are reported below.

2. Tests on 1/36 sectional model

(*a*) *Bucket of radius 15.24 m (50 ft), lip angle 35°, invert El 140.208 m (460 ft).*—Since roller buckets normally prove effective when tailwater depth exceeds the sequent depth by twenty *per-cent*, the bucket invert was kept at *El* 140.208 *m* (460 *ft*) for a preliminary check. The dissipating roller was characterized by erratic movements, heavy hurdling action and disturbed flow conditions downstream. The stabilizing ground roller formation was also far from satisfactory. The performance on the whole was not acceptable. *Photo 20* shows the bucket action for 8.239 *m* (27 *ft*) depth of flow.

(*b*) *Tests with R = 18.288 m (60 ft), = 35°, invert El 140.208 m (460 ft).*—This design worked well for all discharges. The ground roller formation was quite effective and downstream flow disturbances minimised. The maximum scour reached *El* 138.35 *m* (454 *ft*) at a distance of 47.54 *m* (156 *ft*) from the bucket lip. Even under retrogression conditions the action was found satisfactory. *Photo 21* shows the action of the spillway for maximum discharge.

However, the conditions for low discharges clearly showed a very high margin over the tailwater depths. This indicated the possibility of raising the bucket invert by .609 *m* to .91 *m* (2 to 3 *ft*) without affecting the conditions adversely. The invert of the bucket was raised to *El* 141.12 *m* (463 *ft*) and the tests repeated.

(*c*) *Tests with R = 21.945 m (72 ft), θ = 35°, invert El 141.12 m (463 ft).*—The bucket action was satisfactory for all discharges under both normal and reduced tailwater levels. The maximum scour reached *El* 138.684 *m* (455 *ft*) at 51.816 *m* (170 *ft*) from the bucket lip. *Photo 22* shows the conditions for maximum discharge. *Fig 1* shows the water surface profiles and scour patterns for various discharges.

3. Tests on 1/72 three dimensional composite model

The bucket with *R* = 21.9 *m* (72 *ft*), θ = 35° and invert *El* 141.12 *m* (463 *ft*) found satisfactory in the sectional model tests was experimented

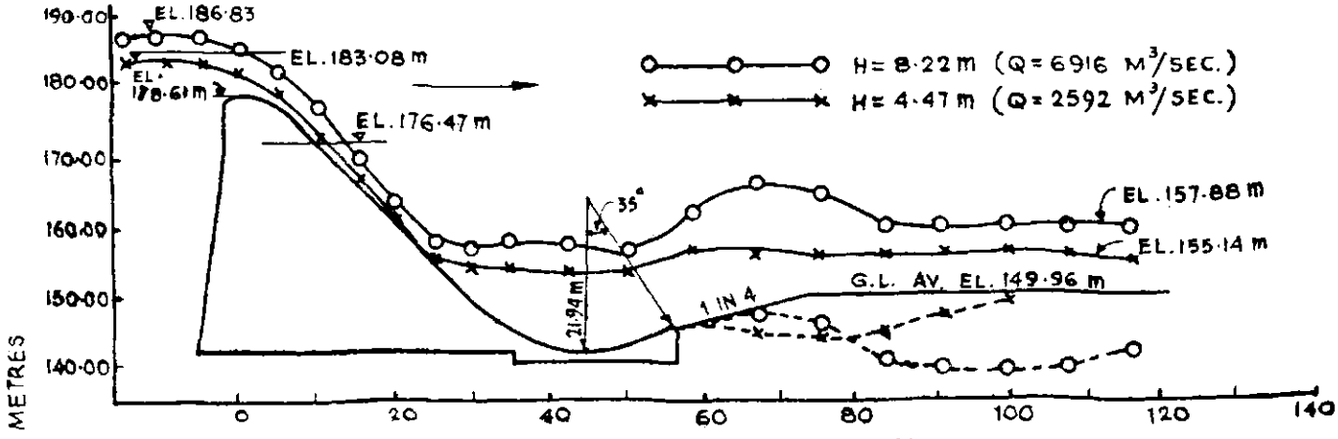

WATER PROFILES AND SCOUR PATTERN WITH ROLLER BUCKET
INVERT AT EL. 141·12 m, R = 21·94 m, θ = 35°

FIG. 1(a)

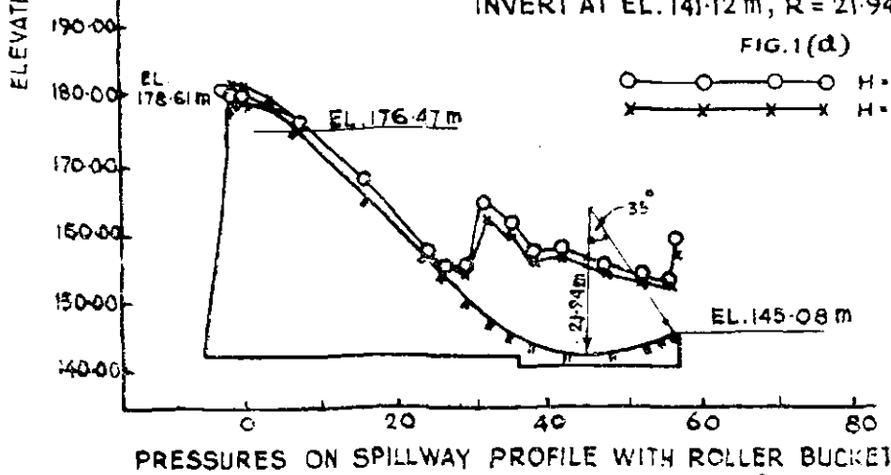

PRESSURES ON SPILLWAY PROFILE WITH ROLLER BUCKET
INVERT AT R.L. 141·12 m, R = 21·94 m, θ = 35°

FIG. 1(b)

with, in the composite model. With the high ground levels existing downstream at present, it was observed that high water levels prevailed particularly on the left bank where a submerged whirling action, drawing in sand laden water into the bucket was seen. The test was performed with a mobile bed.

There are a number of huge boulder outcrops downstream of the spillway interspersed on the high ground particularly on the left side. As this type of configuration would adversely affect the flow downstream of the spillway, the test was repeated with the entire ground downstream reproduced with rigid bed. The performance was marred by severe cross waves, hurdling action, partly submerged flow and flow fanning out irregularly in several directions downstream. The divide walls were overtopped. *Photo 23* shows the spillway in action for 8.229 *m* (27 *ft*) depth of flow. These indicated the necessity for lowering the ground level downstream to an extent which would obtain better flow conditions. From various trials, the ground levels for satisfactory flow conditions were obtained as below:

Downstream of bucket, left side of spillway.	First 15.24 *m* (50 *ft*) at bucket lip level and then ground sloping up the lip at 1 in 4 to *El* 150.876 *m* (495 *ft*).
Downstream of bucket, right side of spillway.	First 15.24 *m* (50 *ft*) at bucket lip level and then the ground level sloping at 1 in 4 to an average *El* 148.98 *m* (492 *ft*).

From the flow conditions it was further observed that the long lengths of guide walls provided in the *CDO* design on the extreme flanks could be easily curtailed. The curved lengths of the walls retaining the earthen envelope were removed and the earthen slopes continued to join the natural ground level. Since flow concentration was slightly more towards the right side, extension of the right end wall straight by 22.86 *m* (75 *ft*) proved adequate. But the walls required raising by .914 *m* (3 *ft*) *ie* to *El* 150.32 *m* (526 *ft*) at the ends; sloping up to *El* 163.08 *m* (535 *ft*) at the line of bucket lip as shown in *fig 2* and *figs 3* (*a*) and *3* (*b*). The left end wall was given a curved alignment with a radius of curvature of 126.49 *m* (415 *ft*) and having an overall length of 126.49 *m* (415 *ft*) of which 92.9 *m* (305 *ft*) was straight so that the high banks of the canal could be satisfactorily retained. The downstream slopes of the earth dam if pitched to about .914 *m* (3 *ft*) above the maximum tailwater level would suffice to protect the slopes from wave wash *etc.*

At this stage of the tests, the project authorities informed that the rock levels particularly over the left side between distance 1447.8 *m* — 1371.6 *m* (*Ch* 4750 — 4500) were higher than intimated earlier. They also suggested that a combination of ski-jump bucket (over the left portion) and roller bucket (over the remaining spans) would prove more economical and might be tried in the model.

Since rock levels were higher, *El* 145.39 *m* (477 *ft*) between distances 1447.8 *m* and 1371.6 *m* (*Ch* 4750 and 4500), raising the invert of the bucket and converting it into a ski-jump bucket could easily be effected over 5 spans from the left end of the spillway. Initially a bucket of 15.24 *m* (50 *ft*) radius with invert at *El* 146.30 *m* (480 *ft*) was tried over the 5 spans combined with the roller bucket, as tested earlier over the remaining 6 spans and a divide wall between the two buckets.

With the ground levels laid as at present, again the haphazard flow conditions were in existence. Even on lowering the ground level to *El* 152.4 (500 *ft*) downstream of high bucket only ski-jump action was obtained only for relatively high discharges. *Photo 24* shows the flow conditions for 8.22 *m* (27 *ft*) depth of flow. This led to raising the invert to obtain better flow conditions downstream.

The next series of tests was performed with the ski-jump raised to *El* 147.82 *m* (485 *ft*), radius and lip angle remaining same as before *viz* *R* = 15.24 *m* (50 *ft*), = 35° with the ground level dressed down to *El* 152.4 *m* (500 *ft*) downstream of the high bucket. The performance was satisfactory. The ski-jump formation was obtained for all but very low discharges. The ground level opposite the roller bucket was kept as recommended earlier at *El* 149.96 *m* (492 *ft*). The maximum throw-off and rise of the jet were 51.816 *m* (170 *ft*) away from and 16.76 *m* (55 *ft*) above the lip of the bucket. The combinations of the high level ski-jump bucket and low level roller bucket worked well. *Photos 25* and *26*

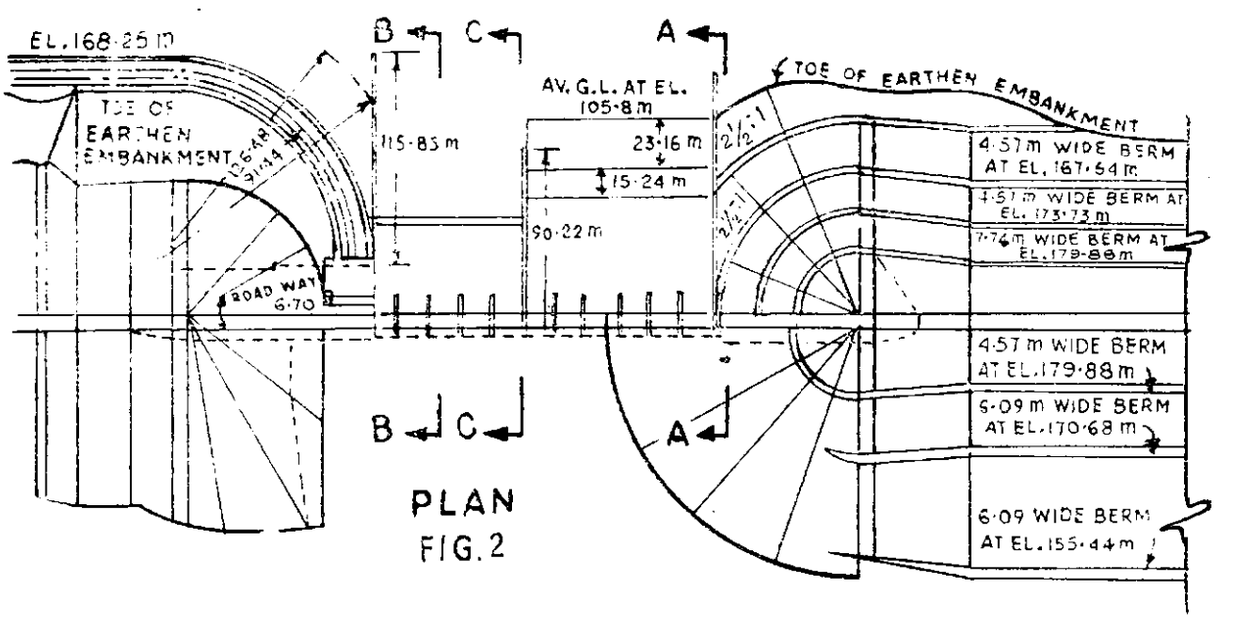

FIG.2

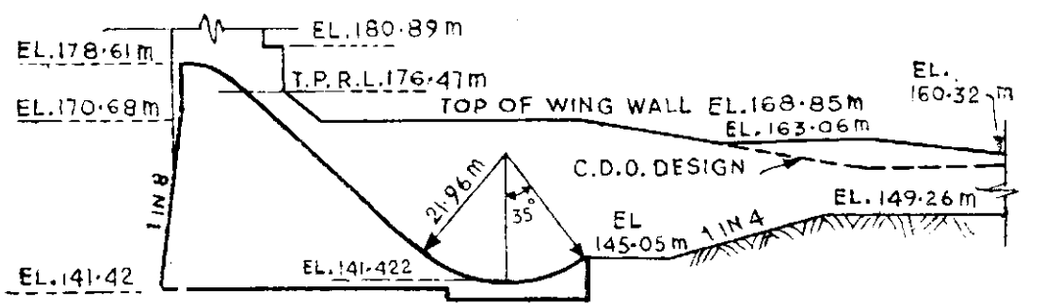

FIG.3(a) SECTION A-A

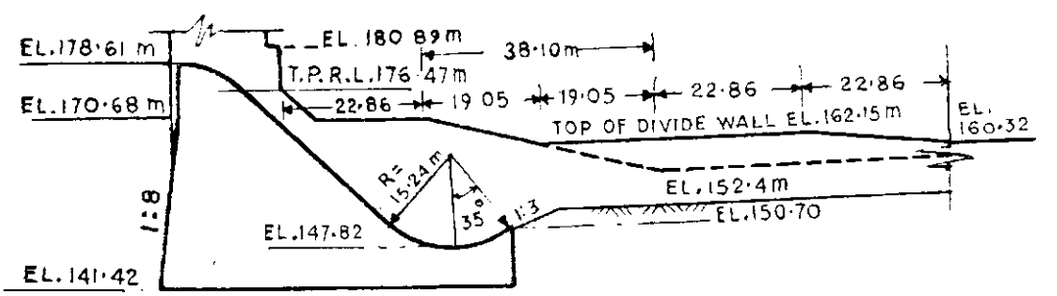

FIG. 3 (b) SECTION B-B

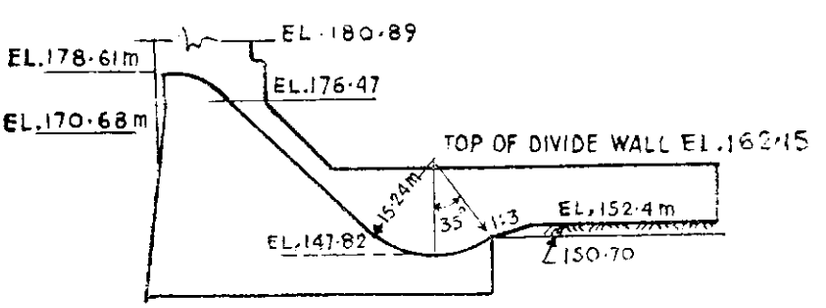

FIG.3(c) SECTION C-C

RECOMMENDED DESIGN

show the conditions for different depths of flow.

The required length of the divide wall from various trials was found to be 38.1 *m* (125 *ft*) beyond the end of the high bucket. The top of the wall was suitably fixed at *El* 162.15 *m* (532 *ft*). The details of the final design of divide wall are shown in *fig 3 (c)*. The guide walls at either end of the spillway remained unchanged.

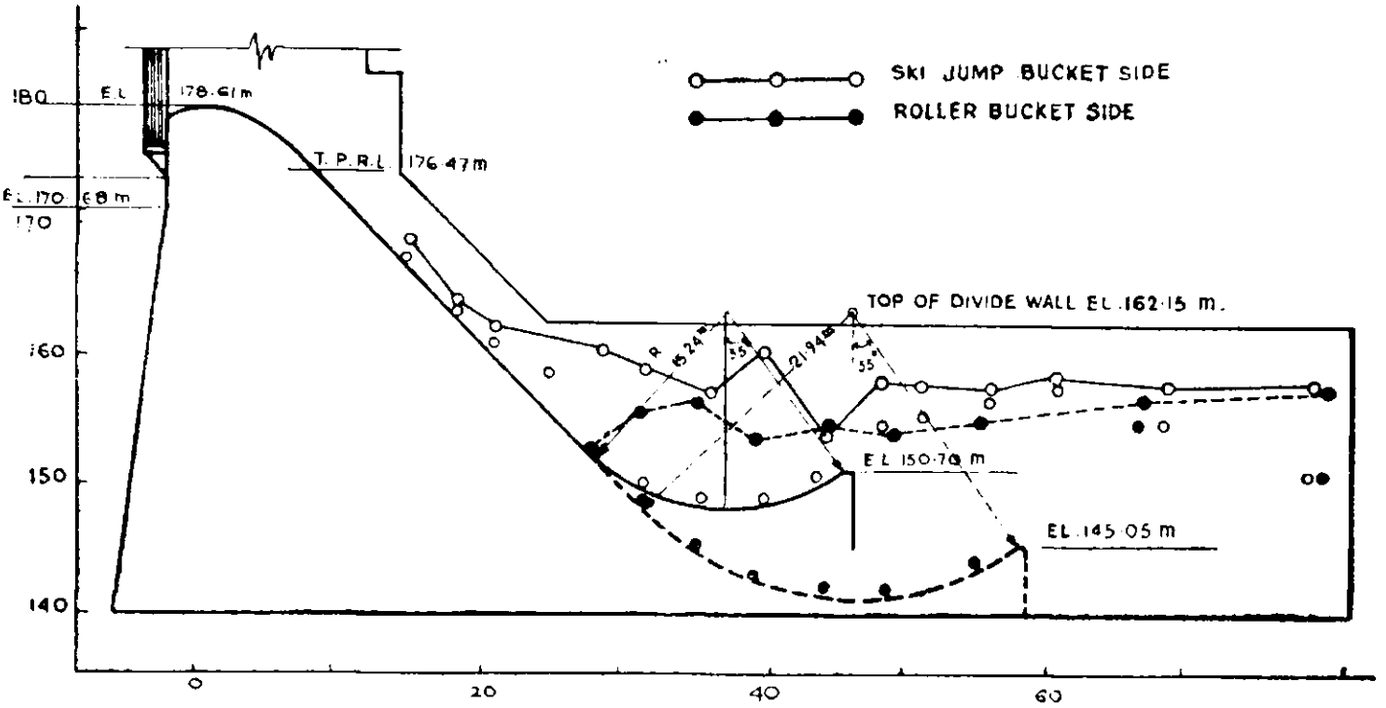

Fig 4 : Pressure distribution on sides of the divide wall between the buckets.

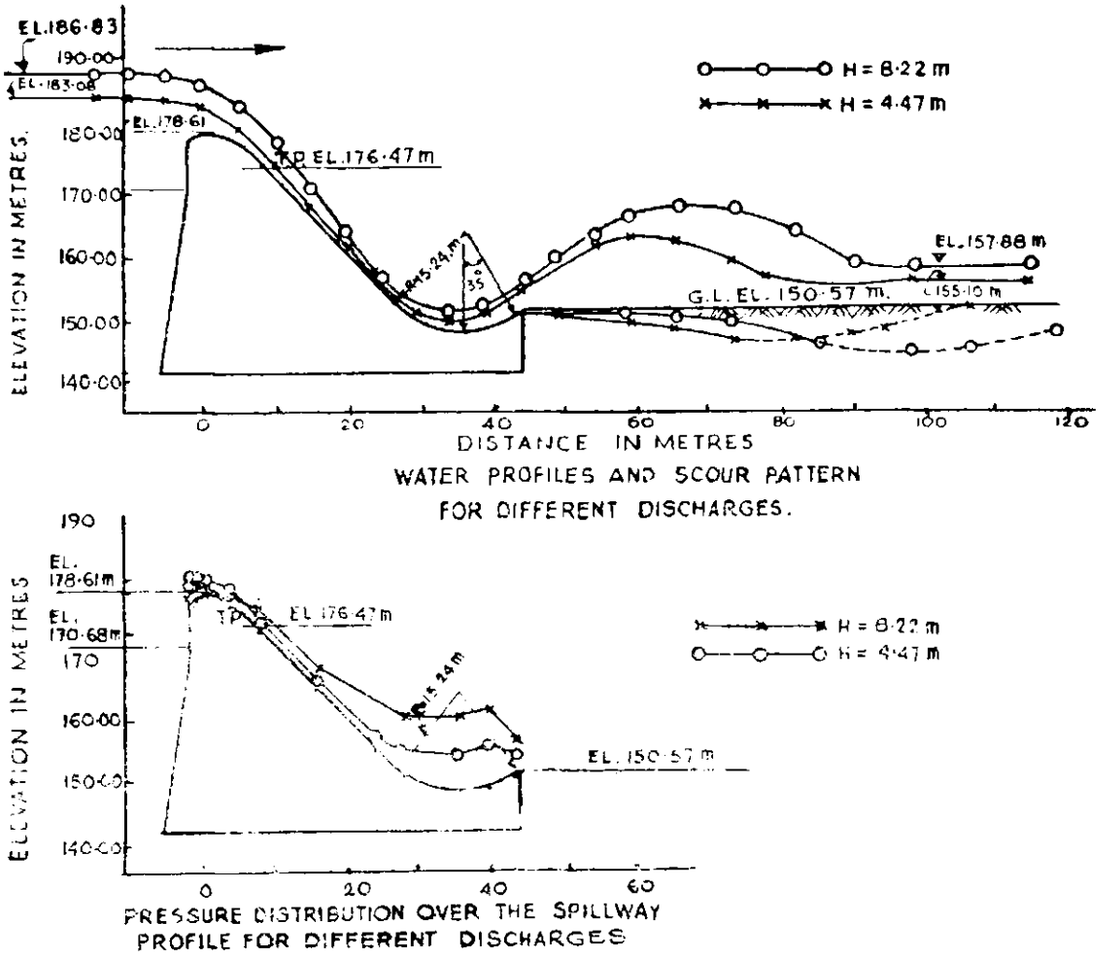

Fig 5: Pressure distribution over the spillway profile for different discharges.

4. Differential pressure on divide wall

The lateral pressures on divide wall between the two buckets were observed in detail in the sectional model. From *fig 4* showing the pressure observations on the sides of the divide wall the maximum side pressure was found to be 6.09 *m* (20 *ft*) of water for the maximum discharge. Observations indicated that it would suffice if the top of the wall was kept at *El* 162.154 *m* (532 *ft*).

The water surface profiles and scour patterns recorded for the ski-jump bucket are shown in *fig* 5. The maximum scour reached *El* 143.5 *m* (470 *ft*) at a distance of 51.81 *m* (170 *ft*) beyond the bucket indicating the safety of the spillway from undermining. The pressures on the divide wall were checked in the three dimensional composite model and results agreed.

5. Conclusions and recommendations

(*i*) The discharging capacity of the spillway was adequate for passing the design flood of 6650 m^3/sec (2,35,000 *cfs*).

(*ii*) The profile of the spillway was safe from negative pressures except at the starting point of curvature *ie* point (1) in *fig* 5, where a slight negative pressure of .914 *m* (3 *ft*) was observed which could be considered as harmless.

(*iii*) The action of the horizontal apron designed by *CDO* showed that the design was over safe. As stated earlier a combination of ski-jump and roller buckets would be both hydraulically efficient and economical. It was recommended that for the left 5 spans a ski-jump bucket $R = 15.24$ *m* (50 *ft*), $\theta = 35°$ with invert *El* 147.8 *m* (485 *ft*) may be adopted and a roller bucket $R = 21.95$ *m* (72 *ft*), $= 35°$ invert *El* 141.12 *m* (463 *ft*) may be adopted for the remaining 6 spans (*fig 3*).

(*iv*) The divide wall between the two buckets may be extended to 38.1 *m* (125 *ft*) beyond the end of high bucket with its top at *El* 162.15 *m* (532 *ft*).

(*v*) The ground levels downstream of the ski-jump bucket should be sloping up from the bucket tip at 1 in 3 and then dressed down to an average level, *El* 152.4 *m* (500 *ft*). The ground immediately downstream of the roller bucket should be kept at lip level over the first 15.24 *m* (50 *ft*) and then sloped up at 1 in 4 to reach an average level *El* 149.96 *m* (492 *ft*).

(*vi*) The guide walls at the two ends need not be carried round the earthen envelopes as in the *CDO* design. Straight guide walls extended by 22.86 *m* (75 *ft*) from the starting point were found to be more effective. The left end guide wall could alternatively be curved as shown in *fig 3* to retain the slope of the high banks. The earth slopes on either side should be sloped down to the natural bed level and the slope pitched upto *El* 158.95 *m* (521.5 *ft*) *ie* .914 *m* (3 *ft*) above the maximum tailwater level. However the top of the walls had to be raised and the final details are shown in *fig 3*.

(*vii*) The maximum lateral pressure on the divide wall between the two buckets was found to be equivalent to 6.1 *m* (20 *ft*) of water for which it may be designed.

Note : The project authorities have subsequently informed that the entire spillway is proposed to be shifted towards the right by 17.373 *m* (57 *ft*). However no change in the design of the spillway is anticipated because of the shift. Check tests in the model are in progress in this connection.

V. Badua Dam Project

THE BADUA dam project aims at harnessing the Badua river for irrigating areas in Bhagalpur and Monghyr districts by constructing an earthen dam across a gap of 457.2 *m* (1500 *ft*) in a range of hills at the northern escarpment of the Chota-Nagpur plateu. The spillway has been proposed to be located in a saddle on the right bank as shown in the index plan in *fig 1*. The *salient features* of the scheme are:

(i)	Catchment area ...	492.0 *sq km* (185.6 *sq miles*).
(ii)	Length of earth dam.	457.2 *m* (1500 *ft*).
(iii)	Maximum height of dam.	40.233 *m* (132 *ft*).
(iv)	Length of upstream weir (circular).	141.427 *m* (464 *ft*).

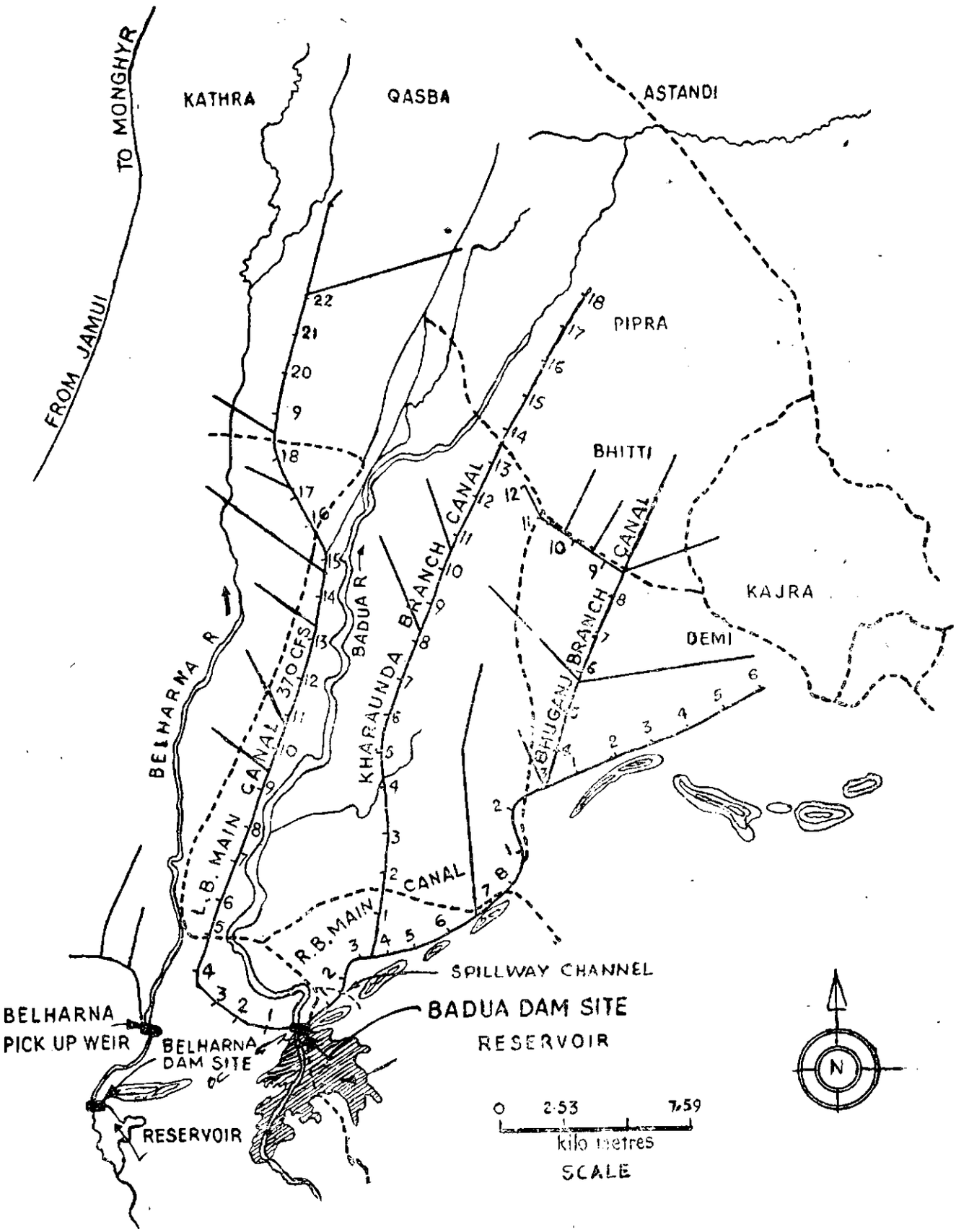

Fig 1: Badua dam project index plan.

(v)	Top of upstream weir=*FRL.*	*El* 128.626 *m* (422 *ft*).
(vi)	Design maximum flood discharge.	2122.5 m^3/sec (75,000 *cfs*).
(vii)	Maximum water level.	*El* 132.359 *m* (434.25 *ft*).
(viii)	Slope of chute ...	1 in 6.
(ix)	Crest of subsidiary spillway.	*El* 100.584 *m* (330 *ft*).
(x)	Gross storage ...	128.28 million m^3 (1,04,000 *acre ft*).
(xi)	Total area irrigated.	32536.7 *hectares* (80,400 *acres*).

2. Spillway design

The original spillway design along with the existing ground levels and rock levels are shown in *fig 2*. The design consisted of an upstream circular weir, a chute and a subsidiary spillway at the end of the chute. The crest of circular weir was kept at *El* 128.626 *m* (422 *ft*). Allowing for a maximum depth of overflow of 3.733 *m* (12.25 *ft*) over the weir to pass the design flood of 2122.5 m^3/sec (75,000 *cfs*) the *MWL* was fixed at *El* 132.359 *m* (434.25 *ft*). The upstream weir was provided with a horizontal apron at *El* 121.92 *m* (400 *ft*) and a curved end sill .762 *m* (2.5 *ft*) high. This was followed by a chute sloping at 1 in 6 meeting a horizontal floor 15.24 *m* (50 *ft*) long at *El* 96.01 *m* (315 *ft*) at the end of which at 213.36 *m* distance (*Ch* 7) a subsidiary spillway was provided. The spillway consisted of 16 spans each 5.9 *m* (19 *ft* 4.5 *inches*) in width separated by 1.828 *m* (6 *ft*) thick piers intended to carry a canal aqueduct. To dissipate the energy downstream of the spillway a 1 in 20 sloping apron with a 2.74 *m* (9 *ft*) high end sill was provided. The chute had a converging-diverging form in plan, as shown in *fig 2*. As the ground levels downstream of the spillway were high, a pilot cut was intended to lead the flow from the spillway into the river about 609.16 *m* (2000 *ft*) downstream. The maximum water level in the river was reported to be *El* 94.79 *m* (311 *ft*) at the proposed junction with the cut. Model tests were undertaken for checking the hydraulic design of the composite spillway.

3. Model experiments

Model experiments were conducted on a 1/40 scale geometrically similar three dimensional model.

(*i*) *Design of circular weir and chute*: Tests with the original design indicated that the spillway design was hydraulically unsatisfactory and required modifications. Owing to the existence of non-submersible high ground upstream of the weir, the approach to the weir was of the side-channel type resulting in concentration of discharge on the left flank. The low end sill of the weir apron proved ineffective in distributing the flow uniformly over the chute. With the supercritical flow on the chute inducing oblique wave fronts, the convergence-divergence of the chute proved objectionable. The divergence was too excessive to be followed by the downcoming high velocity flow which resulted in the formation of strong eddies on the sides and unequal concentration of flow upstream of the subsidiary spillway. The flow actually hurdled over the piers for all discharges. *Photos 27* and *28* show the conditions for maximum discharge. It was essential that the following conditions were satisfied:

(i) Straight and uniform approach to the weir.
(ii) Uniform distribution of flow over the circular weir end sill.
(iii) Uniform width of chute throughout its length.
(iv) Adequate depth and length upstream of subsidiary spillway to create and contain the hydraulic jump fully.

Taking into account these factors the upstream hillock in the reservoir was dressed down to *El* 128.016 *m* (420 *ft*) by which the approach conditions improved considerably. The circular end sill was replaced by a straight vertical sill 1.98 *m* (6.5 *ft*) high which effectively distributed the flow uniformly over it by creating a hydraulic jump in the stilling basin of the weir. The chute slope was steepened to 1 in 5 to meet a horizontal floor 28.194 *m* (92.5 *ft*) long at *El* 96.01 *m* (315 *ft*), at its toe, which gave sufficient depth for clear jump formation. The uniform chute width of 121.92 *m* (400 *ft*) brought about uniform flow down the chute. But increasing the chute width would result in excessive excavation. Thus in order to limit the chute width to 91.44 *m* (300 *ft*) and maintain the discharge intensity as before, it was decided to do away with the piers over the subsidiary spillway and locate the aqueduct separately downstream. To avoid formation of cross waves the side walls of the chute were kept vertical.

The tests for discharging capacity of the circular weir showed that the maximum flood discharge could be passed with a head of 3.9 *m* (12.45 *ft*) against 3.733 *m* (12.25 *ft*) design head. The difference was considered too small to warrant any change in the length of the weir. *Fig 3* shows the plots of *Cd* versus *H* and *H* versus *Q*.

On finalising the dimensions of the end sill of the circular weir, slope and width of chute, the design on subsidiary spillway together with the floor level upstream and the energy dissipating devices downstream were tested exhaustively in the subsequent experiments.

(*ii*) *Design of subsidiary spillway*: During the progress of the experiments, additional bore hole data became available which disclosed sand rock existing at 213.36 *m* (*ch* 7) at *El* 93.26 *m* (306 *ft*). The original design was based on the assumption that rock was available at 33.39 *m* (290 *ft*). This enabled raising of the entire spillway by 4.87 *m* (16 *ft*). In addition the project authorities argued in favour of locating the aqueduct as a separate structure downstream from both economical as well as structural considerations. A suggestion was made by them to keep the spillway crest at *El* 106.68 *m* (350 *ft*) and to flatten the chute slope to 1 in 8. to save excavation. On scrutiny it was not found to be an economical proposal as the economy achieved by saving in excavation did not offset the cost of concrete/masonry for building up the spillway. However a test made with crest of spillway at *El* 106.68 *m* (350 *ft*) chute slope 1 in 5 and upstream floor at *El* 100.58 *m* (330 *ft*) giving a horizontal length of 50.597 *m* (166 *ft*) proved the design oversafe for all discharges thereby indicating the possibility of lowering the spillway crest.

The following combinations of crest level and upstream floor level proved satisfactory.

Crest	*Upstream floor*
El 104.35 *m* (344 *ft*) ...	*El* 99.36 *m* (326 *ft*)
El 108.20 *m* (335 *ft*) ...	*El* 96.01 *m* (315 *ft*)

The crest was further lowered by .3048 *m* (1 *ft*) *ie.* to *El* 101.80 *m* (334 *ft*) keeping the upstream floor at *El* 96.01 *m* (315 *ft*). For the maximum discharge the turbulence upstream of the spillway was severe which gave rise to negative pressures ranging from −3.96 *m* (−13 *ft*) to + 2.438 *m* (8 *ft*) of water over the spillway profile in the crest region. However conditions rapidly improved for lower discharges, the jump progressively shifting up the chute to give stable conditions upstream of spillway. This indicated that an optimum combination of levels had been reached.

To reduce the negative pressures an overdesigned Creager profile for 6.096 *m* (20 *ft*) head was tested in substitution of the previous 5.18 *m* (17 *ft*) head profile. With this design the negative pressure, which occurred only for discharges greater than 1556.5 m^3/sec (55,000 *cfs*), fluctuated between −2.438 *m* (−8 *ft*) and + 2.13 *m* (7 *ft*) of water which were within allowable limits. The negative pressures ceased to develop for discharges below 1556.5 m^3/sec (55,000 *cfs*). As the possibility of the occurrence of maximum flood discharge was remote, this design was accepted. *Fig* 4 shows the water surface profiles, scour patterns and pressure distribution over the spillway for different discharges. *Photo* 29 shows condition for 2122.5 m^3/sec (75,000 *cfs*) discharge.

4. Energy dissipation downstream of subsidiary spillway

A hydraulic jump type stilling basin was chosen to dissipate the energy downstream of the spillway. Assuming 1.219 *m* (4 *ft*) to be the thickness of the concrete apron and rock at *El* 96.317 *m* (306 *ft*), the top of the apron was fixed at *El* 94.488 *m* (310 *ft*). With an average water level at *El* 106.37 *m* (349 *ft*), upstream of the spillway for the maixmum discharge condition, calculations showed that 6.82 *m* (22.4 *ft*) depth of tailwater would be required for the hydraulic jump to form. Since the ground levels downstream were very high and no data regarding tailwater levels was available, the design of the apron involved certain assumptions. The depth of flow in a channel under regime conditions was obtained from Lacey's formula as $R = 0.9\ (q^2/f)^{1/3}$ On this basis, for a 91.44 *m* (300 *ft*) wide channel the depth for maximum discharge worked out to be 6.705 *m* (22 *ft*) which would just suffice even if retrogression reached rock level.

Assuming the tailwater to be at *El* 100.584 *m* (330 *ft*) an apron 27.43 *m* (90 *ft*) long with an end sill 1.83 *m* (6 *ft*) high having its upstream face sloping at 1 to 1 was found sufficient and satisfactory for proper jump formation. The divide walls at the two flanks of the apron extended to the end of the apron. Tests with higher tailwater level, that might occur initially, showed that due to excessive submergence no adverse effects take place. However, to account for the high water level that might occur initially, the top of the divide walls were kept at *El* 103.63 *m* (340 *ft*). *Fig* 5 shows the details of the spillway.

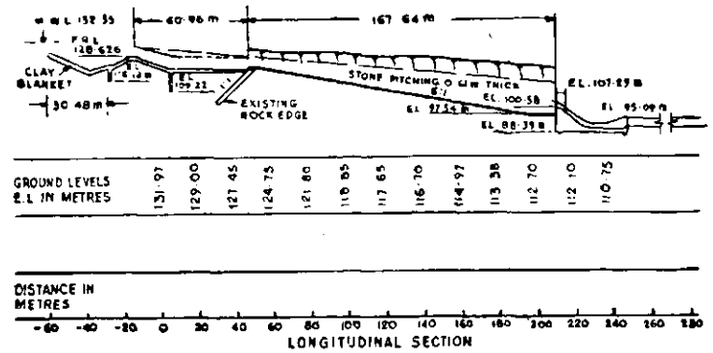

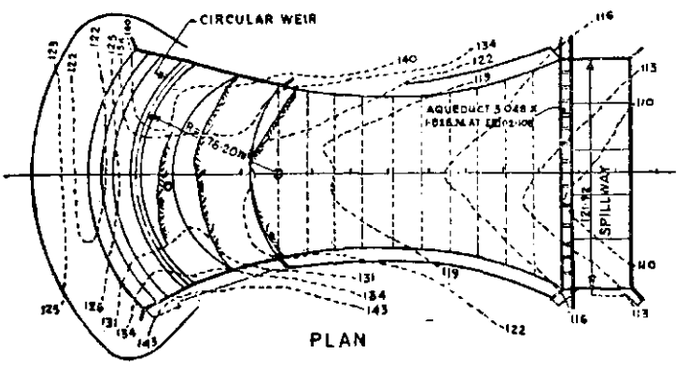

Fig 2

5. Pilot channel downstream

The ground levels downstream were very high and a certain minimum lowering was essential for satisfactory flow conditions downstream. In the model lowering was done upto *El* 97.536 *m* (320 *ft*) which may be done in the prototype as well, over a width of 91.44 *m* (300 *ft*) provided the material so obtained would be useful for earth dam construction. In the other case the cost of excavation would be prohibitive. It was, therefore, decided to explore the possibility of giving a pilot cut downstream which would automatically scour to form a stable channel. Two trials were made.

(i) A pilot cut 91.44 *m* (300 *ft*) wide over 60.96 *m* (200 *ft*) length beyond which it converged to 30.48 *m* (100 *ft*) bed level at *El* 97.536 *m* (320 *ft*).

(ii) A pilot cut 91.44 *m* (300 *ft*) wide over 15.24 *m* (50 *ft*) in length and then converging to 15.24 *m* (50 *ft*) width, bed level at *El* 97.536 *m* (320 *ft*) as shown in *fig 5*.

In the first case the velocity observed in the pilot cut reached a maximum value of 6.096 *m/sec* (20 *ft/sec*) which would be sufficient to scour the channel for the maximum discharge. The tailwater levels, though high initially, did not affect the jump formation on the chute. *Photo 30* shows the condition for maximum discharge.

In case (*ii*) the maximum velocity reached a value of 7.62 *m/sec* (25 *ft/sec*) indicating scour would take place at a faster rate. However the jump formation on the chute was affected by the high tailwater levels and resulted in overtopping the side walls by creation of eddies. *Photos 31* and *32* show the condition for two different discharges. It would be desirable to pitch the slopes over the region marked *XY* in *fig 5* to about 6.096 *m* (20 *ft*) height so that there would be no initial damage. This would be the cheapest of the three proposals. The final decision in this regard would, however, depend upon the site conditions.

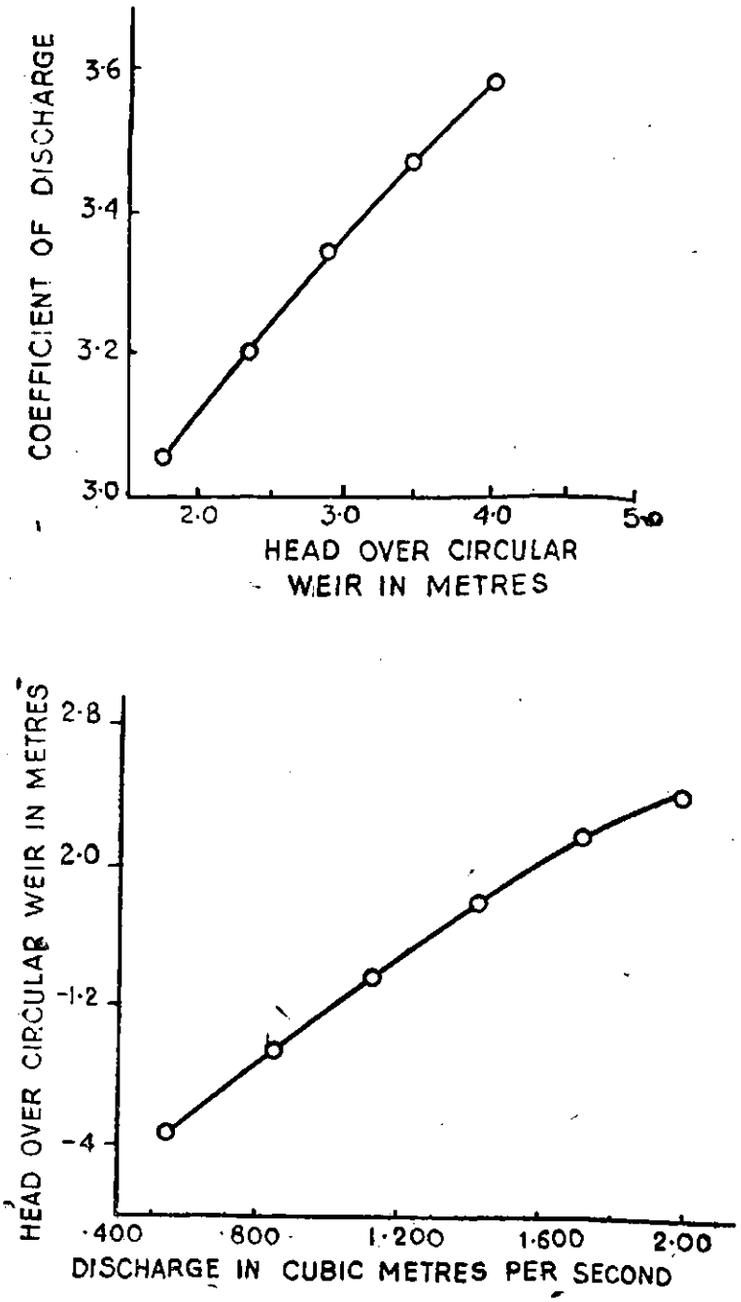

Fig 3

6. Conclusions and recommendations

(*i*) The upstream circular weir as designed would not require any modification. The hillock upstream of it should be dressed down to *El* 128.01 *m* (420 *ft*) to allow for satisfactory approach conditions.

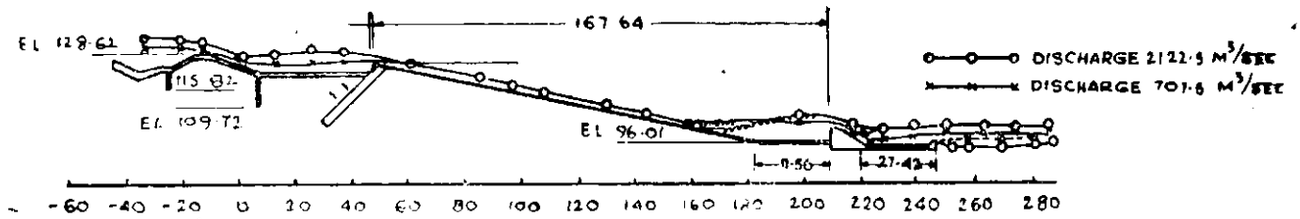

WEIR PROFILES AND SCOUR FOR DIFFERENT DISCHARGES

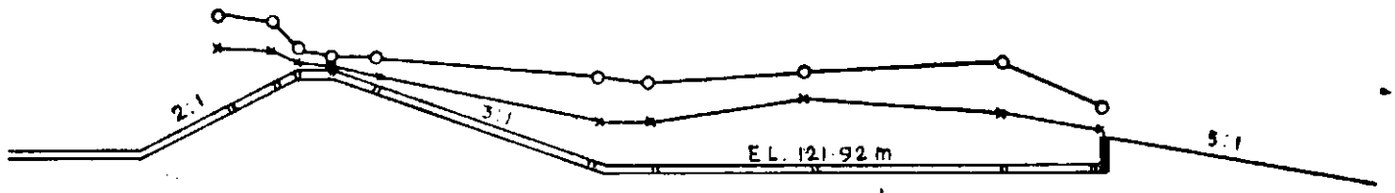

PRESSURE DISTRIBUTION ON U/S WEIR

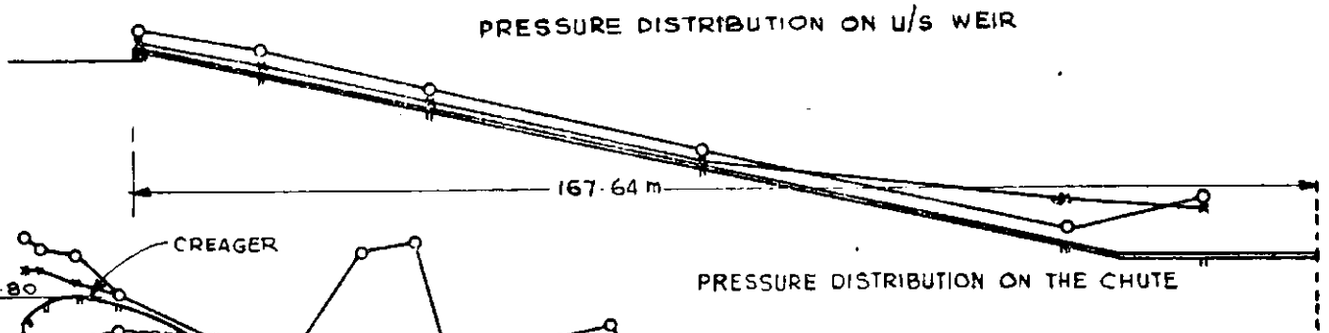

PRESSURE DISTRIBUTION ON THE CHUTE

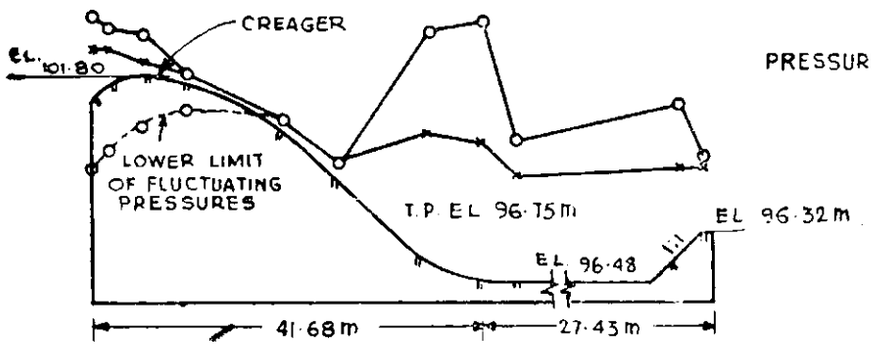

PRESSURE DISTRIBUTION ON THE SPILLWAY PROFILE

FIG. 4
BADUA DAM PROJECT

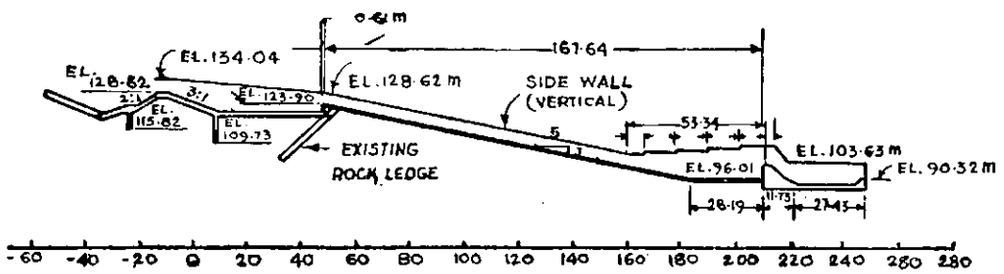

DISTANCE IN METRES

LONGITUDINAL SECTION

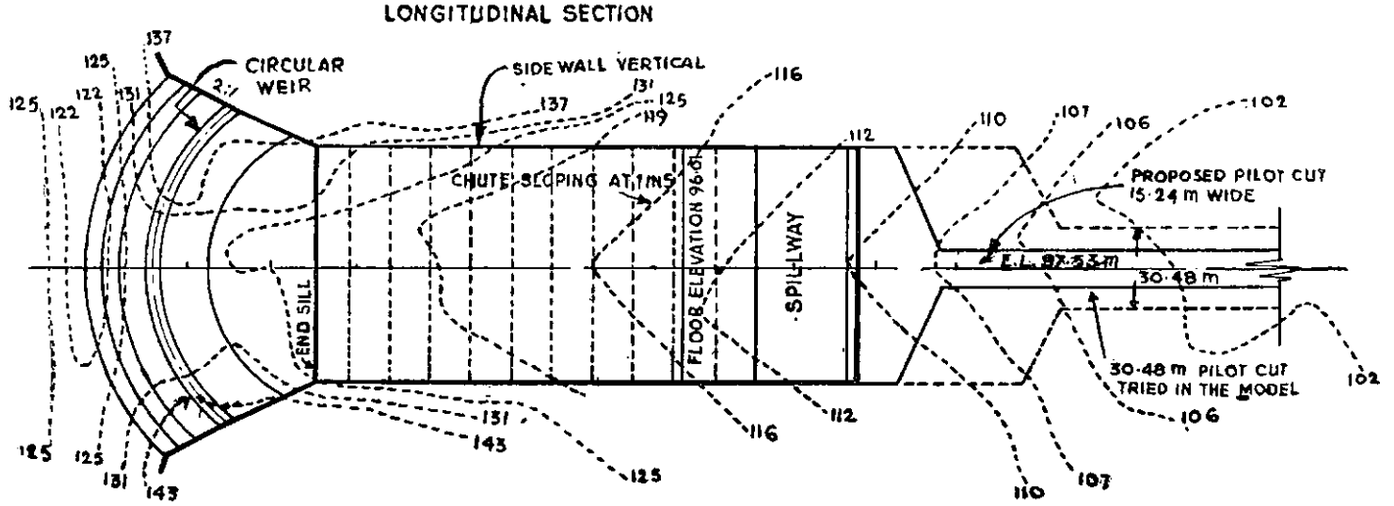

PLAN

Fig 5

(*ii*) The vertical end sill of the circular weir apron should be made straight in plan and constructed to a height of 1.981 *m* (6.5 *ft*) to provide uniform distribution of flow at the starting point of the chute (*fig* 5).

(*iii*) The chute width should be 91.44 *m* (300 *ft*) with a slope of 1 in 5, the toe joining the horizontal floor downstream at *El* 96.01 *m* (315 *ft*) (*fig* 5).

(*iv*) All side walls should be kept vertical with top levels as shown in *fig* 5.

(*v*) The subsidiary spillway should be 91.44 *m* (300 *ft*) in length and without any piers. It should conform to Creager profile for 6.1 *m* (20 *ft*) depth of overflow (*fig* 5).

(*vi*) The apron downstream of the spillway should be 27.43 *m* (90 *ft*) long at *El* 94.488 *m* (310 *ft*). A 1.82 *m* (6 *ft*) high end sill with its upstream side sloping 1 to 1 should be provided at the end of the apron (*fig* 5).

(*vii*) The top of side walls along the two sides of the apron would be at *El* 103.63 *m* (340 *ft*) to account for probable high tailwater levels initially.

(*viii*) The high ground levels downstream of the spillway should be lowered to *El* 97.536 *m* (320 *ft*) in the region of the channel downstream where levels are higher. If the excavated material could be profitably used in the earth dam construction then the lowering may be done over a width of 91.44 *m* (300 *ft*), extending downstream to *El* 97.536 *m* (320 *ft*) contour. If this is not feasible, it is suggested that a pilot cut 15.24 *m* (50 *ft*) wide as shown in *fig* 5 may be made. In the latter case it would be desirable to pitch the side slopes above the vertical side walls between the region marked *XY* in *fig* 5. The final decision in regard to this rests with the project authorities.

Note : On further exploration of the rock ledge at the upstream weir site design of the weir has since been changed slightly. Further the design office has once again proposed to carry the aqueduct over the subsidiary spillway. The tests are being continued with these changes.

VI. Yeldari Spillway, Purna Project

WHILE LAST year's tests were in progress, (*ibid* 1959) the *CDO* modified their design as suggested by the *CWPRS* eliminating the high level bucket and increasing the depth of overflow to 40 *ft* by lowering the crest by 7 *ft* to *RL* 1477. The energy dissipation arrangement remained the same as before . *Fig 1* shows the section of spillway for the modified design.

2. Tests with modified design

It was found during tests with this design that with maximum overflow depth of 40 *ft* and with the corresponding tail water level of *RL* 1447, (*photo 33*) the behaviour of the bucket was not stable. It changed from roller action to ski-jump action with slight lowering of tail water level the water level rising very high during transition. This condition was considered undesirable.

Fig 2 shows the water profiles for 40, 35, 30 and 20 *ft* depths of overflow with corresponding tail water levels, according to the curve supplied by the Project authorities. *Fig 3* shows the pressure distribution at the centre of the span for high overflow depths. The pressures were generally positive on the downstream side of the spillway profile. On the upstream side of the crest, however, the pressures were negative of the order of 10 *ft* because the curve for the upstream portion, as given by *CDO*, was different from the standard curve, according to the Army Corps of Engineers practice for the designed depth of overflow. The *CDO* curve was starting 1.48 *ft* above the standard curve resulting in sharper bend. *Fig 4* shows the standard curve and the *CDO* curve designed for 40 *ft* overflow depth. The pressures became positive when the standard curve replaced the *CDO* curve. *Fig 5* shows the pressures at mid span and on the bucket for the recommended design for higher depths of overflow. *Fig 6* shows the pressures on the spillway profile near piers.

The scour observed for 40 *ft* and 35 *ft* depth of overflow with corresponding *TWLs* was of the order of 13 *ft* and 3 *ft* at about 120 *ft* from the end sill (*Photo 34*). Since good rock is exposed in the

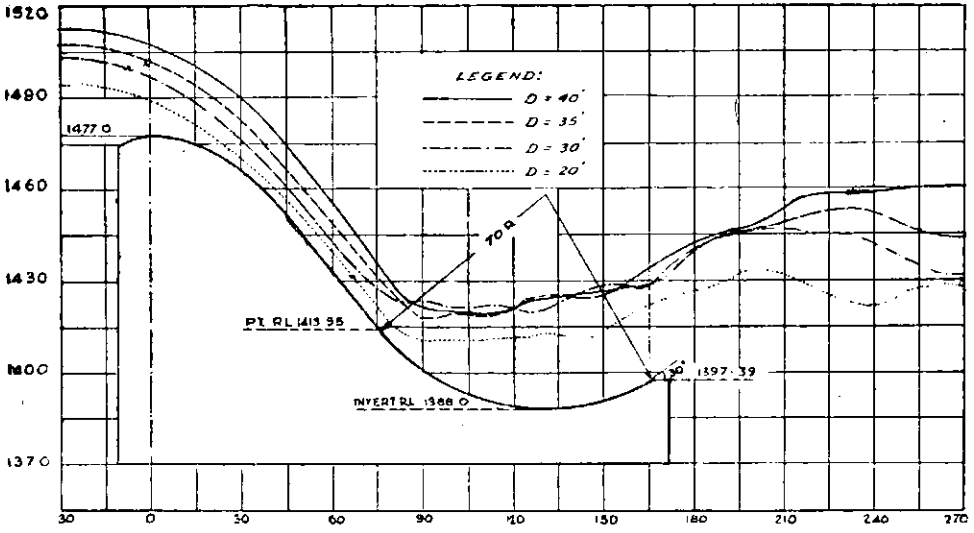

Fig 2: Water profiles for 70 *ft R* bucket at invert *RL* 1388 and 30° exit angle.

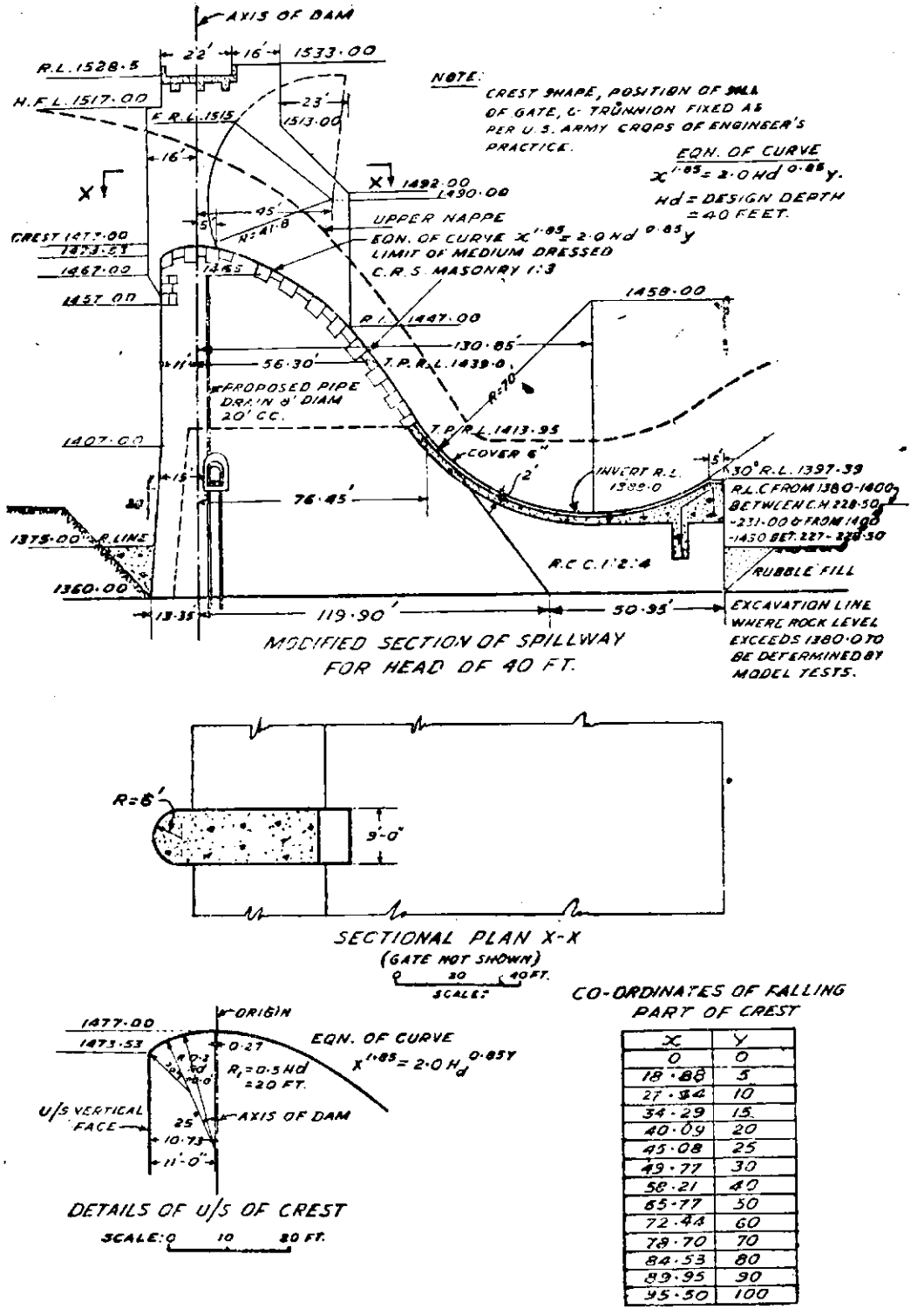

X	Y
0	0
18·88	5
27·54	10
34·29	15
40·09	20
45·08	25
49·77	30
58·21	40
65·77	50
72·44	60
78·70	70
84·53	80
89·95	90
95·50	100

Fig 1: Yeldari dam overflow section.

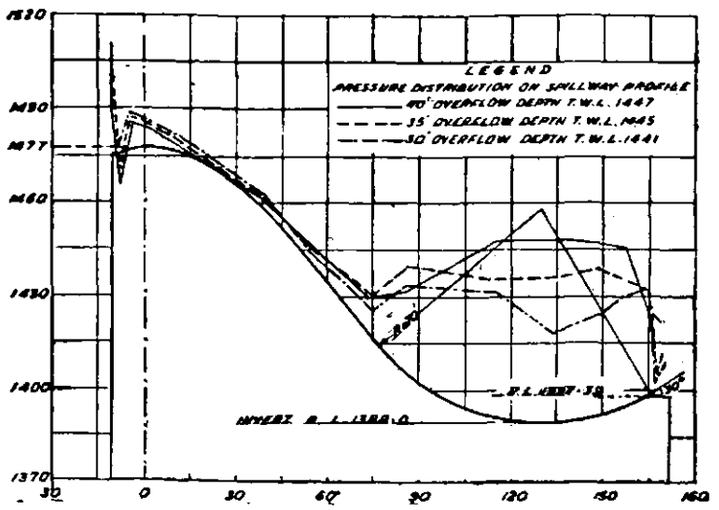

Fig 3: 1/35 scale sectional model of Yeldari spillway.

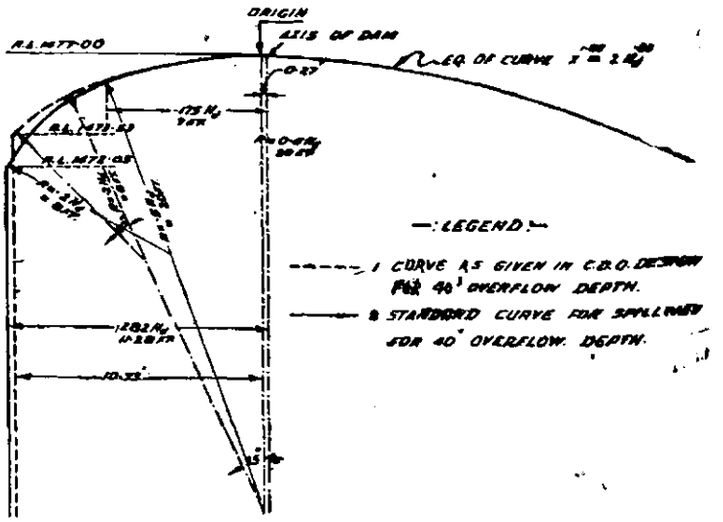

Fig 4: Yeldari dam overflow section.

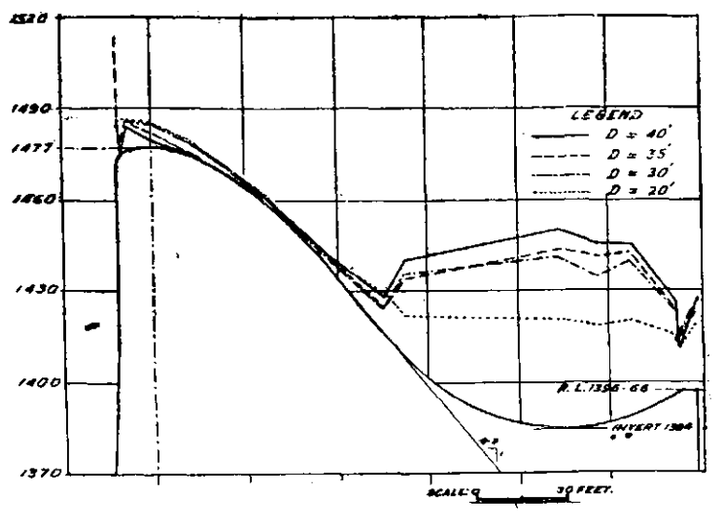

Fig 5: Minimum pressure along centre of spillway span. 70 *ft R* bucket at invert 1384, exit angle 35°.

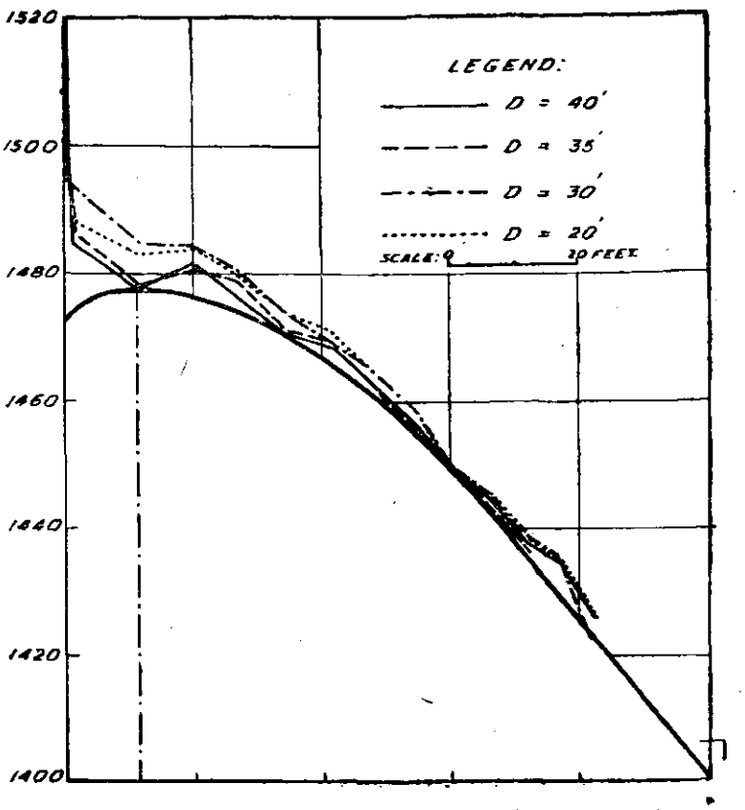

Fig 6: Pressures along pier side.

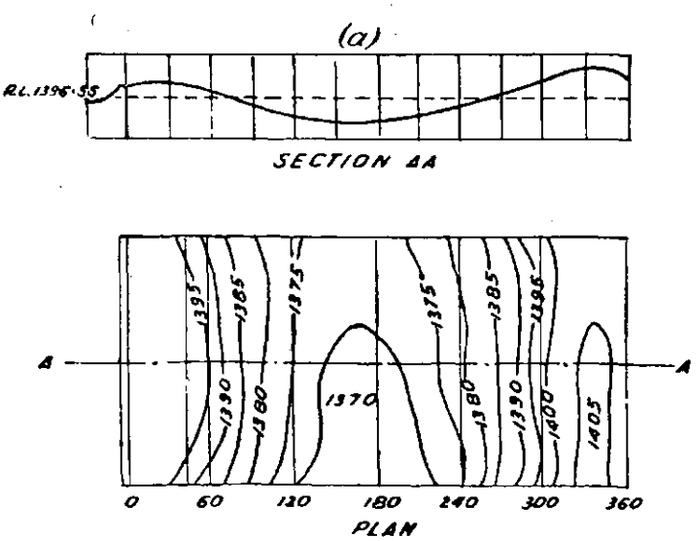

Fig 9 (b): Scour for $D = 35$ *ft TWL* 1445 for 70 *ft R* bucket at invert *RL* 1384 exist angle 30°.

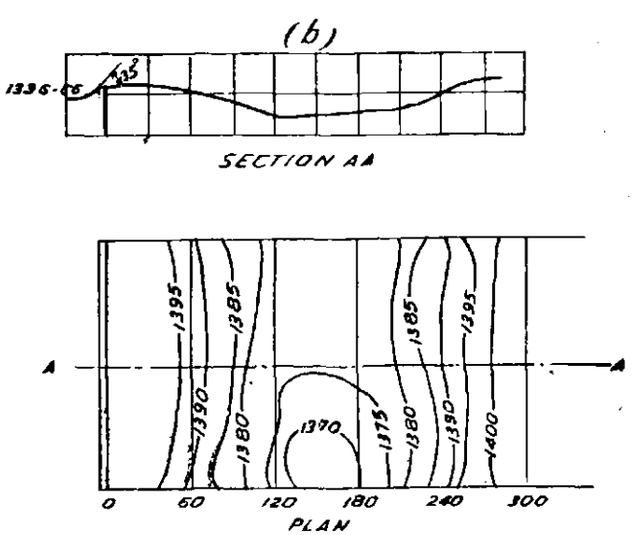

Fig 9 (b): Scour for $D = 35$ *ft TWL* 1445 for 70 *ft R* bucket at invert *RL* 1384 exist angle 30°.

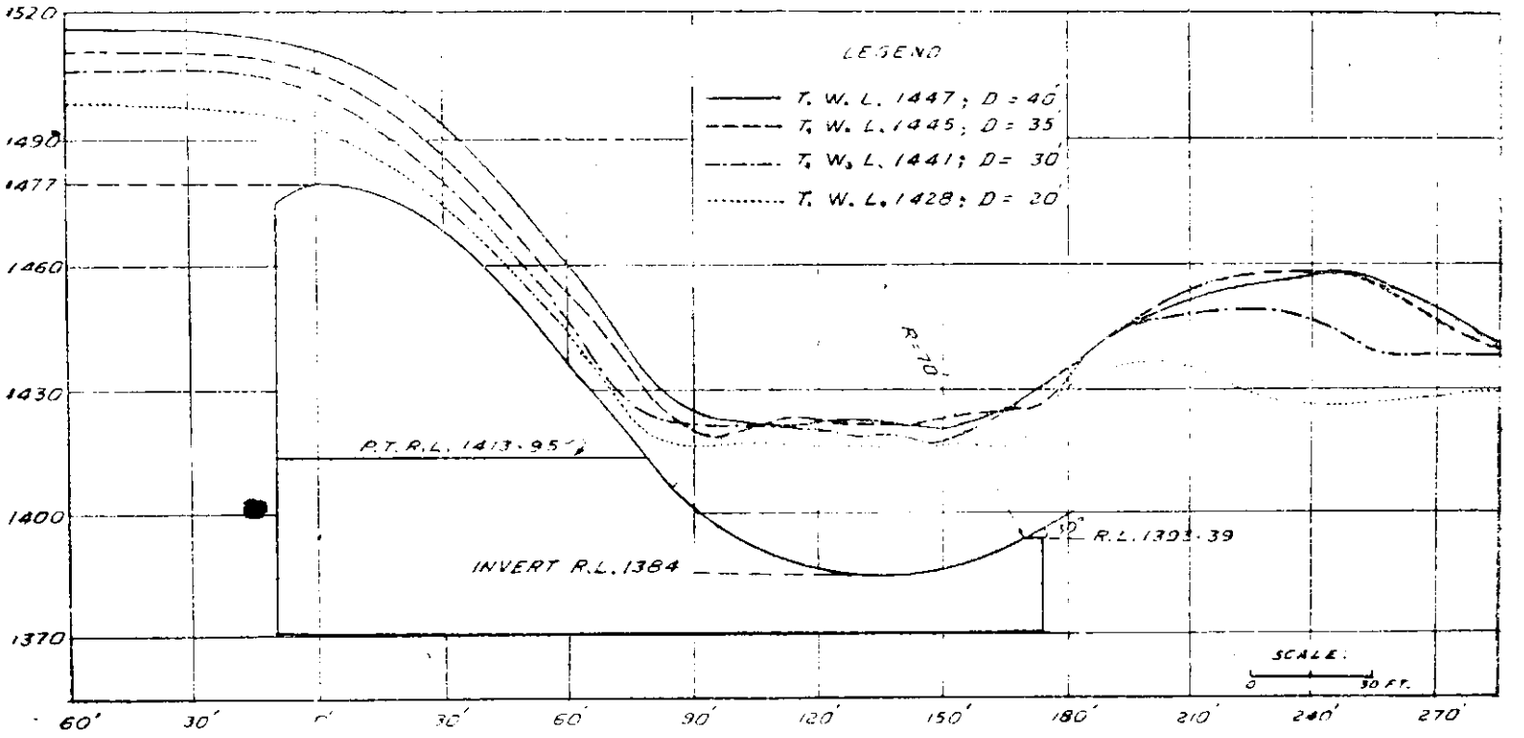

Fig 7 : Profiles of water at invert *RL* 1384, exit angle = 30°.

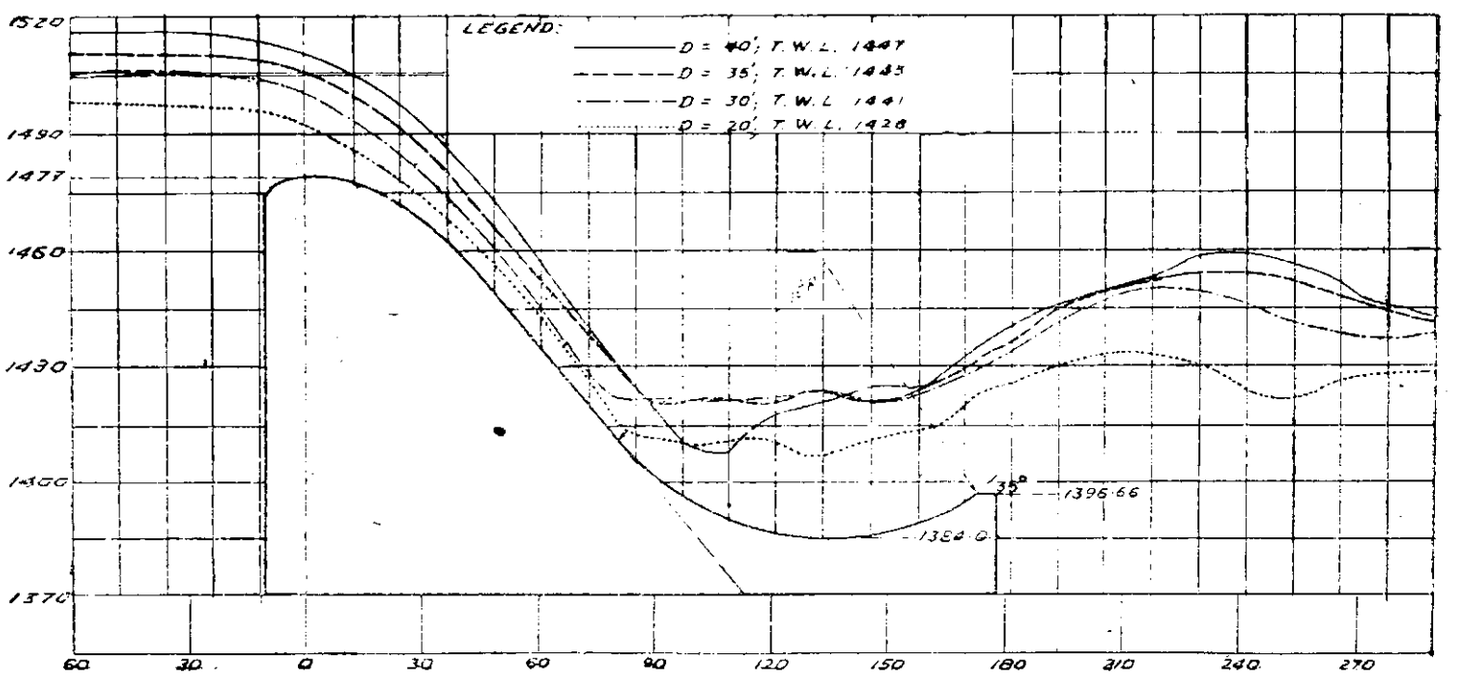

Fig 8: Water profiles of water invert *RL* 1384, exit angle = 35°.

river bed corresponding action on the prototype will be minor.

3. Tests with modifications

To ensure the roller action of the bucket even under possible retrogression of 7 *percent* in the depth of flow in the river channel downstream for a discharge of 50,000 *cfs* to 4 *percent* retrogression for the maximum discharge, it was considered desirable to keep the invert *RL* of the bucket at *RL* 1384.

Fig 7 shows the profiles of water for 40, 35, 30 and 20 *ft* overflow depths with corresponding *TWLs* for the 70 *ft* radius upturned bucket at invert *RL* 1384 and exit angle of 30° (*photo 35*). This action remained of roller type even after lowering the *TWL* by 3 *ft* (*photo 36*).

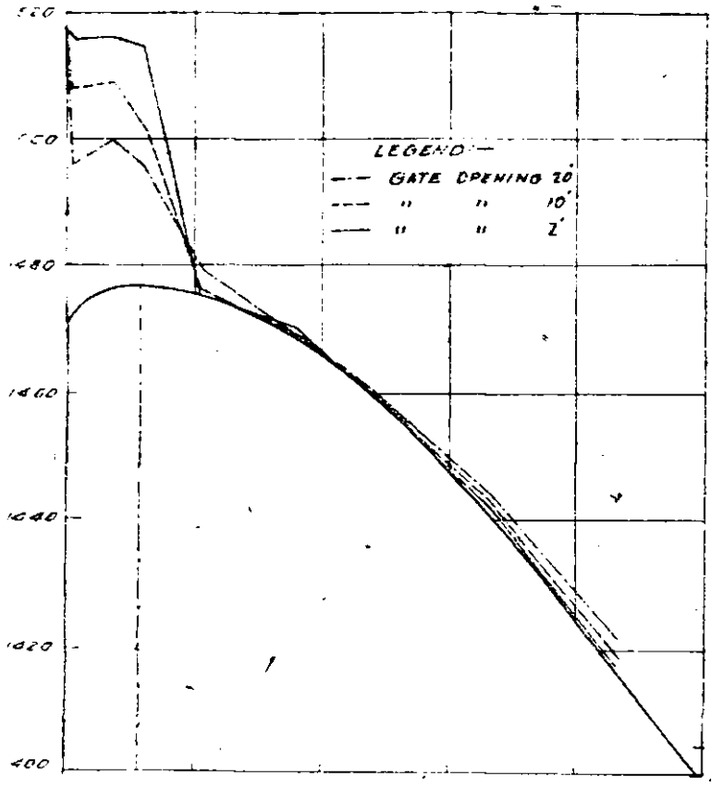

Fig 10 : Partial gate opening—pressures.

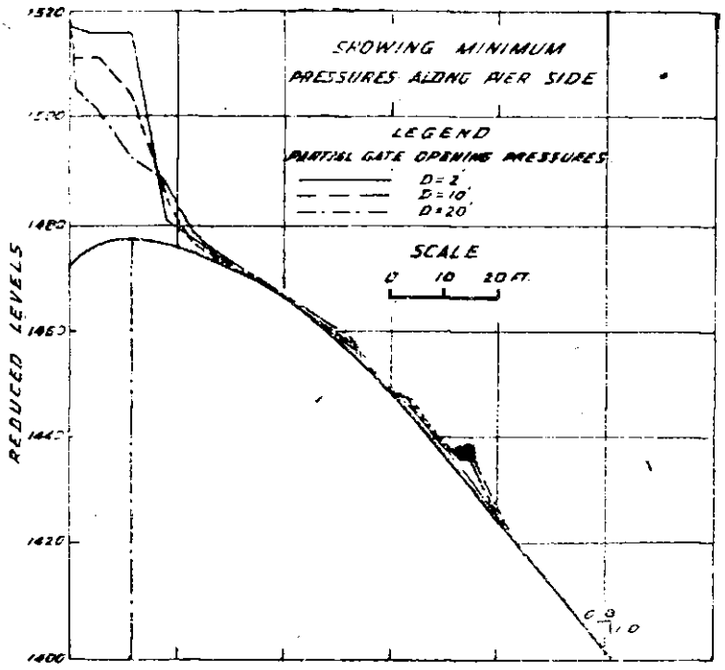

Fig 11

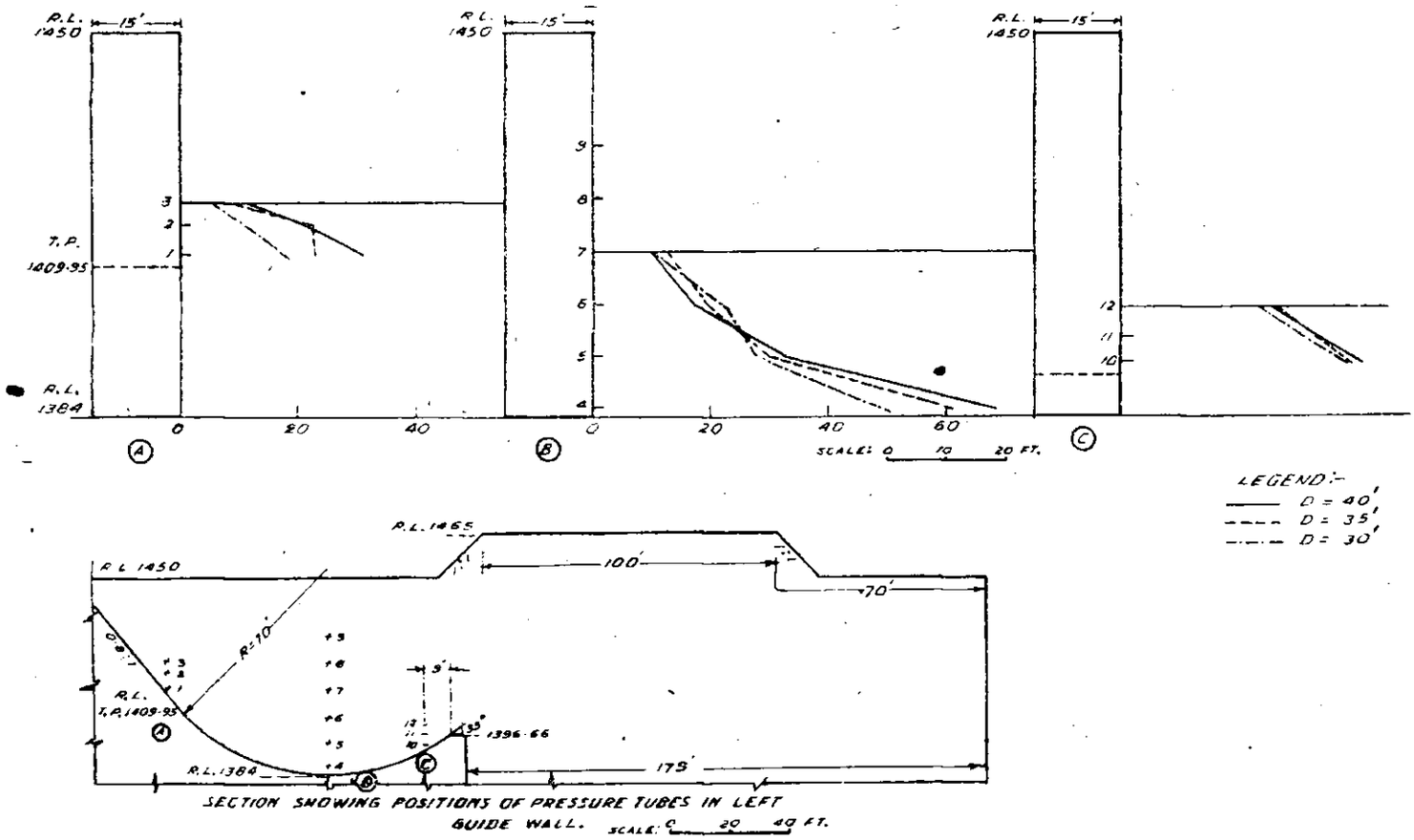

Fig 12: Pressures on left guide wall and position of pressure tubes.

The scour for 40 and 35 *ft* depths of overflow with corresponding *TWLs* was of the order of 18 *ft* and 13 *ft* below the river bed at *RL* 1388 at a distance of about 150 *ft* from the end sill.

4. Tests with 35° exit angle

With an intention of further improving the roller action of the bucket, the exit angle was raised from 30° to 35°. *Fig 8* shows the profiles

of water for various depths. The roller action was found to be good. (*photos 37* and *38*).

Fig 6 shows the pressure observations on the bucket, the pressures on the end sill were quite positive.

Fig 9 shows the scour (*photo 39*) observations for 40 *ft* and 35 *ft* depths of overflow. Though the extent of scour and its distance from the end sill remained almost the same, the piling up of material near the end sill was more indicating that the return roller was stronger than in the previous case.

5. Tests with partial gate openings

A series of tests were conducted to study the pressures on the profile of the spillway for partial gate openings of 2, 10 and 20 *ft*, the gate opening being defined as the vertical distance between the crest and lower lip of the gate. *Fig 10* shows the minimum pressures observed at mid-span for the partial gate openings and *fig 11* shows the pressures near the pier. The pressures were positive.

6. Pressures on the divide wall

Since the differential pressures on the divide wall at the left were not likely to be appreciable, the pressure on the divide wall when spillway was working with various overflow depths were taken to facilitate its design. The pressures on the wall, as recorded, have been shown in *fig 12*.

7. Recommendations

(1) A 70 *ft* radius bucket with invert *RL* 1384 and exit angle of 35° was found satisfactory and hence may be adopted for dissipation of energy for designed depth of overflow with corresponding tail water levels according to the curve supplied by *CDO*.

(2) The design of the crest may be modified according to the standard practice of the US Army Corps of Engineers, as tested

VII. Sone Barrage, Amarkantak Thermal Scheme

FOR WATER supply to Amarkantak Thermal Power Station, the Madhya Pradesh Electricity Board have proposed construction of a barrage across the river Sone near Chachai village of Shahdol District (*MP*). At the instance of the *CWPC*, who prepared the designs and drawings of the barrage, experiments to test the adequacy of the discharging capacity and energy dissipation at the barrage were conducted at the *CWPRS*.

2. Design data

In the absence of any observed gauge and discharge data, a maximum flood discharge of 7079.20 m^3/s (2.5 lakh *cfs*) was worked out from Dicken's formula.

$$Q = CM^{3/4}$$

the value of *C* assumed being 1200 and the catchment area *M*, 3144.24 km^2 (1214 *sq miles*). Salient levels were:

Average bed level	...	1489
Crest level of spillway	...	1494
Crest level of undersluice	...	1489
Minimum Pond level	...	1511.5

The bed is sandy upto *RL* 1474 at which good sand stone was reported to be met with. Downstream water level at the design flood, after construction of barrage has been estimated by assuming bed retrogression down to *RL* 1474 *ie* by 4.57 *m* (15 *ft*) over a width of 144.78 *m* (475 *ft*) with side slopes of $2\frac{1}{2}$: 1 on the left bank and $\frac{1}{2}$: 1 on the right bank. Values of surface slope and Manning's '*n*' assumed were 1/2640 and .03 respectively. Downstream retrogressed *HFL* under these conditions worked out to 1519 and with a limiting affluxed *HFL* of 1526 on the upstream, the design discharge intensity worked out was 60.39 m^3/s *per m* (650 *cfs/ft*) over the spillway and 70.05 m^3/s *per m* (754 *cfs/ft*) hrough the undersluice. To provide for the maximum flood discharge, the barrage has been designed to consist of 2 undersluices bays and 12 spillway bays each of 9.14 *m* (30 *ft*) span separated by 2.13 *m* (7 *ft*) thick piers and provided with vertical lift gates.

For testing energy dissipation at lower discharge stages, the downstream gauge discharge curve (*fig 1*) was worked out in the *CWPRS* based on the assumptions made by the *CWPC*.

3. Model and experiments

A geometrically similar sectional model to a scale of 1/45 was constructed in a .76 *m* (2.5 *ft*) wide flume in which two bays of 9.14 *m* (30 *ft*) and two part bays of 4.80 *m* (15.75 *ft*) of the barrage were incorporated. Bed upstream of the barrage was filled with coarse sand upto *RL* 1489, while on the downstream, 1.91 *cm* ($\frac{3}{4}$ *in*) size broken stone was laid upto *RL* 1474 to correspond to the

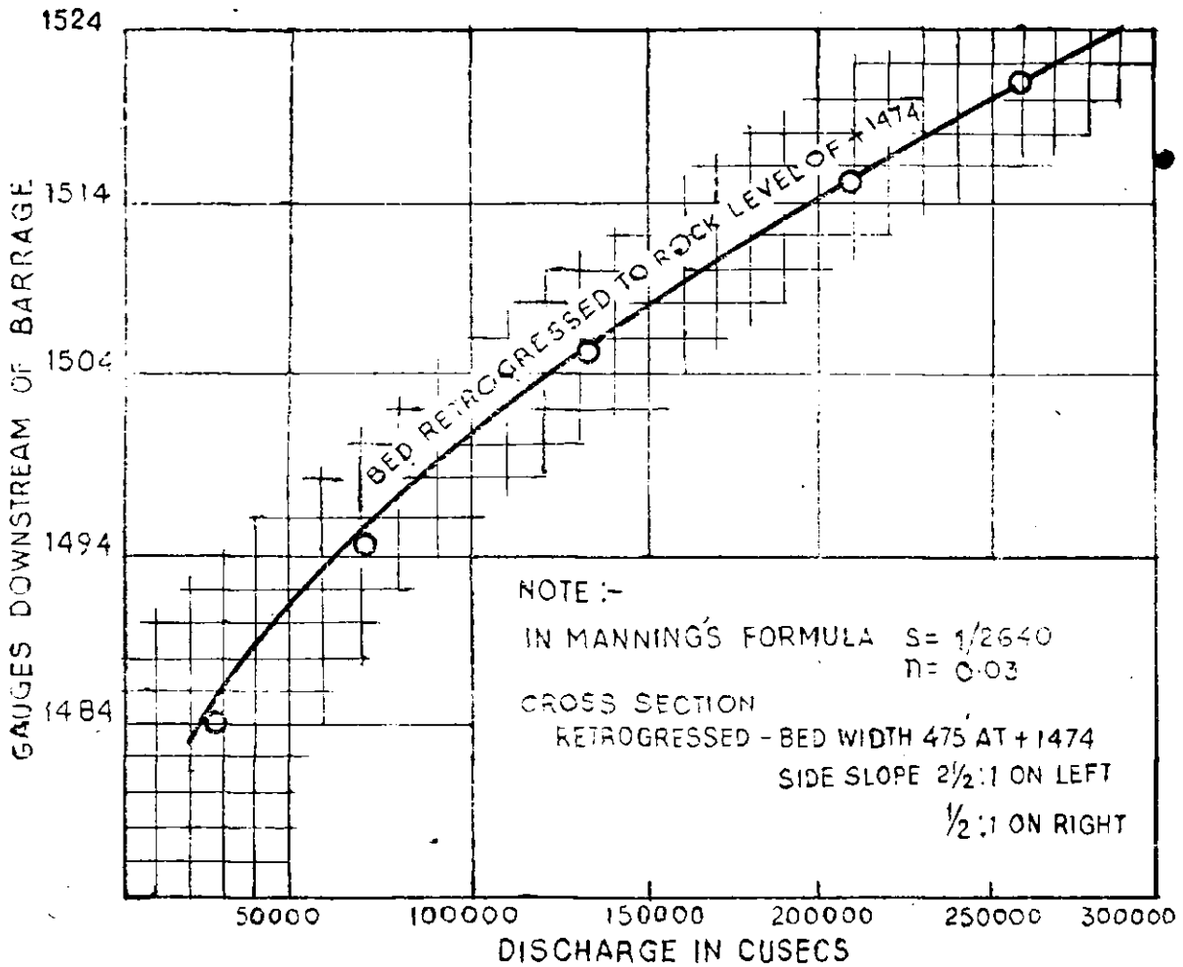

Fig 1: Approximate gauge discharge curve below barrage.
(Worked out at *CWPRS Poona*)

rock level, above which fine sand of mean diameter .4 *mm* was laid upto *RL* 1489.

(*i*) *Spillway*: (*a*).—With a discharge intensity corresponding to 60.39 m^3/s *per m* (650 *cfs/ft*) between the peirs, downstream water level was maintained at *RL* 1519 and the corresponding upstream water level was noted. The value of discharge coefficient obtained from

$$C = \frac{q}{(h + h_v)^{3/2}}$$

was 3.62 as against 3.12 adopted in the design. Under the conditions assumed in the design, the spillway capacity would, therefore, be more than adequate. However, the assumption of bed retrogression from *RL* 1489 to 1474 with a corresponding lowering of water level may not be realised in practice. As such for the discharge intensity of 60.39 m^3/sec *per m* (650 *cfs/ft*) between piers, a relationship between downstream water level varying from *RL* 1519 to 1529 and the corresponding upstream energy level and coefficient of discharge was experimentally established *vide fig 2.*

(*b*) Energy dissipation below the barrage was studied under three different river stages *viz,* 7079.20 m^3/s (2.5 lakh *cft*), 4955.44 m^3/s (1.75 lakh *cfs*) and 2831.68 m^3/s, (1 lakh *cfs*) corresponding downstream water levels maintained in the model being as in *fig 1.* Under the first two stages, flow over the barrage was uncontrolled while at 2831.68 m^3/s (1 lakh *cfs*) stage, discharge had to be throttled by the operation of gates for maintaining the pond level of 1511.5. Energy dissipation for these three stages was found to be generally satisfactory with a clear standing wave forming below the barrage. A secondary wave was, however, found to occur below the primary wave at 2831.68 m^3/s (1 lakh *cfs*) stage. To improve the performance, provision of friction blocks of various dimensions were tested. Finally blocks 1.52 *m* (5 *ft*) high, 1.52 *m* (5 *ft*) wide, .76 *m* (2.5 *ft*) wide at top and 2.29 *m* (7.5 *ft*) at bottom spaced at 2.54 *m* (8.33 *ft*) centre to centre and with their vertical upstream face 14.33 *m* (47 *ft*) from the barrage axis were found to give best results. The water and scour profiles observed in the model

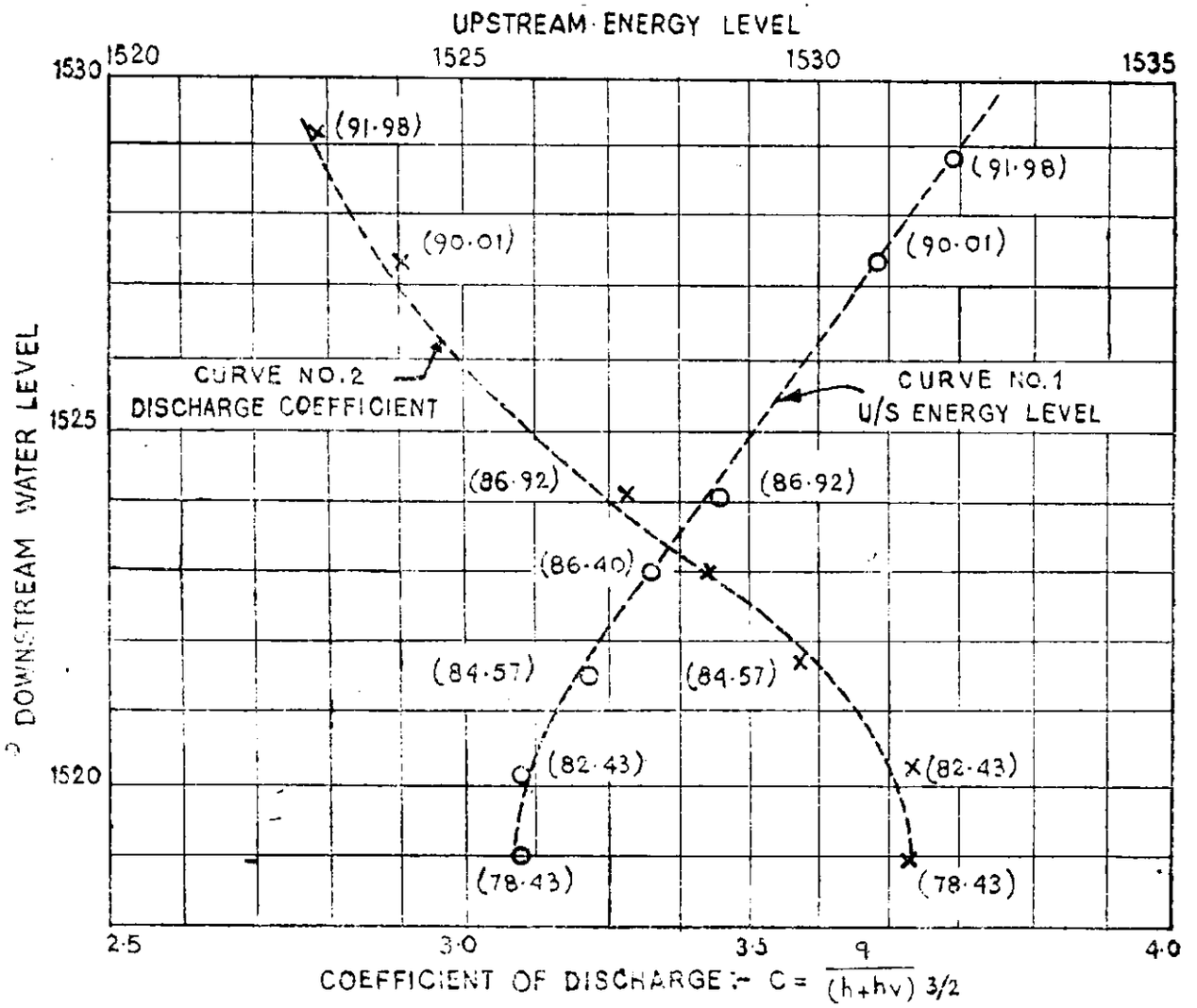

Note:—

1. Standing wave forms at all downstream water levels between *RL* 1519 and *RL* 1529.
2. Discharge was kept constant. Discharge intensity 650 *cfs/ft.*
3. Figures in brackets indicate percent submergence *i e*

$$\frac{\text{Depth of water above crest downstream.}}{\text{Energy head above crest upstream.}}$$

Fig 2: Downstream water level against discharge coefficient and also upstream energy level for design flood of 2.5 lakh *cfs.*

without and with friction blocks at 2831.63 and 7079.20 m^3/s (1.0 lakh and 2.5 lakh *cfs*) stage are reproduced in *figs 3* and *4* respectively.

(*ii*) *Undersluice*: (*a*).—During tests with the undersluice profile, discharge run in the model for each downstream water level between *RL* 1519 and 1529 was varied till the upstream energy level obtained was the same as given by the curve 1 of *fig 2*. Corresponding intensity of discharge and discharge coefficient for each set of upstream energy—downstream water level conditions were then worked out and the relationship plotted in *fig 5*. As can be seen therefrom, intensity of discharge obtained in the model was about the same as adopted in the design, under the design downstream *HFL* of 1519.

(*b*) As for the spillway, energy dissipation below the undersluice was tested for river stages of 7079.20, 4955.44 and 2831.68 m^3/s (2.5 lakh, 1.75 lakh and 1.0 lakh *cfs*). The flow was ungated and energy dissipation was found to be satisfactory. Regulation of undersluice gates would be done

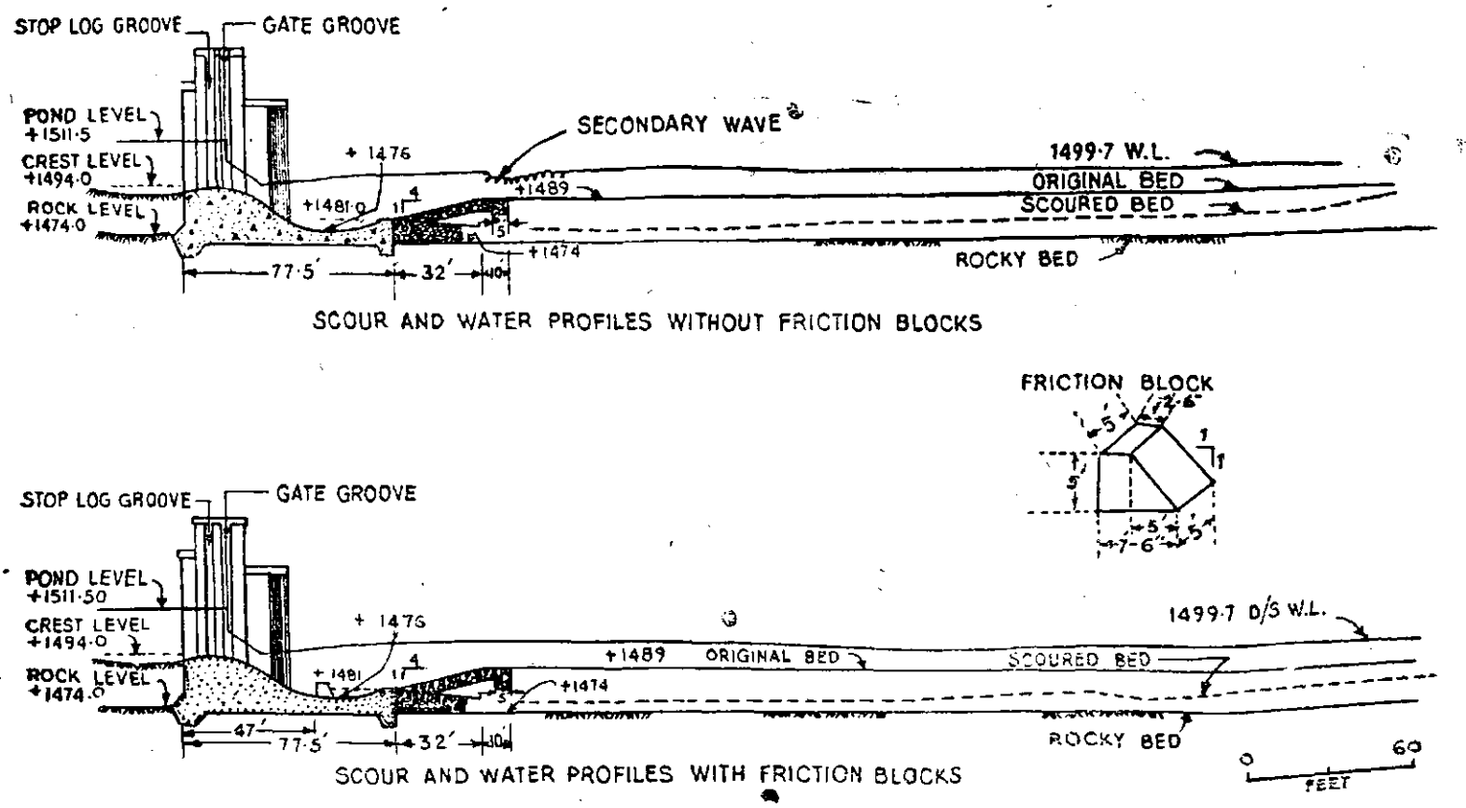

Fig 3 : Energy dissipation below spillway, river stage 1 lakh *cfs*, discharge intensity 238 *cfs/ft.*

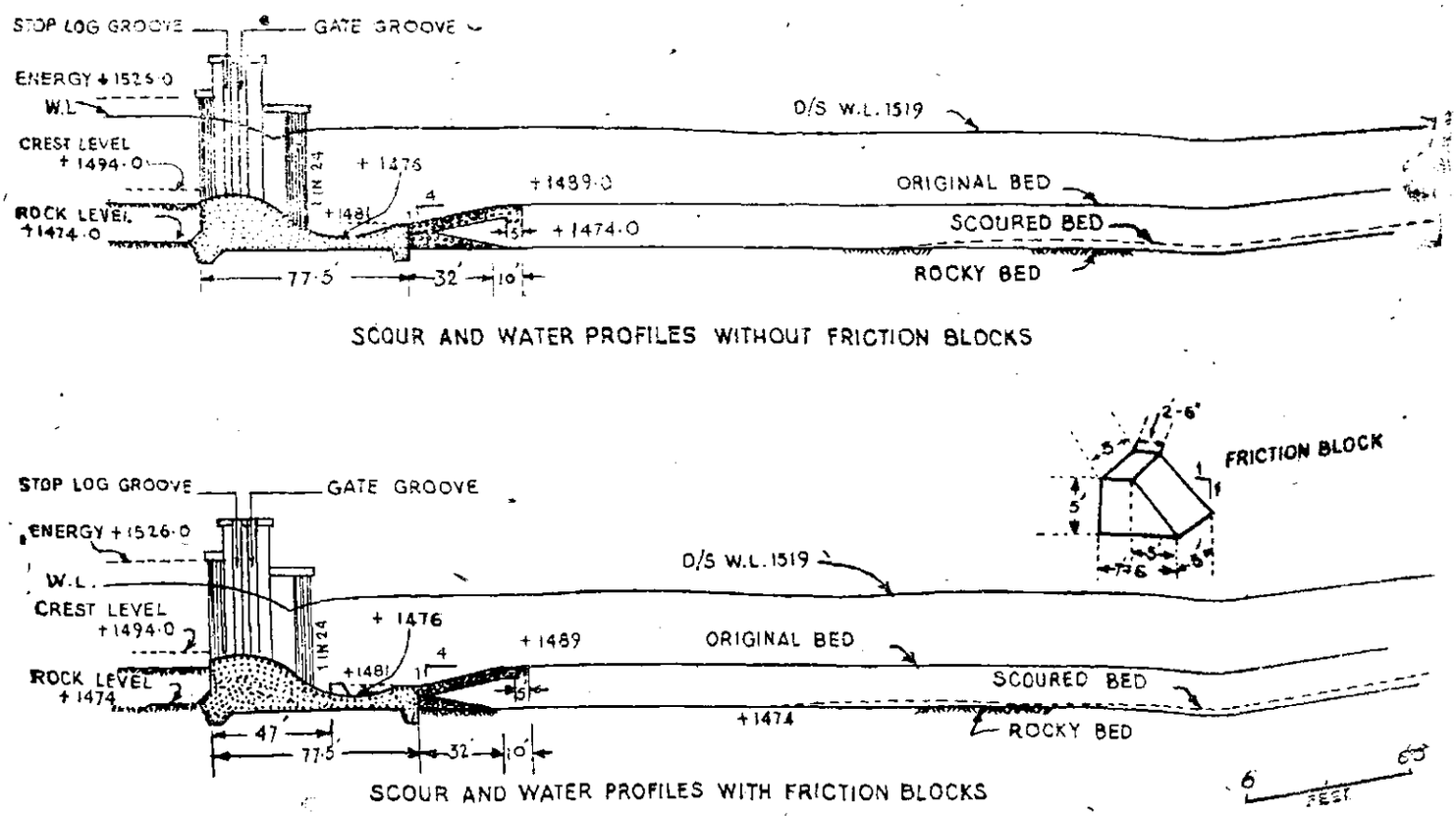

Fig 4 : Energy dissipation below spillway, river stage 2.5 lakh *cfs*, discharge intensity 650 *cfs/ft.*

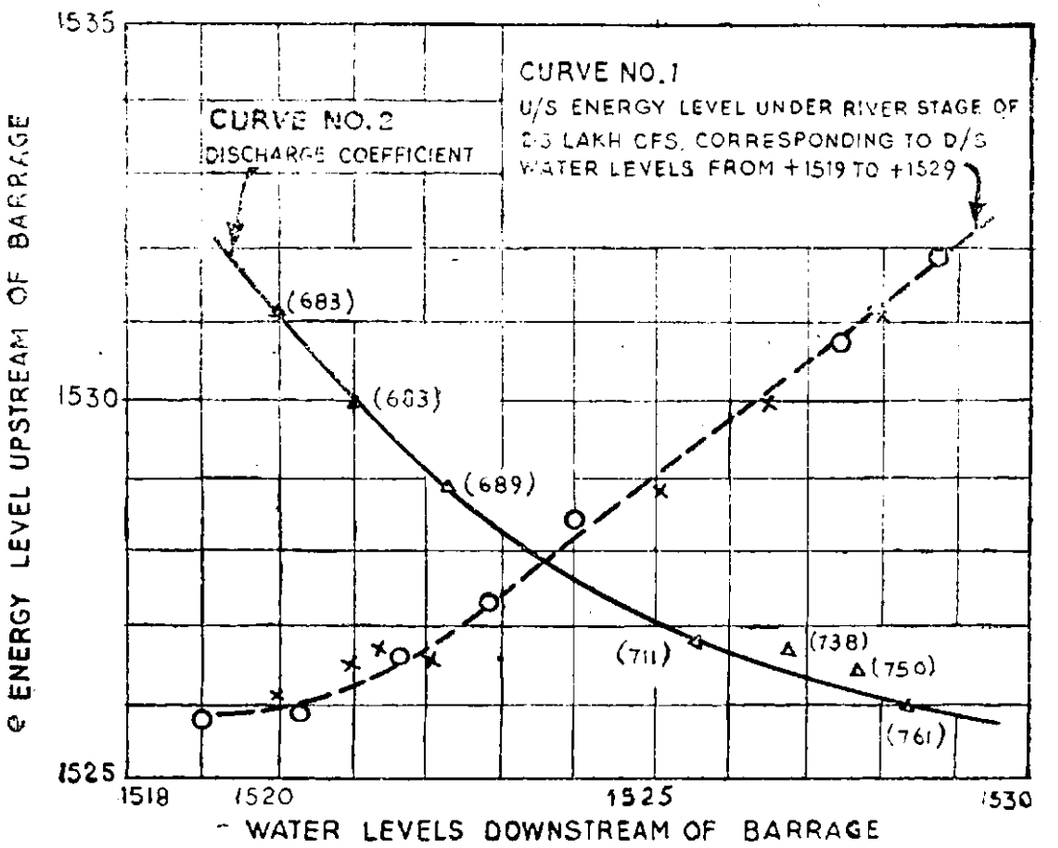

Note:— 1. Curve *No* 1 reproduced from *fig 2*.
2. Points marked thus × indicate *U/S, D/S*, conditions under which observations were made for discharge coefficient.
3. Figures within brackets indicate discharge intensity per foot.

Fig 5: Discharge coefficient of undersluice under river stage of 2.5 lakh *cfs* at upstream energy levels resulting from downstream water levels varying from 1519 to 1529.

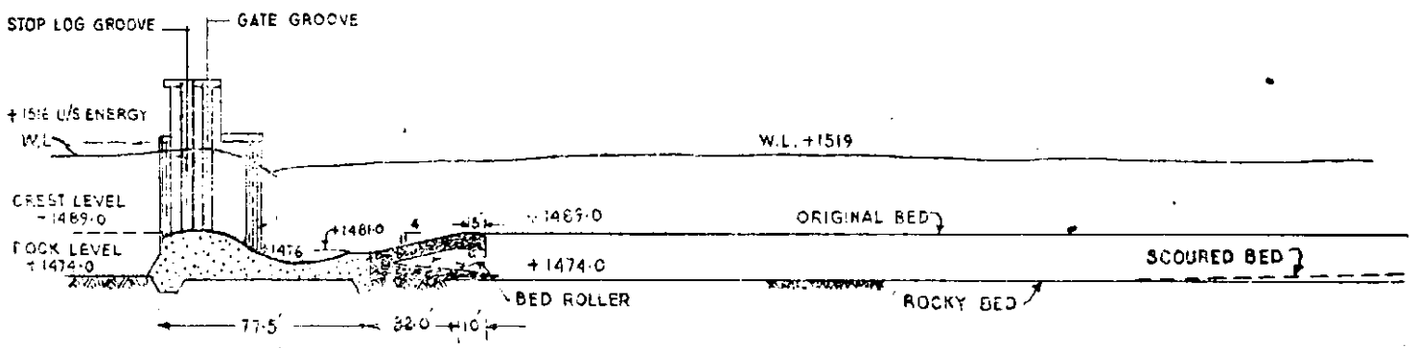

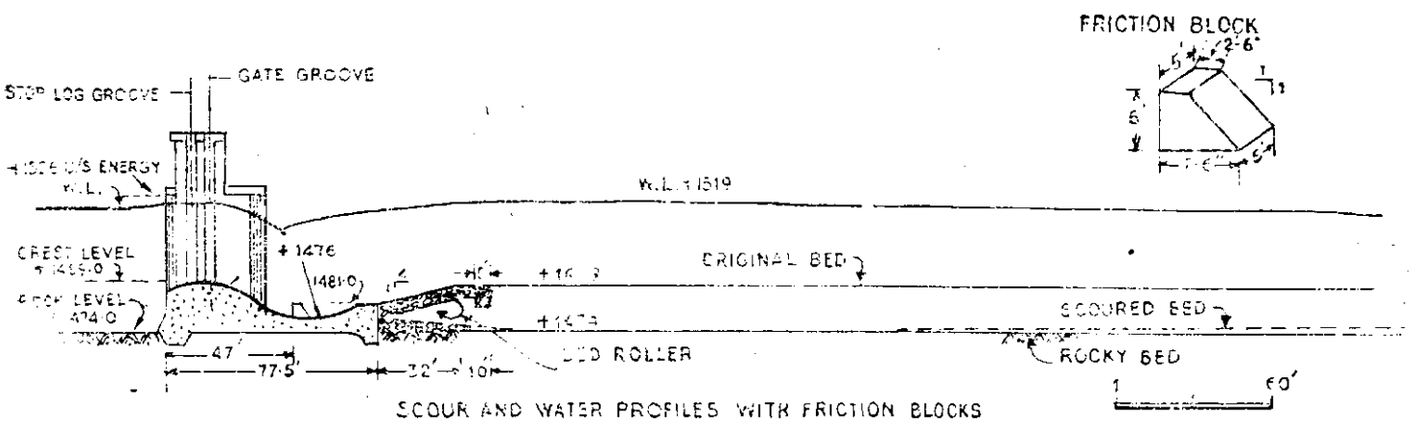

Fig 6: Energy dissipation below undersluice, river stage 2.5 lakh *cfs*, discharge intensity 787 *cfs/ft.*

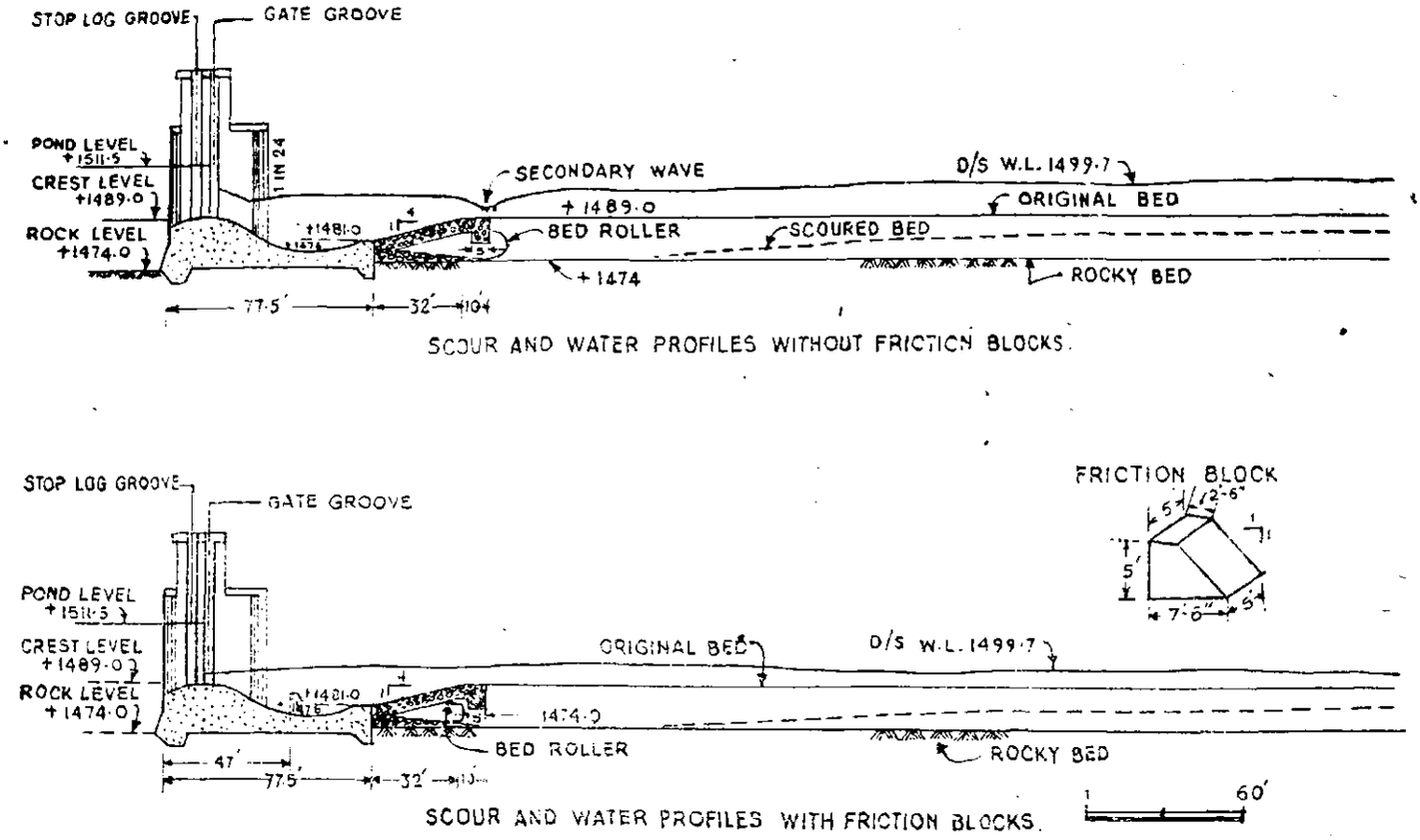

Fig 7 : Energy dissipation below undersluice, river stage 1 lakh *cfs*, discharge intensity 238 *cfs/ft.*

when discharge was low enough to make their partial closing essential to maintain the pond level. Under this condition, however, a pronounced secondary wave was observed to form. Among different correctives tests, provision of friction blocks of the size, spacing and location adopted earlier for the spillway was found to result not only in the elimination of the secondary wave, but in a satisfactory distribution of velocities below the barrage. *Figs 6* and *7* show the water and scour profiles below the barrage under conditions corresponding to river stages of 7079.20 m^3/s (2.5 lakh *cfs*) and 2831.68 m^3/s (1.0 lakh *cfs*) respectively.

4. Conclusions and recommendations

(*i*) Discharging capacity of the barrage (both spillway and undersluice) was found to be adequate, under the conditions assumed in the design. If, however, retrogression below the barrage to the extent assumed did not occur possibility of the design *HFL* being exceeded could not be ruled out.

(*ii*) Under conditions of ungated flow over the barrage, energy dissipation was satisfactory. Under gated flow conditions, however, and specially at river stage of about 2831.68 m^3/s (1.0 lakh *cfs*) a secondary wave formed below the end sill. To eliminate the secondary wave, provision of 1.52 *m* (5 *ft*) high friction blocks located with their upstream face 14.33 (47 *ft*) from the axis of barrage and spaced 2.54 *m* (8.33 *ft*) centre to centre across the direction of flow would be necessary.

(*iii*) Model indicated that the apron below the end sill sloping upto bed level, provided in the design would serve no purpose and could preferably be replaced by an apron sloping down to rock level.

13. Discharging capacity and design of toe protective works

I. Yeldari Spillway, Purna Project

TESTS WERE conducted in 1957 on the original project design along with suggested modifications, (*ibid* 1957). Subsequently the Central Designs Organisation, Bombay sent an alternative design in which the designed maximum discharge was taken as 3,80,000 *cfs* as against 3,14,000 *cfs* in the original project design. The depth of overflow was increased from 30 *ft* to 33 *ft*. This spillway now consisted of ten spans of low level bucket of 70 *ft* radius with invert at *RL* 1388 and an exit angle 30°, and three spans of high level bucket of the same radius and exit angle with invert at *RL* 1440. This high level bucket was designed to come into operation for high overflow depths only, and work as ski-jump bucket. The stage discharge curve was also provisionally further modified on the conservative side the new curve showing stages higher than the ones originally supplied, from about 5 *ft* for lower discharges of 1 lakh *cfs* to 13 *ft* at the maximum discharge of 3.8 lakh *cfs*. Tests were conducted on *CDO* design (*ibid* 1959).

It was suggested, however, that the high level buckets could be eliminated, by increasing the depth of overflow from 33 *ft* to 40 *ft* keeping the maximum *WL* the same as before. This would also eliminate the 18 *ft* thick divide wall between the two buckets. The *CDO* Bombay, modified the design accordingly. With the 40 *ft* maximum depth of overflow in which, the 70 *ft* radius upturned bucket was provided with invert at *RL* 1388 with 30° exit angle for dissipation of energy. *Fig 1* shows the modified design.

2. 70 *ft R* bucket at invert *RL* 1388

The tests were carried out with the design thus supplied. *Fig 2* shows the profiles of water for 40, 35, 30 and 20 *ft* depths of overflow with corresponding tail water levels according to the curve supplied. It was observed that with 40 *ft* depth of overflow and *TWL* 1447 the action of the bucket was very close to ski-jump action, indicating that in prototype the corresponding action could tend to be of ski-jump type. With slight lowering of *TWL* ski-jump action in the model was observed. During transition from ski-jump action to roller action or *vice versa* water level rose very high. *Photo 40* shows the behaviour of the bucket with 40 *ft* depth of overflow and *TWL* 1447 and *photo 41* shows the same depth of overflow with *TWL* 1445.

For depths of overflow of 35 *ft* and less, the action was that of roller type though the roller was somewhat suppressed in the three spans at the left.

Fig 3 shows the scour on the erodible bed for 40 *ft* depth of overflow with corresponding *TWL*. The general scour is of the order of 18 *ft* about 150 *ft* away from the end sill.

In the modified *CDO* design the overflow depth was increased from 33 to 40 *ft* thus increasing the discharge intensity from 720 to 965 *cfs/ft*. This in turn, increased the depth of water necessary for good roller action of the bucket. Hence the 70 *ft* radius upturned bucket acting as roller bucket for 33 *ft* overflow depth was nearly acting as skijump bucket for 40 *ft* overflow depth.

To ensure the roller action of the bucket even under possible retrogression of about 7 *percent* in depth of flow in the river channel downstream for a discharge of 50,000 *cfs* reducing to 4 *percent* retrogression, for the maximum discharge, it was found necessary to keep the invert *RL* at 1384. The roller action then became just good for maximum discharge with 4 *percent* retrogression (*see* curves 2 and 3 of *fig 4*). If the retrogression was not taken into account as the downstream channel mainly consisted of exposed rock then the bucket at invert *RL* 1384 would give satisfactory results for all depths of overflow with corresponding tail water levels as supplied. Hence further tests were conducted with 70 *ft* radius bucket at invert *RL* 1384.

3. 70 *ft R* bucket at invert *RL* 1384

Exit angle 30°.—*Fig 5* shows the profiles of water for 40, 35, 30 and 20 *ft* depths of overflow with corresponding tail water levels. Though the bucket acted as roller bucket for 40 *ft* overflow depth and *TWL* 1447 the action was nearly ski-jump type when the *TWL* was lowered to *RL* 1445. For 35 *ft* and lower depths of overflow the jet from the bucket continued to be suppressed (*photo 42*).

L—S 3401—10

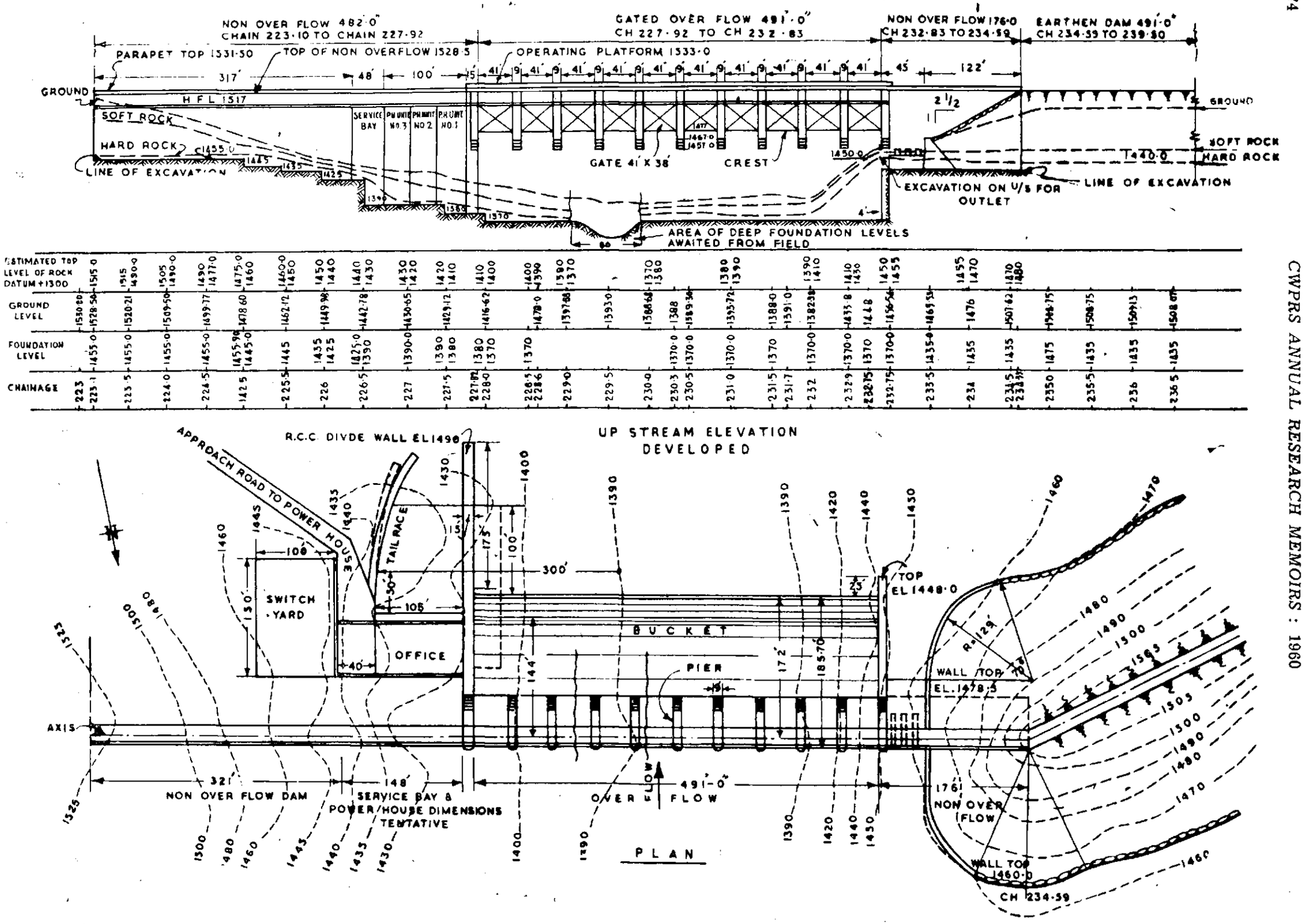

Fig 1: Plan and elevation upstream of masonry dam.

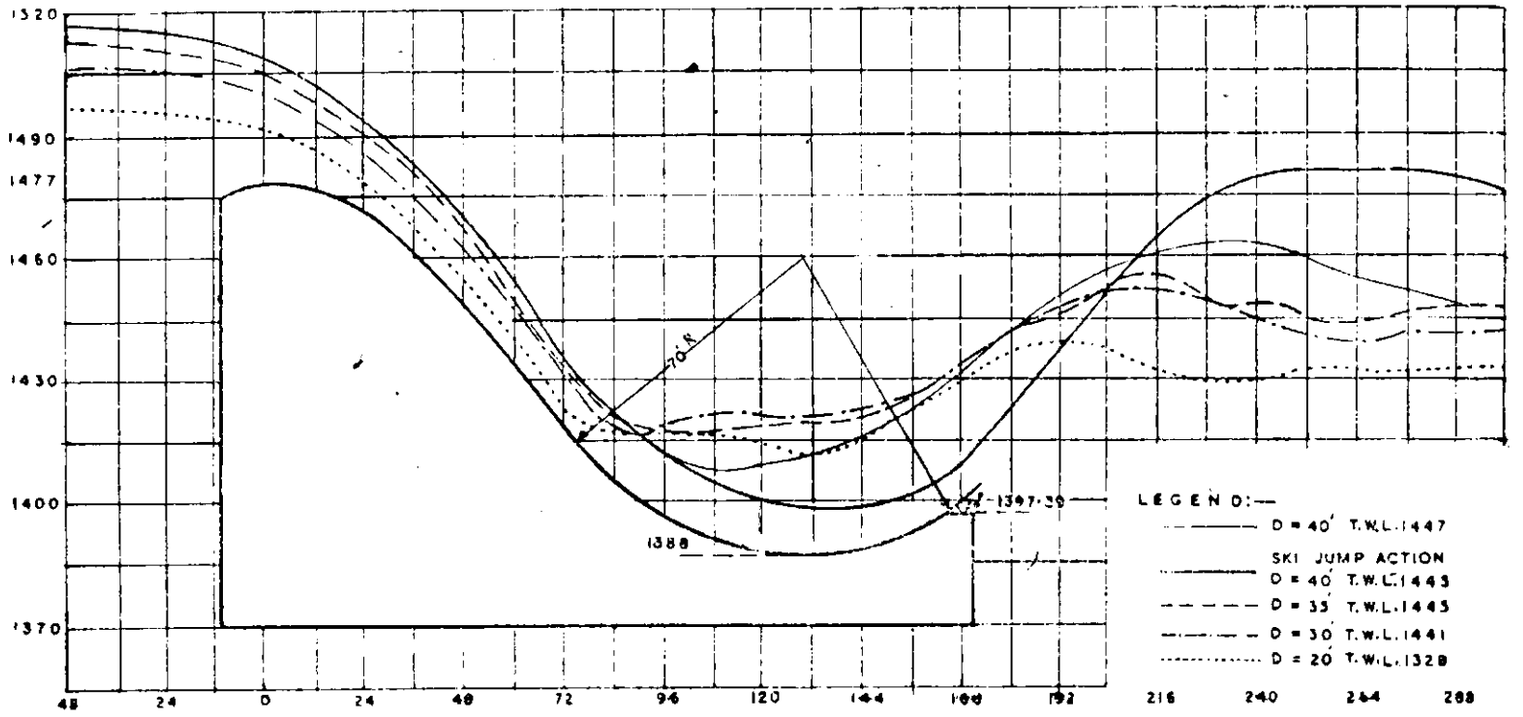

Fig 2: Profiles of water, crest *RL* 1477, 70 *ft R* bucket at *RL* 1388, exit angle 30°.

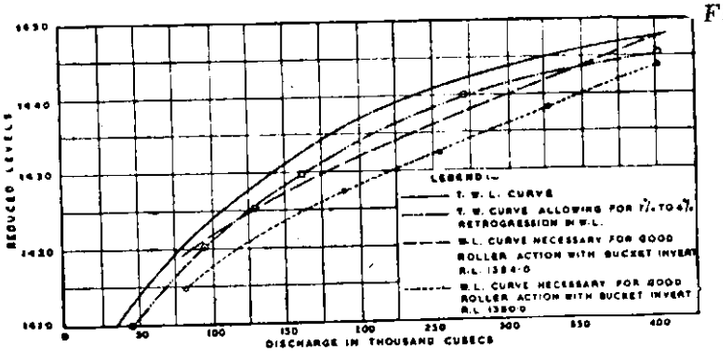

Fig 4: *TW* curves and *WL* curves at invert *RL* 1384.0 and 1380.0 for good roller action.

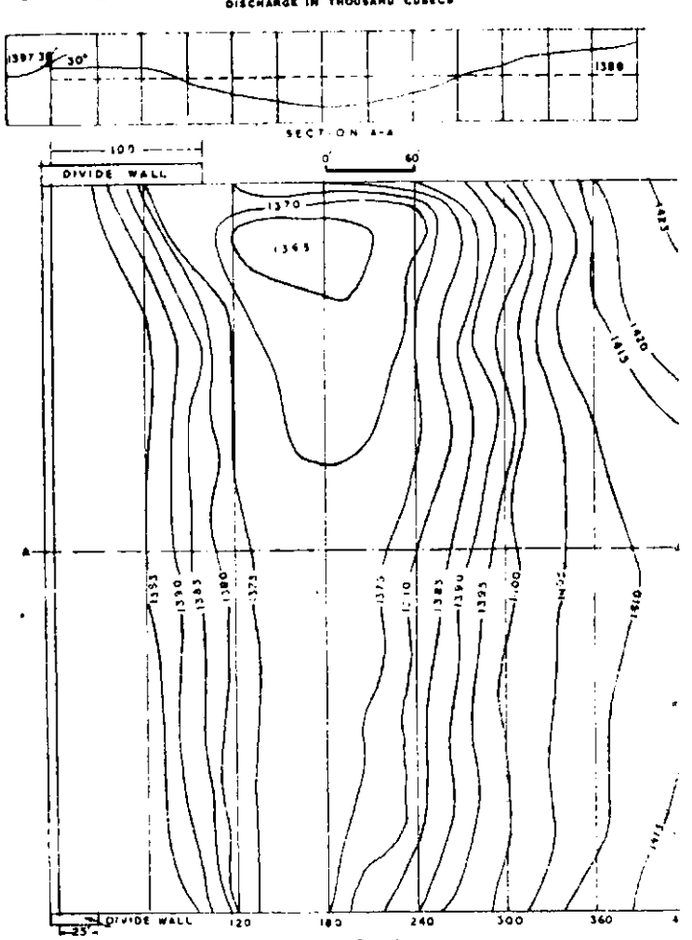

Fig 3: Scour for $D = 40'$ *TWL* 1447, 70 *ft R* bucket at invert 1388 exit angle 30°.

L—S 3401—10-a

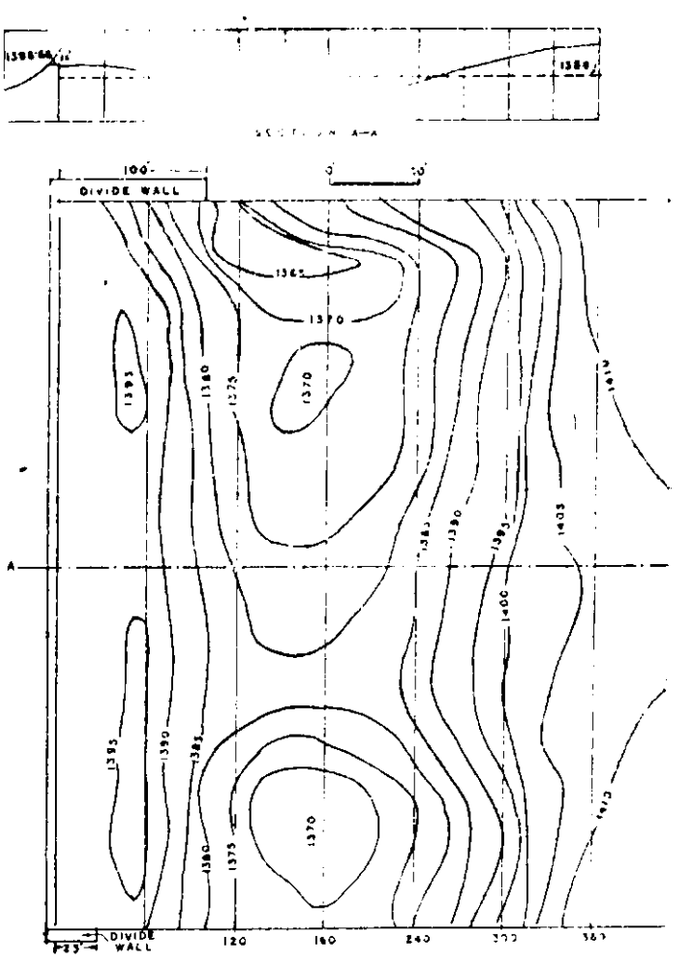

Fig 7: Scour for $D = 40'$ *TWL* 1447, for 70 *ft R* bucket invert *RL* 1384. exit angle 35°.

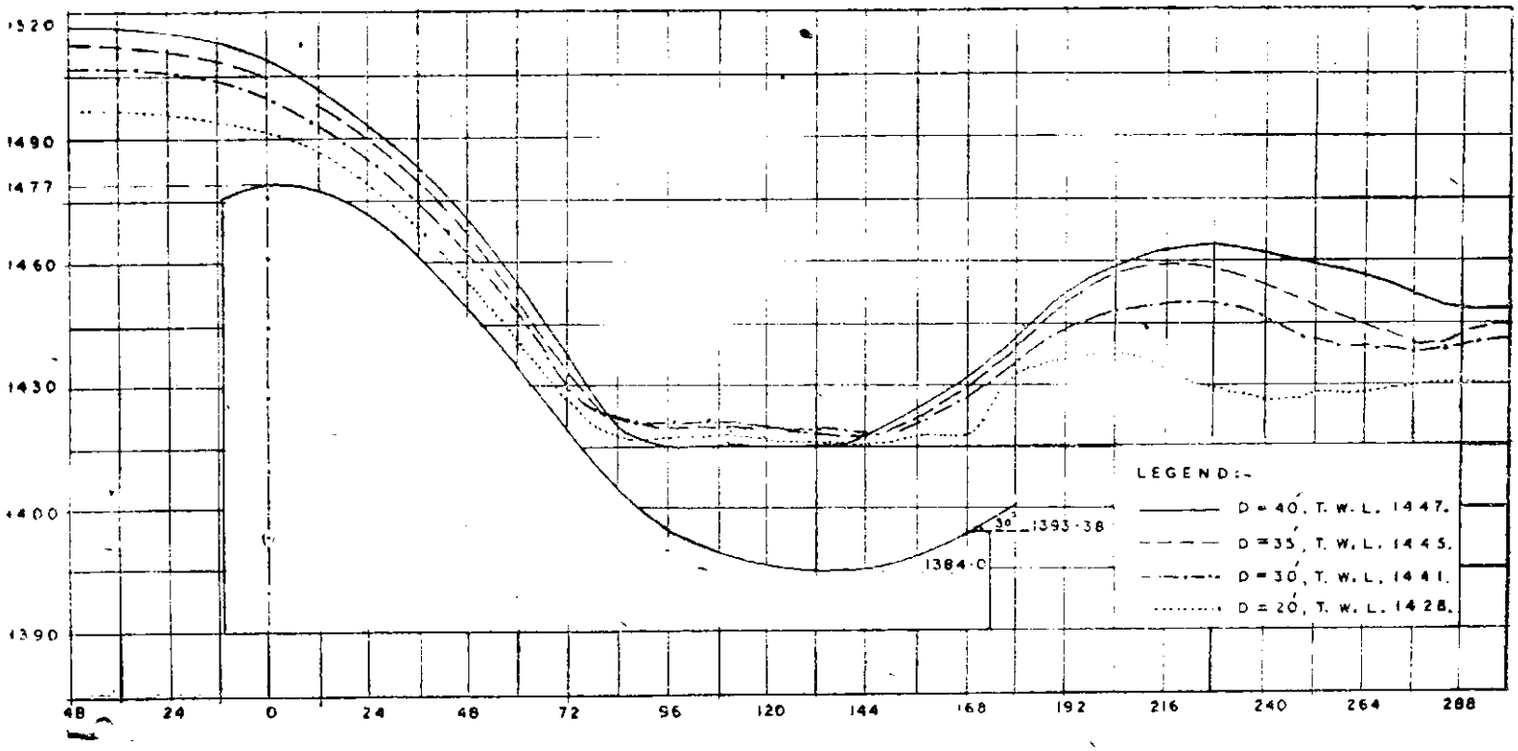

Fig 5: Profiles of water crest *RL* 1477; 70 *ft R* bucket at *RL* 1384.0, exit angle = 30°.

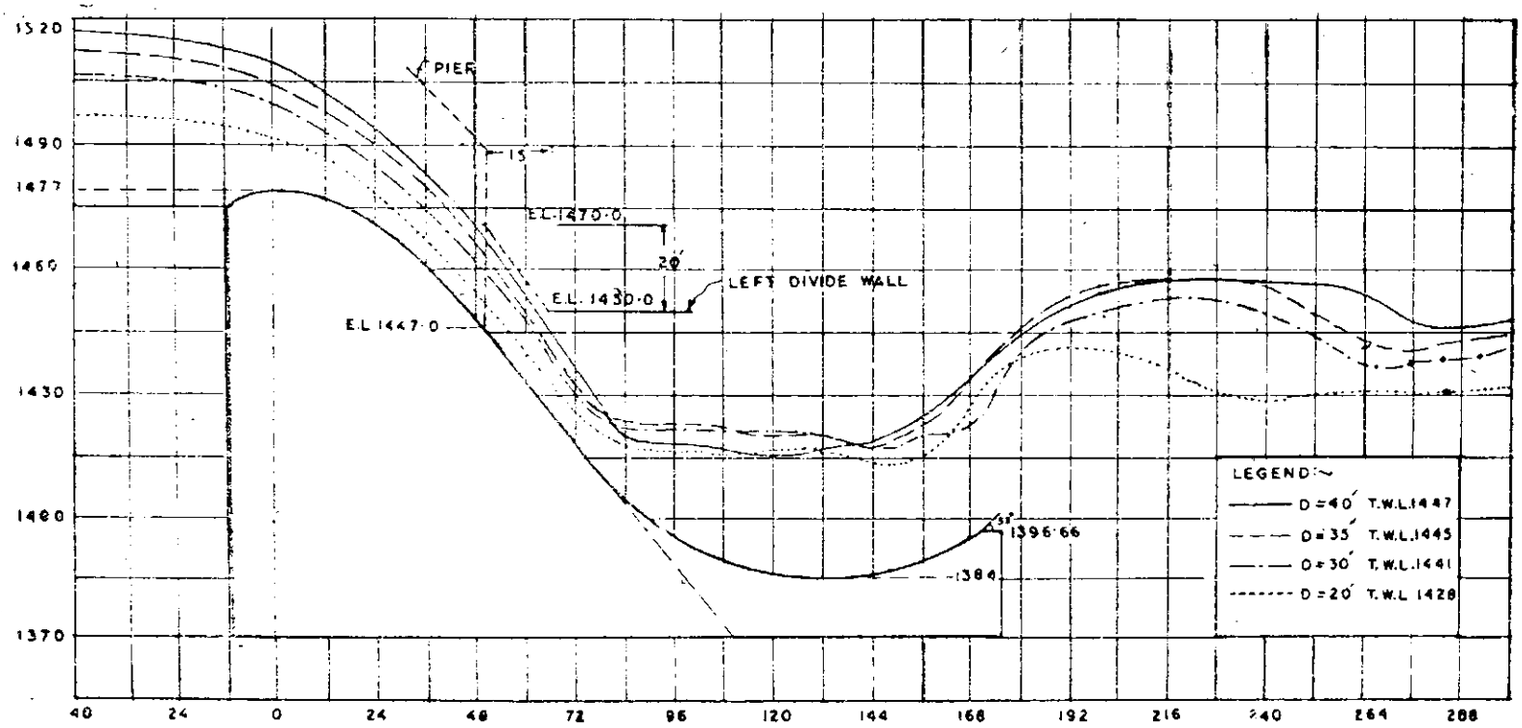

Fig 6: Profiles of water, crest *RL* 1477; 70 *ft R* bucket at *RL* 1384.0; exit angle = 35°.

35° Exit Angle.—To further improve the roller action of the bucket the exit angle was raised from 30° to 35°. It was found the roller action became more stable due to raising of the end sill. *Photo 43* shows the roller action of the bucket for 40 *ft* overflow depth. It was found that with 4 *ft* retrogression the bucket continued to act as roller (*photo 44*). For 35 *ft* and lower depths the suppression of the jet from the exit disappeared with this raised exit angle.

Fig 6 shows the profiles of water for, 40, 35, 30 and 20 *ft* overflow depths with corresponding tail water levels. *Fig 7* shows the scour for 40 *ft* (*photo 45*) overflow depth with corresponding

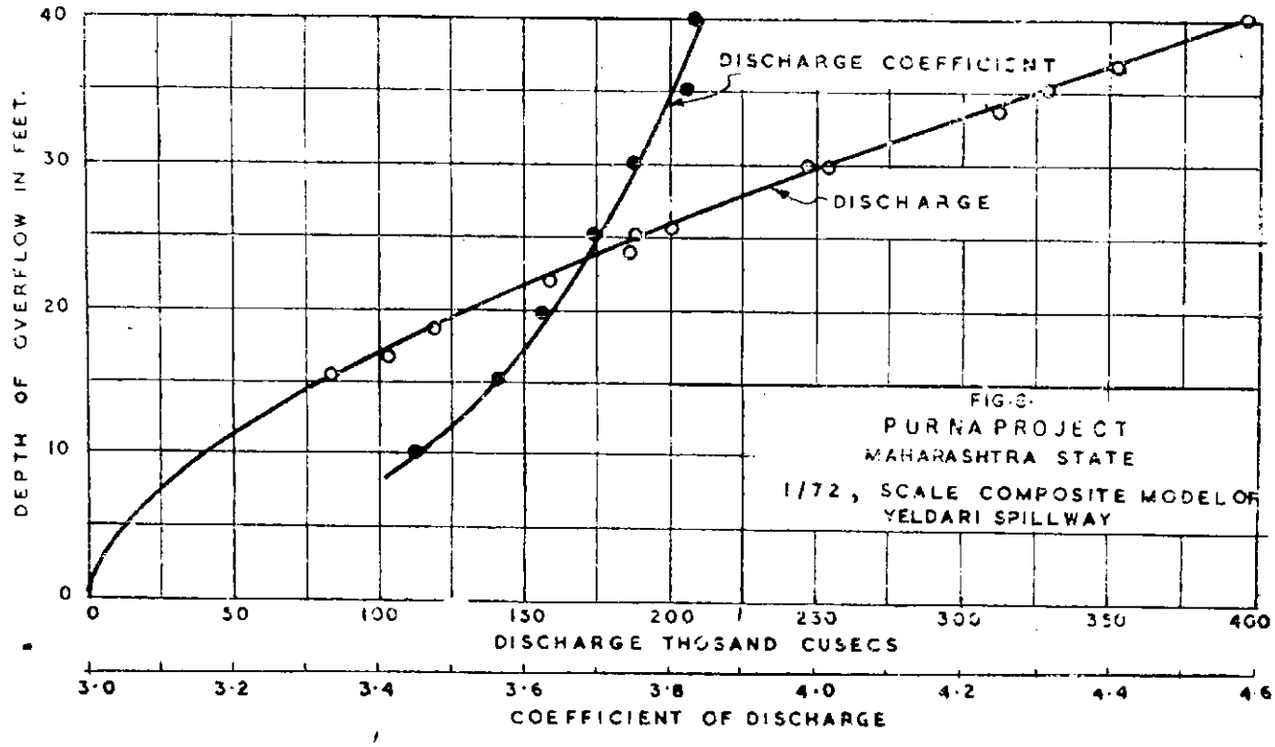

TWL. There was no appreciable change in the scour except the stronger return roller resulting in the 1395 contour near the end sill. The 70 *ft* radius bucket with 35° exit angle was preferred because of the stability of roller action for designed discharge with lower tail water levels and absence of suppression of roller for lower depths of overflow.

4. Discharging capacity of spillway

It was observed that the spillway was able to discharge equivalent of 3,98,000 *cfs* with 40 *ft* overflow depth. Hence the length of spillway to surplus 3,80,000 *cfs* was considered sufficient. *Fig 8* shows the discharge and coefficient of discharge for different depths of overflow. The coefficient varied from 3.44 for 10 *ft* depth to 3.83 for 40 *ft* depth.

5. Divide wall

In the modified *CDO* design the divide wall at the left was extended 100 *ft* beyond the end sill, its top kept at *RL* 1350. It was observed that the length of the divide wall was not sufficient as the surface roller was hitting the river bed beyond this wall and its spread-out was causing cross flow in the mouth of tail race channel (*photo 46*). There was considerable spilling over this wall which was also adding to the cross flow.

To improve the flow conditions (*photo* 47) divide wall was extended 175 *ft* beyond the end sill and its top was raised to 1365 *ft* for a length of 100 *ft* starting from 5 *ft* beyond the end sill. This completely stopped the spilling of water over the divide wall and the cross flow in the mouth of tail race channel was considerably reduced. The following table gives the minimum to maximum fluctuations observed in the tail race channel by an electronic recorder for various extensions of the divide wall, tested in the model.

Conditions for observations	Beyond end sill (*ft*)		
	150	175	200
Depth of overflow 400 *ft*	+ 2·1 to −	+ 1·7 to −	+ 1·6 to −
TWL 1447	+ 4·0 −	+ 3·2 −	+ 2·3 −

It was found from the above observations that an extension of 175 *ft* of wall would bring the fluctuation in the tail race channel close to the permissible limits of ± 3 *ft* set by Superintending Engineer (Hydro).

6. Recommendations

(1) The Yeldari spillway with crest at *RL* 1477 and over-all length of 491 *ft* was found adequate to surplus the designed discharge of 3,80,000 *cfs* with 40 *ft* overflow depth and hence this design may be adopted.

(2) A 70 *ft* upturned bucket with invert *RL* 1384 and exit angle of 35° was found to be satisfactory and may be adopted for dissipation of energy for designed depth of overflow with corresponding *TWLs* according to the curves supplied by *CDO*.

(3) Where the river bed is higher than the end sill it may be dressed to the level of the end sill for a length of 50 *ft* and be given a gentle slope to the existing level beyond.

(4) The divide wall may be extended 175 *ft* beyond the end sill and its top may be raised from *RL* 1450 to *RL* 1465 for a length of 100 *ft* starting 5 *ft* beyond the end sill. The raised portion may be joined to the lower level by 1:1 slope on both the sides. Also on the upstream end, it may be joined to the pier at *El* 1470 with slope of .75 *H* to 1 *V* to avoid any spill in the tail race channel (*fig 6*).

II. Kadana Spillway, Kadana Project

After a series of tests were conducted (*ibid* 1957) on the alignment and design of Kadana Spillway, the tests were suspended pending a major revision of alignment design and crest levels *etc.* The

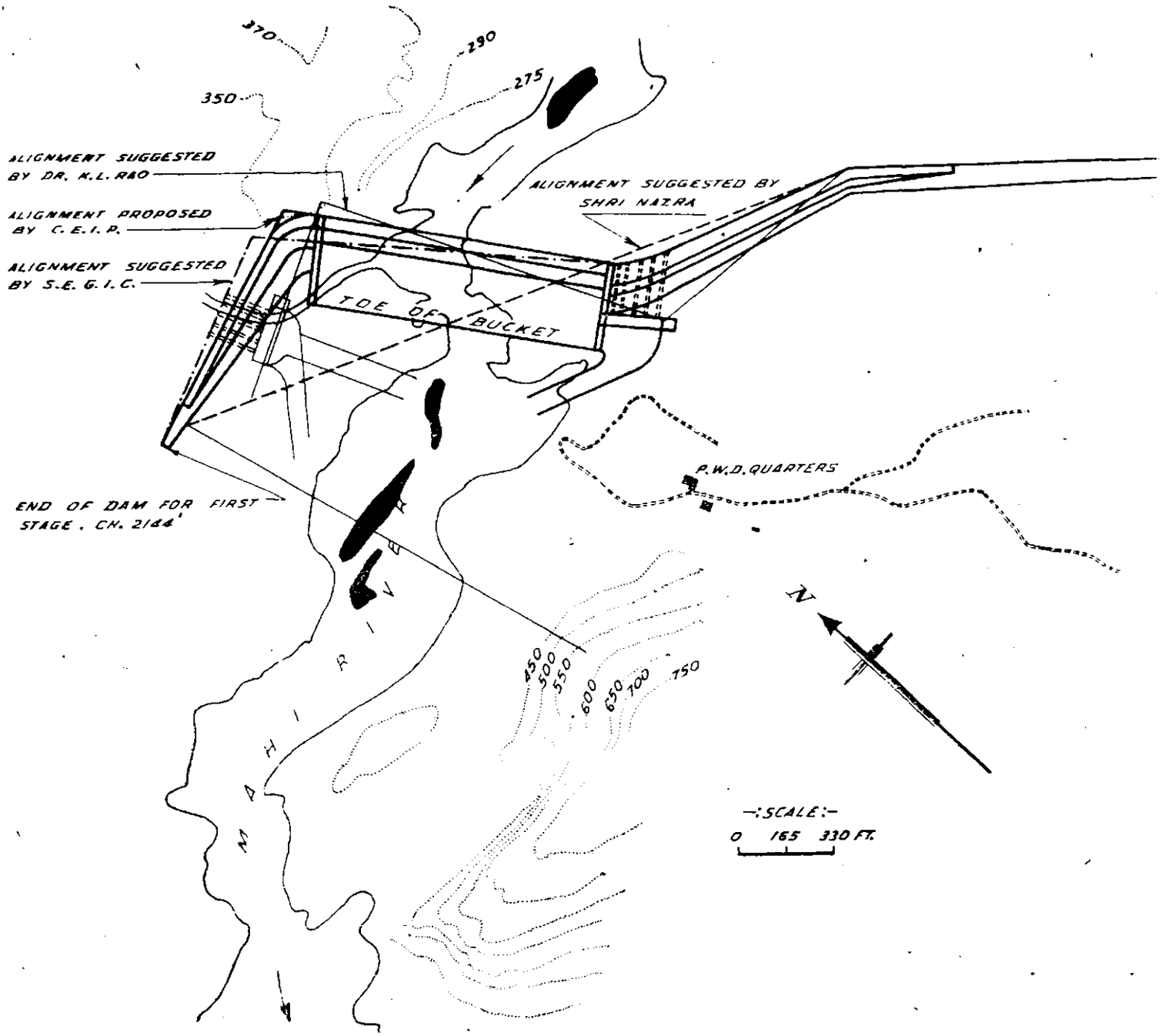

Fig 1: Mahi river and dam alignments.

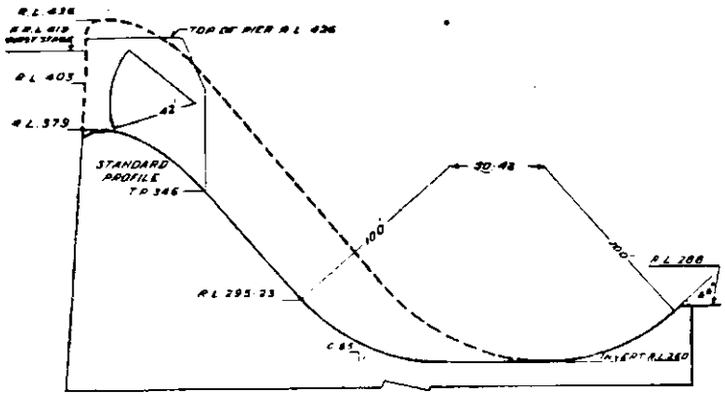

Fig 2: Spillway section (two stages).

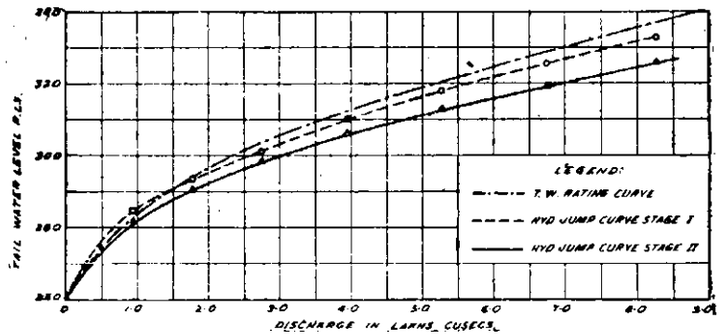

Fig 4: Assumption for curve No 1, $n = .0375$, $s = 1/2112$ or $2.5/mile$, $Q = 13.04$ lakhs with *TWL RL* 358.83.

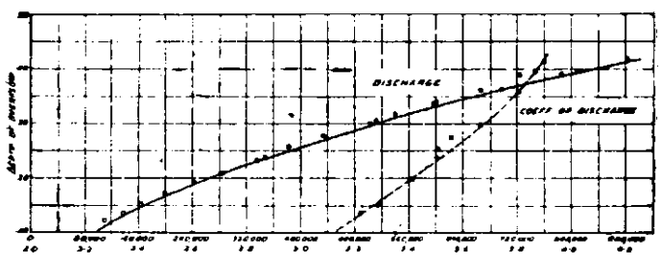

Fig 6: Kadana reservoir project (1st stage).

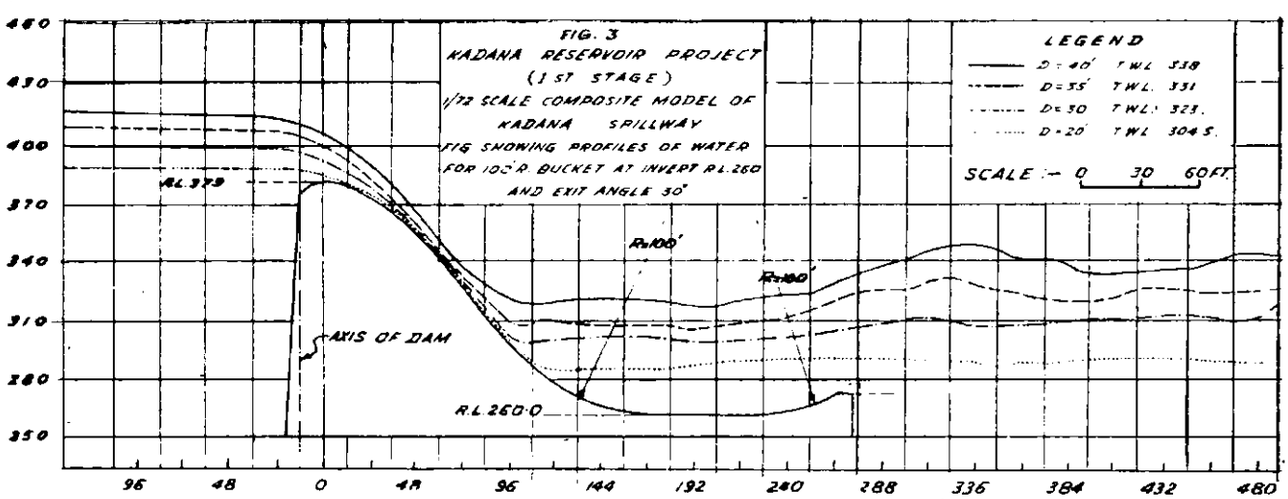

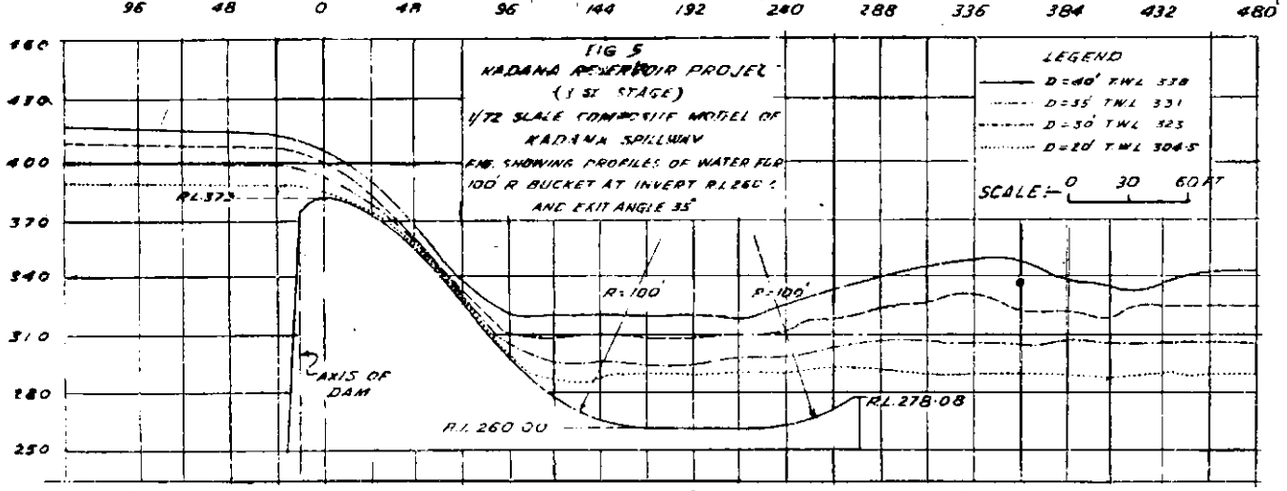

	Crest *RL*	Depth of over-flow (*ft*)	*HFL RL*	Spill-way length (total) (*ft*)	Width of span (clear) (*ft*)	Designed discharge (*cfs*)
Original design ...	425	40	465	1240	40	8,15,000
Modified design } Stage I.	379	40	419	1035	45	,,
Modified design } Stage II.	436	40	476	1035	45	,,

particulars of the modified design (in two stages) along with the original project design are given for comparison.

The alignment of the spillway suggested by *CWPC* based mainly on hydrodynamic consideration was also slightly modified by the Chief Engineer (Irrigation Projects) giving due considerations to the foundation conditions. *Fig 1*

shows the alignment suggested by *CE (I & P)* along with the *CWPC* alignment and the original project alignment. *Fig 2* shows the spillway section for the first stage.

2. Tests and results

The first stage of the *CDO* design of the spillway was reproduced to a scale of 1/72 according to the new alignment the dissipation of energy downstream, general flow conditions and adequacy of the spillway to surplus the designed discharge *etc.*

The exit angle of the 100 *ft* radius upturned bucket (in the II stage) proposed for dissipation of energy by *CDO* was of the order of 44° the end sill being 28 *ft* above the invert *RL* of the bucket. This exit angle was considered very high. The tests were therefore, started with 30° exit angle.

Fig 3 shows the profiles of water for various depths of overflow with corresponding tail water levels according to the curve shown in *fig 4*. The roller action was considered generally good for the first stage (*photo 48*).

Fig 5 shows the profiles taken for the same depths of overflow with the exit angle of the bucket raised to 35°. The roller action showed some improvement for this stage (*photo 49*).

The roller action of the bucket has to be studied for both the stages for the best and most economical design.

Fig 6 shows the graph of depth of overflow vs. discharge and discharge coefficients. It was observed that a discharge of 8.34 lakh *cfs* could be surplussed with 40 *ft* overflow depth. The length of the spillway was therefore, considered adequate for the designed discharge of 8.15 lakh *cfs*.

III. Bhadar Spillway

AFTER THE 1956 tests on the Project design of Bhadar spillway were conducted (*ibid* 1956), the *CDO* Bombay further modified the design as under:

Description	Original Design	*CDO Design*
Length of spillway overall.	2200 *ft*	1239 *ft*
Length of spillway clear.	2200 *ft*	1015 *ft*
Number of spans ...		29
Designed discharge ...	2 lakh *cfs*	2 lakh *cfs*
Depth of overflow ...	8 *ft*	14 *ft*
High flood level ...	*RL* 362	*RL* 362
Crest ...	*RL* 354	*RL* 348
Spillway profile ... Standard Creager's downstream slope.	.78:1	.85:1

For dissipation of energy a horizontal apron 110 *ft* long was proposed in the *CDO* design as compared to 5 different aprons in the original project design and 3 roller buckets recommended by the Research Station. *Fig 1* shows the plan and elevation of spillway of the *CDO* design. *Fig 2* shows the details of overflow section.

2. CDO design

Sectional model.—*Fig 3* shows the profiles of water for 14 *ft*, 10 *ft* and 6 *ft* depths of overflow with corresponding tail water levels according to *fig 4* (curve 1). It was observed that the jump was submerged for higher depths of overflow of 10 and 14 *ft* (*photos 50, 51*) . This was expected as the tail water curve was higher than d_2 curve for the apron at *RL* 283.

Fig 5 shows the pressures on the profile of spillway for the *CDO* design. The pressures were positive for 6, 10 and 14 *ft* depths of overflow and corresponding tail water levels.

Composite model.—A composite model was constructed to a scale of 1/60 to study the general flow conditions downstream of spillway especially with a view to protect the temple just downstream of spillway.

Fig 6 shows the profiles of water for 14, 10 and 6 *ft* depths of overflow with corresponding tail water levels, according to curve 1 shown in *fig 4*. It was observed that the jump was submerged (*photos 52, 53*). *Fig 7* shows depth of overflow plotted against discharge for both sectional and composite model. It was found that the length of spillway was adequate for the designed discharge. *Fig 8* shows the coefficient of discharge against overflow depths. The velocities observed near the hillock on downstream on which the temple is situated were of the order of 7.75 *ft/sec* minimum to 16 *ft/sec* maximum.

3. Other modifications

As the tail water curve was higher than d_2 curve for apron at *RL* 283, it was considered that a roller bucket would act better for dissipation of energy because roller bucket acts better when the tail water depths are higher than hydraulic jump depths. Curve 3 in *fig 4* shows the tail water curve necessary for good roller action with

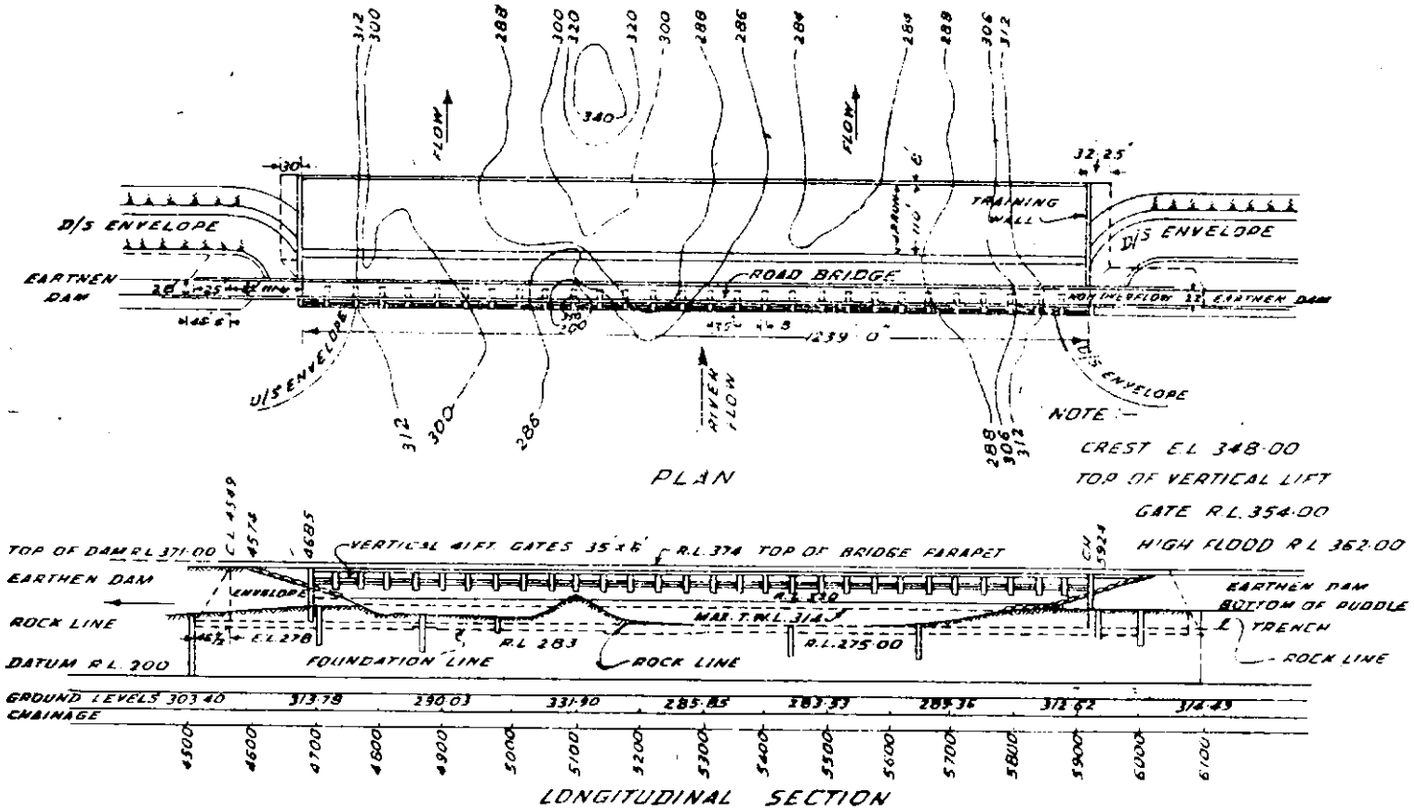

Fig 1 : Bhadar project plan and L. section.

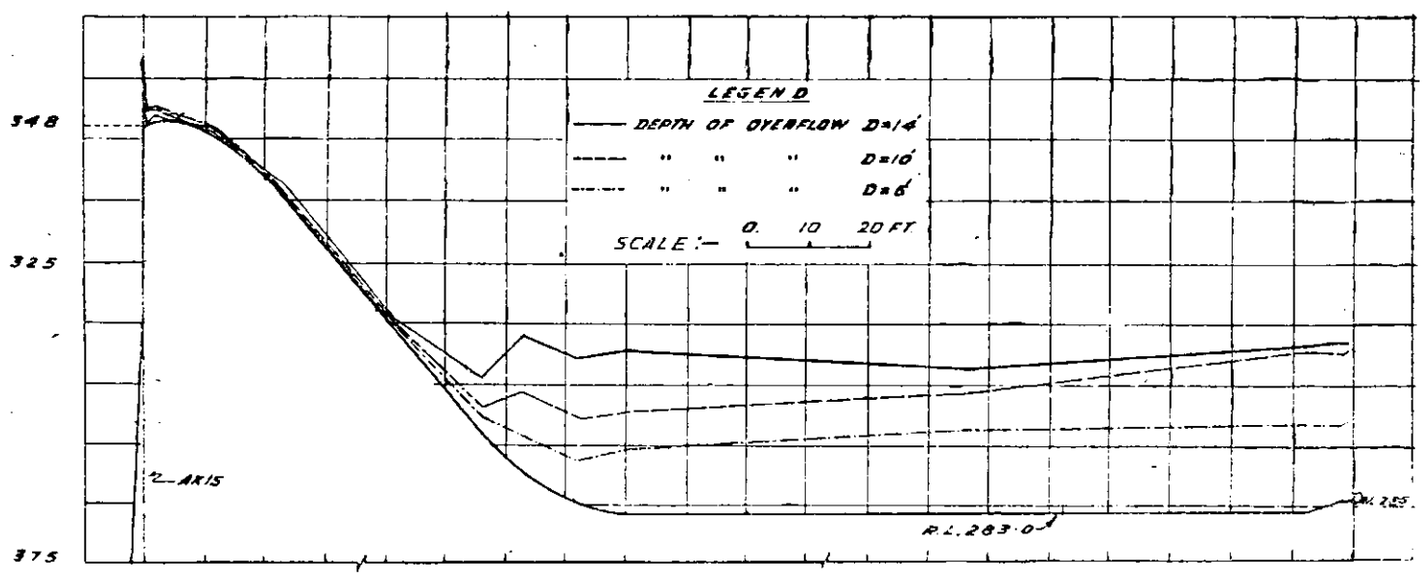

Fig 5: Minimum pressures along section of spillway for CDO design; 1/24 scale sectional model.

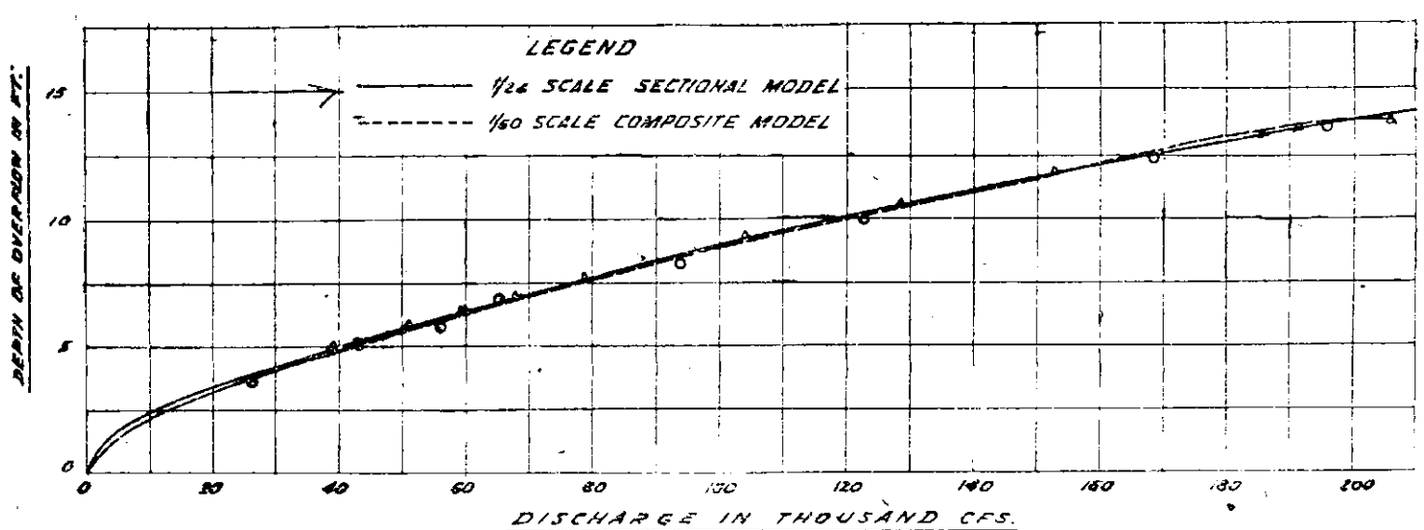

Fig 7

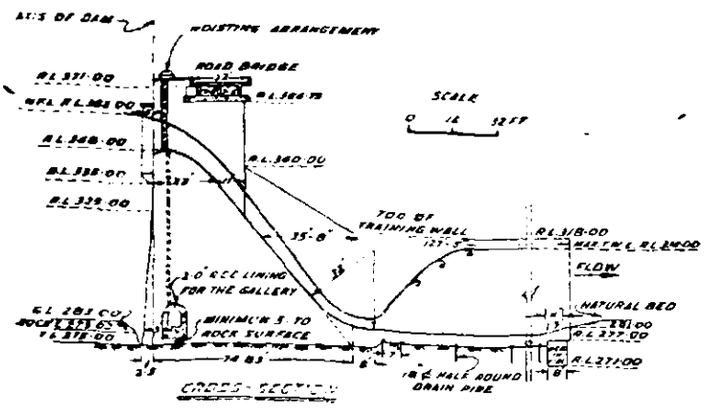

Coordinates of napee	
X (o U/S + ace)	Y (o at RL 348 crest)
0.0	1.76
1.4	0.50
2.8	0.09
4.2	0.00
5.6	0.09
8.4	0.88
11.2	2.14
14.0	3.37
16.8	5.74
19.0	8.20
23.8	12.80
28.0	18.34

Fig 2: Bhadar project details of overflow section.

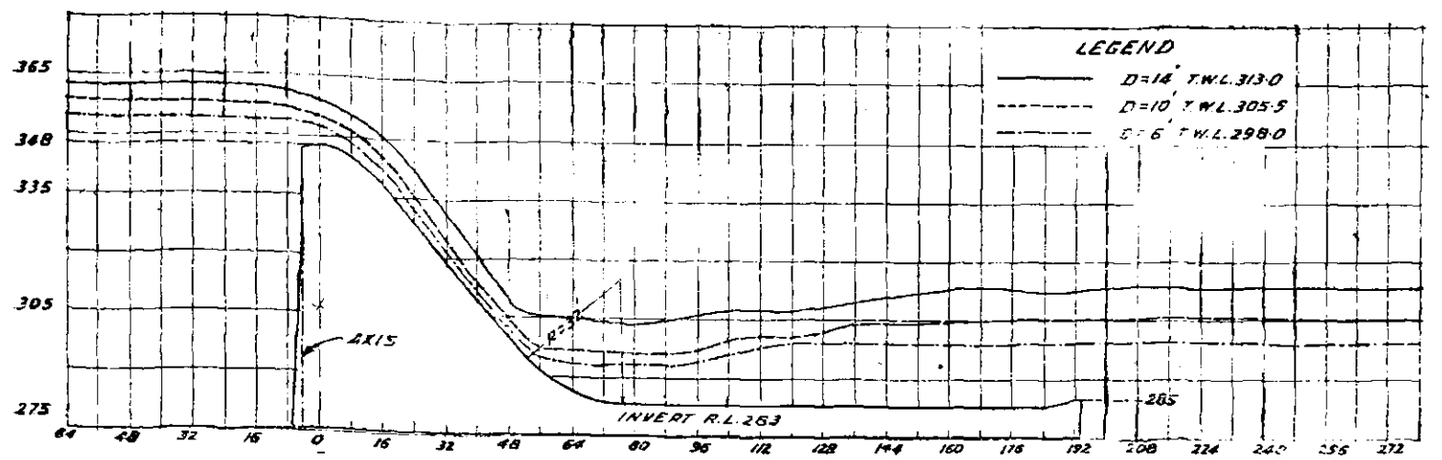

Fig 3: Profiles of water.

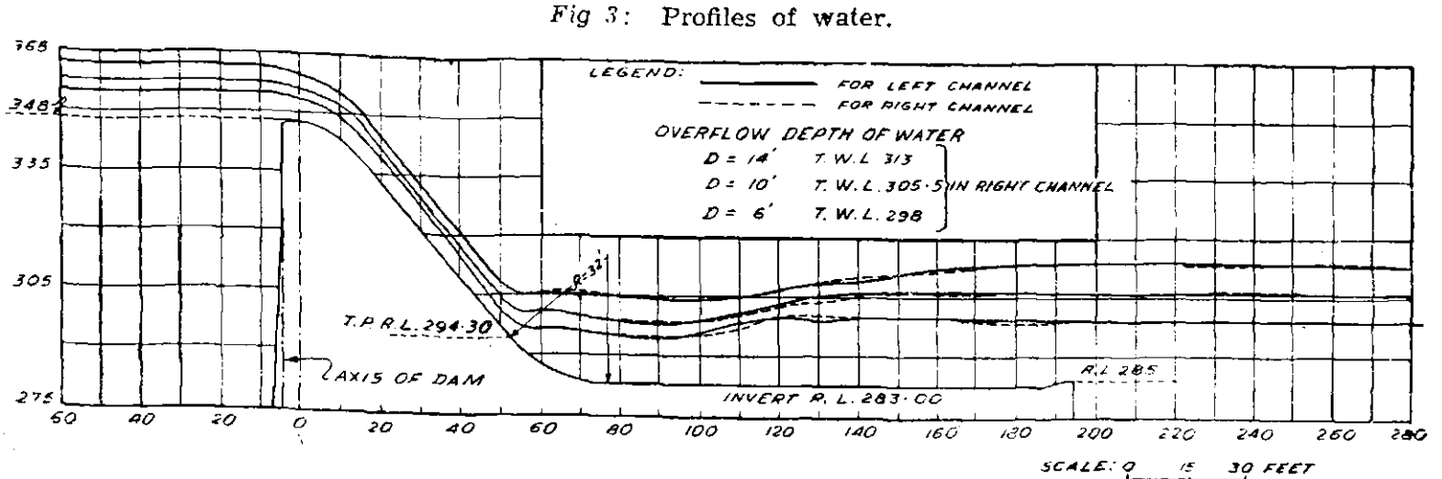

Fig 6: Water profiles; 1/60 scale composite model.

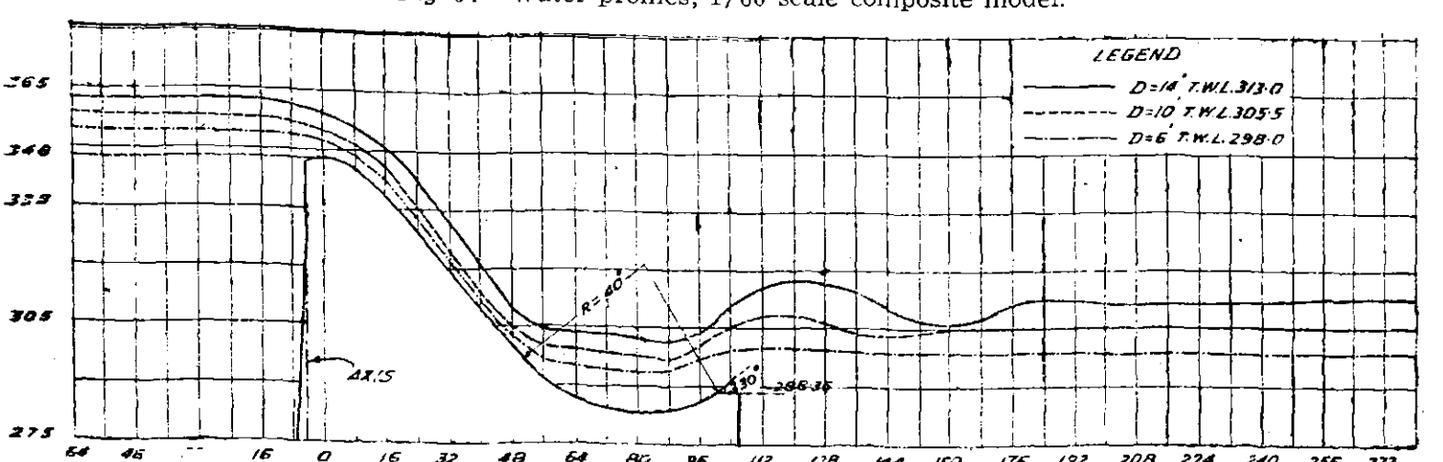

Fig 9: Profiles of water at invert *RL* 283, bucket $R = 40$ *ft* exit angle 30°; 1/24 scale sectional model.

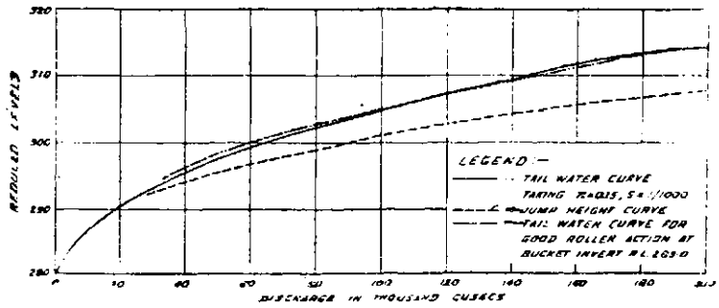

Fig 4

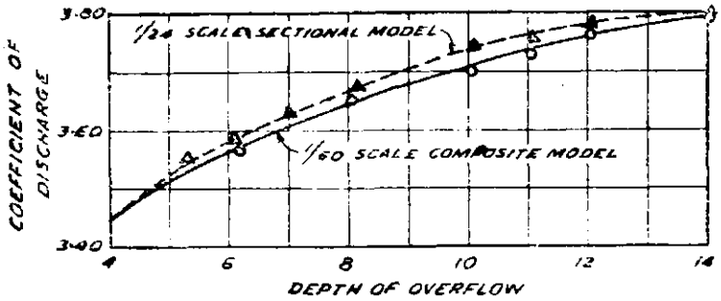

Fig 8

bucket at invert *RL* 283. A 40 *ft* radius upturned bucket at invert *RL* 283 with exit angle 30° was then tested.

Fig 9 shows the profiles of water for 14, 10 and 6 *ft* overflow depths with corresponding *TWLs*. *Photos 54* and 55 show the roller action of bucket for 14 and 10 *ft* overflow depths with corresponding *TWLs*. *Fig 10* shows the pressure distribution (minimum pressures) on bucket and end sill. The experiment showed that the 40 *ft* upturned bucket at invert *RL* 283 was not satisfactory, little lowering the invert *RL* would work satisfactory.

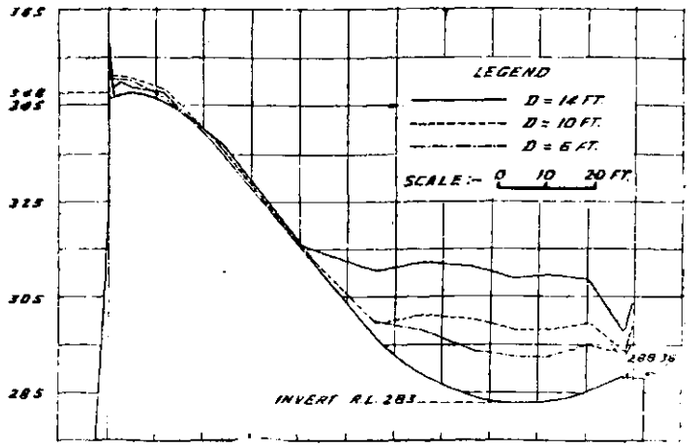

Fig 10: Pressures along the spillway at invert *RL* 283, exit angle 30°;

As the extrapolated values of tail water rating curve do not permit more fluctuations and as during the visit of Executive Engineer, Bhadar Irrigation Project for discussions it was mentioned that the work has already started and is in progress, the hydraulic jump apron was considered suitable.

The *CDO* design as tested worked out to be satisfactory. The design is subject to minor changes in protective works on downstream, depending upon the availability of rock on right end span of spillway. Further experiments are in progress.

IV. Koyna Sluice, Koyna HE Project

In continuation of the previous tests (*ibid* 1958), supplementary experiments were performed to observe the flow conditions, discharging capacity, and pressure distribution in the entrance bellmouth and conduit of the Koyna Sluice. The tests were made with different openings of the service gate, for reservoir water levels of *KRL* 2100 (640.080 *m*), *KRL* 2060 (627.888 *m*) and *KRL* 2020 (615.696 *m*). The upstream maximum reservoir level of *KRL* 2165 (659.892 *m*) corresponding to the final stage, was also tested, for the present sluice profile. Photos show the 1/16 scale model fabricated in perspex.

With the *modified entrance bellmouth design*, (*figs 1, 2* and *2a*) and sluice length corresponding to 73,000 *m cft* (2067.126 m^3) section. tests with different reservoir water levels, were conducted to observe pressures, under different conditions, including the case, when the air vent just stopped functioning.

2. Experiments with modified design

Series I: *Sloping invert corresponding to final stage* : *No outlet constriction.*—The air vent as reproduced in the model, is shown in *fig 2a*. *Fig 3* gives a typical profile, showing the pressure distribution, in entrance bellmouth, and in sluice conduit system, for critical service gate opening of 98 *percent* for reservoir water level ≡ *KRL* 2100 (*KRL* 640.08 *m*).

The local negative pressures observed in the roof, at a section, just upstream of air vent, and downstream of service gate, corresponding discharges, and gate openings, at the different reservoir water levels, are given in *table 1*.

It was observed, in these preliminary experiments that the highest equivalent local negative pressure, is of the order of 30 *ft* (9.144 *m*) for reservoir water level ≡ *KRL* 2165 (659.892 *m*) under critical gate opening of 96 *percent*.

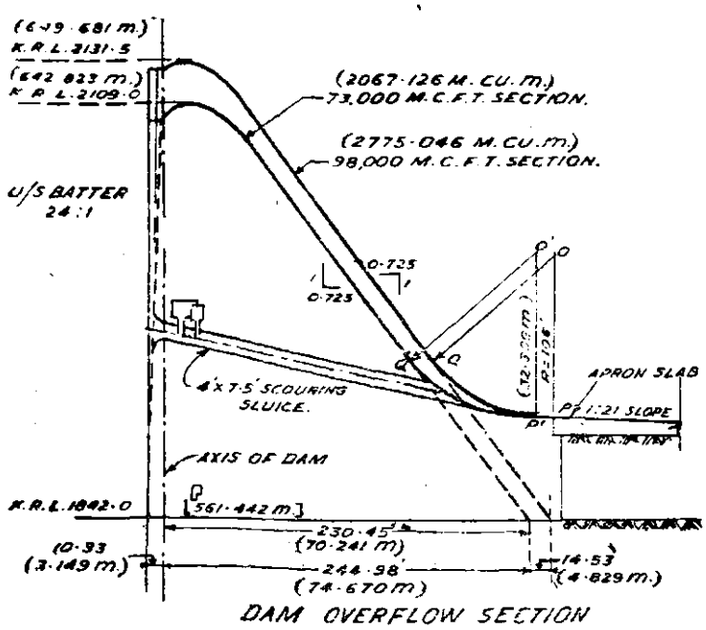

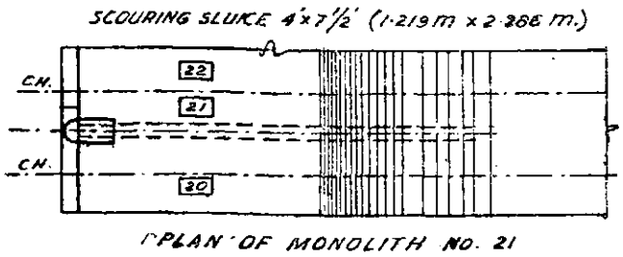

Co-ordinates of bucket points.

Point	73000 *m cft*		98000 *m cft*	
	CH	Level	*CH*	Level
Centre of curvature *O* & *O'*	237·85' 272·497 *m*	2012·46 613·393 *m*	252·83' 77·063 *m*	2011·78 613·190 *m*
Apron tangent point (*P*-*P'*)	232·81' 70·960 *m*	1906·58 581·126 *m*	247·80' 75·529 *m*	1905·87 580·909 *m*
Upper tangent point (*Q* & *Q'*)	151·98' 46·323 *m*	1950·24' 594·433 *m*	167·01' 50·945 *m*	1949·53 594·226 *m*

Fig 1 : Dam overflow section and plan of sluice monolith

Series II : Sluice invert, provided with transition, at outlet to the profile corresponding to Stage I (fig 4a). Also no constriction at the outlet.—The air vent, as used in the model, is shown in *fig 2a*. *Fig 5* gives a typical profile, showing the pressure distribution, in entrance bellmouth, and in sluice conduit system, for critical gate opening of 97.8 *percent* for reservoir water level ≡ *KRL* 2165 (650.892 *m*).

The local negative pressures observed in the roof, at a section, just downstream of service gate and upstream of air vent, corresponding discharges, and gate openings, at the different reservoir water levels, are given in *table 2*.

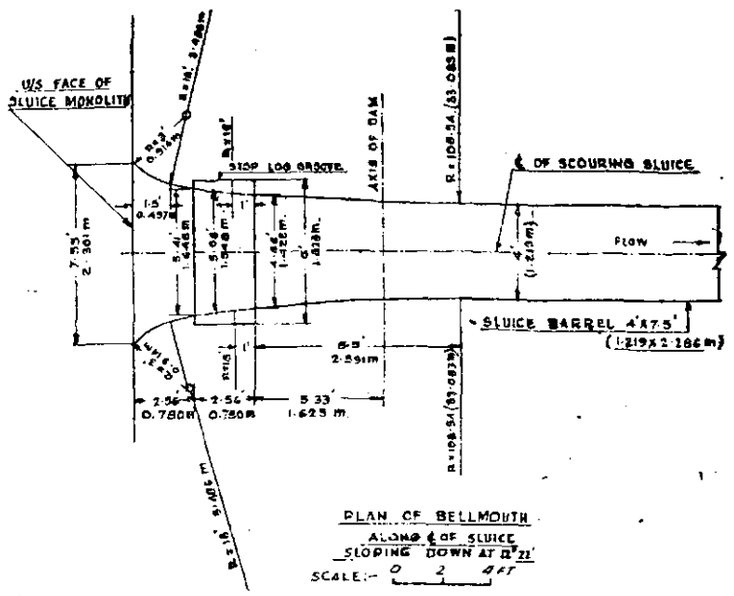

Fig 2

It was observed, that the highest, equivalent local negative pressure, in this series, was of the order of 10 *ft* (3.048 *m*) for reservoir *WL* ≡ *KRL* 2165 (659.892 *m*) under a critical gate opening of 97.8 *percent*.

At this stage in order to test the optimum modifications required, outlet constrictions of 12.25 *percent* and 22.75 *percent* in area were tried in model, to cause sufficient back pressure to improve the local negative pressure, in the roof, just upstream of air vent position, and downstream of service gate.

Series III : 22.75 percent constriction at the outlet [fig 4 b] and also the air vent position same as in series II, fig 2a.—*Fig 6* shows the pressure distribution, under critical gate opening, for the reservoir water levels, equivalent to *KRL* 2165 (659.892 *m*) and *KRL* 2020 (615.696 *m*) respectively. Also *fig 7* shows the pressure distribution for full opening of service gate, for reservoir water levels, of *KRL* 2165 (659.892 *m*) and *KRL* 2020 (615.696 *m*) respectively.

Table 3 gives the local equivalent negative pressures observed in the roof just downstream of service gate, the corresponding critical gate openings, and the discharges observed.

It was observed, that the worst local negative pressure, for this series, was of the order of 4 *ft* (1.219 *m*) only, occurring for critical service gate opening of 93.6 *percent* for reservoir water level ≡ *KRL* 2020 (615.696 *m*).

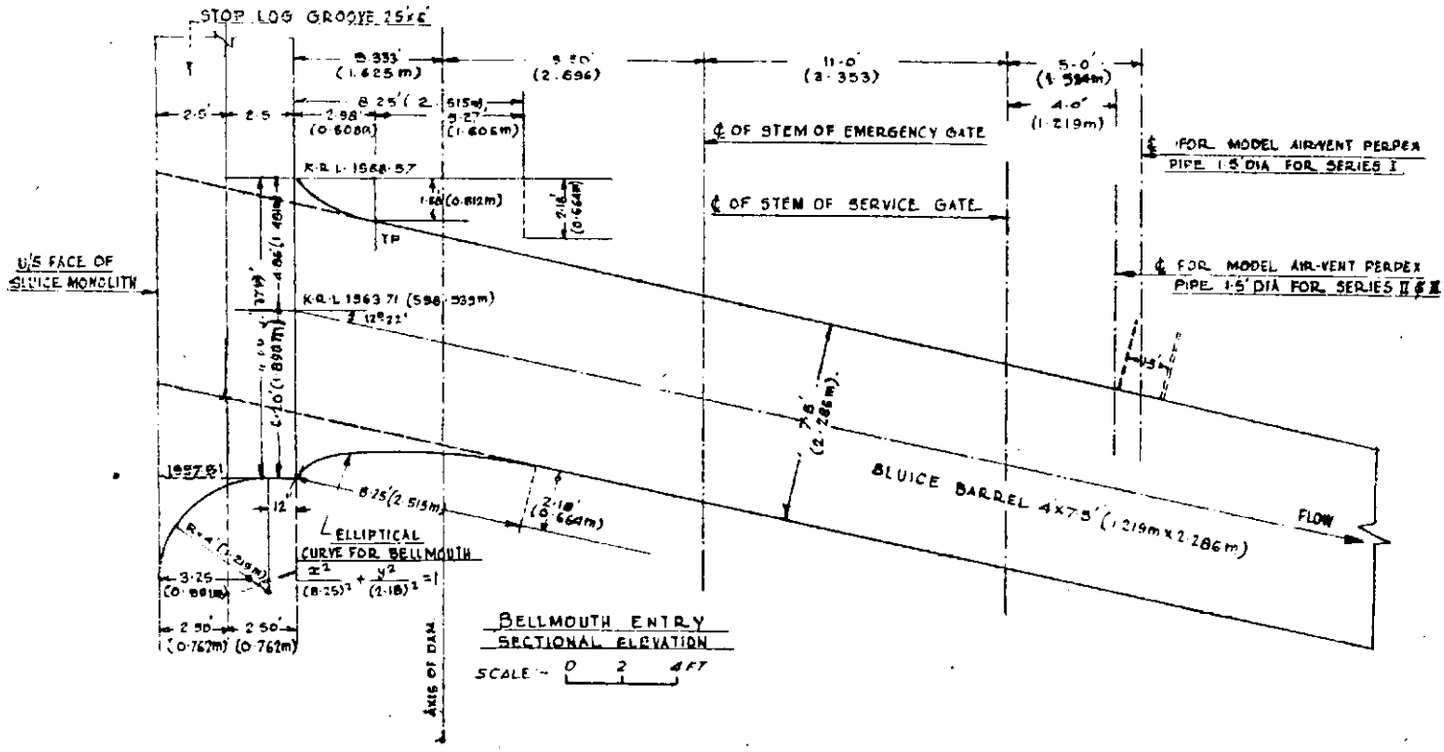

Fig 2a: Details of bellmouth entry (sectional elevation) and model air-vent pipe positions.

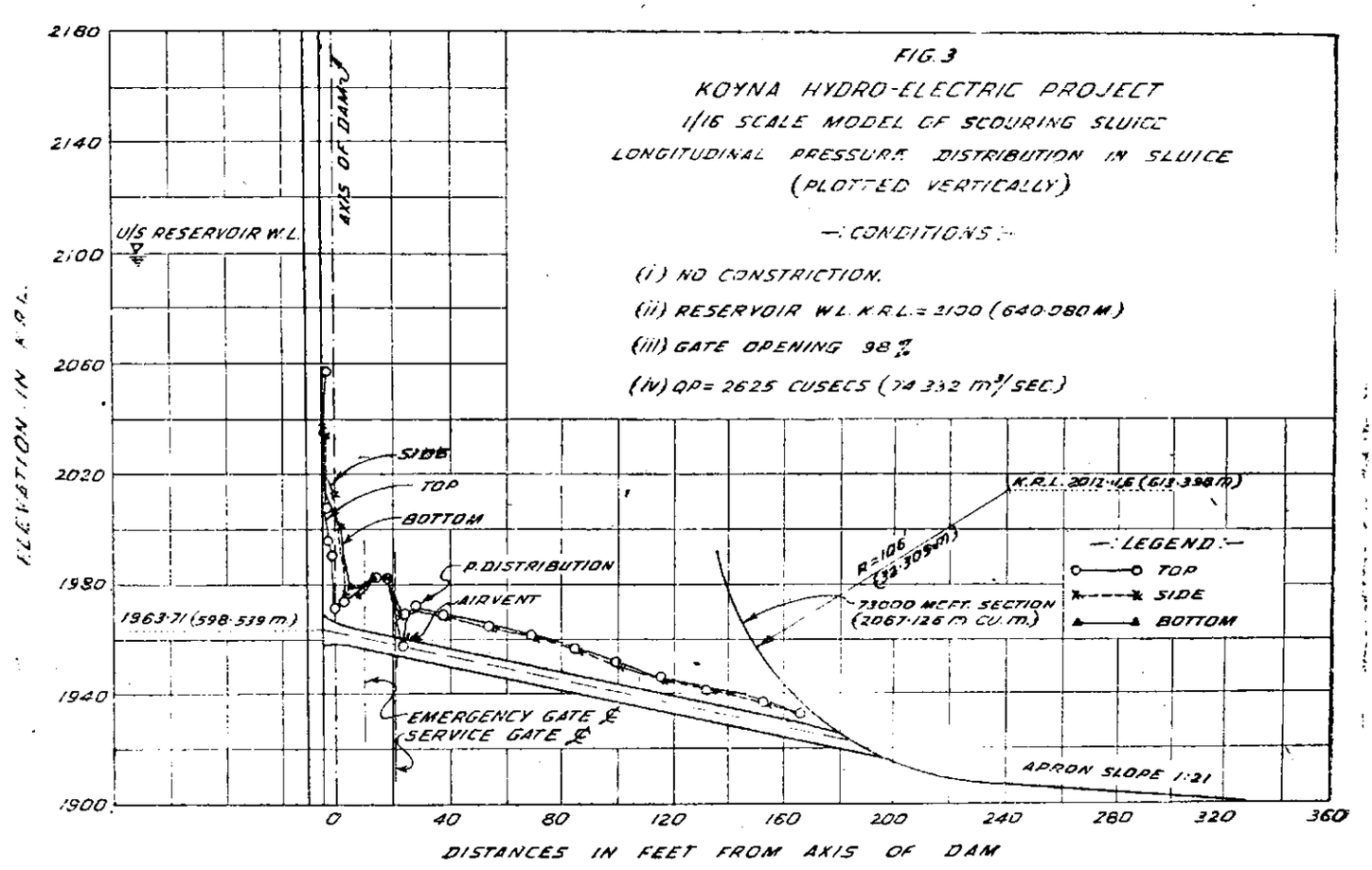

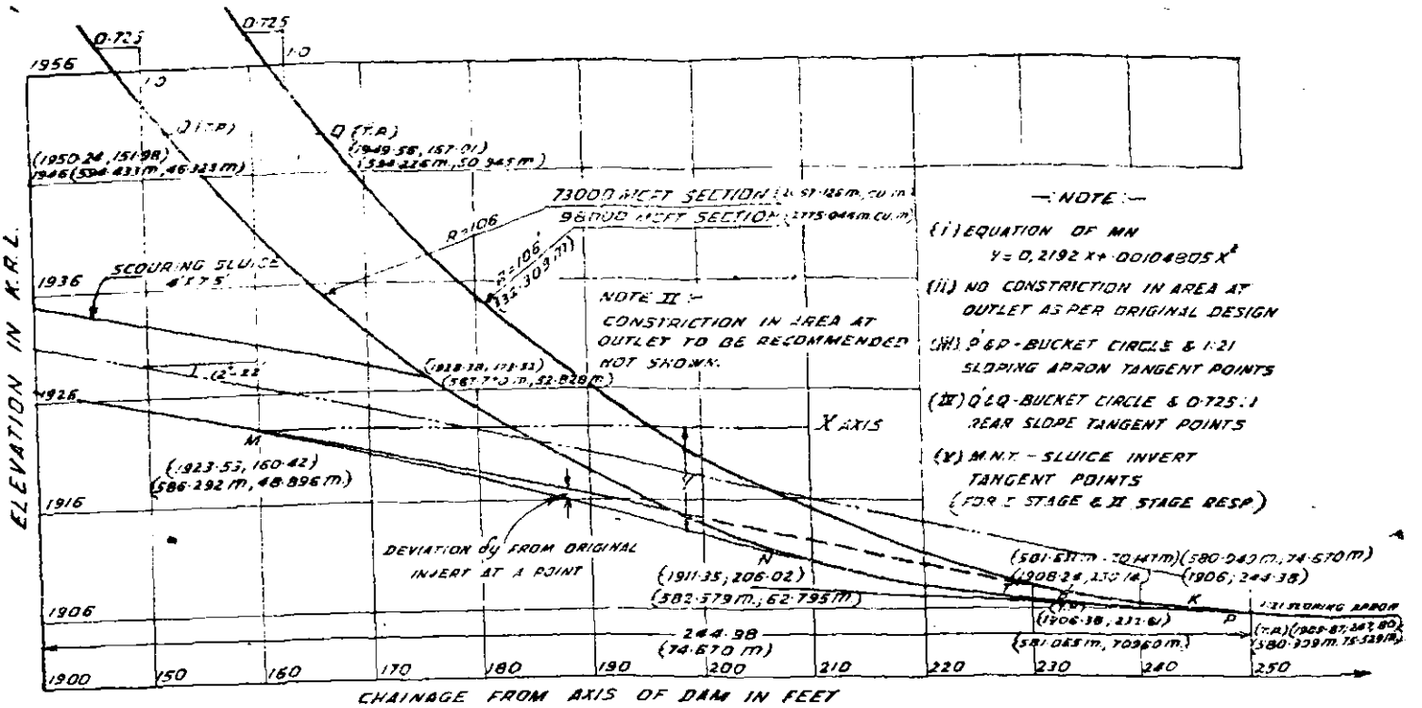

Fig 4a: Details of tail-end parabola at invert of sluice for 73,000 *m* cft section.

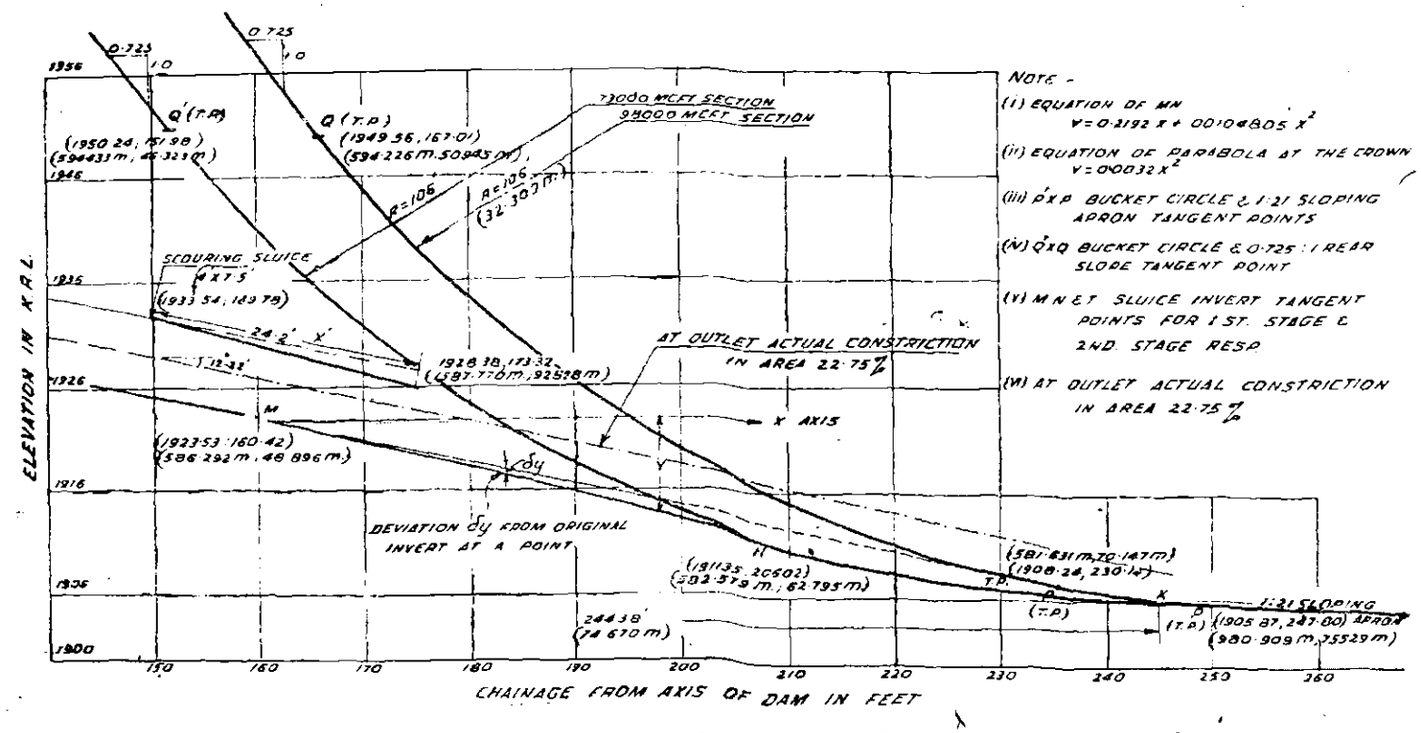

Fig 4b: Details of tail-end parabola at invert and at crown for 73,000 *m* cft section.

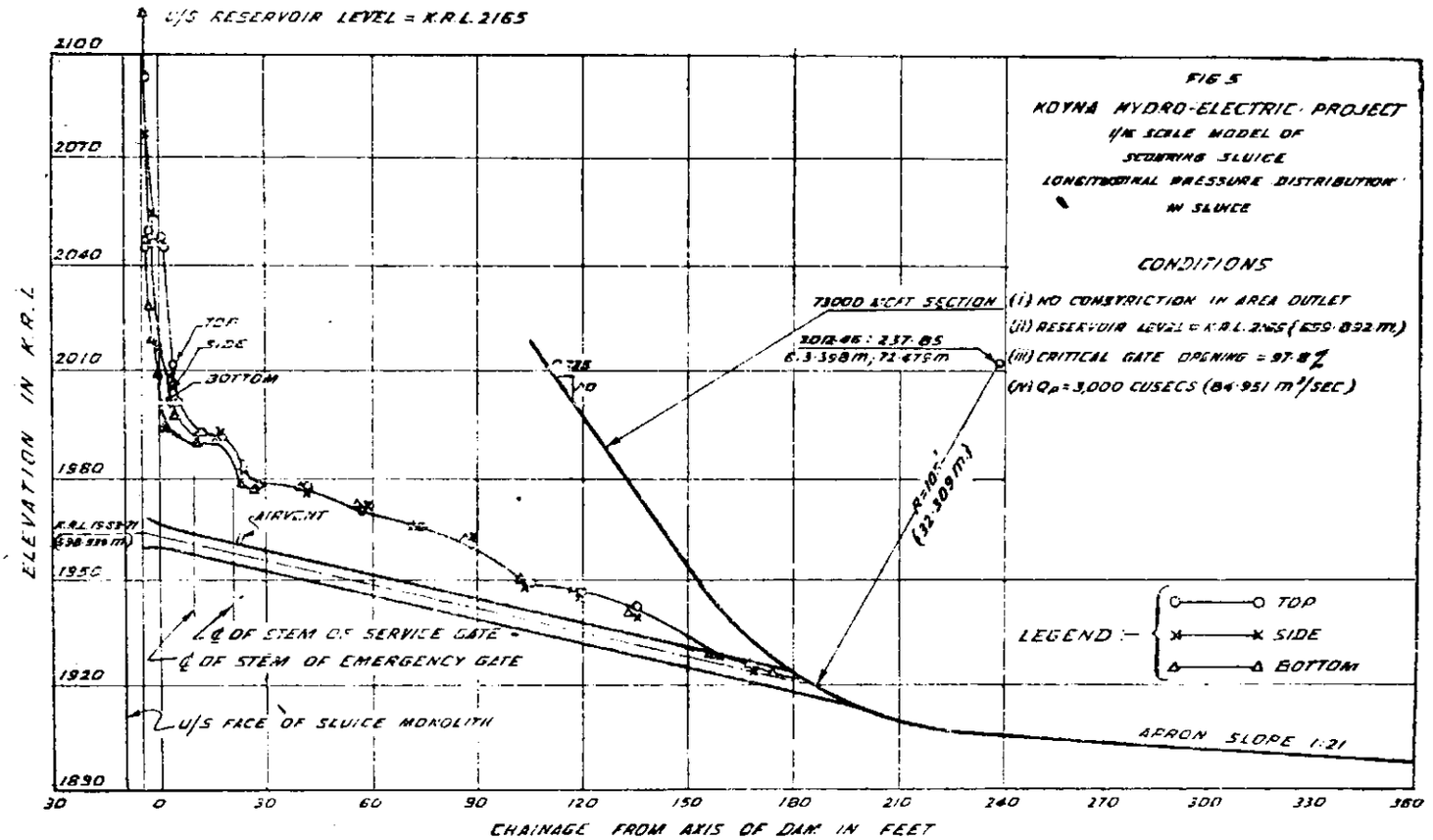
U/S RESERVOIR LEVEL = K.R.L. 2165
ELEVATION IN K.R.L.
CHAINAGE FROM AXIS OF DAM IN FEET
TOP
SIDE
BOTTOM
AIRVENT
73000 M.CFT SECTION
℄ OF STEM OF SERVICE GATE
℄ OF STEM OF EMERGENCY GATE
U/S FACE OF SLUICE MONOLITH
APRON SLOPE 1:21
LEGEND :-
TOP
SIDE
BOTTOM
FIG 5
KOYNA HYDRO-ELECTRIC PROJECT
1/16 SCALE MODEL OF
SCOURING SLUICE
LONGITUDINAL PRESSURE DISTRIBUTION
IN SLUICE
CONDITIONS
(i) NO CONSTRICTION IN AREA OUTLET
(ii) RESERVOIR LEVEL = K.R.L. 2165 (659.832 m.)
(iii) CRITICAL GATE OPENING = 97.8%
(iv) Qd = 3,000 CUSECS (84.951 m³/SEC.)

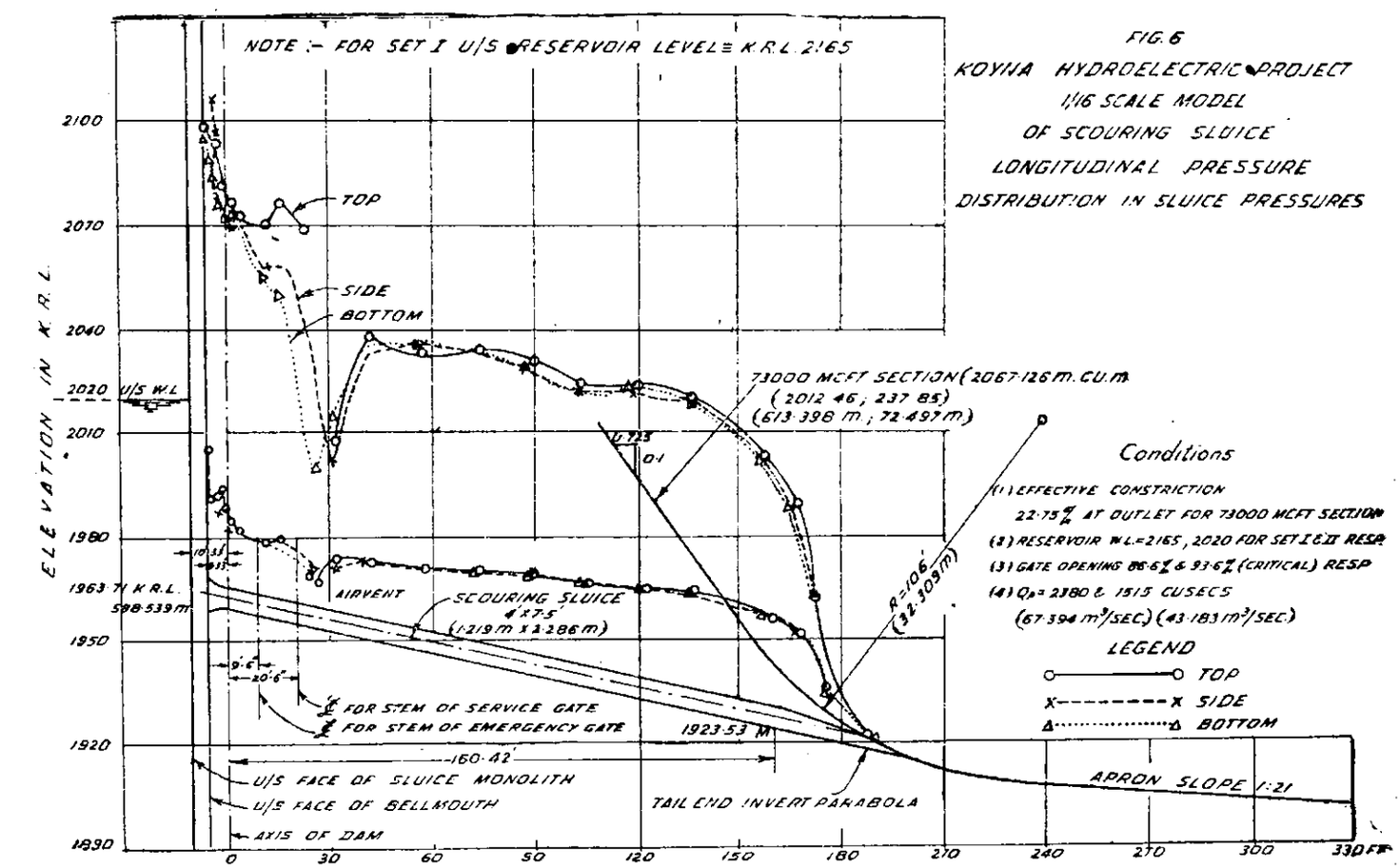
NOTE :- FOR SET I U/S RESERVOIR LEVEL = K.R.L. 2165
ELEVATION IN K.R.L.
TOP
SIDE
BOTTOM
U/S W.L
AIRVENT
SCOURING SLUICE
73000 MCFT SECTION (2067.126 m. CU.m.
(2012.46 ; 237.85)
(613.398 m ; 72.497 m)
℄ FOR STEM OF SERVICE GATE
℄ FOR STEM OF EMERGENCY GATE
160.42'
U/S FACE OF SLUICE MONOLITH
U/S FACE OF BELLMOUTH
AXIS OF DAM
TAIL END INVERT PARABOLA
APRON SLOPE 1:21
Conditions
(1) EFFECTIVE CONSTRICTION
22.75% AT OUTLET FOR 73000 MCFT SECTION
(3) RESERVOIR W.L.=2165', 2020 FOR SET I & II RESP.
(3) GATE OPENING 86.6% & 93.6% (CRITICAL) RESP.
(4) Qd = 2380 & 1515 CUSECS
(67.394 m³/SEC.) (43.183 m³/SEC.)
LEGEND
TOP
SIDE
BOTTOM
FIG. 6
KOYNA HYDROELECTRIC PROJECT
1/16 SCALE MODEL
OF SCOURING SLUICE
LONGITUDINAL PRESSURE
DISTRIBUTION IN SLUICE PRESSURES

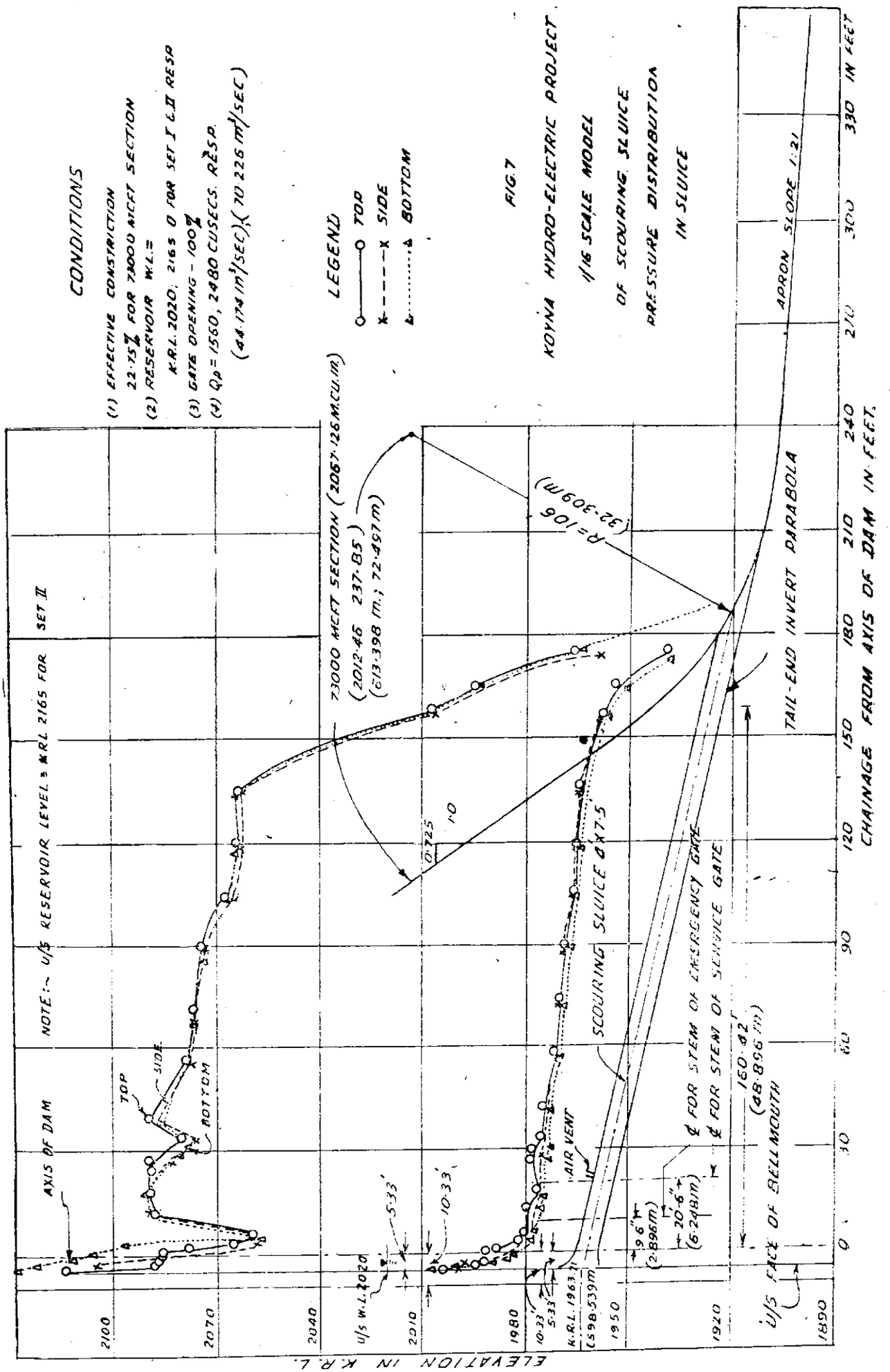
CONDITIONS
(1) EFFECTIVE CONSTRICTION 22·75% FOR 73000 MCFT SECTION
(2) RESERVOIR W.L.= K.R.L. 2020, 2165 & FOR SET I & II RESP.
(3) GATE OPENING - 100%
(4) Qb = 1560, 2480 CUSECS. RESP. (44·174 M³/SEC), (70·226 M³/SEC)
LEGEND
TOP
SIDE
BOTTOM
FIG. 7
KOYNA HYDRO-ELECTRIC PROJECT
1/16 SCALE MODEL
OF SCOURING SLUICE
PRESSURE DISTRIBUTION
IN SLUICE
NOTE:- U/S RESERVOIR LEVEL = K.R.L. 2165 FOR SET II
AXIS OF DAM
TOP
SIDE
BOTTOM
73000 MCFT SECTION (2067·126 MCU.M.)
(2012·46 237·85')
(613·398 m.; 72·467m)
R=106' (32·309m)
0·725
1·0
SCOURING SLUICE 6'X7·5'
AIR VENT
5·33'
10·33'
U/S W.L. 2020
K.R.L. 1963·1'
(598·539m)
9·6" (2·896m)
20·6" (6·248m)
℄ FOR STEM OF EMERGENCY GATE
℄ FOR STEM OF SERVICE GATE
160·42'
(48·896m)
TAIL-END INVERT PARABOLA
APRON SLOPE 1:21
U/S FACE OF BELLMOUTH
ELEVATION IN K.R.L.
CHAINAGE FROM AXIS OF DAM IN FEET.
2100
2070
2040
2010
1980
1950
1920
1890
0
30
60
90
120
150
180
210
240
270
300
330 IN FEET

Tables 1, 2 and 3

Reservoir level in *KRL*		Gate opening	Discharge Q_p		Negative pressure observed on tube upstream of air vent in *ft.* of water		Remarks
ft	*m*	%	*cfs*	*m3/sec*	*ft*	*m*	
			Series I: Sloping invert corresponding to final stage: No outlet constriction				
2165	659·89	96	3000	84·95	−30	−9·14	Critical gate opening the flow at air vent pipe just pressurised.
2100	640·08	98	2625	74·33	−15	−4·57	
2060	627·89	100	2315	65·55	−15	−4·57	
2020	615·70	100	1860	52·67	−14	−4·27	Air vent functioning.
2165	659·89	100	3150	89·20	...	...	Fully pressurised flow.
2020	615·70	100	1860	52·67	−14	−4·27	Air vent functioning.
			Series II: No constriction in area at outlet—invert parabola at the tail end				
2165	659·89	97·8	3000	84·95	−8 to −10	−2·44 to −3·05	Critical gate opening the flow at air vent pipe just pressurised with fluctuations.
2100	640·08	98·9	2625	74·33	−6 to −8	−1·83 to −2·44	
2060	627·89	100·0	2275	64·42	Do.	Do.	Air vent functioning.
2020	615·70	100·0	1830	51·82	Do.	Do.	
2165	659·89	100·0	3150	89·20	...	...	Fully pressurised flow.
2020	615·70	100·0	1830	51·82	−6 to −8	−1·83 to −2·44	Air vent functioning.
			Series III : 22·75 % constriction in area at outlet.				
2165	659·89	86·6	2380	67·39	+4 to +6	+1·22 to +1·83	Critical gate openings in all cases.
2100	640·08	89·9	2065	58·47	0 to +4	0 to +1·21	
2060	627·89	91·5	1850	52·39	−1 to −3	−0·30 to −0·91	
2020	615·70	93·6	1525	43·18	−3 to −5	−0·91 to −1·52	
2165	659·89	100·0	2480	70·23			Fully pressurised flow.
2020	615·70	100·0	1560	44·17			

3. Discussion of results

With full gate opening, the discharging capacity and overall pressure distribution are generally satisfactory for different reservoir water levels. However, local high negative pressures were observed in the roof, at a section just downstream of the service gate and upstream of air vent, under critical gate openings. The constrictions at the outlet tried in the model showed, that a 22.75 *per-cent* outlet constriction improved the local negative pressure, to a safe value, causing sufficient back pressure. With this constriction, the minimum discharge requirements, of the Project authorities are also satisfied.

Some further revision of the bellmouth design, has been received from the Project, and tests are in progress.

14. Hydraulic model studies of surge tanks

Sharavathi HE Project

THE SHARAVATHI river rises on the eastern slopes of the Western Ghats near Amburthirtha in the North-West corner of Thirthahally Taluka in Shimoga District. The river flows through the Western Ghats, and empties itself into the Arabian sea, after flowing through a short length of 82 *miles* (131.97 *km*). The total drainage area of the river is 1017 *sq miles* (2634.03 *sq km*). This area is sparsely populated and subjected to very heavy rainfall. The average annual yield as estimated over a period of 14 years from 1944-45 is 1,78,000 *m cft* (5097 million m^3 of which nearly 70 *percent* is realised during the months of July and August.

The river flows for about 64 *miles* (103 *km*) in hilly gorge and then drops down vertically by about 836 *ft* (254.313 *m*) creating a natural fall of great beauty known as the Jog Falls.

The existing Mahatma Gandhi Hydroelectric Station with an installed capacity of 1,20,000 *kw* makes use of a regulated flow of 1150 *cfs* (32.57 m^3/sec) which is roughly 16 *percent* of the available average yield. It is this balance of 84 *percent* that is proposed to be utilised by the Sharavathi Hydroelectric Project (*fig 1*).

2. Salient features

The project is proposed to be completed in several stages; ultimately ten units of 89,100 *kw* each will be installed utilising the full yield of the river at a site about three miles downstream of the present Mahatma Gandhi Hydroelectric Station. The gross head available at the site is 1525 *ft* (464.82 *m*) which is about 300 *ft* (91.44 *m*) more than that at the Mahatma Gandhi Hydroelectric Station site.

(i) Formation of a storage reservoir to store 1,56,000 *m cft* (4417.42 million m^3) of water by constructing a dam 194 *ft* (59.131 *m*) above foundations, at Linganamakki.

(ii) Construction of a power channel from the main dam to Talkalale balancing reservoir of a length of 14,190 *ft* (4325.112 *m*) and a free flow tunnel 1980 *ft* (603.504 *m*) long designed for a discharge of 6200 *cfs* (175.56 m^3/sec).

(iii) Formation of a balancing reservoir across Talkalale stream by constructing a dam 198 *ft* (60.35 *m*) above the river bed.

(iv) Construction of two pressure tunnels 22 *ft* (6.706 *m*) diameter and about 3400 *ft* (1036.32 *m*) long each, with suitable approach cut 2000 *ft* (609.6 *m*) long. Each tunnel is designed for 5200 *cfs* (147.25 m^3/sec).

(v) Construction of a vertical surge tank 50 *ft* (15.24 *m*) in diameter at the end of each of the two pressure tunnels.

(vi) Penstocks, Powerhouse, receiving stations *etc* (*figs 2, 3* and *4*).

In the first stage now in progress for completion by first quarter of 1963, only two units of 89,100 *kw*, each are proposed to be installed. The second stage contemplates installation of five more such units.

The water conductor system from the Talkalale balancing reservoir to the power house has been designed for a maximum discharge of 10,400 *cfs* (294.494 m^3/sec). In view of the huge capacity of the station of 891 *mW* it is proposed to have two tunnels taking off from the balancing reservoir to feed two independent surge tanks. This would facilitate inspection of the tunnel without complete shut down of the station. Each surge tank is a simple vertical shaft 50 *ft* (15.24 *m*) in diameter feeding five penstocks 8 *ft* (2.438 *m*) diameter each.

3. Terms of reference

The inter-play of various design factors was taken up in the complete design calculations made for the surges, by the project authorities under the most severe design assumptions envisaged. To check the various features, model tests are proposed for the surge system with the following terms of reference by the Project authorities:

(i) To check maximum and minimum water levels reached in the surge tanks under critical upsurge and downsurge conditions analysed by the Project authorities.

(ii) To eliminate or to minimise the formation of various rollers, suction of air into any of the take offs and head race tunnel etc. under steady as well as surging conditions.

(iii) To check and if necessary to modify the shape of the entry of the head race tunnel to surge tanks, shapes of the take offs, alignment of take offs and head race tunnel *etc.*

(iv) To suggest means to ensure uniform flow of water through all the take offs involving minimum loss of head.

(v) (*a*) To find out the time taken for the surges under the worst conditions to die out.

(*b*) To find the period of interval recorded from the moment of instantaneous shut-down, for commissioning the various units safely.

(vi) To estimate the magnitude of water hammer wave entering into the Head Race Tunnel, if any and to minimise it.

(vii) To investigate the stability of the surge tank so as to function successfully under all partial load variations.

(viii) To study the effect of waves in the approach channel due to variations in discharge of the head race tunnel.

(ix) To study any other modifications to improve conditions of flow, to minimise losses and to ensure stability and quick damping of oscillations for all conditions.

4. Design criteria

In view of the importance of the Sharavathi Station in the inter-connected grid system and its sensitivity to variations in load, the following criteria have been adopted in the design of the surge tanks, by the Project authorities.

(A) Worst upsurge to occur under the following conditions:

(i) Talkalale reservoir water level to be at its maximum *viz* 1695.0 (516.636 *m*).

(ii) Friction and other losses in the system to be minimum (n_m) = 0.011)

(iii) The whole station running at full over-load [Q = 5200 *cfs* (147.25 m^3/sec) per surge tank] is shut off instantaneously

(iv) No spill-over is allowed in the design.

(B) The worst downsurge to occur under the following conditions:

(i) The reservoir to be at its minimum water level *viz* 1690 (515.112 *m*)

(ii) The friction and other losses in the system to be maximum (n_m = .016)

(iii) Load on five units fed by each of the surge tanks is all thrown off instantaneously when running at full overload capacity of 5,34,500 *kW*, corresponding to a discharge of 5200 *cfs* (147.25 m^3/sec) and load corresponding to a capacity of one unit, which is 1,06,900 *kW*, is accepted, instantaneously at the worst moment of the swing *ie* when the velocity in the head race tunnel is minimum.

(iv) Under these conditions the level of the most severe downsurge is to be at least 15 *ft* (4.57 *m*) over the crown of the take offs and above the crown of the tunnel inlet.

5. Constant power output curves and graphical analysis of surges

The power output is given by the formula.

Output $N = \eta\, w\, Q\, (H - kV^2)$ *ft lbs/sec*

Where η = turbine efficiency.

W = Wt of water per *cft*

H = gross head on turbines (surge tank WL – nozzle level)

kV^2 = losses in penstocks where V-velocity in tunnel

Q = discharge in *cfs*.

$$N \text{ output in } kW = \frac{A_T \cdot V}{C} (H - kV^2)$$

A_T = area of tunnel.

With Talkalale *WL* of 1690 (515.112 *m*) and maximum friction in the tunnel, taking 5200 *cfs* (147 25 m^3/sec) as the necessary discharge for producing an output of 5,34,500 *kW* including overload capacity, the value of *C* works out to be 13.99.

With this formula, the discharges necessary for various surge tank water levels, for the outputs of 5 turbines *ie* 5,34,500 *kW* were calculated. The corresponding discharges for outputs of 1, 2 and 3 turbines were also computed. *Fig* 5 shows these curves of the surge tank water levels and discharges for various constant power outputs.

The computations of the maximum and minimum surges under the design conditions have been done by arithmetical step-by-step method and by graphical method. The results of graphical computations are shown in *fig 6*. *Table 1* shows the maximum and minimum levels during surge under different load changes.

6. Basic design equations

The governing equations of flow in the surge-system as provided in the *SHEP* can be written as:

$$\frac{Le.}{g} \cdot \frac{dV}{dt} = -Z - hf. \quad \text{... Equation of momentum}$$

$$a \cdot V = A. \frac{dZ}{dt} + qp. \quad \text{... Equation of continuity}$$

where

Le = equivalent length of the head race tunnel

q = representative area of cross-section of the *HRT*

V = velocity in the cross section a of the *HRT*

g = acceleration due to gravity

Z = water levels in the surge measured from the steady reservoir level.

A = Area of surge tank

t = time

qp = discharge in penstocks

$$hf = \frac{f \cdot Le \cdot V^2}{2gm} = \frac{n_m^2 Le \cdot V^2}{1{\cdot}486^2 \cdot m^{4/3}}$$

where

m = hydraulic mean radius of the cross-section a

f = friction coefficient

n_m = Manning coefficient

7. Scales adopted

The governing conditions for the model prototype relations, using suffix (s) for the scale, can be written from the above basic equations as:

(1) from frictional loss scale:

$$\frac{n_s^2 \cdot L_s \cdot V_s^2}{D_s^{4/3}} \times \frac{1}{Z_s} = 1$$

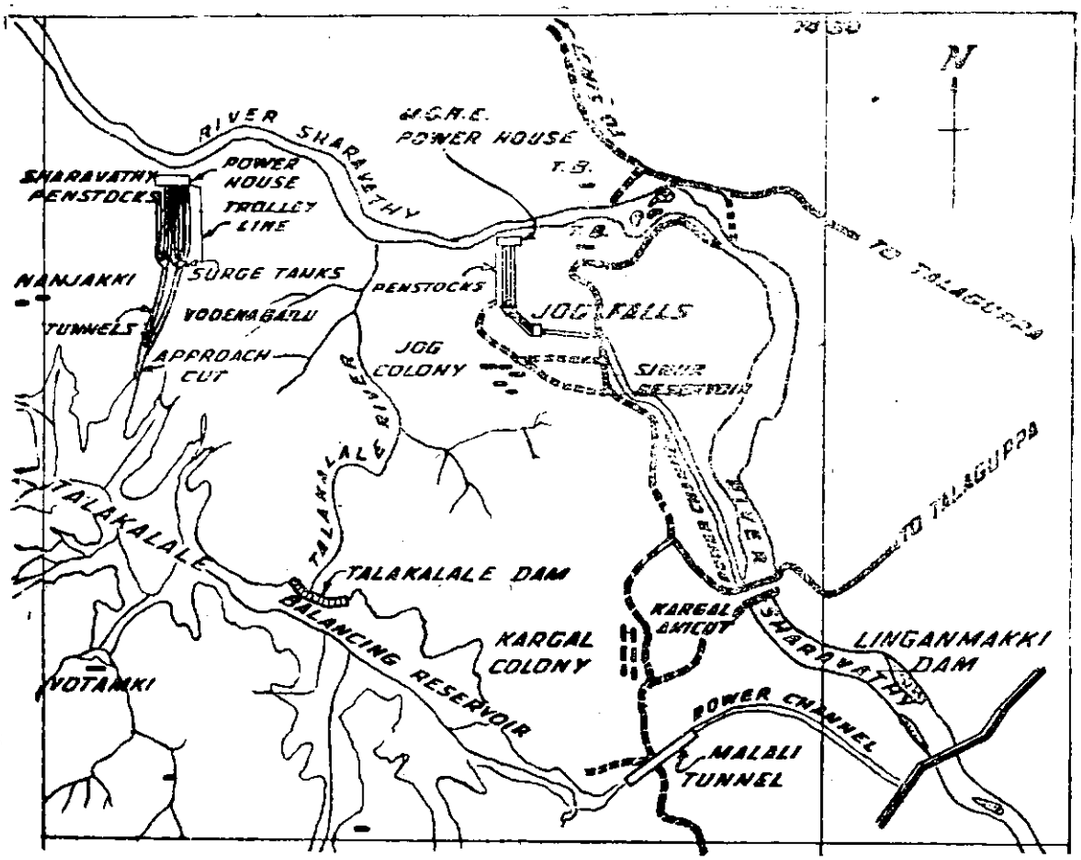

Fig 1: Sharavathi valley hydro-electric project layout plan.

(2) from acceleration scale:

$$\frac{V_s L_s}{T_s} = Z_s$$

(3) Storage scale:

$$\frac{A_s Z_s}{T_s Q_s} = 1$$

From (1), (2) and (3) by rearrangement we get the major deciding scales;

$$\text{(i) } Z_s = \frac{D_s^{10/9}}{n_s^{2/3}} \qquad \text{(ii) } T_s = \frac{Z_s \sqrt{L_s}}{D_s}$$

$$\text{(iii) } V_s = \frac{Z_s^2}{D_s \sqrt{L_s}} \qquad \text{(iv) } Q_s = D^2{}_s \times V_s$$

The diameter scale ($D_s = 22$) was chosen at the ready availability of 12 *in dia.* hume pipes. (.305 *m dia.*). The length scale $L_s = 22$ was decided so as to keep the model geometrically similar for the approach channel and tunnel portion.

The appropriate surge scales for the minimum and maximum friction were based on the friction losses actually obtained in the model. These are discussed along with actual distribution of head losses in the tunnel.

It will be seen that a surge scale of $Z_s = 22$ corresponding to a completely geometrically similar scale is obtained in the model for very nearly the maximum friction case used in the downsurge tests.

8. Model layout

A geometrically similar model to the scale 1/22 decided on the ready availability of the 12 *in* (.305 *m*) *dia* hume pipes for tunnels was constructed with appropriate arrangements for discharge by gravity. The model reproduced the power channel about 2000 *ft* (609.6 *m*) long downstream of Talkalale reservoir, the intake features at the entry of the tunnels, the twin tunnels, 22 *ft dia* (6.7 *m*) each about 3400 *ft* long (1306.32 *m*) and the twin surge tanks 50 *ft dia* (6.7 *m*) each with five take offs.

The pressure tunnels are reproduced by 12 *in* (.305 *m*) *dia* hume pipe incorporating the bends *etc.* The surge tanks are partly of steel and partly of masonry with perspex windows to observe the inside flow conditions.

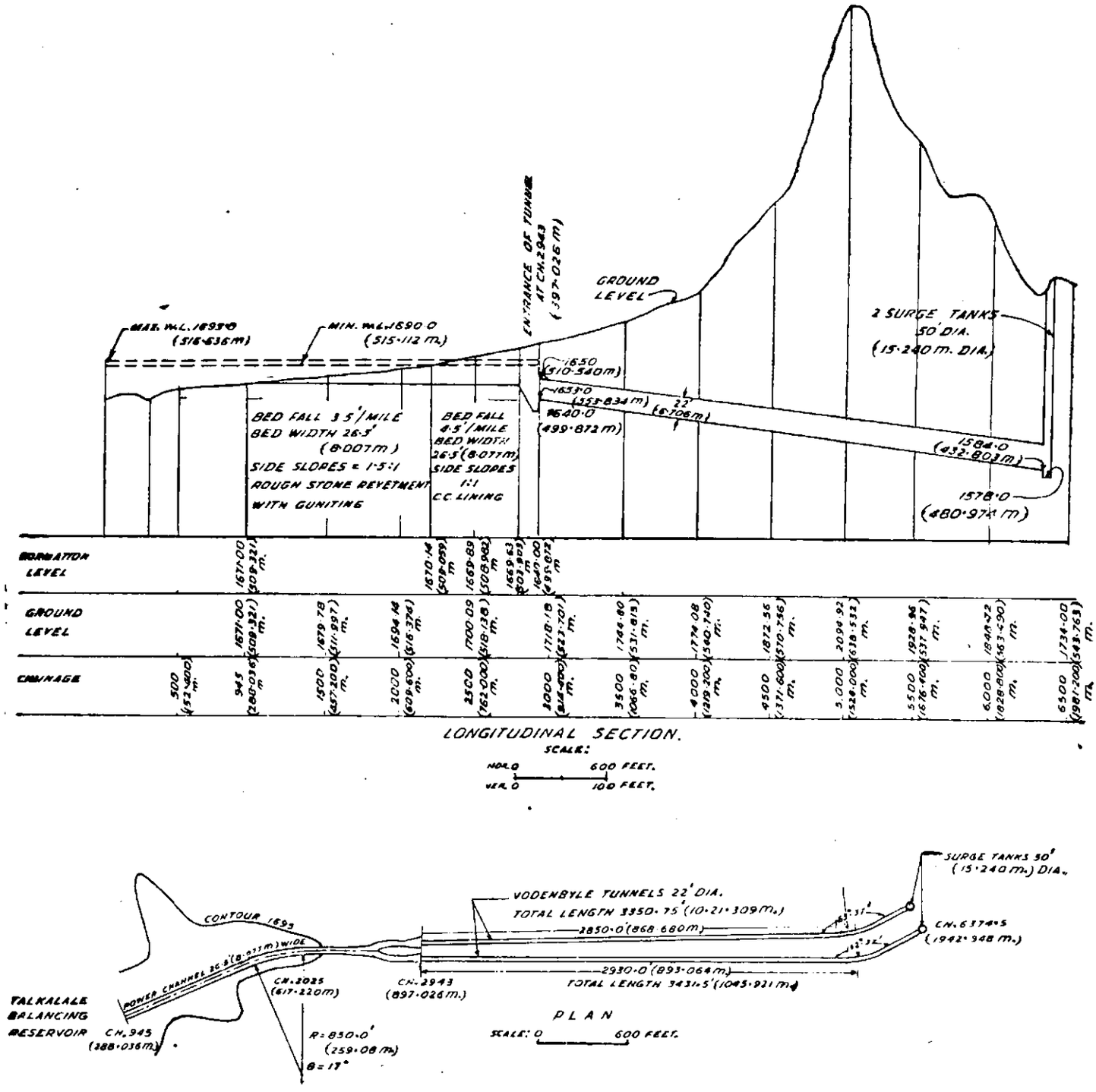

Fig 2: Plan and L-section of power channel tunnels and surge tanks.

The five take-offs from each surge tank in steel and perspex lead to a common pressure chamber and then to a 8 *in dia* sluice valve, to regulate the discharge flowing through each tunnel, which will be ultimately measured on a standing wave flume, one for each surge tank. *Fig 7* (*photos 58* to *61*).

9. Frictional loss tests

To study the frictional coefficient values of the tunnels in the model, water levels at the intake 1 and the surge tank 1 were observed over a complete range of 2000-7000 *cfs* (56.63-198.22 m^3/sec). The total loss of head as observed against the discharge and the design head drop for maximum and minimum friction are plotted in *fig 8*. It is seen that the actual head loss corresponds very nearly to the design head loss with maximum friction.

In order to study the distribution of losses along tunnel 1 in the model, a number of piezometers were installed at controlling points such as entry, exit, either side of bend *etc* and pres-

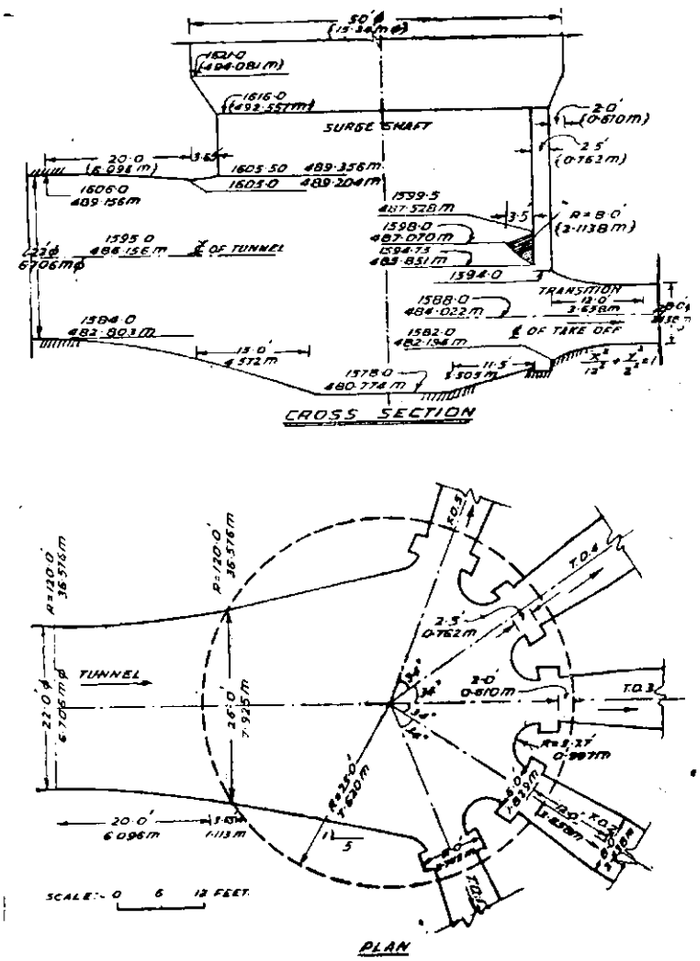

Fig 3: Surge tank details; alternative 1.

sure readings on these piezometers were recorded for the design discharge of 5200 *cfs* (147.25 m^3/sec). The observed pressure drop against the design drop for minimum and maximum friction is shown in *fig 8*. As observed from the graph, the pressure gradient has very nearly the same slope as the one for design maximum friction.

The friction of the tunnel and the surge tank water level in the model thus correspond nearly to the case of the maximum friction and are capable of reproducing precise downsurge conditions.

10. Upsurge tests

Upsurge tests for the minimum friction case were conducted with scales of $Ls=Ds=Hs=22$, $Zs = 43.88$ and $Qs = 4528$, to give the actual friction of tunnel in model. The variations of water levels were taken at both surge 1 and intake 1 for a sudden load rejection of 534.5 mW-0 *ie* 5200 *cfs* (147.247 m^3/sec) to 0 *cfs*. The graphical analysis for this case was also done with intake water level variations accounted for. The following *table 2* shows the values as per project design as against the values actually observed and graphically computed.

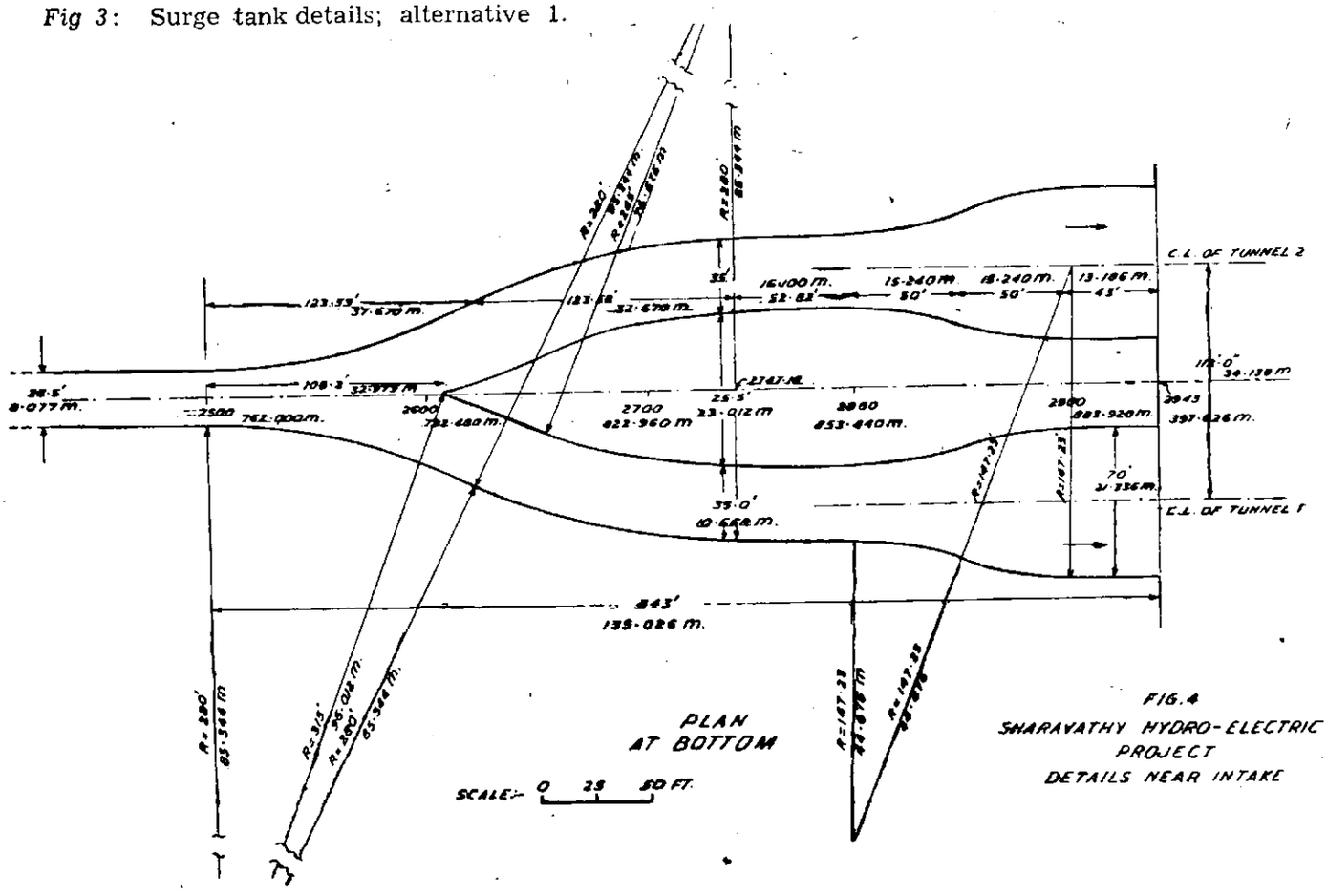

FIG. 4
SHARAVATHY HYDRO-ELECTRIC PROJECT
DETAILS NEAR INTAKE

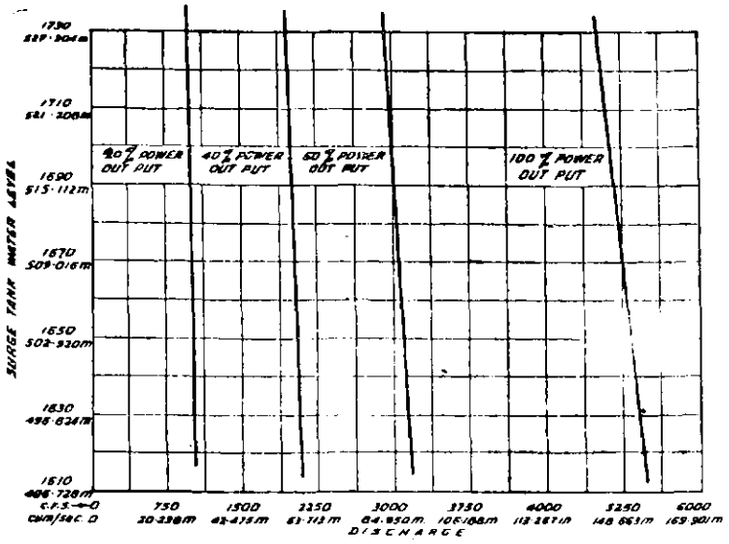

Formula:—$N = [AV/13.99]\ [H - O - 373V^2]$

H = Surge tank WL — Hozzle level. Total power = 5,34,500 KW including 15% over load capacity.

Fig 5: Constant power output curves.

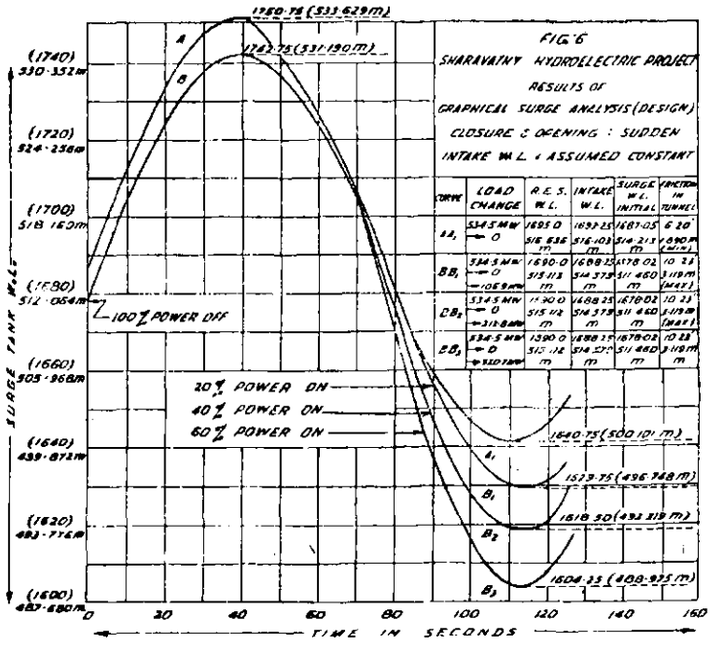

Upsurge tests were also conducted with the geometrically similar scale of 1/22, with the actual friction in tunnel in the model. The variations at surge tank 1 and intake 1 for total load rejection of 534.5 $mW - 0$ *ie* 5200 *cfs* (147.247 m^3/sec) — 0 are shown in *fig 9*.

11. Downsurge tests

The design criterion for the critical downsurge in Talkalale WL = 1690.0 (515.112 m); Tunnel friction loss = maximum; Load change — Instantaneous full load rejection of 5200 *cfs* followed by demand of one unit corresponding to 20 *percent* total power output at the worst moment of the swing *ie* when the tunnel velocity is minimum.

It is found that for the discharge 10,400 *cfs* (294.494 m^3/sec) (corresponding to full load output of 1069 mW including 15 *percent* overload) in the power channel with Talkalale WL at 1690 (515.112 m), the given section of the power channel is inadequate. For this Talkalale WL, the designed channel in the model carried a discharge equivalent to 9600 *cfs* (271.841 m^3/sec) with the

Table 1 :—Sharavathi Hydroelectric Project—Results of Surge Analysis

Load change		Reservoir WL	Intake WL	Frictional drop in tunnel	Initial surge tank WL	Maximum WL during surge		Minimum WL during surge		Min. WL with constant Q corres. to 20 percent 40 percent, 60 percent power in steady state	Diff.
						Arithmetical	Graphical	Arithmetical	Graphical		
534·5 MW—0 (5200 *cfs*—0)	*ft*	1695	1693·25	5·70	1687·55	1752·05	1750·75	1640·66	1640·75	...	...
	m	516·636	516·103	1·737 (min.)	514·365	534·025	533·629	500·073	500·101	...	...
534·5 MW—0—106·9 MW (Const. Q=1040 *cfs*)	*ft*	1690	1688·25	9·73	1678·52	1743·74	1742·75	1628·84	1629·25	...	...
	m	515·112	514·579	2·966 (max.)	511·613	531·492	531·190	496·470	496·595	...	...
534·5 MW—0—106·9 MW (const. power)	*ft*	1690	1688·25	10·23*	1678·02	1743·73	1742·75	1629·20	1629·75	...	...
	m	515·112	514 579	3·118 (max.)	511·460	530·489	531·190	496·608	496·748	...	...
534·5 MW—0—213·8 MW (const. power)	*ft*	1690	1688·25	10·23	1678·02	1743·73	1742·75	1616·52	1618·50	1617·63	+0·93
	m	515·112	514·579	3·118 (max.)	511·460	531·489	531·190	492·715	493·319	493·054	+0·283
534·5 MW—0—320·7 MW (const power)	*ft*	1690	1688·25	10·23	1678·02	1743·73	1742·75	1603·26	1604·25	1605·16	+1·70
	m	515 112	514·579	3 118 (max.)	511·460	531·489	531·190	488·674	488·975	489·253	+0·518

* Frictional loss as modified later by the Project Authorities.

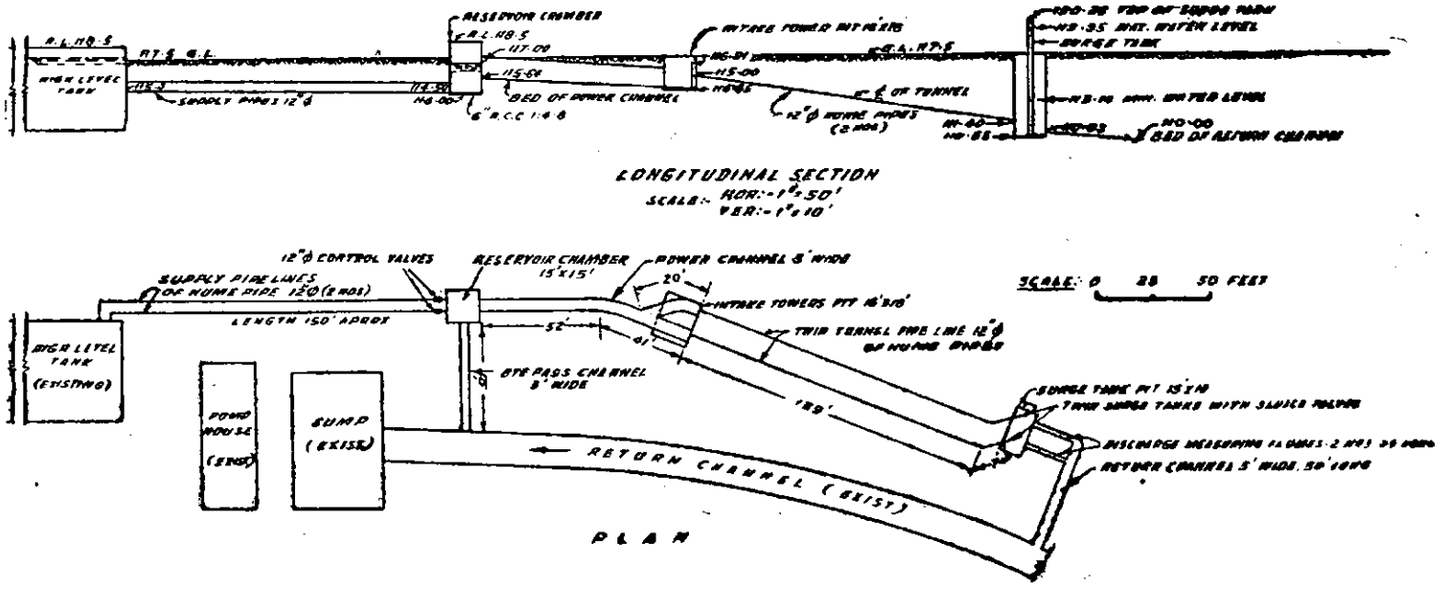

Fig. 7

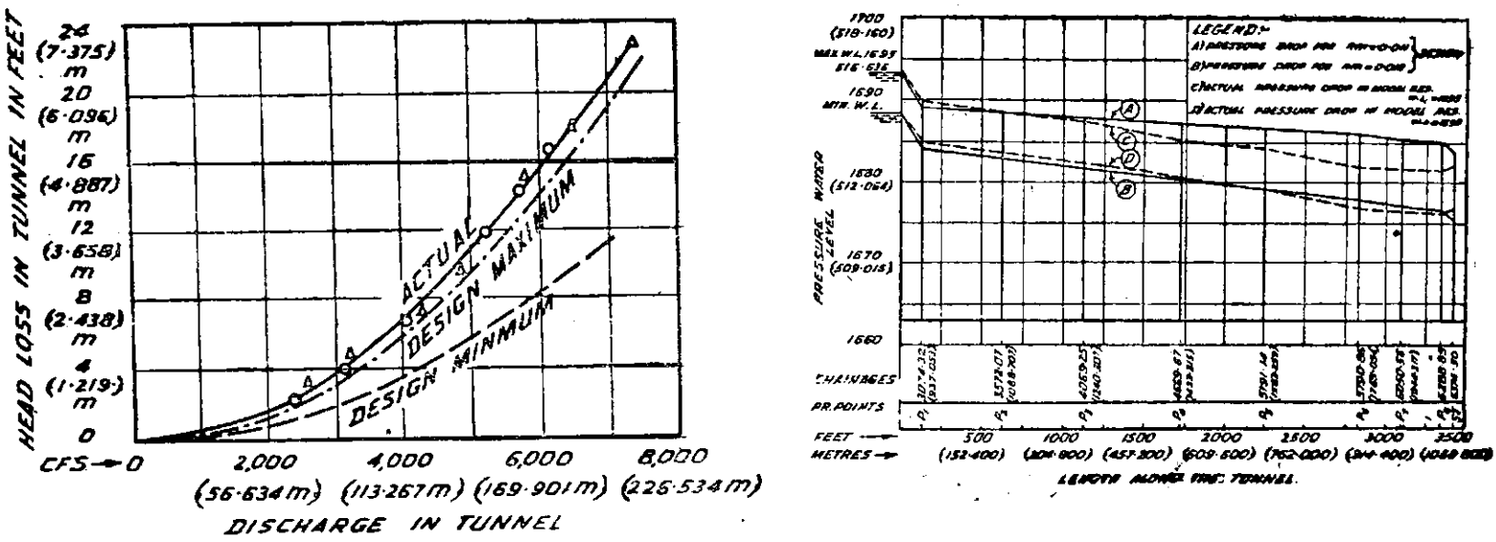

Fig 8: Pressure drop between Reservoir. WL and surge.

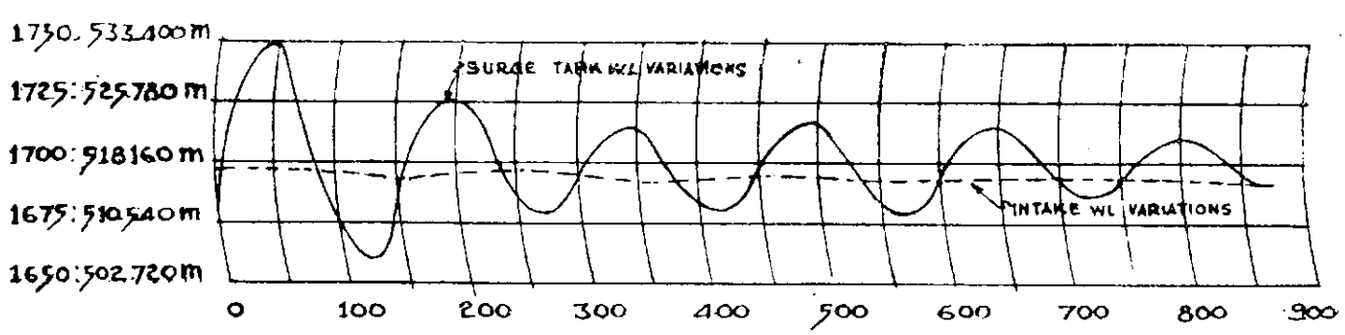

Fig 9 : Upsurge test with actual model friction load change 534.5 *MW*. $\rightarrow 0$

[5200 *cfs* (147.25 m^3/sec)]
Talkalale Reservoir *WL* = 1695.0 (516.63 *m*)
Intake *WL* = 1694.7 (516.545 *m*)
Initial Surge table *WL* = 1684.0 (513.283 *m*) closure sudden.

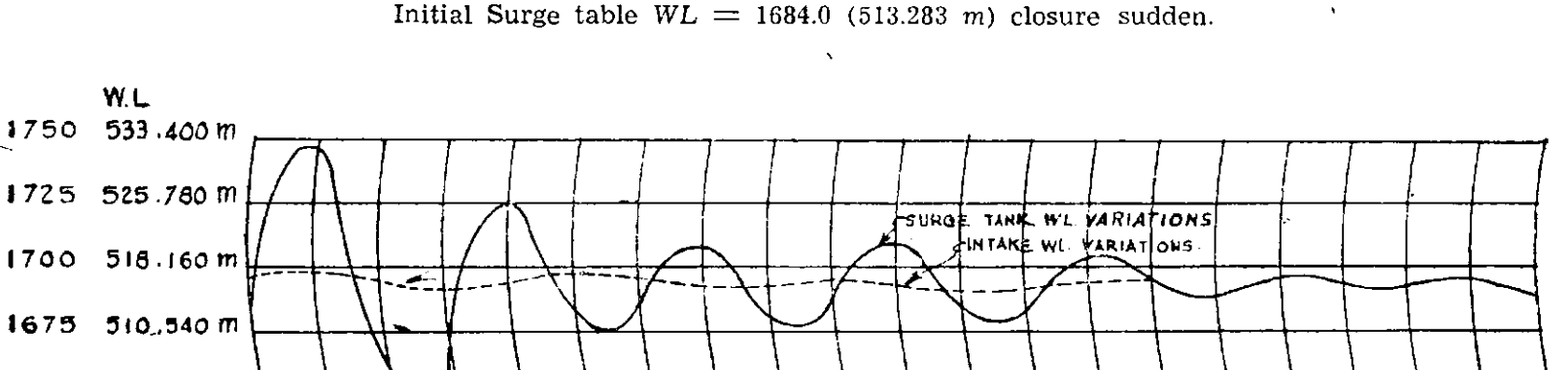

Fig 10: Critical downsurge test load change. 534.5 *MW* $\rightarrow$ 0 $\rightarrow$ 106.9 *MW*

(Average discharge)

Talkalale Reservoir *WL* = 1695.0
Intake *WL* = 1694.7
Initial Surge tank *WL* = 1684.0
Closure and opening : Sudden

Table 2

	Talkalale *WL*	Intake *WL* (initial)	Surge Tank *WL* (initial)	Maximum *WL* in surge tank during up-surge	Max. rise in surge tank over initial steady level Z_{max}
Project Analysis ...	1695.0 (516.636 *m*)	1693.25 (516.103 *m*)	1687.55 (514.365 *m*)	1752.05 (534.025 *m*)	58.8 (17.922 *m*)
Graphical Analysis (*CWPRS*)	,,	1694.9 (516.606 *m*)	1689.2 (514.868 *m*)	1753.2 (534.375 *m*)	53.3 (17.77 *m*)
Test results ...	,,	,,	,,	1752.4 (534.132 *m*)	57.5 (17.526 *m*)

Note: (i) Sudden closure (ii) Intake *WL* constant at 1693.25 (516.103 *m*) for Project Analysis while for other two intake *WL* varying (iii) Tunnel friction loss = 5.70 *ft* (1.737 *m*) design (minimum)

Table 3

	Talkalale *RL*	Intake *WL* (initial)	Surge tank *WL* (initial)	Minimum *WL* in surge tank during down surge.
Project Analysis ...	1695·0	1693.25	1683·52	1633·84
	(516·64*m*)	(516·10*m*)	(513·14*m*)	(497·99*m*)
Graphical Analysis.		1694·50	1683·0	1643·0
		(516·48*m*)	(512·93*m*)	(500·79*m*)
Test results ...	,,	,,	,,	1645·0
				(501·40*m*)

Conditions: (i) Sudden closure and opening
(ii) Intake water level constant at 1693.25 (516.10 *m*) for Project Analysis and varying for the other two
(iii) Tunnel friction loss = 9.73 *ft* (2.966 *m*) (design maximum) for Project Analysis
and = 11.5 *ft* (3.505 *m*) (nearly design maximum) for the other two
(iv) Load change 5200-0-1040 *cfs* for all.

formation of hydraulic jump. This resulted in free flow in the tunnel. This condition disappeared for Talkalale *WL* of 1692 and above.

Pending suitable modifications in the depth of power channel, the preliminary critical downsurge test was conducted with Talkalale *WL* at 1695 (516.636 *m*). *Table 3* gives comparative results :

Fig 10 shows the variations of water level in surge tank 1 and at intake 1, for critical downsurge test with actual model friction for a load change of 534.5 *mW* - 0 - 106.9 *mW* (average discharge).

The loss in the power channel as per design is 1.75 *ft* (.533 *m*). The loss obtained on the model for Talkalale *WL* = 1695.0 (516.636 *m*) was .5 *ft* (.152 *m*) resulting in slight difference in initial intake *WL*.

The intake *WL* is assumed to remain steady in the design calculations. In the model however, this also varies during downsurge and this variation contributes to the higher minimum surge level obtained both in the graphical computation and in the model. Further experiments are in progress.

15. Supplementary tests on Kota Barrage model

PRIOR TO 1959 flood season, the construction of the Kota Barrage along with the Earthen dam was completed except the erection of the radial gates. During the flood season, the highest water level recorded in the pool upstream of the Barrage was *RL* 834.5 (*RL* 254.356 *m*). With all the 19 spans of the barrage freely discharging the maximum discharge under this water level was estimated to be 7930 m^3/sec (2.8 lakh *cfs*).

During high floods the flow issuing from the barrage concentrated towards the right bank due to the existence of cross slope from the barrage towards the deeper section of the channel on its rights. (*photo 62*). This resulted in right bank erosion to a depth of 15 to 20 *m* (about 50 to 75 *ft*) between 37 *m* to 76 *m* (*Ch* 1200 to *Ch* 2500) downstream of the barrage. Two bathing ghats in this reach were partly undermined.

The model results reported previously had indicated the existence of such concentration under normal floods and to prevent damage pitching of the bank was recommended. This, however, was not carried out.

To prevent further erosion of the right bank the Project authorities proposed an extension of the right downstream retaining-*cum*-training wall by 396.25 *m* (1300 *ft*). According to the original design the wall was extended to 114.3 *m* (375 *ft*) from the axis of the earth dam.

Supplementary tests were, therefore, conducted in 1 : 100 scale composite model to study the efficacy of the proposed extension and possi-

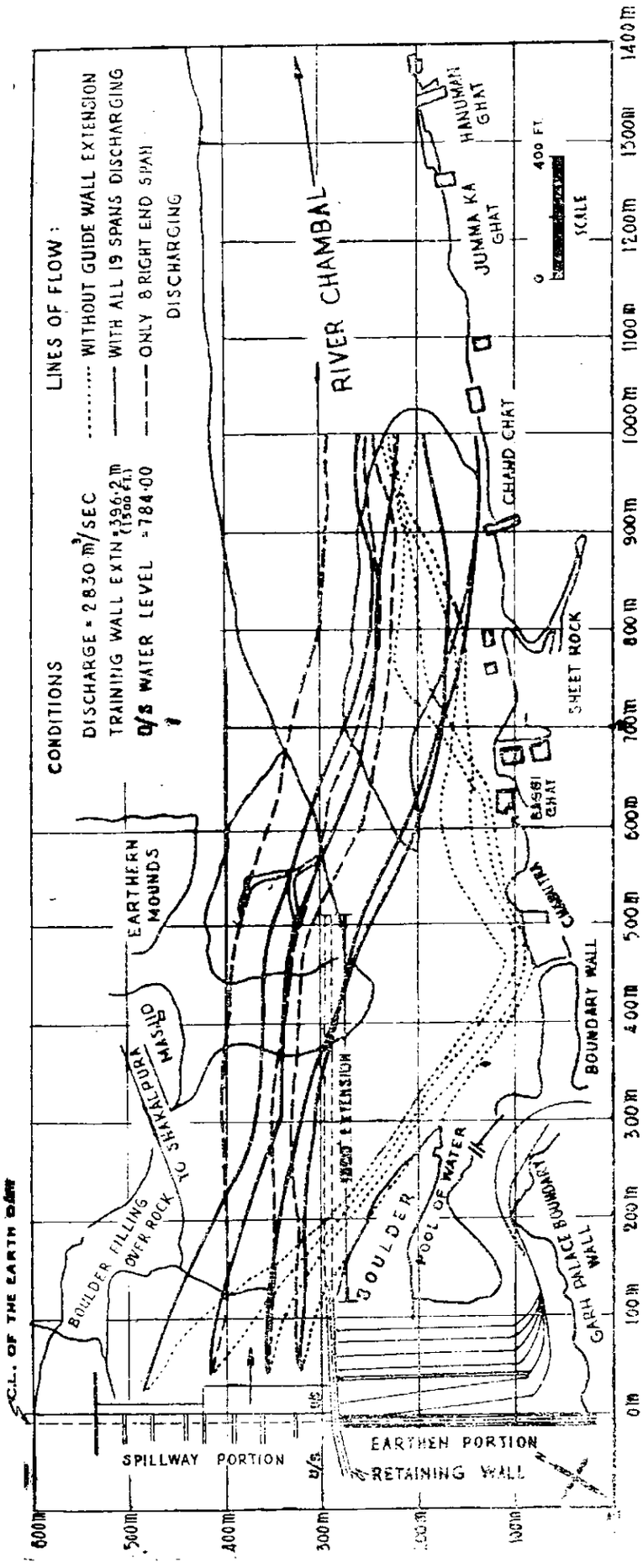

Fig 1

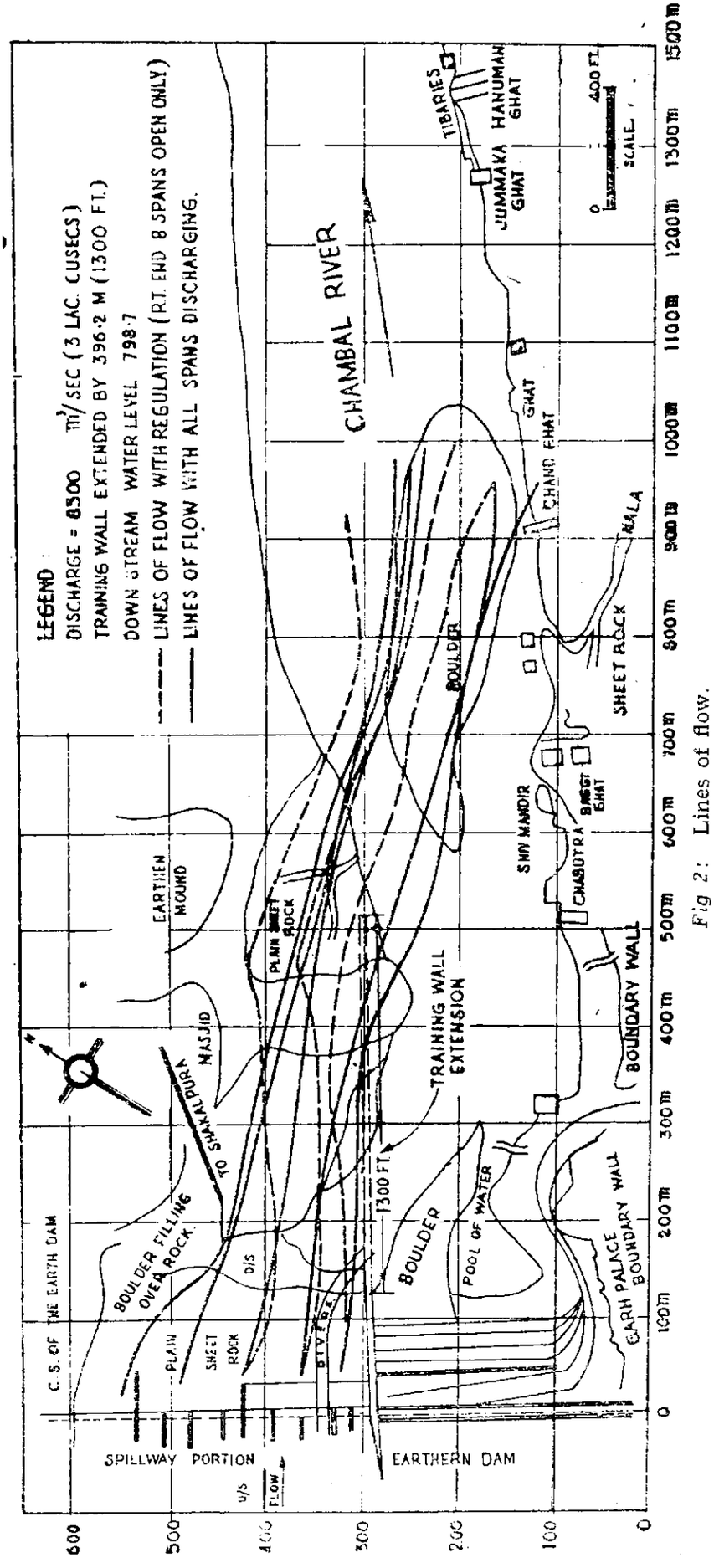

Fig 2: Lines of flow.

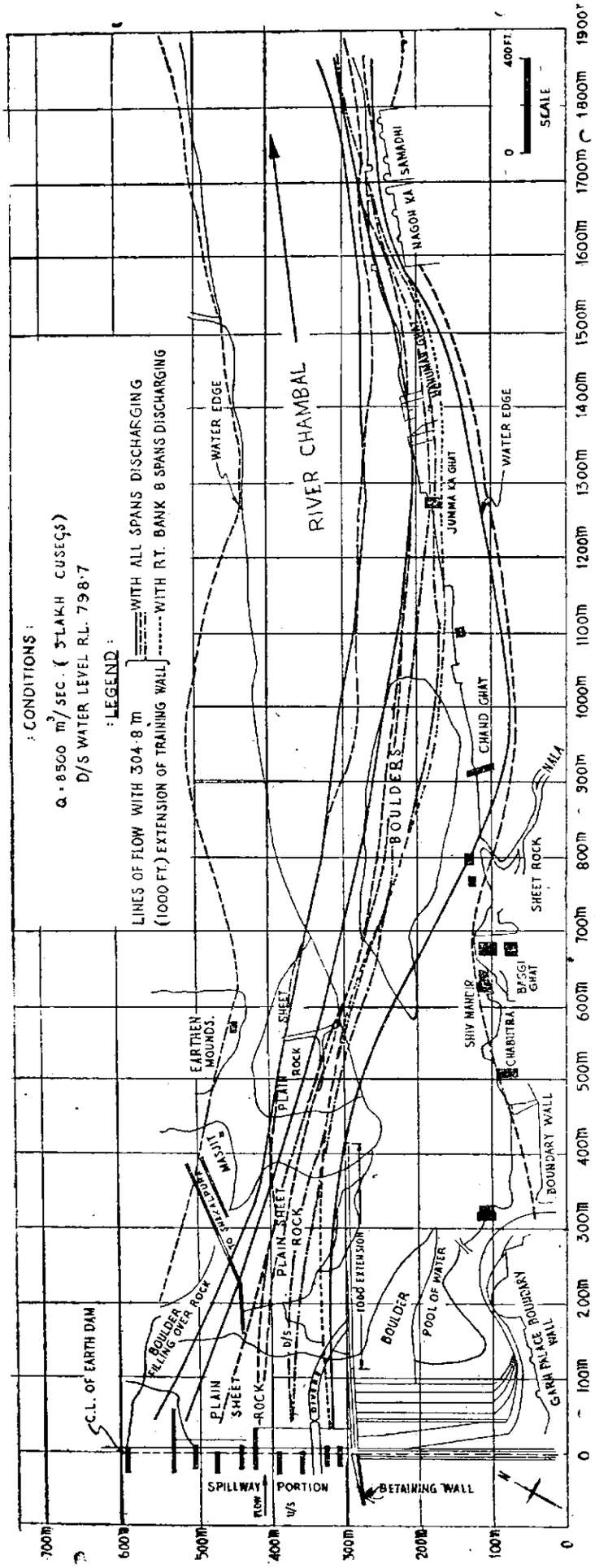

Fig 3: Lines of flow.

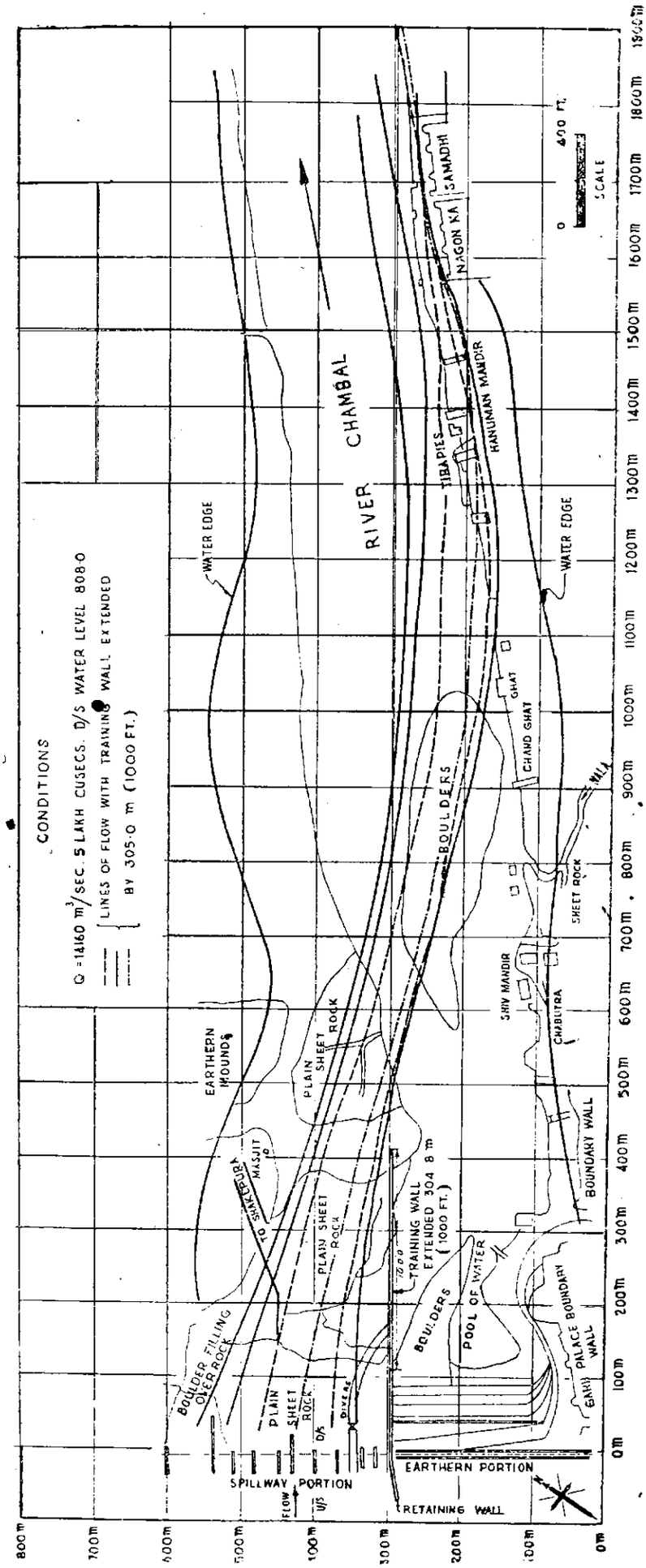

Fig 4: Lines of flow.

ble modifications. The top levels of this stepped training wall in the various reaches were as under :

Distance from Axis of Earth Dam.	Top level *RL*
114.3 to 175.25 *m* (*Ch* 375 to *Ch* 575) ...	820
175.3 to 358.15 *m* (*Ch* 575 to *Ch* 1175) ...	814
358.14 to 510.55 *m* (*Ch* 1175 to *Ch* 1675)...	790

The river channel downstream of the barrage was reproduced in the model according to recent survey by the Project authorities.

2. Experimental results

Discharges from equivalent from 2830 m^3/sec to 19,820 m^3/sec (1 lakh to 7 lakh *cfs*) were run in the model and the lines of flow and general flow conditions in the channel downstream, especially along the right bank were studied.

With discharge through the barrage of the order of 8500 m^3/sec (3 lakh *cfs*) and less, higher forward velocity was obtained in the flow leaving at the end of the extended training wall by regulation of the barrage gates. This helped to increase the protected reach of the right bank to a certain extent.

Fig 1 shows the surface lines of flow with $Q \equiv$ 2830 m^3/sec (1 lakh *cfs*) with and without the proposed extension. Lines of flow with regulation (with spans *Nos* 1 to 8 on right only open) are also given for comparison.

It will be seen that under the existing conditions the right bank between 366 *m* to 762 *m* downstream (*Ch* 1200 to *Ch* 2500) was attacked by the flow from the barrage. With the 396 *m* (1300 *ft*) extension of the training wall the right bank was protected down to 914 *m* (3000 *ft*) below the barrage. *Fig 2* shows lines of flow with $Q \equiv$ 8500 m^3/sec (3 lakh *cfs*). For discharges higher than this, the conditions along the right bank improved due to natural centralisation of the main flow in the downstream channel.

In the next series an extension of 305 *m* (1000 *ft*) only was tested. Please see *figs 3* and *4*. It will be noted that with this extension, the protected length of the right bank materially remains unaltered. The velocities of flow near the bank at 915 *m* (*Ch* 3000) downstream varied from 2.13 to 3.35 *m/sec* (7 to 11 *ft/sec*), for a discharge variation from 2830 to 19,820 m^3/sec (1 lakh to 7 lakh *cfs*). It may be however, pointed out that for a flood discharge of about 8500 m^3/sec (3 lakh *cfs*) the flow at the end of the training

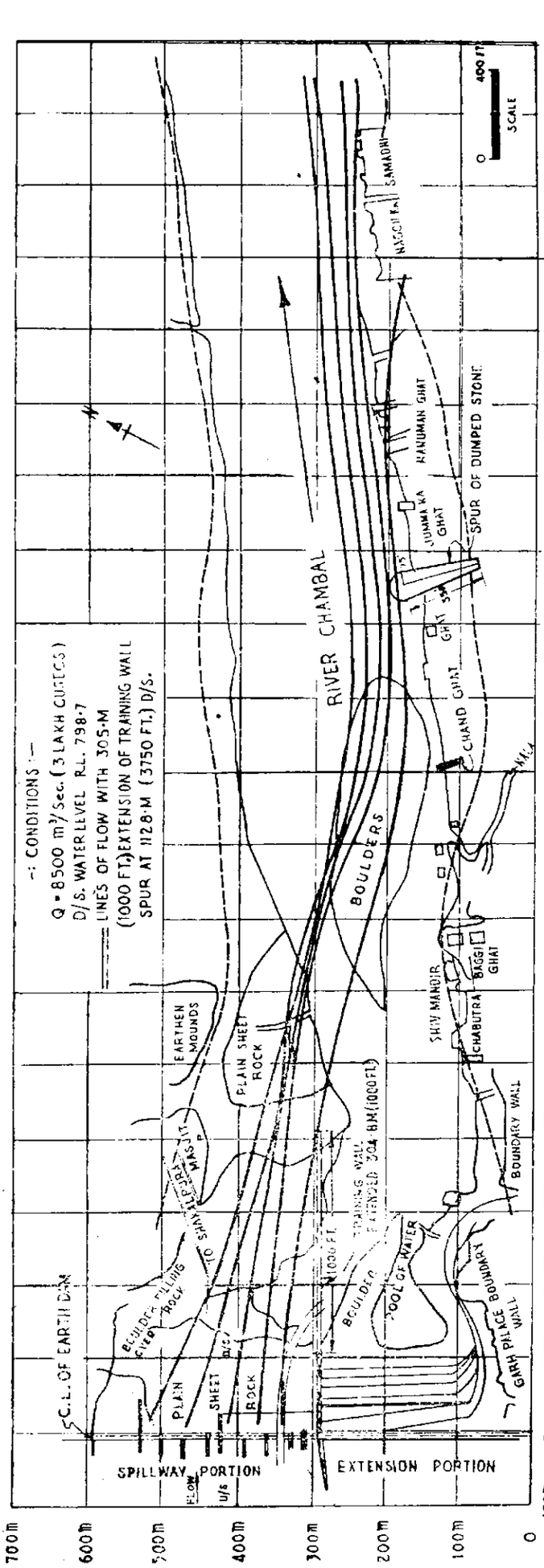

Fig 5: Lines of flow.

wall, fans out naturally and meets the right bank at about 1070 *m* (3500 *ft*) below the barrage. The flow meeting the right bank was not acute and was not expected to cause any serious erosion.

A spur made out of dumped stone extending 25 *m* (75 *ft*) in the river channel with its top level at *RL* 820 may be constructed if conditions of flow are more severe than predicted by the model in the ensuing floods. The lines of flow with such a spur in position are shown in *fig 5*.

3. Differential heads on extended training wall

Due to the extension the flow from the barrage is confined between the training wall and the left bank of the river.

The difference of water levels on the two sides of the training wall depends on the discharge through the barrage and gauge in the channel downstream corresponding to the discharge. A maximum differential head of about 6 *m* (20 *ft*) was observed in the first 274 *m* (900 *ft*) extension with a discharge of 8500 m^3/sec (3 lakh *cfs*). In the remaining length the differential head was about 4.5 *m* (15 *ft*).

The top levels of the training walls recommended in the various reaches are :

Distance from the Axis of the earth dam.	Top level *RL*
114.3 to 175.26 *m* (*Ch* 375 to *Ch* 575) ...	820
175.26 to 358.14 *m* (*Ch* 575 to *Ch* 1075) ...	814
358.14 to 510.14 *m* (*Ch* 1075 to *Ch* 1375)...	804

16. Misalignments in excluder walls of Kosi barrage

DURING construction of excluder tunnels in the left pocket of Kosi barrage, misalignment was reported to have occurred in the walls of vent numbers 3, 5, 6, 7 (*figs 1* and *2*). It was desired by Kosi Project authorities that

(i) effect of the misalignments on the efficiency of excluders in respect of sand exclusion, and
(ii) possibility of cavitation in the tunnels

may be experimentally studied. Effect on the performance of the excluder vents in respect of silt exclusion was studied in 1/10 scale geometrically similar models of individual vents by comparison of the velocities and rugosity coefficients obtained with and without misalignments. Aspect of cavitation could not be studied for want of a cavitation tunnel.

2. Model experiments and results

Model tests were conducted with both the shortest vent (vent *No 3*) and the longest vent (vent *No 5*) each one with and without misalignments in the side walls. Experiments were carried out with pond at *RL* 245 as well as at *RL* 255 and under both retrogressed and unretrogressed conditions downstream. Square, as well as, rounded entrances of the vents were successively tested to assess possible improvement in the performance with the latter type of entrances.

Experimental observations consisted of

(i) Measurement of discharge through the tunnel under given upstream and downstream water levels, by means of a .61 *m* (2 *ft*) *SWF* located on the upstream side.
(ii) Assessment of hydraulic gradient in the tunnel, by reading piezometers located in the top of the excluder tunnel as shown in *fig 1*. A typical set of piezometer observations is given in *fig 3*.

Values of rugosity coefficient '*n*' of the vents were next calculated with and without misalignments, by using Manning's formula under all conditions. These are given in *table 1*.

At the critical stage of operation of the excluders, *viz* with the pond level at *RL* 245 under minimum available head of .9 *ft* (.27 *m*) at the river stage of 11327 m^3/sec (4 lakh *cfs*) with unretrogressed water level downstream, no measurable difference in '*n*' value was observed between straight and defective walls. Velocity obtained through the vent was (5.25 *ft/sec*) 1.6 *m/sec* with and without misalignments.

Model tests thus indicated that the existing misalignments may not reduce working efficieney of the tunnels. This was also borne out by theoretical calculations by assuming the irregularities to correspond to a series of convergences and divergences. Velocities thus computed at selected flood stages are given in *column* 6 of *table 2*.

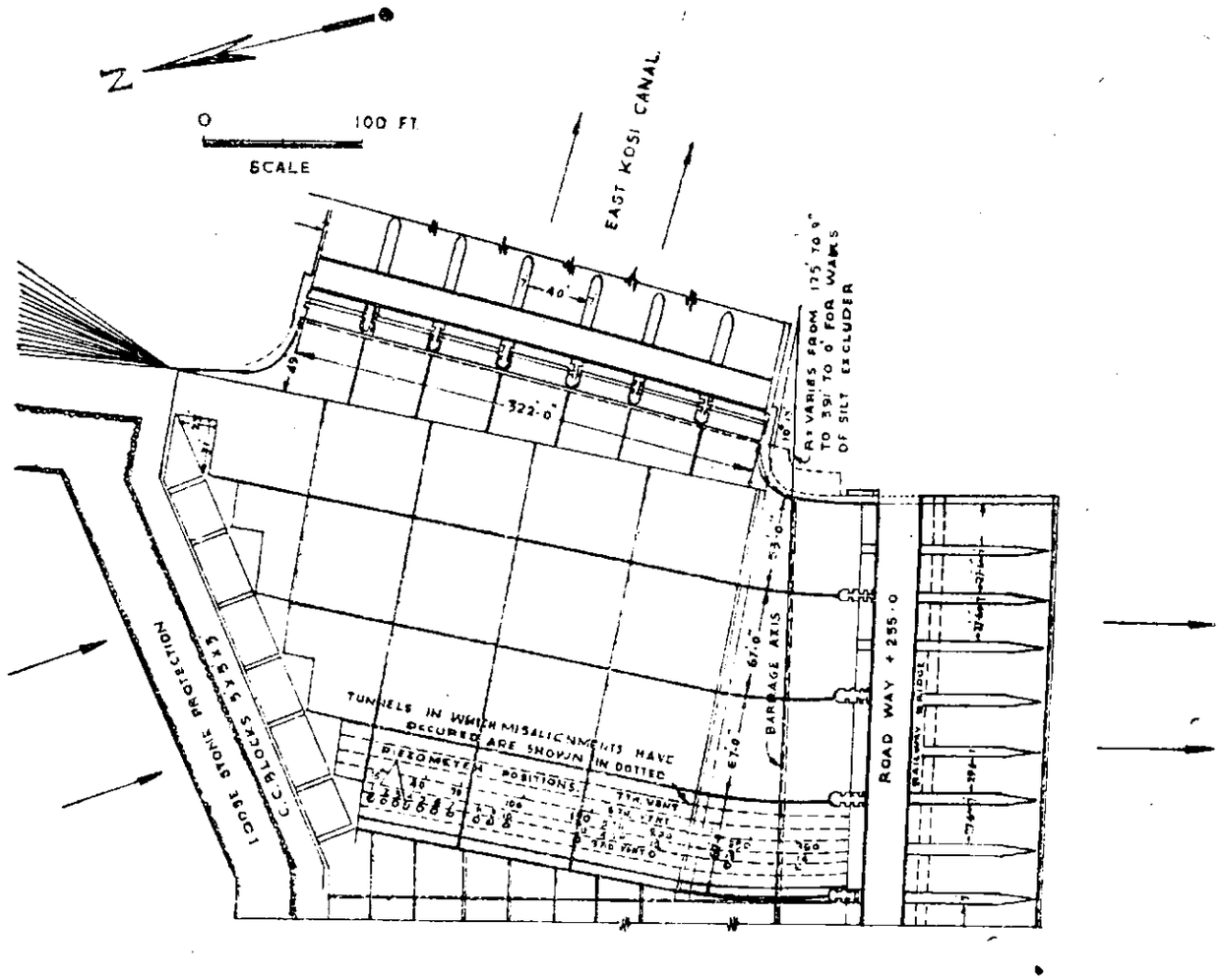

Fig 1: Plan of silt-excluder in the left pocket of Hanumannagar barrage.

Reference:—Positions of piezometers are indicated by circles and their distances from the upstream end of vent are marked.

Velocities computed in absence of misalignments are given in *column* 5 of the same statement. Comparison of *columns* 5 and 6 would indicate that no appreciable change in velocities may be expected owing to the misalignments.

Results with a rounded entrance are presented in *columns* 6, 8, 10, and 12 of *table 1*. It will be noted that velocities through the vent increased with a rounded entry, the maximum increase being of the order of about 16 *percent* at pond level of 255 at 21238 m^3/sec (7.5 lakh *cfs*) flood stage with retrogressed downstream water level.

Results of experiments with vent *No* 5, the largest one, were similar and also failed to indicate any measurable changes in velocities and the '*n*' values.

3. Conclusions

(*i*) Performance of the vent *Nos* 3 to 7 in the left pocket excluder may not worsen on account of the misalignments resulted due to faulty casting of inside walls as in *fig 2*.

(*ii*) Misalignment of side walls has occurred in only five tunnels out of a total number of 32, on the divide wall side of the pocket. Tunnels located here have even otherwise lesser efficiency than those near the canal head regulator, as indicated by experience as well as model tests.

(*iii*) Improved performance of the tunnels was indicated with a rounded entrance.

(*iv*) Bed sand at barrage site was reported to be coarse with mean diameter of .437 *mm*. Kosi is also known for heavy sediment load. Suffi-

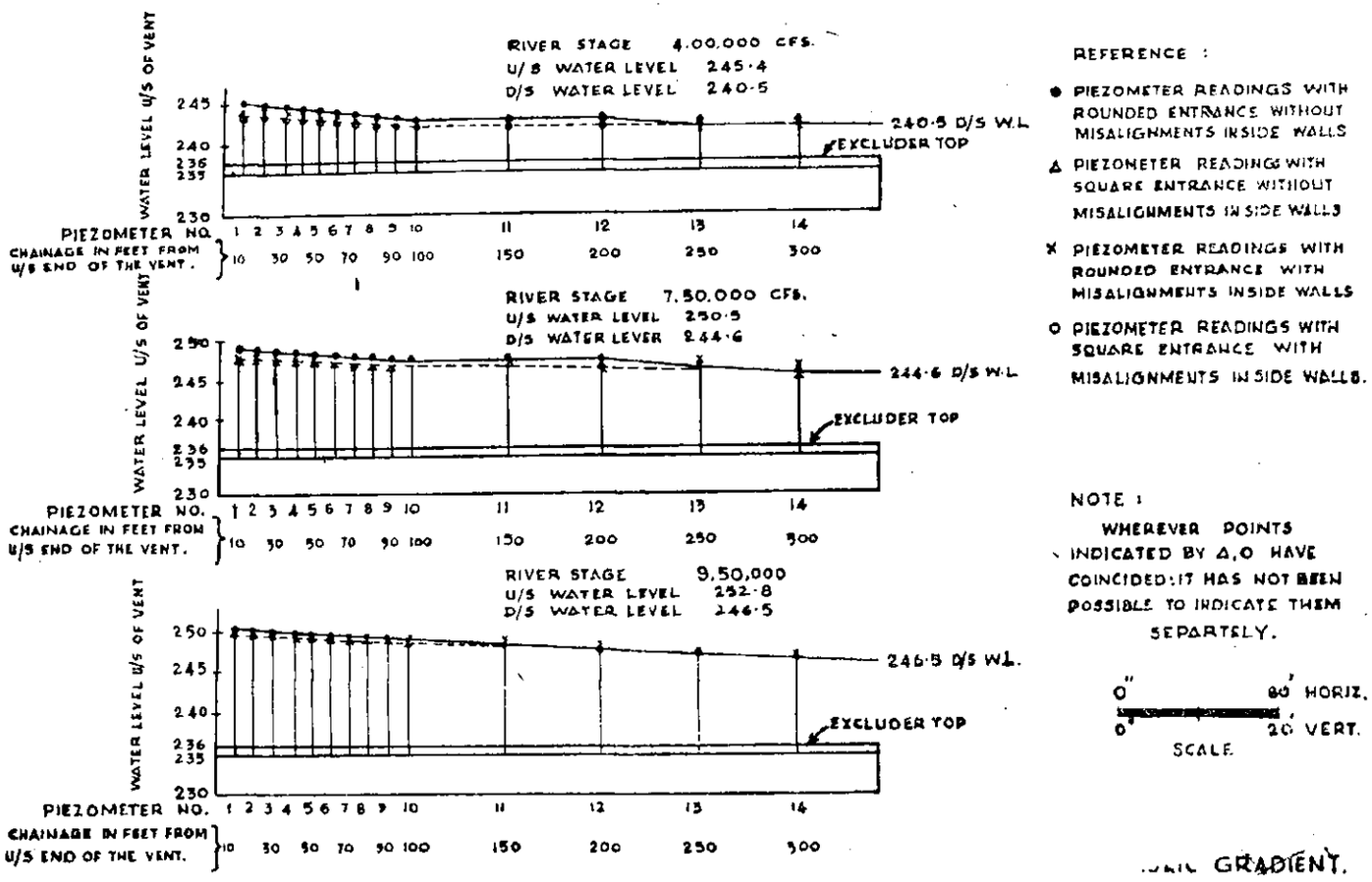

Fig 3: Plot showing hydraulic gradient in vent number 3 under low pond with retrogressed water levels downstream.

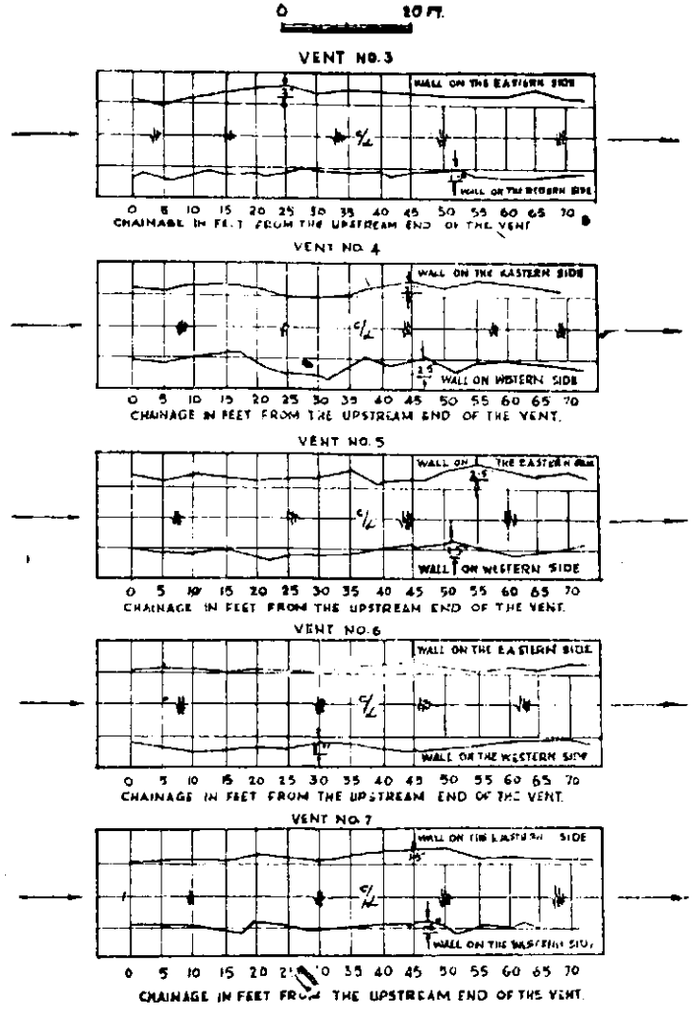

Fig 2: Plan of profile showing misalignments in silt excluder walls in the left pocket of Hanumannagar barrage on the Kosi cast during the working season 1958-59.

Table 1 : Model Velocities through vent *No* 8 of the left pocket excluders of Kosi Barrage and its '*n* values. Submerged flow downstream of vent

Length: 339′ 4″ (103·43 *m*) Size: 7·125′ × 5′ (2·17 *m* × 1·524 *m*)

River Stage in lakh *cfs*, (m^3/*sec.*)	U/s water level *RL*	D/s water level *RL*	Head available in *ft* (*m*)	Velocity through tunnel in *ft/sec* (*m/sec*)				Overall '*n*' (Manning's)			
				without Misalignment		with Misalignment		without Misalignment		with Misalignment	
				Square Entry	Round Entry	Square Entry	Round Entry	Square Entry	Round Entry	Square Entry	Round Entry
At lower Pond level of RL 245											
(*i*) Downstream water levels retrogressed											
4·0 (11327)	245·4	240·5	4·9 (1·49)	10·8 (3·29)	11·5 (3·51)	10·8 (3·29)	11·4 (3·47)	·017 (·0052)	·018 (·0055)	·017 (·0052)	·017 (·0052)
7·5 (21238)	250·5	244·6	5·9 (1·80)	11·4 (3·47)	12·5 (3·81)	11·4 (3·47)	12·4 (3·78)	·016 (·0049)	·017 (·0052)	·017 (·0052)	·017 (·0052)
9·5 (26901)	252·8	246·5	6·3 (1·92)	11·75 (3·58)	12·8 (3·90)	11·7 (3·57)	12·6 (3·84)	·017 (·0052)	·018 (·0055)	·017 (·0052)	·017 (·0052)
(*ii*) Downstream water levels unretrogressed											
3·0 (8495)	245·0	243·75	1·25 (·38)	5·65 (1·72)	6·37 (1·94)	5·65 (1·72)	6·35 (1·94)	·017 (·0052)	·018 (·0055)	·017 (·0052)	·017 (·0052)
4·0 (11327)	245·4	244·5	·9 (·27)	5·25 (1·60)	5·9 (1·80)	5·25 (1·60)	5·9 (1·80)	·017 (·0052)	·017 (·0052)	·017 (·0052)	·017 (·0052)
5·0 (14159)	246·86	245·0	1·86 (·57)	6·65 (2·03)	7·26 (2·21)	6·6 (2·01)	7·25 (2·21)	·017 (·0052)	·018 (·0055)	·017 (·0052)	·016 (·0049)
9·5 (26901)	252·8	247·5	5·3 (1·62)	11·10 (3·38)	11·4 (3·47)	11·1 (3·38)	11·4 (3·47)	·017 (·0052)	·018 (·0055)	·017 (·0052)	·017 (·0052)
At higher pond level of RL 255											
(*i*) Downstream water levels retrogressed											
4·0 (11327)	255	240·5	14·5 (4·42)	17·7 (5·40)	19·0 (5·7)	17·7 (5·40)	19·0 (5·79)	·017 (·0052)	·017 (·0052)	·017 (·0052)	·017 (·0052)
7·5 (21238)	255	244·6	10·4 (3·17)	14·4 (4·39)	16·7 (5·09)	14·4 (4·39)	16·6 (5·06)	·017 (·0052)	·017 (·0052)	·017 (·0052)	·017 (·0052)
9·5 (26901)	255	246·5	8·5 (2·59)	13·5 (4·11)	13·8 (4·21)	13·5 (4·11)	13·50 (4·11)	·018 (·0055)	·018 (·0055)	·018 (·0055)	·017 (·0052)
(*ii*) Downstream water levels unretrogressed											
3·0 (8495)	255	243·75	11·25 (3·43)	16·7 (5·09)	17·0 (5·18)	16·5 (5·03)	16·9 (5·15)	·017 (·0052)	·017 (·0052)	·016 (·0049)	·017 (·0052)
4·0 (11327)	255	241·5	10·5 (3·20)	15·3 (4·66)	15·5 (4·72)	15·3 (4·66)	15·5 (4·72)	·017 (·0052)	·018 (·0055)	·016 (·0049)	·017 (·0052)
5·0 (14159)	255	245·0	10·0 (3·05)	15·1 (4·60)	15·2 (4·63)	15·0 (4·57)	... ...	·017 (·0052)	·018 (·0055)	·016 (·0049)	... ...

Table 2 : Computed velocities through Vent No 3 of left pocket excluders of Kosi Barrage assuming the misalignments to correspond to successive convergences and divergences.

River stage in lakh *cfs*	U/S WL RL	D/S WL RL	Head available in *ft*	Velocity in *ft/sec*		Eddy loss in *ft.** $= .C03 \frac{V^2}{2} . N$
				Without misalignment	With misalignment	
1	2	3	4	5	6	7
			At lower pond level of RL 245·0			
			(i) Downstream water levels retrogressed			
·5 (1416)	245	243.3	10.7 (3.26)	15.1 (4.60)	15.0 (4.57)	.102 (0.0311)
4 (11327)	245.4	240.5	4.9 (1.49)	10.40 (3.17)	10.35 (3.15)	.051 0.0155)
7 (21238)	250.4	244.6	5 9 (1.79)	11.34 (3.45)	11.30 (3.44)	.060 (0.0183)
9 (26901)	252.8	246.5	6.3 (1.92)	11.70 (3.57)	11.65 (3.55)	.064 (0.0195)
			(ii) Downstream water levels unretrogressed.			
3 (8495)	245	243.75	1·25 (0.38)	5·8 (1.77)	5·8 (1.77)	.015 (0.0046)
4 (11327)	245.4	244.5	0·90 (0·27)	5·2 (1·58)	5·2 (1·58)	.0125 (0.0038)
5 (14159)	246.86	245.0	1·86 (0·56)	6·8 (2·07)	6·8 (2·07)	.0125 (0.0038)
9 (26901)	252.8	247.5	5·30 (1·62)	10·8 (3·29)	10·75 (3·28)	.0545 (0.0036)
			At higher pond level of RL 255·0			
			(i) Downstream water levels retrogressed			
·5 (1416)	255	234.3	20.7 (6.31)	20.7 (6.31)	20·52 (6·25)	.2 (0·0610)
4 (11327)	255	240.5	14.5 (4.42)	17.4 (5.30)	17·25 (5·26)	.14 (0.0417)
7 (21238)	255	244.6	10.4 (3.17)	14.9 (4.54)	14.8 (4.51)	.103 (0.0314)
9 (26901)	255	246.5	9.5 (2.89)	13.5 (4.11)	13.45 (4.10)	.085 (0.0259)
			(ii) Downstream water levels unretrogressed			
·5 (1416)	255	239.5	15.5 (4.72)	18.0 (5.49)	17.9 (5.45)	.152 (0.0463)
3 (8495)	255	243.75	11.25 (3.43)	15.4 (4.6)	15.3 (4.66)	.11 (0.0335)
4 (11327)	255	244.5	10.5 (3.20)	14.9 (4.54)	14.80 (4.51)	.103 (0.0314)
5 (14159)	255	245.0	10·0 (3·05)	14.6 (4.45)	14.52 (4.42)	.01 (0.3078)

*·C03 = loss coefficient. N = number of divergences. V = Velocity in excluder tunnel in *ft/sec* (Refer page 412 of Engineering Hydraulics by Hunter Rouse)

ciently high velocities in the excluder vents are, therefore, warranted. *Column* 4 of *table* 1 indicates that head available for Kosi excluders at 8495, 11327, 141591 m^3/sec (3, 4, 5 lakh *cfs*) flood stages would be .38 *m* (1.25 *ft*) .27 *m* (0.9 *ft*) and 0.57 *m* (1.86 *ft*) respectively under unretrogressed conditions downstream, with pond level of 245. As against these, design heads of other barrages were as in the *table*. Comparison will reveal that in the intervening period till retrogression occurs on the downstream of Kosi barrage, efficiency of sand exclusion may be expected to be low. The conditions, however, would improve with retrogression.

Excluders on	Design head	Nature of bed material
Kalabagh barrage on Indus.	3 *ft* (.9144 *m*)	Shingle
Gudu barrage on Indus (provided in the original design).	2 *ft* (.6096 *m*)	Fine sand (0.14 *mm*)
Kotri barrage on Indus (provided in the original design).	2 *ft*	Fine sand (0.32 *mm*)
Khanki weir on Chanab...	3 *ft*	Fine sand
Harike barrage on Sutlej...	3 *ft*	Fine sand and clay

(*v*) As previously mentioned cavitation aspect could not be experimentally studied. Considering, however, the hydraulic conditions, under which excluder tunnel would be working, possibility of cavitation was not apparent.

17. Silting in relation to Hirakud Lake model

FURTHER tests were conducted with an average discharge of 6 lakh *cfs* in the Mahanadi with reservoir *WL* at *RL* 620. Normal unfractioned red silt was used for injection at the rate of 4.8 parts/1000 (by weight). A number of samples of silt in suspension was collected at depth .6 *D* at various places in the reservoir and a collection of sediment deposits was done regionwise at the end of the test. The results of measurements for this and the subsequent tests are shown in *table 1* and the silt sediment being shown as a percentage of the total injection of silt.

The further two tests were conducted with discharge in the Mahanadi maintained at 6 lakh *cfs*, but the reservoir *WL* was raised to *RL* 630. (*photo* 63; *fig 1*). There was no overflow, the discharge being allowed to pass through the left sluices.

In a further series of tests the discharge was maintained at an average of 9 lakh *cfs* and the reservoir *WL* at *RL* 620, the duration of each test being the only variable.

2. Results

Fig 2 shows the amount of silt in suspension against longitudinal distance from the dam upstream for the above tests, along with the tests reported in 1959. The average curves in the two cases are similar. *Fig 3* shows the regionwise bed deposits as a percentage of the total injection.

Fig 4 shows the mean size of the silt particles in the bed deposits, against the longitudinal distance from the dam upstream for the above tests as also for tests reported in 1959. The average curves are similar. *Fig 5* shows the location at each cross-section where the samples of silt in suspension was obtained.

Some of the features of the passage of the silt laden stream through the lake, the pattern of deposits, and the nature of exclusion from the sluices are elucidated in the results of these experiments. The comparative usefulness of keeping the lake levels low is indicated in the experiments for the lake level at 630 and lower lake levels. The average silt concentration in the discharge passing through the sluice is about 1 *percent* of the charge, as injected, in the model for higher water levels, rising to about 4 *percent* for lower water levels tested. A fuller series of

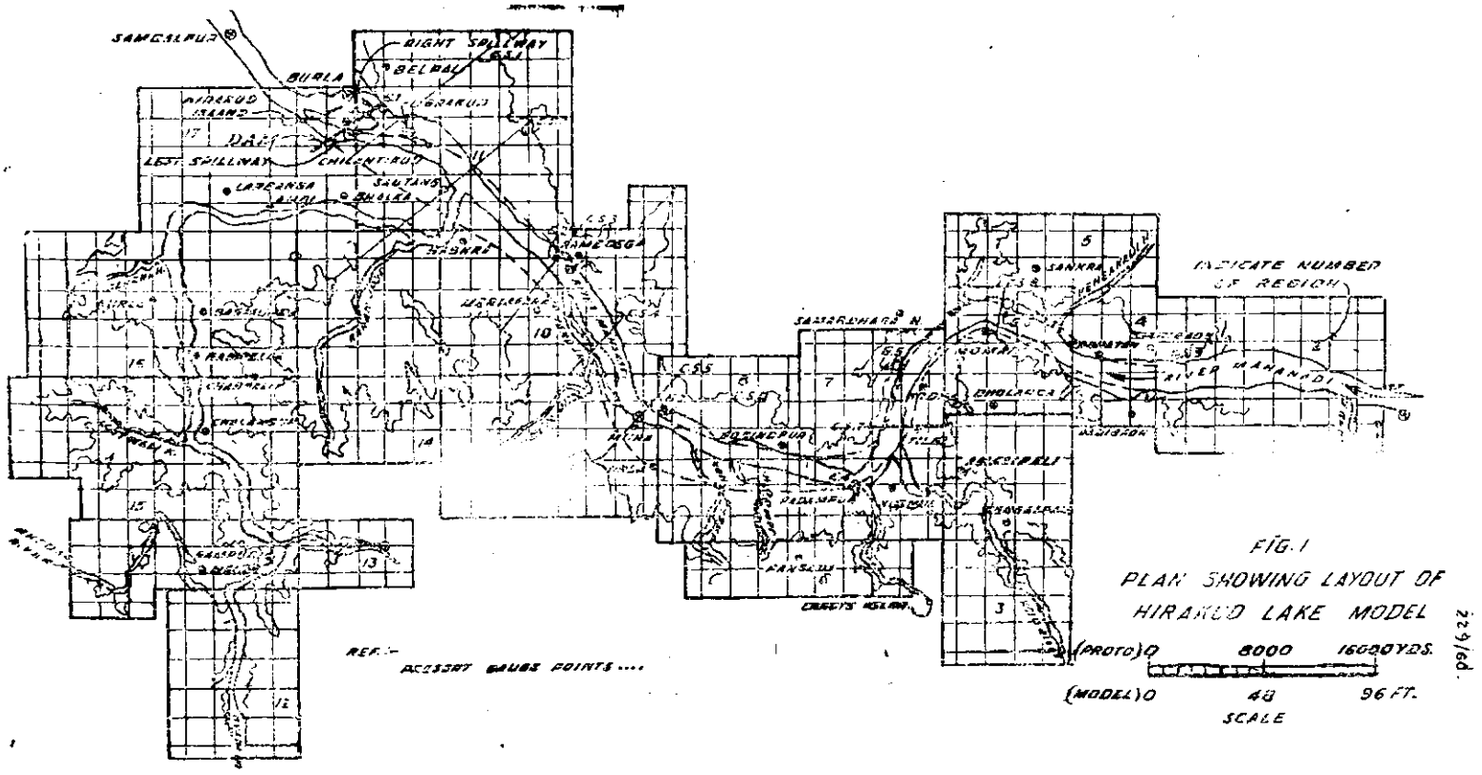

FIG. 1
PLAN SHOWING LAYOUT OF HIRAKUD LAKE MODEL

229/60.

Table 1 : Results of tests with normal unrefractioned red silt injected at rate of 4·8 parts/100

Test No		COMPARTMENTS													Silt passing through the sluice						
		2	4	7	8	9	10	11	14	16	17 U/S	17 D/S	Sluice	River	Chamber	Right Spillway					Left Spillway	
		CROSS SECTION																				
		9	8	7	6	5	4, 3	2, 1								1	2	3	4	5	6	7
Sluices 1, 2, 3 full and 4th half open; Q = 6 lakhs *cfs* *u/s WL* 620; time in hours = 16																						
1	*a*	8·13	17·93	15·22	15·22	7·48	5·03	5·03	0·37	0·13	0·26			0·39	0·39	0·2388	0·2055	0·2610	0·2277			
	b	0·195	0·055	0·083	0·047	0·035	0·034,0·036	0·038,0·038				0·183			0·027							
		0·146	0·101	0·063	0·073	0·044	0·030,0·028	0·023,0·025	0·029		0·112	0·079			0·087							
	c	0·7721	0·6943	0·6277	0·4388	0·4499	0·3388,0·1722	0·1944,0·0722			0·029	0·2811		0·2611	0·1906							
		0·5905	0·5943	0·7728	0·4366	0·4488	0·3810,0·1453	0·1417,0·1173						0·1928		0·2609	0·0855	0·1895	0·2393			
Sluices 1, 2, 3 and 4th 3/4th open; Q = 6 lakhs *cfs* *u/s WL* 630; Time in hours = 23½																						
2	*a*	15·40	24·29	17·47	9·62	3·81	5·05	5·88	0·778	0·35	0·96			0·28	0·18							
	b	0·150	0·139	0·050	0·079	0·030	0·023	0·040	0·093	0·164	0·094	0·172	0·093	0·137	0·152							
							0·020	0·030								0·2933	0·0955	0·0814	0·865			
	c	2·963	0·7643	0·4310	0·2844	0·2997	0·3844	0·0599						0·1444								
							0·2333	0·0599														
Sluices 1, 2, 3 and 4th 3/4th open; Q = 6 lakhs *cfs* *u/s WL* = 630; Time in hours = 19																						
3	*a*	14·858	26·179	14·150	11·32	5·07	5·189	6·014	2·122	1·650	1·533											
	b	0·219	0·133	0·056	0·035	0·035	0·028	0·045	0·066	0·122	0·037	0·064		0·055								
							0·038	0·029								0·044	0·034	0·024	0·032			
	c	1·378	0·858	0·534	0·452	0·189	0·278	0·070						0·078								
							0·218	0·064														

Sluices 1, 2, 3, 4, 5, 6, 7th half open ; Q = 9 lakhs *cfs* *u/s WL* = 620; Time in hours = $22\frac{1}{4}$

4	*a*	7·59	16·49	16·34	30·78	11·82	7·44	5·69	0·58	0·14	0·72								
	b	0·391	0 268	0·327	0·188	0·066	0·047	0·031,0·029	0·044				0·082	0·276					
							0·036	0·031,0·031							0·062	0 140	0·094	0·284	0·222	0·180	0.038	0·192
	c	1·072	1·042	0·946	0·546	0·438	0·332	0·184				0·098	0·140	0·120		0·110						
							0·148	0·054														

Sluices 1, 2, 3, 4, 5, 6 and 7th half open; Q = 9 lakhs *cfs* *u/s WL* = 620; Time in hours = $24\frac{3}{4}$

5	*a*	8·22	16·60	13·12	35·19	10·36	8·23	6·24	0·797	0·134	0·124									
	b	·264	·235	·295	·251	·080	·045	·032	·144	·209	·058			·092	·135							
							·037	·027,·035								0 252	0·062	0·116	0·128	0·128	0·120	0·030
	c	0·108	0·402	0·558	0·186	0·414	0·382	0·442				0·052	0·150	0·018	0·018	0 514	0·388	0·046	0·256	0·150	0·150	0·182
		0·248					0·194	0·352														
		0·622																				

Sluices 1, 2, 3, 4, 5, 6 and 7th half open; Q = 9 lakhs *c/s* *u/s* WL = 620; Time in hours = 10

6	*a*	13·24	27·155	16·39	14·24	8·28	7·29	6·95	0·995	0 331	0·165									
	b																			
	c																			

a = % of silt deposits; b = size of silt deposit (in *mm*) ; c = silt in suspension *gm*/1000*c e*.

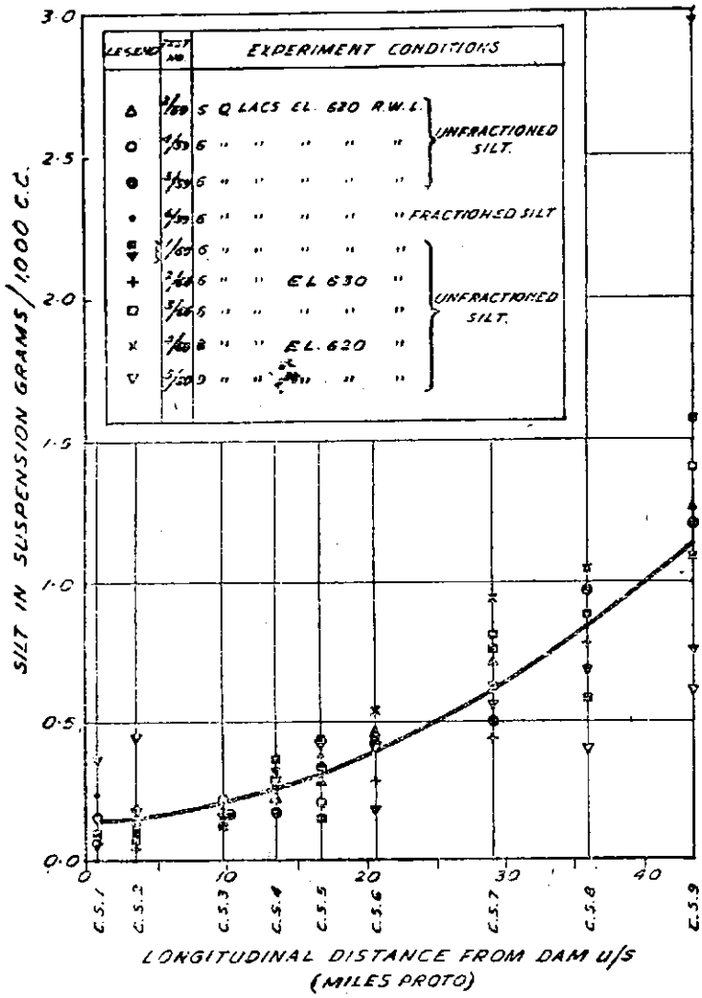

Fig 2 :

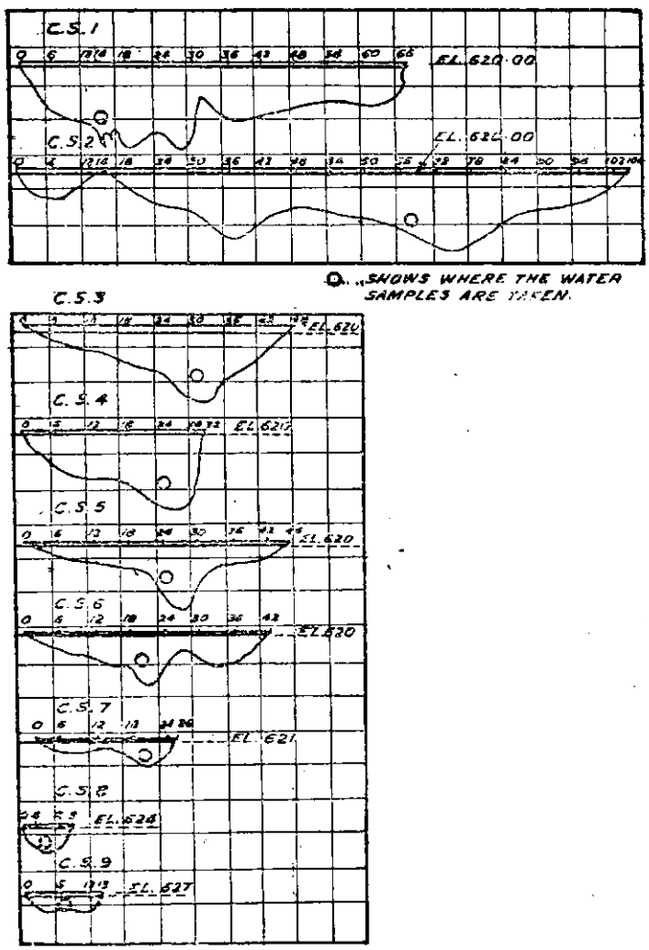

Fig 5 : Location of silt samples.

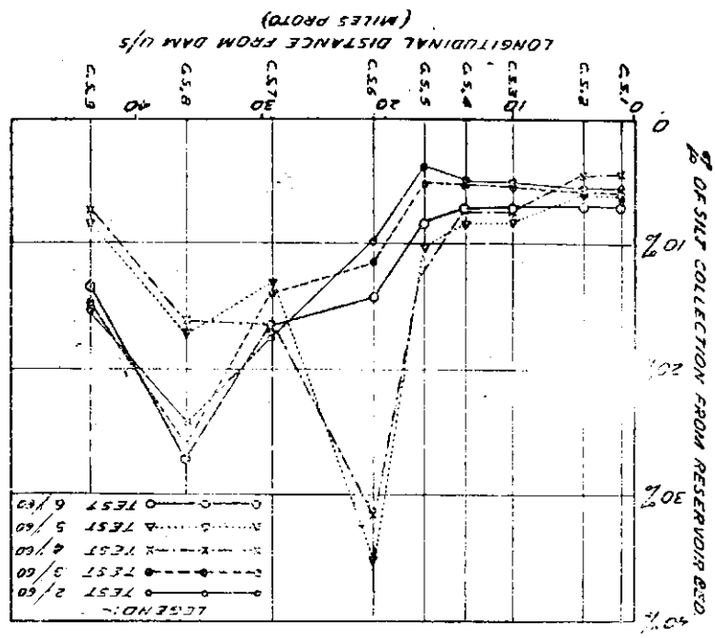

Fig 3: Test 11 D. Q = 6.0 lakhs *cfs* WL EL 630.00 silt charge 4.8 parts per 1000

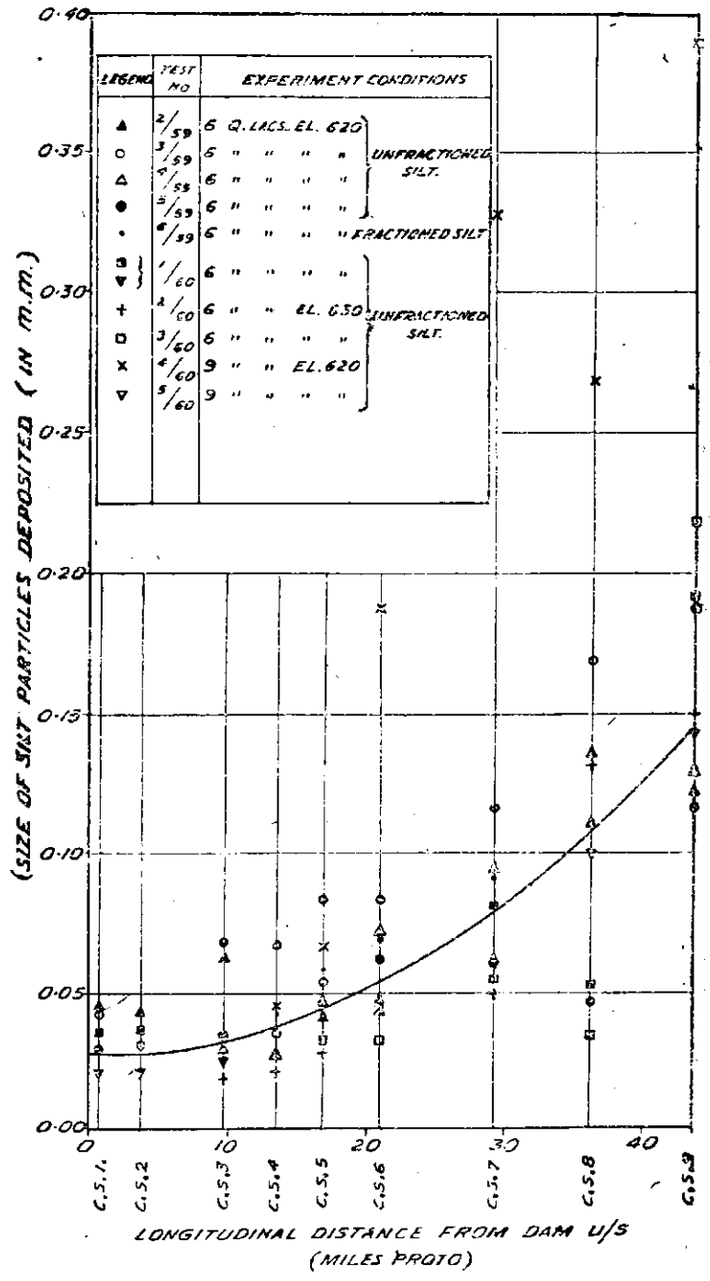

Fig 4

measurements will have further data on this, along with the effects of different discharge.

The distribution of deposits shows well defined trends. For comparatively lower water levels the deposits are less in the upper reaches of the river, tend to increase nearer the dam. In the particular cases tested, good percentage of the finer silt traverses right through the lake to reach the regions upstream of the dam.

Further work on this with different concentrations are required to evaluate the potentialities of this effect in obtaining an optimum exclusion, as well as other features of the distribution of silting patterns, in the lake for different inflow and flow disposal.

18. Two dimensional photoelastic analysis

I. Gandhisagar Spillway Piers

GANDHISAGAR dam spillway piers have been made hollow to enable operation of gates from the top of the piers. The piers support a spillway bridge of 18.3 *m* (60 *ft*) clear span. Bridge carries a 75 *ton* gantry crane in addition to *IRC* class *A* loading. Each pier is provided with rectangular opening 6.4 *m* × 3.5 *m* (21 *ft* × 11.5 *ft*) leaving a width of .76 *m* (2.5 *ft*) on each side. Two dimensional photoelastic tests were carried out to determine

(i) Stresses along a horizontal section due to vertical load from the bridge.

(ii) Shear stress distribution on gate slot sides.

Technical Details: The three dimensional structure could for the shear tests be reduced to a two dimensional model by adopting the following scales :

Vertical and horizontal scale : 1/192
Lateral (thickness) Scale : 1/1200

The model was constructed out of an Araldite-D plate 2.54 *cm* (1 *inch*) thick, according to the dimensions shown in *fig 1* by proper milling. To simulate the vertical load from the bridge, two circular discs of equal diameter made from photoelastic material were placed over the piers. A known load was applied at the centre of the distance between the two discs and the equal distribution of the applied load in the bridge piers was confirmed by measuring the load coming in the each disc.

(i) *Analysis of stresses along horizontal section X-X in fig 1* : Isochromatic fringe pattern for the vertical load is given in *photo 64*. The measurement of the fringe order along the horizontal section *X-X* (*fig 1*) was carried out by Tardy's method. From the isochromatic pattern given in *photo 64*, the distribution of the load intensity along the section *X-X* was calculated. This

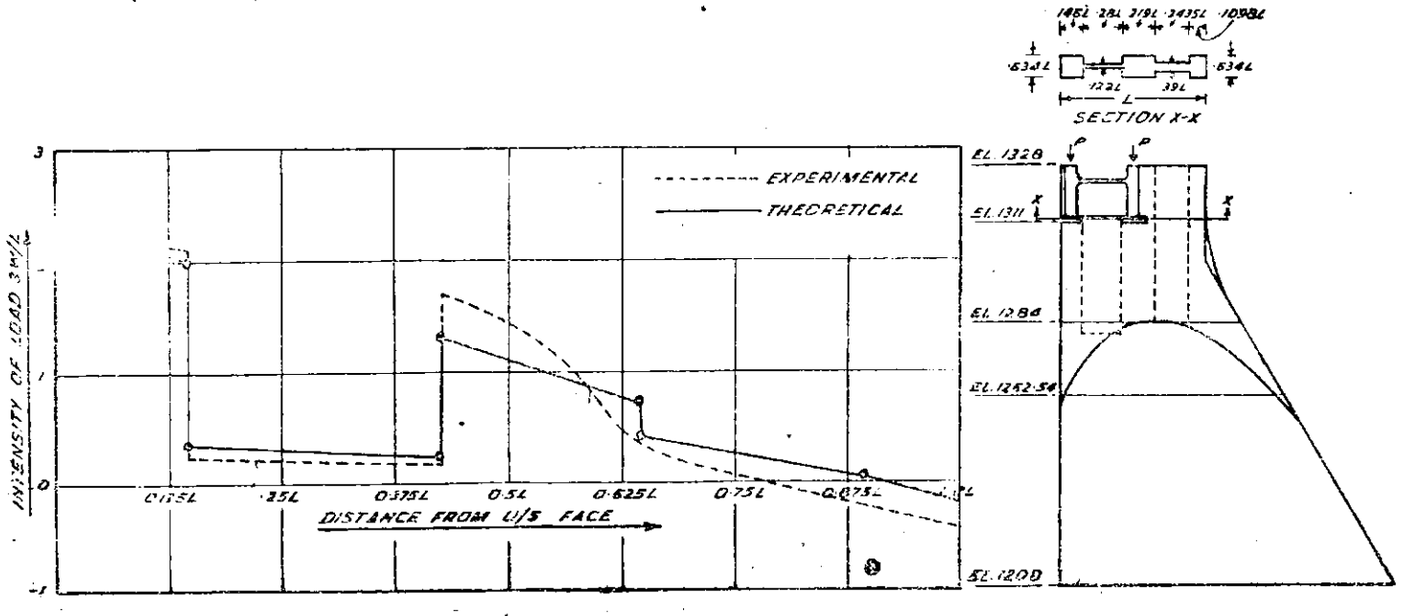

Fig 1: Load distribution diagram for section X-X.

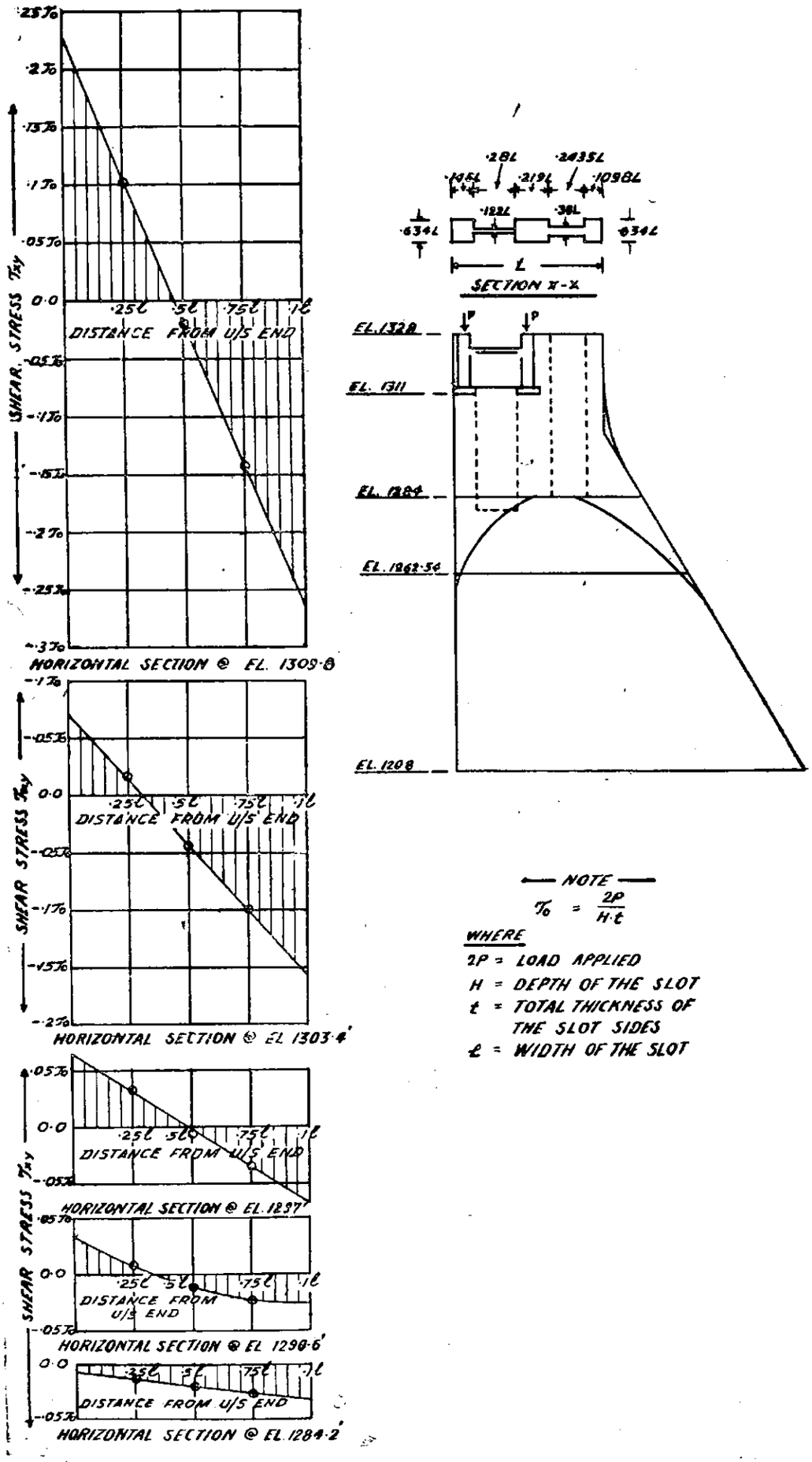

Fig 3 : Shear stress in the sides of the gate slots.

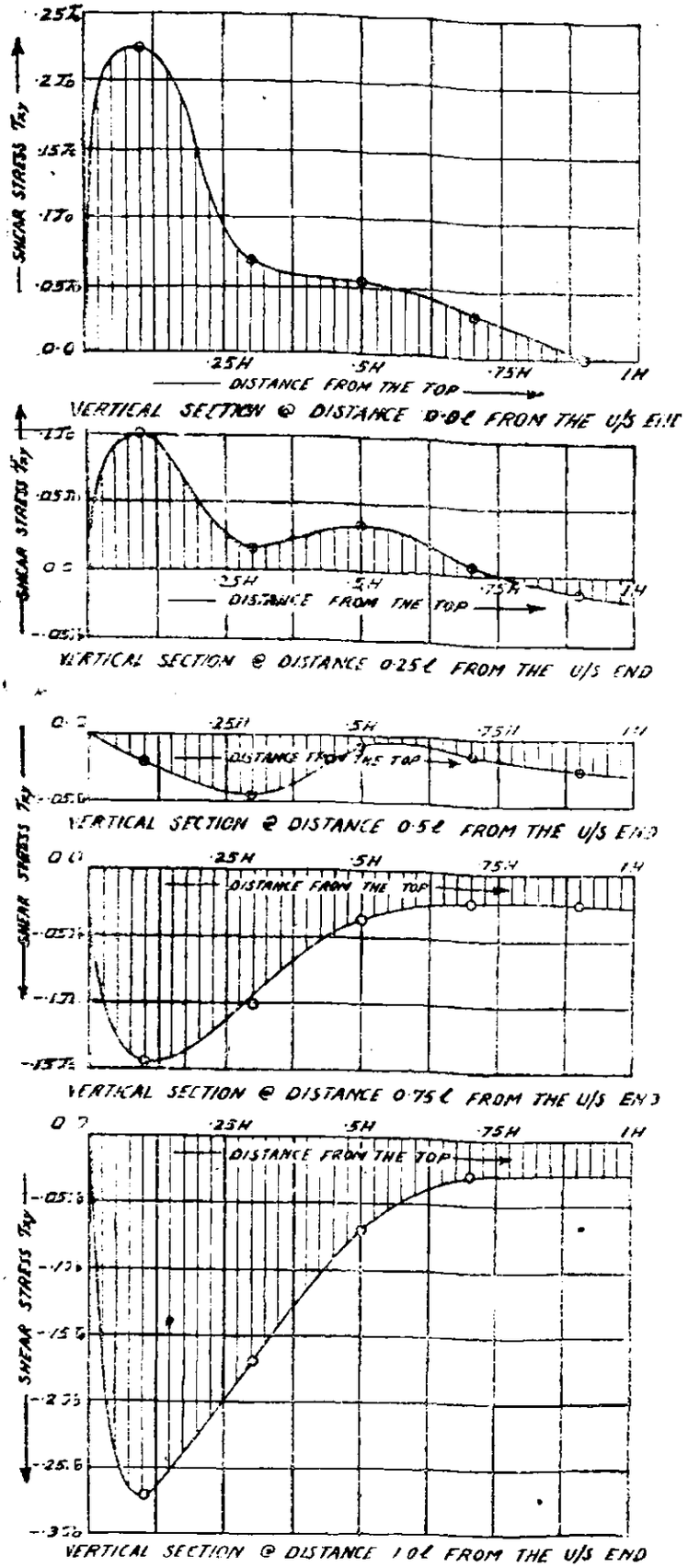

Fig 4 Shear stress in the sides of the gate slots.

agreed very well with the distribution of load calculated by ordinary method of analysis and it can be concluded that the analytical method is adequate for design purposes.

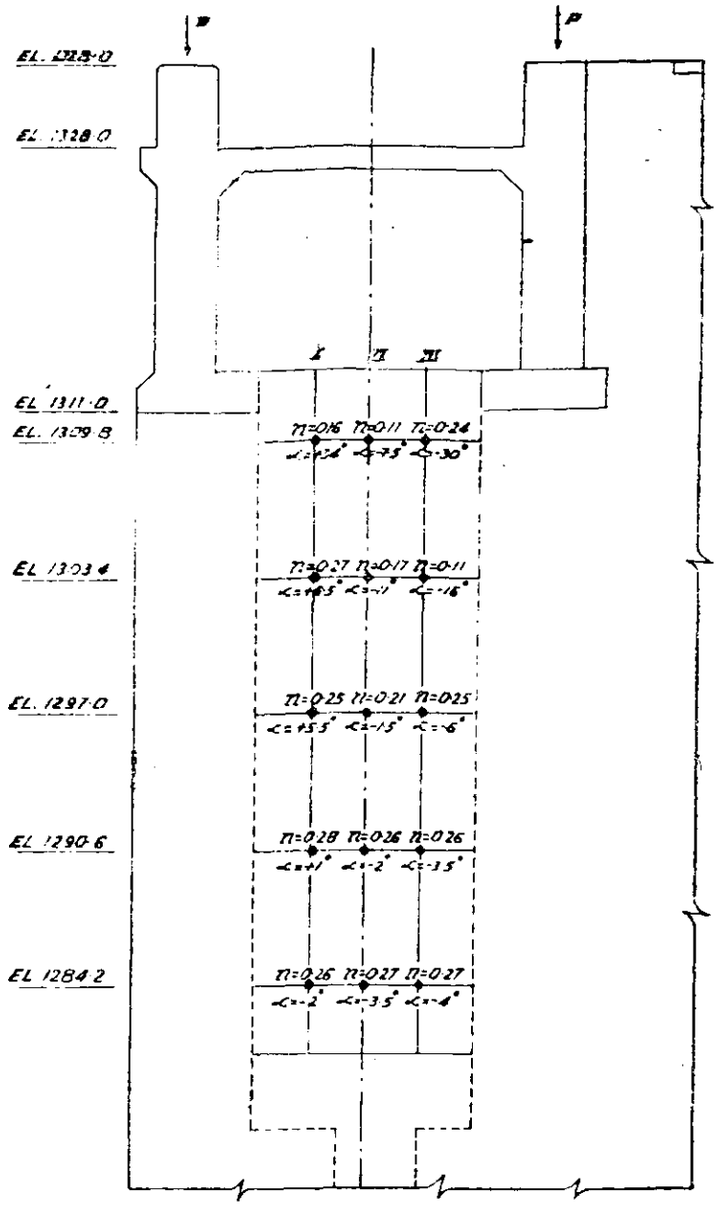

Fig 2: Fringe orders and isoclinic parameters.

(*ii*) *Analysis of shear stress distribution on gate slot sides* : The fringe orders and the isoclinic angles were measured along five horizontal sections at different elevations shown in *fig 2*. The shear stress at each point was computed from this data and a plot of shear stresses along horizontal and vertical lines was obtained in *figs 3* and *4* respectively. The maximum shear stress intensity was found to occur towards the downstream end of the slot side and a little below the top. The value of this shear is

$$(Txy)\ max = \cdot 27 \times 2p/Ht$$

Where $2P$ = the load applied

H = depth of the slot

t = total thickness of the sides.

Which corresponds to 14 *psi* in the prototype.

II. Stresses in the vicinity of 'no stress meters' in dams

FOR THE MEASUREMENT of stresses at various location in concrete dams a rosette of unbonded electrical resistance strain gauges of Carlson type is embeded in concrete. The strains measured by these gauges are developed not only on account of loads on the structure but are also due to temperature, moisture, movement and chemical action in the concrete. To isolate the effect, strains due to loads from those due to other factors it is usual to use a no stress meter. This *no stress meter* is a strain gauge attached to a block of concrete which is free from stress yet is placed closed to the location of other gauges and is subjected to the same temperature and shrinkage. To satisfy the latter requirement it is necessary that the concrete surrounding the no stress meter be continuous with the rest of concrete. A typical arrangement for no stress meter installation is shown in *fig 1*. The portion in which the strain meter is installed is isolated from rest of the concrete by a groove. The radius r of the isolated portion is decided on the basis of the size of gauge and the aggregate but very little information is available about the minimum depth of the slot that is necessary to isolate the gauge most effectively from the stress field. Photoelastic tests were, therefore, carried out for obtaining this information. The present note describes the two dimensional studies carried out in this connection.

2. Experimental procedure

A two dimensional model was prepared out of columbia Resin sheet .365 *cm* thick. The following cases were studied.

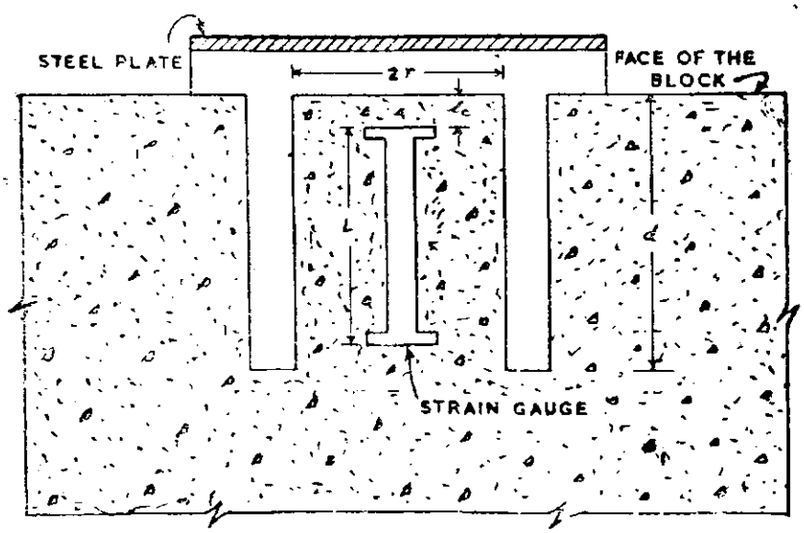

Fig 1 : Typical arrangement for no stress meter installation.

Case	d/r	Case	d/r
1	.0786	8	.8660
2	.2050	9	1.0250
3	.2838	10	1.2600
4	.3780	11	1.5420
5	.5050	12	1.8100
6	.5970	13	2.0600
7	.7245		

where d is the depth of the groove and r is the radius of the isolated portion. The model strip of size 30.5 *cm* × 12.7 *cm* was loaded in uniform tension by distributing the load at four equidistant points along the top and bottom boundaries of the model. The uniformity in the distribution of load at the middle section of the plate was

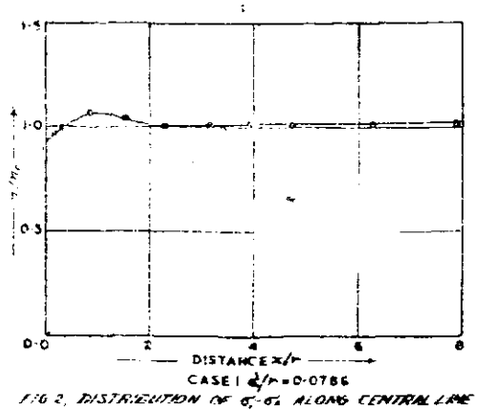

FIG 2. DISTRIBUTION OF σ_t/σ_t ALONG CENTRAL LINE

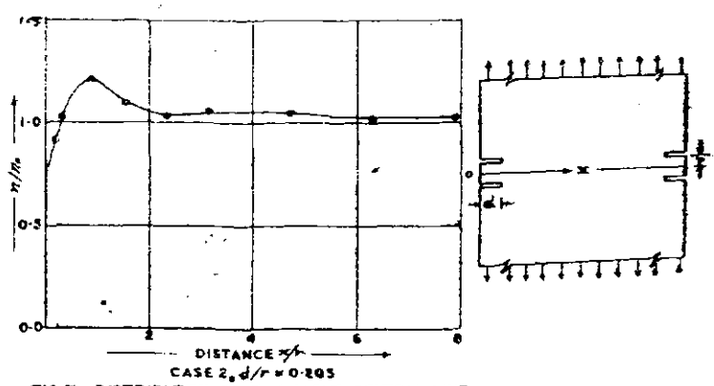

FIG 3. DISTRIBUTION OF σ_t/σ_t ALONG CENTRAL LINE

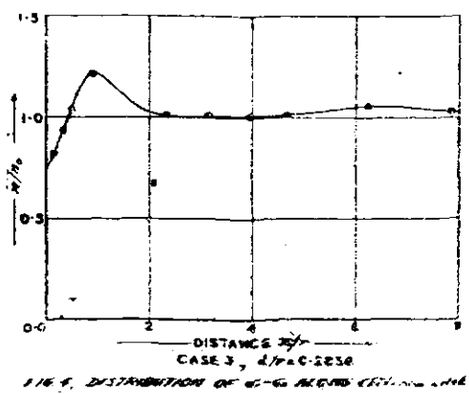

FIG 4. DISTRIBUTION OF σ_t/σ_t ALONG CENTRAL LINE

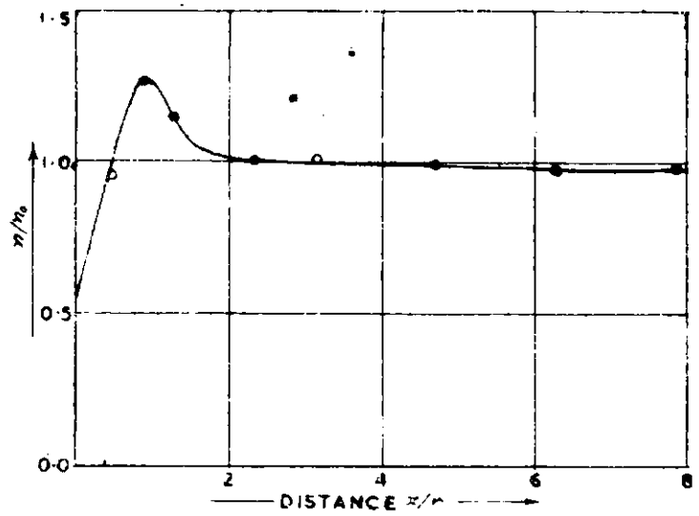

CASE 4, $d/r = 0.378$

FIG. 5. DISTRIBUTION OF $\sigma_1 - \sigma_2$ ALONG CENTRAL LINE

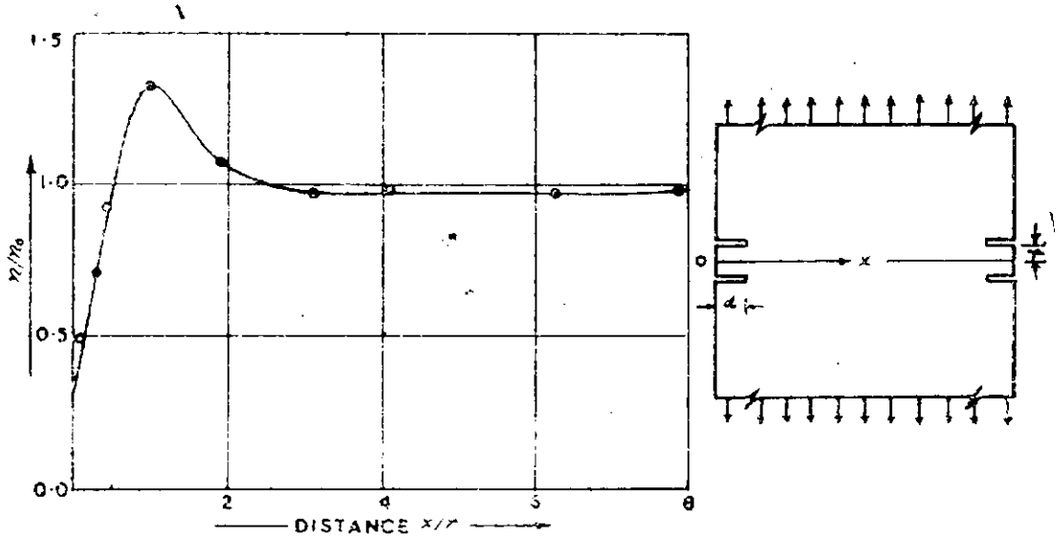

CASE 5 $d/r = 0.505$

FIG 5. DISTRIBUTION OF $\sigma_1 - \sigma_2$ ALONG CENTRAL LINE

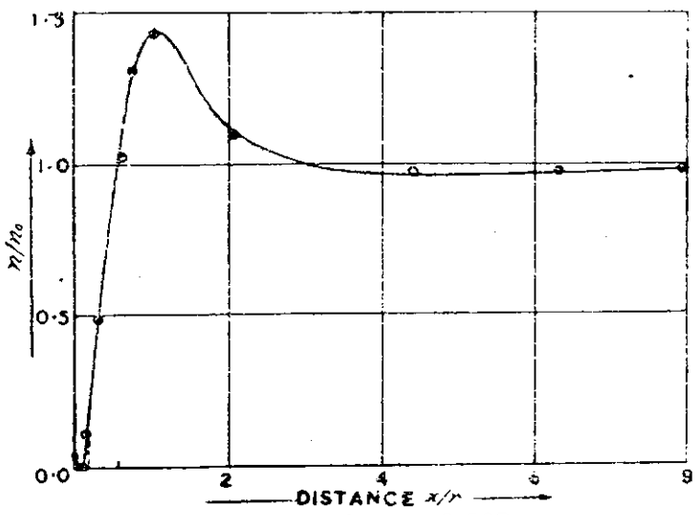

CASE 6, $d/r = 0.597$

FIG 7, DISTRIBUTION OF $\sigma_1 - \sigma_2$ ALONG CENTRAL LINE

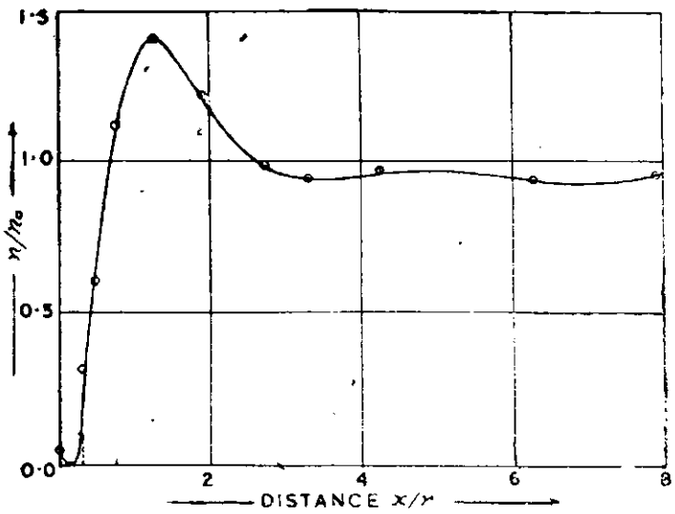

CASE 7, $d/r = 0.7245$

FIG. 8. DISTRIBUTION OF $\sigma_1 - \sigma_2$ ALONG CENTRAL LINE

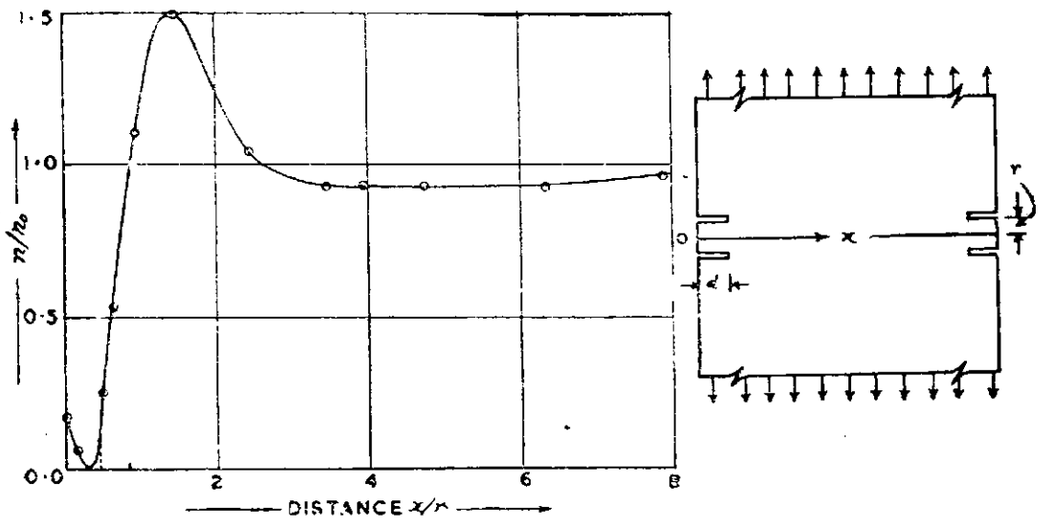

CASE 8, $d/r = 0.956$

FIG. 9. DISTRIBUTION OF $\sigma_1 - \sigma_2$ ALONG CENTRAL LINE

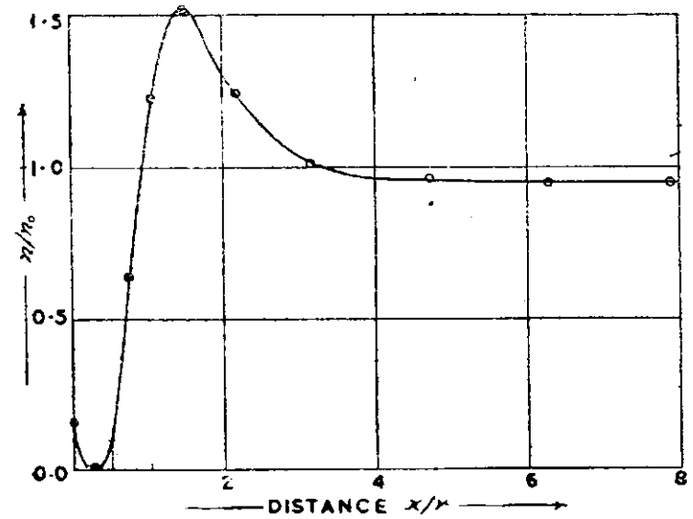

CASE 9, $d/r = 1.025$

FIG. 10, DISTRIBUTION OF $\sigma_1 - \sigma_2$ ALONG CENTRAL LINE

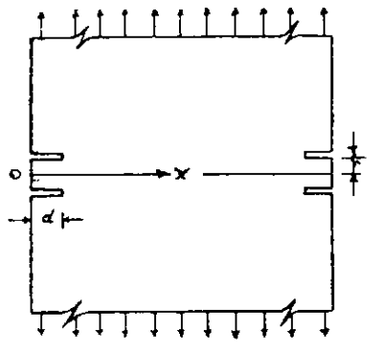

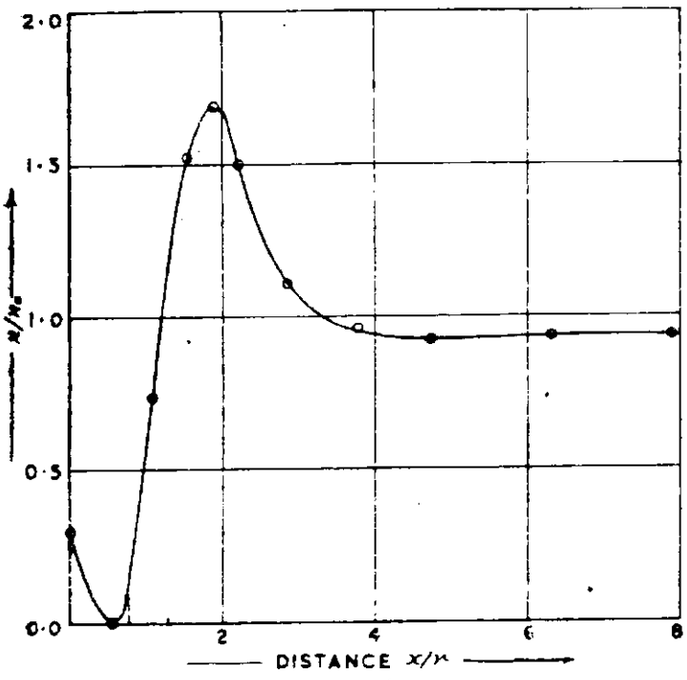

CASE 10, $d/r = 1{\cdot}26$

FIG 11, DISTRIBUTION OF $\sigma_1 - \sigma_2$ ALONG CENTRAL LINE

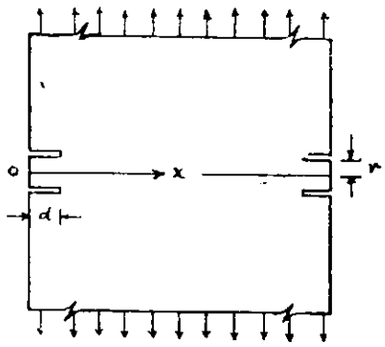

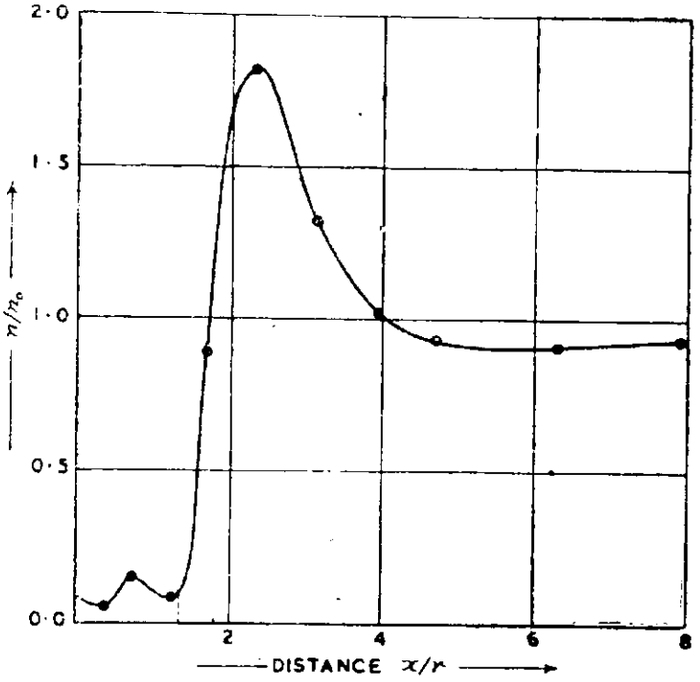

CASE 12, $d/r = 1{\cdot}81$

FIG 13, DISTRIBUTION OF $\sigma_1 - \sigma_2$ ALONG CENTRAL LINE

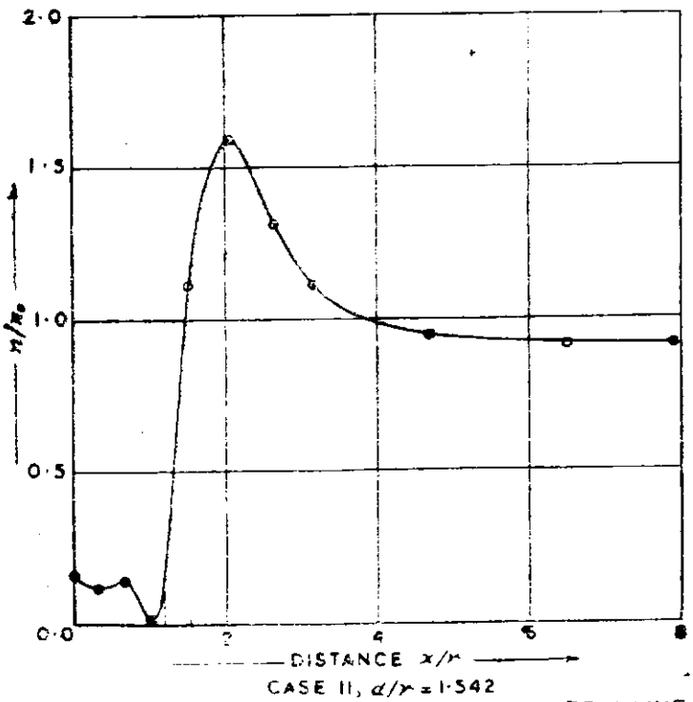

CASE 11, $d/r = 1{\cdot}542$

FIG. 12, DISTRIBUTION OF $\sigma_1 - \sigma_2$ ALONG CENTRAL LINE

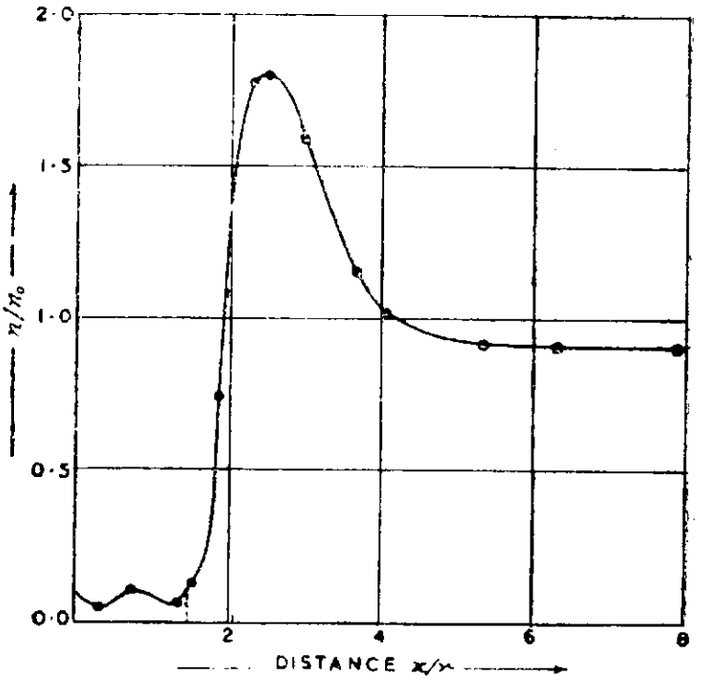

CASE 13, $d/r = 2{\cdot}06$

FIG. 14, DISTRIBUTION OF $\sigma_1 - \sigma_2$ ALONG CENTRAL LINE

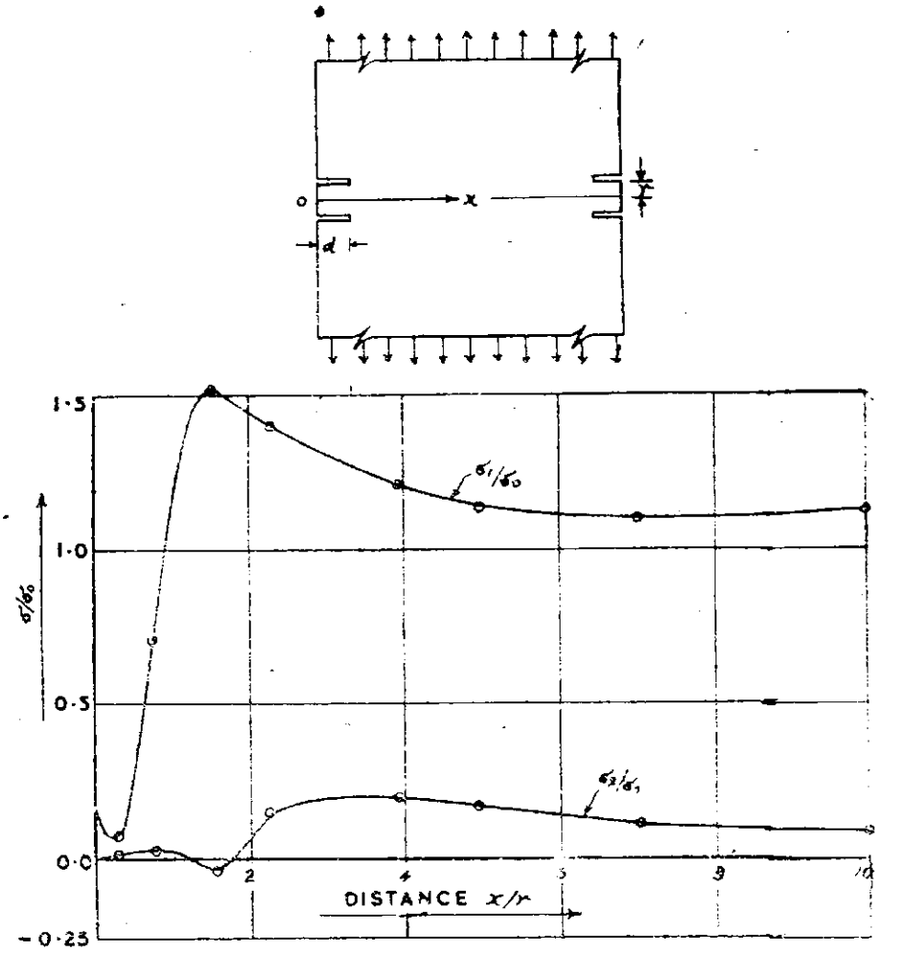

d/r = 1

FIG. 15. DISTRIBUTION OF PRINCIPAL STRESSES σ_1 & σ_2 ALONG CENTRAL SECTION

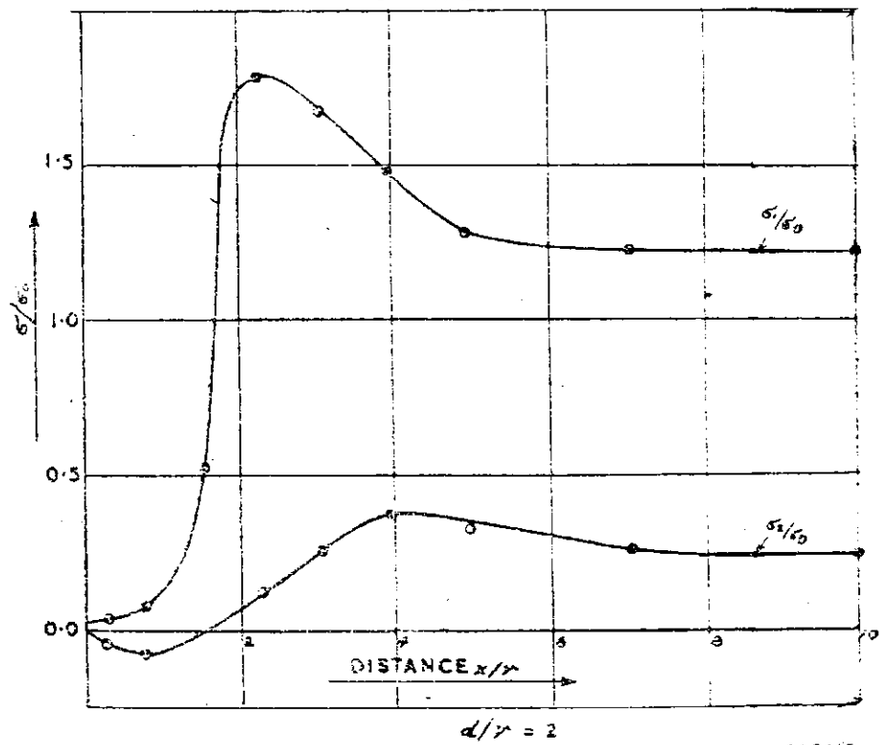

d/r = 2

FIG. 16, DISTRIBUTION OF PRINCIPAL STRESSES σ_1 & σ_2 ALONG CENTRAL SECTION

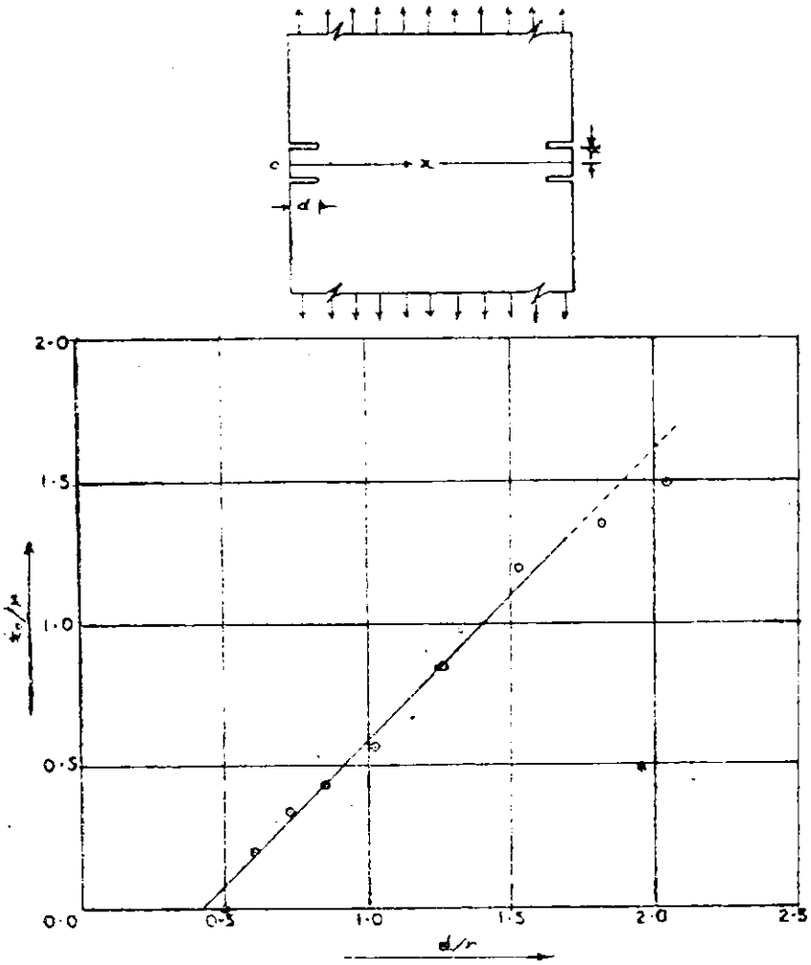

FIG 17. VARIATION OF x_0/r WITH d/r

confirmed by observing the fringe order distribution without the grooves. The grooves were made on both sides. Typical isochromatic patterns for cases d/r = .25, .5, 1 and 2 are given in *photos 65* to 72. For each case the fringe orders were measured accurately by Tardy's method at several points along the central line. Also for each case the lateral extension was measured by Hiltscher's lateral extensometer. The difference in the principal stresses was obtained from the formula

$$\sigma_1 - \sigma_2 = n F \qquad \ldots \qquad (1)$$

where n is the fringe order at point under consideration and F is the model fringe value. The sum of the principal stresses was obtained from the formula

$$\sigma_1 + \sigma_2 = k \times \delta \qquad \ldots \qquad (2)$$

where k is constant for the lateral extensometer used and d is the lateral extension. The principal stresses at each point were separated by using the relations (1) and (2).

3. Discussion

The principal stresses along the central section for cases d/r = 1 and 2 are given in *figs 15* and *16*. It is observed from these curves that in the isolated region the major principal stress is small near the face of the isolated portion remains constant for a certain distance and then rapidly rises to a peak at a point approaching the end of the groove. Beyond that there is a gradual reduction in stress and uniform conditions are obtained at a distance of the order of twice the depth of the groove from the face.

The distribution of the major principal stress and the difference in principal stresses is almost of the same nature as the minor principal stress and is of the small magnitude. It was, therefore, sufficient to study only the difference in the principal stresses to get the point beyond which the stresses rise very rapidly.

The main purpose of these tests, as already stated, was to determine the distance from the face up to which the isolated portion could be considered free from stress. To arrive at a quantitative estimate of this distance the criterian was adopted that the stresses should not be more than ten *percent* of the average at the end.

The distance where the stresses go beyond 10 *percent* of the average is denoted as x_{10}. This is marked in each of the curves in *figs 2-14* by the dotted line. This stress is acting normal to the axis of the strain gauge and hence even a 10 *percent* stress would affect the strain gauge very slightly. The effect will depend on the Poisson's ratio of the concrete used. If Poisson's ratio of concrete is assumed as .1, the effect of this stress would be only 1 *percent* of that given by the

average stress in the direction of the strain gauge. The minor principal stress is always less than 1 *percent* and hence need not be considered.

The veriation of x_0/r with d/r is given in *fig 17* and is practically a straight line in the region $d/r = 2$. The no stress meter strain gauge must in all cases be placed within a distance x_0 which can be considered as free from stress. Knowing the length of the strain meter and the diameter of the cylinder scooped out the x_0/r ratio can be determined after allowing for the cover at the top. A suitable value of the depth of the isolated portion can be read off from the curve given in *fig 17*.

It may be noted, however, that these results are based on two dimensional analysis and are not strictly applicable to the actual three dimensional cases.

4. Conclusions

From the above study the following relation may be obtained for finding out the depth to which the groove is to be taken for obtaining reliable results from no stress meters.

$$d = L + l_c + r/2 \quad \ldots$$

where d — minimum depth of the groove
L — length of the strain meter
lc — cover at the top
r — radius of the isolated portion

---

19. Three dimensional photoelastic analysis

Gandhisagar Spillway Piers

SPILLWAY piers of the Gandhisagar dam include large openings to facilitate operation of sluice gates in the body of the dam from the top of the spillway bridge. The piers are spaced at 26.21 *m* (86 *ft*) centre to centre and support a spillway bridge of 18.28 *m* (60 *ft*) clear span with .91 *m* (3 *ft*) thick beams. The bridge carries a 7.62×10^4 *kg* (75 *ton*) Granty crane in addition to *IRC* Class *A* loading. The girders are provided with sliding bearings on the piers. No major problem arises in the design of the piers for the vertical loads coming from the bridge or for the water pressure. However, the analysis for transverse forces due to the thermal expansion of the bridge and friction of the bearing is very complicated. A transverse load of the order of 40.9×10^3 *kg* (90 *kips*) may develop due to thermal expansion of the bridge. This eccentric load goes down to the foundation with the following alternative action.

(i) Cantilever action of the upstream portion of the pier.
(ii) Portal action of a horizontal section of the pier.
(iii) Torsion of the whole section.

The purpose of the three dimensional photoelastic studies was to determine the proportion of the loads transferred in each of the modes.

2. Preparation of the model

A three dimensional model of the spillway pier (*photos 73* and *74*) was made from an araldite block (Araldite D + 40 *percent* phthalic anhydride) to a scale 1/200. The dimensions of the model are given in *fig 1*. The top of the spillway was simulated by a block of 15 *cm* length × 13 *cm* width and 7.5 *cm* height of the same material. The former was then pasted to

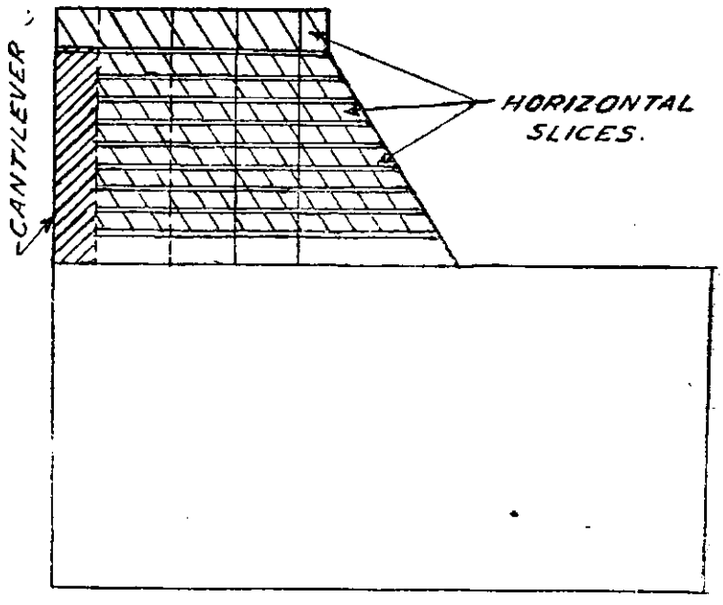

Fig 1: Plan of slicing.

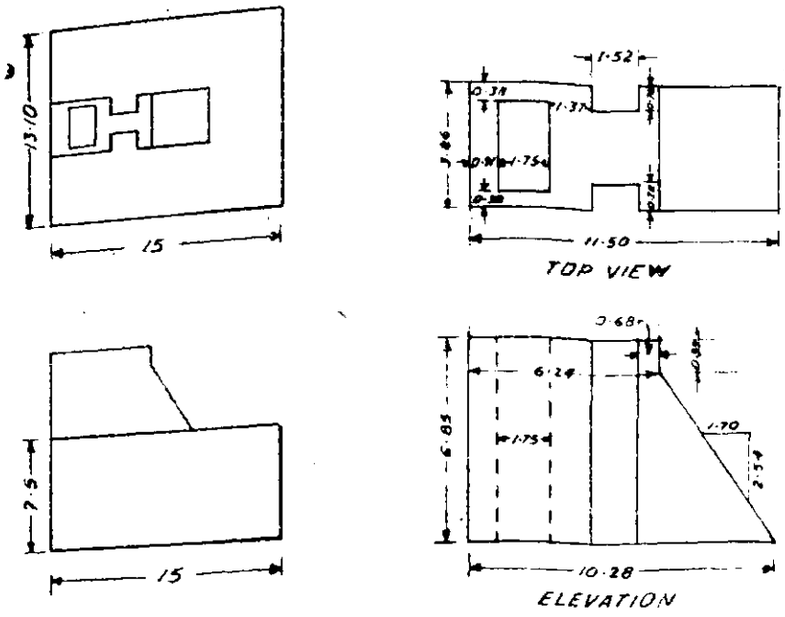

Fig 2: Dimensions of model.

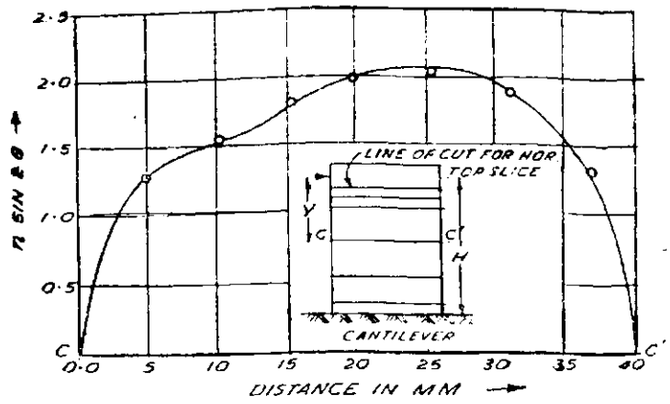

Fig 5: Shear stress distribution in section CC' ($y/H = 0.500$) (side width $2\frac{1}{2}$ *ft*).

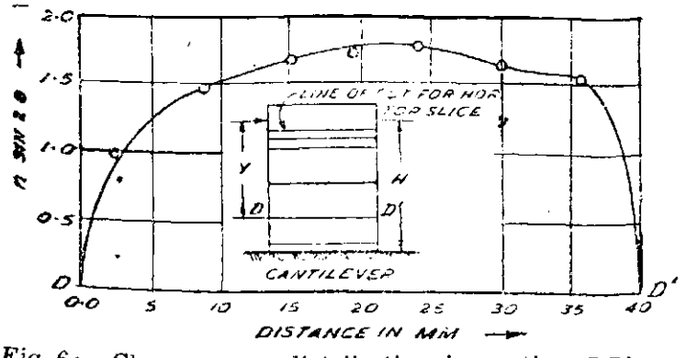

Fig 6: Shear stress distribution in section DD' ($y/H = 0.75$) (side width $2\frac{1}{2}$ *ft*).

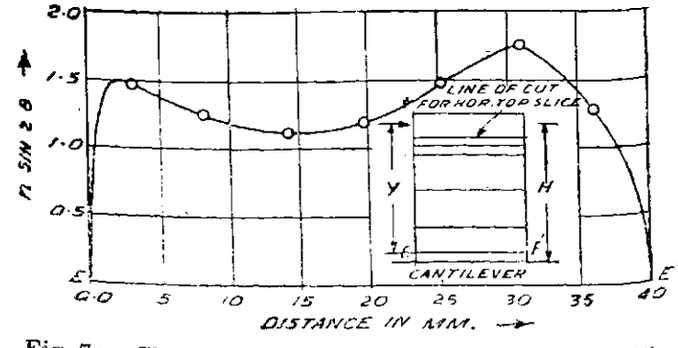

Fig 7: Shear stress distribution in section EE' ($y/H = 0.938$) (side width $2\frac{1}{2}$ *ft*).

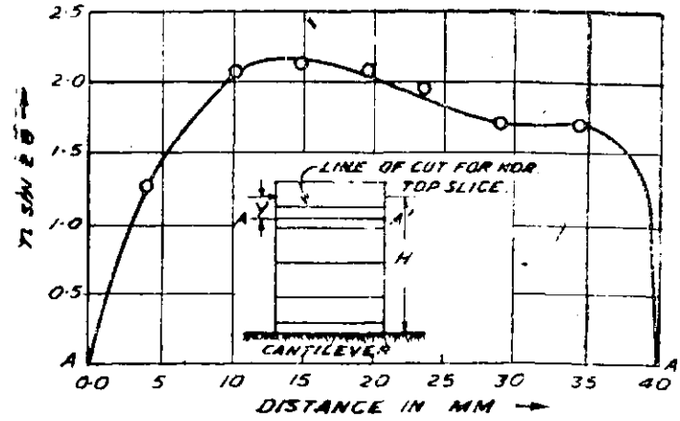

Fig 3: Shear stress distribution in section AA' ($y/H = 0.188$) (side width $2\frac{1}{2}$ *ft*).

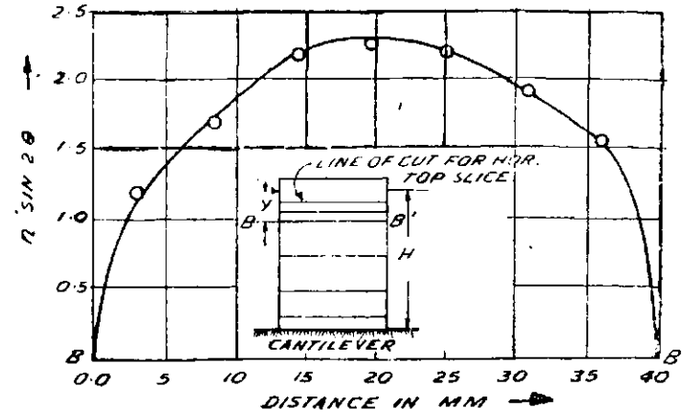

Fig 4: Shear stress distribution in section BB' ($y/H = 0.250$) (side width $2\frac{1}{2}$ *ft*).

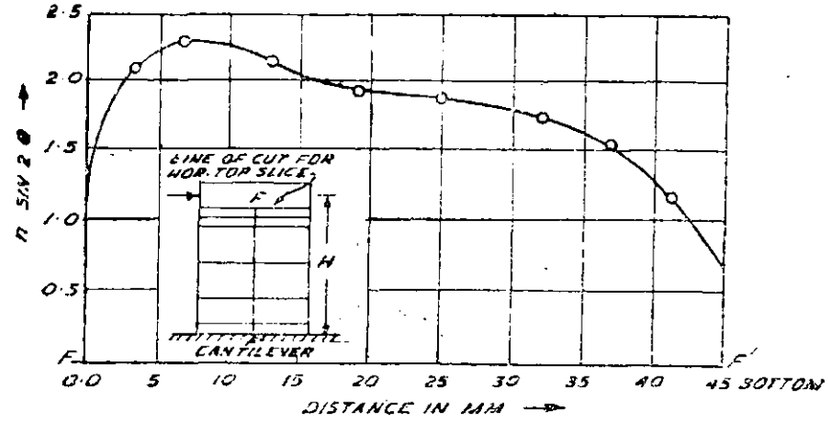

Fig 8: Shear stress distribution in section FF' (side width $2\frac{1}{2}$ *ft*).

this block using Araldite D and hardener 951. The whole assembly was cemented to 1.25 *cm* thick and 20 *cm* in diameter iron plate.

Loading : The transverse concentrated load was applied by a lever arrangement shown in *photo* 75. The lever ratio was 2:1. A load of 2.5 *kg* was applied to the lever, the load going on the model being 1.25 *kg*.

Stress freezing : The model with loading arrangement was kept in the oven, having programme controller and the temperature was

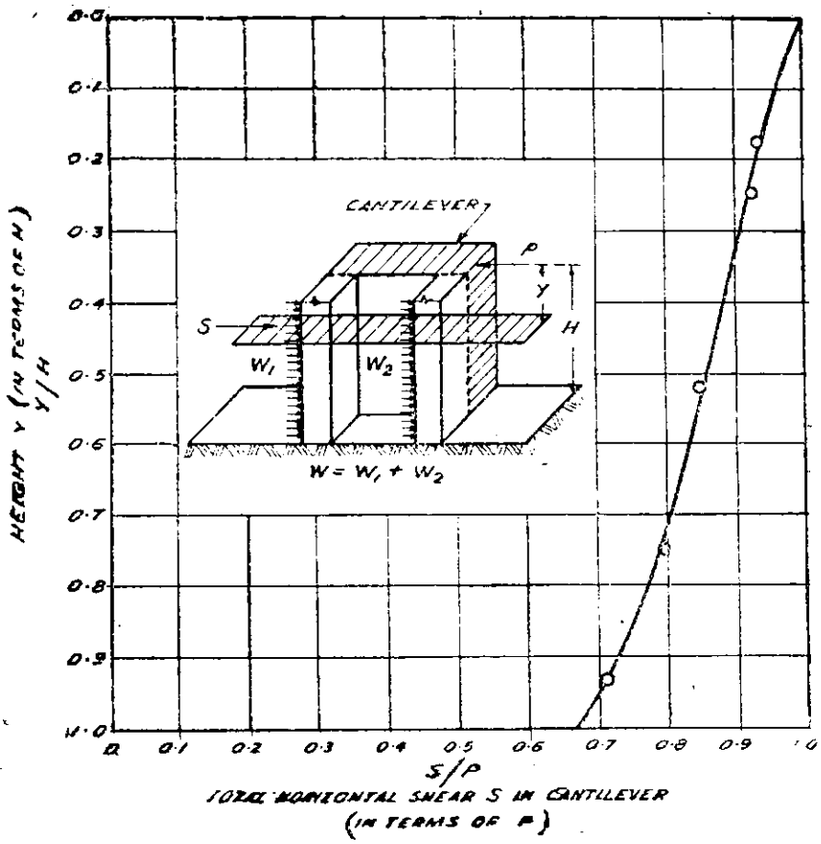

Fig 9: Load taken by cantilever.

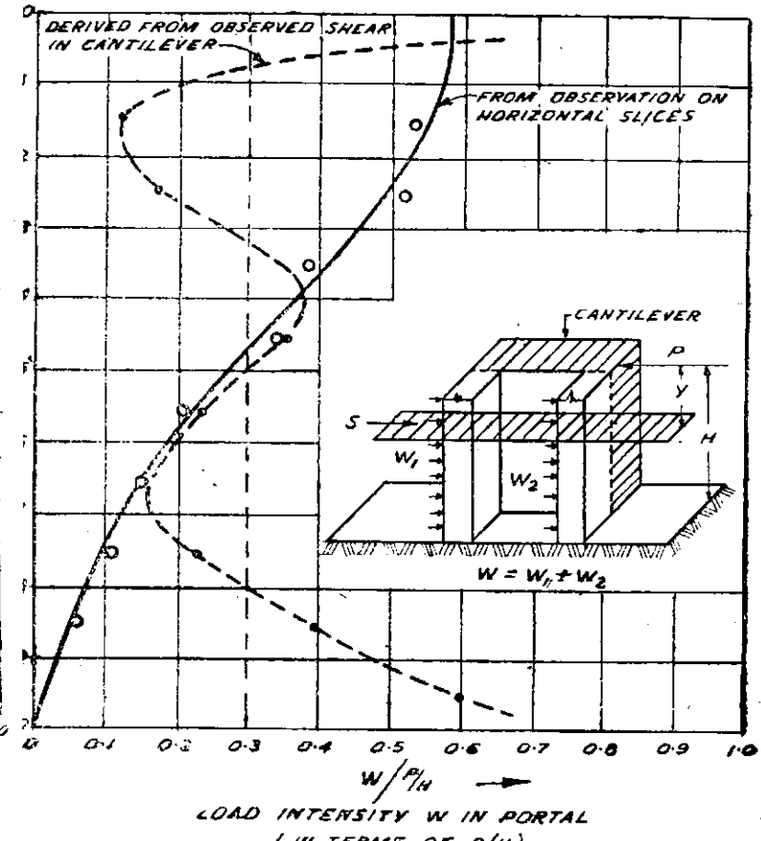

Fig 10: Load taken by portals.

raised at the rate of 2° C per hour to 130° C. The model was kept at this temperature for 8 hours in order to soak the temperature. The model was loaded and the temperature was lowered to room temperature at the rate of 2° C per hour.

Slicing : The plan of slicing is shown in *fig 2*. Top horizontal slice was cut first and then vertical slice of cantilever was cut. Eight more horizontal slices were taken from the remaining model.

8. Analysis and results

The slice was examined in the polariscope and the measurement of the fringe orders along the sections *AA'*, *BB'*, *CC'*, *DD'*, *EE'*, and *FF'* (*figs 3* to *8*) were taken using Trady's method. *Photo 76* shows the stress pattern for vertical cantilever slice (isochromatic - dark field). Shear stresses on horizontal planes at various sections of the cantilever were computed and the total shear at any section was calculated. This is plotted in *fig 9*. About 70 *percent* of the load is transferred to the foundation directly by cantilever action. This information would enable the economical design of the cantilever reinforcement. The shear stress diagram is practically linear and shows that the rate of transfer of the shear to the portals is practically constant and equal to about $\frac{\cdot 3 \times 90}{38.3}$ .81 *kips ft* (12.11 *kg/cm*) on the average (*fig 10*). A more detailed analysis of this data however gives the distribution of load intensity as shown by the dotted curve in *fig 10*.

4. Horizontal portal sections

The horizontal slices were also examined in the polariscope and the measurement of fringe orders and isoclinics were made on the central sections of the narrow sides of the slots. Isochromatics for the top slice are shown in *photo* 77.

Analysis of the horizontal slices showed that the maximum load was transferred to the top slice where the intensity was (considering the minimum slice of .91 *m ie* 3 *ft* in prototype) 22.44 *kg/cm* (1.5 *kips/ft*). This drops down to about one third at height of about 4.8 *m ie* 16 *ft*. The distribution of intensity is given in *fig 10* by the continuous line. Near the base (top of spillway) there is practically no portal action. In spite of this, an increasing amount of the shear from the cantilever is transferred to the narrow sides of the portal. This is understandable if we realise that the narrow sides of the slots are fixed at the bottom and offer increasing torsional restraint. The shear from the cantilever therefore

passes directly to the foundation through the narrow sides. No portal action occurs. The intensity of load in this lower part of about 1.8 to 2.1 *m* (6 to 7 *ft*) is 29.92 to 44.88 *kg/cm* (2 to 3 *kips/ft*). The ideal reinforcement would be at 45° but vertical and horizontal bars providing equal area would be adequate.

5. Recommendations

Based on the above studies the following can be recommended as design loads for a total transverse load of 90 *kips*.

Distance from load point *ft*		Intensity (*kip/ft*) of load per *ft* portal	
0-8	...	2	
8-16	...	1·5	
16-24	...	1·0	
24-base	...	Little portal action. Vertical reinforcement important.	1·5 in vertical cantilever.

20. Experimental stress analysis

I. A 40 ft Steel Tower

IN THE DESIGN of steel towers consisting of several individual columns braced together by horizontal and diagonal members, it is assumed that each plane frame acts as a truss and the columns are subjected to simple tensile and compressive forces even when the tower is being subjected to lateral loads (wind or earthquake). It is obvious, however, that this unit action of the tower will only take place if the columns and the other members are proportioned properly. For example if the diagonals and the cross members are very slender and flexible, each column will behave as a cantilever and will be subjected to a very high bending moment near the base. Increase of the section of these columns would only add to the moments and may not reduce the bending stresses. It is, therefore, essential in the design of such structures that proper proportion between the columns and the other members to be maintained to avoid unnecessary waste of material. A similar problem arose while examining the design of a 40 *ft* steel tower proposed to be constructed in this research Station. An experimental study was taken up to arrive at general criteria for proportioning the members in such towers.

2. Problem and experimental procedure

The dimensions of the steel tower together with the design loads are given in *fig 1*. The tower is subjected to a live load of 10 *tons* on each column together with wind load. The analysis, if truss action can be assumed, does not present any problem and is amenable to the routine analytical methods for the analysis of redundant frames. However, if the columns are not well proportioned, truss action and cantilever action in individual columns, both take place and theoretical analysis becomes complicated. An experimental study was, therefore, undertaken. Begg's Deformeter was used for the experimental analysis.

The equipment essentially consists of accurate guages which can be fixed to the structure at the points where loads are to be determined and measurements of deflections are carried out by means of accurate Microscope at the points where the load is applied. The construction of the gauges enables any type of deflection *ie* the direct thrust, shear or rotation to be given at the gauges. Unknown forces at any section can then be found from the relation:

$$F = P_n \frac{\Delta_n}{\Delta}$$

where F = unknown force to be found out at the desired section.

Δ = deflection introduced at the desired section in the direction of F.

P_n = the force acting at any point n, the effect of which is to be obtained at the desired section.

Δ_n = the deflection produced at the point n, in the direction of P_n where the force P_n is supposed to be acting.

Two scales were adopted in the analysis of this model, one for the linear dimensions (1/12) and another for the moment of inertia $1/1.104 \times 10^4$. Three different series of tests were carried out with moment of inertias of the columns 115 in^4, 58.8 in^4 and 24.6 in^4.

3. Results and discussion

The influence curve for thrust at the fixed ends of the columns are given in *fig 2*. The thrust gradually increases as the load moves from the foundation to the top. This is as expected in a cantilever but in a pin connected truss the column should show no moment. Another significant point is that the increase in moment of inertia of the columns decreases the thrust which means, in other words, that the total moment resisted by the reactions is less for columns with higher moment of inertia than from one with less moment of inertia. Consequently high moments will be developed at the foundation ends of the columns having large moment of inertia.

This point is further clarified in *fig 3* wherein the influence curves for the moments at the foundation are given for the three different sizes of columns. For column with moment of inertia equal to 115 in^4 the moment rapidly increases with the distance of the load from the base. It shows that the columns are behaving as independent cantilevers and high bending moments have, therefore, been developed. As against this the column with I = 24.6 in^4 shows practically no increase in the bending moment when the load moves towards the top. This shows that the columns behave as a part of the truss and do not act as an independent cantilevers. It may be mentioned that the constant bending moment shown by each of the columns at the foundation is due to the portal action and has nothing to do with the cantilever action discussed above.

In order to elucidate the structural behaviour better for the case of columns with I = 24.6 in^4, loads were analysed in the bottom panel of one of the columns and also in the diagonals. The influence curves for these cases are given in *figs 4*, 5 and 6. These show that the structure behaves as a truss and the moments are negligible.

4. Conclusions

The above study clearly shows that the increase in section of the columns beyond a certain

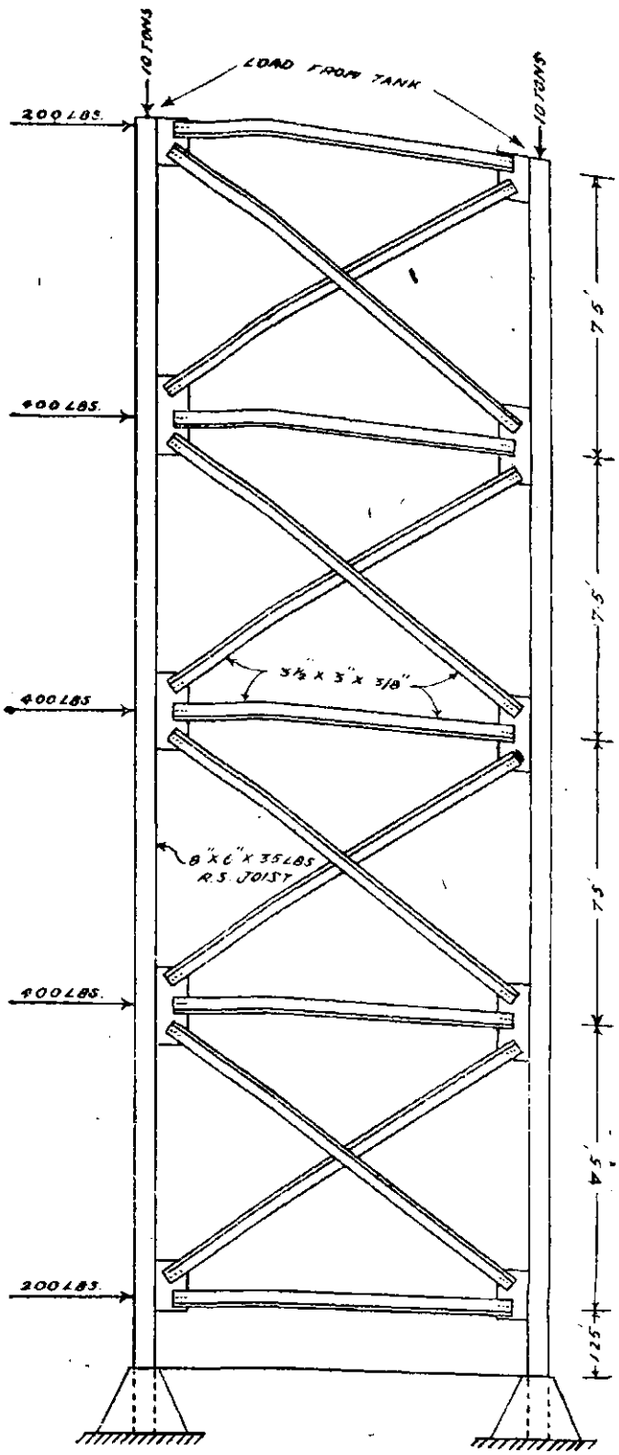

Fig 1: Dimensions and design loads.
Note: Wind load of 2500 *lbs* acts at 37.5 *ft* from the base.

limit only leads to the increase in moments and results in waste of material. In this particular case, the columns proposed were 8 *in* × 6 *in* at 35 *lbs* joists and the experimental study showed that these were too heavy. Increase in sections of columns did not increase the safety factor in the structure as there was corresponding increase in the bending stresses. *Fig* 7 shows how an increase in the moment of inertia of the columns increases the end moments in the columns. The

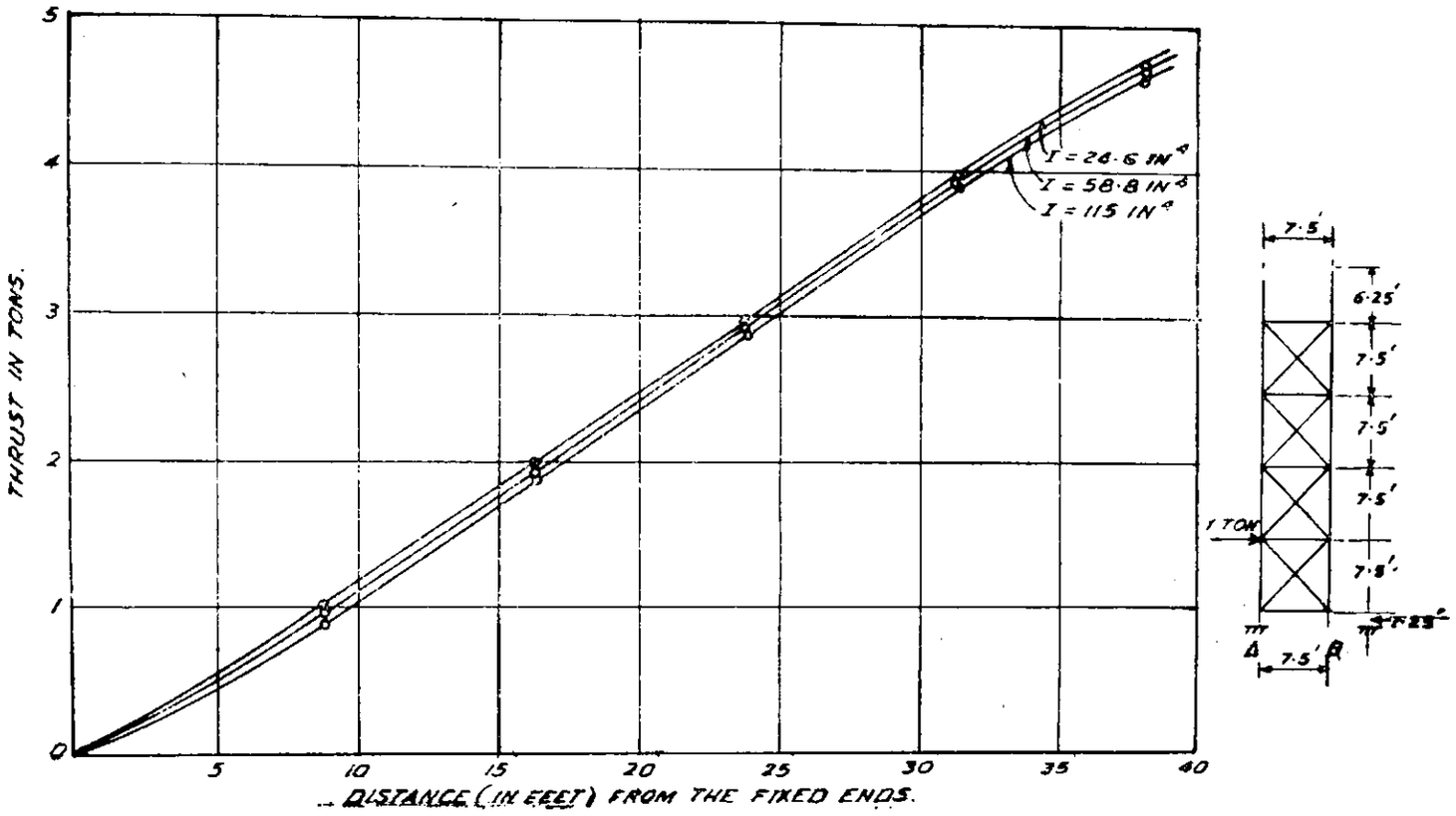

Fig 2: Influence curve for thrust at "A" due to load acting horizontally. The figure at the right shows Cavitation tank tower analysis by Beggs Deformeter. I = Moment of inertia of the column.

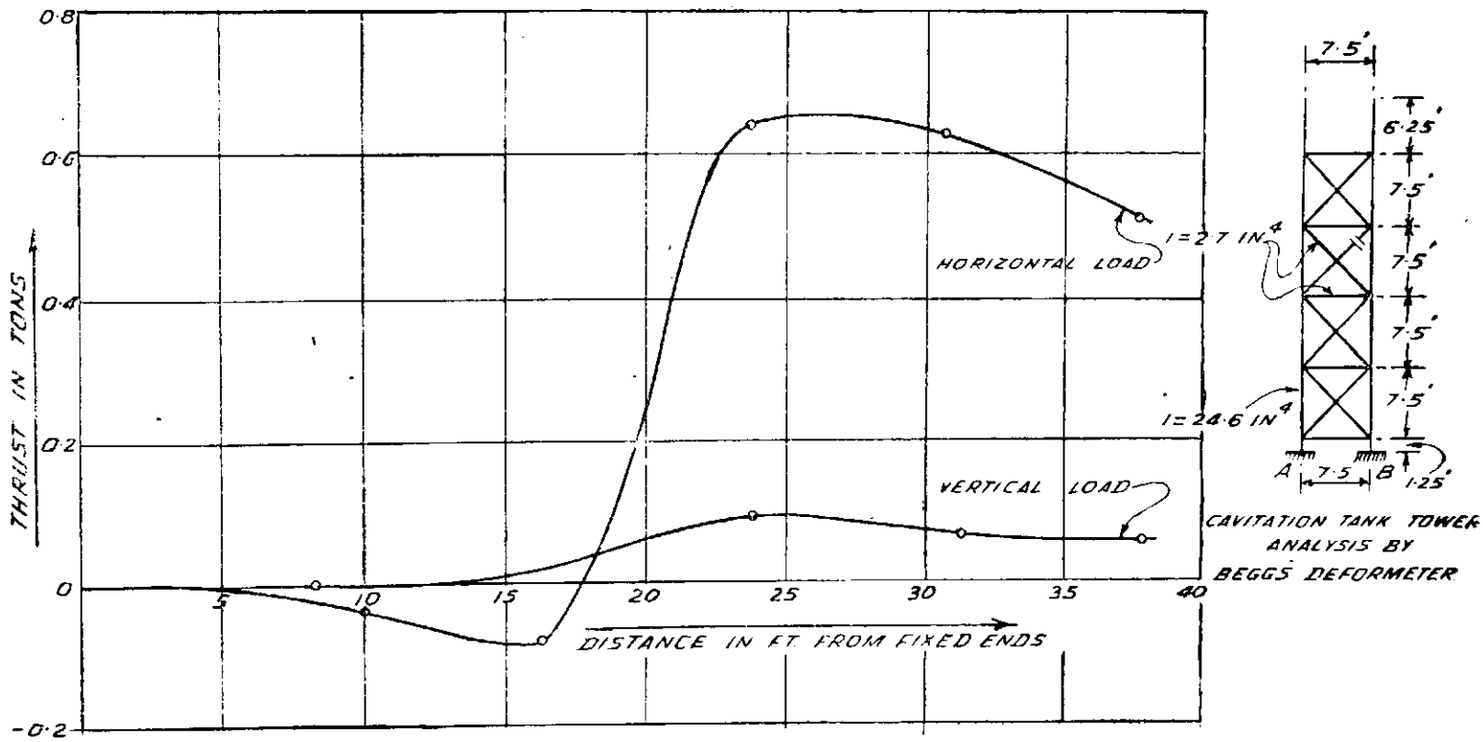

Fig 6: Influence curves for diagonal member shown cut in the *fig* for thrust due to vertical and horizontal loads acting separately.

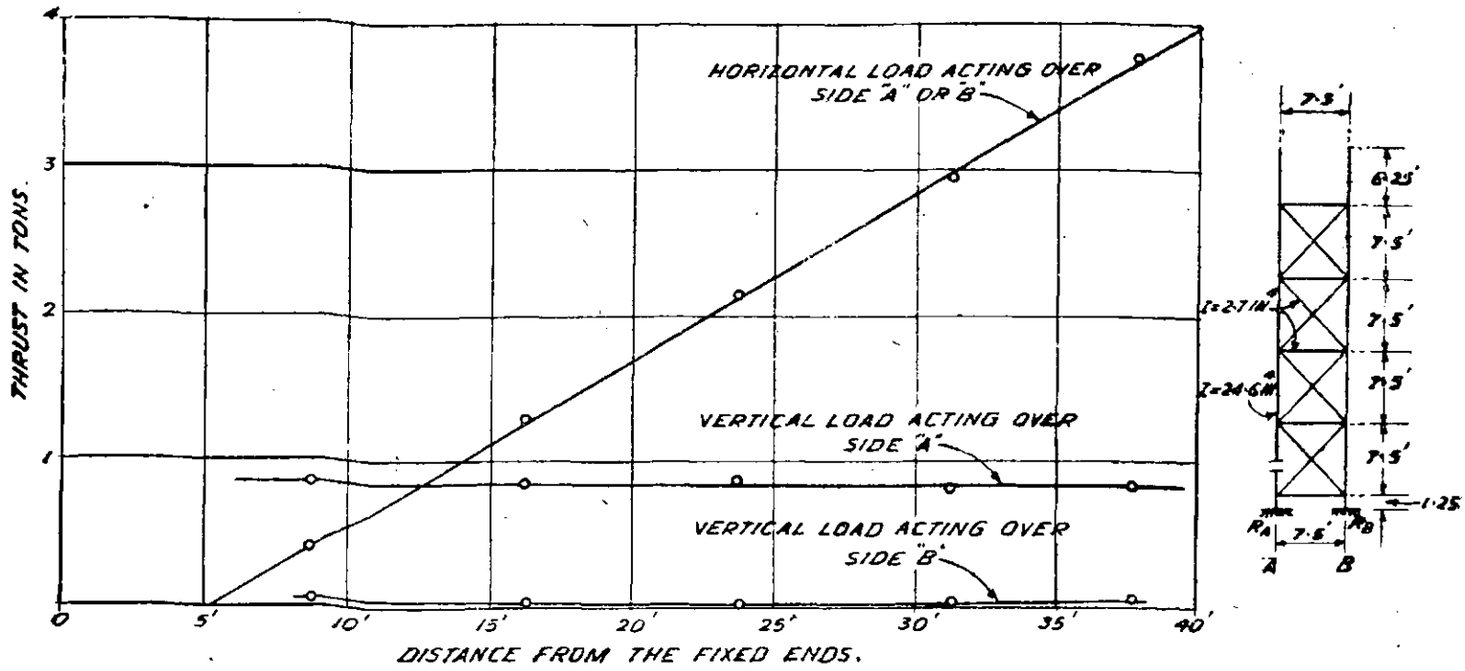

Fig 4: Influence curves for the member shown cut in *fig* for thrust due to vertical and horizontal loads acting separately. The figure at the right shows Cavitation tank tower analysis by Beggs' Deformeter.

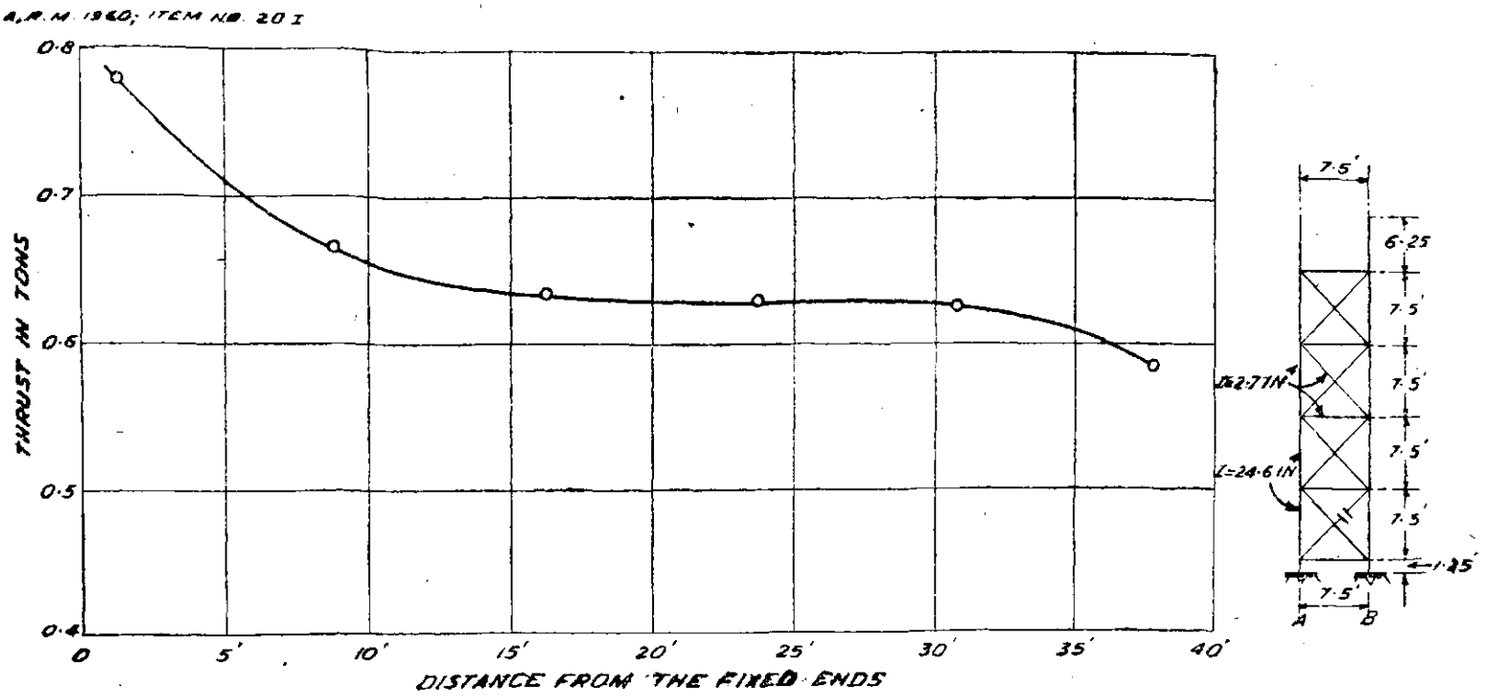

Fig 5: Influence curve for the diagonal member shown cut in the *fig* for the thrust due to load acting horizontally. The figure at the right shows Cavitation tank tower analysis by Beggs' Deformeter.

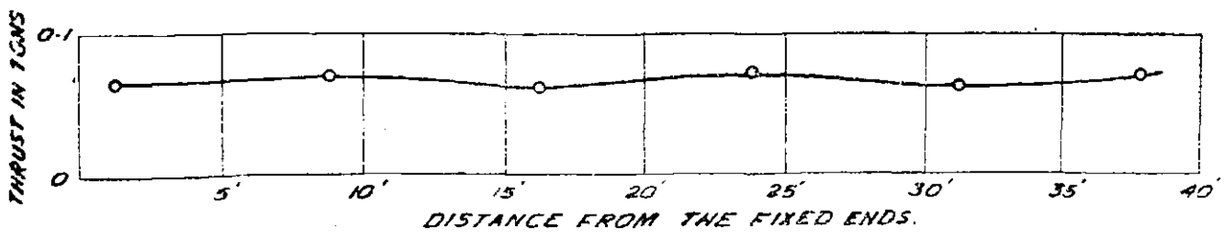

Fig 5: Influence curve for diagonal member shown cut in the *fig* for the thrust due to vertical load.

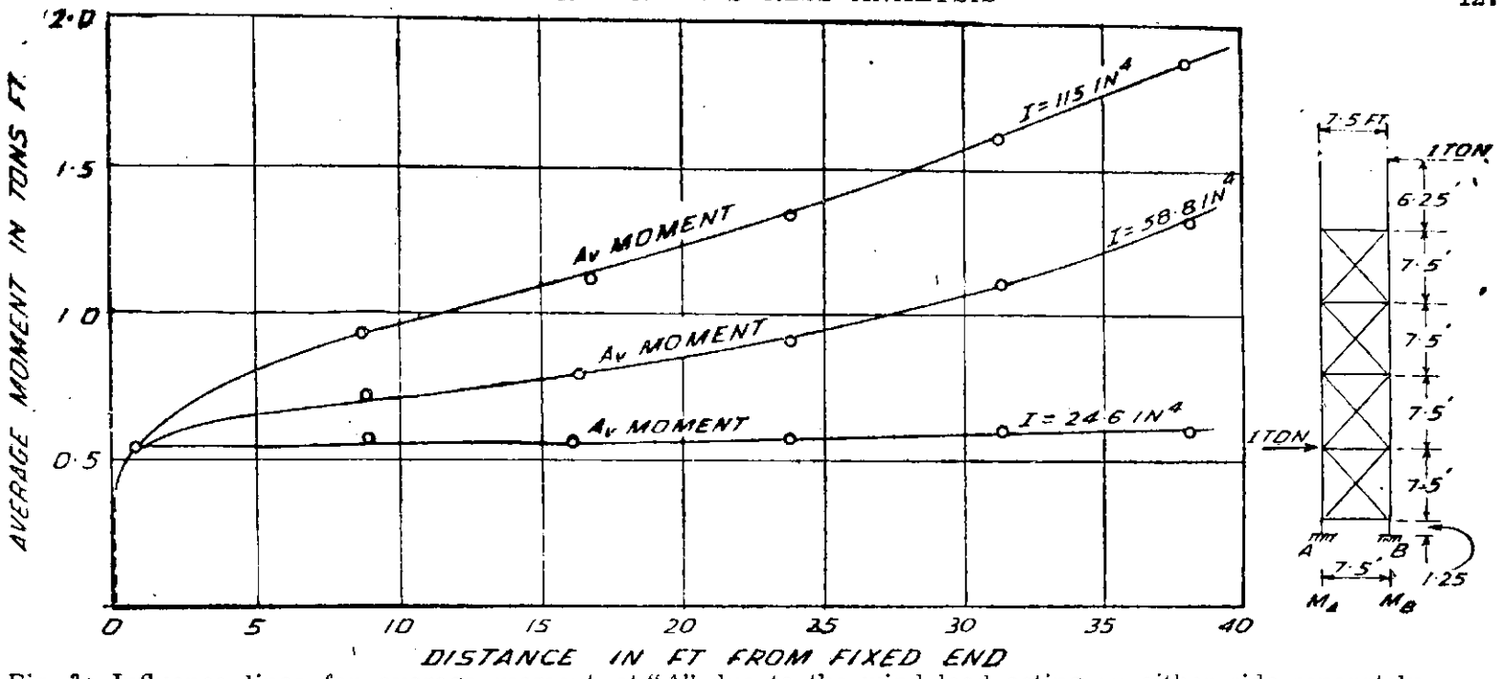

Fig 3: Influence lines for average moment at "A" due to the wind load acting on either side separately.

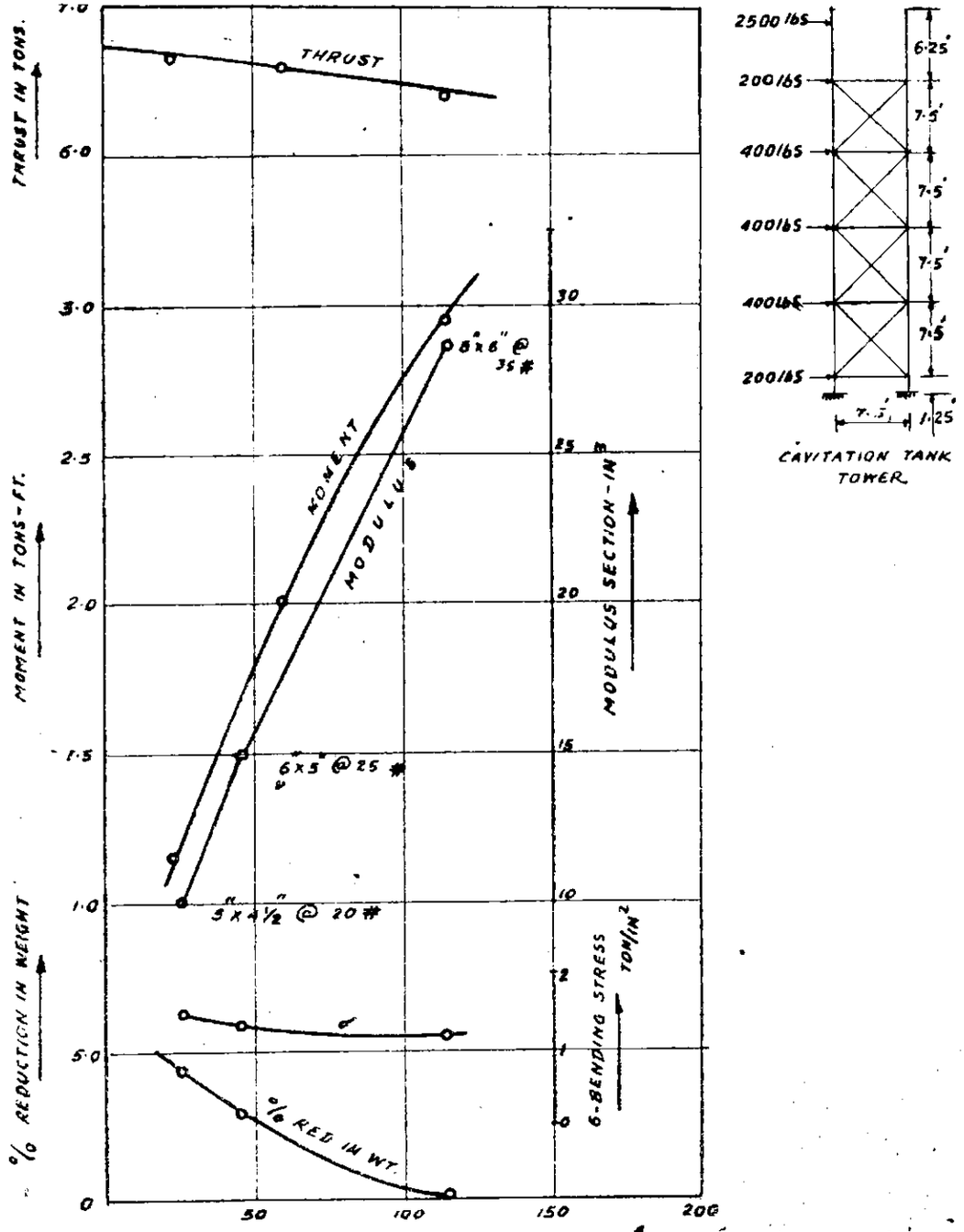

Fig 7

modulus of the section for various joists ranging from 5 *in* × 4½ *in* at 24 *lbs* to 8 *in* × 6 *in* at 35 *lbs* are also given. A decrease in the column section although decreasing the modulus of the section, reduces the moment and the maximum stress in the columns remains practically the same. It was, therefore, possible to reduce the weight of the columns by about 40 *percent* without decreasing the strength of the structures.

The above results can easily be generalised and can be used to find out the economical sections of the columns for structures of similar dimensions.

II. Nagarjunasagar--Construction Trestle Bridge

IN ORDER to facilitate the movement of material during the construction of the Nagarjunasagar Dam, it is proposed to construct a steel trestle bridge 3600 *ft* long. The bridge is composed of trestle towers which carry the crane girders and walkway girders. The elevation of the top of

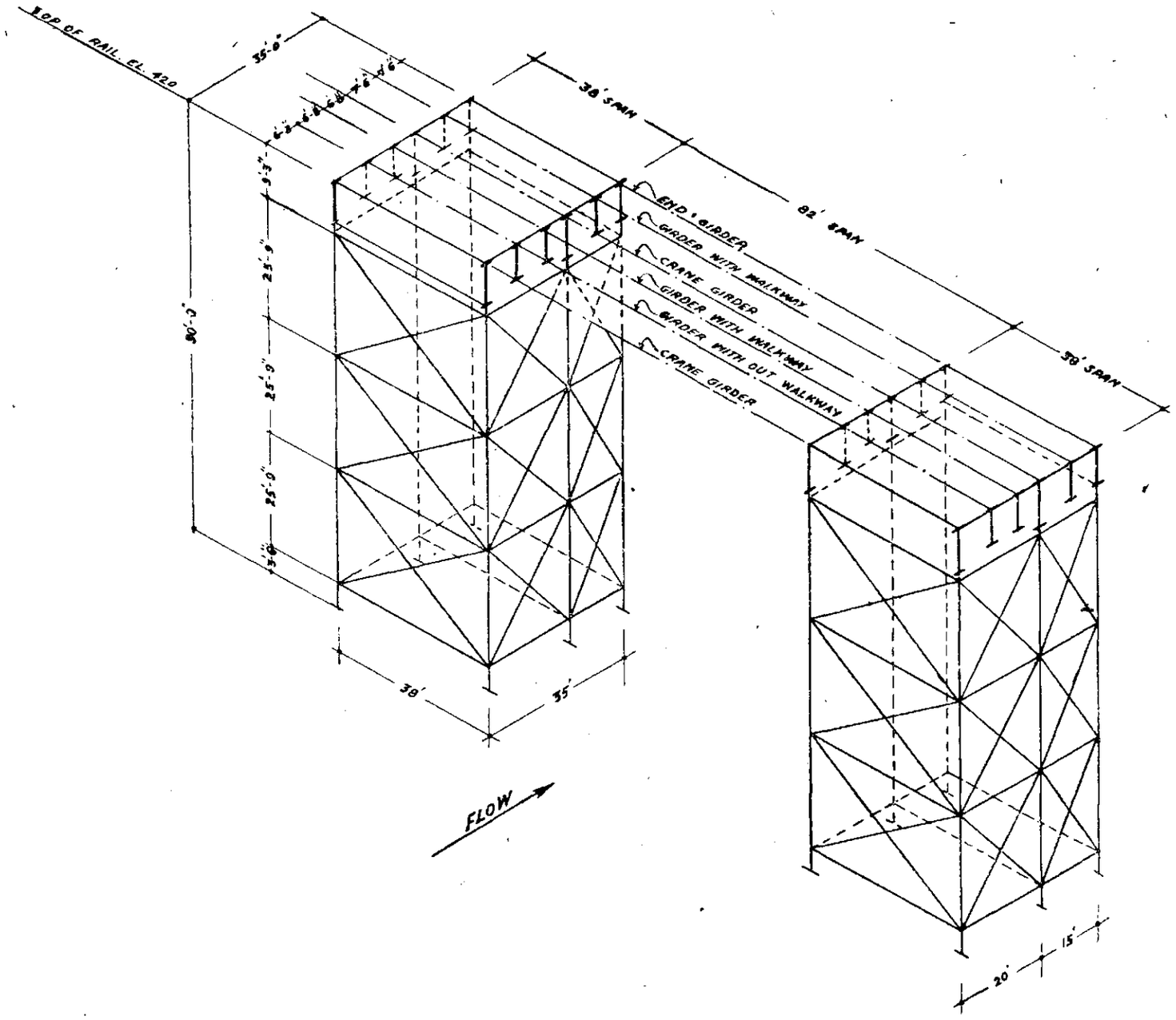

Fig 1

rail is *RL* 420. A line sketch showing the position of the two typical trestle towers and bridge girders is given in *fig 1*. Details of the tower are given in *fig 2*.

In order to provide clearance for the erection of the girders and to accommodate the end

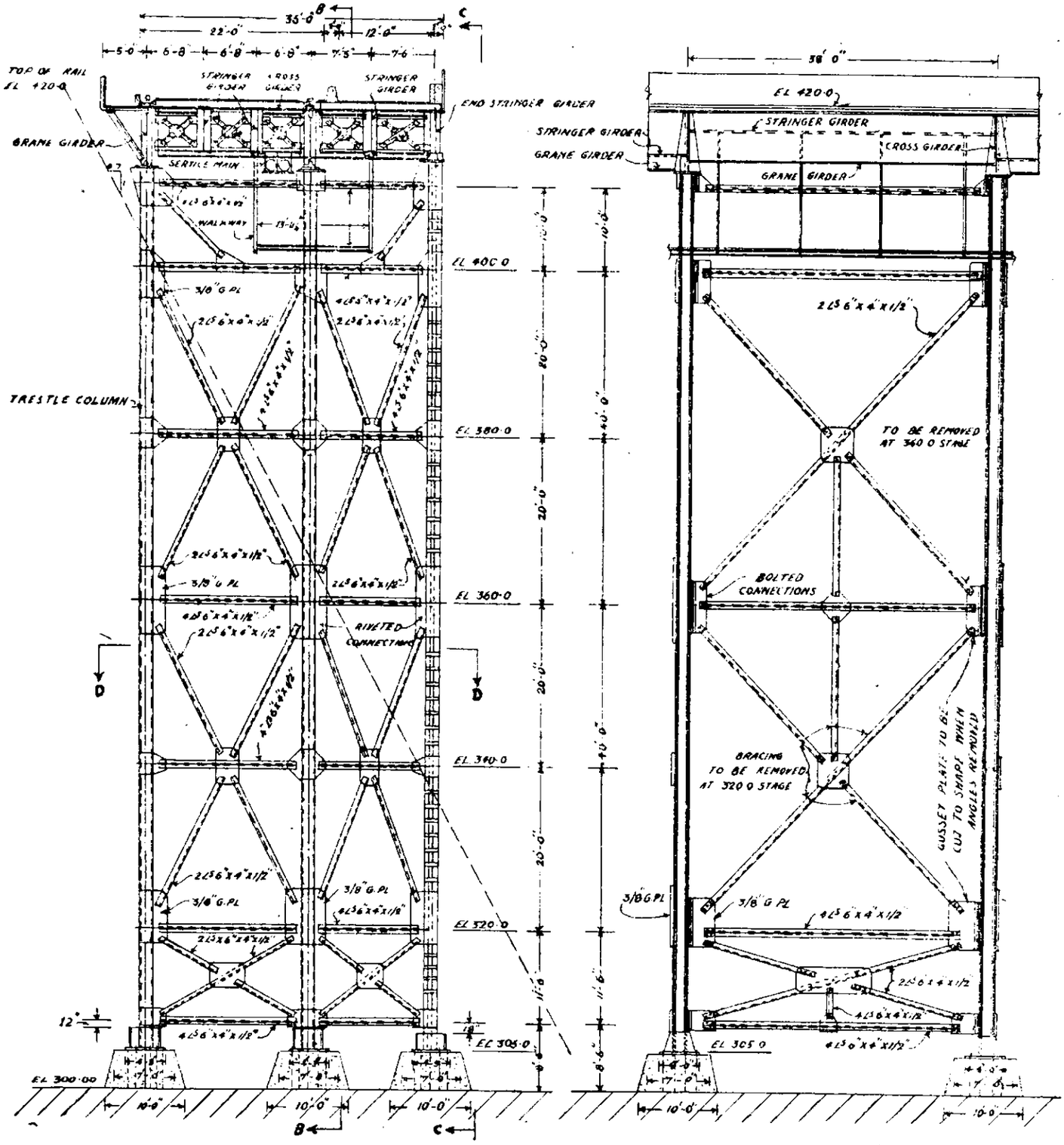

Fig : 2

Section A-A *Section B-B*

stiffners some eccentricity has been allowed between the centroids of the column sections and the bearing of the girders. In the design of the tower, it is assumed that all the six columns with the deck system over the tower will act as one unit. The bending moments, lateral sway, longitudinal and wind forces will induce direct loads in the columns and no bending moment. In case any bending moment is to be resisted, it will be resisted by all the six columns acting together. The indeterminate moment in the columns because of eccentricity of connection has not been taken into account in the design.

In view of the high value of loads and large value of eccentricity, it was considered necessary to verify the validity of the design

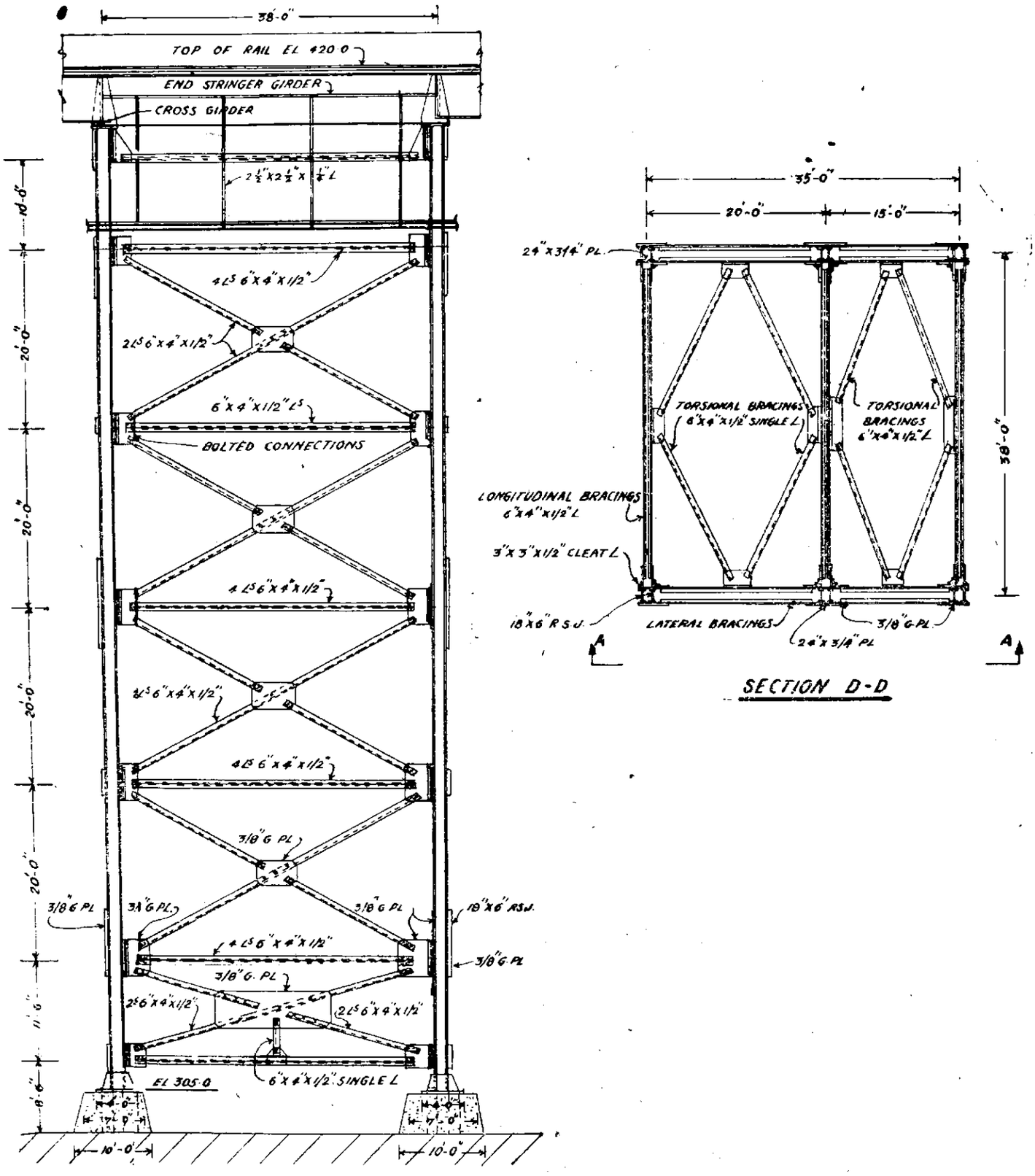

Section C-C

Fig 2: General arrangement; spillway portion.

Notes

1. Designs are based on construction stages before the monsoon breaks 320.0 and 420.0 masonry should not be stopped at intermediate levels.
2. Bracing facing the direction of flow will be joined by bolted connections.
3. During various stages of construction bracings obstructing flow of water will be removed before the monsoon starts.
4. Cut waters to be provided and the details will be furnished.

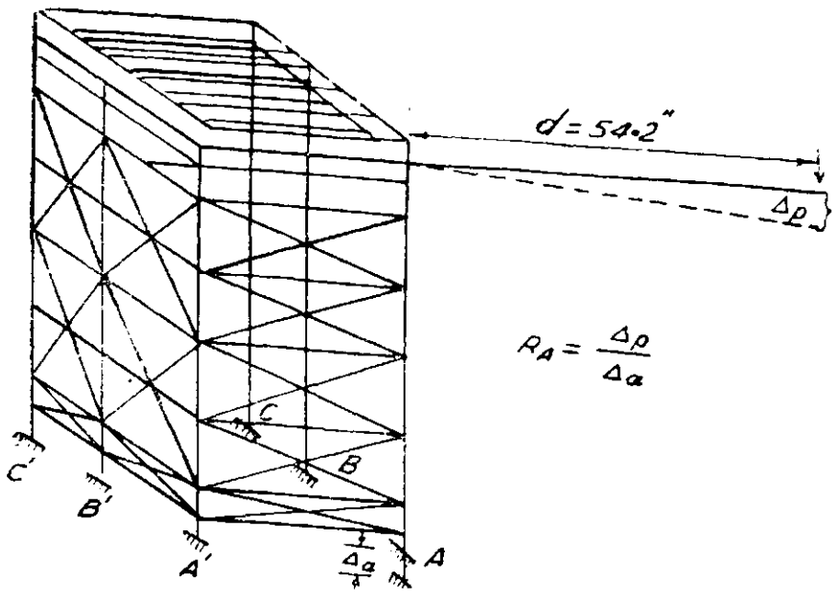

Fig 3

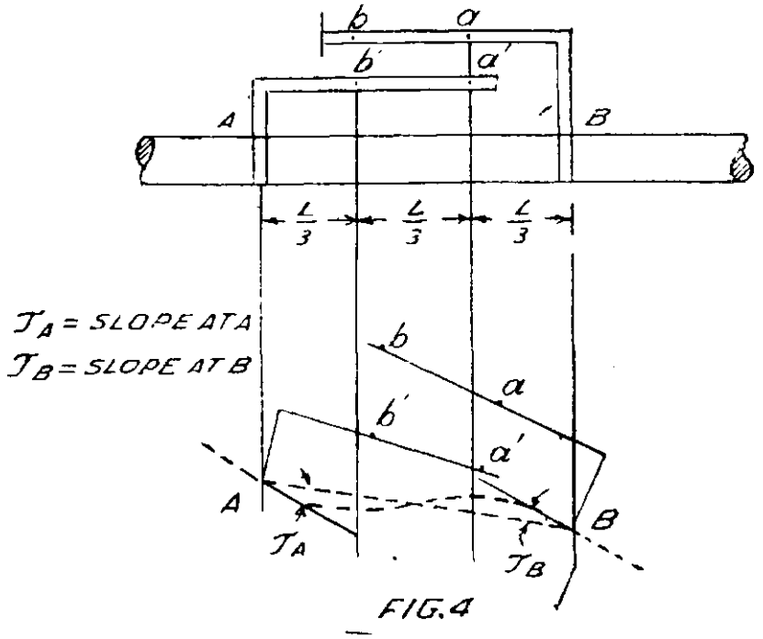

FIG. 4

assumptions by expedimental investigation. The results of such investigation are reported in this note.

2. Problem and model

The main assumptions to be verified are:

(i) Whether at the base of the columns the reactions are direct compression or tension and whether these could be obtained by considering the tower as a rigid body.

(ii) Whether at the top of the columns where the girders join the chair with an eccentricity, the columns are subjected to a moment. If so what would be the order of magnitude of these moments. It is obvious that in the absence of the deck system the eccentric load will induce the full moment at the top of the columns. However, in presence of the deck system the moment could be redistributed among the different members and full moment is not expected to be developed at the top of columns. The magnitude of this moment will also depend on the nature of the joints.

Considering the creep and other qualities of plastics it was considered necessary to have brass wire model for this particular case. The chief advantages of such a model were the ease in fabrication, ready availability of the sections and direct indication of the moments in the members by moment indicator. The linear scale adopted was 1/30 and it gave a model about 44 *in* high on a base of 15.2 × 14 *in*. The columns were proportioned mainly in relation to their moment of inertia. As the moments of inertia about both the *XX* and *YY* directions are practically the same, it was justifiable to use circular sections instead of actual built up section as used in the prototype. The other members of the structure were also made proportional to the moment of inertia. The moment of interia scale was $1/(7.5 \times 10^5)$. In the deck system rectangular brass sections were used and the value of *Ixx* and *Iyy* were correctly simulated. This was to ensure that both the bending stiffness and torsional stiffness of the girder were correctly represented. All joints were made perfectly rigid by using a cold setting plastic as a jointing material. The cold setting plastic consisted of liquid Araldite D with 10 *percent* hardner. About 3 coats of this cold setting plastic were given on each joint so as to have proper strength.

All the six columns were anchored to rigid steel foundation by means of special devices which at the same time enabled vertical movement to be introduced at any of these columns. The vertical movement device consisted of steel block having a central bolt which could be moved vertically by means of a nut (*photo 78*).

3. Reactions and moments at column bases

The Maxwell's reciprocal theorem was used for determining the reactions at the base on the columns. A known vertical displacement Δ_o was given at the base of the columns where the reaction was to be determined. The corresponding vertical deflection Δ_p on a point on a long light arm attached to the column under consideration was measured by a microscope. The ratio $\frac{\Delta_p}{\Delta_o}$ gave the reaction at the particular

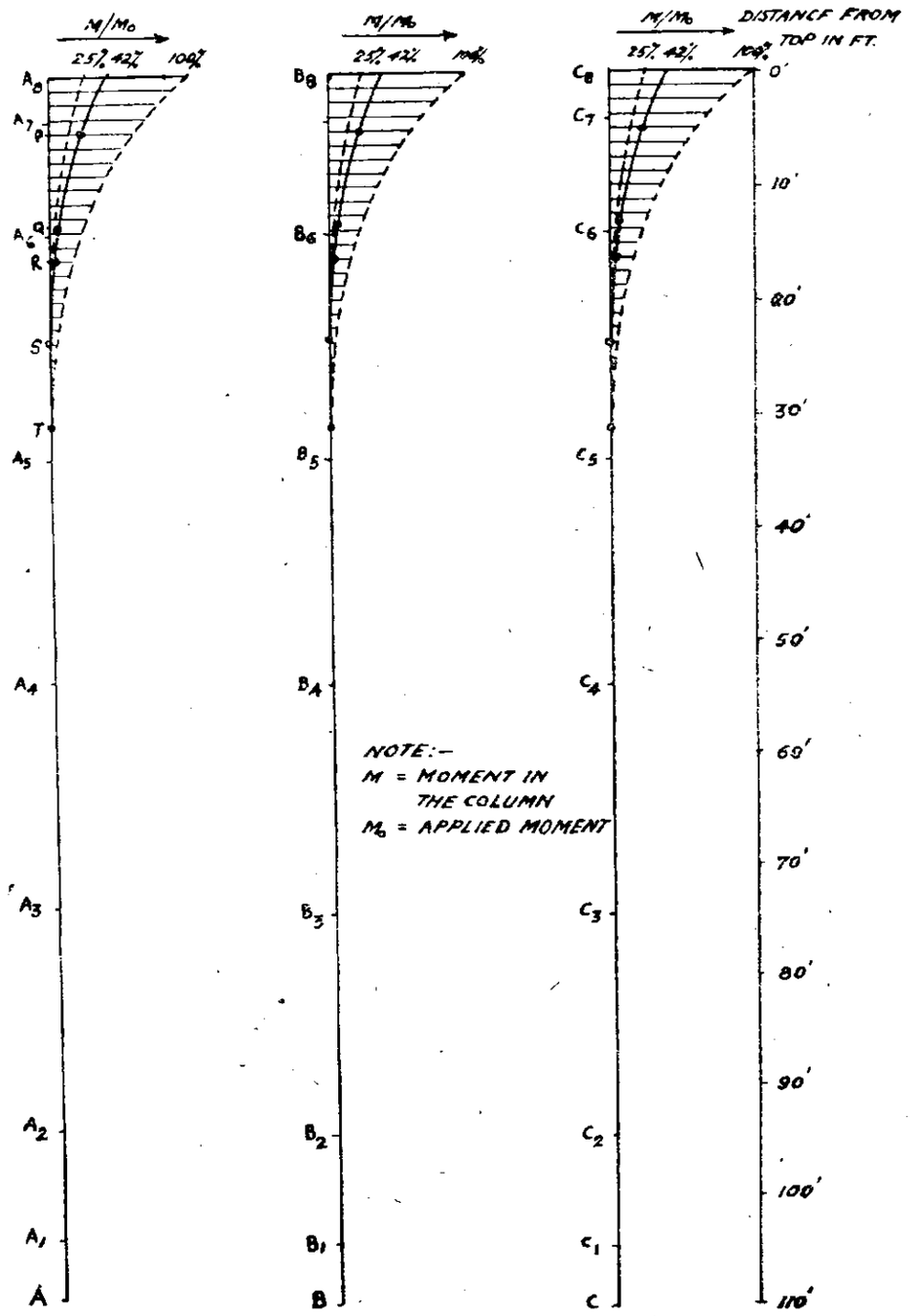

Fig 5: Moment in the column *A*, *B*, *C* due to applied moments.

column base when unit load was applied to the arm. To know the reactions on the other columns, similar displacements were given at each of the bases of the columns and the corresponding vertical displacement of the point on the arm were measured and the ratios of the displacements were calculated, thereby giving the respective reactions in each of the columns. The unit load on the arm was equivalent to a moment $M = l \times d$ *lb in*, where d = distance of the point from column and a direct load of l *lb* applied at the joint between the column and the deck system (*photo 79* and *fig 3*). The results obtained by a unit load and a moment at *A* are given in *table 1*.

In *table 1* the result of the analysis on the assumption that only direct load occurs in the column bases and the tower can be treated as a rigid body for calculating the reactions are also included. There is a general agreement between the experimental and calculated values indicating the assumptions in the theoretical analysis are reasonable.

That the moments at the base were negligible was further confirmed by direct measurement

Table 1: Reaction measurement (experiment and theoretical) when load is on the end crane girder

Load	Unload	Difference	Load	Unload	Difference	Load	Unload	Difference
10·625	10·653	·028	10·640	10·664	·024	10·633	10·645	·012
10·627	10·654	·027	10·639	10·663	·024	10·634	10·644	·010
10·620	10·654	·028	10·637	10·661	·024	10·633	10·644	·011
	$R_A = 2·200$			$R_B = 1·820$			$R_C = 0·868$	
Exprimental (corr). value.	$R_A = 2·020$			$R_B = 1·670$			$R_C = 0·800$	
Theoretical value.	$R_A = 2·070$			$R_B = 1·100$			$R_C = 1·010$	
10·581	10·559	0·022	10·593	10·579	0·014	10·608	10·593	0·015
10·583	10·561	0·022	10·592	10·578	0·014	10·605	10·591	0·014
10·580	10·557	0·023	10·590	10·578	0·012	10·602	10·590	0·012
	$R'_A = -1·76$			$R'_B = -1·05$			$R'_C = -1·075$	
Experimental (corr.) value.	$R'_A = -1·53$			$R'_B = -0·94$			$R'_C = -0·98$	
Theoretical value.	$R'_A = -1·18$			$R'_B = -1·18$			$R'_C = -1·18$	

with moment indicator (*see* below) which gave practically no deflection.

4. Moments at top of columns

To measure the moments at the different panel points of the columns, caused by the eccentric loads a moment indicator was prepared. A brief description is given below.

The moment indicator is a convenient instrument which furnishes a direct method of obtaining bending moments in a model. The theory of this instrument is based on Manderla-Winkler equations. These equations are applicable to a member or a portion thereof which is initially straight and has constant E and I and to which no external loads are applied between ends of the portion under consideration.

Let M_{AB} be the moment acting on the A end of the member AB and M_{BA} be the moment on the B end. Let T_A and T_B be the slope of the tangent to the elastic curve at points A and B.

$$\left.\begin{aligned} M_{AB} &= \frac{2EI}{L}(2T_A + T_B) \\ M_{BA} &= \frac{2EI}{L}(T_A + 2T_B) \end{aligned}\right\} \quad \ldots 1$$

Referring to *fig 4*, suppose two arms were attached at points A and B of a member. As the model was loaded and distorted by loads applied outside this segment, the two arms would rotate through the same angles as the tangents to the elastic curve at their point of attachment. Let $\triangle_a$ and $\triangle_b$ represent the relative movements of the points a, a' and b, b'.

Then

$$\left.\begin{aligned} \triangle_a &= \frac{2L}{3}T_A + \frac{L}{3}T_B = \frac{L}{3}(2T_A + T_B) \\ \triangle_b &= \frac{L}{3}T_A + \frac{2L}{3}T_B = \frac{L}{3}(T_A + 2T_B) \end{aligned}\right\} \ldots (2)$$

From (1) and (2)

$$M_{AB} = \frac{6EI}{L^2}\triangle_a$$

$$M_{BA} = \frac{6EI}{L^2}\triangle_b$$

The deflection Δ_a and Δ_b were measured, by a dial gauge calibrated for known moment. The dial guage was calibrated by attaching it on a beam under constant bending moment and was checked for a known cantilever moment. The calibration constant is 12.28 *lb in/division* of the dial guage whose least count is .01 *mm* on a 0.5 *in* diameter brass wire (*photo 80*).

The moment at the top of the columns were measured directly by means of moment indicator (*photo 81*). The moment was applied by means of light balanced cantilever attached to the top of the column. This introduced a known moment to the top of the column.

In absence of deck system the full moment was developed at the top of the columns but this reduced to less than 5 *percent* below the first joint where diagonal members joined (*ie* about 15 *ft* below the top in the prototype).

When the deck system was erected the moments in the columns were reduced depending upon the effectiveness of the joints between

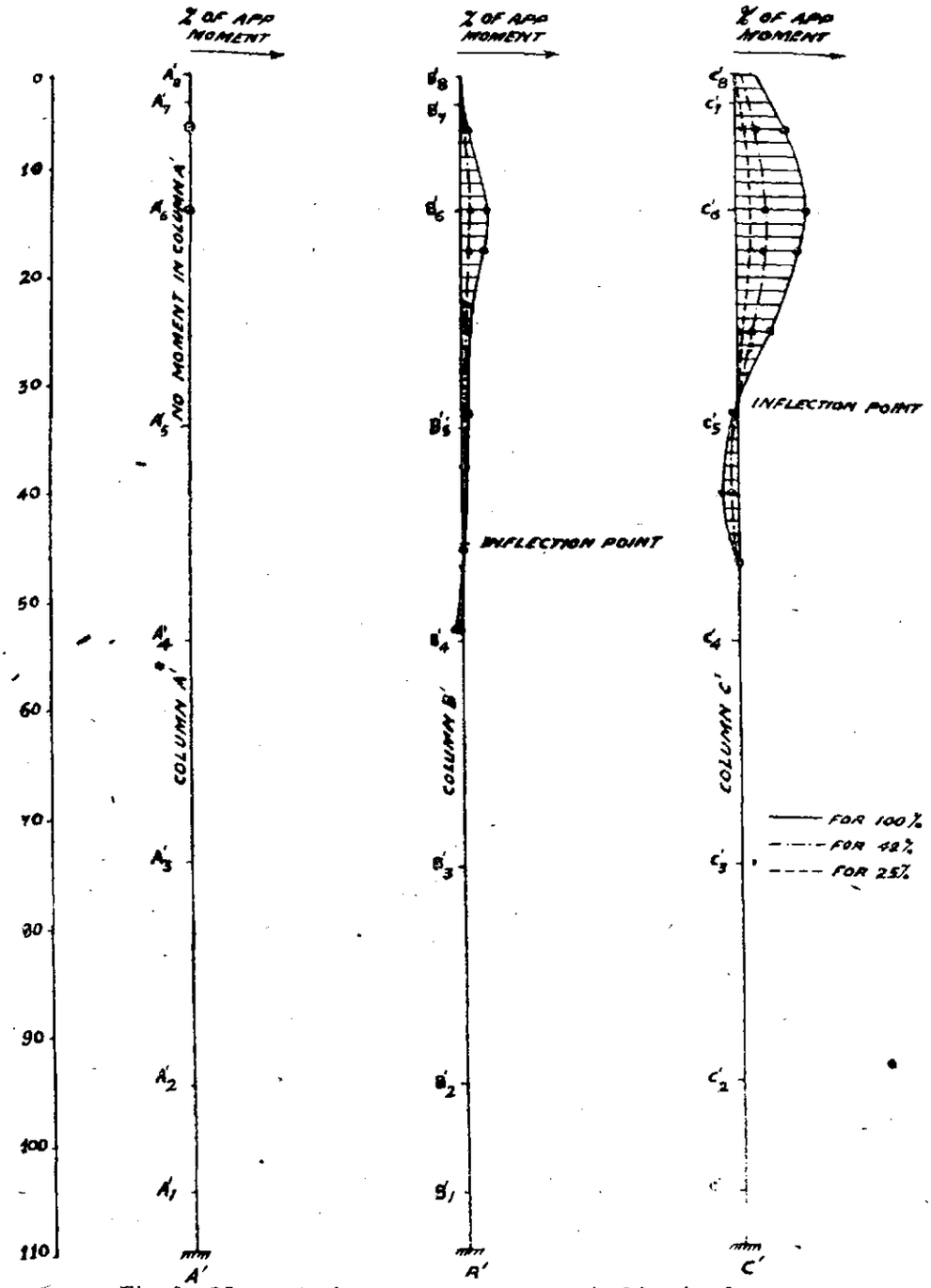

Fig 6: Moment in rear columns *a'*, *b'*, *c'*, for an applied moment at the joint c_s of column *c* (c_s is joint between deck and column *c*).

the girders and the columns. For perfectly rigid joints the moments in the columns were well below 25 *percent* whereas for a pin connected joint the moments were practically 100 *percent*. The moments in the various columns with an external moment at the top are given in *fig 5*. Moments in the opposite columns *A'*, *B'*, *C'* were also measured and are given in *fig 6*.

5. Discussion

Although complete similarity between the results of the model and the prototype cannot be expected in such a model, the general behaviour of the structure is fairly well indicated.

At the base of the columns very little moment is developed due to the eccentric loading at the top. The experimental results for an eccentric load on the top of the columns indicated that the reactions calculated on the basis of bending as a rigid body give fairly good indications of the actual stresses occurring. This requires further confirmation for other position of loads.

The column tops, however, could, if the joint was not rigid, be subjected to the full external

moment. But this moment dies down very rapidly as we go down along the columns. The moments due to the wind and traction are small at the top of the columns and hence even if full moment is taken for design purposes the section of the columns may not be different from that at the base.

6. Conclusions

From the observations made on the brass wire model of the Nagarjunasagar trestle bridge for checking the design assumptions, the following conclusions may be arrived at:

(*i*) Even with eccentric loads coming at the top of the columns, the reactions at the base are vertical direct stresses which can be determined fairly well on the basis of a rigid body displacements of the tower as a whole.

(*ii*) The moment developed at the top of the column with a known external moment applied at the joint between deck system and the columns depends largely on the nature of the joint. If the deck system is simply supported the full moments will be developed at the top of the column and if the joint is perfectly stiff the moment may be reduced to less than 25 *percent.* In view of the uncertainty occurring in the prediction of the behaviour of the rivetted joints in the prototype it would be desirable to design top panel of the columns for the full eccentric moment (wind and traction moments being least there). The moments are reduced practically to zero near about the first joints from the top where the diagonal members meet.

---

21. Optimum number of years for computing mean annual precipitation

LARGE VARIATIONS in the incidence, intensity and time-to-time depths of rainfall occurrences in the vast tropical sub-continent of India are too well-known a feature. But, happily regular long-term data obtain for no less than about 3500 raingauge stations maintained by the India Meteorological Department and a similar number of additional raingauges maintained by local bodies for studying these aspects. But the 3500 and odd stations were not all instituted simultaneously; their existing density has been reached in fact by a steady-growing process continued for over 100 years. *Fig 1* shows the absolute and percentage growth of the number of raingauges in the different States.

2. Varying lengths of data

The voluminous data maintained by all these raingauges over their several years have been found greatly useful in the valuable work of irrigation engineers for the estimation of the total water potential capacities of different basins. But the data of different stations as already mentioned cover different numbers of years. For example, only about 1700 odd raingauges out of the 3500 maintained by the *IMD* have records extending to 60 years. Just over a 2250 stations or so have records extending to 35 years.

On account of the time-to-time changes simultaneously contained in individual raingauges' data, the mean rainfall depths computed from varying numbers of years of observations for the different raingauge will not be strictly comparable. Comparable estimates for the different gauges can be computed at best by strictly limiting the coverage of all the gauges' data to their common years of observation, which in turn may not extend very long. The question thus arises: "How many years' observed data are absolutely necessary for yielding reliable mean estimates of the phenomenon's characteristic variable features of interest for any desired period (not exceeding 12 months)?" The analysis below aims to provide an answer.

3. Variations at 100 selected raingauges

Instead of analysing the data of all the 3500 odd raingauges with their different coverages of years, some 100 raingauges were picked out in the first instance by an approximate method of stratified random sampling to cover all the anticipated heterogeneities in the land. The 100 raingauges

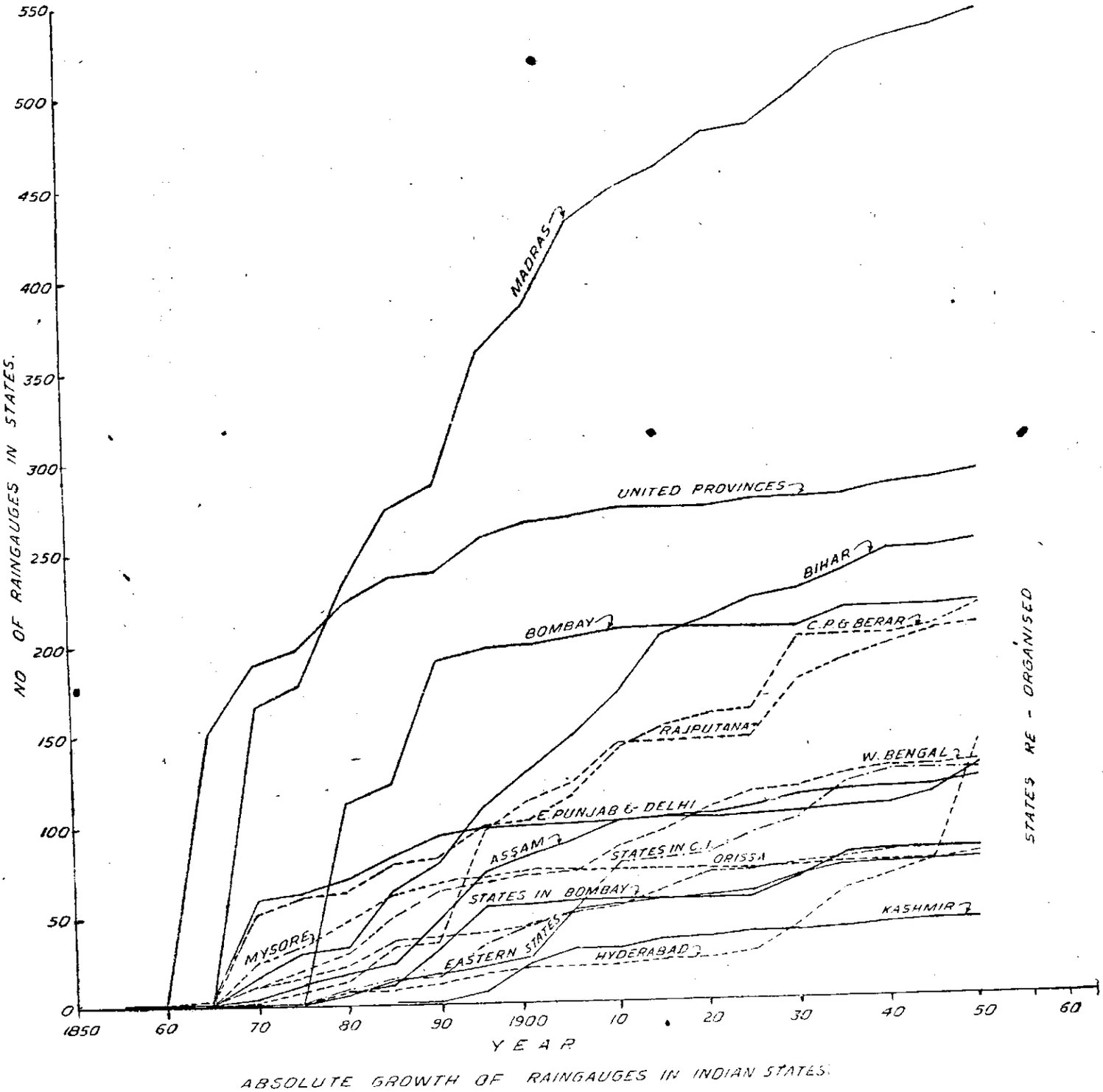

Fig 1: Growth of raingauges in pre-reorganized States (India).

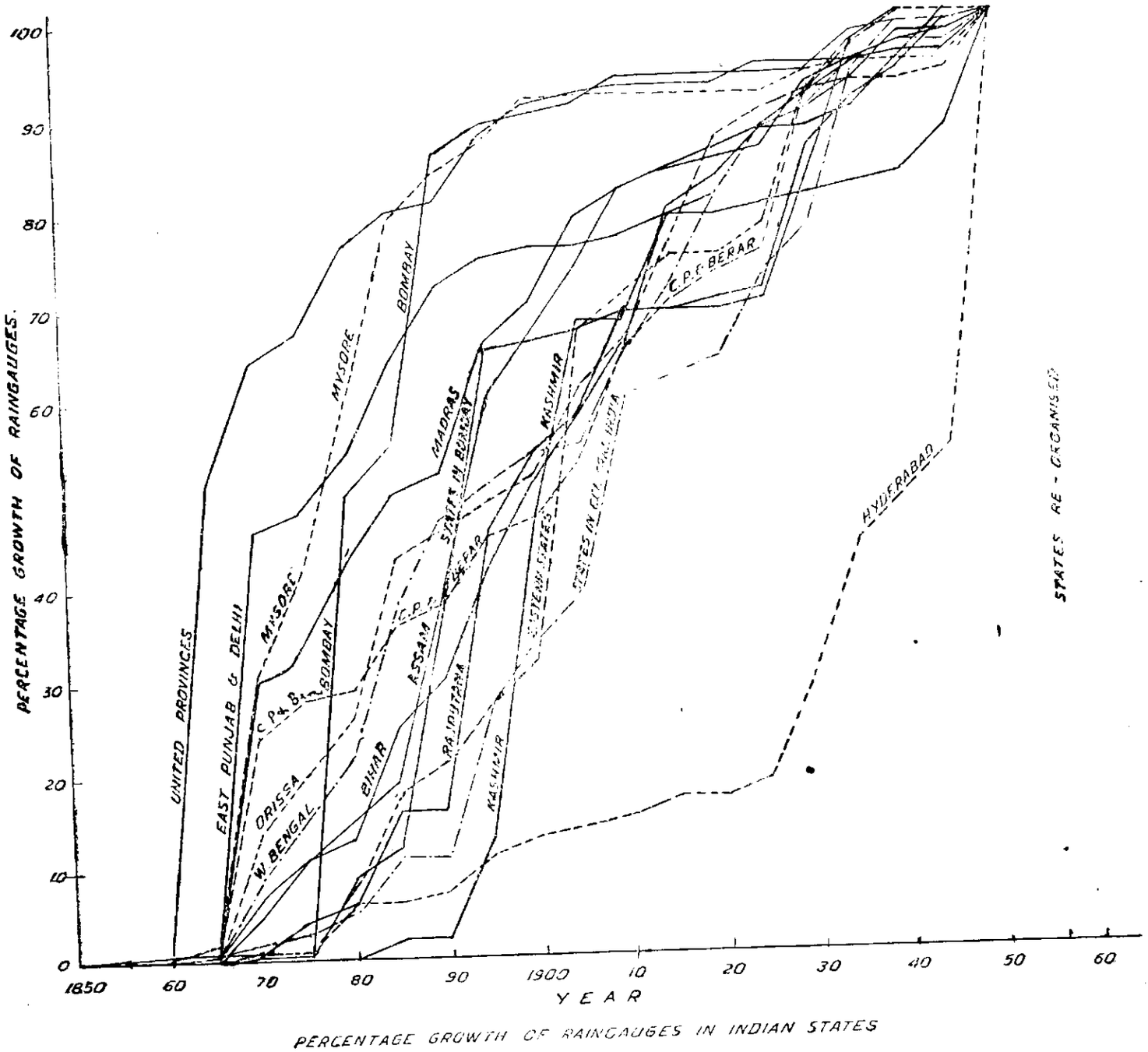

PERCENTAGE GROWTH OF RAINGAUGES IN INDIAN STATES

Fig 1: Percentage growth of raingauges in pre-reorganized States (India).

all have their data available from 1901 onwards. The mean annual (Jan-Dec) precipitation depths computed for the 100 stations are shown in *fig 2*. But the means alone of the 55 individual years precipitation depths cannot suffice to disclose the full information contained in the data. For, the total rainfall depths registered over specified intervals of time (not exceeding 12 months) at any raingauges, exhibit considerable variations from year to year. Thus, in order to bring out this year-to-year variability aspect about the long-term means, some additional information has to be presented as well. The standard statistical medium of " standard deviation" perhaps fulfils this role very effectively. The values of the standard deviation of all the 100 selected rainguages are also accordingly shown in parantheses in *fig 2*.

4. Coefficient of variation as a tool

The extents of both the variations in *fig 2* cover very wide ranges. But there is no method of reducing the magnitudes of the absolute values of the mean yearly precipitation depths, as reproduced in *fig 2*. They are actually irreplaceable. For the sake of convenience, the large range of the variation observed can be compressed at best into a small number of graded classes suitably designated as high rainfall zones, low rainfall zones, and so on. But the numerical magnitudes of the standard deviation measures (*fig 2*) as such have no similar use by themselves; for, identical standard deviation value of s units will have different meanings for different raingauges respectively with different mean depths for corresponding periods of the year. Thus, the common standard deviation values for the stations respectively paired below, though indicating comparable extents in absolute units of the year-to-year departures from their respective long-term means, present different pictures of the same variations in terms of their percentage measures relative to the means.

Annual Mean Precipitation (*mm*)		Standard Deviation *mm*	%	%
Amraoti (869) Hazaribagh	(1463)	254	29.2	17.3
Kolhapur (1011) Janjipur	(1397)	279	27.6	20.0
Villipuram (1138) Drug	(1280)	257	22.6	20.1

In other words the same constant value 254 *mm* of the standard deviation can mean 17.3 *percent* variation from the mean for Hazaribagh and 29.2 *percent* for Amraoti. It may mean even other larger or smaller percentage variations for other raingauges. In order to have a clear picture of these percentage variations obtaining from respective means for the 100 raingauges, these values of the percentage coefficients of variation are shown in *fig 3*. Their range extends from 14 for Mangalore to about 67 for Jaisalmer. It is believed, their range for the 6000 odd raingauges in India is not much unlike.

The practical use of the coefficients of variation is rather limited unless the frequency distributions of the parent data follow the Gaussian law. The early hydrologists have found that such data do not strictly conform to the Normal type. Despite the limitation, the means evaluated of such data for 30 or larger number (n) of years' observations nevertheless approximately follow the normal law of errors with standard deviation equal to $s/\sqrt{n}$. Since the means in *fig 2* have all been evaluated from 55 years' observations, their respective coefficients of variation can be easily deduced on dividing the earlier values in *fig 3* by $\sqrt{55}$. The new set of values so obtained (*fig 3*, in parantheses) are all seen to be tolerably small. Their range extends from 1.9 for Mangalore to 9.0 for Jaisalmer.

5. Optimum number of years

It follows from the hypothesis of normal distribution of the means that the mean annual rainfall depths evaluated from fresh batches of 55 years' data are not likely to differ from the means observed for 1901 to '55 by more than twice the respective coefficients of variation in 95 *percent* cases. This implies that the means reproduced in *fig 2* of 55 years' data are fairly stable for certain raingauges and not so for others on account of the large year-to-year fluctuations inherent to different localities. But, for the purpose of design of engineering works involving expenditures of vast sums of money, it is not usual to subject the mean estimates to errors exceeding ± 5 *percent*. In order to ensure the 20:1 odds of the errors due to causal reasons, not exceeding ± 5 *percent*, the means must be based on sufficient number (N) of years' observations. In other words, the values in *fig 3* of

$$\frac{100s}{\bar{x}\sqrt{n}} \not> \frac{5}{t} = 2.5 \quad \text{or} \quad N > \left(\frac{40s}{\bar{x}}\right)^2$$

MEAN ANNUAL PRECIPITATION

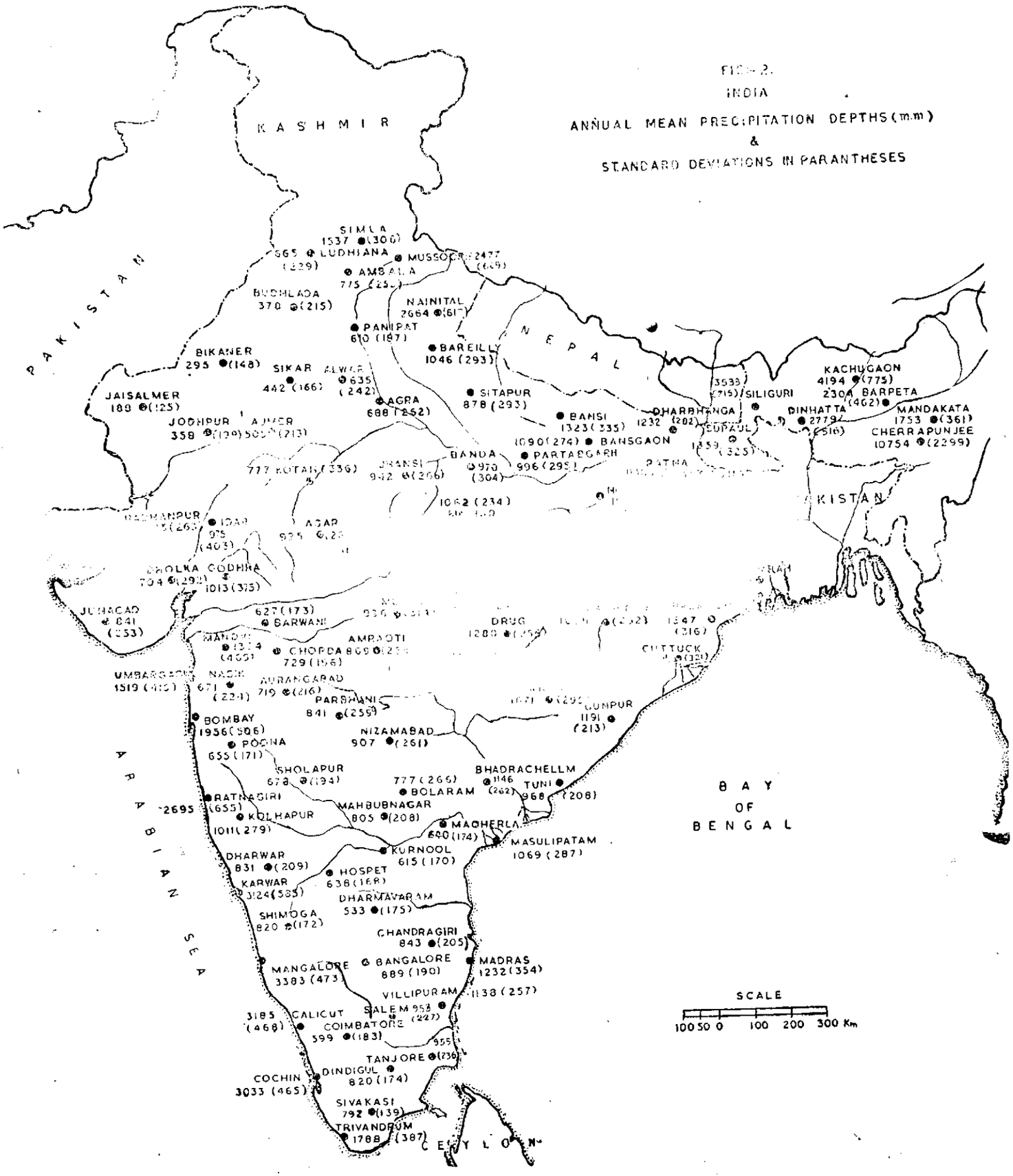

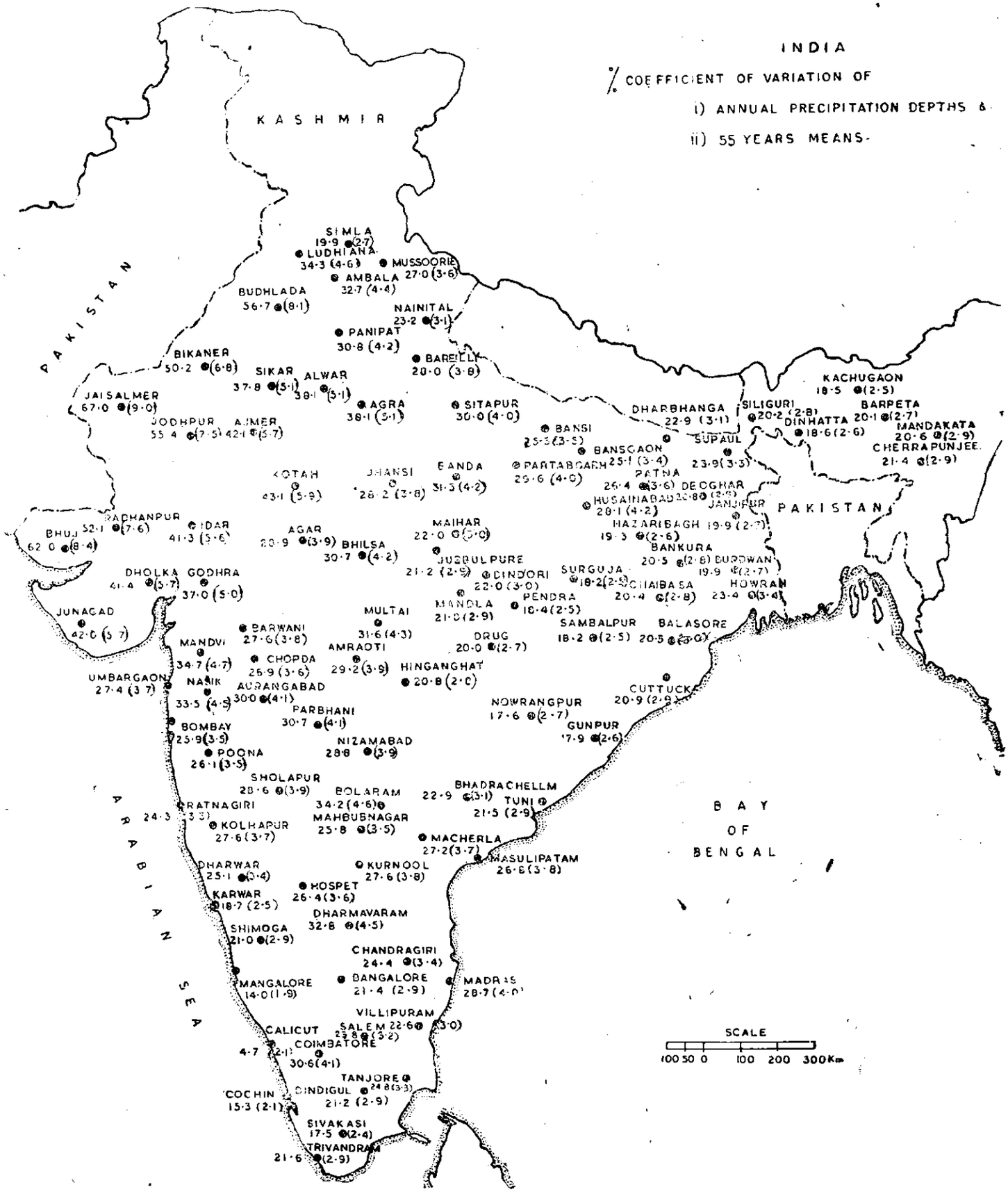
INDIA
% COEFFICIENT OF VARIATION OF
i) ANNUAL PRECIPITATION DEPTHS &
ii) 55 YEARS MEANS.
KASHMIR
PAKISTAN
PAKISTAN
SIMLA 19·9 (2·7)
LUDHIANA 34·3 (4·6)
MUSSOORIE 27·0 (3·6)
AMBALA 32·7 (4·4)
BUDHLADA 56·7 (8·1)
NAINITAL 23·2 (3·1)
PANIPAT 30·8 (4·2)
BIKANER 50·2 (6·8)
BAREILLY 20·0 (3·8)
SIKAR 37·8 (5·1)
ALWAR 38·1 (5·1)
JAISALMER 67·0 (9·0)
AGRA 38·1 (5·1)
SITAPUR 30·0 (4·0)
JODHPUR 55·4 (7·5)
AJMER 42·1 (5·7)
BANSI 25·5 (3·5)
DHARBHANGA 22·9 (3·1)
SILIGURI 20·2 (2·8)
KACHUGAON 18·5 (2·5)
DINHATTA 18·6 (2·6)
BARPETA 20·1 (2·7)
MANDAKATA 20·6 (2·9)
CHERRAPUNJEE 21·4 (2·9)
SUPAUL 23·9 (3·3)
BANSGAON 25·1 (3·4)
PARTABGARH 29·6 (4·0)
PATNA 26·4 (3·6)
DEOGHAR 20·8 (2·8)
HUSAINABAD 28·1 (4·2)
JANJPUR
KOTAH 43·1 (5·9)
JHANSI 28·2 (3·8)
BANDA 31·3 (4·2)
PALANPUR
BHUJ 52·1 (7·6)
62·0 (8·4)
IDAR 41·3 (5·6)
AGAR 20·9 (3·9)
BHILSA 30·7 (4·2)
MAIHAR 22·0 (3·0)
HAZARIBAGH 19·9 (2·7)
BANKURA 20·5 (2·8)
BURDWAN 19·9 (2·7)
JUBBULPURE 21·2 (2·9)
DINDORI 22·0 (3·0)
SURGUJA 18·2 (2·5)
CHAIBASA 20·4 (2·8)
HOWRAH 23·4 (3·4)
DHOLKA 41·4 (5·7)
GODHRA 37·0 (5·0)
MANDLA 21·0 (2·9)
PENDRA 18·4 (2·5)
JUNAGAD 42·0 (5·7)
MULTAI 31·6 (4·3)
BARWANI 27·6 (3·8)
SAMBALPUR 18·2 (2·5)
BALASORE 20·5 (2·8)
DRUG 20·0 (2·7)
MANDVI 34·7 (4·7)
AMRAOTI 29·2 (3·9)
CHOPDA 26·9 (3·6)
HINGANGHAT 20·8 (2·0)
UMBARGAON 27·4 (3·7)
NASIK 33·5 (4·5)
AURANGABAD 30·0 (4·1)
CUTTUCK 20·9 (2·9)
NOWRANGPUR 17·6 (2·7)
PARBHANI 30·7 (4·1)
GUNPUR 17·9 (2·6)
BOMBAY 25·9 (3·5)
NIZAMABAD 28·8 (3·9)
POONA 26·1 (3·5)
SHOLAPUR 28·6 (3·9)
BOLARAM 34·2 (4·6)
BHADRACHELLM 22·9 (3·1)
TUNI 21·5 (2·9)
RATNAGIRI 24·3 (3·3)
MAHBUBNAGAR 25·8 (3·5)
KOLHAPUR 27·6 (3·7)
MACHERLA 27·2 (3·7)
MASULIPATAM 26·8 (3·8)
DHARWAR 25·1 (3·4)
KURNOOL 27·6 (3·8)
HOSPET 26·4 (3·6)
KARWAR 18·7 (2·5)
DHARMAVARAM 32·8 (4·5)
SHIMOGA 21·0 (2·9)
CHANDRAGIRI 24·4 (3·4)
MANGALORE 14·0 (1·9)
BANGALORE 21·4 (2·9)
MADRAS 28·7 (4·0)
VILLIPURAM
SALEM 22·6 (3·0)
CALICUT 23·8 (3·2)
COIMBATORE 30·6 (4·1)
TANJORE
DINDIGUL 24·8 (3·3)
COCHIN 15·3 (2·1)
21·2 (2·9)
SIVAKASI 17·5 (2·4)
TRIVANDRAM 21·6 (2·9)
ARABIAN SEA
BAY OF BENGAL
SCALE
100 50 0 100 200 300 Km

Fig 3

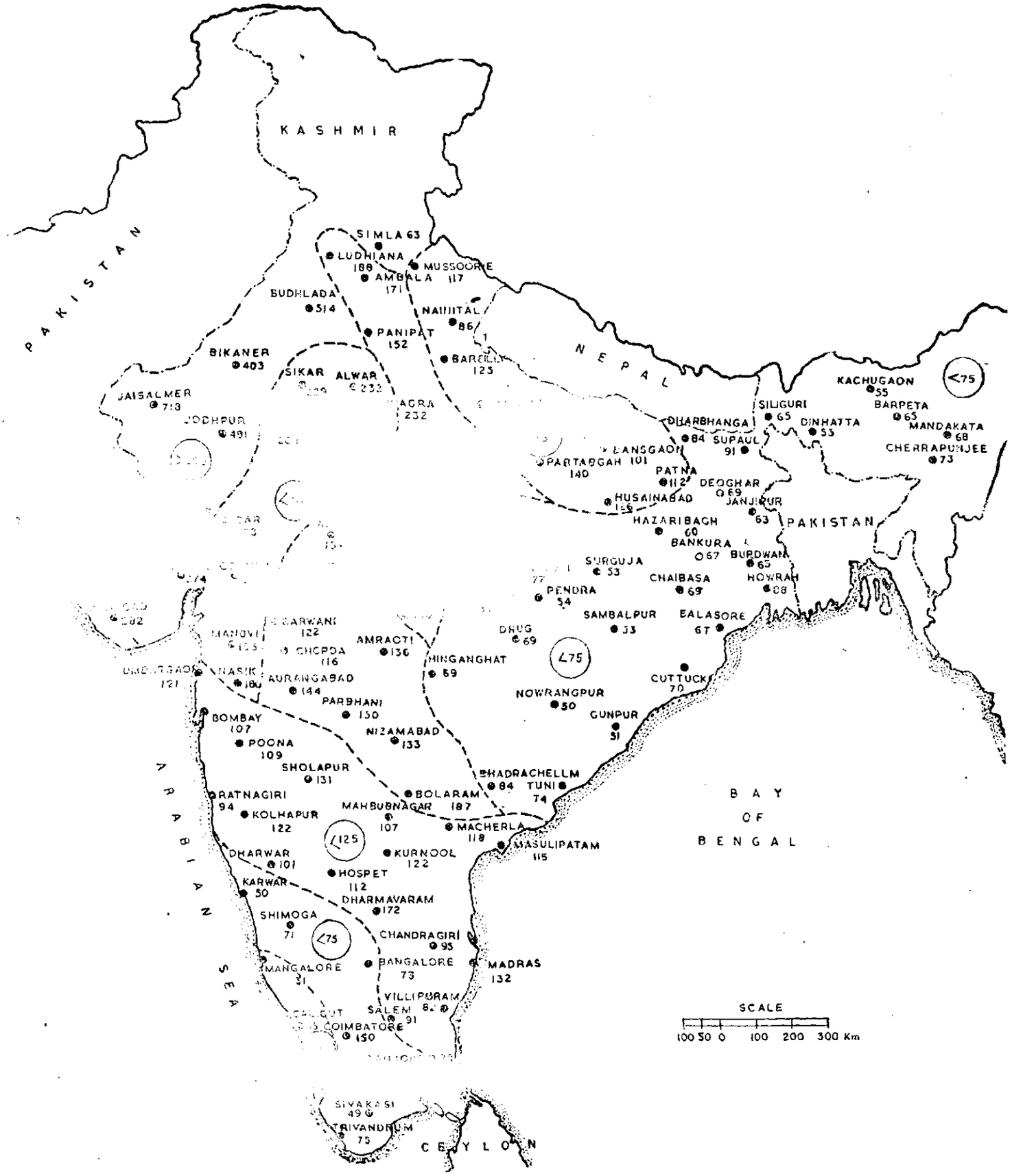

Fig 4: 95% optimum number of years for computing mean annual precipitation depth within ±5% reliability.

The values of N so evaluated for the 100 raingauges (*fig 4*) show that about 50-75 years' observations in the least are easily required for computing the mean annual precipitation depth for any raingauge with the reliability of its being out by not more than $\pm$ 5 *percent*. A fewer number of years' observations may suffice for a few localities with smaller fluctuations in the phenomenon's year-to-year variational patterns. But an appreciably larger number of years' observations may be necessary for quite a large number of other localities. In the arid tracts particularly even 200 years' observations may not suffice for yielding the desired degree of accuracy for the mean.

6. Conclusion

The statistical concept of the percentage coefficient of variation has been utilized for determining the optimum number of years' observations necessary for computing the mean annual precipitation depth for any raingauge. The same concept can be utilized for similarly determining the optimum number of years necessary for computing the mean depth for any other desired period smaller than 12 months.

---

22. Effect of temperature and boundary on currentmeter ratings*

CONSIDERABLE research has been done in the last five decades or so towards improving the accuracy of measurement of velocities. An instrument known as the currentmeter with which most engineers of today are familiar was developed as a standard device for measuring velocities. This type of instrument generally falls under two categories:

(i) propeller-type currentmeter in which turning movement is obtained by the lift developed on the blades by water

(ii) cup-type currentmeters in which differential drag on cups in opposite directions rotates the cup assembly

The cup-type currentmeters (*fig 1*) are comprised of six hollow conical cups mounted on a vertical shaft held between bearings at the two ends. A set of guide vanes keeps the axis of the wheel perpendicular to the current and the entire assembly parallel to the direction of flow. The wheel is geared to a mono or penta contact arrangement for counting the number of its revolutions through a headphone or a counter by making or breaking a contact of the electrical circuit at the end of every one or five revolutions.

For very low velocities of 0.5 *ft/sec* and less the friction in the bearing of the currentmeter is comparable to the moving forces of water. The form of relation, therefore, of such low velocities with the corresponding number of the revolutions/*sec* is different from that for higher velocities. The general relation also called the rating curve, is evaluated for velocities more than 0.5 *ft/sec* by calibrating the currentmeters in rating or towing tanks by towing them in still water at different velocities and counting the number of revolutions per *sec* for each run.

2. Necessity of present investigation:

The conditions with regard to temperature of water and boundary *ie* distance at which the currentmeter is held from the side or from the bottom may be different in actual streams as compared to that under which the currentmeter is calibrated in a towing tank.

No standardized procedure is so far known to have been prescribed in respect of specific temperature(s) to be maintained, or of holding the currentmeter at specified distance(s) from the bottom and/or from the sides for ensuring immunity from boundary effect during the course of calibration and actual observations in the field. Actually, there may be differences in either or both the factors on different occasions. It may be noted that temperature variation over rivers is fairly wide in India, generally ranging between 5° to 40°C.

It was thought pertinent, therefore, to investigate the variations due to such extraneous differences of temperature or distances from bottom and sides on the rating tables or equations of rating curves obtaining for currentmeters. The information so procured would

*Separately published as Technical Memorandum *HLO*, 1 Sept 1960.

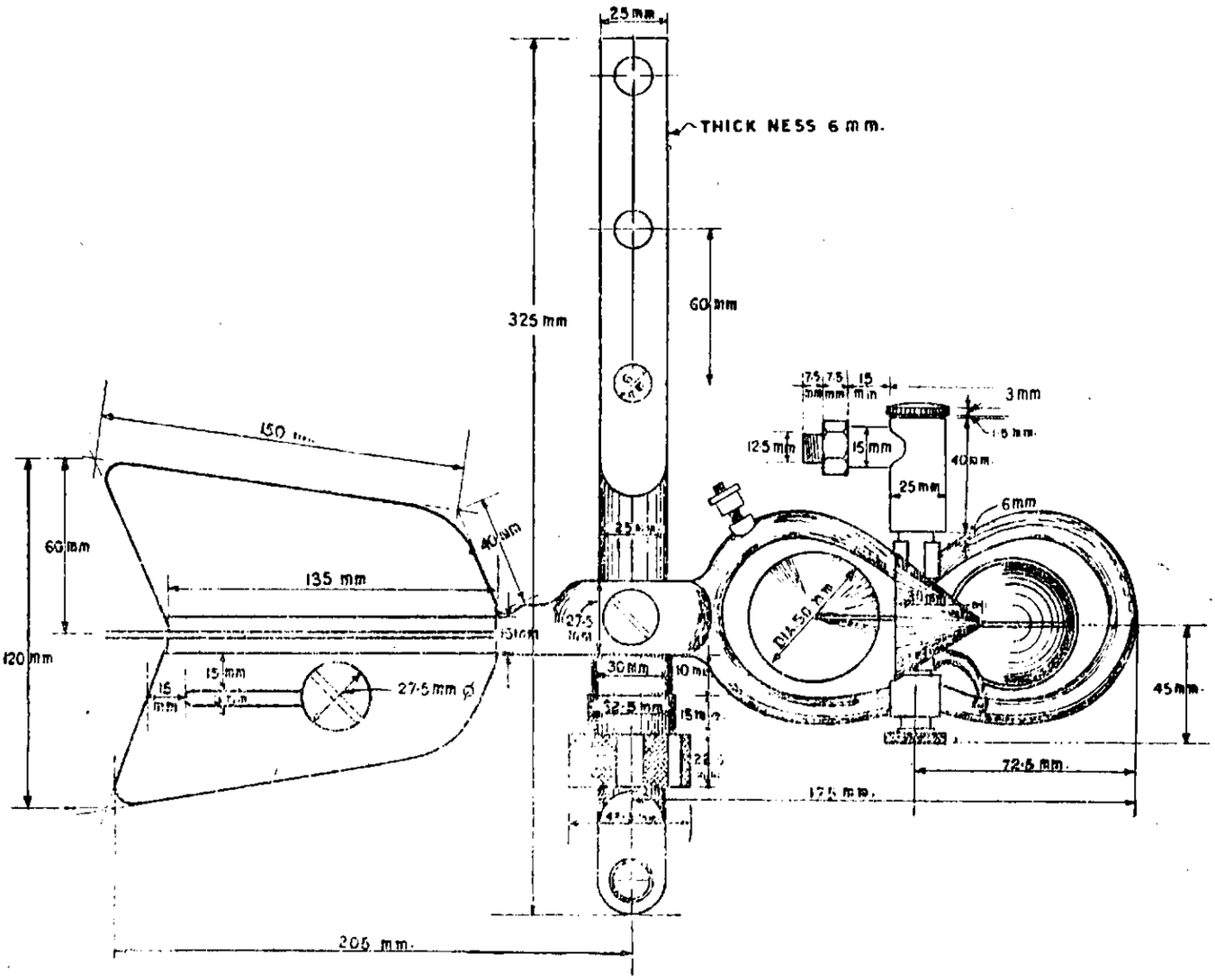

Fig 1 : Watts Currentmeter *No* 91391 (not to scale).

serve as a valuable guide for standardisation of conditions under which rating should be made and also for introducing appropriate corrections, if any, to the respective rating expressions of the currentmeters whenever the field conditions differed from those under which they might have been calibrated.

3. Facilities available

Facilities for calibrating currentmeters are well provided at the Ship Testing Tank at the *CWPRS*. The tank is 500 *ft* long, 12 *ft* wide and 7 *ft* deep. Sixty pound rails are laid to the curvature of the earth on either sides of the tank. A towing carriage with the facility of an Electronic Speed Control arrangement can run on the rails at any constant speed(s) between .06 to 6 *m* (.2 to 20 *ft*) *per sec* (*photo 82*). An Automatic Recorder (*photo 83*) fitted on board keeps the continuous data of the time, distance and the resolutions of the currentmeter wheel during the runs of the carriage.

The extent of boundary effects up to different distances was investigated by a series of experimental ratings made in this tank.

It was difficult to raise and lower the temperature of water over the desired range in the large tank. For the purpose of ratings under regulated temperature conditions, therefore, the experiments were confined to the *small-fixed* circular tank of rectangular section 15 *in* wide and 17.75 *in* deep having a central radius of 3 *ft* (*photo 84*). An arm provided at the centre of the tank rotates at different velocities through a gear box by a synchronous motor (*fig 2*). Baffles are provided at eight radial positions in the tank to prevent water from acquiring circular motion during calibrations.

The experimental calibrations made in the two tanks for evaluating the effects of controlled variations of temperature and boundary, their procedure, the data collected, their analysis and the conclusions drawn are described in the following paragraphs.

Temperature Effect

4. The procedure adopted for regulating the temperature (T) of water in the circular tank is described first.

Initially the temperature of water in the circular tank was brought down to about 3°C by adding ice. Water was then fully stirred to ensure uniformity of temperature and absence of differential currents on account of temperature difference. Care was taken that no circulation or residual velocity was present in the tank on account of stirring. Temperature of water was allowed to rise gradually to the room temperature of 23.6°C. It was noted that the time taken for each degree of rise of temperature was between 30-50 *min*. This ensured that the variation of temperature during the period of observation (3-5 *min*) was less than 0.1°C. Calibrations were next done with the rise of temperature from 3°C to room temperature as described above.

Temperatures of water higher than the room temperature were produced by heating water electrically at three different places and stirring it constantly to ensure uniformity of temperature. Actually, temperature readings of water were taken at 8 different points along the periphery of the tank, and all *inter-se* differences were within a variational latitude of 0.1°C.

5. Observation of data

With these arrangements of temperature (T) control, a set of experimental calibrations were made of one pygmy-type Gurley currentmeter (*No* 541273) for assessing the effect of changing

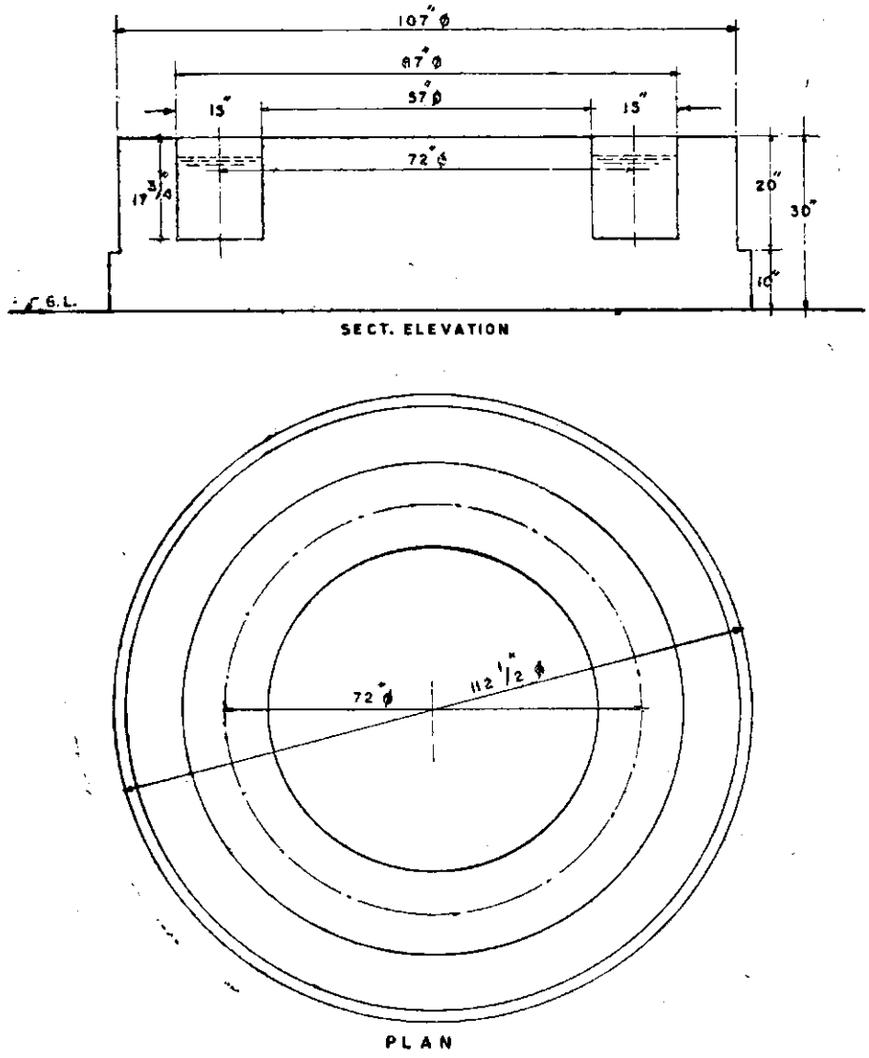

Fig 2: Circular Tank for Midget Currentmeter.

temperature of water. A 12 *in* constant depth of water was maintained in the tank all through and the currentmeter immersed to a constant depth of 3 *in* under water. The currentmeter was rated six times under six different controlled ranges of temperature of

5-6, 13-14, 20-21, 27-28, 34-35 and 39-40°*C*

covering between them nearly the full range of water temperatures in Indian streams. For each rating five sets of the R, V data were obtained at five speeds of

2.61, 1.44, .86, .51 and .29 *ft/sec*

Observations of V and R were started only after the currentmeter had completed two revolutions of the circular tank and stable conditions were reached. Following procedure was adopted thereafter.

For each separate run of the currentmeter the time intervals taken for five complete rounds of the tank were observed repeatedly until their two successive values (t) were obtained as nearly identical. The number of revolutions recorded of the currentmeter wheel were also counted for equal intervals of time (t_o) until two successive counts (n) were steady. The values of V and R for the 30 runs so made with different combinations of the six constant temperature ranges and the five speeds were derived from

$$V = \frac{\text{Length of five rounds}}{t} \text{ and } R = \frac{n}{t_o}$$

and set in *table 1* below:

Table 1

V	T(°C)						Maximum% variation of R
	5-6	13-14	20-21	27-28	34-35	39-40	
1	2	3	4	5	6	7	8
2·61	2·270	2·270	2·250*	2·300†	2·250‡	2·300*	2·22
1·44	1·256†	1·247	1·245	1·247	1·236‡	1·242	1·62
0·86	0·772†	0·763	0·758	0·761	0·755‡	0·761	2·25
0·51	0·420	0·422‡	0·430†	0·423	0·424	0·423	1·89
0·29	0·206	0·201‡	0·206	0·209†	0·206	0·208	3·98

*Obtained for $V = 2.60$ *ft/sec*

†Maximum value of R

‡Minimum value of R

6. Analysis of data

The analysis of such data usually proceeds by fitting expressions of the type $V = f_1(R)$..... .....$V = f_6(R)$ to the six sets of the data respectively for the six ranges of temperature values. Preliminary to this, however, plot of the (R, V) data *vide fig 3* showed a fairly linear lie of the five points in all the batches separately. On evaluating exact expressions, the dispersions of the individual points about the respective lines are seen to go up to ± 3 *percent*. Subject to this measure of observed variability, the six lines all drawn against a common pair of co-ordinate axes in *fig 4* show themselves as very nearly coalescent over the length of the observed data. In other words the linear expressions descriptive of the R, V relations ($.29 \leqslant V \leqslant 2.61$) are not appreciably different from each other for temperature variations between 5-40°*C*. *Col* 8 of *table 1* shows the maximum percentage variation of revolutions for different velocity values. It will be observed that this variation is of the order of about 2 *percent* except in the case of lowest velocity of .29 *ft/sec*, which is very small and boosts up the difference.

Thus the variation in revolutions for the range of temperatures tested is within the tolerance limit for rating of currentmeters. Independent statistical analysis of variance carried out for evaluating the rating expressions also confirms that the effect of temperature variations from 5-40°*C* on the R, V data is not significant as under:

From variations of	Degrees of freedom	Sum of squares	Mean square	Standard Deviation *ft/sec*	Conclusion
1	2	3	4	5	6
Temperature ...	5	·000809	·000162	·013	Insignificant
Velocity ...	4	16·185443	4·046361	2·012	Significant
Error ...	20	·002215	·000111	·011	
Total ...	29	16·188467			

Thus the standard deviation measure of the velocity values due to temperature variations namely .013 *ft/sec* equals only about half *percent* for $V = 2.6$ *ft/sec* and 4.5 *percent* for $V = .29$ *ft/sec*

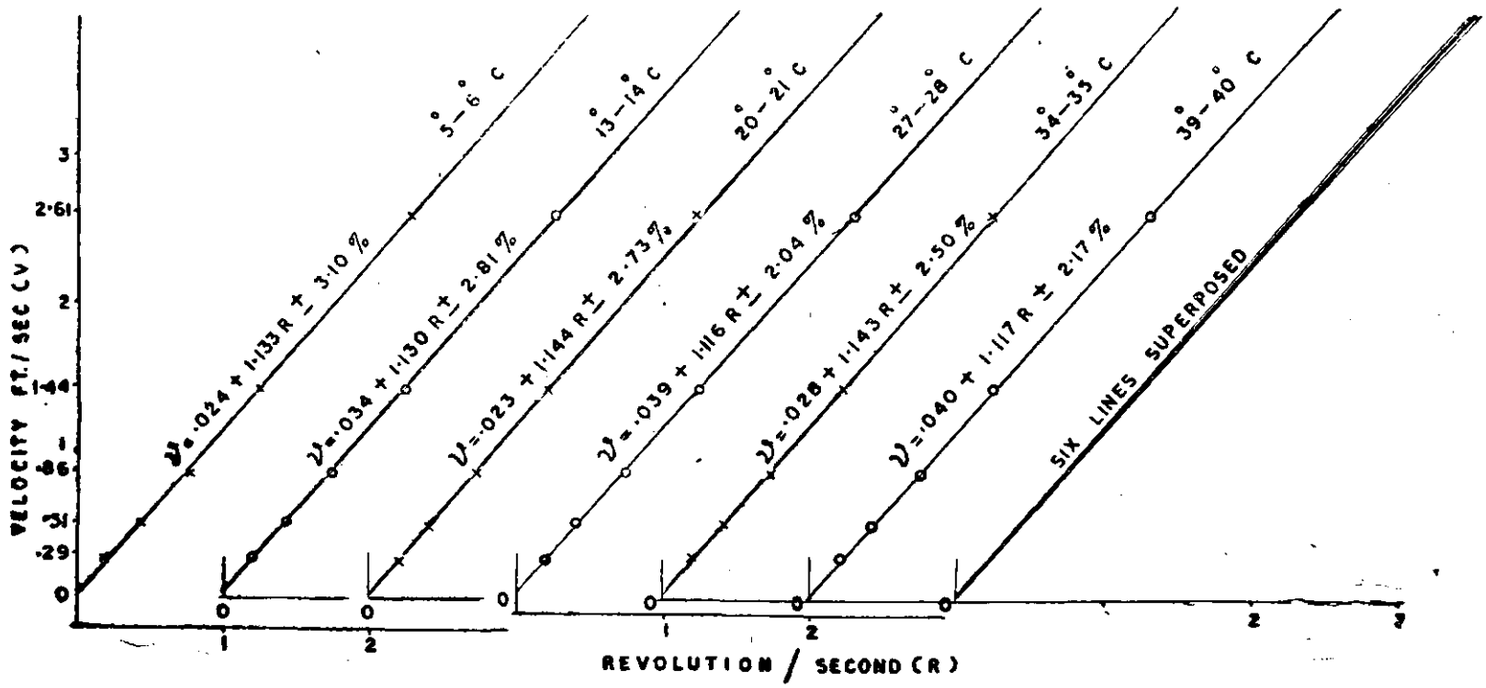

Fig 3: Rating expressions ($V = a + b\,R$) for Pygmy type Gurley Currentmeter *No* 541273 calibrated in circular tank at different temperatures.

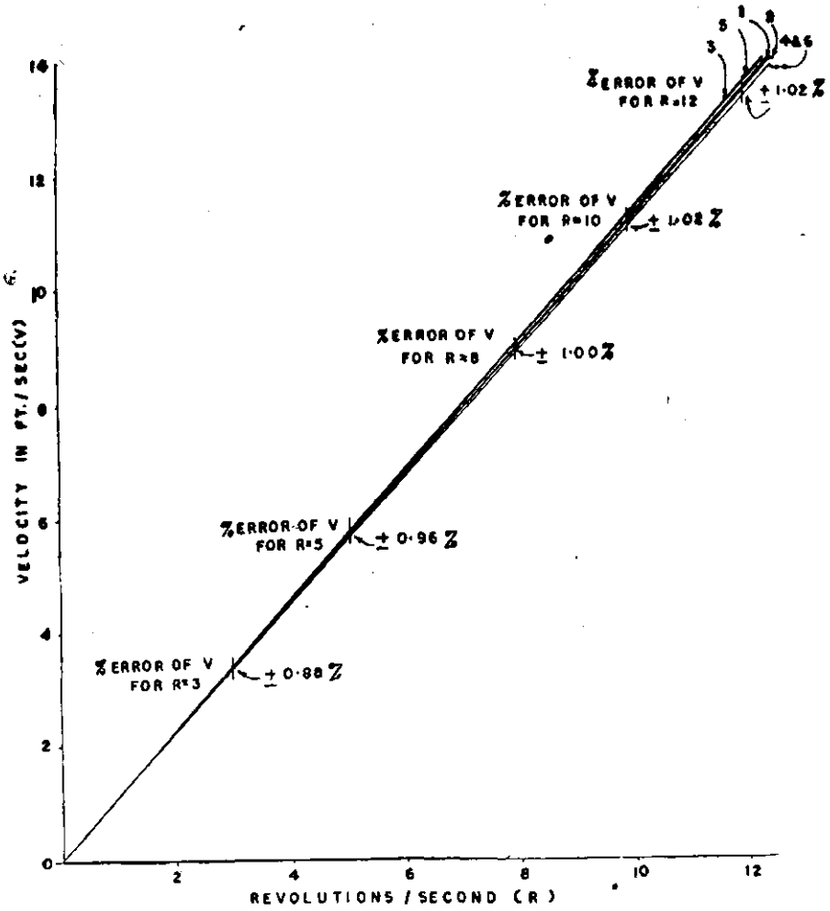

Fig 4: Extensions of rating expressions for $V > 2.16$ *ft/sec* (*ie* outside observed range).

7. Extrapolations

But the limitations particularly in respect of the small range of variation of the observed velocity data was rather serious. The inference drawn about the invariability of the V, R relation will have little importance, if similar invariability did not hold for the higher velocities as well. Higher velocity runs could not be made in the circular rating tank due to limitations already mentioned. Thus pending further obser-

vations an inductive approach was made to see if it could provide an answer.

Normally velocity encountered in stream gauging does not exceed 14 to 15 *ft/sec*. When the lines for the six sets of expressions in *fig 4* are extended to a velocity of 14 *ft/sec* the maximum *inter-se* difference in the region of 14 *ft/sec* velocity is found to be sensibly small, limited to ± 1 *percent* only.

Thus, despite the six expressions having been derived from observed data of only five points each from the lower values of V not exceeding 2.61 *ft/sec*, their divergence within a strictly narrow band in upper reaches of the R-V field indicates that in case of higher velocities also, the effect of temperature on rating may not be of any consequence.

Boundary Effect

8. Experimental precautions

Experiments were undertaken for investigation of boundary effects in the larger Ship Model Testing Tank. The following precautions were taken to ensure freedom from any experimental variations:

(1) The currentmeter was oiled and cleaned before each set of runs.

(2) Spin tests of the currentmeter was taken regularly before beginning each set of runs to ensure that friction in the bearings was minimum. While the spin test gave a period of at least 90 *sec* many ratings were carried out with spin-test values of 100 *sec* and more up to 140 *sec*. This ensured that the effect of friction at velocities of 1 *ft/sec* was negligible.

(3) The currentmeter was held tightly to the carriage by securing it at 2 points so that vibrations due to suspension of rod were reduced to the minimum.

(4)* Sufficient interval of time was allowed to lapse between two consecutive runs in order to induce stillness to the water mass in the tank and so ensure freedom from disturbance to the following run.

9. Design of the experiment

Twenty positions of immersing the currentmeter during its experimental runs in the tank comprised of points at four depths along each of the five selected verticals *vide fig 5*. All the 20 positions were selected from a half portion of the cross-section, as their symmetry about the central vertical suggests similar V-R behaviour over the second half also. The observations for any individual vertical will be capable of yielding separately information about the influence of the nearness of the bottom. Similarly the observations along any one depth on the five verticals can also yield information about the influence of the nearness of side wall; these may again differ for the 4 different depths. The advantage of this method of collection of data lies in the utilization of a large number of compounded observations to yield information on each feature of investigation and their interaction of differcombinations. For example, whenever disproportionately increased bias due to depth is obtained along some verticals alone, the feature will be properly highlighted by the interaction mean square term in the analysis of variance.

10. Observations

A constant depth of 7-0 *ft* of water was maintained in the tank and a Watt currentmeter (*No* 91891) was used for the experimental ratings. Following series of tests were conducted:

(1) Currentmeter held in the centre of the tank and velocities observed at 6, 12, 66 and 72 *in* above the bed

(2) Currentmeter held at 5, 12, 18 and 24 *in* from the side wall of the tank and the velocity observations made in each case at 6, 12, 66 and 72 *in* above the bed

to minimise the effect of any residual disturb-

*When a run is taken in a tank for rating a currentmeter, waves and drift are generated. It takes certain time for this disturbance to reduce to a reasonably low value before next run can be taken. These intervals were actually decided from a separate experiment in which the absence of movements in water were checked by observing the reflection of 4.0 *ft* long fluorescent tube suspended about 13.0 *ft* from the surface of water. The movement of the image of the tube is greatly exaggerated, if the water has even the slightest movement. With a view to minimise the effect of any residual disturbance and make its effect equal on all calibrations, regnite intervals were allowed between successive runs at different speeds as given below:

These were maintained in all the experiments that are described in the note.

Velocity (*ft/sec*)	1	1.5	2	2.5	3	4	5	6	7	8
Time interval (*min*)	3	3	3	5	5	6	9	11	14	16

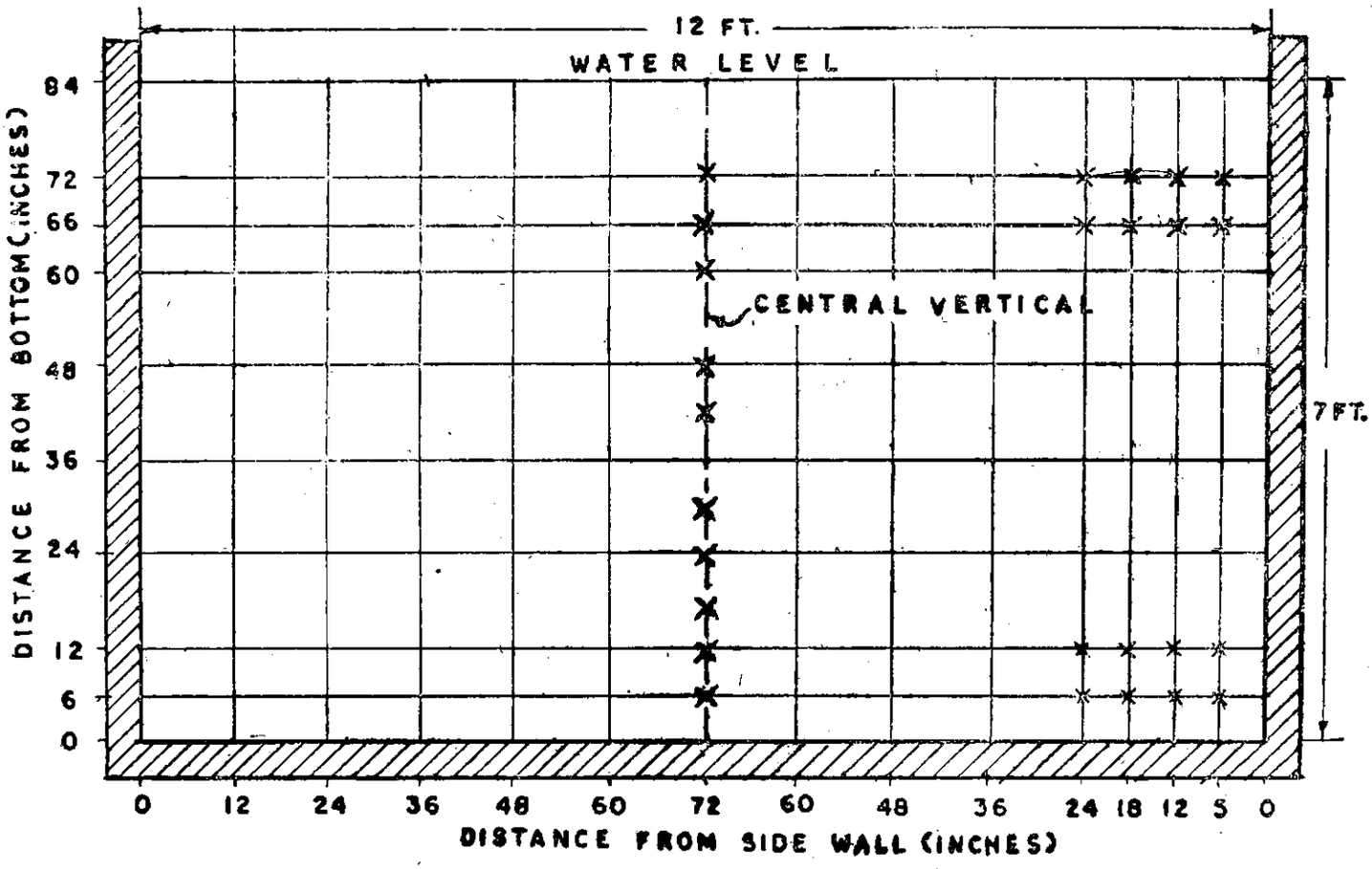

Fig 5: Cross-section of Ship model testing tank showing immersion positions of Currentmeter for calibrations looking towards the end of the tank.

(2) Additional tests with currentmeter at the centre of the tank and velocities observed at 6, 12, 18, 24, 30, 42, 48, 60, 66 and 72 *in* above the bed. For evaluating rating expressions corresponding to 20 different positions replicate observations were made *vide* items (1) and (2) above. About 10 runs were made for each by running the carriage at different velocities between .95 $<V<8.44$ *ft per sec.*

11. Analysis of data

The numerical values of the R and V for all the several runs are reproduced in *table 2* and shown plotted in *fig 6*. Straight line expressions evaluated by the method of least squares are drawn on the respective sets to show their goodness-of-fits. The average departures of individual points from the respective lines do not exceed about 3 *percent* except in a single case when it goes up to 6.9 *percent* for the extreme immersion position *viz* six inches from the bottom and five inches from the side of the tank. The large departure may more probably be ascribed to some mechanical maladjustment during the experiment rather than to the immersion position.

12. Differences between replicate calibrations

Replicate ratings for each different position were made solely to provide the measure of consistency between repeated calibrations, other things being equal.

The paired presentation of replicate lines in *fig 6* discloses very effectively the varying degrees of their coalescence generally. These random differences between repeated calibrations usually provide the base for computing the upper limits which normal differences between calibrations for different positions should not exceed.

If there were no differences between replicate calibrations or between calibrations for different immersion positions of the currentmeter, the values by the 40 lines for $R = 1$ (and similarly 3 or 5) should all be identical. The format of *table 3* offers a means for examining as well as for computing the concrete differences between replicate calibrations or calibrations with positions of other features in common. Thus, for example a glance at the mean values line discloses the steadily-decreasing trend for decreasing depth of immersion of the currentmeter.

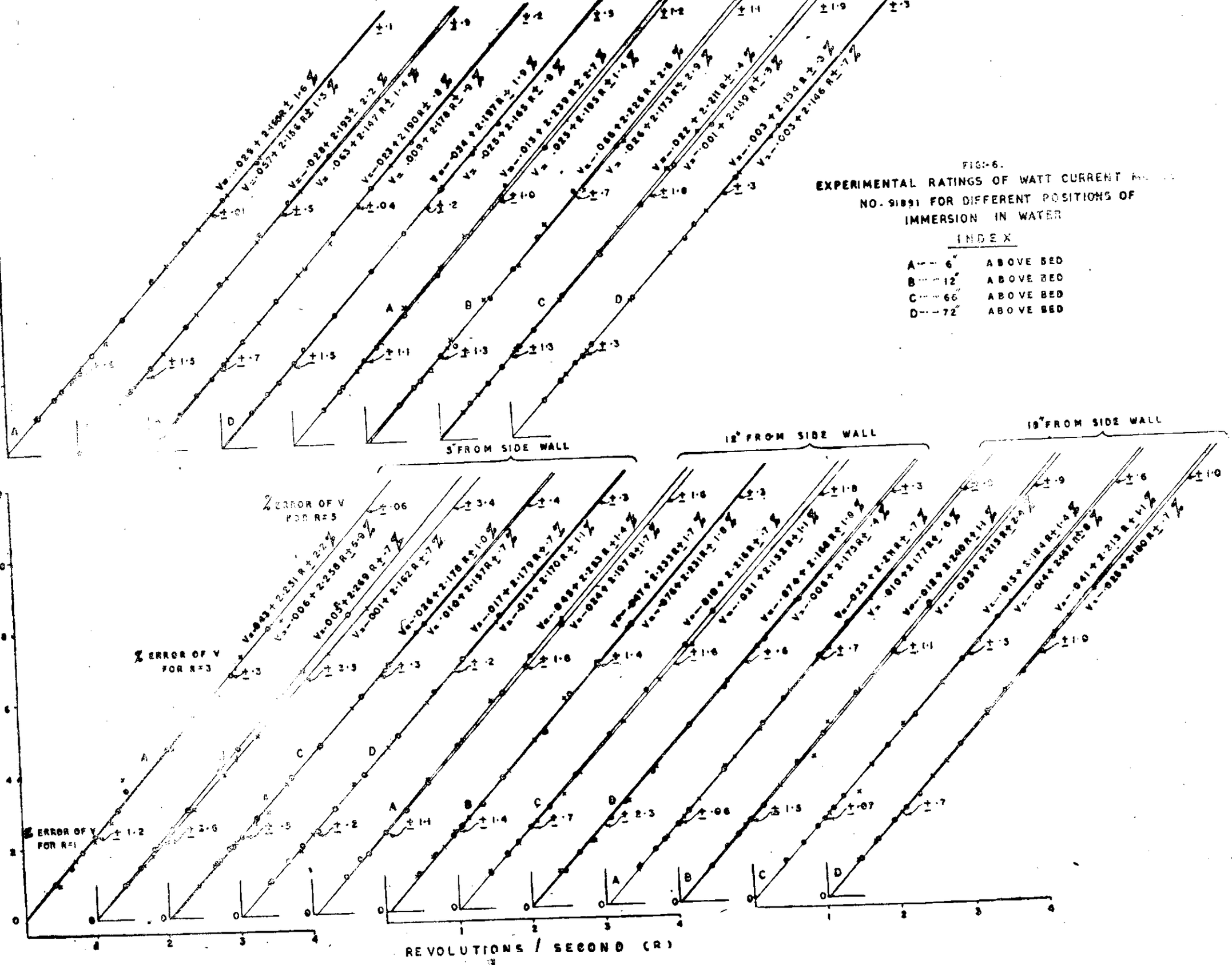

FIG-6.

EXPERIMENTAL RATINGS OF WATT CURRENT [illegible] NO. 91891 FOR DIFFERENT POSITIONS OF IMMERSION IN WATER

INDEX

A — 6" ABOVE BED
B — 12" ABOVE BED
C — 66" ABOVE BED
D — 72" ABOVE BED

Table 2 : Revolution (R) / *sec* and velocity (V) *ft* / *sec* observed for experimental calibration runs of Watts type currentmeter *No* 91891

Distance from side wall (*inches*)	DISTANCE FROM BOTTOM (*Inches*)															
	6				12				66				72			
	REPLICATE															
	1		2		1		2		1		2		1		2	
	R	V	R	V	R	V	R	V	R	V	R	V	R	V	R	V
	.44	.99	.50	1.00	.43	.98	0.46	1.01	.70	1.54	.44	.95	.46	1.01	.43	.98
	.66	1.47	.69	1.50	.64	1.47	0.69	1.51	.88	1.93	.68	1.49	.69	1.52	.69	1.47
	.85	1.93	.76	1.66	.86	1.95	0.82	1.79	.91	1.99	.76	1.61	.89	1.91	.87	1.81
	1.03	2.33	1.02	2.22	1.12	2 52	1.01	2.18	1.05	2.27	.96	2.10	1.10	2.38	1.03	2.24
	1.35	3.06	1.28	2.74	1.33	3.02	1.41	3.03	1.28	2.74	1.26	2.65	1.35	2.89	1.35	2.90
5	1.50	3.61	1.45	3.94	1.80	4.07	1.86	3.98	1.78	3.87	1.71	3.69	1.77	3.83	1.64	3.59
	2.07	4.71	2.16	4.70	2.07	4.67	2.34	5.01	2.19	4.67	2.17	4.66	2.24	4.83	2.12	4.54
	2.43	5.60	2.60	5.86	2.62	6.00	2.73	5.93	2.77	5.96	2.62	5.66	2.77	6.00	2.66	5.76
	3.01	6.73	3.16	7.26	2.97	6.76	3.34	7.24	3.16	6.83	3.11	6.78	3.17	6.91	3.14	6.84
	3.53	7.95	3.71	8.21	3.64	8.23	3.90	8.44	3.68	7.96	3.56	7.74	3.70	8.08	3.66	7.92
	.47	1.01	.46	1.02	.48	1.01	.44	.97	.43	.97	.43	1.02	.46	1.01	.40	1.03
	.67	1.50	.68	1.53	.69	1.51	.66	1.48	.68	1.52	.67	1.52	.68	1.49	.66	1.53
	.78	1.64	.81	1.74	.96	2.05	.83	1.77	.82	1.81	.81	1.76	.84	1.82	.87	1.87
	1.02	2.21	1.08	2.40	1.06	2.30	.98	2.15	1.03	2.28	1.13	2.44	1.11	2.40	1.06	2.49
	1.32	2.80	1.26	2.72	1.38	2.91	1.20	2.57	1.30	2.82	1.50	3.17	1.33	2.86	1.36	2.91
12	1.63	3.54	1.63	3.63	1.65	3.64	1.74	3.81	1.66	3.68	1.73	3.74	1.70	3.67	1.76	3.83
	2.02	4.52	2.11	4.66	2.25	4.83	2.13	4.63	2.14	4 73	2.36	5.11	2.25	4.90	2.26	4.95
	2.70	5.96	2.53	5.76	2.61	5.86	2.55	5.76	2 67	5.92	2.87	6.18	2.72	5.91	2.77	6.10
	3.05	6.64	3.10	6.93	3.03	6.67	3.02	6.75	3.24	7 14	3.31	7.17	3.30	7.18	3.20	7.02
	3.56	7.76	3.57	7.99	3.51	7.78	3.48	7.67	3 62	8.04	3.85	8.35	3.80	8.26	3.75	8.23
	.47	1.04	.45	1.00	.45	1.01	.46	1.02	.46	1.07	.46	1.00	.47	1.02	.45	.99
	.69	1.53	.68	1.49	.68	1.52	.68	1.52	.69	1.51	.69	1.50	.71	1.53	.68	1.48
	.83	1.79	.87	1.87	.83	1.84	.85	1.87	.90	1.94	.89	1.92	.95	2.05	.96	2.08
	1.01	2.20	1.12	2.44	1.00	2.21	.94	2.09	1.00	2.13	1.08	2.32	1.11	2.39	1.06	2.28
	1.17	2.53	1.33	2.89	1.19	2.60	1.44	3.15	1.13	2.42	1.13	2.44	1.29	2.71	1.49	3.27
18	1.68	3.70	1.83	3.99	1.66	3.80	1.89	3.91	1.27	2.76	1.68	3.64	1.88	4.09	1.69	3.66
	2.21	4.85	2.18	4.76	2.03	4.52	2.20	4.83	1.89	4.10	2.12	4.76	2.27	4.93	2.26	4.90
	2.51	5.50	2.61	5 74	2.51	5.57	2.58	5.75	2.28	4.91	2.69	5.85	2.77	6.03	2.51	5.58
	3.03	6.66	3.16	6.86	3.02	6.76	3.18	7.04	2.95	6.41	3.19	6.92	3.22	6.97	3.21	7.09
	3.45	7.65	3.77	8.20	3.56	7.99	3.57	7.90	3.47	7.52	3.66	7.99	3.78	8.22	3.41	7.51
	.46	1.02	0.41	1.01	.46	1.02	.41	1.03	.45	1.00	.45	1.00	.44	.98	.45	.99
	.69	1.52	.68	1.53	.70	1.52	.67	1.51	.68	1.49	.69	1.52	.67	1.47	.69	1.51
	.81	1.76	.94	2.02	.77	1.70	.83	1.84	.90	1.96	.73	1.54	.81	1.78	.81	1.73
	1.05	2.26	.99	2.16	1.06	2.29	1.07	2.30	1.08	2.35	.94	2.04	1.05	2.28	1.04	2.29
	1.26	2 75	1.44	3.10	1.20	2.43	1.25	2.68	1.37	2.98	1.17	2.50	1.18	2.65	1.18	2.36
24	1.71	3.70	1.69	3.68	1.57	3.42	1.75	3.78	1.82	4.04	1.59	3.47	1.65	3.58	1.74	3.77
	2.12	4.72	2.34	5.19	2.08	4.55	2.17	4.71	2.27	4.88	2.18	4.71	2.17	4.71	2.18	4.72
	2.60	5.76	2.80	6.16	2.65	5.86	2.62	5.78	2.66	5.83	2.60	5.68	2.63	5.71	2.63	5.71
	3.17	6.92	3.24	7.02	3.06	6.72	3.25	7.04	3.21	7.01	3.02	6.60	3.16	6.88	3.18	6.95
	3.67	7.87	3.72	8.02	3.68	7.97	3.69	7.98	3.79	8.25	3.49	7.65	3.61	7.85	3.66	8.03
	.44	1.00	.46	1.01	.45	.99	.46	.99	.45	.97	.34	.76	.46	1.00	.46	.99
	.67	1.49	.69	1.52	.67	1.48	.69	1.49	.70	1.50	.55	1.20	.70	1.51	.70	1.49
	.70	1.56	.92	2.01	.77	1.62	.91	1.98	.91	1.93	.91	1.97	.92	1.96	.79	1.70
	1.03	2.28	.94	2.07	1.06	2.31	1.17	2.51	1.16	2.51	1.10	2.40	1.00	2.16	1.08	2.32
	1.19	2.61	1.27	2.73	1.28	2.59	1.20	2.74	1.37	2.93	1.33	2.92	1.16	2.46	1.16	2.49
72	1.59	3.50	1.59	3.67	1.77	3.85	1.69	3.84	1.78	3.83	1.71	3.73	1.73	3.73	1.70	3.64
	2.08	4.55	2.12	4.78	2.13	4.63	2.20	4.75	2.31	4.94	2.29	5.04	2.47	5.26	2.28	4.92
	2.50	5.61	2.47	5.61	2.47	5.51	2.57	5.82	2.90	6.24	2.58	5.69	2.64	5.64	2.77	5.99
	3.00	6.65	3.03	7.03	2.98	6.70	3.13	6.74	2.36	7.29	3.27	7.22	3.19	6.87	3.25	7.00
	3.63	7.93	3.06	6.96	3.61	7.89	3.72	8.02	3.91	8.34	3.71	8.20	3.82	8.19	3.71	7.98

Nearly similar variation of the side effect is also perceivable in the series of the mean values in *table 3* for different horizontal distances from the side wall. Thus, when the currentmeter is closest to the side wall, higher velocities are again registered for same R's. But the side effect does not continue in a steady sense beyond a 5 *in* distance. The casual differences noticed between the mean values for other distance of 12, 18 and 24 *in* from the side wall are not larger than what may be expected between repeated calibrations for any random immersion position.

For the comparison of overall means for $R = 1$, $R = 3$ and $R = 5$ *vide cols* 6, 11 and 16 (*table 3*) with the mean values for observations at 6 and 12 *in* from the bottom *vide cols* 2, 3, 7, 8, 12 and 13 and at 5 and 12 *in* from the side, *vide* items 1 and 2 of *cols* 6, 11 and 16 values are extracted as under:

		Mean velocity ($\overline{V}$) and its difference for distance (*inches*) from				All distances mean velocity V_o.
		bottom		side wall		
		6	12	5	12	
$R=1$	$\overline{V}$	2·215	2·192	2·202	2·190	2·188
	$\overline{V}-V_o$.	·027	·004	·014	·002	
	% diff. to V_o.	1·23	·18	·64	·09	
$R=3$	$\overline{V}$	6·635	6·609	6·608	6·597	6·573
	$\overline{V}-V_o$.	·062	·036	·035	·024	
	% diff. to V_o.	·94	·55	·53	·36	
$R=5$	$\overline{V}$	11·056	11·027	11·014	11·003	10·959
	$\overline{V}-V_o$.	·097	·068	·055	·044	
	% diff. to V_o.	·89	·62	·50	·40	

Table 3 : Values of V from rating expressions for different immersion positions of the currentmeter

Distance from side wall (*inches*)	$R=1$					$R=3$					$R=5$				
	DISTANCE FROM BOTTOM (*Inches*)														
	6	12	66	72	Mean	6	12	66	72	Mean	6	12	66	72	Mean
1	2	3	4	5	6	7	8	9	10	11	12	13	14	15	16
5	2·293	2·273	2·197	2·162		6·795	6·810	6·481	6·519		11·297	11·348	10·794	10·876	
	2·253	2·161	2 151	2·137	2·202	6·770	6 485	6·506	6·497	6·608	11·287	10·809	10 862	10·837	11·014
12	2·173	2·154	2·206	2 109		6·567	6·616	6·687	6·520		10·861	11·077	11·068	10·870	
	2·207	2·186	2·184	2·242	2·190	6·713	6·652	6·488	6·579	6·597	11·218	11·118	10·793	10·915	11·003
18	2·185	2 228	2·176	2·154		6·606	6·709	6·500	6·615		11·028	11·190	10 823	10 815	
	2·187	2 180	2·174	2·175	2 182	6·541	6·610	6 542	6·605	6·578	10 894	11·041	10·910	11·035	10·974
24	2·194	2·165	2·187	2·197		6·525	6·551	6·542	6·520		10·855	10·936	10·898	10·849	
	2·215	2·210	2·166	2·144	2·184	6·524	6·504	6·546	6·538	6·531	10·835	10· 98	10·925	10·833	10·879
72	2·220	2·160	2 150	2·143		6·609	6·612	6·498	6·414		10 999	11·063	10·747	10·725	
	2·224	2·199	2·189	2·152	2·180	6·703	6·555	6·611	6·460	6·553	11·182	10·892	11·033	10·769	10·926
Mean	2·215	2·192	2·175	2·169	2·183	6·635	6·609	6·540	6·519	6·573	11·056	11·027	10·885	10·868	10·959
Marginal random difference between two	Mean V's	·024	·026				·061		·068			·113			·126
	Unit V's	·074					·192					·356			

From variations of	Degrees of freedom	Sum of squares	Mean square		Sum of squares	Mean square		Sum of squares	Mean square	
Distance from bottom ...	3	·012823	·004274	significant	·029935	·033142	significant	·75153	·09·719	significant
Distance from side ...	4	·000641	·000660		·031509	·007892		·101903	·025325	
Residual I	22	·032216	·01007		·201 33	·006310		·609967	·0 90 1	
Residual II ...	56	·034 56	·000968	$s=\cdot031$	·233502	·006186	$s=\cdot081$	·7·1208	·022·27	$s=$ 149
Total ...	39	·047680		$=\pm$ 1·42%	·333498		$=\pm$ 1·2·%	·986426		$=\pm$ 1·36%

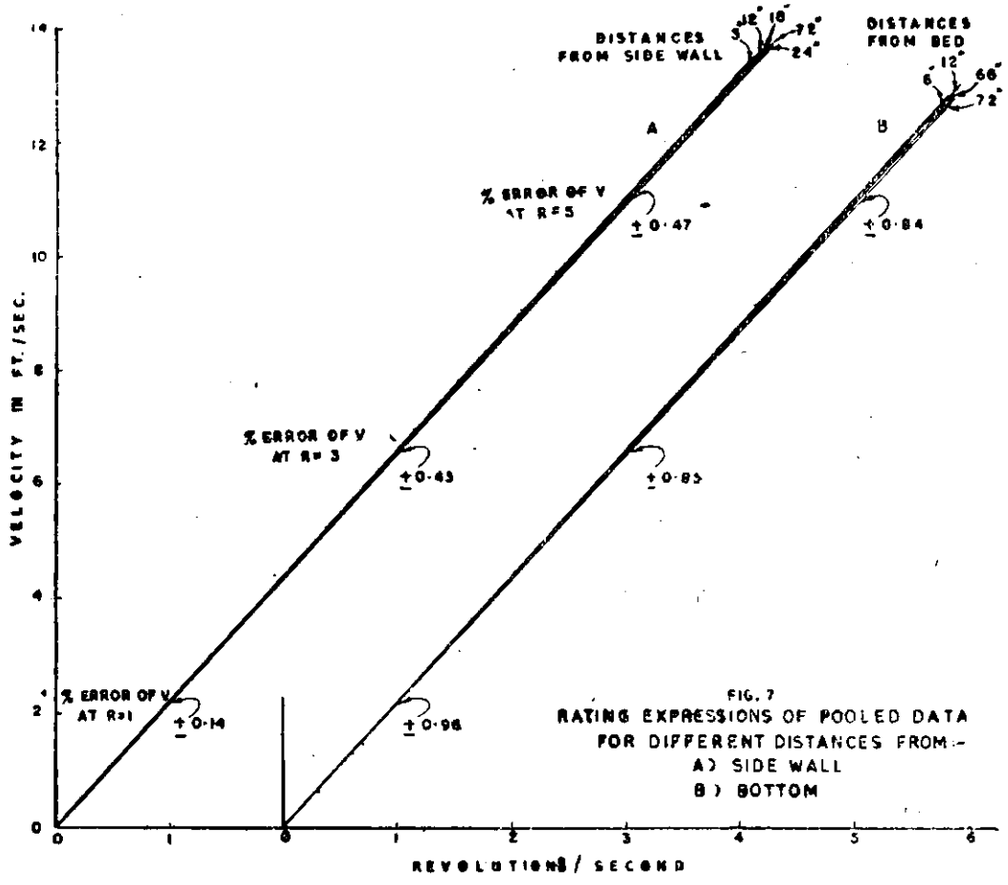

FIG. 7
RATING EXPRESSIONS OF POOLED DATA FOR DIFFERENT DISTANCES FROM:-
A) SIDE WALL
B) BOTTOM

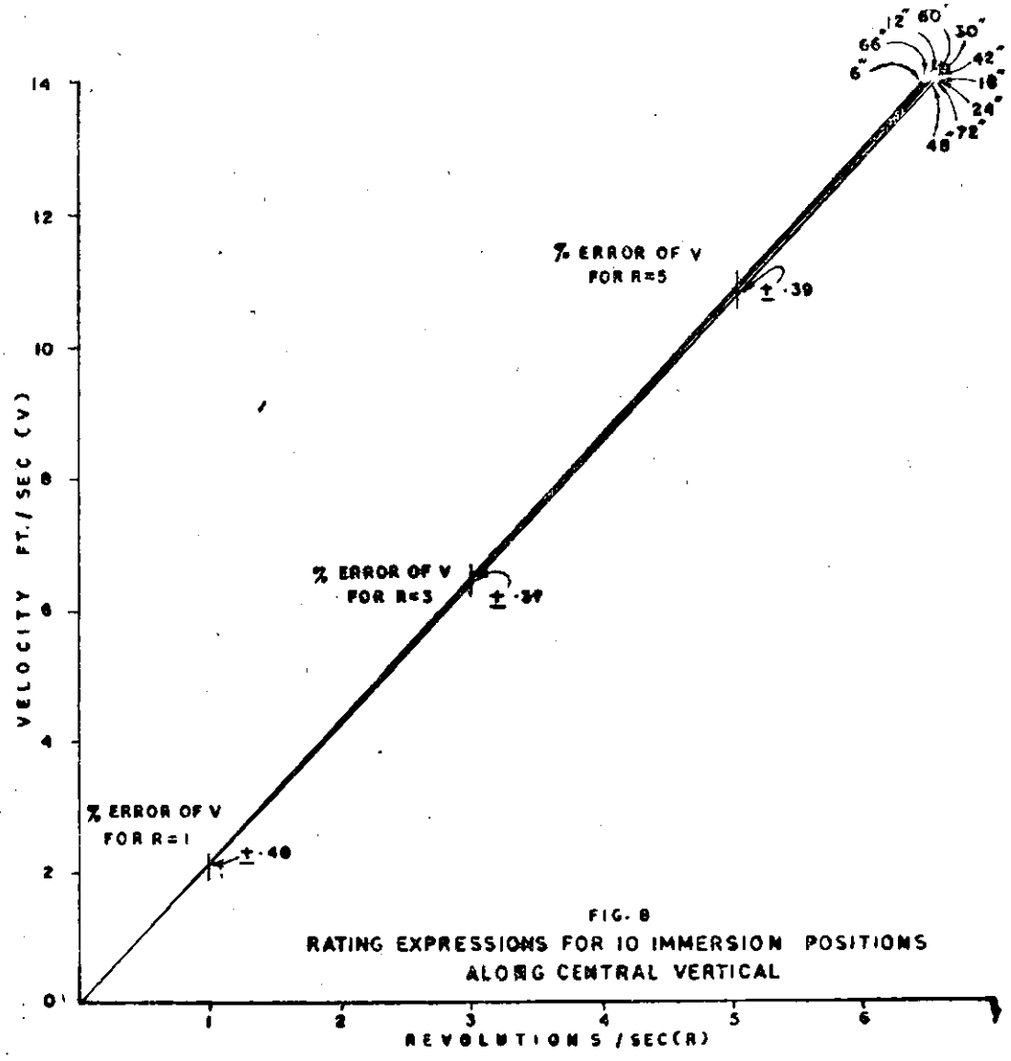

FIG. 8
RATING EXPRESSIONS FOR 10 IMMERSION POSITIONS ALONG CENTRAL VERTICAL

Table 5 : Values of V from rating expressions for different immersion positions of current-meter along central vertical

Distance from bottom (*Inches*)	$R=1$							$R=3$							$R=5$						
	REPLICATES																				
	1	2	3	4	5	6	Mean	1	2	3	4	5	6	Mean	1	2	3	4	5	6	Mean
1	2	3	4	5	6	7	8	9	10	11	12	13	14	15	16	17	18	19	20	21	22
6	2·220	2·223	2·182	2·159	2·181	2·188	2·192	6·609	6·618	6·544	6·552	6·562	6·539	6·571	10·999	11·013	10·906	10·946	10·943	10 891	10.950
12	2·160	2·199	2·159	2·226	2·168	2·183	2·183	6·612	6·545	6·463	6·548	6·551	6·515	6·539	11·063	10·892	10·767	10·870	10·958	10.847	10.895
18	2·154	2·214	2·142	2·180	2·174	2·197	2·177	6·468	6·585	6·452	6·482	6·538	6·544	6·512	10·781	10·957	10·763	10·784	10·902	1 .890	10.846
24	2·157	2·199	2·165	2·185	2·181	2·180	2·178	6·519	6·513	6·489	6·512	6·519	6·494	6·508	10·881	10·826	10·813	10·839	10·857	10.809	10.838
30	2·179	2·188	2·181	2·177	2·208	2·194	2·188	6·584	6·564	6·557	6·480	6·520	6·497	6·534	10·990	10·940	10·933	10·782	10·832	10.801	10.860
42	2·176	2·150	2·141	2·195	2·210	2·145	2·169	6·471	6·456	6·442	6·661	6·678	6·453	6·527	10·766	10·763	10·743	11·127	11·146	10·761	10.884
48	2·158	2·159	2·173	2·173	2·192	2·158	2·169	6·469	6·466	6·457	6·498	6·641	6·469	6·500	10·781	10·768	10·791	10·824	11·050	10·779	10.830
60	2·171	2·109	2·156	2·158	2·157	2·135	2·164	6·528	6·573	6·534	6·524	6·535	6·454	6·527	10·904	10·937	10·912	10·850	10·914	10·718	10.890
66	2·150	2·189	2·213	2·180	2·159	2·185	2·179	6·448	6·611	6·629	6·562	6·532	6·590	6·562	10·747	11·033	11·046	10·944	10·904	10·995	10.945
72	2·143	2·152	2·201	2·175	2·153	2·178	2·167	6·434	6·460	6·532	6·558	6·482	6·540	6·501	10·725	10·769	10·864	10·942	10·811	10·901	10.835
Mean							2·177							6·528							10.879
Marginal random difference between two — mean V's							·022							·056							
Marginal random difference between two — unit V's							·053							·138							

From variations of	Degrees of freedom	Sum of squares	Mean square		Sum of squares	Mean square		Sum of squares	Mean square	
Distances	9	·004594	·000510		·032152	·003572		·100774	·011197	
Residual	50	·024808	·000496		·168112	·003362		·519 91	· 103 4	
Total	59	·029402	·000498	s=·022 = ±1·01%	·2002b4	·003394	s=·058 = ±·89%	·620465	·010516	s=·102 = ±·94%

L—S 3401—20

Table 4 ; Revolution (R)/*sec* and velocity (V) *ft*/*sec* observed for experimental calibration runs of Watts type currentmeter *No* 91891 at different depths along central vertical

Distance from bottom (*Inches*)	REPLICATE											
	1		2		3		4		5		6	
	R	V	R	V	R	V	R	V	R	V	R	V
6	.44	1.00	.44	1.01	.45	.98	.47	.99	.46	1.01	.45	1.00
	.67	1.49	.82	1.82	.68	1.47	.69	1.50	.69	1.53	.65	1.49
	.70	1.56	1.17	2.57	.86	1.85	.97	2.04	.86	1.85	.92	1.97
	1.03	2.28	1.67	3.66	1.10	2.35	1.21	2.57	1.05	2.28	1.06	2.29
	1.19	2.61	2.12	4.71	1.37	2.94	1.48	3.17	1.26	2.68	1.35	2.95
	1.59	3.50	2.62	5.84	1.63	3.59	1.91	4.12	1.81	3.93	1.85	4.02
	2.08	4.55	3.22	7.10	2.20	4.87	2.17	4.78	2.15	4.72	2.16	4.76
	2.50	5.61	3.48	7.63	2.53	5.72	2.62	5.88	2.53	5.64	2.57	5.64
	3.00	6.65			3.10	6.73	3.15	6.91	3.06	6.68	3.11	6.78
	3.63	7.93			3.67	7.87	3.82	8.25	3.57	7.75	3.64	7.91
12	.45	.99	.46	.99	.36	.78	.44	.99	.45	1.00	.46	1.00
	.67	1.48	.69	1.49	.79	1.72	.77	1.73	1.14	2.50	.75	1.65
	.77	1.62	.91	1.93	1.24	2.67	1.18	2.63	1.23	2.70	1.27	2.77
	1.06	2.31	1.17	2.51	1.48	3.19	1.60	3.53	1.71	3.64	1.68	3.65
	1.28	2.59	1.20	2.74	2.14	4.59	2.07	4.53	2.15	4.55	2.13	4.62
	1.77	3.85	1.69	3.84	2.75	5.93	2.61	5.75	2.63	5.80	2.67	5.80
	2.13	4.63	2.20	4.75	3.15	6.80	3.20	6.97	3.02	6.65	2.85	6.18
	2.47	5.51	2.57	5.82	3.76	8.10	3.60	7.82	3.56	7.77	3.43	7.44
	2.98	6.70	3.13	6.74								
	3.61	7.89	3.72	8.02								
18	.45	.98	.44	.99	.44	.95	.44	.97	.44	.98	.45	1.01
	.80	1.71	.67	1.48	.86	1.84	.79	1.72	.79	1.73	.78	1.72
	1.21	2.62	.72	1.58	1.29	2.75	1.30	2.81	1.28	2.76	1.23	2.68
	1.59	3.41	1.08	2.40	1.65	3.52	1.53	3.31	1.76	3.79	1.60	3.47
	2.24	4.83	1.24	2.69	2.26	4.82	2.17	4.67	2.08	4.52	2.20	4.78
	2.61	5.62	1.68	3.65	2.61	5.66	2.67	5.83	2.81	6.08	2.63	5.77
	3.06	6.61	2.00	4.60	3.24	6.94	3.19	6.89	3.20	6.96	3.15	6.91
	3.55	7.66	2.59	5.66	3.67	7.91	3.54	7.62	3.98	8.72	3.94	8.56
			2.98	6.59								
			3.61	7.82								
24	.45	.97	.42	.98	.44	.96	.46	.99	.45	.97	.45	.99
	.80	1.73	.87	1.97	.83	1.80	.86	1.92	.85	1.86	.77	1.67
	1.24	2.66	1.25	2.67	1.20	2.62	1.24	2.70	1.19	2.59	1.17	2.57
	1.71	3.68	1.70	3.67	1.78	3.83	1.73	3.75	1.54	3 34	1.80	3.90
	2.17	4.70	2.13	4.60	2.25	4.87	2.18	4.71	2.17	4.72	2.20	4.77
	2.75	5.93	2.71	5.91	2.60	5.62	2.76	5.98	2.43	5.25	2.54	5.51
	3.07	6.76	3.00	6.56	3.29	7.10	3.04	6.67	2.94	6.47	2.89	6.28
	3.66	7.91	3.65	7.91	3.76	8.16	3.72	8.06	3.80	8.20	3.64	7.85
30	.46	1.01	.46	1.02	.45	1.00	.44	.99	.44	.99	.45	1.00
	.67	1.46	.71	1.54	.90	1.98	.79	1.73	.76	1.70	.89	1.99
	1.04	2.24	1.01	2.19	1.23	2.68	1.08	2.35	1.13	2.48	1.22	2.64
	1.14	2.46	1.15	2.48	1.82	3.94	1.62	3.50	1.76	3.87	1.76	3.83
	1.30	2.84	1.29	2.89	2.19	4.75	2.06	4.47	2.07	4.52	2.19	4.75
	1.73	3.76	1.71	3.81	2.79	6.07	2.73	5.99	2.68	5.83	2.78	6.05
	2.30	5.04	2.31	4.99	3.24	7.13	3.31	7.15	3.13	6.82	3.19	6.91
	2.71	6.06	2.65	5.81	3.77	8.24	4.01	8.66	3.83	8.30	3.60	7.76
	3.13	6.83	3.27	7.14								
	3.77	8.25	3.61	7.90								

Table 4—contd.

Distance from bottom (*Inches*)	REPLICATE											
	1		2		3		4		5		6	
	R	*V*	*R*	*V*	*R*	*V*	*R*	*V*	*R*	*V*	*R*	*V*
42	.31	.69	.38	.81	.49	1.04	.34	.76	.35	.81	.51	1.09
	.49	1.08	.59	1.28	.68	1.47	.52	1.16	.35	.78	.64	1.37
	.81	1.78	.83	1.80	.85	1.80	.76	1.69	.61	1.34	.95	2.01
	1.06	2.31	1.50	3.21	1.09	2.34	1.00	2.21	.86	1.89	1.10	2.37
	1.20	2.61	1.70	3.64	1.31	2.79	1.25	2.76	1.03	2.26	1.25	2.66
	1.59	3.49	1.63	3.49	1.63	3.51	1.59	3.52	1.22	2.59	1.91	4.13
	2.73	5.86	2.22	4.79	2.21	4.71	2.11	4.68	1.60	3.53	2.16	4.63
	3.14	6.78	2.57	5.51	2.72	5.82	2.54	5.67	2.07	4.66	2.76	5.96
	3.68	7.93	3.14	6.77	3.18	6.83	3.01	6.70	2.58	5.74	3.16	6.78
			3.69	7.93	3.71	8.00	3.56	7.94	3.07	6.83	3.69	7.95
48	.32	.71	.37	.80	.39	.87	.37	.85	.37	.83	.39	.85
	.80	1.72	.59	1.30	.56	1.24	.58	1.27	.56	1.23	.63	1.36
	.99	2.16	.88	1.88	.78	1.72	.81	1.74	.79	1.74	.82	1.76
	1.22	2.62	1.00	2.18	1.04	2.26	1.06	2.28	1.02	2.23	1.08	2.33
	1.66	3.57	1.31	2.81	1.24	2.68	1.27	2.76	1.27	2.77	1.27	2.73
	2.22	4.77	1.76	3.80	1.66	3.59	2.22	4.84	1.63	3.55	1.71	3.71
	2.59	5.59	2.22	4.76	2.16	4.70	2.69	5.81	2.22	4.87	2.12	4.57
	3.11	6.71	2.70	5.83	2.69	5.65	3.19	6.92	2.62	5.79	2.73	5.91
	3.66	7.89	3.21	6.91	3.10	6.71	1.69	3.66	3.11	6.89	3.27	7.04
			3.69	6.96	3.60	7.78	3.73	8.08	3.59	7.98	3.75	8.08
60	.37	.84	.36	.81	.35	.81	.29	.65	.37	.81	.38	.82
	.65	1.48	.62	1.36	.56	1.23	.59	1.31	.64	1.39	.64	1.38
	.81	1.77	.90	1.95	.94	1.98	.92	1.97	.94	2.04	.87	1.83
	1.16	2.56	1.12	2.42	1.17	2.49	1.17	2.50	1.15	2.43	1.13	2.42
	1.25	2.76	1.30	2.79	1.38	2.92	1.40	2.97	1.43	3.10	1.33	2.80
	1.50	4.04	1.69	3.65	1.80	3.92	1.90	4.13	1.70	3.64	1.90	4.12
	2.20	4.81	2.17	4.71	2.28	4.98	2.21	4.80	2.22	4.82	2.21	4.72
	2.85	6.28	2.59	5.67	2.74	5.97	2.89	6.31	2.80	6.12	2.79	6.00
	3.23	7.08	3.12	6.79	3.17	6.90	3.23	7.02	3.08	6.70	3.30	7.09
	3.76	8.19	3.76	8.22	3.69	8.07	3.68	8.02	3.73	8.16	3.71	8.01
66	.45	.97	.34	.76	.47	1.01	.45	.98	.48	1.02	.45	1.00
	.70	1.50	.55	1.20	.67	1.48	.80	1.73	.68	1.51	.67	1.49
	.91	1.93	.90	1.97	.88	1.85	1.16	2.54	.89	1.90	.79	1.73
	1.16	2.51	1.10	2.40	1.06	2.61	1.58	3.44	1.05	2.33	1.17	2.54
	1.37	2.93	1.33	2.92	1.33	2.87	2.12	4.64	1.37	2.93	1.32	2.85
	1.78	3.83	1.71	3.73	1.72	3.78	2.72	5.94	1.76	3.69	1.73	3.80
	2.31	4.94	2.29	5.04	2.27	4.98	3.04	6.65	2.18	4.79	2.08	4.53
	2.90	6.24	2.58	5.69	2.65	5.83	3.78	8.27	2.85	6.29	2.76	6.06
	3.36	7.29	3.27	7.22	3.12	6.94			3.18	6.76	3.05	6.70
	3.91	8.34	3.71	8.20	3.61	7.93			3.62	7.97	3.60	7.94
72	.46	1.00	.46	.99	.44	1.04	.45	1.00	.46	.98	.44	.97
	.70	1.51	.70	1.49	.81	1.77	.89	1.91	.81	1.76	.72	1.56
	.92	1.96	.79	1.70	1.12	2.44	1.24	2.70	1.34	2.88	1.17	2.51
	1.00	2.16	1.08	2.32	1.61	3.50	1.62	3.53	1.72	3.69	1.68	3.69
	1.16	2.46	1.16	2.49	2.18	4.76	2.00	4.37	2.23	4.82	2.23	4.87
	1.73	3.73	1.70	3.64	2.59	5.65	2.56	5.60	2.73	5.91	2.72	5.92
	2.47	5.26	2.23	4.92	2.90	6.32	3.13	6.85	3.14	6.81	3.01	6.58
	2.63	5.60	2.77	5.99	3.72	8.08	3.58	7.82	3.73	8.03	3.68	8.00
	3.19	6.87	3.25	7.00								
	3.82	8.19	3.71	7.98								

Thus

(1) For the 6 *in* position above bottom the mean velocity estimates may be subject to an upward variation between .9 to 1.23 *percent*.
(2) For the 12 *in* position from bottom the effect remains between .18 to .62 *percent*.
(3) For positions of 5 *in* from the side wall the mean velocities may be similarly subject to an upward bias ranging between .5 to .64 *percent*.
(4) For the 12 *in* position from side wall the velocities will vary between .09 to .4 *percent*.

The broad inferences above are confirmed as correct by exact analyses variance subjoined in *table 3*.

The percentage standard error differences between the respective pairs of V's in *table 3* for all replicate calibrations are shown in *fig 6*. Their numerical magnitudes generally do not exceed 1.5 *percent* except for only one position (12 *in* from bottom and 5 *in* from side wall when the replicates have a standard error equal to about 3.5 *percent*. But a minute scrutiny of the data has disclosed that the rating runs for one of the two sets for the supposed position of 12 *in* from bottom might in all probability have been made at the 6 *in* position.

Pooling the primary data of all depths positions for each fixed distance from the side wall separately the five mean lines respectively obtaining are drawn in *fig 7*. Similarly the 4 mean lines computed from all primary data for each of the 4 different depths irrespective of the positions distances from side wall are also shown as a separate set. The two sets of mean lines together provide a graphical demonstration of the larger dispersion due to the effects of different distances from the bed than of similar effects from the side wall. Obviously, further observations were necessary for investigating the depth at which the bottom effects were the least if not totally absent.

13. Additional observations along central vertical

Fresh observations were therefore made as stated in *para* 11 *supra* with their scope limited to the central vertical only, as side effects had been found totally absent along three verticals close to the side wall and nearly absent at 5 *in* distance. The primary data of the R, V, values for the different rating runs made for 6 repeated calibrations for 10 different depths of immersion respectively at 6, 12, 18, 24, 30, 42, 48, 60 66 and 72 *in* are reproduced in *table 4*.

Table 5 shows three sets of V's as before for $R = 1$, 3 and 5 together with their respective analyses of variance. Study of mean value lines for the 3 sets of velocities shows that bottom effects do not perceivably continue beyond more than 12 *in* as inferred from the mean value lines in *table 3*.

At the central vertical mean velocity at 6 *in* above bottom may be subject to a maximum variation of .67 *percent* and the difference at 12 *in* above bottom is not likely to exceed .27 *percent*.

Thus, the mean V's for only two positions distant from the bottom by not more than 12 *in* are consistently higher than the rest. The higher mean V's uniformly obtaining for the position 66 *in* from bottom seem to be more casual than systematic, as no similar tendency is observed for the positions 72 *in* or 60 *in* from the bottom.

Fig 8 shows the 10 mean lines separately evaluated for the 10 depths each by pooling all the respectively replicate ratings data. The compact lie of the 10 lines, indicates the very negligible bottom effects on currentmeter ratings at different heights above 12 *in* along the central vertical.

14. Conclusions

From a set of observed data of experimental calibrations of a pygmy-type currentmeter with 2 *in* diameter bucket wheel towed at a circular rating tank the following conclusions can be derived:

Temperature effect :

(i) Under constant temperature conditions, R-V relations are sensibly linear for $.89 < V < 2.61$ *ft/sec* subject to standard deviation random variations of 3 *percent*

(ii) Estimates of V deduced from different relations for $5° < T < 40°C$ have a ± standard deviation variability between them not exceeding 1 *per cent*. In other words, R-V relations remain sensibly invariable to normal temperature changes.

(iii) The variability measure between different R-V relations does not increase even when they may be extended beyond their observed range up to nearly $V = 14$ *ft/sec*. Thus, the invariability of the R-V relations to temperature changes is inferred also up to $V = 14$ *ft/sec* provided their linearities hold; the latter aspect is amply borne out by the voluminous data collected for the experiments in the larger towing tank.

The effect of the proximity of boundary was assessed with a Watt currentmeter having 5 *in* diameter bucket wheel, in the large tank.

The following conclusions were drawn :

Boundary effect :

(iv) The linearity of the *R-V* relations for $.75<V<8.$ *ft/sec* holds for all positions of immersing the currentmeter in the towing tank, subject to ± standard deviation random variations of 3 *percent*

(v) Estimates of *V* from replicate ratings expressions, other conditions being equal, have a ± standard deviation random variability between them not exceeding 1.5 *percent*

(vi) Estimates of *V* from rating expressions for different immersion positions more than 5 *in* from side wall or 12 *in* from bottom also have comparable ± standard deviation variability and are less than 1.5 *percent*

(vii) For the 6 inches position above bottom the mean velocity estimates may be subject to an upward bias of from 0.9 to 1.2 *percent*. At the central vertical the bias is of the order of .67 *percent*.

For the 12 *in* position from bottom the bias remains between .2 to .6 *percent*

For positions of 5 *in* from the side wall the mean velocities may be similarly subject to an upward bias ranging between .5 to .64 *percent*. For the 12 *in* position from side wall the bias varies between .1 to .4 *percent*

(viii) From conclusions *v* to *vii* it follows that current meter observations in the field as well as calibration in the rating tank will be subject to a negligible boundary effect (which will be less than 6 *percent*)provided the velocities are observed at a distance of not less than 12 *in* from the sides as well as bottom.

(ix) An error up to 1.2 *percent* may be expected if velocity observations are taken six inches above the bottom and 5 *in* from the side.

---

23. Number of constant velocity runs for rating currentmeters

THE CONSTANT speed towing facilities provided at the *CWPRS* Ship Model Testing Tank are often availed for calibrating and/or recalibrating standard type currentmeters. For this, the currentmeter is fastened from the towing carriage to a desired immersed position under water and a number of runs made of the carriage along the tank. The constant velocities(*V*) of the separate and/or repeated runs and the corresponding numbers of the currentmeter wheel's revolutions (*R*) are recorded each time. The *R, V* data so collected for the complete range of velocities for which the currentmeter has been designed are then plotted and superposed over by a mean line. While the general lie of the points is often found as not very perceptibly different from linear, a few points, may however, be observed to lie not quite strictly on the mean line. The magnitudes of such departures of individual points are generally small and are attributed to unavoidable random observational errors. Nonetheless their precise extents have to be measured or evaluated before accepting their tolerableness in practice. But, prior to that the most probable form itself of the mean lie has to be determined first from the observed *R, V* points in such a way as to minimise effectively all the random departures. The procedure and the issues arising are described below:

The *R, V* data observed for repeated ratings of a Watt's type currentmeter *No* 91891 by immersing it to different positions under water are shown in *tables 2* and *4* (*p* 150, 154-55, *chap* 22). The tentative straight-line expressions fitted to the data for the several immersion positions as well as the different repeated ratings are also shown separately in *fig 6 cp* 149, *chap* 22). The reader can clearly see that the points for each individual rating set do not actually all lie on the respective straight lines. But by virtue of the different departures not bearing any systematized or conceivable other relations with respect to their exact location along the respective line, there remains no choice but to style them as random. Accordingly, their average magnitudes for each 8 or 10 points representing as many runs made for the individual calibrations from which the 40 mean lines have all been derived are also shown in *fig 6*.

In terms of the percentage coefficient of variation as they are expressed, the average departures have values between −3 and +3 barring a single case when the immersion position of the currentmeter was nearmost to the corner of the tank bottom. Excluding such extreme positions, therefore, which are generally not availed for standard rating immersions, *table 1* presents about 72 values of the coefficients of variation obtained for the 72 repeated calibrations made of the currentmeter. The *table* shows the values of a and b also for the several valibration expressions fitted of the type $V = a + bR$. The number of constant velocity runs for each calibration remained between 8 and 10 as before with the coefficients of variation values also ranging between ± 3 *percent.*

But, from practical tolerance considerations in stream flow measurements a ±3 *percent* variational range for the coefficient of variation of a calibration expression constitutes rather too wide a margin. It will be definitely desirable to have the calibration expression evaluated more precisely. But having secured and analysed the data of as many as 72 separate calibrations of a single currentmeter under controlled conditions, there appears to be no conceivable way of accomplishing the desired improvement. The question naturally arises whether a straight-line expression gives the best possible fit to the lie of the 8 or 10 observed points. The correct

Table 1

S. No.	Sample size.	a	b	Mean V *ft/sec.*	Coefficient of variation.	S. No.	Sample size.	a	b	Mean V *ft/sec.*	Coefficient of variation.
1	10	−.026	2.195	3.72	.86	37	9	.002	2.156	3.97	.30
2	8	.025	2.197	4.29	1.21	38	10	.007	2.152	3.82	.41
3	10	.001	2.181	3.84	2.32	39	10	.080	2.142	3.72	1.43
4	10	−.038	2.197	4.02	1.94	40	10	.011	2.163	3.82	.35
5	10	−.009	2.190	3.81	1.37	41	10	−.032	2.224	3.79	.70
6	10	.013	2.176	3.88	.95	42	10	.003	2.155	3.83	.30
7	10	−.066	2.226	3.76	1.83	43	10	.027	2.182	3.98	.86
8	10	.026	2.173	3.88	.49	44	10	−.012	2.183	3.84	.60
9	8	.007	2.152	4.22	.74	45	10	−.032	2.189	3.93	1.20
10	8	.065	2.161	4.24	2.64	46	10	−.025	2.183	3.97	.96
11	8	−.023	2.191	4.33	.36	47	10	−.032	2.189	3.92	.77
12	8	.017	2.166	4.14	.48	48	10	−.026	2.161	3.92	.69
13	8	−.002	2.157	4.18	.20	49	10	−.001	2.149	4.05	.35
14	10	.028	2.186	3.74	.68	50	10	−.022	2.211	3.91	2.71
15	8	−.013	2.155	4.30	2.05	51	10	.005	2.208	3.93	.14
16	8	−.029	2.151	4.23	.55	52	8	−.010	2.191	427	.82
17	8	−.001	2.182	4.44	.53	53	10	−.027	2.186	3.92	2.25
18	8	.023	2.173	4.36	.65	54	10	−.017	2.202	3.86	.80
19	8	.024	2.181	4.29	1.13	55	10	−.003	2.146	3.88	.40
20	8	.042	2.157	4.28	1.18	56	10	−.003	2.154	3.85	.43
21	8	.003	2.162	4.37	.27	57	8	.035	2.166	4.20	.69
22	8	.022	2.164	4.35	.86	58	8	−.017	2.192	4.22	.28
23	8	.012	2.169	4.18	.97	59	8	−.011	2.164	4.36	.58
24	8	.022	2.158	4.19	.42	60	8	−.003	2.181	4.26	.31
25	10	−.024	2.203	4.00	.32	61	8	−.036	2.201	4.24	.32
26	10	.000	2.188	4.00	.54	62	8	.078	2.216	4.23	1.15
27	8	−.007	2.188	4.48	1.36	63	8	−.088	2.217	4.20	1.14
28	8	.026	2.151	4.36	1.06	64	8	.137	2.134	4.32	.64
29	8	.052	2.156	4.31	.55	65	8	−.027	2.159	4.25	.21
30	8	.042	2.152	4.37	.29	66	7	.012	2.153	3.95	.13
31	9	.028	2.147	3.61	.63	67	10	.001	2.146	3.92	.69
32	10	−.003	2.153	3.92	.44	68	8	.068	2.185	4.34	.80
33	10	−.009	2.150	3.83	.46	69	8	.068	2.190	4.49	1.07
34	10	−.022	2.233	3.71	.36	70	8	.001	2.178	4.24	.25
35	10	−.009	2.154	3.90	1.68	71	8	−.026	2.167	4.29	.31
36	10	−.024	2.234	3.05	.53	72	8	−.014	2.159	4.30	.40

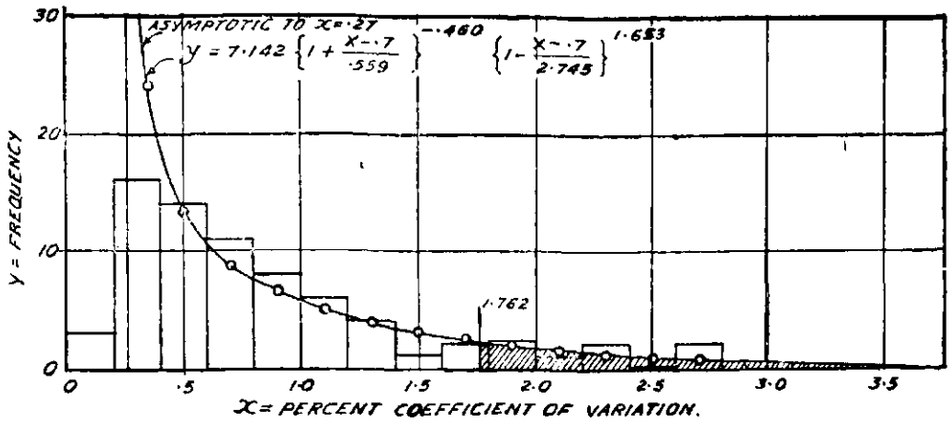

Fig 1 : Distribution of coefficients of variation.

theoretical relation between R and V may not be strictly linear at all, though only slightly differing from it. Thus, with the very fundamental form itself of the lie not fully known or defined, the least square method can be availed for fitting infinite types of expressions to the small basic data of the 8 to 10 points.

Since the whole discussion on the subject was initiated by the large values of the coefficients of variation obtaining for a uniform size of the basic data namely at between 8 and 10 points, it was thought appropriate to examine the frequencies of the different magnitudes of the 72 values. *Fig 1* accordingly presents their frequency histogram which is seen to conform to a skew type. On proceeding in accordance with the usual methods of frequency curve fittings the distribution is found to be of a Pearson Type I form with equation

$$y=7\cdot142\left(1+\frac{x-\cdot7}{\cdot559}\right)^{-\cdot460}\left(1-\frac{x-\cdot7}{2\cdot745}\right)^{1\cdot653}$$

The distribution of the frequency curve in *fig 1* shows that, for a size of the ratings data equal to about 9 points, the value of the percentage coefficient of variation about the rating expression will go up to 1.762 in about 90 *percent* of the ratings and will exceed it only in 10 *percent* or less number of times. But a variational range of ±1.762 *percent* is also considered large in velocity measurements while a $\pm.5$ *percent* would be tolerable. To achieve the desired degree of accuracy, therefore, the size of the data for deriving each calibration expression will have to be increased.

Probably a new series of experimental rating observations may have to be designed for this objective. In the mean time, an attempt is made here to derive an approximate estimate of the desired large size of N by an indirect process from the present data. The small value of a in *table 1* are utilized as a useful adjunct to lend the necessary help in this direction. For, by neglecting the a term the linear rating expression will simply reduce to

$$V=bR$$

In other words, any errors in the estimation of the regression coefficient b will be directly reflected in V. Conversely, each value of coefficients of variation of the rating expressions for V can be effectively reduced by reducing the corresponding standard errors of the b values. Without being very rigorous, the desired objective may as well be achieved alternatively by reducing the 90 *per cent* limiting value found above of 1.762 to 1 or, when necessary, to .5. For this purpose, the average value of the 72 bs and the average value of the 72 " $\bar{V}_s$ " (*ie*, $\bar{\bar{V}}$) are utilised, and the required value deduced of the N as

$$N=\frac{t^2}{\left(1-\frac{\beta}{b}\right)^2}\times\left(\frac{S_V}{b\cdot S_R}\right)^2$$

where,

t is the 90 *percent* value of the student's t distribution $=1\cdot895$, for $n-2=7$ df

b is the estimate of the population 'β' obtained by averaging all the 72 sample values of b $=2\cdot176$,

S_R denotes the average departures of R values $=1\cdot141$, and $S_V=1\cdot762\times\bar{\bar{V}}=\cdot0706$

Thus,

$$N=\frac{(1\cdot895)^2}{(\cdot01)^2}\times\left(\frac{\cdot0706}{2\cdot176\times1\cdot141}\right)^2=29$$

No doubt, 29 runs is a rather large size for the observational runs to be made for individual ratings of currentmeters. But when 72 rating expressions each derived from about 8-10 runs' data have yielded coefficients-of-variation values randomly lying between ±3 *percent*, there seems no other way of controlling the variability to within ±1 *percent* but by increasing the number of runs. But new data to the increased size as indicated or suitably moderated will definitely be useful for corroborating the nearness of the value found above of *N*. Increased size new data will incidentally prove useful for a second purpose also for examining the strict linearity of the *V*, *R* relation over the entire or limited parts of the coverage of the data. In order to ensure the consistency of the new experimental data, a precaution, if exercised, of securing at least two or more repeat observational runs with each constant velocity will be found very useful.

24.. Quality of irrigation waters

I. Indian Rivers

A SYSTEMATIC study of Indian river waters was started in the year 1955 and this is the last year of study. During the year, water samples have been collected monthly from various sites for *rivers Ganga, Gandak, Brahmaputra, Kopili, Yamuna, Chambal, Narmada, Tapi, Godavari* and *Cauvery*. The samples after filtration have been tested for conductivity, pH, sodium, potassium, calcium, magnesium, carbonate, bicarbonate, chloride etc. The results are presented in the accompanying statement.

There are four sites on the *river Ganga*, namely Hardwar, Patna, Bhagalpur and Faracca. The salt concentration is least at Hardwar. One peculiarity observed during the year is that at all sites of the *river Ganga*, the salt concentration has been highest during January or February. In other years salt concentration has been found highest in summer months. The pH was always on the alkaline side varying from 7.7 to 8.7. The predominant cation is calcium followed by magnesium. The predominant anion is bicarbonate which is generally more than 90 *percent* of total anion. The maximum sodium concentration is 26.4 *ppm* at site Faracca in April 1960 and minimum is .8 at Hardwar in July 1960. Hardness number is above 150 for samples at Patna during December to March 1960, and for sample at Bhagalpur during April 1960, in rest of the samples, hardness number is below 150. Calcium and magnesium are the predominant cations; sodium percentage is generally low, maximum being 30 *percent* at Faracca in April 1960.

Water samples of the *river Gandak* at Hajipur show that as in other years the salt concentration is quite low throughout the year. Calcium is the predominant cation and bicarbonate the main anion . Hardness number is below 150 and maximum sodium percentage is only 13.

Samples of water from Gauhati on the *river Brahmaputra* show that salt concentration is quite low as in other years. However, samples from Dibrugarh on the same river show that salt concentration during the year was higher than corresponding samples from Gauhati and also of previous years. The reason for this is under investigation. Both hardness number and sodium percentage are low.

Samples from the *river Kopili* at Garampani indicate that the water contains least soluble salts of all Indian river water samples tested.

Water samples from the *river Yamuna* at Agra show that from December to June salt concentration is very high. The highest conductivity of 1485 has been found during December 1959. Hardness number is above 200 for samples other than July, August and September. Sodium percentage is also fairly high. It is of the order of 50 for five to six months.

Water samples for the *river Chambal* show that salt concentration is fairly high during winter and summer months. However, the maximum

Date of collection.	Conductivity.	pH	Parts per Million of							Hardness No.	Sodim Percent.
			Na	*K*	*Ca*	*Mg*	*Cl*	CO_3	HCO_3		
Ganga at Hardwar											
16-11-59	195	8·4	3·3	1·8	24·9	7·2	4	...	98	93	6·8
-12-59	210	8·6	3·7	1·9	23·2	10·6	4	...	101	102	7·0
25-1-60	310	8·4	5·4	2·8	29·7	8·3	5	...	122	109	9·3
16-3-60	255	8·5	4·5	2·0	23·8	8·3	3	5	98	107	8·4
19-4-60	205	8·4	3·8	1·8	24·1	6·5	4	2	89	87	8·7
20-5-60	158	8·4	2·7	2·0	27·5	5·2	3	3	82	91	5·5
16-6-60	170	8·5	1·6	2·3	24·1	5·2	2	2	67	82	4·0
20-7-60	130	7·8	0·8	2·6	16·8	3·9	1	2	55	58	5·4
25-9-60	140	8·3	2·1	1·6	19·4	4·4	2	...	64	67	6·0
4-10-60	148	8·4	2·5	1·6	22·8	5·9	2	...	83	82	6·1
Ganga at Patna											
16-12-59	305	8·6	14·5	3·2	21·5	23·2	10	2	201	150	16·9
15-2-60	500	8·4	23·4	3·5	39·6	16·0	13	5	220	166	23·1
16-3-60	395	8·6	24·8	3·7	38·3	15·7	17	...	238	161	24·1
17-4-60	420	8·5	22·4	4·4	36·6	13·2	15	...	232	146	24·4
27-5-60	380	8·0	21·3	3·8	32·7	12·9	12	8	163	135	24·9
21-6-60	330	8·0	17·8	2·8	29·2	11·6	11	6	143	122	23·5
30-8-60	141	7·7	5·5	2·1	25·8	...	5	...	79	126	8·5
29-9-60	200	8·2	7·3	2·4	25·8	7·2	5	3	120	93	14·3
Ganga at Bhagalpur											
26-12-59	315	8·4	12·4	3·2	18·5	24·5	10	...	193	148	15·0
28-1-60	405	8·4	16·1	3·3	39·1	11·9	9	...	204	148	18·7
22-2-60	490	8·7	17·3	3·5	26·6	17·6	12	5	128	123	22·7
23-3-60	390	8·6	20·6	4·5	38·3	11·1	14	...	214	142	23·4
20-4-60	410	8·5	21·8	3 8	29·2	20·4	13	8	183	153	22·5
15-5-60	360	8·5	19·3	4·1	29·7	14·2	13	8	153	134	23·2
1-7-60	265	8·6	7·0	4·0	34·0	7·7	5	5	125	117	10·9
30-8-60	155	8·4	5·4	2·1	22·8	3·1	4	2	88	70	13·6
24-9-60	255	8·7	8·9	...	34·4	6·2	14	3	134	112	13·4
31-10-60	232	8·6	11·0	3·0	28 0	8·0	6	3	128	103	18·3
Ganga at Faracca											
5-11-59	230	8·7	10·2	2·7	29·7	7·0	9	2	140	103	17·1
11-12-59	280	8·5	11·4	3·0	28·0	14·2	9	2	168	129	15·5
20-1-60	500	8·3	12·6	4·6	37·0	10·6	10	...	180	137	16·1
20-2-60	395	8·4	15·9	3·6	36·1	13·2	11	3	186	145	18·7
20-3-60	380	8·7	17·1	3·8	36·6	10·1	13	...	198	133	21·2
14-4-60	350	8·7	26·4	4·9	34·8	9·6	14	3	201	127	30.1
25-5-60	320	8·7	14·6	4·1	31·8	11·1	10	6	146	124	19·5
20-6-60	230	8·5	7·9	3·2	26·2	5·7	5	3	110	89	15·4
23-7-60	270	8·0	9·1	3·2	35·3	6·7	3	5	140	116	14·2
16-8-60	200	8·2	7·5	3·4	25·4	5·4	6	3	98	86	15·4
28-10-60	225	8·5	9·1	3·2	28·4	8·0	5	3	131	105	15·2
Gandak at Hazipur											
26-2-60	340	8·7	7·5	3·9	18·0	13·9	7	3	122	103	13·2
21-3-60	290	8·6	6·3	3·9	32·3	6·7	8	...	134	109	10·6
27-4-60	290	8·4	4·4	3·8	30·5	7·0	8	...	122	106	7·9
17-5-60	275	8·6	4·9	3·6	33·5	7·2	6	6	165	114	8·1
-6-60	240	8·3	3·3	3·7	42·0	7·7	4	5	134	118	4·7
26-7-60	320	8·1	1·8	4·0	33·0	5·7	5	5	110	107	3·4
29-8-60	208	8·4	2·6	3·6	30·5	7·0	3	3	104	106	4·7
29-9-60	225	8·6	3·1	3·2	34·4	7·5	3	3	128	117	5·1
23-10-60	225	8·3	2·8	3·2	32·3	8·0	3	...	137	114	4·8
Brahmaputra at Dibrugarh											
22-12-59	450	8·5	21·5	...	21·1	31·7	24	...	275	185	18·6
25-1-60	390	8·3	22·0	3·0	23·2	7·7	39	...	61	90	33·5
28-2-60	265	8·4	4·4	3·1	26·7	5·7	3	...	98	90	9·2
26-4-60	500	8·3	3·3	4·0	35·3	13·7	89	...	58	145	25·0
23-5-60	465	8·3	23·9	0·9	33·1	15·2	83	3	76	147	24·5
24-6-60	435	8·3	21·8	0·8	35·7	16·0	83	2	82	156	23·2
-8-60	465	7·7	23·0	1·1	34·4	16·0	84	3	70	153	24·5
1-9-60	400	8·5	22·9	0·7	36·6	15·0	85	2	70	154	24·2
6-10-60	420	8·3	25·0	1·9	34·8	16·5	83	...	79	156	25·4

Date of collection	Conductivity.	pH	Parts per million of							Hardness Number	Sodium *percent*
			Na	*K*	*Ca*	*Mg*	*Cl*	CO_3	HCO_3		
Brahmaputra at Gauhati											
17-11-59	170	8.0	4.4	3.0	23.2	4.1	3	...	95	75	10.7
18-12-59	190	8.6	4.4	2.8	25.4	4.9	3	...	104	84	9.7
20-1-60	275	8.5	4.9	3.2	31.8	3.4	5	...	110	94	9.7
29-3-60	210	8.3	4.4	3.4	24.1	4.1	5	...	89	77	10.4
21-4-60	190	8.1	3.8	5.6	21.9	0.8	3	...	79	58	10.9
13-5-60	175	8.2	2.6	3.2	22.8	3.9	3	2	73	76	7.7
14-6-60	150	7.7	2.6	2.9	18.9	2.3	1	...	67	57	9.7
Kopili at Garampani											
5-9-59	75	7.9	1.6	1.1	8.2	1.6	3	...	37	27	10.9
5-10-59	70	7.9	0.9	1.2	10.8	0.5	3	...	37	29	6.1
6-11-59	75	8.2	1.2	0.7	10.8	1.3	2	...	40	33	6.3
5-12-59	55	8.1	2.1	1.1	8.2	0.3	2	...	28	23	16.4
6-1-60	110	7.9	2.8	1.0	10.8	1.5	2	...	46	34	14.6
6-2-60	75	8.2	2.4	1.0	5.2	3.6	3	...	28	28	14.5
6-3-60	80	8.2	2.8	1.2	7.2	1.8	3	...	37	26	18.1
6-4-60	90	8.2	2.6	1.0	15.1	...	2	...	64	38	13.4
13-5-60	90	8.0	3.0	1.3	7.7	2.1	2	...	40	28	18.0
6-6-60	75	7.9	1.2	0.7	9.9	...	2	...	31	35	8.7
5-7-60	70	7.7	0.8	0.7	10.3	2.3	2	...	40	49	3.5
5-8-60	65	7.8	0.8	0.7	15.9	0.5	2	...	37	42	3.4
4-9-60	105	8.5	1.1	0.6	17.6	2.1	3	...	76	53	4.4
4-10-60	50	7.9	1.1	0.6	6.5	1.8	2	...	31	24	9.4
Yamuna at Agra											
17-11-59	390	8.8	22.4	5.6	23.7	23.5	24	2	162	157	22.8
26-12-59	1485	9.0	140.0	9.5	84.3	50.8	314	11	223	422	41.2
22-1-60	1355	8.6	117.0	7.4	61.5	34.8	172	...	211	299	45.2
2-3-60	1160	8.6	101.7	9.0	28.4	32.5	148	3	122	207	50.3
13-4-60	1350	8.6	128.5	9.6	54.2	34.1	171	3	232	278	48.9
30-5-60	1310	8.4	144.0	14.1	47.3	37.9	168	11	214	277	51.5
11-6-60	1080	8.7	106.0	10.1	32.7	32.8	134	8	162	218	49.9
14-7-60	340	8.3	27.2	5.6	29.7	8.5	...	5	137	110	33.6
11-8-60	310	8.1	14.6	6.1	26.2	12.6	15	5	122	118	21.5
15-9-60	325	8.9	18.7	5.4	41.3	10.3	16	6	146	146	20.9
Chambal at Kota											
14-12-59	390	8.7	36.2	2.9	22.4	20.4	25	2	217	141	35.2
-1-60	690	8.8	74.8	2.8	25.8	18.6	62	6	159	143	52.5
15-2-60	495	8.6	38.7	3.4	31.4	15.7	24	5	204	146	35.9
-3-60	420	8.7	39.7	4.0	31.8	11.9	28	...	223	130	39.1
14-4-60	420	8.8	41.1	3.4	16.8	15.5	30	3	198	107	37.2
10-5-60	560	8.6	57.9	10.0	26.7	16.8	42	9	211	137	45.7
11-6-60	460	8.5	41.7	3.9	22.8	16.5	28	6	177	126	40.8
7-7-60	270	8.0	16.1	3.2	24.9	8.0	17	5	110	96	25.9
12-8-60	145	8.2	8.9	2.0	19.4	2.3	4	3	64	58	12.3
17-9-60	260	8.5	21.8	4.9	24.1	7.2	14	3	131	90	32.9
25-10-60	252	8.5	20.3	2.6	23.7	8.5	13	5	119	95	30.9
Narmada at Mortakka											
12-11-59	310	8.7	21.7	2.0	34.0	16.8	12	3	211	155	22.9
11-12-59	305	8.8	22.9	1.8	26.7	19.6	11	6	201	148	24.8
24-1-60	435	8.6	22.0	1.7	24.5	19.4	11	...	226	142	24.8
15-2-60	500	8.4	26.9	1.9	30.5	22.2	11	...	268	169	25.4
15-3-60	410	8.8	32.3	2.7	29.2	23.0	11	...	278	169	28.9
15-4-60	440	8.2	36.2	2.1	28.8	19.9	12	6	262	155	33.2
16-5-60	470	8.6	35.6	2.1	23.2	25.8	11	14	226	166	31.5
14-6-60	495	8.2	39.9	2.6	22.8	27.1	13	14	244	170	33.2
7-7-60	275	8.3	25.8	2.1	37.8	8.2	4	6	156	129	29.8
12-8-60	190	7.7	5.5	1.9	25.8	4.6	3	2	110	85	12.1
11-9-60	270	8.2	10.9	1.4	35.3	10.1	5	6	159	130	15.1
17-10-60	186	8.1	6.1	1.4	23.7	7.2	4	...	125	89	12.5

Date of collection	Conductivity	pH	Parts per million of						Hardness Number	Sodium *percent.*
			Na	*K*	*Ca*	*My*	*Cl*	CO_3	HCO_3		
Narmada at Akteshwar											
6-11-59	305	8.3	21.6	1.8	30.5	17.0	12	2	220	148	23.8
20-1-60	460	8.7	27.6	1.7	21.1	19.6	18	...	223	134	30.6
28-2-60	515	8.5	34.1	2.2	24.1	23.2	16	5	238	157	31.6
24-3-60	505	8.8	36.7	2.2	27.5	24.3	19	...	281	170	31.6
26-4-60	460	8.8	33.6	2.1	17.2	25.3	18	12	211	148	35.8
28-5-60	490	8.1	44.3	2.4	23.2	24.3	22	14	223	159	37.3
20-6-60	480	8.3	43.2	2.2	24.1	20.1	21	8	232	144	39.0
28-7-60	245	8.0	7.1	1.7	34.4	6.7	4	6	122	114	11.7
11-9-60	254	8.5	13.7	1.9	27.5	11.1	10	6	134	115	20.1
Krishna at Karikal											
12-11-59	425	8.6	40.9	2.1	29.2	13.9	46	6	98	131	40.0
15-12-59	325	8.8	39.3	1.8	25.8	5.2	25	...	137	86	49.1
7-1-60	840	8.4	77.1	2.6	34.4	20.6	88	...	186	172	49.3
22-3-60	1125	8.7	151.9	4.2	24.1	31.7	130	...	192	192	65.0
22-4-60	1090	8.6	125.0	4.3	22.4	27.6	138	2	107	171	60.6
7-5-60	1390	8.6	178.0	5.4	28.4	37.9	205	8	150	229	62.1
5-6-60	610	8.3	73.9	2.9	29.7	10.1	63	6	134	116	57.3
5-7-60	285	8.1	6.9	1.9	38.7	7.7	14	6	116	129	10.2
-8-60	135	7.8	4.7	0.9	17.2	3.1	7	2	70	56	14.9
7-9-60	150	8.3	7.5	2.4	18.9	4.4	10	2	70	66	19.2
Krishna at Nagarjunasagar Dam											
10-12-59	490	8.9	64.3	3.1	22.8	14.5	44	3	198	117	53.5
22-2-60	620	8.4	62.6	2.3	21.5	12.6	52	...	150	108	49.9
22-3-60	450	8.3	50.3	1.8	21.5	9.1	42	...	134	93	53.4
16-4-60	515	8.6	60.3	3.1	19.8	9.0	47	2	107	88	58.8
14-5-60	550	8.4	72.1	2.5	22.4	8.3	51	5	131	91	62.6
11-6-60	560	8.1	76.7	2.6	24.1	7.0	45	3	143	89	62.8
9-7-60	240	8.0	9.4	1.2	28.8	7.0	10	3	116	101	16.6
18-8-60	260	8.3	7.0	1.2	19.4	3.9	10	3	70	65	18.5
19-9-60	290	8.6	32.5	2.1	23.2	7.2	16	5	128	88	43.8
Godavari at Nanded											
9-11-59	505	8.8	66.6	3.2	28.4	18.8	33	6	220	150	43.6
9-12-59	600	8.9	73.6	3.7	30.5	22.2	38	6	250	169	47.9
30-1-60	965	8.7	104.0	4.5	26.2	24.5	58	2	259	168	56.6
24-2-60	1150	8.7	127.4	5.3	28.0	29.7	67	6	274	194	58.0
11-3-60	980	8.9	130.9	5.5	30.5	27.6	71	6	250	192	58.9
28-4-60	1400	8.8	187.0	8.0	35.7	34.3	106	8	281	233	62.5
25-6-60	320	8.6	30.8	2.4	22.4	8.5	15	6	128	92	42.7
21-7-60	290	8.4	25.1	2.9	23.2	7.2	14	6	113	88	37.3
-9-60	280	8.6	31.0	2.2	23.2	7.2	13	6	128	88	42.5
-10-60	580	8.0	79.2	5.6	33.1	12.8	37	...	250	136	54.6
Tapi at Kakrapar											
5-11-59	420	8.7	43.2	2.3	30.5	19.9	30	3	247	160	36.6
14-12-59	550	8.7	61.9	2.8	19.4	30.2	43	3	290	175	43.0
13- 1-60	770	8.7	68.9	3.1	29.2	23.7	50	...	305	172	45.9
10- 2-60	720	8.8	72.5	3.1	29.2	23.5	50	6	275	171	47.3
10- 3-60	690	8.9	81.8	3.4	11.6	25.8	62	6	250	137	55.7
12- 4-60	790	9.0	88.8	3.6	22.4	19.4	67	8	268	136	57.9
12- 5-60	820	8.6	104.0	4.3	21.9	28.1	74	21	259	170	56.2
9- 6-60	870	8.6	112.0	4.3	24.5	28.4	82	18	268	180	56.7
8- 7-60	280	8.4	23.8	2.2	23.2	7.0	14	5	131	70	36.3
11- 8-60	290	8.1	17.4	2.1	27.5	9.3	11	8	134	108	25.6
14- 9-60	310	8.9	32.0	2.7	25.4	9.3	20	5	168	102	39.7
14-10-60	270	8.1	26.9	2.2	23.2	8.3	17	...	162	95	37.5
Cauvery at Bhavani											
13-11-59	185	8.5	15.5	1.7	14.6	6.5	11	2	101	64	33.8
22-12-59	260	8.8	21.9	1.9	19.4	9.5	13	2	153	83	34.4
21- 1-60	330	8.6	22.4	1.8	20.2	5.4	15	...	156	73	39.2
19- 2-60	355	8.7	26.4	2.0	18.9	10.6	14	3	146	92	37.9
12- 3-60	320	8.7	36.4	2.4	20.6	10.3	17	3	156	97	36.6
27- 4-60	340	8.7	26.4	2.2	22.4	9.6	17	...	177	96	36.8
17- 5-60	325	8.4	29.0	2.0	22.8	11.6	15	8	150	106	36.8
10- 6-60	325	8.2	27.0	2.3	21.9	10.6	17	8	140	104	36.4
22- 7-60	145	8.1	9.4	1.9	13.3	4.6	8	2	76	53	26.9
12- 8-60	125	7.8	9.1	1.6	9.9	3.6	9	...	55	40	32.2
14- 9-60	153	8.6	10.9	1.3	14.6	4.9	8	2	73	51	23.0

concentration obtained this year is in January 1960. Hardness number is below 150 in all the samples. Sodium percentage, however, lies between 30-50 for most of the samples. Sodium percentage is above 50 for one sample.

Water samples for the *river Narmada* at Martakka and Akteshwar show that maximum salt concentration occurs during February 1960 at both the sites. Appreciable amount of calcium, sodium and magnesium is present in all the samples, though calcium is the predominant on during monsoon. The main anion is bicarbonate. Hardness number of more than 150 occurs in a number of samples. Sodium percentage is, however, always below 50.

Water samples of the *river Krishna* at Karikal and at Nagarjunasagar Dam Sites show that whereas maximum conductivity of 1390 has been obtained in May 1960 at Karikal, the maximum conductivity of only 620 has been obtained during February 1960 at Nagarjunasagar Dam Site. Hardness number is above 150 in 3 samples at Karikal. Sodium percentage is higher than 50 in a number of samples at both the sites.

The highest conductivity of 1400 has been obtained for the sample colleted in April 1960 for the *river Godavari*. Appreciable amount of sodium, calcium and magnesium is present in the samples. Both hardness number and sodium percentage are higher than 150 and 50 respectively for a number of samples.

The maximum conductivity of 870 has been obtained for a sample of water at Kakrapar on the *river Tapi*. Sodium percentage and hardness number is more than 50 and 150 respectively for a number of samples.

The maximum conductivity of 355 has been obtained for a sample at Bhavani on the *river Cauvery* during the year. Maximum hardness number is 106 and sodium percentage is 39.

II. Wells and Tube-wells

FURTHER WORK on the collection and analysis of well and tube-well waters from various states was continued. About 300 samples were collected this year and analysed for their conductivity, *pH* value, individual cations and anions. The water samples (including last year's samples) have been grouped according to ranges of individual ions, in which they fall. The groupings for different states is given in *table 1*. *Table 2* contains the classification of water samples for irrigation purposes according to conductivity and *SAR* as proposed by the staff of the *US* Salinity Laboratory in their Agriculture Handbook *No* 60 "Diagonosis and Improvement of Saline and Alkali Soils". The results are discussed below.

2. Maharashtra

It will be seen that most of the samples have sodium plus potassium and also calcium less than 150 *ppm* and magnesium less than 50 *ppm*. Carbonate plus bicarbonate content is high in majority of the samples and they contain a fair amount of sulphate. *Table 2* shows that most of the samples fall in C_2S_1 and C_3S_1 classes for irrigation. Waters falling in C_3S_1 class should be used on salt tolerant crops only.

3. Gujerat

It is seen that sodium plus potassium content of the water samples is high, most of the samples having sodium content more than 50 *ppm* and about 50 *percent* samples have sodium content more than 150 *ppm*. Calcium content is moderate, most of the samples having less than 50 *ppm*. Magnesium like calcium is low and amounts to less than 50 *ppm*. Carbonate plus bicarbonate is very high ranging from 150 *ppm* onwards. About 80 *percent* of the samples have carbonate plus bicarbonate more than 300 *ppm* and about 20 *percent* samples have more than 500 *ppm*. Chloride content is considerable, most of the samples lying in higher ranges. A fair amount of sulphate is present in most of the samples. *Table 2* shows that most of the samples fall in C_2S_1, C_3S_1 and C_3S_2 classes for irrigation. Waters falling in C_3S_1 class should be used for salt tolearnt crops and those falling in C_3S_2 class should be used on quite permeable soils and for salt tolerant crops only. About 14 *percent* of the samples are having either high salinity or high *SAR* or both and should only be used under restricted conditions.

Table 1.—Number of samples falling in various ranges for different ions as *ppm*

State	Ions	Upto 25	25-50	50-150	150-300	300-500	above 500
Maharashtra (73 samples)	Na + K	14	22	23	9	3	2
	Ca	15	36	21	1	...	—
	Mg	38	25	9	1	...	...
	CO_3 + HCO_3	...	1	4	33	29	6
	Chioride	24	23	15	8	1	2
	SO_4	51		12	7	...	3
Gujerat ... (116 samples)	Na + K	3	11			19	7
	Ca	52	47	17	...	...	...
	Mg	49	47	19	1	...	...
	CO_3 + HCO_3	...	...	1	25	67	23
	Chloride	16			14	15	9
	SO_4	82	..	.	12	...	...
Andhra ... (29 samples).	Na + K	...	8	13	8	...	...
	Ca	4	11	14	...	..	...
	Mg	12	14	3	...	..	...
	CO_3 + HCO_3	...	...	1	6	20	2
	Chloride	5	5	15	3	1	—
	SO_4	27		2	...	...	...
Madras ... (68 samples).	Na + K	2	4	48	6	1	7
	Ca	16	18	17	3	5	7
	Mg	34	11	13	7	3	...
	CO_3 + HCO_3	...	...	11	40	17	—
	Chloride	7	12	28	6	5	10
	SO_4	45			16	...	7
Bihar ... (63 samples)	Na + K	22	14	26	1	...	...
	Ca	16	32	15	...	...	...
	Mg	44	16	3	...	...	...
	CO_3 + HCO_3	—	—	3	41	19	—
	Chloride	44	13	6	...	...	...
	SO_4	54		9	...	...	...
Madhya Pardesh (9 samples)	Na + K	2	6	1	...	...	...
	Ca	...	6	3	...	...	...
	Mg	...	1	8	...	...	...
	CO_3 + HCO_3	...	...	...	6	2	1
	Chloride	4	3	2	...	...	...
	SO_4	7		1	1	...	...
(Total 358 samples).	Na + K	43	65	148	63	23	16
	Ca	103	150	87	4	5	7
	Mg	177	114	55	9	3	...
	CO_3 .. HCO_3	...	1	20	151	154	32
	Chloride	100	74	110	31	22	1
	SO_4	266		36	36	...	0

Table 2.—Classification of samples according to conductivity and SAR for different states:

Classes	Maharashtra	Gujarat	Andhra	Madras	Bihar	Madhya Pradesh
C_1S_1	3			3	1	
C_2S_1	33	23	10	27	48	8
C_2S_2	1					
C_3S_1	27	44	17	23	13	1
C_3S_2	4	28	1		1	
C_3S_3		6				
C_3S_4	1	1				
C_4S_1		4		2		
C_4S_2	2		1	2		
C_4S_3		2				
C_4S_4		5				
C_5S_1		1		1		
C_5S_2				6		
C_5S_3		1		1		
C_5S_4		3				
C_6S_1				1		
C_6S_2				1		

Notation for conductivity in micromhos/cm

C_1 = upto 250
C_2 = 250-750
C_3 = 750-2250
C_4 = 2250-4000
C_5 = 4000-6000
C_6 = above 6000

S_1, S_2, S_3, etc. are increasing sodium hazards.

4. Andhra

Individual cations in most of the samples are less than 150 *ppm*. Sodium plus potassium content for some samples is higher than 150 *ppm*. Carbonate plus bicarbonate of the samples is high, majority of the samples falling in 300-500 *ppm* range. Chloride content is moderate and sulphate content of most of the samples is on the lower range. Most of the samples fall in C_2S_1 and C_3S_1 classes for irrigation (*table 2*). Waters falling in C_3S_1 class should be used for salt tolerate crops only.

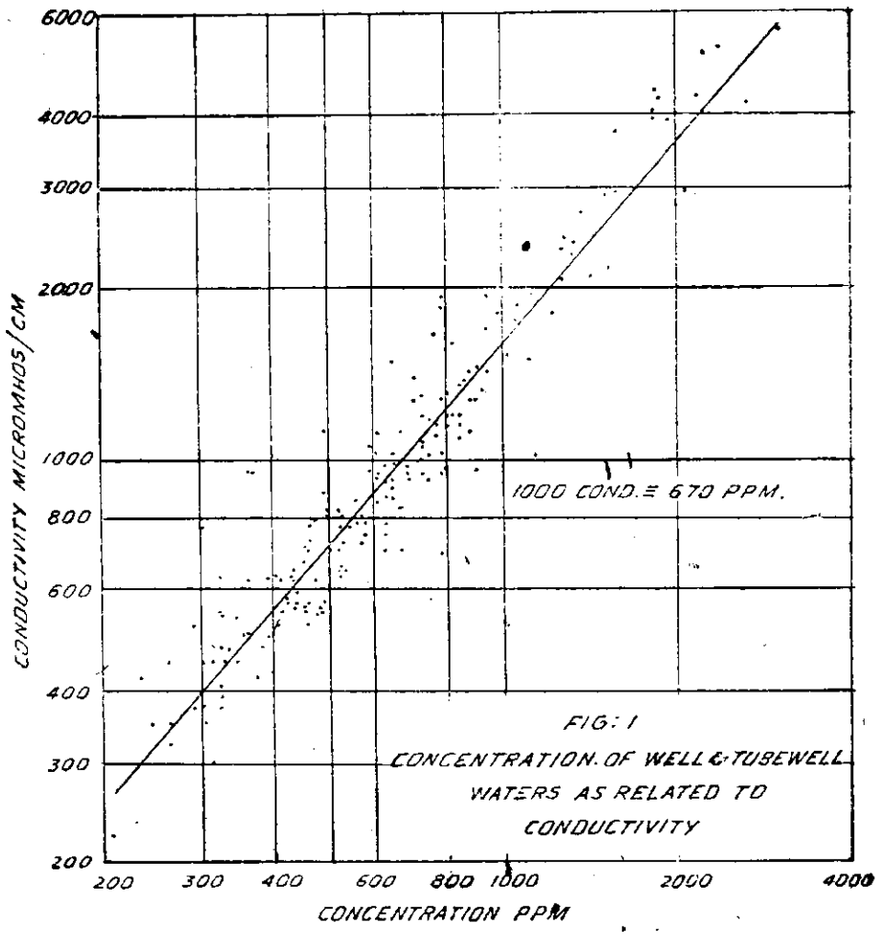

FIG: 1
CONCENTRATION OF WELL & TUBEWELL WATERS AS RELATED TO CONDUCTIVITY

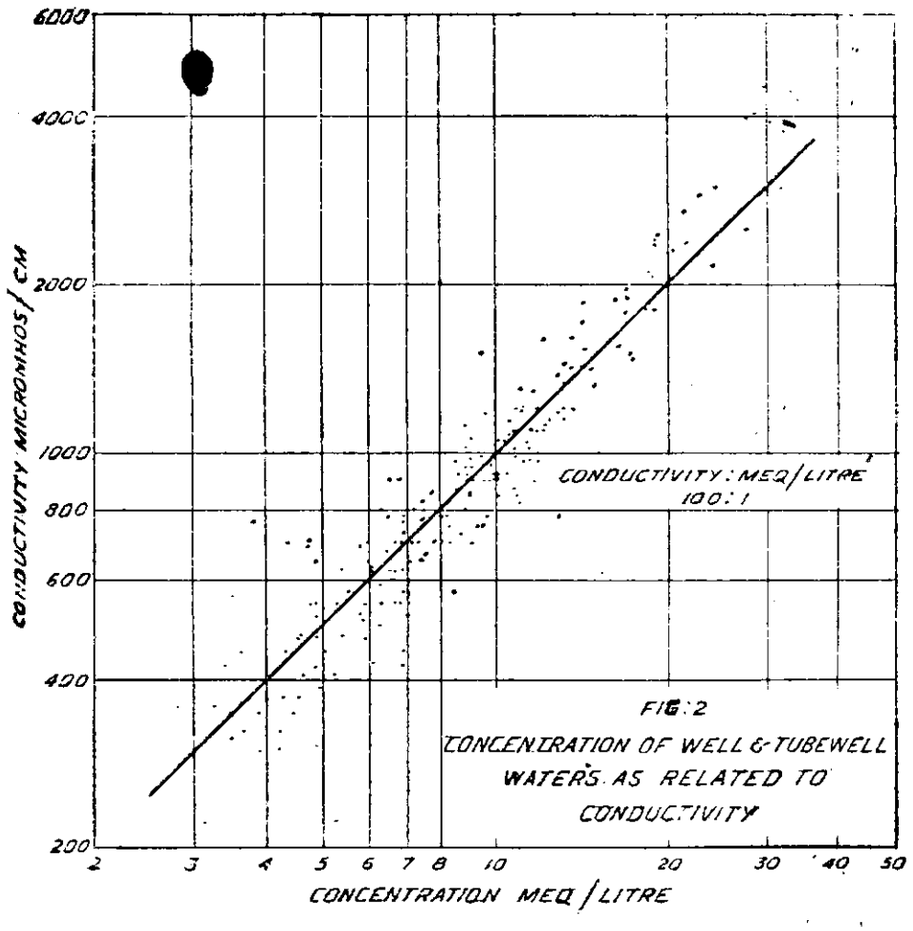

FIG: 2
CONCENTRATION OF WELL & TUBEWELL WATERS AS RELATED TO CONDUCTIVITY

5. Madras

Sodium plus potassium content of the samples is on the higher range, majority of the samples having more than 50 *ppm*. About 20 *percent* of the samples have more than 150 *ppm*. As regards calcium content, samples are well distributed in all the ranges. 50 *percent* of the samples have low magnesium content and other 50 *percent* are well distributed in all the ranges. No sample has more than 500 *ppm* of magnesium. Carbonate plus bicarbonate is high and all samples lie in 50-500 *ppm* ranges. Chloride content of majority of samples is in the higher ranges, about 15 *percent* samples have more than 500 *ppm*. Majority of the samples have low sulphate content. About 35 *percent* samples have high to very high sulphate content. About 75 *percent* of the samples fall in C_2S_1 and C_3S_1 classes of irrigation purposes. Remaining samples have either high salinity or high *SAR* or both and should be used only under restricted conditions.

6. Bihar

Sodium plus potassium content of majority of the samples is less than 150 *ppm* and so is calcium and magnesium. Carbonate plus bicarbonate is high, majority of the samples lying in 150-300 and 300-500 *ppm* ranges. Chloride and sulphate are on lower ranges. Waters fall in C_2S_1 and C_3S_1 classes for irrigation. Waters falling in C_3S_1 class should be used on salt tolerant crops.

7. Madhya Pradesh

Samples have been received only from one site and most of them contain low salts as majority of the samples fall in C_2S_1 class for irrigation. Individual cations are less than 150 *ppm* and the predominant anion is bicarbonate.

It was intended to collect about 4 samples from each well or tube-well during the year. It is only from Maharashtra, Andhra and Madras that 2nd and 3rd samples have been received from some of the sites. It has been seen from the results that the samples received from the same tube-wells during the year do not vary much. But the samples received from the same well vary considerably. Most of the samples from wells have high to very high salinity.

Figs 1 and *2* give the relation of conductivity with salt concentration expressed as *ppm* and with salt concentration expressed as *meq/litre* respectively. It is seen from *fig 2* that the ratio of conductivity to concentration as *meq/litre* is 100: 1 which agrees with the usual value accepted for this ratio. *Fig 1* shows that for these samples 1000 conductivity should be taken to mean 670 *ppm* which is slightly higher than the usual value of 640 *ppm*. Slightly higher value is due to the predominance of carbonate plus bicarbonate ions in these waters.

---

25. Development of Cuddalore port

THE HISTORY of the problem, salient features of the prototype and experiments carried out for proving the model have been described in *Annual Research Memoirs 1958*. Experiments subsequently carried out for testing various proposals for stabilising the entrance channel and maintaining adequate depths in it are discussed in this note.

2. Experiments were first carried out for finalising proposals for the first stage of development. While finalising these proposals it was borne in mind that it should be possible to evolve layout for second stage of development which would key in with the first stage without incurring any infructuous expenditure.

3. Test conditions

(*i*) Experiments with various proposals were carried out with two sets of freshet discharges (*in cfs*) *viz*

		Q Gadilam	Q Paravanar
I set	...	5,000	500
II set	...	2,000	1,000

These discharges were considered to represent the worst conditions of freshets which could be reasonably expected.

(*ii*) Following sequence of waves and discharge conditions was operated in the model.

Sl. No.	Equivalent period (months) in the prototype	Waves and discharge conditions
1	9 ...	Waves from *SSW*—no freshet
2	1 ...	Waves from *NE*—no freshets
3	1 ...	Waves from *NE*—with freshets
4	1 ...	Waves from *NE*—no freshets

Other details of model operation were the same as described previously.

4. Following three proposals (*fig 1*) were tested in the model for the first stage of development with an entrance channel dredged to 9 *ft* below *LWOST* from 9 *ft* contour in the sea to the Port office.

(i) Proposal *A*,
(ii) Proposal *B*,
(iii) Proposal *C*: evolved after a series of tests and discussions with the Port authorities and other agencies concerned.

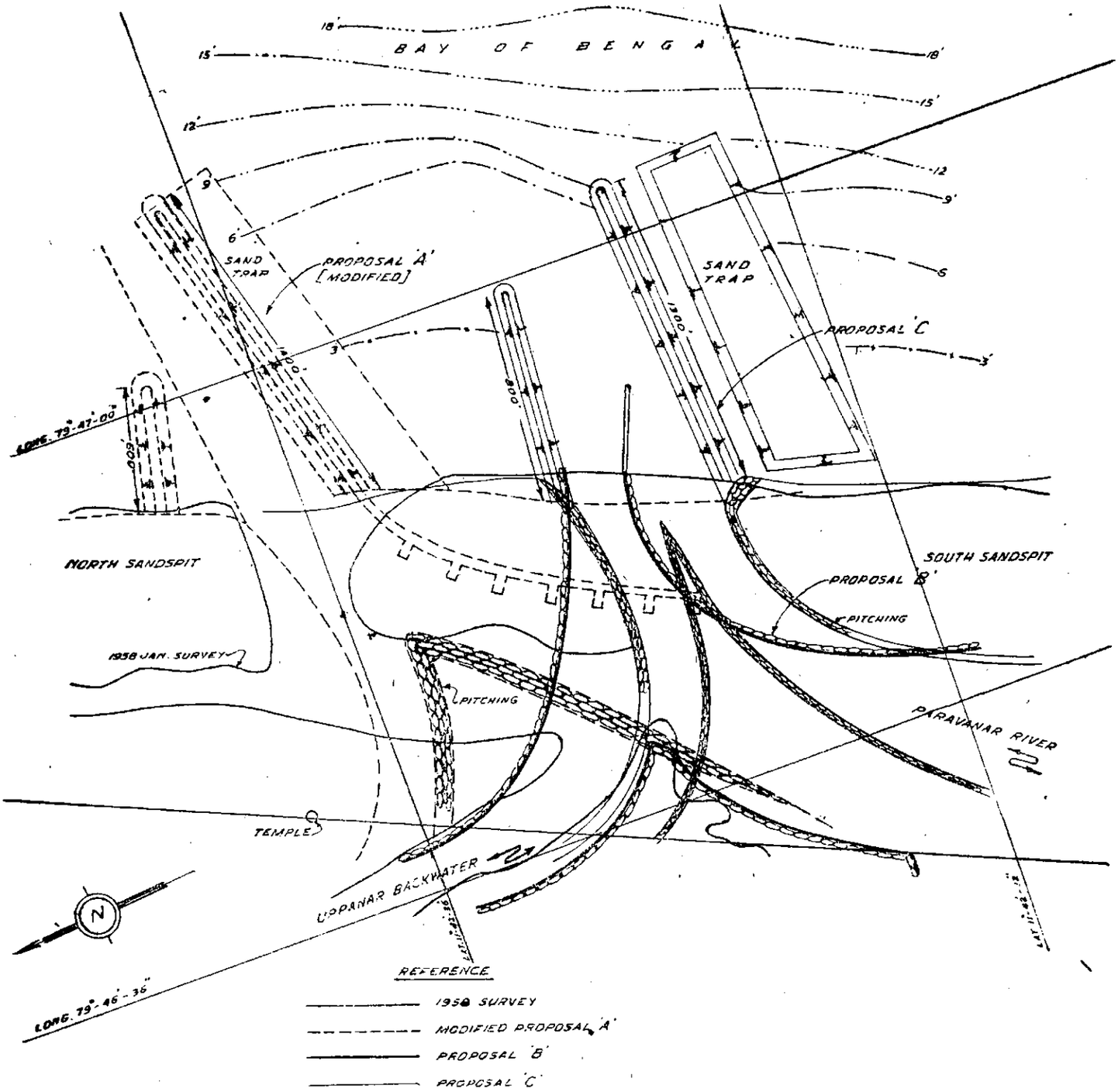

Fig 1: Plan showing the various propopsals considered.

5. Proposal *A*

Examination of observations, carried out in respect of flow pattern, velocities and bed changes in the model after laying the model to 1958 survey, revealed the following:

(*i*) The sharp curvature given to the training wall along the Uppanar channel at Gori Point appeared to cause return flow during flood tide along its left bank near Gori temple and also along the western bank immediately after its confluence.

(*ii*) Further, at the confluence, slack water region was observed and velocities dropped considerably. This was considered undesirable from the point of view of siltation.

(*iii*) Experiments conducted with both the sets of discharges and with sea side works revealed that depths in the navigation channel upto confluence of the two rivers would be maintained. There would, however, be a heavy silting in the entrance and in the navigation channel between the breakwaters. The alignment of the channel which was directly exposed to the wave disturbance during monsoon was mainly responsible for this deterioration. The material, agitated by waves was, therefore, pushed in by waves during flood tide and this could not be flushed out by the ebb tidal currents.

6. Proposal *B*

Same observations as in the case with proposal *A* were carried out. A study of these revealed the following:

(*i*) Since the Paravanar has bigger tidal absorption capacity, the flow, instead of following the straight navigation channel, was sligthtly inclined towards north and south during ebb and flood respectively. During freshets also, this tendency persisted, indicating that instead of having a straight entrance channel it would be desirable to make it slightly inclined towards north. Some return flow was also observed in the Paravanar and Uppanar channels.

(*ii*) Bed contours observed after running the model without any sea side works or operations showed that, as expected, entrance channel outside and inside the sea silted up very rapidly. The model was not, therefore, run further after an equivalent period of one year.

(*iii*) Further experiments performed with sea side works consisting of two breakwaters and a sand trap, in combination with river training works, as shown in *fig 1*, indicated considerable improvement over (*ii*) above. The improvement was, however, not as complete as desired.

The experiments with an open jetty and a sand trap for transportation of drift to the north side could not be conducted in the model due to model limitations. The merits, demerits and feasibility of such a proposal have, however, been discussed at length subsequently.

7. Proposal *C*

From the foregoing it was observed that in order not to impede navigation, the alignment of training works should be such that navigation channel would be, as far as possible, free from any return flow or eddies and that the flow should be guided very smoothly. The axis of the channel if made to coincide with predominant direction of flow, would be conducive to self maintenance of the channel. Finally, the entrance formed by breakwaters should not be unduly exposed to the disturbance from predominant waves.

(*i*) Keeping this in view, several experiments were conducted till a satisfactory layout (*fig* 1) was evolved. The flow pattern observed was very satisfactory (*photo 85*).

(*ii*) *Proposals tested in the model*: With the layout of training works thus finalised various proposals mentioned below were tested in the model for stabilising an entrance channel to sea and maintaining a 9 *ft* depth in it.

(i) An approach channel only, dredged to 9 *ft* depth below *LWOST* from the port office to 9 *ft* contour in the sea.

(ii) An approach channel, as above, with a southern breakwater 1300 *ft* in length.

(iii) An approach channel as in (i) above, with two breakwaters, one on the southern side 1300 *ft* in length and the other on the northern side 600 *ft* in length.

(iv) An approach channel as in (i) above with a southern breakwater 1300 *ft* in length and a northern breakwater 800 *ft* in length.

(v) An approach channel as in (i) above with a sand trap only.

(vi) Same as in (v) above with a southern breakwater 1300 *ft* length only.

(vii) Same as in (v) above with a southern breakwater 1300 *ft* in length and a northern breakwater 800 *ft* in length.

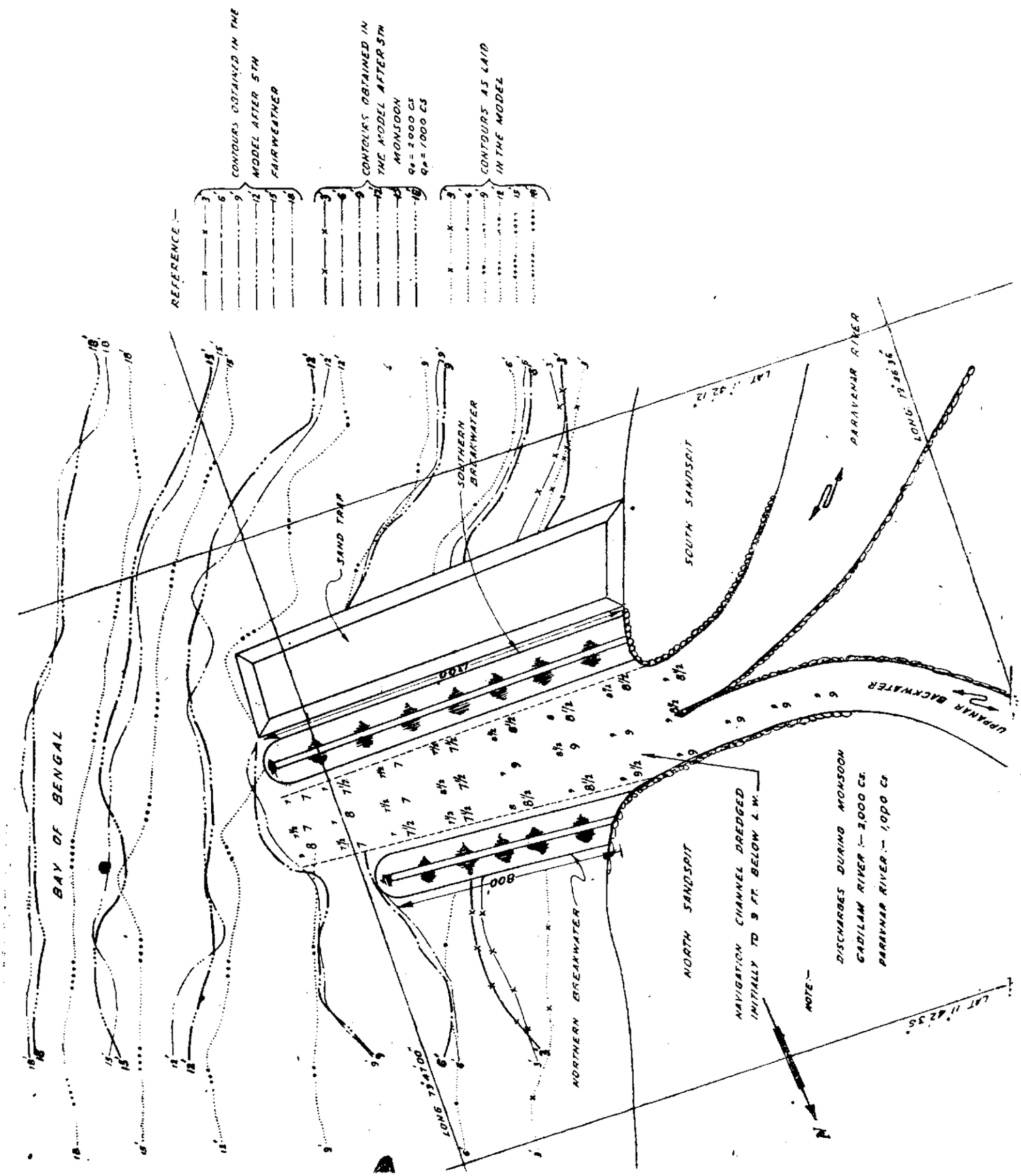

Fig 2 (i): Contours obtained in the model with proposal 'C' [I stage] for an equivalent period of five years.

Note.—Width of the Uppanar channel at — 9′ = 232′. Experiment conducted without pedio dic dredging of sand trap.

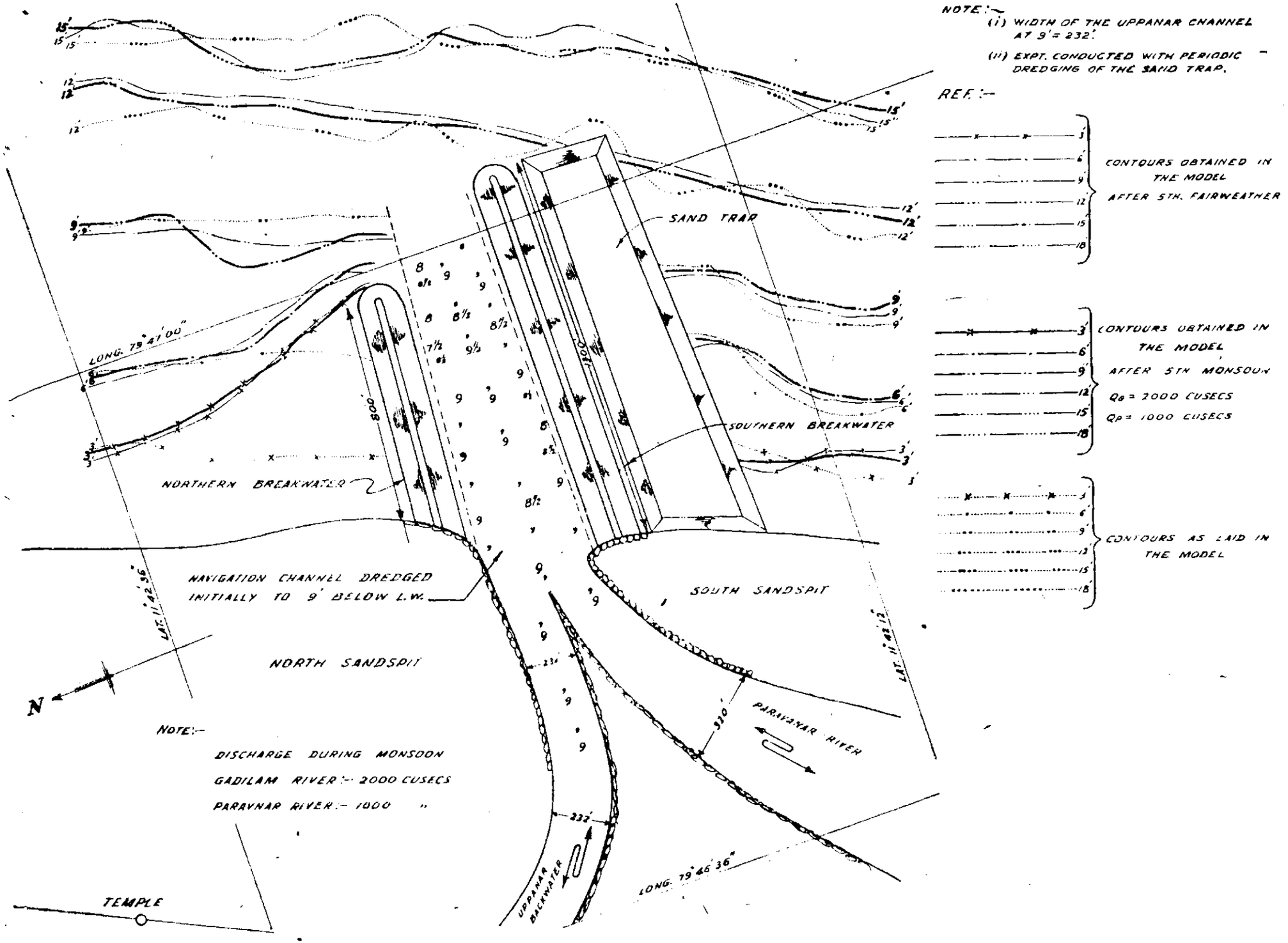

Fig 2 (ii): Contours obtained in the model with proposal 'C' (I stage) after an equivalent period of five years.

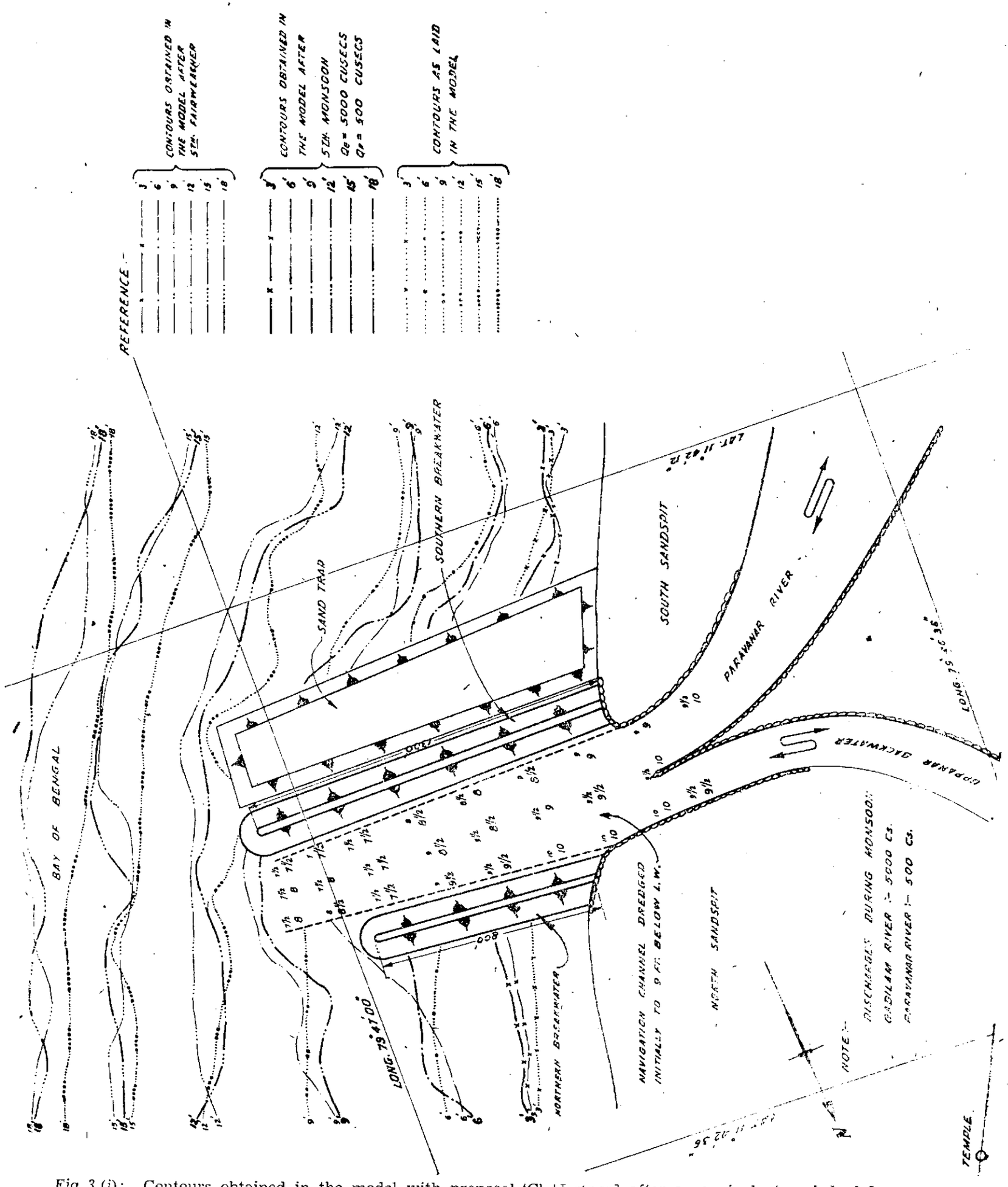

Fig 3 (i): Contours obtained in the model with proposal 'C' [I stage] after an equivalent period of five years. Width of Uppanar channel at a depth of — 9′ = 232′.

Note.—Experiment conducted without periodic dredging of the sand trap.

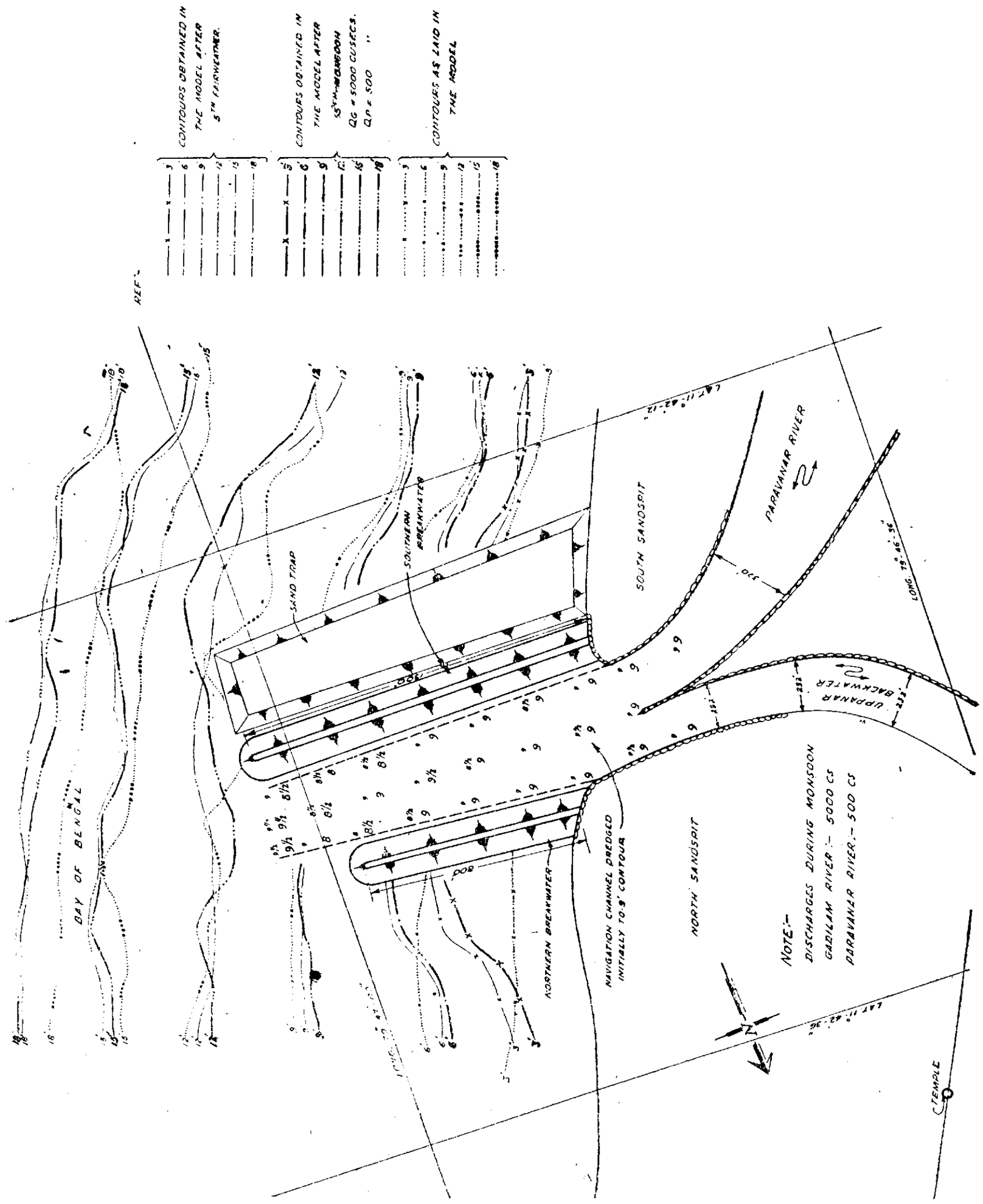

Fig 3 (ii): Contours obtained in the model with proposal 'C' [I stage] after an equivalent period of five years.
Note.— (i) Width of the Uppanar channel at — 9′ = 232′.
(ii) Experiment conducted with periodic dredging of the sand trap and nourishing the coast on the northern side.

(*a*) *Experiments and results*: All the proposals mentioned above were tested under the test conditions described in *para* 3 above. The model prior to commencement of every test was laid to 1958 survey and then run for both the fair weather and monsoon conditions.

Out of the various proposals tested, proposal (vii) *viz* an approach channel upto 9 *ft* contour and two breakwaters one on the southern side 1300 *ft* in length and the other on the northern side 800 *ft* in length with a sand trap behind the southern breakwater was found promising. Long period tests were, therefore, conducted with this layout under two sets of river discharges mentioned in *para* 3 (*ii*) above with periodic dredging of the sand trap and nourishing coast on the northern side and without any dredging for five years. The results obtained after an equivalent period of five years are presented in *figs* 2 (*i*), (*ii*) and 3 (*i*), (*ii*).

These tests showed that with periodic dredging the desired depths are likely to be maintained throughout the length of navigation channel. Dredging would also be required at the point of bifurcation of discharges between the Paravanar and the Uppanar channels, where the deterioration might be more than that in the rest of the channels. Periodic dredging at these places was, therefore, indicated. In case, no dredging was done, there might be silting at the entrance which would reduce the efficiency of the port.

This layout was, therefore, considered suitable for the development of port for maintaining 9 *ft* depths below *LWOST*.

(*iii*) Velocity observations taken in the model showed that these gradually increased from confluence of the two channels towards the sea indicating that flow of the rivers was guided properly and smoothly. Maximum surface velocities observed during monsoon (with *Q* Gadilam = 5000 *cfs* and *Q* Paravanar = 500 *cfs*) were 3.55 *ft/sec* and 1.80 *ft/sec* in the Gadilam and Paravanar rivers respectively. The velocities obtained in the model were well within the permissible range of velocities, *viz* 5 *ft/sec* for lighters and boats using this port. Hence the alignment of breakwater needed no change and could, therefore, be considered satisfactory.

(*iv*) *Wave disturbance in the area enclosed by breakwaters*: This was one of the important aspects in governing the final lengths of breakwaters and their alignments. The test was carried out by maintaining water level in the model at *HW* and waves of equivalent predominant height of 4 to 5 *ft* and 3 to 4 *ft* were generated in the model from *SSW* and *NE* directions respectively. Wave heights in the area under consideration were recorded with and without breakwaters for both the wave directions. Observations with rubble mound breakwaters showed that there was a considerable reduction in height of waves inside the area included by breakwaters. Maximum wave height was only one foot which was considered quite safe for lighters using the port. The lengths and alignment of breakwaters were, therefore, considered suitable from this aspect also.

8. Second stage of development for 17 *ft* depths below *LWOST* at entrance

The layout fianlised for 9 *ft* depths below *LWOST* was maintained and the lengths of southern and northern breakwaters were increased in steps with the channel dredged upto 17 *ft* contour. The following combinations of lengths of breakwaters were tested with a sand trap of suitable dimensions behind the southern breakwater.

S. No	Length of breakwater in *ft*	
	northern	southern
1	1150	1400
2	1400	1600
3	1500	1800
4	1500	1900
5	1700	1900

(*i*) The combination designated *No* 5 above was found to give good results.

Long period tests were conducted with two sets of discharges mentioned in *para* 3 (*i*) and with and without periodic dredging of the sand traps. Results of these tests showed that since the cross-sectional area provided was much more than the one commensurate with the tidal influx observed, the flow was very sluggish and thus might induce silting.

(*ii*) As in the first stage of development flow pattern in the navigation channel between the breakwaters and through the Uppanar channel was observed to be very satisfactory.

(*iii*) Though, in general, velocities were much less, the flow was observed to have been guided

smoothly and nowhere a slack water region was observed.

(*iv*) Wave heights under similar conditions mentioned in *para* 7 (*iv*) were observed without and with rubble mound breakwaters. Observations showed that the area inside the breakwaters was adequately protected and the layout considered satisfactory.

9. Results and recommendations

(*i*) Taking first the proposal *A*, it will be seen that slight return flow was observed in the navigation channel for some period during flood tide. Next the curvature given to the navigation channel was sharp which was an undesirable feature for further development of the port for bringing in coasters. The flow at the confluence of two rivers was also observed to be slack which was not favourable for maintaining depths. Further due to the alignment of breakwaters and the navigation channel facing the north-east direction, too much of wave disturbance was felt inside the channel, resulting in deterioration of depths. The proposal *A* could not, therefore, be considered suitable.

(*ii*) As regards proposal *B* with breakwaters, it would be noticed that the navigation channel was at right angles to the coast line. Experience of the Research Station which was corroborated by the model showed that a channel at right angles to the direction of predominant littoral drift was less efficient than the one inclined slightly in its direction. This inclination appeared necessary since the alignment should give more consideration to the direction of flow from the Paravanar river which had a bigger tidal influx.

The proposal of a sand pump moving over a jetty, as at Madras Port, could not be studied in the model. It had, however, inherent limitations. Firstly, the pump could not be designed for the maximum rate of littoral drift and, for economical running it had to be designed for the average rate of littoral drift. It was well known that the rate of littoral drift varied according to energy of waves and hence would obviously be different during different months (*fig 4*). Thus the pump will always have some backlog of littoral drift, which it would not handle. This quantity of littoral drift passing over the channel, would cause channel to silt up and lose depths. The proposal of a sand pump and a jetty did not, therefore, appear to be sound.

(*iii*) After taking into consideration the shortcomings of the proposals tested above, the proposal evolved by the Station shown in *figs 5* and *6* appear to be satisfactory. The flow was observed to be smooth and without any return flow, and the depths also maintained to reasonable expectations.

(*a*) The layout finalised for first stage (*fig 5*) envisaged construction of two breakwaters *viz* 1300 *ft* long on the south side and 800 *ft* long on the north side of the entrance and a sand trap of the dimensions shown in the figure provided behind the southern breakwater. A navigation

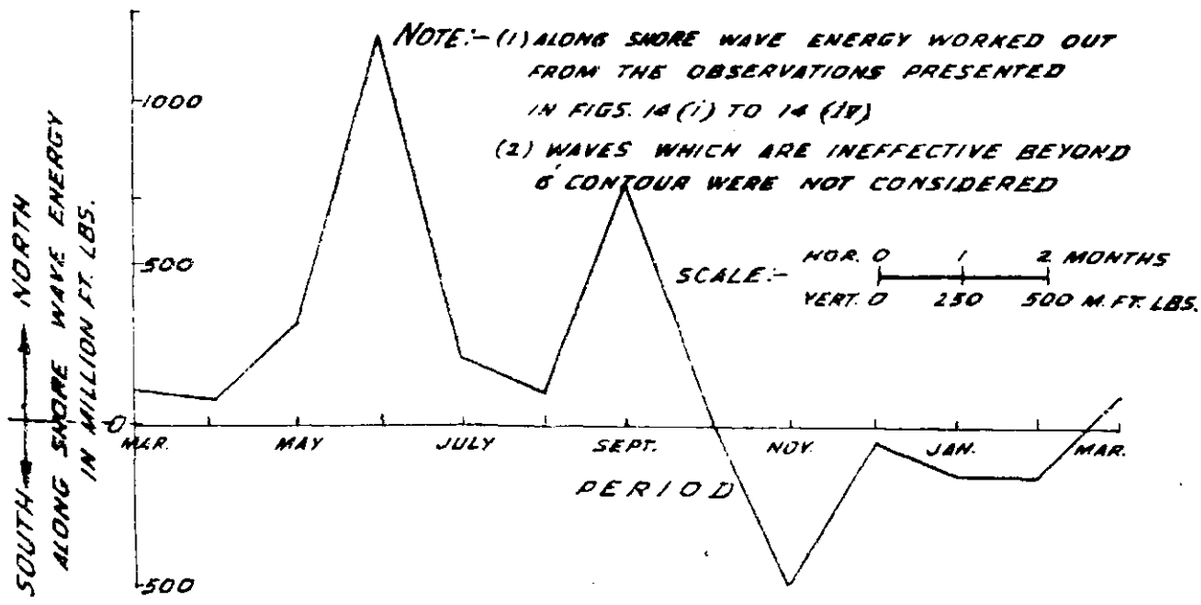

Fig 4: Graph showing the direction and magnitude of wave energy at Cuddalore.

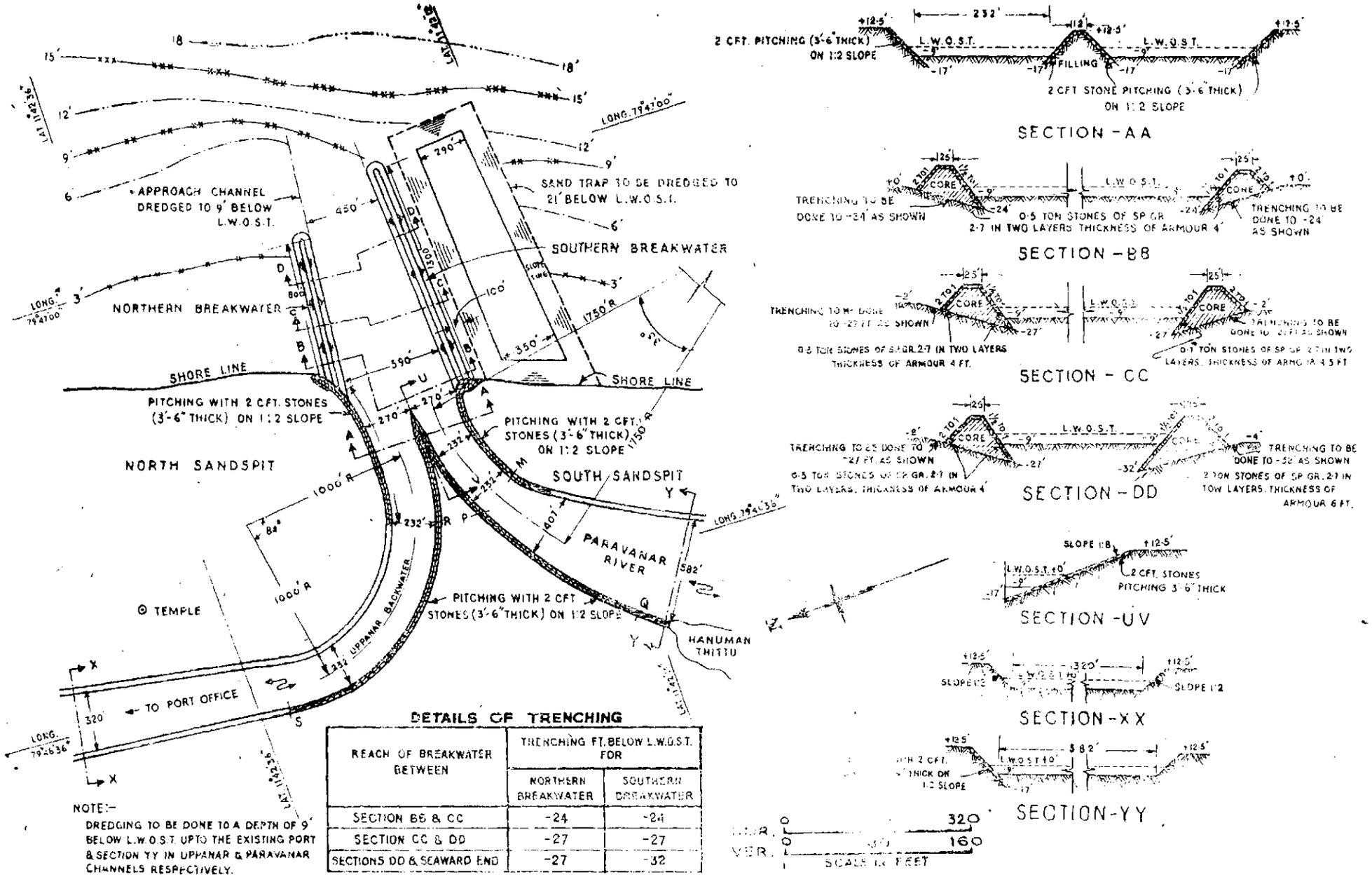

DETAILS OF TRENCHING

REACH OF BREAKWATER BETWEEN	TRENCHING FT. BELOW L.W.O.S.T. FOR	
	NORTHERN BREAKWATER	SOUTHERN BREAKWATER
SECTION BB & CC	-24	-24
SECTION CC & DD	-27	-27
SECTIONS DD & SEAWARD END	-27	-32

Fig 5: Layout of first stage of development.

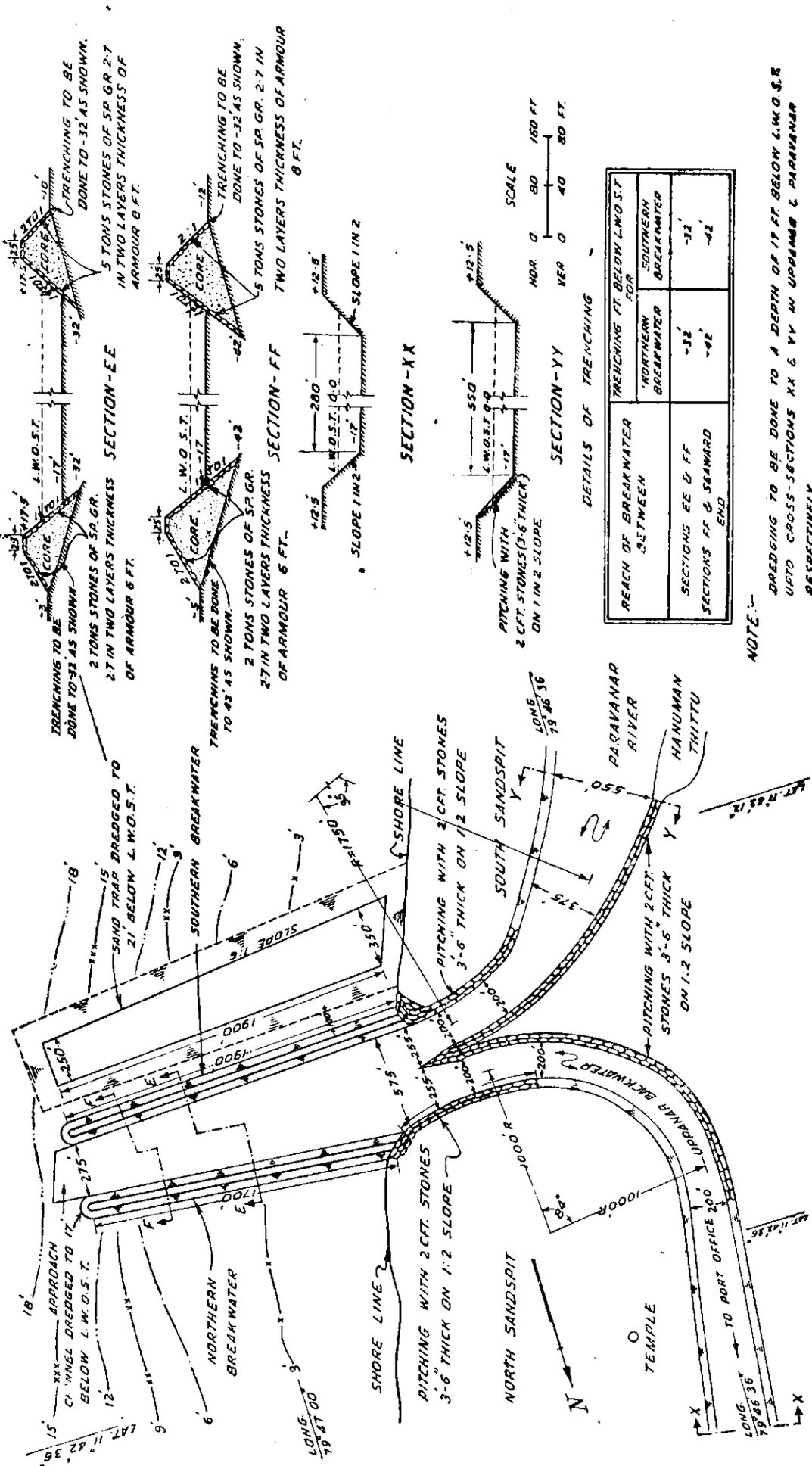

REACH OF BREAKWATER BETWEEN	TRENCHING FT. BELOW L.W.O.S.T. FOR	
	NORTHERN BREAKWATER	SOUTHERN BREAKWATER
SECTIONS EE & FF	-32'	-32'
SECTIONS FF & SEAWARD END	-42'	-42'

Fig 6: Layout of second stage of development.

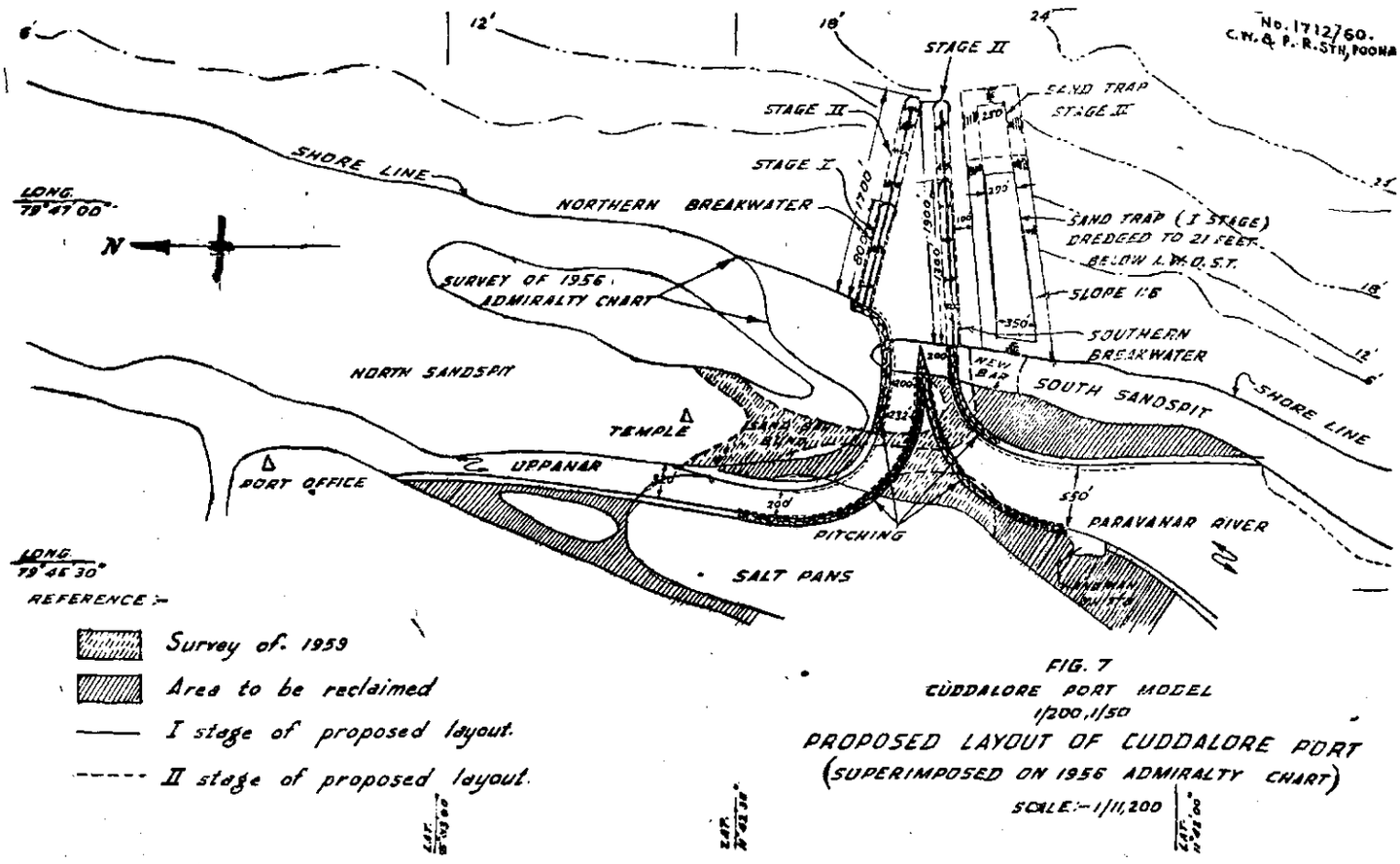

FIG. 7
CUDDALORE PORT MODEL
1/200, 1/50

channel commencing from the entrance formed by the breakwaters to the existing port on the Uppanar channel was dredged to 9 *ft* below *LWOST*. The Paravanar river was also dredged to this depth upto the place known as Hanuman Thittu to provide for additional berths if required in the region marked *PQ*.

(*b*) *Fig* 7 shows the same layout superimposed on the 1956 admiralty chart. It will be seen from this figure that the channel on the western side of the Hanuman Thittu would be required to be closed. Similar reclamations as shown in this figure would also have to be carried out for training the Uppanar.

(*c*) Though dredging was carried out upto the existing port, it was suggested that the port might now be shifted to anywhere along the reach marked *RS* in *fig* 5. This would reduce the to and fro distance appreciably from the present distance of 4.5 *miles* and thereby increase the number of trips leading to quicker turnover of the cargo.

(*d*) It was suggested that breakwaters of first stage might not be extended in the beginning of the second stage of development. Instead, only the sand trap upto 17 *ft* depth should be provided and periodic dredging carried out in the sand trap. Extensions of the breakwaters should be decided after watching conditions in regard to silting of the entrance in the prototype.

26. Development of Kelva-Mahim Fishing Port

Protection of coast against erosion

THE FISHING PORT at Kelva located at the mouth of the Mahim creek, is about 7 *miles* south of Satpati fishing port and 55 *miles* north of Bombay. It is served by a road from Palghar station on the Western Railway (*fig 1*).

The port caters for the needs of Kelva and Mahim villages, the population of which is about 8,000. This was a small flourishing port till about 1920, when vessels of draft 6 to 8 *ft* could enter even at low stages of the tide. Due to certain reasons, discussed subsequently in the note, the Mahim Creek started deteriorating and shifting its course. It was eventually lost to the fishermen as a navigation channel and the port was gradually getting out of use. As a result, severe erosion of the coast near Dadarpada devastating the rich fertile land occurred.

2. Problem

The course of the creek, as reported to have existed sometime back, is shown as an inset in *fig 2*. This creek started deteriorating and meandering probably due to obstruction to the natural waterway caused by the bridge connecting Kelva and Mahim villages across the channel. Another probable reason may be construction of an earthen bund across the creek to bring about 600 *acres* of land, affected by saline water, under cultivation. This bund cut off one of the tidal compartments (*viz D* in *fig 2*) of the creek. Progressive deterioration and consequent meandering of the creek damaged rich paddy fields and coconut gardens of Dadarpada area near Kelva village (*fig 2*). Considerable silting and shifting of the mouth was also observed as a result of which even small fishing boats could not use the port safely.

Besides, if the erosion along the coast near Dadarpada continued, safety of the village itself would be endangered. The groynes and a sea wall over a length of 1200 *ft* constructed by the Bombay State *PWD*, were severely damaged during June-July 1957 due to heavy action of waves on the coast.

3. Terms of reference

The model tests were required to be carried out :—

(i) To find the alignment of a new cut for the creek providing adequate depths for navigation of fishing boats and assessing the necessity of removing the salt water barrier and increasing the waterway of the bridge, and

(ii) To evolve suitable measures to arrest coastal erosion.

4. Available data

(*i*) *Hydrographic survey* : Hydrographic survey of the creek and the sea portion upto 26 *ft* contour carried out in 1957 showed that the seaward bed of the creek was 4 *ft* above *LWOST* while at the bridge it was 6 *ft* above *LWOST*. Thus the average slope of the creek below the bridge worked out to 2 *ft per mile*. The average width of the creek as shown on the plan, was about 100 to 120 *ft*.

(*ii*) *Cross-sections of the foreshore* : *Fig 3* shows 1957 and 1959 *HW* lines in the reach under erosion. The *HW* line receded along the entire length marked between *X* and *Y*. The groynes and sea wall constructed in 1957 did not, therefore, appear to have afforded any protection to the foreshore. The creek also shifted towards the shore in some reach.

The foreshore at this place appeared to be steep as compared to other stable foreshores. The slope between +17 and +10 contours varied between 1 in 20 to 1 in 50. The waves might, therefore, be approaching very close to the foreshore during high water, and carry away the material while breaking, thus receding the *HWOST* line.

The erosion, as one would expect for obvious reasons, had been maximum during monsoon. The material dislodged by the waves was carried away by the ebb tidal currents of the creek which was occupying a position very close to the foreshore.

(*iii*) *Tidal data* : Maximum tidal ranges observed during the period 30th November 1957 to 18th December 1957 for which observations were carried out, were 7 and 14.05 *ft* at the bridge and towards the sea *ie* at tidal stations *Nos* 1 and 3 respectively shown in *fig 2*. Analysis of these observations showed that tide with 8 to 10 *ft* range at the seaward tidal station had higher frequency during the period of observations; and the ebbing period was in general more than flooding period by about one hour. This could

L—S 3401—23-a

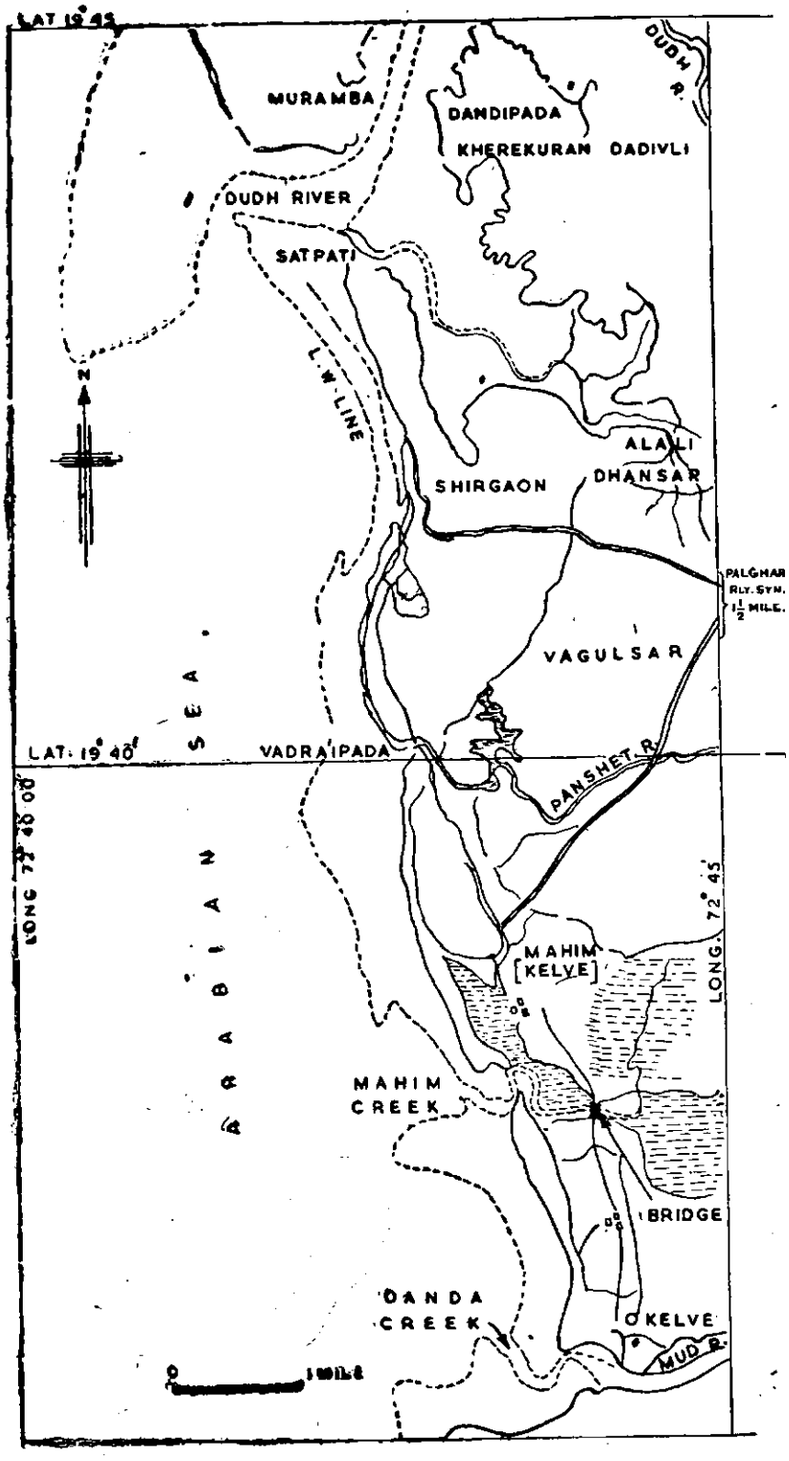

Fig 1 : Index plan showing location of Kelva-Mahim.

also be considered one of the causes for deterioration of depths in the creek. The mean spring and neap tidal ranges were, however, reported to be 17 *ft* and 10 *ft* respectively, the *HWOST* being shown on the hydrographic survey chart as +17.

Analysis of tidal observations carried out at two stations east and west of the Kelva-Mahim bridge, showed no afflux at the bridge.

(*iv*) *Influx* : Influx worked out for a mean spring tidal range of 17 *ft* for the different com-

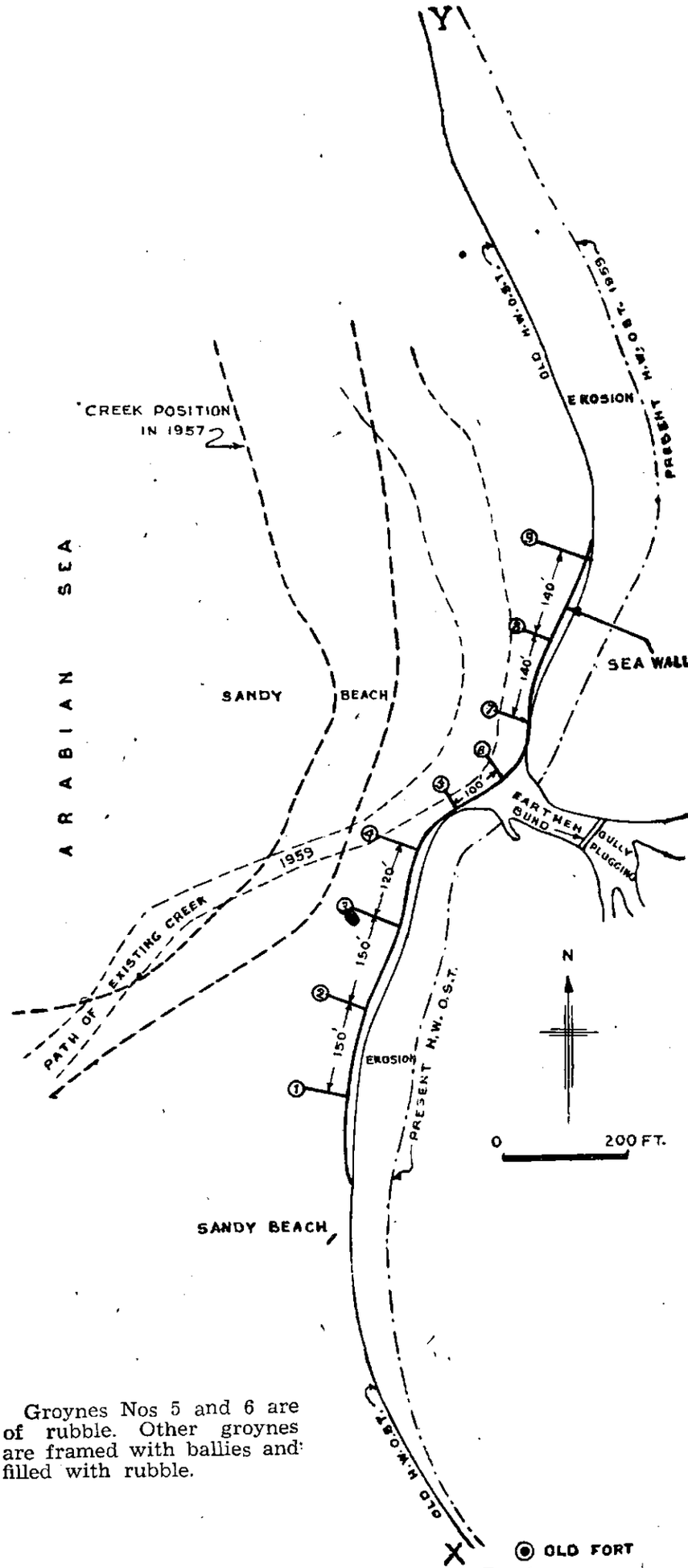

Groynes Nos 5 and 6 are of rubble. Other groynes are framed with ballies and filled with rubble.

Fig 3: Groynes and seawall constructed by Bombay *PWD* in 1957.

partments *A*, *B*, *C* and *D* above *M-N*, shown in *fig 2*, are given below:

Compt. *No*	Influx in *million ft*^{3}	Percentage of tidal influx
A	20.66	17.1
B	18.16	15.0
C	28.24	23.5
D	49.75	44.4
Total	116.81	100.0

Total influx with and without the volume absorbed by the compartment marked *D* is 2675 and 1540 *acre ft* respectively.

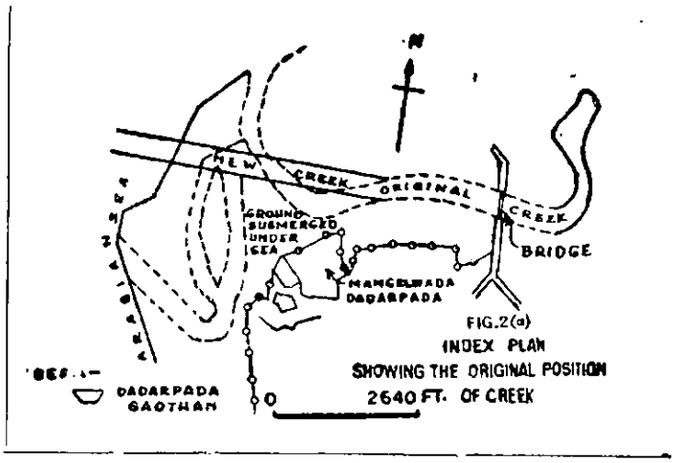

FIG.2(a)
INDEX PLAN
SHOWING THE ORIGINAL POSITION

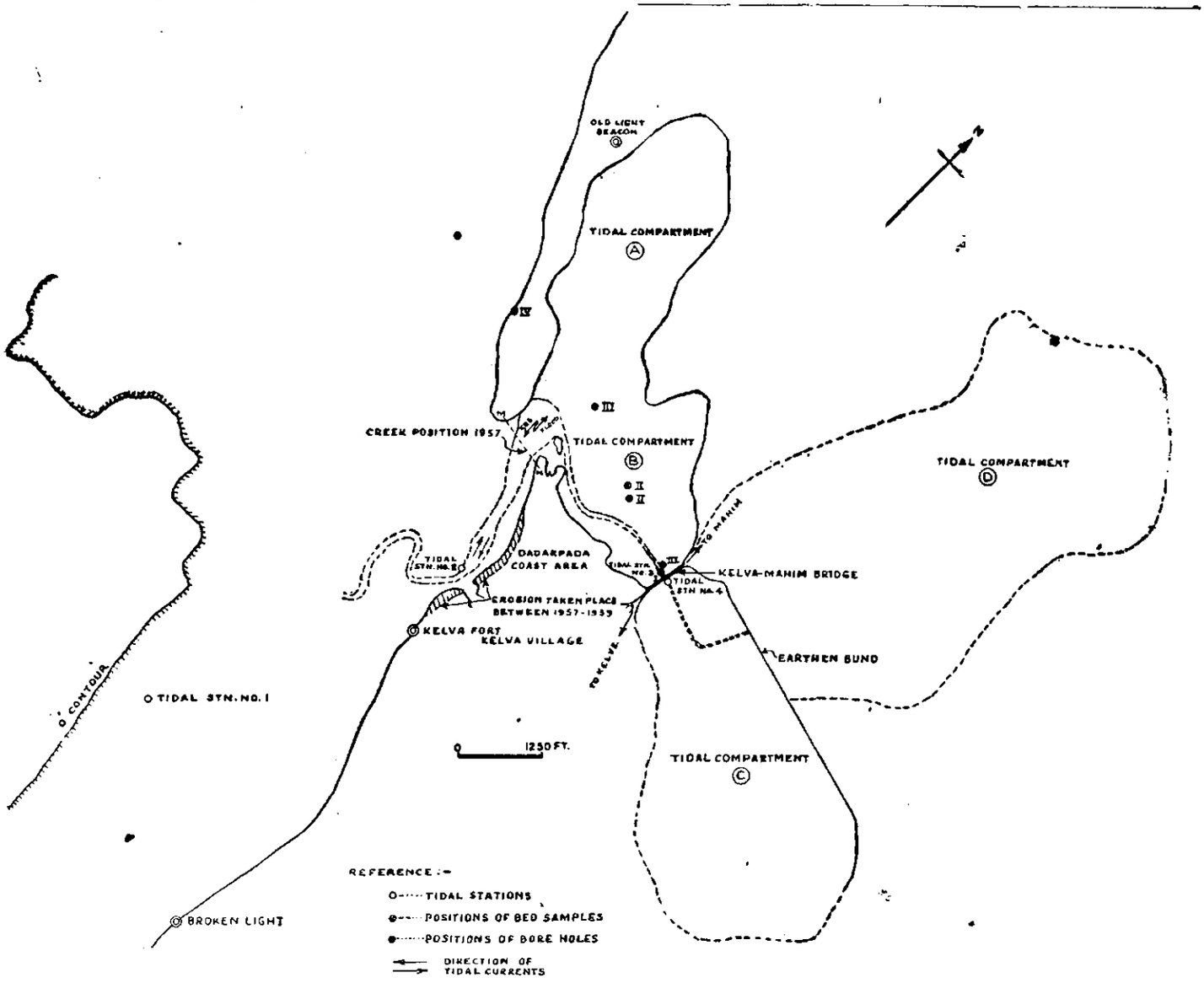

Fig 2: Plan showing tidal stations, positions of bore holes, bed samples and erosion along the shore at Kelva-Mahim.

From the above, it would be seen that 44 *percent* of the influx had been cut off by the bund.

(*v*) *Wave data* : Wave data in the vicinity of this place was made use of to arrive at the predominant wave height and wave direction. The analysis of these data showed that the predominant direction of waves was from west to southwest, predominant wave heights ranging between 3 to 6 *ft*.

(*vi*) *Bore-hole data* : Bore holes were taken at four places shown in *fig 2*, along the alignment of a new cut tentatively proposed in 1955.

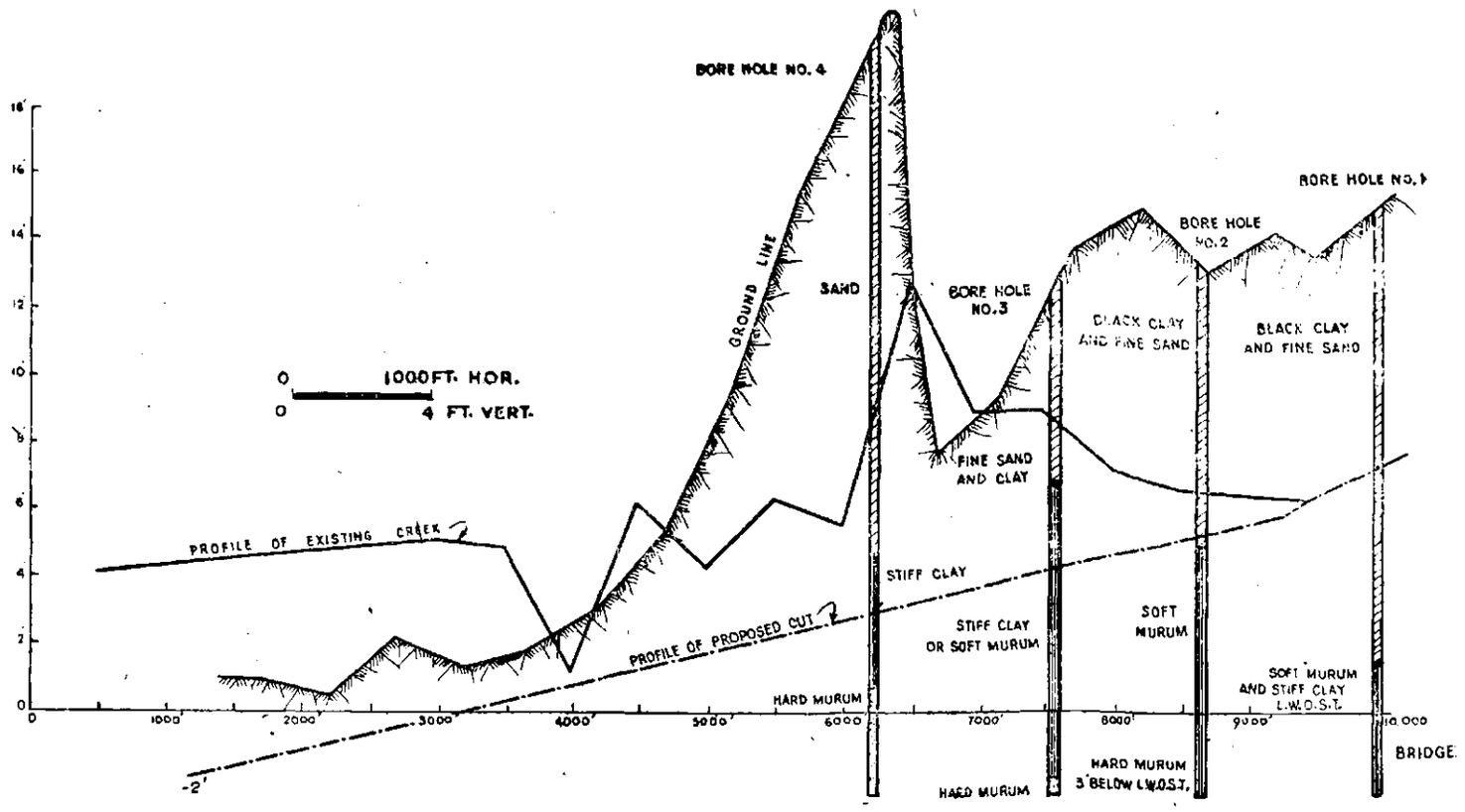

Fig 4: Plan showing profiles of ground, existing creek and proposed cut with positions of boreholes.

The strata from top to bottom consisted of fine sand and black clay and soft murum and hard murum ranging in various thicknesses, (*fig 4*).

(*vii*) *Bed samples* : Some bed samples were taken at the places shown in *fig 2*. Analysis of these samples showed that mean size of sand increased from .076 *mm* in the sea portion to 2.27 *mm* near the bridge. Carbonate content also increased from 1.9 *percent* in the sea portion to 58.6 *percent*, near bore hole *No* 3. The rocky reef in the sea was of sedimentary calcareous rocks.

5. Model

The general plan of the model and its limits are shown in *fig* 5 and *photo 86*.

Various materials were tested for laying the model bed. Eventually following combination was found most suitable for proper reproduction of conditions in respect of erosion of the foreshore. The creek and sea portion was laid in Ninan sand and the foreshore was laid in powdered coal passing through 20 *mesh* sieve and retained on 40 *mesh* sieve. This gave a satisfactory movement and consequently a closer reproduction of bed and shore line changes.

The scales adopted for the model were:

Length scale:	1/250
Depth scale:	1/50
Velocity scale:	1/7.07
V. E. :	5

With the above scales, time scale worked out to 1/35.5, giving a tidal period of 22 *minutes* in the model. The vertical exaggeration was kept 5 to fulfil the requirements of simultaneous reproduction of tides and waves as well as to keep the model and prototype ratio of rugosity coefficient nearer to unity to minimise adjustments of roughness.

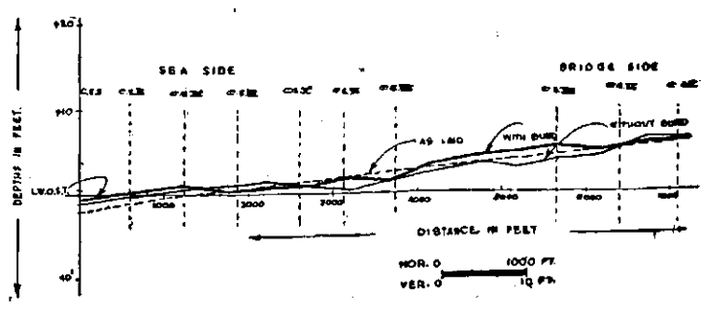

Fig 8: Longitudinal section of the cut along alignment *No* 3 [(150 *ft* width of the channel] after experiment with and without bund.

Before taking up experiments with various proposals the model was proved in respects of tides, waves and erosion of the coast.

6. Experiments and results

Various experiments conducted were divided into two series.

First series dealt with the alignment of the diversion of the creek to provide adequate depths for navigation throughout the channel. *Inter alia* an effect of diversion of the creek and removal of bund constructed for reclaiming 600 *acres* of land on coastal erosion was also studied. Second series of experiments was carried out to evolve protective measures to arrest the coastal erosion at Dadarpada.

(*i*) *Experiments for alignment of new diversion of creek* : The existing course of the creek was a very tortuous one (*fig 2*). Though seaward end of the creek was at the level of +4, the upstream reaches of the creek were very shallow particularly at the bends. The fishing crafts had, therefore, to wait for a tide to rise to transport their catch from sea to the village. In order to improve these conditions, suitable diversion of the creek which would maintain adequate depths for navigation was contemplated. After discussions with the concerned authorities, it was decided that seaward end of the cut should be kept at 2 *ft* below *LWOST* and joined to the existing levels of the creek at the bridge. The slope of the new cut worked out to 5.25 *ft per mile* approximately.

Two sections of the diversion cut suitable for the tidal influx with and without the salt water bund were tested. The bed width in these two cases was kept as 100 *ft* and 150 *ft* respectively with side slopes *1 V* to *6 H*.

The model was operated with tides only to decide upon the optimum alignment of diversion cut. The final alignment of the cut was, however, tested with both waves and tides. Observations were taken in respect of velocities and cross-sections of the creek. In all the experiments with diversion cuts existing creek was suitably closed. The various experiments conducted are described below.

(*a*) *Existing creek with and without bund*:— Removal of the bund would increase the tidal influx of the creek. In order to assess its effect on the development of the creek, this experiment was conducted. Representative cross-sections and *HWOST* near Dadarpada were observed after experiments under both the conditions *viz* with and without bund. It was seen from these observations that by removing the bund, though velocities, in general, increased no appreciable deepening of the creek took place. On the contrary, creek widened and *HWOST* line was observed to have receded towards east, *ie* Dadarpada area. Removal of the bund might thus accentuate erosion of this coast. A tendency of the creek to flow straight to the sea over the low lying area near the northern sandspit was also observed.

Velocities considerably reduced by construction of the bund must have led to the silting of the creek as well as of the surrounding area. This was also corroborated by the bore hole data shown in *fig 4*. There was a layer of sand or fine clay over the strata of soft murum and stiff clay and that sand obtained in the bore hole *No* 4 was coarser than that from other bore holes.

(*b*) The various alignments of the diversion cuts shown in *fig 6* were, therefore, next tested. Two sections of the diversion cut suitable for the tidal influx with and without the salt water bund were tested. The bed width in these two cases was kept as 100 *ft* and 150 *ft* with side slopes *1V* to *6H*.

Out of the various alignments tested in the model, alignment 3 was found to be suitable.

(*c*) *Alignment 3 with 100 ft bed width of the cut*: Experiments with this alignment were conducted with and without bund. Longitudinal section of this cut as laid and as observed after experiments is shown in *fig 7*, and cross-sectional areas along cross-sections shown in *fig 6* tabulated in *table 1*. The results showed that this alignment of the cut, with bund,

Table 1

Cross section No. (Ref. *fig* 6).	Areas of cross section in *sq ft*			% increase (+) or decrease(−) over *col* 2.	
	as laid.	After experiment.		of *col* 3.	of *col* 4.
		Without bund.	With bund.		
1	2	3	4	5	6
	Bed width of Channel = 100 ft.				
I	7100	7050	7040	− ·7	− ·85
II	6600	6850	6600	+ 3·8	0
III	6200	6490	6250	+ 4·7	+ ·8
IV	5800	5750	5900	− ·45	+ 1·73
V	5400	5160	5400	−4·45	0
VI	4400	4200	4400	−4·55	0
VII	2425	2570	2500	+ 6·0	+ 3·1
VIII	1810	1760	2440	− 6·1	+ 35·0
IX	1220	1440	1980	+18·0	+ 62·0
X	950	1530	1515	+61·0	+ 70·0
	Bed width of Channel = 150 ft.				
I	7150	6570	6410	− 8·10	−10·35
II	6650	6090	6210	− 8·42	− 6·62
III	6440	5960	5600	− 7·46	−13·00
IV	6350	5500	5470	−13·38	−13·85
V	5915	5120	5120	−13·45	−13·45
VI	5280	4820	4870	− 8·72	− 7·75
VII	3785	4350	3990	+14·92	+ 5·42
VIII	1565	2280	2575	+45·60	+64·50
IX	1365	1138	1250	−16·50	− 8·45
X	1250	1125	1240	−18·00	− ·80

Note.—Areas considered over a width of 500 *ft*. (*i.e.* 250 *ft* on either side of the centre line of cut) and below + 13.

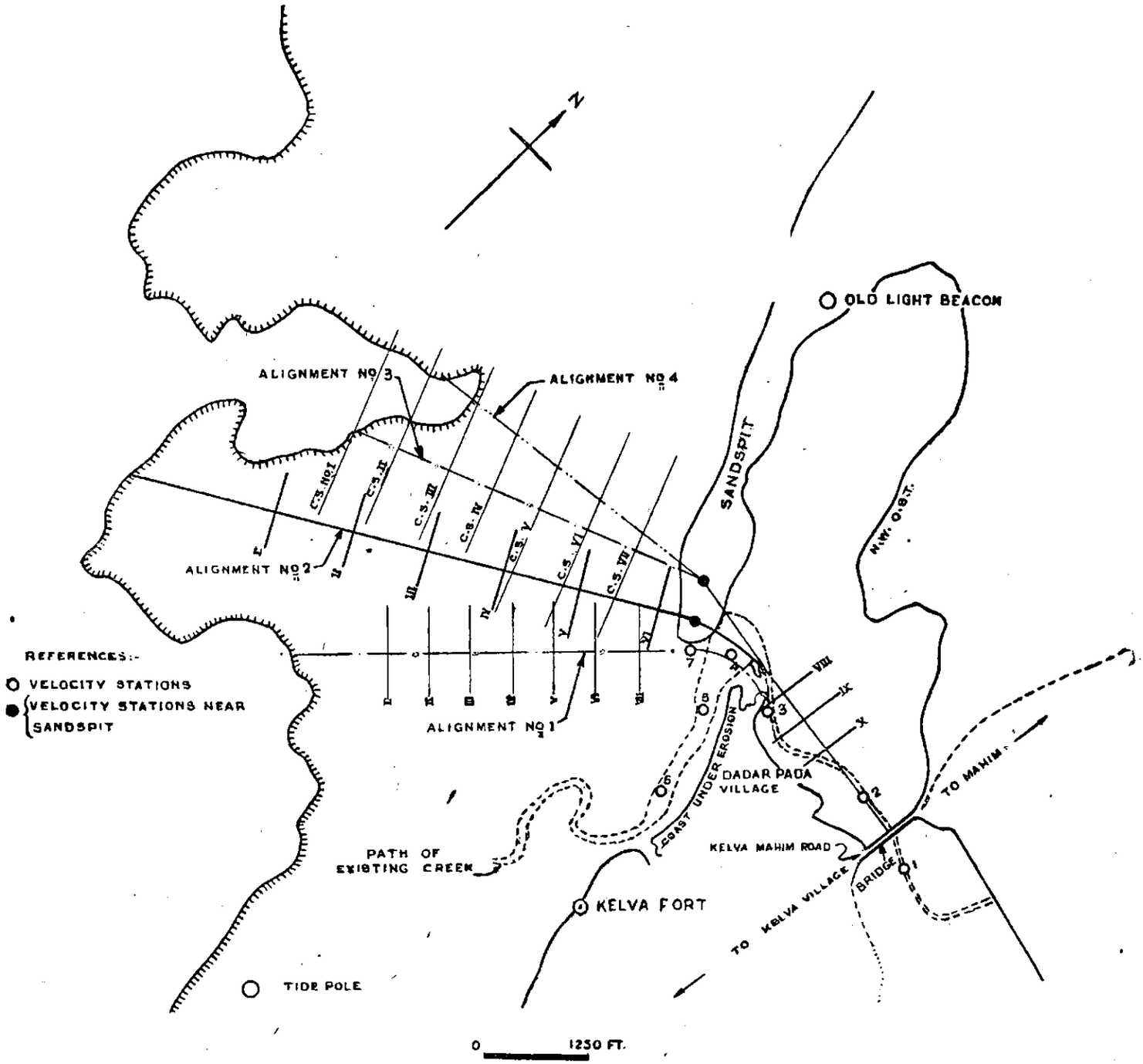

Fig 6: Plan showing the various alignments tested in the model, velocity stations and positions of cross-sections.

could maintain depths along its entire reach and was even observed to have developed in some reaches. Without bund, however, the cut showed signs of deterioration.

(*d*) *Alignment 3 with 150 ft bed width of the cut*:— As mentioned above, it was observed that alignment 3 without salt water barrier did not show any promising results with 100 *ft* bed width of the cut. This was considered to be due to insufficient cross-sectional area as compared to the influx absorbed with the removal of salt water bund.. In this experiment, therefore, more cross-sectional area was provided by increasing the bed width from 100 *ft* to 150 *ft*. The side slopes were the same as before *viz* 1*V* to 6*H*. The quantity of dredging in this case worked out to 9.16 *m ft*^{3}. The longitudinal section is plotted in *fig 8* and cross-sectional areas tabulated in *table 1* which showed that the cut deteriorated with bund, while the results without bund were not comparatively better than those with bund and 100 *ft* bed width of the cut. Besides, it would be costlier as the quantity of dredging would be more and would also require acquisition of land protected by salt water bund at present.

(*e*) *Long period tests with alignment 3*:—Before finalising the alignment 3, it was subjected to long period test. Results of this test showed that the creek would not deteriorate much and may require slight maintenance dredging.

The alignment 3 was, therefore, considered to be satisfactory.

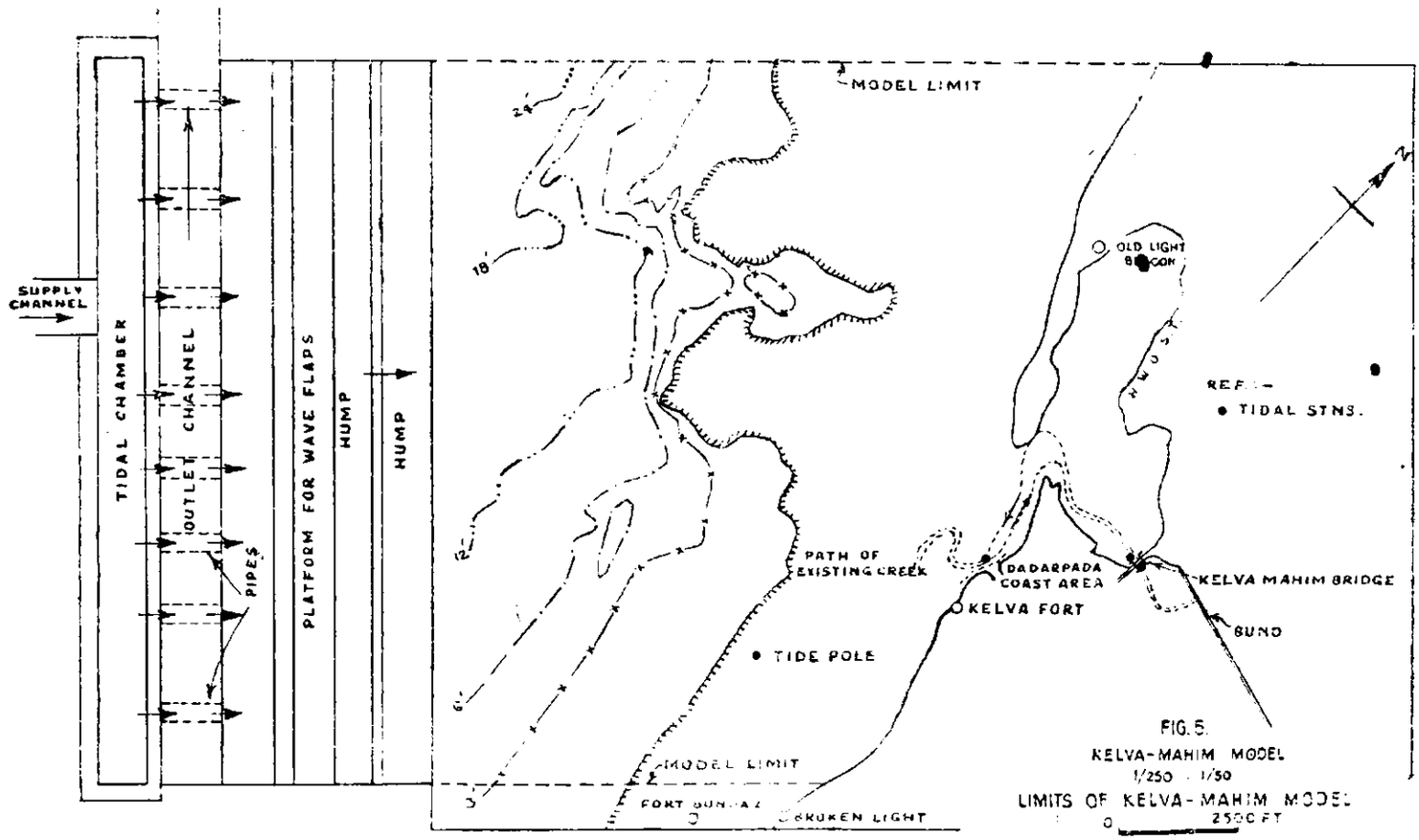

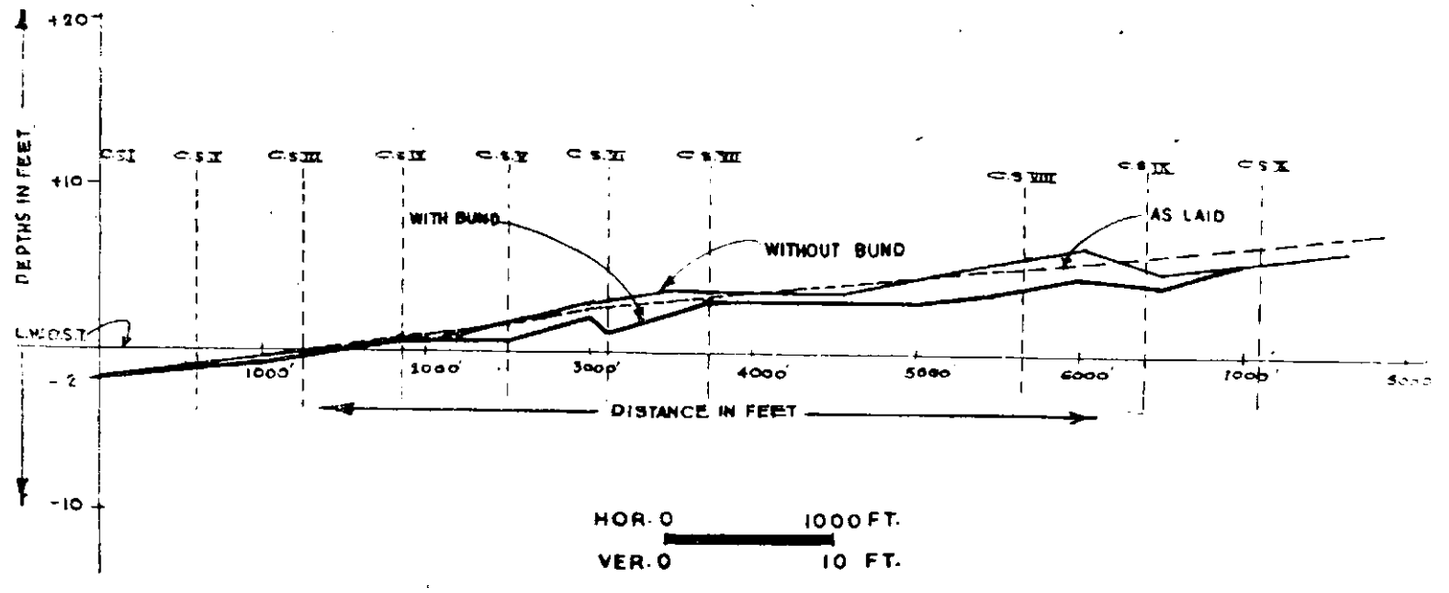

Fig 7: Longitudinal section of the cut along alignment *No* 3 after experiment with and without bund.

(*f*) *Alignment 3 as in 6 (i) (c) and model run with waves and tides*:—As mentioned in para 6 (*i*) *supra* final alignment was tested with model run with both waves and tides and the observations taken. The longitudinal section observed after the experiments, showed that some silting would take place in the creek as a result of agitation due to waves. Some periodical clearance of the channel was thus indicated.

(*ii*) *Experiments for evolving coastal protective measures* : Experiments were performed with the present alignment of the creek and the creek diverted along a suitable alignment discussed previously in para 6 (*i*)(*c*).

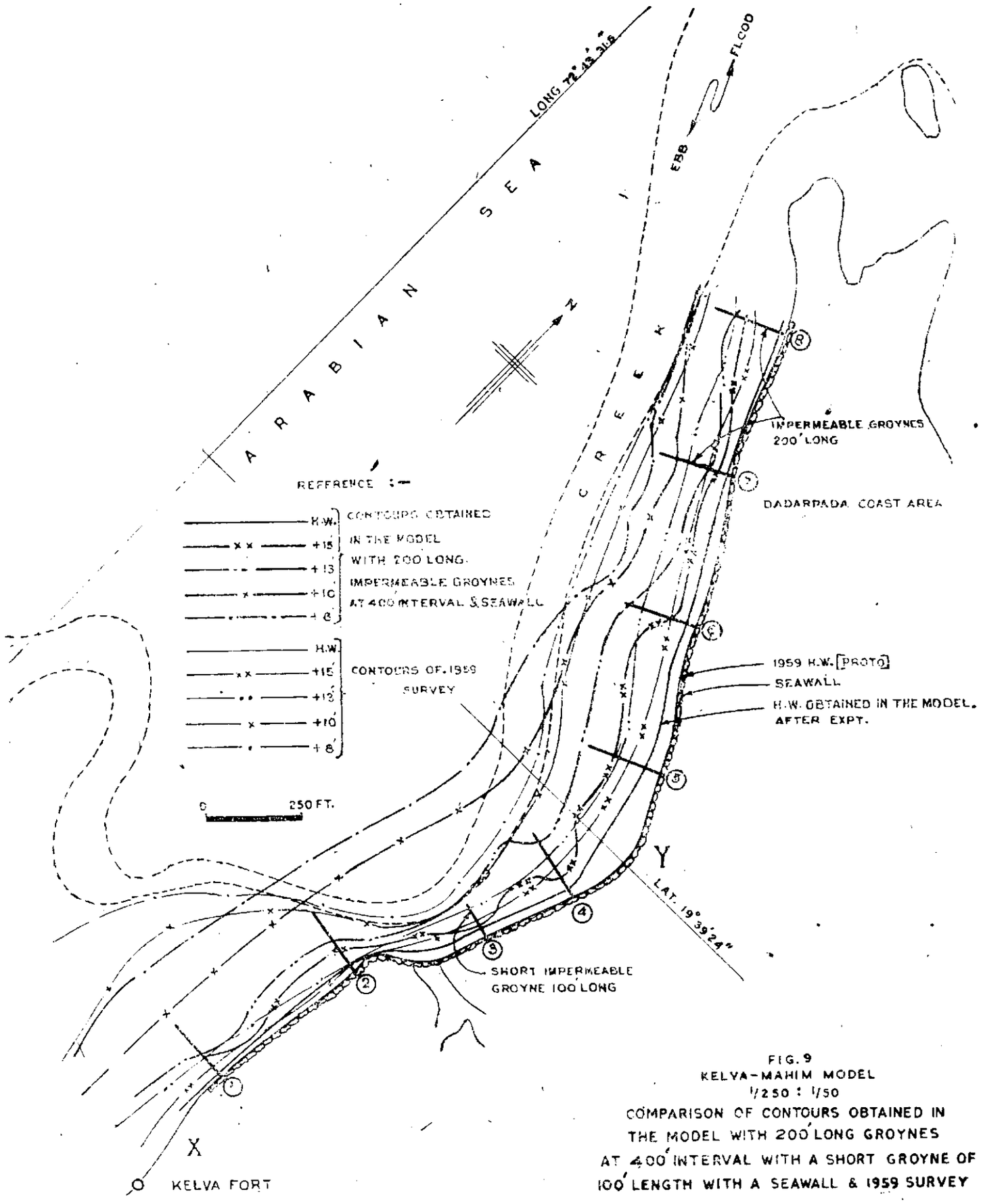

FIG. 9
KELVA-MAHIM MODEL
1/250 : 1/50
COMPARISON OF CONTOURS OBTAINED IN THE MODEL WITH 200' LONG GROYNES AT 400' INTERVAL WITH A SHORT GROYNE OF 100' LENGTH WITH A SEAWALL & 1959 SURVEY

The various protective measures tested in the model were as follows :—

(i) 9 short groynes as constructed in 1957
(ii) 100 *ft* long groynes at 300 *ft* interval
(iii) 100 *ft* long groynes, at 200 *ft* interval
(iv) 150 *ft* long groynes at 350 *ft* interval
(v) 200 *ft* long groynes at 500 *ft* interval
(vi) 200 *ft* long groynes at 400 *ft* interval with a sea wall
(vii) 200 *ft* long groynes at 400 *ft* interval without a sea wall

(viii) 250 *ft* long groynes at 500 *ft* interval with a sea wall

(ix) 200 *ft* long groynes at 400 *ft* interval with local diversion of the creek

(x) Diversion of the creek along an alignment in 6 (i) (c) above without protective works.

In all these experiments model was laid according to 1959 cross-sections along the coast, while in the rest of the portion it was laid to the 1957 hydrographic survey. Both, the tides and waves, were generated in the model .

(*a*) Out of the various proposals mentioned above, 200 *ft* long groynes at 400 *ft* interval with one short groyne 100 *ft* long with a sea wall, provided adequate protection to the coast under erosion. Results of experiments with this proposal and the groyne field are shown in *fig 9*.

(*b*) Experiments with 200 *ft* long groynes at 400 *ft* interval were further continued to see if the cost could be reduced by omitting either part or the whole length of the sea wall. Results of these experiments revealed that it was essential to have the entire length of the sea wall as shown in *fig 9*. This could probably be due to a fairly steep slope of foreshore. The foreshore continued to erode and high water line receded. Though the eroded material deposited in between the groynes at lower contours, it could not prevent outflanking of the groynes due to continued recession of the high water line.

(*c*) *200 ft long groynes at 400 ft interval with local diversion of the creek*: As mentioned in para 6(*ii*)(*a*) above, groyne 3 was kept only 100 *ft* in length to prevent blocking of the creek by a longer groyne. In order to assess the advantage that would be derived by increasing the length of this groyne also to 200 *ft* by way of additional silting in between the groynes along the coast, the creek was diverted in the region of groynes 2 to 5. Arrangement of groynes had also to be suitably altered to accommodate the longer groyne 3.

The results of these tests showed that there was no appreciable improvement.

(*d*) *Diversion of the creek along an alignment in 6(i)(c) above without protective works* : This experiment was conducted with a view to assess the effect of diversion on the extent of erosion of the coast and to see whether the protective measures could be dispensed with. Results of this experiment without protective measures showed that coastal erosion was not reduced to a considerable extent and that the action of waves was confined to a region marked *X* — *Y* in the *fig 9*. It did not, therefore, appear feasible to dispense with the protective measures.

(*e*) *Diversion of the creek as above and with 200 ft long groynes at 400 ft interval with a sea wall* : Though the diversion of the creek could not dispense with protective measures, it was thought that it would be helpful in reducing attack on the groyne-field by way of inducing more silt in between groynes along the coast since the material dislodged would not be carried away by the tidal current of the creek. This was borne out by the model, indicating that the diversion of the creek along an alignment might reduce considerably the maintenance required for protective measures.

7. Conclusions

It could be seen that the existing creek would not be suitable for navigation of fishing crafts even after the bund was removed. Removal of the bund under existing conditions might, on the contrary, accentuate erosion of the coast near Dadarpada village. By blocking the existing creek and by making a new diversion cut, erosion of the Dadarpada coast could be reduced to a certain extent but it would not completely eliminate the necessity of protective works. The maintenance of protective works would, however, be reduced.

If the navigation facilities at the Kelva-Mahim port were to be improved, it would be necessary to develop the creek along the new alignment by blocking the creek and making a new diversion cut along an alignment 3 shown in *fig 6*. Removal of the bund in this case also, would not have a distinct advantage in maintaining a wider and deeper channel.

Though initial deterioration of the creek was due to construction of the bund and the bridge it appeared that the creek had adjusted to these modified conditions. This could be inferred from the tidal observations upstream and downstream of the bridge supplied by the Bombay *PWD*. It was, therefore, not considered necessary to widen the bridge at present.

A groyne field consisting of 200 *ft* long groynes at 400 *ft* interval with one short groyne 100 *ft* long and with a sea wall, as shown in *fig 9* would be necessary to prevent coastal erosion at Dadarpada.

27. Resonance tests for coastal harbour at Paradip

AS AN ALTERNATIVE to the proposal of developing an estuarine harbour in the *river Mahanadi*, a coastal harbour 5.65 *km* (3½ *miles*) south of the *Mahanadi river* mouth was proposed by the *CWPRS* for more reasons than one. The orientation, shape and size of this coastal harbour were decided by conducting tests in a geometrically similar model. Two breakwaters, one 762 *m* (2500 *ft*) long on the north and second 1920 *m* (6300 *ft*) long on the south and east, enclosed an area equivalent to 65.2 *hectares* (161 *acres*), out of which 53 *hectares* (131 *acres*) was dredged to 12.2 *m* (40 *ft*) below *LWOST*. The harbour thus constituted an artificial harbour with vertical quay walls on the western side and sloping rubble mound breakwaters on the remaining three sides. Such artificial harbours undergo resonance due to presence of certain long period waves. Resonance is dangerous to ships moored at the berths particularly at the nodal points. They undergo excessive longitudinal and transverse movements resulting in breaking of mooring ropes and damage to the wharves or the ship itself.

2. Resonant periods and nodal points

The probable periods of resonance and the positions of nodal points were worked out theoretically for the harbour basin for its known geometry as summarised in *table 1*. These theoretical values are, however, only a rought guide and sometimes differ from the actual values because of many complicated factors such as nature and slope of reflecting surface, sudden irregularities in bed configuration and friction on the bed. A model study was therefore essential to detect probable reasonant period and places of nodal points.

3. The hydraulic model was constructed in this case to a scale of 1/150 (*GS*) and waves of periods varying from 20 to 96 *sec* were reproduced with height of .457 *m* (1½ *ft*) in the deep sea. This range of periods covers the probable dangerous periodicities for most of the ships of commercial sizes. Observations of movements of water mass in the basin were made with wooden floats of very light weight with pointers attached to them. Movements of ships were observed by actually

Table 1

	Period of resonance (in *seconds*)				Distance (*meters*) from northern to southern break waters and *SE* break water to wharf			
	Fundamental	Harmonic			Fundamental	Harmonic		
		1st	2nd	3rd		1st	2nd	3rd
Open ended basin (between entrance and southern break-water). Length $L=516$ *m*	163.	54.4	32.6	23.3	516	172	103	73.6
							310	221
								368.5
Closed ended basin (between northern and southern break-water). Length $L=755$ *m*	119.2	59.6	39.8	29.8	377	188.5	126	94
							377	283
							640	472
								659
Closed ended basin (between wharf wall and eastern part of southern break water) Length $L=972$ *m*	154.2	77.1	51.4	38.5	496	243	162	121
							486	364
							810	606
								850

berthing ship models along the wharves by elastic rubber strings simulating the characteristics of manila rope.

4. Tests conducted

(*i*) Float movements at various places in the basin and for different periods were made. *Table 2* gives float movements at the entrance for periods for which fairly large movements were obtained. It would be seen from these results that the maximum movement of the watermass was associated with a wave period of 90 *sec* and was of the order of 4.57 *m* to 6.1 *m* (15 to 20 *ft*). For other periods the movements rarely exceeded 3.66 *m* (12 *ft*). The float movements were, however, only of indicative nature and ship movements were essential for accurate information.

Table 2

Sl No	Wave period in seconds	Float movement in *meters*					
		Berth 1	Berth 2	Berth 3	Berth 4	Entrance	Turning Basin Point 5
1	42	1·33	1·33	1·79	1·41	3·62	2·29
2	44	1·33	1·71	1·71	1·33	3·85	2·67
3	66	1·27	1·33	1·33	1·33	2·09	1·33
4	75	3·44	2·29	1·56	2·29	3·01	1·705
5	84	4·57	3·24	2·09	2·6	3·24	2·09
6	86	4·18	2·47	1·91	2·63	4·2	1·91
7	88	4·76	3·05	1·91	3·2	3·44	2·48
8	90	6·1	4·18	3·24	4·76	4·95	4·76
9	92	5·07	3·24	2·67	3·44	3·66	2·86

(*ii*) Ships of different tonnages were, therefore, moored at the berths (*fig 1*) and inside the turning circle. Their vertical, longitudinal and transverse movements were observed at the bow and the stern for different periods of waves. It would be seen from the results in *table 3* that either the longitudinal or transverse movement of the ship in any case did not exceed 1.91 *m* (6.25 *ft*), although the float movement observed was of the order of 6.1 *m* (20 *ft*). Movements for 90 *sec* period were comparatively more than for any other periods.

(*iii*) For detecting the positions of nodal points, ships were moored at places where maximum float movements inside the basin were observed; and their movements recorded (*table 4*) . It would be seen that for periods of 44 and 75 *sec* the nodal points happended to be at 136 and 191 *m* (446 and 625 *ft*) respectively from the eastern breakwater

Table 3

Position of the ship at	Wave Period in *sec*	Ship movements in *meters*				Vertical
		Longitudinal		Transverse		
		Stern	Bow	Stern	Bow	
Berth 1	42	1·33	1·14	·76	·57	·57
	44	1·41	1·33	·76	·76	·57
	75	1·52	1·33	·76	·76	·38
	84	1·33	1·33	·57	·76	·57
	86	1·52	1·52	·76	·57	·57
	88	1·33	1·33	·76	·57	·57
	90	1·91	1·71	·95	1·14	·76
	92	1·28	1·41	·91	·76	·38
Berth 2	42	1·14	1·14	·76	·57	·38
	44	1·33	·95	·95	·84	·76
	75	1·33	1·33	·76	·57	·57
	84	1·14	1·14	·76	·565	·38
	86	1·14	1·14	·57	·57	·57
	88	1·14	1·14	·57	·57	·38
	90	1·64	1·52	·80	·76	·68
	92	1·52	1·33	·46	·38	·38
Berth 3	42	1·14	1·14	·57	·57	·38
	44	·95	1·14	·95	·99	·76
	75	1·33	1·33	·76	·76	·57
	84	1·33	1·14	·76	·57	·38
	86	1·14	1·14	·57	·76	·57
	88	1·33	1·14	·76	·57	·37
	90	1·71	1·52	1·29	·91	·57
	92	1·14	·99	4·18	·38	·38
Berth 4	42	1·33	1·14	·76	·57	·38
	44	·95	·95	·95	1·14	·57
	75	1·33	1·33	·57	·57	·38
	84	1·33	1·14	·76	·57	·57
	86	1·33	1·33	·76	·57	·57
	88	1·33	1·14	·76	·57	·57
	90	1·52	1·71	1·22	1·29	·57
	92	1·38	1·33	·53	·57	·38
Turning basin point 5.	42	1·71	1·52	·95	·57	·38
	44	1·71	1·71	1·03	1·03	·57
	75	1·33	1·14	1·14	1·03	·46
	84	1·52	1·33	·95	·76	·38
	86	1·71	1·52	·95	·76	·46
	88	1·52	1·52	·95	·72	·57
	90	2·02	1·91	1·30	1·07	·57
	92	1·64	1·60	·76	·76	·38

Note: Details of Ship: Displacement ... 4970 *m ton*
Length ... 145 *m*
Beam ... 19·1 *m*

(positions *A* and *B* on *fig 2*) for which the maximum movements observed were of the order of 2.06 and 1.68 *m* (6.75 and 5.3 *ft*) respectively. For a period of 90 *sec*, however, the movements were much larger and were of the order of 2.21 *m* (7.25 *ft*) longitudinal and 4.9 *m* (16.1 *ft*) transverse at a distance of 318 *m* (1041 *ft*) (Position *C* on *fig 2*). Transverse movements of this order specially are dangerous and remedial measures were considered necessary.

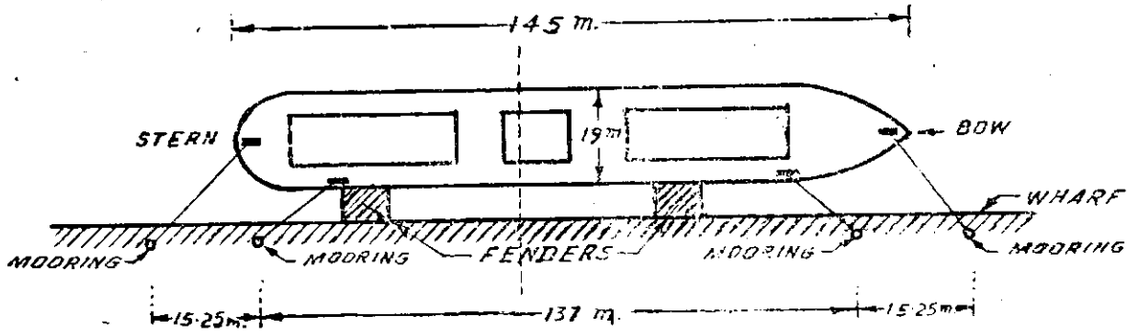

Fig 1: General arrangement of berthing for study of ship movement in the model.

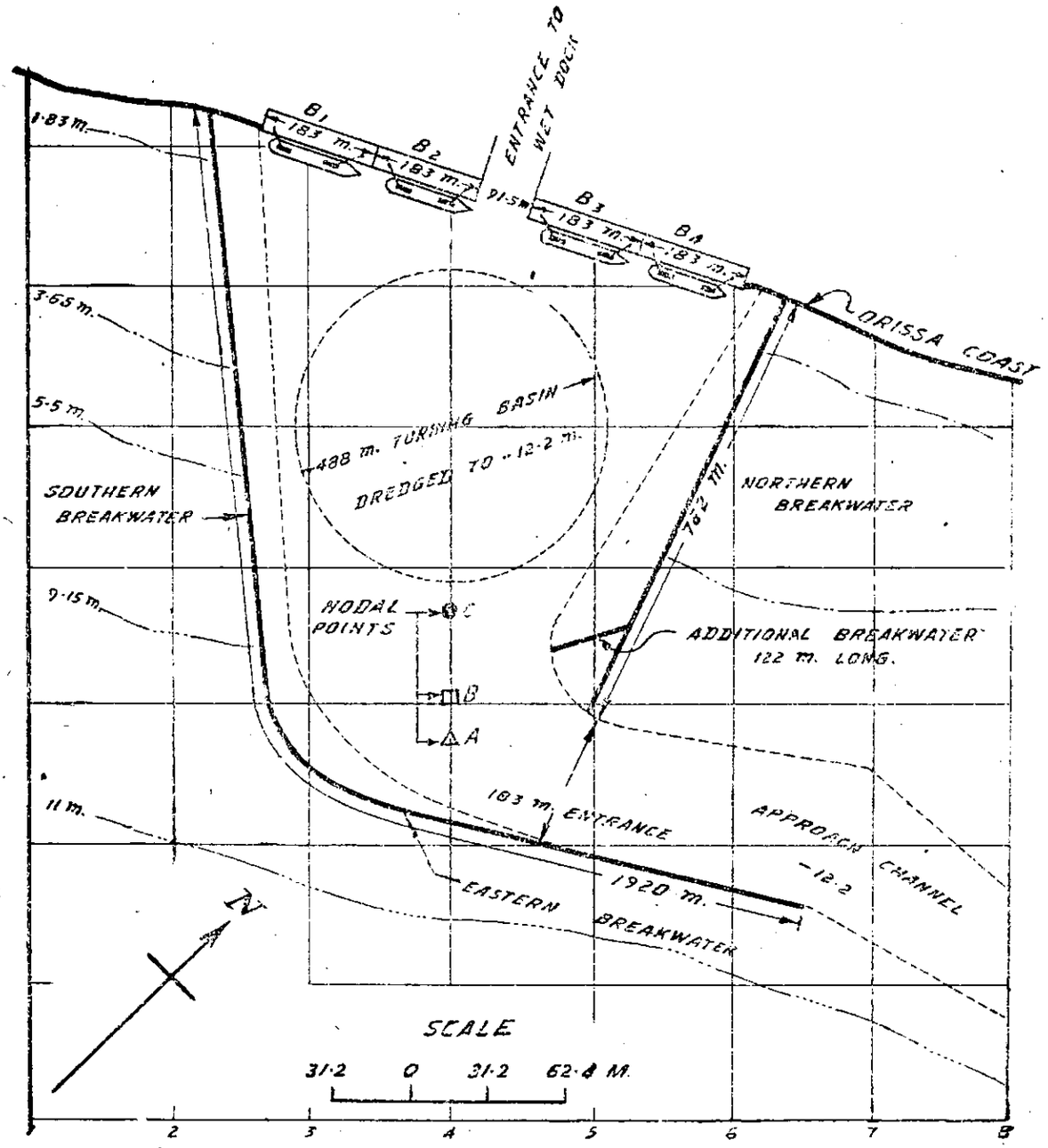

Fig 2: Experiments with long period waves from east.

Table 4

Position of Nodal point in *meters* from Eastern Breakwater or Berth *No*	Period (*secs*)	Ship movement in *meters*				
		Longitudinal		Transverse		Vertical
		Stern	Bow	Stern	Bow	
Without Additional Breakwater						
136	44	2.06	2.06	1.52	1.56	.57
408	44	1.33	1.22	.84	.76	.38
680	44	1.22	1.1	.57	.57	.189
190	75	1.64	1.56	1.37	1.255	.417
583	75	1.56	1.52	.46	.46	.38
307	90	1.67	2.21	4.91	4.38	.57
With Additional Breakwater						
136	44	1.38	1.4	1.22	1.22	.417
408	44	1.22	1.22	.57	.57	.38
680	44	1.13	1.06	.57	.57	.15
190	75	1.45	1.38	1.22	1.14	.417
573	75	1.33	1.22	.46	.46	.38
317	90	1.295	1.48	1.14	1.03	.495
Berth 1	90	.95	.95	.46	.45	.38
„ 2	90	.95	.95	.46	.38	.38
„ 3	90	.95	.95	.46	.512	.38
„ 4	90	.95	.95	.417	.38	.38
Turning Basin Point 5	90	1.25	1.14	.57	.57	.38

Details of ship : (*a*) Displacement ... 4970 *m ton*
(*b*) Length ... 145 *m*
(*c*) Beam ... 19.1 *m*

(*iv*) The remedial measure consisted of modification of the geometry of the harbour. An addition of a 122 *m* (400 *ft*) long breakwater arm to the northern breakwater as shown in *fig 2*, improved the conditions markedly. As would be seen from *table 4*, the transverse movement of 4.9 *m* (16.1 *ft*) was reduced to 1.15 *m* (3.75 *ft*) only.

The *table* also shows that with the addition of this breakwater conditions at other places would not deteriorate but on the contrary improve slightly.

In case of short period waves also this breakwater acted as a trap for the diffracted waves and hence resulted in the reduction of wave heights near the berths.

5. Conclusions

(1) Ship movements would not be of excessive order near the berths for long and short period waves.

(2) There will be a nodal point at a distance of 318 *m* (1040 *ft*) from the eastern breakwater near the entrance for long period waves of 90 *sec* period.

(3) A considerable reduction in ship movement could be achieved by the introduction of a breakwater as shown in *fig 2*.

28. Distributions of wave heights

Bay of Bengal (1949-59)

HIGH TIDES and waves over the ocean area are caused by gusty winds blowing for limited period of time or steady winds blowing for continued periods. The heights of the sea-wave, therefore, vary accordingly for different reaches as well as times, depending on their respective incidental causes. The conditions in the Indian Ocean are very peculiar. Waves are generated by regular seasonal winds of lesser intensities blowing over longer durations. The high intensity winds associated with storms also generate higher waves depending on the fetch area, decay distance and path of storm tract, etc. The latter may be superimposed on the waves caused by seasonal winds. The exact distributional features of these variations thus have considerable interest for navigational purposes in the open seas as well as for the maintenance of ports and harbours and also for purposes of saving the coastal beaches from erosion.

The data of the day-to-day wave heights obtaining over different reaches are thus being collected constantly by the large numbers of the commercial and other vessels while streaming in different directions in their normal course over the boundless oceans. These commercial vessels which follow the common trade routes alone collect the wave heights' information along their limited tracks only and not for the entire lengths and breadths of the vast oceans. Thus they

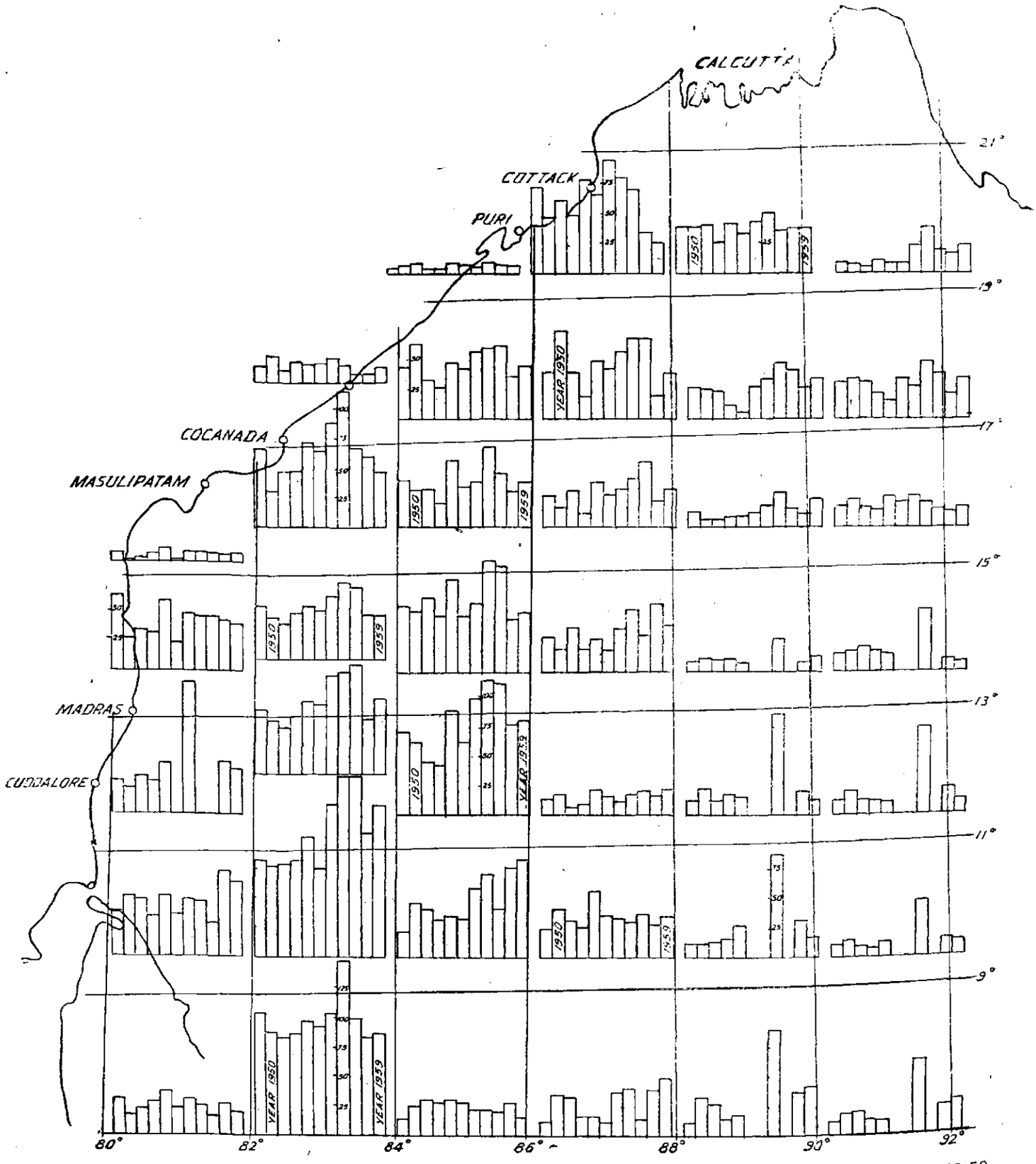

Fig 1: Yearwise distributions of ship —days observed for 2° lat. × 2° long. areas in Bay of Bengal 1949-59.

provide the basis of some representative samples only of the variations occurring over the wide seas. The data are maintained in some of the developed countries for long periods and have been analysed as well for evolving their variability laws and formulating suitable expressions for their related variations with other climatological factors. The India Meteorological Department at Poona also have arrangements for maintaining such data as pertain to the oceanic areas bordering the Indian coasts. An analysis was made of the broad features of the variational

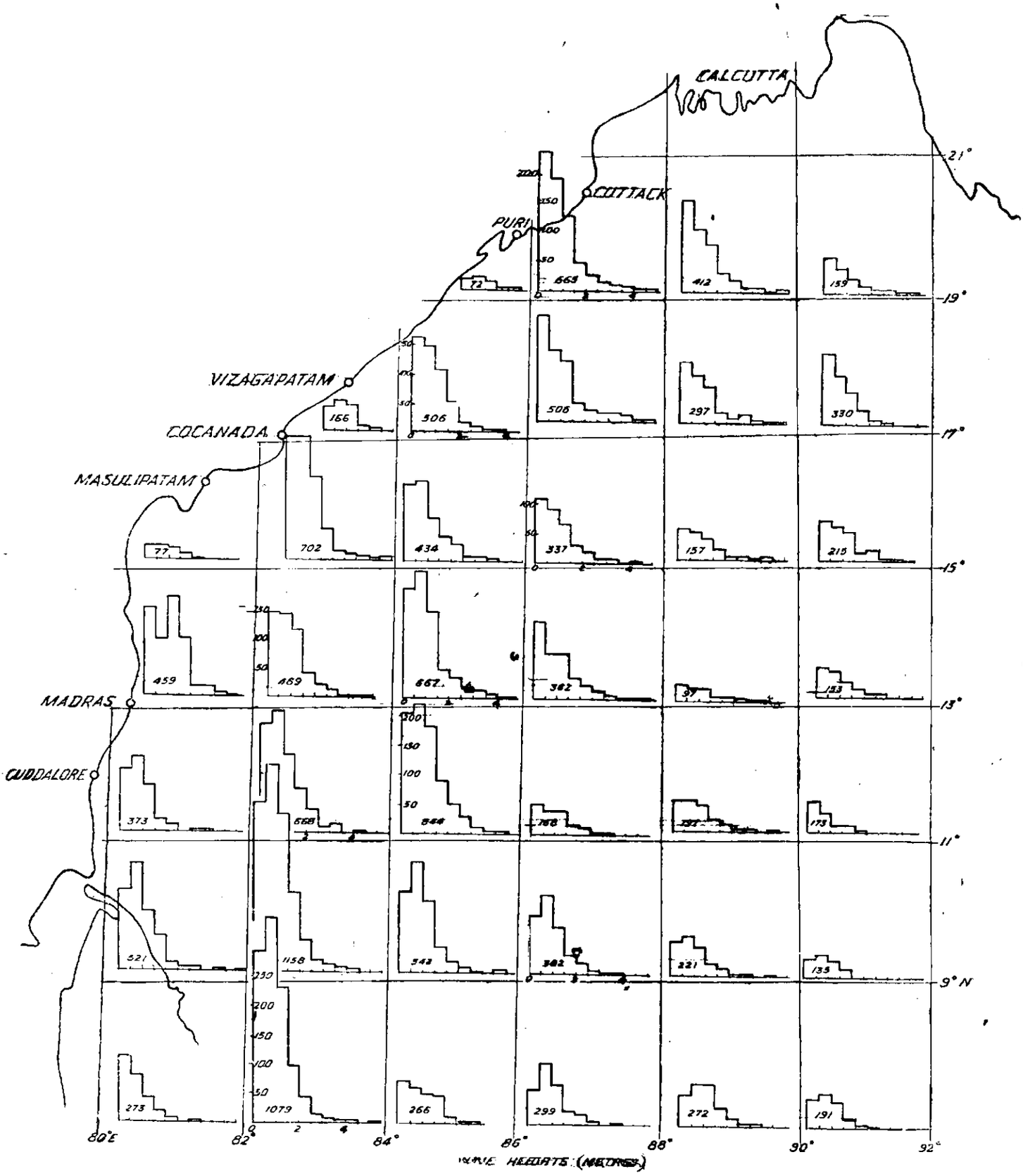

Fig 2: Frequency histograms of pooled wave heights for 2° lat. × 2° long. areas in Bay of Bengal.
Note: Numbers inset in Histograms connote total frequency.

patterns as contained in 4 years' (1954-57) data and described in *Annual Research Memoirs 1959*.

After the evidence secured last year of the limited year-to-year homogeneity patterns obtaining of the frequency distributions of wave heights over selected 1°×1°; 2°×2°; 3°×3° and 4°×4° regions of the Bay of Bengal, the studies were continued during 1960 for all the observed

data for a longer series of years over the same regions. The total length of the data now covered about 11 years from 1949-59. But, in all the 168 or so $1^\circ \times 1^\circ$ regions, the yearly number of ship days observed were rarely found adequate for studying the frequency patterns of the wave heights distributions. For the purpose of deducing reliable inferences about the year-to-year variations in the frequency distribution patterns, the coverages of the data had, therefore, perforce to be extended to wider regions covering about $2^\circ \times 2^\circ$ areas.

The yearwise frequency distributions so obtained for the enlarged regions of the total number of 15,024 ship days' observations made during 1949-59 are presented in *fig 1*. But, no consistency was easily discernible in the patterns of the year-to-year observed number of ship days or from region to region. Their apparent differences possibly reflect only the naturally expected trends from such casually observed data over the commercial ship tracks.

From the detailed yearly wave heights distributions thus of the type† some 9 regions only out of the 39 $2^\circ \times 2^\circ$ wise cut up areas with about 30 or more yearly ship day observations remain eligible for strict analytical studies. On making homogeneity analysis for all the 9 regions, the χ^2 evaluated for only one was observed as significantly large. The respective values for the different regions are shown in *table 1* below. In other words, the differences obtaining between the frequency patterns of the wave heights distributions over the 8 other $2^\circ \times 2^\circ$ regions remained tolerably small.

† YEARS

Wave Height meters	49	50	51	52	53	54	55	56	57	58	59	Total
0 – ½	5	10	7	9	6	7	3	8	14	7	11	87
– 1	9	15	10	15	19	12	35	29	19	21	19	203
– 1	22	20	26	26	35	16	36	48	50	24	50	353
– 1½	21	18	23	17	23	18	26	33	33	18	34	269
– 2	10	10	7	8	6	12	17	24	17	15	9	135
– 2½	6	2	4	2	5	6	6	6	5	12		54
– 3	3		1	1	3	1	4	2	3	4	1	23
– 3½	4			3	1			1	2	2	1	14
– 4	1							1	3	1	2	8
– 4½					1	2		1		1		5
– 5												—
– 5½		1			2							3
– 6					1	1						2
– 6½							1		1			2
– 7												—
Total	81	76	78	81	102	75	128	153	152	105	127	1158

Table 1: Values of x^2 for various regions (1949-59)

Region between Lat	Long	Total No. of ship days observed.	Degrees of freedom	X^2
7- 9	82-84	1079	50	97.48**
9-11	80-82	521	30	36.49
9-11	82-84	1158	50	78.00
11-13	82-84	668	30	35.49
11-13	83-85	858	50	72.66
12-14	80-82	414	20	23.68
12-14	82-84	584	30	38.82
14-16	81-83	688	30	28.02
15-17	85-87	514	40	55.87

The feature appears probably natural from other considerations also, and so lends an acceptable road for pooling the data observed over a long course of years for the purpose of their detailed analysis when the data of single or stray years may be inadequate. *Fig 2* thus shows the regionwise separate frequency histograms so prepared by pooling all the respectively observed 11 years' data, of the wave heights distributions. The study for the determination of any uniform characters contained in the different frequency distributions over the Bay of Bengal and of their regional continuity of variations, if any, in one or more directions thus now remains to be undertaken.

29. Coastal erosion near naval battery at Cochin

THE COAST of Cochin, near Naval Battery immediately to the south of the approach channel is being considerably affected by erosion due to wave action in the sea. Army and Navy Establishments situated close to the coast are being constantly threatened by this erosion. Steps to check the erosion were taken up from time to time by the Port, Naval and State authorities for protecting the areas under their respective control.

The storm of 1958 caused considerable erosion in front of the proposed magazine area and brought the *HW* mark very close to the existing establishment. This necessitated a probe in the matter to investigate the probable causes and recommended suitable measures for arresting erosion.

2. *Fig 1* shows the coast affected by erosion. The contours represent the *HW* marks during various years. During the year 1948-49 the *HW* line was very close to the Army establishment and a temporary Sea wall was constructed in the reach *PQ*. This was subsequently strengthened in 1950-51 and extended upto the reach *QR* in 1956-57. Raising of the wall was done in 1958-59.

In the reach *PQ*, 15.25 *m* (50 *ft*) long groynes at 30.48 *m* (100 *ft*) apart with stones of .085 to .135 m^3 (3 to 4 ft^3) in size were constructed prior to 1959 monsoon. These have withstood the wave attack well and no damage in the reach has taken place. In the reach *QR* also 15.25 *m* (50 *ft*) long groynes 30.48 *m* (100 *ft*) apart were constructed. These have, however, been completely damaged probably because of the small size of stones *viz* .0284 to .056 m^3 (1 to 2 ft^3) used for their construction.

A sea wall was constructed near the Naval Battery in 1954-55. The section of sea wall appears to be inadequate to withstand the wave action and requires strengthening. At present there is a sand cover of not less than 30.48 *m* (100 *ft*) in front of the reach *PQ*, *QR*, *RS*, *ST* and even beyond *T* upto the state boundary.

3. Analysis of data

(*a*) *Study of HW Lines.—Fig 1* shows the *HW* lines in various years, starting from 1922. *Table 1* shows the rate of advancement or recession per year in this particular reach, and *table 2* the distances of *HW* lines with respect to a fixed base line *AB* along the various sections *viz* at cemetery, and at *P*, *Q*, *R*, *S* and T_1. The study revealed no definite trend for progressive erosion or accretion in the reach. In some years the *HW* lines were very close to the Army and Navy establishments, whereas in others they were so far off that one would not think of providing any protective measures. On an average the rate of erosion or accretion is about 6.1 to 9.15 *m* (20 to 30 *ft*) per year.

Table 1

Years	Cemetery	*P*	*Q*	*R*	*S*	T_1
1922-27	-22.6	-19.5	- 5.5	- 1.22	+ 6.7	+ 3.05
1927-32	+13.7	+21.3	+15.2	+15.9	+15.2	+ 9.15
1932-37	- 7.62	-12.2	+ 0.61	+10.7	+15.2	+21.3
1937-42	+25.9	-12.2	+ 1.5	- 1.52	- 6.1	-12.2
1942-47	-18.3	-21.3	-17.7	-16.8	- 6.1	+ 4.6
1947-49	...	- 7.62	-26.5	-22.8	-28.6	-28.6
1949-58	...	+ 0.85	+ 1.68	- 0.397	- 7.62	-11.9
1958-59	+67.0	+76.2	+39.0	+ 7.62	+46.0	+46.0

Table 2

Year	Cemetery	Sections (distances in *meters*)				
		P	*Q*	*R*	*S*	T_1
1922 ...	183	216	192	145	65	76.2
1927 ...	70	119.5	167.5	137	100.5	91.5
1932 ...	148	224	241	219.5	180	140
1937 ...	107	181	247	268	256	253
1942 ...	238	244	255	261	228.5	195
1947 ...	148	134	169	175	193.5	218
1949 ...	...	119	116	131	135.5	160
5-5-1958 ...	81	119	128	135.5	128	115.8
11-8-1958 ...	73.2	119	128	128	109.5	106.5
end of 1958...	...	...	...	137	68.5	53.4
1-6-1959 ...	140	195	167	145	114.5	99

S 3401—25-a

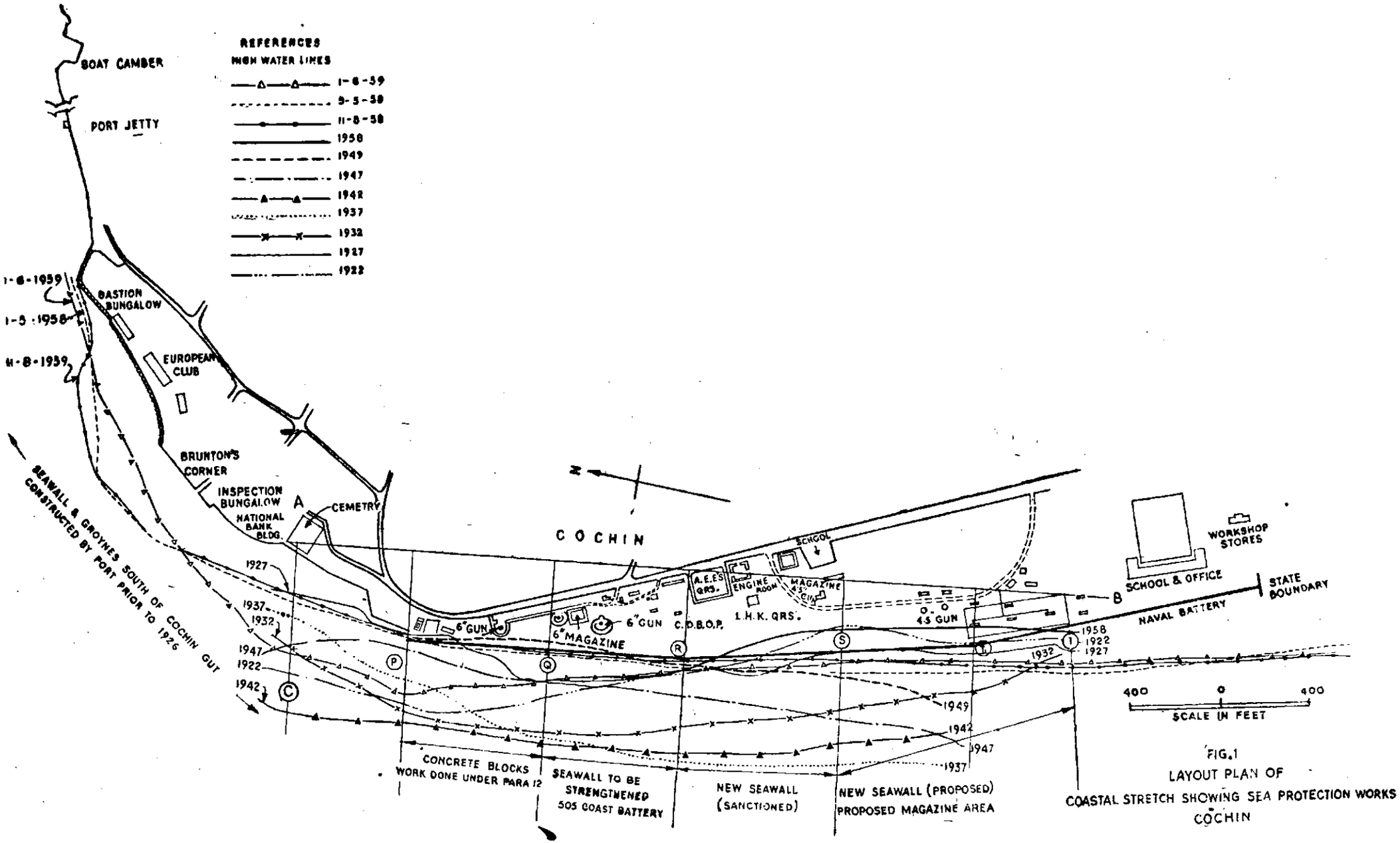

FIG.1
LAYOUT PLAN OF
COASTAL STRETCH SHOWING SEA PROTECTION WORKS
COCHIN

(*b*) *Storm Characteristics.*—Data regarding storms in the Arabian Sea over a period of 1921 to 1959 were analysed to see if storms were responsible for this behaviour. Characteristics of waves such as height, period and direction generated due to these storms were worked out by adopting hindcasting techniques. *Table 3* gives the relevant details. This analysis showed a correlation between the storms and the recession or advancement of *HW* lines. An interesting point brought out by the study was that whenever a storm was located either on the west-north-west or north-west of Cochin, erosion occurred immediately on the south side of the Cochin gut, and that whenever they were centred to the west, south-west or south of Cochin they contributed to accretion in this reach. This is but natural as a strong current through the Cochin gut acts as a partial barrier to the drift. As the coast is not nourished, waves from *NW* pick up the material from the reach, and as it happens to be immediately on the downdrift side the rate of erosion is higher under such conditions.

Table 3: Occurrences of storms in dif erent years and wave characteristics obtained by hindcasting technique (for Cochin)

Period	Position of Storm	Maximum wind-speed (*knots*)	Wave characteristics			Remarks
			H_W (*m*)	P_W (*Sec*)	D_W	
12th; 13th Nov '27.	*NW*	27	1·07	12·2	*NW*	
24th May '32...	*NW*	21	·84	9·15	*NW*	Shoreline advanced in 1932
17th May '33...	*NW*	12	·17	6·49	*NW*	
1st; 3rd Nov '34...	*NW*	21	·54	8·6	*WNW*	
20th; 22nd Oct '35.	*NW*	16·5	·55	7·6	*NW*	
7th Nov '38...	*NW*	32	1·37	13	*NW*	
16th Oct '40...	*NW*	30	·84	11·3	*NW*	Shoreline advanced in 1942
18th Aug '44...	*NW*	20	·37	8·7		
1946...		Local strong centre	depression with winds of 21 knots d at Cochin.			Shoreline receded back
12th Jun '48...	*NW*	30	1·86	13·8	*NW*	
23rd; 28th Sep '48.	*NW*	40	1·99	15·1	*NW*	
20th; 22nd Nov '48.	*NW*	55	3·02	16·8	*NW*	Shoreline receded far back in 1949
19th Apr '51...	*NW*	15	·20	6·25	*W*	
12th; 16th Nov '51.	*WNW*	35	2·24	14·4	*W*	
1st; 2nd May '56.	*NW*	20	·82	9·75	*NW*	
7th; 13th Nov '57.	*NW*	25	1·27	11·8	*WNW*	
9th; 16th Oct '58.	*NW*	30	1·72	13·3	*NW*	
24th; 28th Nov '58.	*WNW*	20	·72	7·9	*WNW*	
20th; 24th May '59.	*W*	55	2·53	14·0	*W*	

(*c*) *Rose Diagrams.*—The analysis of wave characteristics reported by ships steaming in the vicinity of the area during 1958 and 1959 was also made. Rose diagrams for wave heights have been prepared and attached as *figs 2* and *3*.

Calculations were made for the wave energy (in $m\ kgm \times 10^5$) from *N* and *NW* and from *S* and *SW* and reproduced in *table 4*. The analysis shows that there was considerably more energy from south and south-west in the year 1959, which seems to be responsible for accumulation of material just south of the gut which acts as a partial barrier to the drift.

Table 4

Energy from		1958	1959
North	...	3·5	2·49
North West	...	6·55	4·32
Total	...	10·0	6·8
South	...	0·78	5·47
South West	...	3·15	3·77
Total	...	3·95	9·24

On the other hand in the year 1958 there was considerably more energy from north and north-west. This appears to have caused erosion along this reach.

4. Conclusions

(*i*) Erosion as well as accretion is observed along this reach in different years. On an average the rate of erosion or accretion is 6.1 to 9.15 *m* (20 to 30 *ft*) per year. At some places it is even more.

(*ii*) Whenever the storm is located either on the west-north-west or north-west of Cochin the erosion is caused immediately on the down drift side; and when the storm is located on the west,

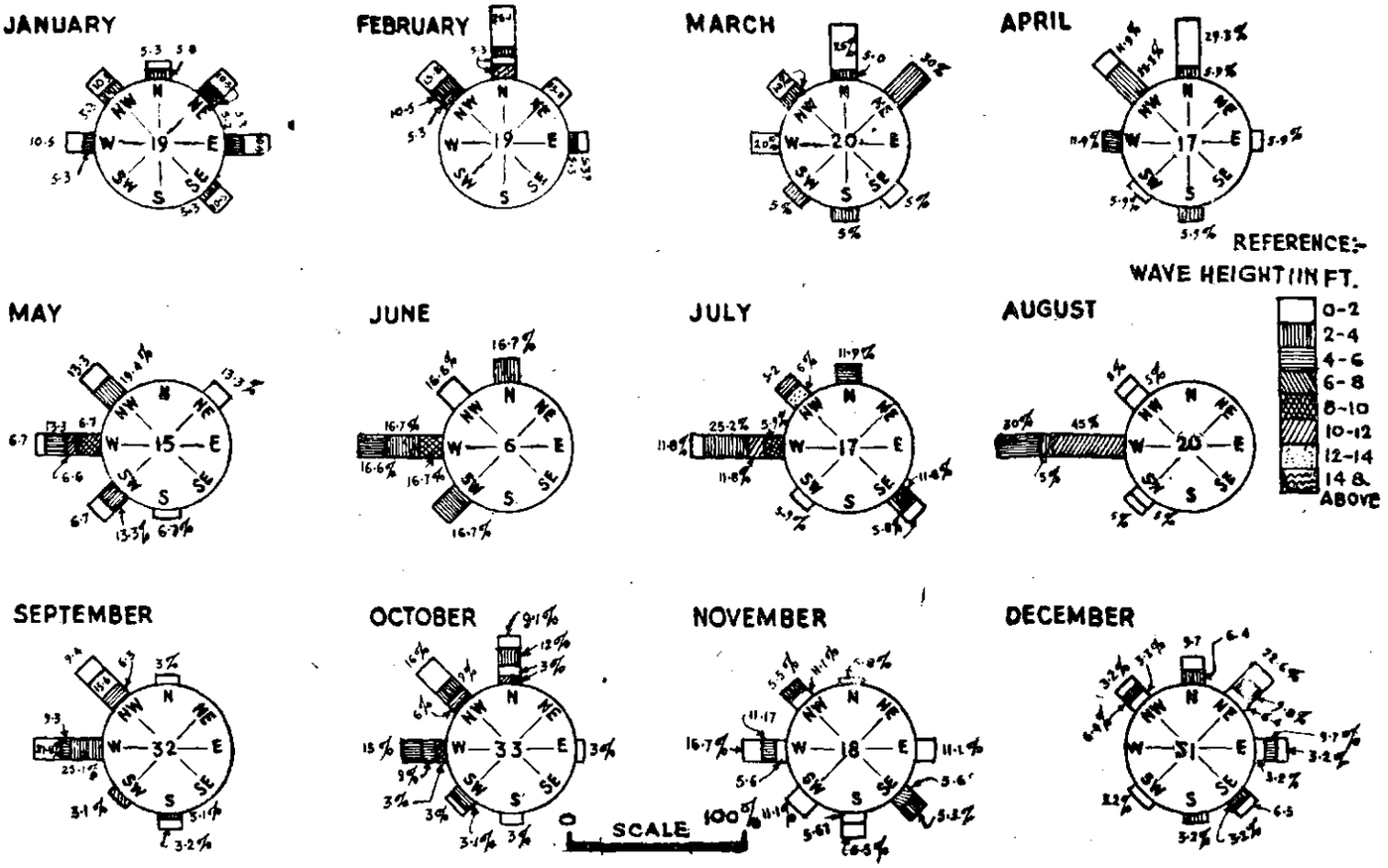

Note:—Figures at the centre of the circles indicate the total number of observations.

Fig 2: Cochin rose diagrams showing wave characteristics between *lat.* 7°-30 to 12° N. and *long.* 72° to 77° E. for the year 1958.

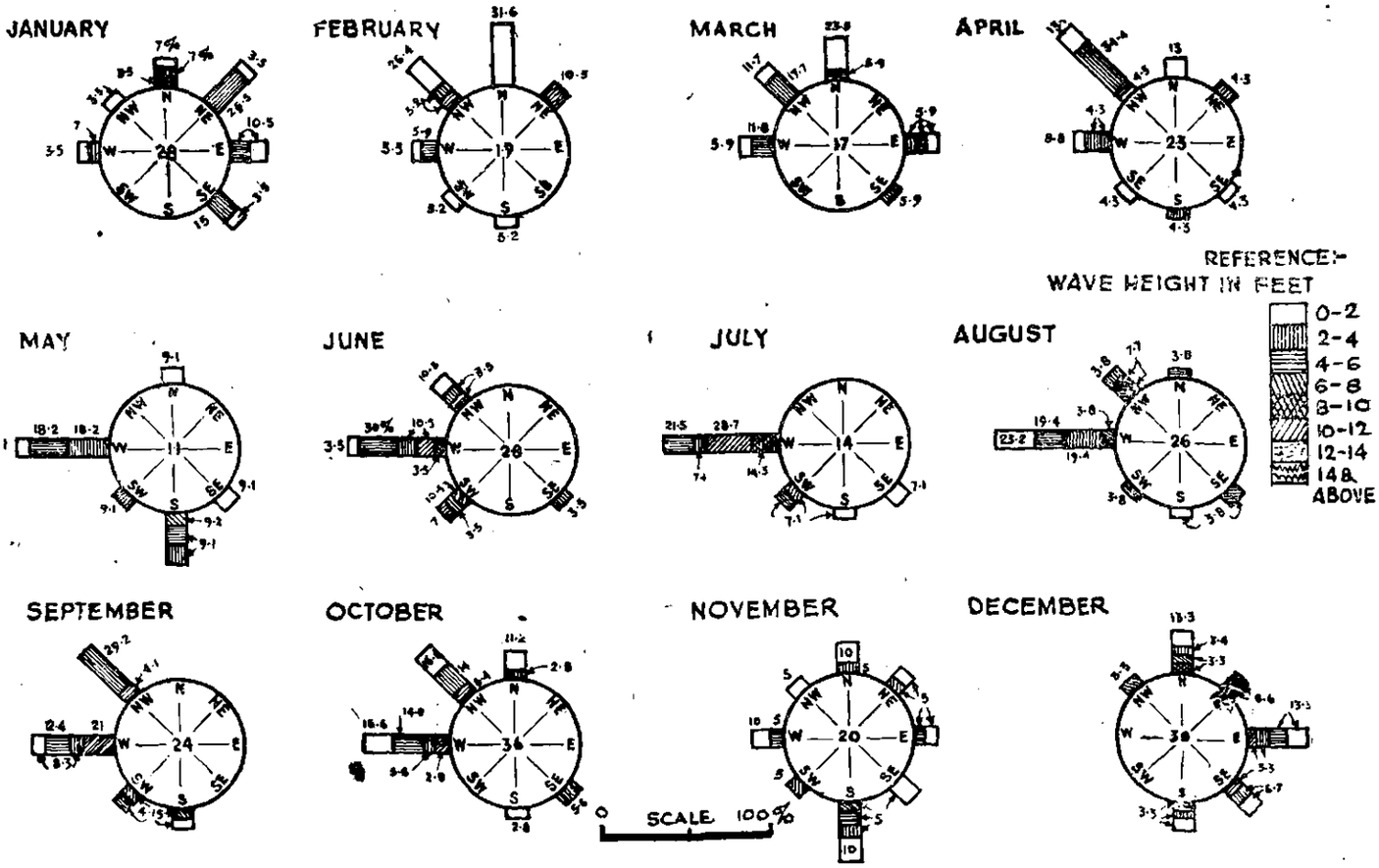

Fig 3: Cochin rose diagrams for the year 1959.

south-west or south side of Cochin accretion appears to take place in this reach.

(*iii*) If the preponderance of wave energy is from south or south-west accretion will take place in this reach.

(*iv*) Depending upon the position and intensity of the storms and the direction of waves, there is always a danger of erosion of the coast line in some portion or the other from point *P* to the State boundary.

5. Recommendations

The following recommendations were made:

(i) A sea wall supplemented with 61 *m* (200 *ft*) long groynes 152.5 *m* (500 *ft*) apart with groyne top sloping from + 2.74 *m* (+ 9 *ft*) at the shore ends, to + 2.14 *m* (+ 7 *ft*) towards the sea was recommended. Stones of weight not less than 277 *kg* (500 *lb*) should be used for the outer layer in particular for the nose of the groynes. The levels mentioned are with respect to the *LWOST* datum.

(*ii*) The top of the sea wall to be kept at +3.35 *m* (+ 11 *ft*) with 2 : 1 side slope on the seaward side and 1 : 1 on the leeward side.

(*iii*) The groynes and sea walls should be constructed on fascine mattresses.

(*iv*) In case it is not possible to finish the construction of groyne and sea walls before the outbreak of monsoon some reserve stones of sufficient size should be kept ready at vulnerable places for dumping as and when required.

---

30. Pore pressure in Triaxial Shear Test

PORE PRESSURE plays an important part in the determination of shear strength of soils by triaxial shear test. In an undrained triaxial test, the total pore pressure developed governs the behaviour of the soils with regard to shear strength characteristics expressed in terms of effective stress. Skempton and Bishop have developed the concept of pore pressure parameters to obtain a clear picture of how pore pressure responds to different combinations of applied stress. It is possible to explain relationship between different types of triaxial test and also provides a basis for estimating the magnitude of pore pressure to be encountered in actual problems by the concept of pore pressure parameters.

An increase in pore pressure in an undrained triaxial shear test can be expressed in the form of following equation :

$$\Delta u = \frac{1}{1 + n\, C_w / C_c} \left[\Delta\sigma_3 + \tfrac{1}{3} (\Delta\sigma_1 - \Delta\sigma_3) \right]$$

Where C_w = compressibility of pore fluid

$C_c = 3 \left(\frac{1 - 2\mu}{E} \right)$ = compressibility of soil skeleton.

E, μ, n are Young's Modulus, Poisson's ratio and porosity respectively.

$\Delta\sigma_1$ and $\Delta\sigma_3$ are increase in major and minor principal stresses.

The pore pressure change in an undrained triaxial test is firstly due to change in all round pressure and secondly from a change in deviator stress. This change can be expressed in terms of two emperical parameters A and B where

$$\Delta u = B \left\{ \Delta\sigma_3 + A \ (\Delta\sigma_1 - \Delta\sigma_3) \right\}$$

For fully saturated soil C_w is a constant and is very small as such $B = 1$ within the limit of experimental accuracy. The value of A depends on stress history of the soil and on the proportion of failure stress applied.

In case of partially saturated soil the value of C_w is much higher because of the presence of air and the value of B is thus less than 1 and varies with the stress range. For this reason, the product $A \times B$ in the above equation is denoted by $\bar{A}$ as

$$\Delta u = B \Delta\sigma_3 + \bar{A} (\Delta\sigma_1 - \Delta\sigma_3)$$

Preliminary studies have been made of pore pressure parameters B and $\bar{A}$ for three soils compacted at Proctor's density and saturation moisture. The mechanical composition and Proctor's density of the samples are given in *table 1.*

The pore pressure measurement had been carried out by null method. The sample was placed on a saturated porous disc connected with the

Table 1

Sample No	Mechanical Analysis					Proctor's Compaction Test	
	Clay < ·002 mm	Silt ·002 to ·02 mm	Fine sand ·02 to ·2mm	Coarse sand ·2 to 2·0 mm	Gravel >2·0 mm	OMC per cent	MDD lbs/cft
2393	23	13·1	19·2	9·2	30·5	18	104·2
2393A	27	25·7	37·5	9·0	·8	18	100·0
2415	45	37·7	12·2	6·8	...	21	97·8

null indicator. Great care was taken to remove air bubbles from the system. Saturated filter strips were placed round the samples to get the pore pressure-equilibrium quickly.

2. Results and Discussion

Fig 1 shows the Mohr Circles drawn with respect to both total stresses and effective stresses. It will be seen from the figure that with respect to total stresses $\phi = 0$ condition exists. When Mohr Circles are drawn with respect to effective stresses for maximum deviator stress, the effective stress circles almost tend to be identical for all the samples of soil tested. As there was no failure plane developed, true shear parameters could not be obtained from these effective stress circles. Skempton's results also show that in undrained test, failure envelope in terms of effective stress cannot be determined as σ'_1 and σ'_3 are independent of cell pressure.

The deviator stress, the effective stress ratio, the pore pressure changes and values of $\bar{A}$ in relation to axial strain are plotted in *figs 2a, b, c.* The value of pore pressure parameter B at different ambient pressures and of $\bar{A}$ at failure are given in *table 2.* The value of B varies from

Table 2

Sample No	25 psi		35 psi		45 psi	
	B	$\bar{A}$	B	$\bar{A}$	B	$\bar{A}$
2393	·88	−·049	·89	−·024	·92	−·085
2393A	·88	−·06	·93	−·045	·93	−·06
2415	·92	−·08	·92	−·05	·91	−·026

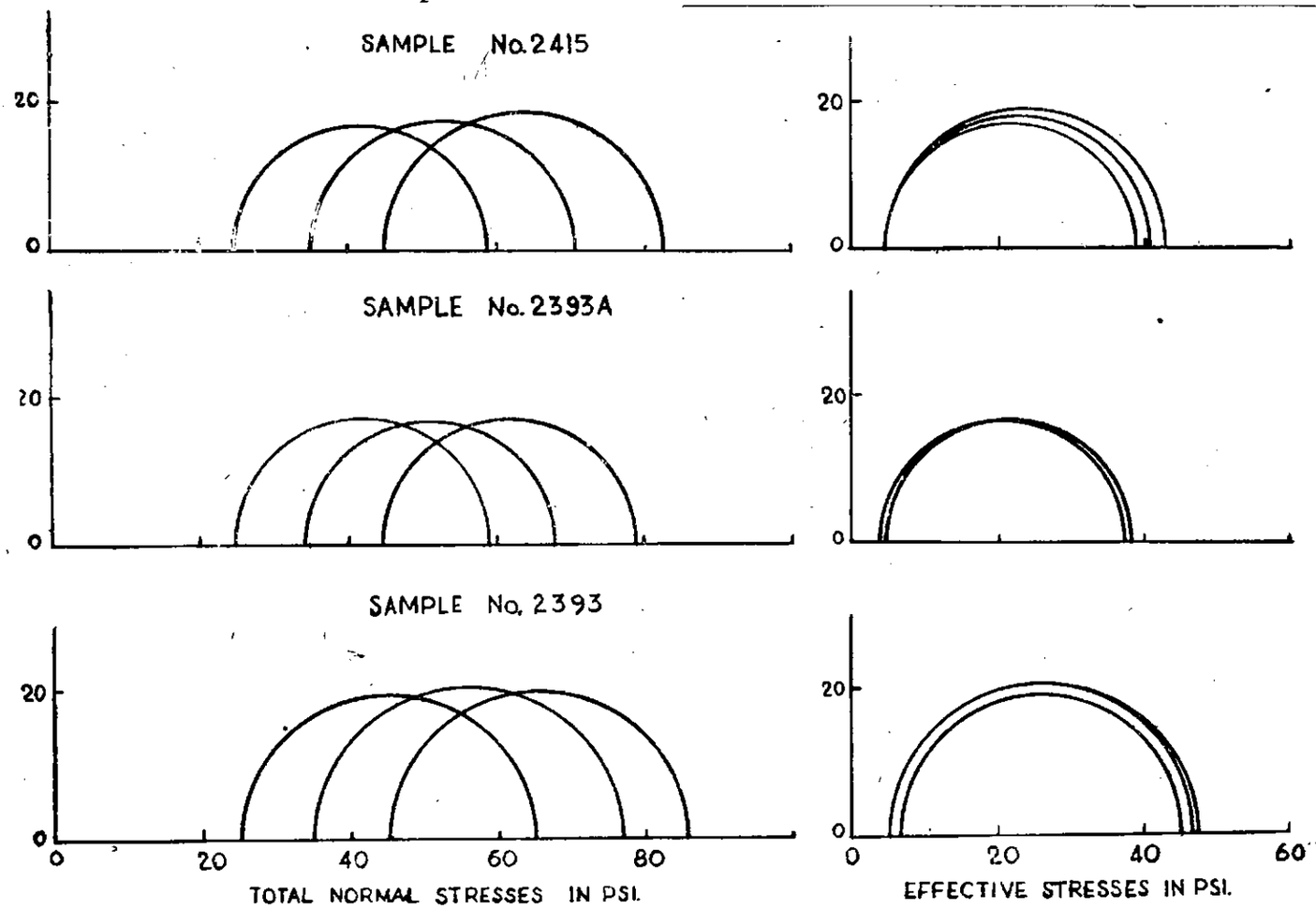

Fig 1: Mohrs circles for total and effective stresses.

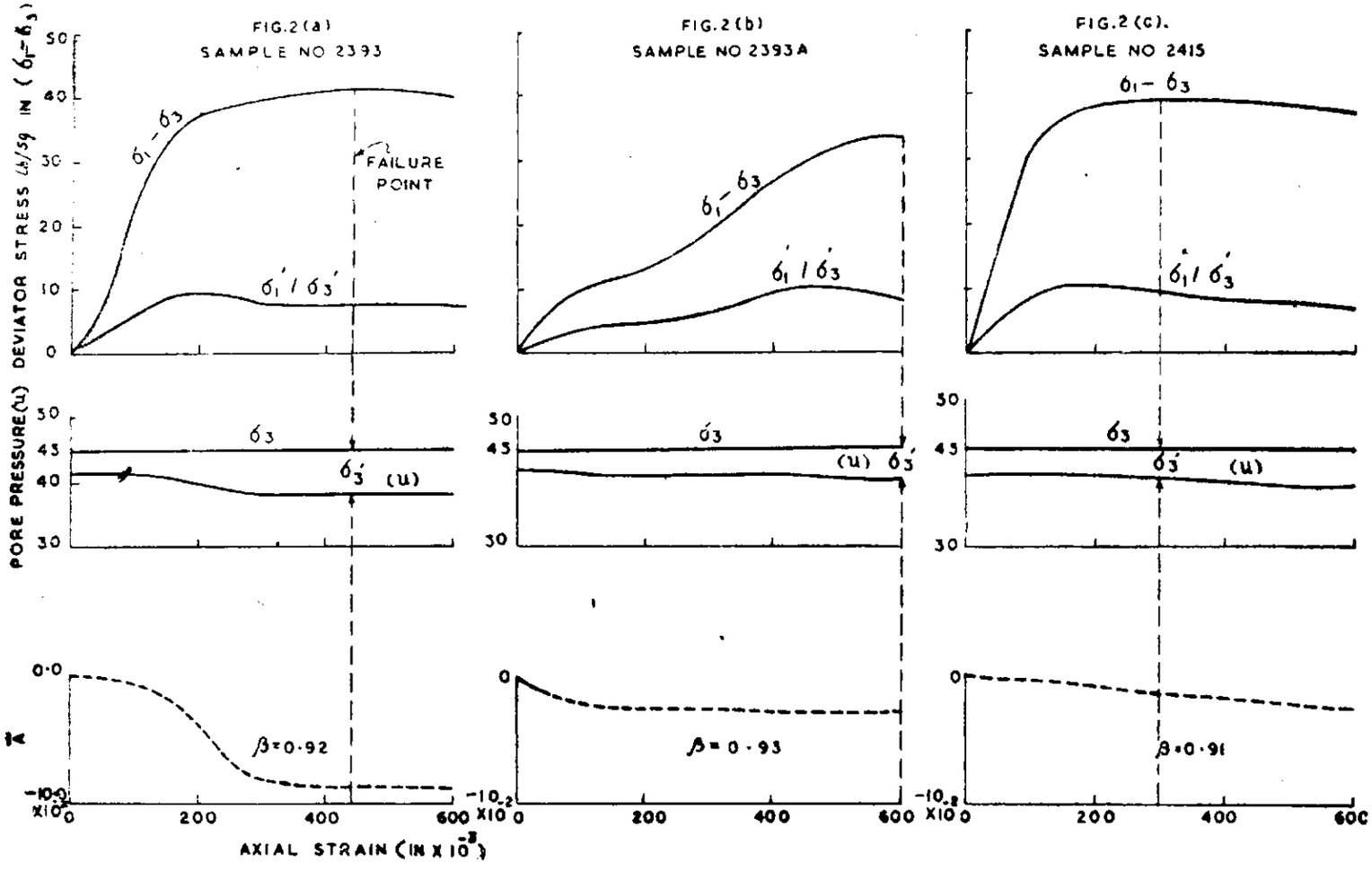

Reference:—

$\sigma_1 - \sigma_3$ Deviator stress in *lb/sq in*

σ_3 Ambient pressure in *psi.*

σ'_1/σ'_3 Effective stress ratio

B & $\bar{A}$ Pore pressure parameters

U Pore pressure in *psi.*

σ_3 Effective ambient pressure.

Fig 2

.88 to .93 instead of theoretical value of unity for saturated soil. The discrepancy is probably due to the method adopted for preparation of saturated samples, where there is likelihood of some air voids being left. As the value of B is not unity, the pore pressure parameter $\bar{A}$ has been calculated instead of A. It will be seen that $\bar{A}$ is always negative and varies from .026 to .085.

The pore pressure assembly is being modified for carrying out consolidated undrained test which is not possible with the arrangement available at present.

31. Compaction and shear strength of soils

THE STANDARD laboratory compaction test was developed by Proctor (1933) and is carried out in 4.6 *in* by 4 *in* diameter mould using 5½ *lb* hammer and 12 *in* fall. The purpose of laboratory compaction test is to find out amount of mixing water necessary to get the maximum density under particular compacting energy. This also serves as a guide for field compaction. Before the second world war the compacting equipment used in the fields were comparatively smaller, so Proctor's standard laboratory compaction test gave comparable results with field compaction. The field equipment for compaction available at present time gives higher densities, necessitating the use of higher compacting energy in the laboratory compaction test. The modified Proctor test using 10 *lb* hammer and 18 *in* fall has been introduced. A comparative study of standard Proctor test and modified test using 10 *lb* hammer and 18 *in* fall, in 3 layers and also in five layers has been made. The compactive energy in the above tests were as follows :

Proctor Test	*Wt.* of hammer *lb.*	Height of fall (*in*)	Number of layers	blows per layer	Compactive energy per volume *ft-lb/cft.*
Standard	5½	12	3	25	12,400
Modified	10	18	3	25	33,800
Modified	10	18	5	25	56,300

In addition to estimation of optimum moisture content and maximum density under each compactive effort, shear strength and permeability of soils were also determined.

2. Results and discussion

The mechanical composition and Atterberg limits of the samples are given in *table 1.* Out of 13 samples tested, 5 samples are sandy and 8 soils are clayey or silty. The liquid limit of only three soils are 50 and above.

The optimum moisture content and density as obtained by different methods are presented in

Table 1

Lab No.	Depth in *ft*	Texture	Atterberg limits				Mechanical Analysis (%)					
			Liquid Limit	Plastic Limit	Plasticity Index	Shrinkage limit	Clay	Silt	Fine sand	Coarse sand	Gravel 2 to 6·4 *mm*	+3/16 *in*
						Barapani Project, Assam						
2092	... 0–7	*CH*	50	30	20	...	40·2	33·4	17·9	7·3	1·2	...
2086	... 0–10	*ML*	50	34	16	29	18·0	31·4	37·9	10·4	2·3	...
2080	... 0–10	*SM*	44	32	12	25	32·1	9·7	41·2	11·8	1·8	3·4
						Bhimghar Dam, Wain Ganga Project, M. P.						
1951	... ...	*SC*	49	31	18	12	5·0	20·8	23·9	26·0	9·4	14·9
1955	... ...	*SM*	33	24	9	15	8·4	13·8	49·3	29·7	...	3·8
1960	... ...	*SM*	52	...	...	19	3·4	7·3	31·0	48·4	6·8	3·1
1994	... ...	*SM*	25	...	...	15	2·3	5·7	67·8	21·9	...	2·3
						Hasdeo, M. P.						
2406	... 0–3	*CL*	23	16	7	15	27·0	12·4	49·1	9·1	2·4	...
2414	... 0–5	*CL*	34	18	16	...	31·6	14·4	28·5	10·4	11·1	...
2410	... 0–8	*CL*	26	16	10	12	44·2	25·4	24·5	4·7	1·2	...
2417	... 0–8	*CL*	21	13	8	...	22·4	22·3	44·7	10·6	...	...
						Aniyarankal Project, Kerala						
2292	... Composite Sample	*CH*	54	31	23	25·8	28·3	23·8	12·5	24·6	10·8	...
						Girna Project, Maharashtra						
2294	... ,,	*SC*	39	23	16	18·6	14·0	20·1	36·4	17·4	18·1	...

table 2, and a typical moisture-density curve is shown in *fig 1*. It will be seen from the *table 2* and the *fig 1* that with the increase in compactive energy, the maximum density increases and moisture content decreases. The maximum increase of 11 *lb/cft* has been obtained for sample *No* 1960 between standard and modified Proctor in three layers. The maximum increase of 16.5 *lb/cft* has been obtained between standard and modified proctor in five layers for sample *No* 2410. Generally decrease in optimum moisture content varies from 2 to 4 *percent*. However the maximum decrease of 7 *percent* moisture has been observed in case of sample *No* 2082.

Triaxial shear tests have been carried with maximum densities as obtained under various compactive energy both at optimum moisture content and at saturation. The permeability tests have also been carried out with some samples. The results are presented in *table 3*.

Table 2 :

Lab No	Standard Proctor Compaction.		Modified Proctor Compaction done in:			
			3 Layers		5 Layers	
	OMC%	*MDD lbs/cft*	*OMC %*	*MDD lbs/cft*	*OMC %*	*MDD lbs/cft*
2082 ...	32	90	24.9	95.3		
2086 ...	26	92.8	21.7	101.5		
2080 ...	25.3	94.8	22.2	98.8		
1951 ..	21	101	20.7	105.7		
1955 ...	22.8	101	20.5	104.8		
1960 ...	20.4	104.2	16.8	115		
1994 ..	18.5	109.7	16.7	115.2		
2406 ...	14	115	11	118	10.2	122.2
2414 ...	14	110	13	117	11	122.4
2410 ..	17	106	14	110	11.7	122.5
2417 ...	13	111	12	117	10.8	124
2292 ...	22.6	97.8	20.4	102.8	19	106.4
2291	20.8	104.7	16.8	111.3	16	118.3

Table 3

Lab. No.	Triaxial Shear Values												Permeability *ft/year*		
	At Standard Proctor at				At Modified Proctor								At Standard Proctor values	Modified Proctor values	
	O. M. C. %		Saturated		3 Layers at				5 Layers at					3 Layers	5 Layers
					O.M.C. %		Saturated		O.M.C.%		Saturated				
	C	(degrees)	C psi	(degrees)	C	(degrees)	C	% (degrees)	C	% (degrees)	C	(degrees)			
2082 ...			8.5	10			20	7							
2086 ...	13	14.5	6	13			18	16							
2080 ...	22	22	4	8			8	25							
1951 ...			12.5				12	11.5					10.8	.1	
1955 ...			5				5	17					15.0	.04	
1960 ...			7	7			6	23					12.0	.3	
1994 ...			0	18			6	21.5					25.12	1.3	
2406 ...	5	10.5	4	5.5	10.5	22	7.5	8	20	25	13.5	14	4.56	.54	.076
2414 ...	6	6.3	6	1.5	23	7.5	12	5	30	17	21	6.5	.004		
2410 ...	9	1	5.2	0	19	5	7	2	20	23	12	17.5	.005	.001	
2417 ...	6	18.5	3.8	4	15	20.5	10	9.5	26	22	18	16.5	.55	.36	.29
2292 ...	30	21.5	20	3.5	36	23	23.5	21	40	27.5	30	22.5	18.2	10.4	.63
2291 ...	12	11.5	8.5	4	20	20.5	16	10.5	24	24.5	17.5	23.0	0.13	0.08	.03

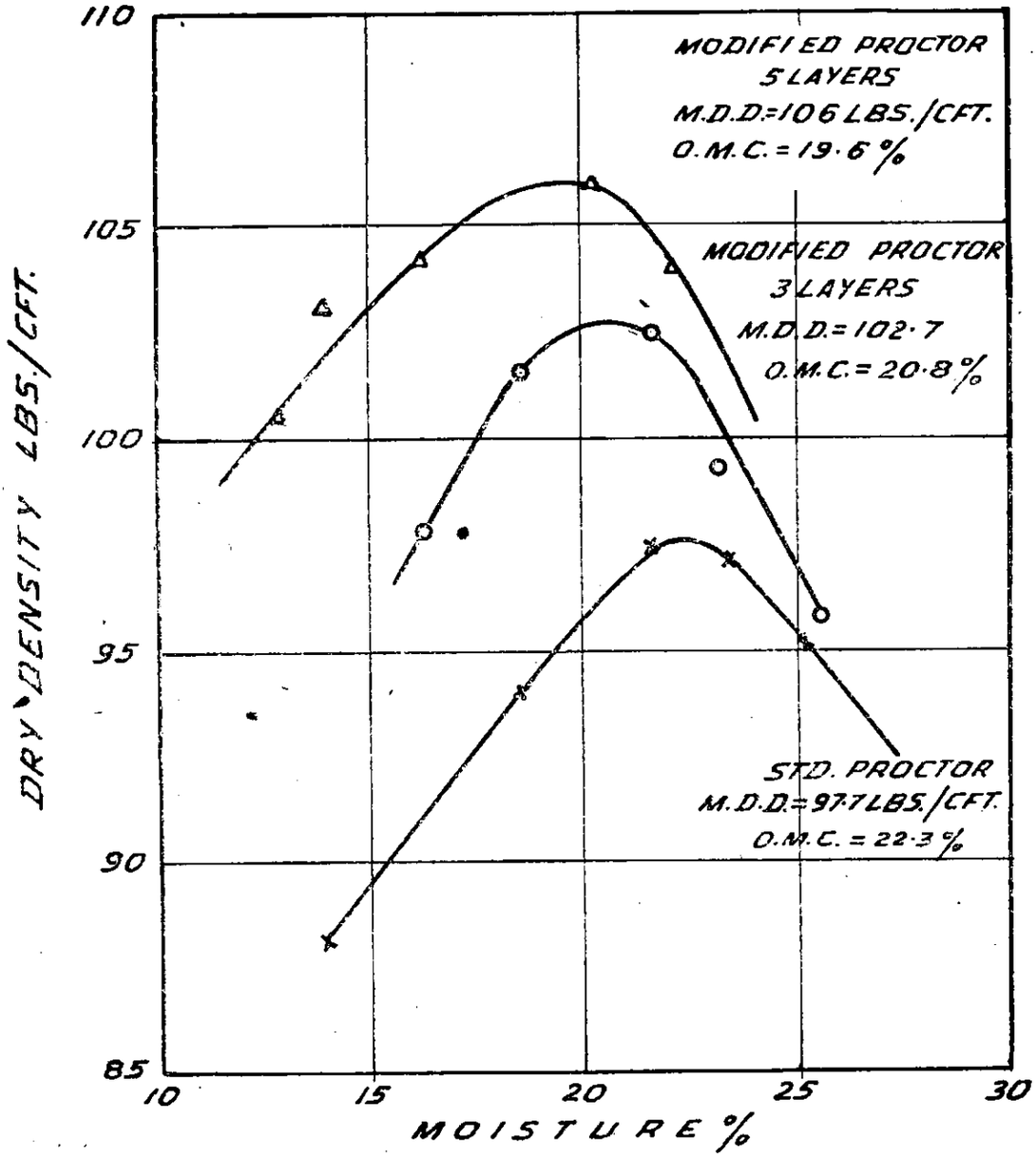

Fig 1.

It will be seen that there is a general increase in both cohesion and angle of internal friction with the increase in compactive energy. This is true for both optimum moisture and saturated moisture content. The increase in shear strength is quite appreciable in many cases. The permeability decreases with increase in compactive energy. In case of sandy soils which are semi-pervious under standard Proctor test became impervious even with modified test in 3 layers.

---

32. Foundation Investigation

I. Tawa Dam Site

A MASONARY *cum* earth dam 2001.32 m (6566 *ft*) long and 54.87 *m* (180 *ft*) high above the deepest foundation is to be constructed across the river Tawa, a tributary of Narmada. The dam site, situated about half a mile downstream of the point of confluence of rivers Tawa and Denva, can be approached from Itarsi and Bagra stations of the Central Railway.

2. Geology and general features

The river Tawa after joining with its major tributary Denva leaves the Satpura ranges at the dam site and flows into the alluvial planes of the Narmada Valley. The main geology at and around the dam site consists of bagra beds and Pachmarhis. The river bed stands at *El* 309.68 *m* (1016 *ft*) whence the terrain rises sharply to *El* 335.28 *m* (1100 *ft*) on the left bank to almost a flat terrace extending 609.6 *m* (2000 *ft*) west to the foot of the hill, beyond which are located the two saddles. On the right bank, however, the land rises gradually to *El* 320.04 *m* (1050 *ft*) with a few depressions in between up to the right abutment. The substratum, which is fissured sand stone, is covered with about 6.10 *m* (20 *ft*) of alluvium on the right bank and river bed, but on the left bank the overburden is quite deep.

3. Foundation investigations

Several pits and bore holes have been made by the Project authorities along the dam axis to ascertain the nature of the foundation material. Further investigations were carried out to ascertain the engineering properties of the overburden with special reference to the permeability characteristics. A series of five deep holes at chainages −304.8 *m* (−10 +00), −213.36 *m* (−7 +00), 15.24 *m* (0 +50), 91.44 *m*(3 +00) and 167.64 *m* (5 +50) and four shallow holes at chainages − 518.16 *m* (− 17 + 00), 259.08 *m* (8 + 50), 350.52 *m* (11 + 50) and 853.44 *m* (28 + 00) were drilled on the left bank to study the nature of the substrata and their permeability characteristics. The substrata were found very hard and dry drilling was not possible with the equipment available. The deep holes were, therefore, drilled by wash boring. The wash materials were continuously observed for logging the strata. Field permeability tests were carried by different methods to suit the local conditions as observed in the different drill holes and pits. All efforts were made to clean the hole by jetting with clean water, brought in limited quantity from a distant source, prior to conducting the field permeability tests. In addition, a few typical block samples from pits already excavated were collected and examined for their texture and permeability.

On the right bank weathered and fissured sand stone was seen at shallow depths in almost all the pits excavated along the axis, except near about chainage 1325.9 *m* (43+50) where the alluvium was fairly deep. No drilling was necessary on this side of the river. Representative soil samples were collected from the pits and examined for their mechanical composition and permeability in undistributed state. In addition, permeability of the deep alluvium at chainage 1325.9 *m* (43 + 50) was determined by filling the pit with water from the adjoining pit at chainage 1386.8 *m* (45 +50). The rates of dissipation and recuperation of the two pits were observed respectively to determine the permeability coefficient of the alluvium.

The test results of the various samples collected are shown in *table 1*. *Table 2* indicates the permeability values as determined at various points by different methods. *Fig 1* shows the plan and *L*-Section of the dam site with location of the bore holes and *fig 2* shows the logging of the bore holes with the permeability values shown against the tested sections.

4. General discussion

The overburden along the dam alignment consists of weathered materials, washed deposits from the adjoining hills and alluvium deposited by the river. The weathered materials are generally sand stone, and purple clay stone which has intruded in the sand stones here and there. The weathered materials are well compacted. The texture of the washed materials varies from sandy clays to silty sands. The river borne materials are classified as medium to coarse sand in the river bed but on the right flank they vary from sandy clay with kankar incrustations to clayey gravels and boulders.

The examination of the trial pits and the drill holes revealed that the hillocks consist partially of weathered sand and clay stone. The valleys along the alignment on the left flank and portions of right flank near the right abutment are covered with washed deposits overlying the weathered materials. The river bed and a part of the right bank is covered with alluvial deposits.

From the examination of pits excavated and bore holes drilled along the alignment, it is evident that the material is suitable for the foundation of an earth dam except near the hillock

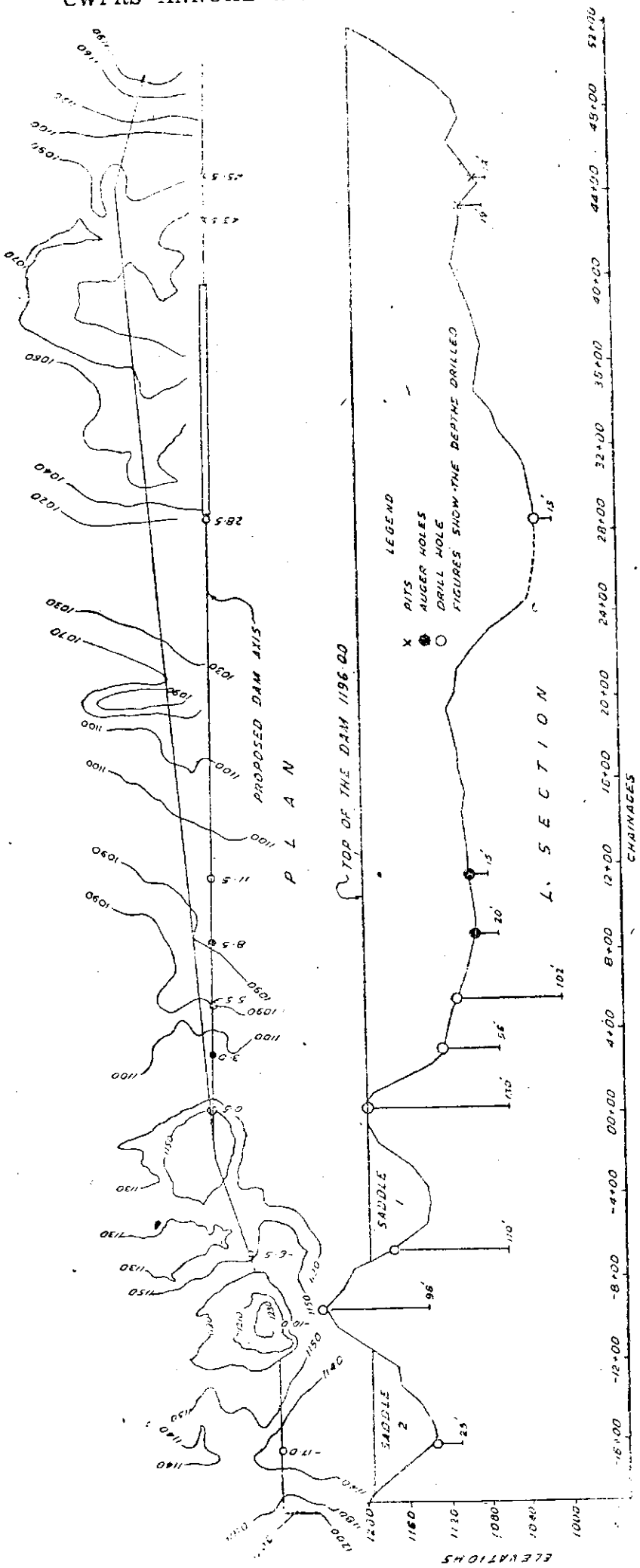

Fig 1: Tawa multipurpose project; showing plan, L. section and location of drill & auger holes and pits tested

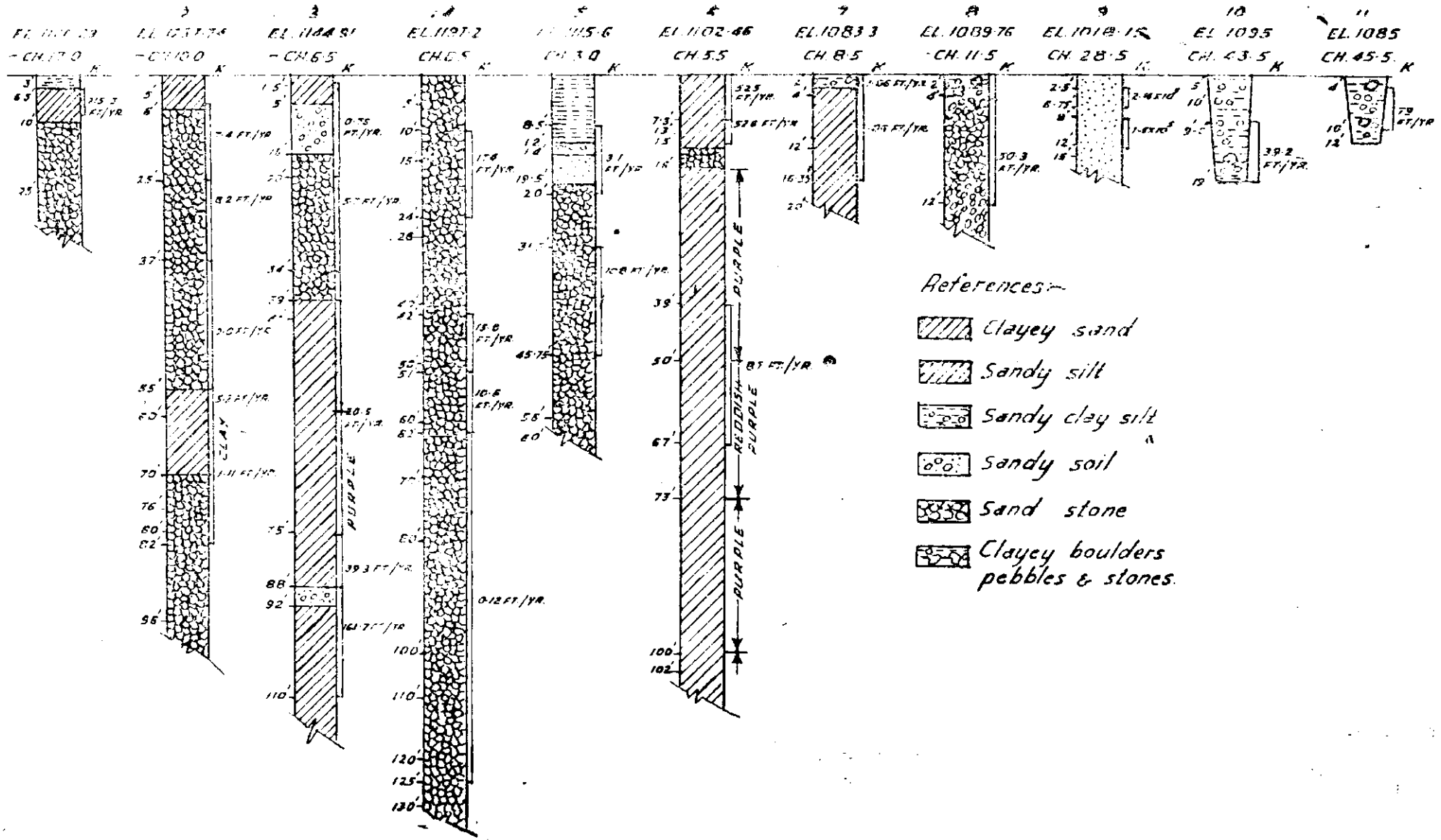

Fig 2: Logging of drill holes (nos 1 to 6 and 9), power auger holes (nos 7 and 8) and pits (nos 10 and 11) along Tawa Dam axis and their respective field permeability values (k).

Table 1 : Results of soil samples from Tawa Project

Sl. No	Lab. No.	Depth ft.	Classification	Mechanical Analysis					Atterberg's Limits		
				Clay .002 mm or less	Silt .002 to .02 mm	Fine sand .02 to .2 mm	.2 to 2 mm	2 mm to 1½"	LL %	PL %	SL %
					D H at Ch —1700						
1	2333	0-2	Clayey sand	10·6	5·5	30.3	47·8	5·8	non-	plastic	...
					Auger hole at zero hill						
2	2330	0-2	Do.	15·1	7.9	18.0	59.0	0	21	...	...
3	2269	0.4	Silty sand	13·0	10.4	16.3	56·3	4	19	not possible	16
4	2270	4-6	Sand	9·2	6.0	17.5	60.1	7.2	36	17	16
5	2271	6-10	Silty sand	14·0	7·3	23.3	50.7	4.7	31	15	15
6	2331	11-12	Sand	2·9	5·3	7.5	83.6	0·7	non-	plastic	...
					D. H at +5·5						
7	2372	0-5	Silty sand	20·3	12·8	19.4	41.1	6.4	28	12	11
8	2373	5-8½	Silty sand	5·8	28·2	12·9	48·2	5·0	32	16	11
9	2374	8½-13	Silty sand	14·5	14·8	12·7	51·0	7·0	26	13	8
10	2375	13-14½	Sandy clay	20·3	20·8	8·8	38·1	2·0	47	22	10
11	2276	15-16	Clay loam	32·7	32·9	9·5	16·5	8·4	44	24	13
12	2257	26½-27½	Clay	35·1	56·9	4·3	3·7	0	43	25	13**
					A. H at 8·5						
13	2277	0-2	Silty sand	21·0	10·2	7·2	37·5	24·1	30	10	13
14	2278	2-4	Sandy clay	33·8	10·0	8·6	37·0	10·6	38	19	11
					Ch. 8·5 Auger hole						
15	2279	4-9	Do.	32·1	15·8	25·4	21·1	5 6	50	24	11
16	2234	9-10	Clay purple	43·3	30.1	7·1	18·7	·8	48	26	12
17	2280	9-16½	Clay purple	47·9	3·3	45·1	3·6	0	49	21	12
					Ch. 11·50 Auger hole						
18	2281	0-2	Sand clay loam	28·3	21·8	22·9	19·3	7·7	41	24	14
19	2282	2-4	Sandy clay	32·3	17.0	17.6	31.0	2·1	43	23	...
20	2283	4-9	Silty sand	18·4	13.0	8.0	52·4	8·2	30	18	11
21	2284	9-11	Sand	11·8	6·3	12·8	52·7	16·4	25	12	10
22	2285	11-15	Sand	11·0	6·5	15·7	57·8	9·0	21	...	...
23	2286	15-21	Sand	13·3	3·2	14·6	61·1	7·8	18	not	possible
					Pit at 45·50						
24	2332	4.5	Sand	3·6	4.5	10.7	76·6	4.6	...	...	...
					Pit at 43·50						
25	2264	0-9½	Clayey sand	17·4	23·3	45·1	7·6	6·6	...	...	...
26	2265	9½ onward	Sandy gravel	8·0	3·4	5·7	6·7	76·2	39	20	12

**C = 8 p. s. i.
ϕ = 32.5°
Dry Density = 122·2 *lbs/cft*
% Moisture = 12.4

at *ch* : 00 *m* (0 + 0) and the portion from *ch* : 1524 to 274.32 *m* (5 + 00 to 9 + 00).

Loose boulders with big cavities in between were observed on the southern and eastern side of the hillock. The bore drilled at *ch* : 15.24 *m* (0 + 50) showed a great water loss at a depth between 7.92 to 12.19 *m* (26 to 40 *ft*) which shows the presence of large cavities. It will be necessary to remove the loose boulders from the foundation here and if found anywhere else on the slope of the two hills.

Table 2: The results of Permeability Test

Sl. No	Chainage	Type of test	Test section in *ft*	Permeability ($=K$) value in *cm/sec*
1	−17	Bl	0–2	*1.06×10^{-3}
2	,,	R	3–6.5	2.08×10^{-4}
3	−10	B	5–32	6.85×10^{-6}
4	−10	R	5–25	7.15×10^{-6}
5	,,	R	25–37	7.92×10^{-6}
6	,,	R	37–55	1.93×10^{-6}
7	,,	R	55–60	5.12×10^{-6}
8	,,	R	60–82	1.07×10^{-6}
9	−6.5	D	1.5–20	7.34×10^{-7}
10	,,	D	20–34	5.5×10^{-6}
11	,,	D	34–75	1.99×10^{-5}
12	,,	B	34–75	2.17×10^{-5}
13	,,	B	75–87	3.79×10^{-5}
14	,,	D	87–110	1.58×10^{-4}
15	·5	Bl	0–2	1.01×10^{-4}
16	·5	Bl	11–12	2.15×10^{-4}
17	,,	D	9.5–24	1.68×10^{-4}
18	,,	D	42–51	1.52×10^{-5}
19	,,	D	52–62	1.02×10^{-5}
20	,,	D	62–125	1.16×10^{-7}
21	3	B	8·5–20	3.00×10^{-6}
22	,,	B	31·5–45.75	1.01×10^{-4}
23	5·5	D	0–7·5	5.07×10^{-4}
24	,,	R	7·5–13	5.08×10^{-4}
25	,,	B	34–67	8.40×10^{-5}
26	8·5	Bl	3–0	1.80×10^{-6}
27	,,	D	4–16.35	5.80×10^{-8}
28	11.5	B	0–11.5	7.50×10^{-5}
29	11.5	D	0–11.5	4.86×10^{-5}
30	28·5	B	2·5–6.75	2.06×10^{-1}
31	28·5	B	8–12	1.35×10^{-1}
32	43.5	Bl	4	1.54×10^{-6}
33	43.5	D	Depth = 9–19	3.79×10^{-5}
34	45 5	R	4–10	7.63×10^{-5}
35	11	Bl	10	1.49×10^{-5}

* The block had holes to give passage to water.

Note:—R = Recuperation test B = B test
D = Dissipation Bl = Block

The depth at which the purple clay layer starts between *ch* 152.4 to 274.32 *m* (5 + 00 to 9 + 00) varies from .61 to 4.88 *m* (2 to 16 *ft*) below the ground level. The clay at shallow depths will get exposed even during stripping and as it is very deep, it is not possible to remove it completely. Undisturbed samples collected from the clay layer show that it had a dry density of 1.95 *gms/cc* (122 *lbs/cft*). One sample collected from a depth of 8.23 *m* (27 *ft*) during the course of drilling the hole at *ch* 167.64 *m* (5 + 50) revealed that shear properties are quite good but the clay is fissured even at that depth. So the clay will crack on exposure to the atmosphere and extra care will be required during construction in this region. Attempt should be made to cover the excavated portions immediately to avoid shrinking and cracking of the clay layer.

To study the perviousness of the foundation, it may be divided in three portions *viz* left bank and saddles, river bed, and the right bank. The characteristics of the three portions are discussed below :

5. Left flank and saddles between *ch* −621.8 to 731.52 *m* (− 20.4 to +24.0)

The overburden mainly consist of weathered materials except in low lying areas where the weathered materials are covered with washed materials from the surrounding hills. The weathered sand stone is fairly compact and has given a maximum permeability of the order of 1.7×10^{-4} *cm/sec* (174 *ft/year*) at *ch* 15.24 *m* (0+50). The permeability of the washed materials is 5.07×10^{-4} *cm/sec* (525 *ft/year*) as determined in the bore hole at *ch* 167.64 *m* (5.5), depth 2.29 to 3.96 *m* (7.5 to 13 *ft*). In the bore at *ch* 167.64 *m* (5.5), depth 11.39 to 20.42 *m* (39 to 67 *ft*), the purple clay had also given a maximum permeability of 7.1×10^{-5} *cm/sec* (84 *ft/year*) and this high value is attributed possibly to the slipping between casing and sides of the drill holes. Even then the permeability figures are not high to require any special treatment and it should be sufficient to embed the cut off trench in the weathered, sand stone or the clay stone.

The drill hole at *ch* 15.24 *m* (0+50) requires a particular mention. It has already been suggested to remove the boulders occurring on the south eastern side, and the depth of cut may be about 12.19 *m* (40 *ft*). Further the upstream side of the hill has got a very steep slope and the weathered sand stone which has given a maximum field permeability of 1.7×10^{-4} *cm/sec* (174 *ft/year*) will get exposed on stripping and may disintegrate further in the course of time when it will come in contact with water. An impervious layer along the upstream side, to avoid further disintegration of the sand stone, would be desirable.

6. River bed between *ch* 731.52 to 944.88 (24 to 31+00)

The bed is covered with a layer of medium to coarse sand, having a maximum depth of about 6.10 *m* (20 *ft*). Rock out crops are also seen near the banks. The permeability test carried out in the sand layer gave a permeability of 2.1×10^{-1} *cm/sec* (2.14×10^{5} *ft/year*) and by Hazen's formula the permeability comes out to be 10^{-1} *cm/sec* (10^{5} *ft/year*). The permeability is very high but the sand layer is fairly shallow. Pumping out water for excavating the foundation and back filling it with clay may be feasible and best. The cut off here should be properly embedded into the left flank to prevent the water from the river course finding an outlet through this junction.

7. Right flank 944.88 to 1615.44 *m* (*ch* 31.0 to 53.0 *ft*)

The spillway and the masonry walls are to be constructed between *ch* 991.06 to 1296.01 *m* (32+51 to 42+52) and hence the foundation is to be excavated upto rock in this reach.

The fissured and partially weathered sand stone occurs at 1.83 to 2.44 *m* (6 to 8 *ft*) depth in the remaining portion coming under the earth dam except between *ch* 1296.01 to 1402.08 *m* (42+52 to 46+00). The depth of the deposit here varies from 2.44 to 6.1 *m* (8 to 20 *ft*). The permeability of the clayey gravel layer as determined at chainage 1325.88 *m* (43 + 50 is 6.7×10^{-5} *cm/sec* (39 *ft/year*) and that of the sandy clay layer as observed at *ch* 1386.84 *m* (45 + 50) is 7.5×10^{-5} *cm/sec* (79 *ft/year*). The permeability values are not very high and can be ignored but for the sake of uniformity, the cut off in the portion between 1296.0 to 1402.08 *m* (42+52 to 46+00) coming under the earth dam should be embedded in the partially weathered and fissured sand stone as will be done in the other reaches.

As the material in the foundation is very heterogeneous and some pockets of pervious materials may exist here and there, a series of grout holes should be done in order to intercept the pervious pockets in the foundation.

II. Thanneermukkom Regulator

THE THANNEERMUKKOM Project envisages the construction of a regulator at Thanneermukkom to regulate the flow of water between Vembanad Lake and the back waters of the sea at Cochin. The main regulator structure is 1244 *m* (4082 *ft*) in length and includes 93 piers. The distance up to 31st pier on the Western side has been enclosed in a ring bund. The piers of the regulator will be founded on a group of 40.6 *cm* (16 *in*) diameter *cast-in-situ* concrete piles. Each pile carries a load of 31.4 *metric tons* (32 *tons*). The piling work is being done by M/s Simplex & Company. Foundation investigation for finding subsoil condition and the depth of hard stratum for pile foundation have been carried out by the Soil Division.

2. General physical features

The regulator is situated in the Vembanad Lake, which lies in the back water zone of the sea at Cochin. The bed of the lake is made up of alluvial deposits brought by rivers and by the back water of the sea and consists of sands, silts, clay, partially decomposed plant residue and organic matter.

3. Programme of work

To find out the depth of hard stratum and subsoil condition and for calculating the frictional resistance and end bearing of *cast-in-situ* concrete piles, following field and laboratory investigations have been carried out.

(i) Bore holes and undisturbed sampling of various strata
(ii) Standard penetration tests and cone penetration tests in the bore holes
(iii) Cone penetration test outside bore holes
(iv) Density, moisture content, unconfined compression test, triaxial tests, atterberg limits and mechanical composition of the samples.

4. Methods adopted for field investigations

(*i*) *Boring and undisturbed sampling.*—Generally dry boring and cleaning by muck barrel was adopted. Occasionally wet methods including jetting, bailing, and sand pumps were used for advancing the bore hole when it was not found possible to advance by dry method. Undisturbed samples were taken at every 1.52 *m* (5 *ft*) interval or at change of stratum. After each undisturbed sampling standard penetration test using Terzaghi's standard split spoon sampler with

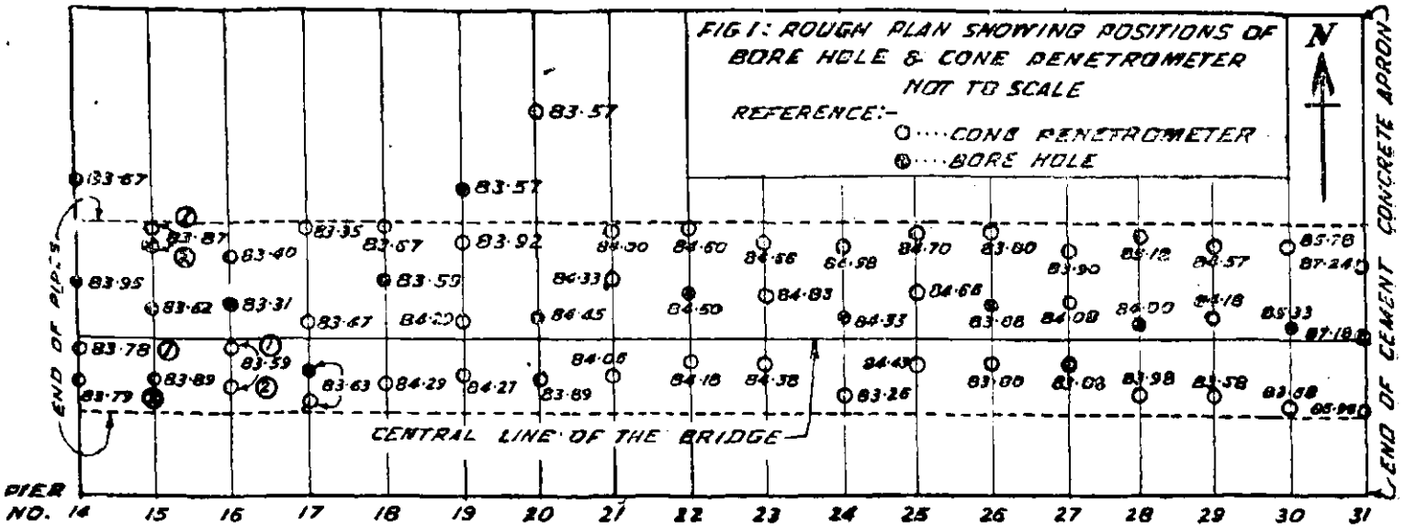

476 *kg/m* (350 *ft/lb*) energy per blow was carried out. Cone penetration tests were also carried out in the bore holes when neither undisturbed sampling nor standard penetration test was feasible.

(*ii*) Cone penetration tests to find the depth of hard stratum were carried out at 2-3 points at each pier site using 63.5 *kg* (140 *lb*) monkey with (30 *in*) .76 *m* fall, .05 *m* (2 *in*) cone (60°) and drill rods of .041 *m* ($1\frac{5}{8}$ *in*) size without casing pipe. Torque was given at every 1.52 *m* (5 *ft*) interval to lessen the friction between rods and soil.

5. Laboratory tests

Mechanical analysis, Atterberg limits for disturbed and undisturbed samples and density, moisture content, unconfined compression test for undisturbed samples were carried out in the laboratory.

Triaxial shear tests have been carried out for a few representative samples. In order to assess the actual friction mobilised between soil and concrete piles, direct shear test using concrete block in the lower box and soil at field density and moisture content in the upper box was conducted. The normal load for direct shear tests was calculated assuming that earth pressure at rest, acts on piles at various depths.

6. Results and discussion

Fig 1 shows the general lay out and location of bore holes and penetration test points. The various strata met with are shown in *fig 2*. The typical logging of bore holes, penetrometer test data and properties of undisturbed samples *etc* are shown in *fig 3*.

It will be seen from *fig 2* that generally soil strata met with are as follows:

(i) Loose sandy soil with little amount of fines. This is the deepest layer of about 7.0 — 8.5 *m* (23-28 *ft*)

(ii) Black soft clay varying in thickness from .3-2.7 *m* (1 to 9 *ft*)

(iii) Black clay with medium sand varying in thickness from .84-2.89 *m* (2.75 to 9.5 *ft*)

(iv) Lateritic clay with and without nodules varying in thickness from 1.83-4.88 *m* (6.5 to 16 *ft*)

(v) Black medium clay varying from 0-6.25 *m* (0-20.5 *ft*)

(vi) Dark-brown clay with organic matter varying from 0-6.4 *m* (0-21 *ft*)

(vii) Hard stratum, indurated sand with small amount of lateritic clay.

Though the nature and sequence of various strata are almost similar in the area investigated, it can, however, be broadly divided into four zones with regard to the depth of hard stratum. The first zone between 14th pier to 19th pier, the hard stratum is met with at a depth of 22.5 to 24.4 *m* (74-80 *ft*). At 20th pier, the hard stratum is met with at 21.3 *m* (70 *ft*). Between 21st to 28th piers the depth of hard stratum lies within 17.2-18.6 *m* (56.5 to 61 *ft*). Hard stratum dips down again from 18.3 *m* (60 *ft*) at 28th pier to 23.2 *m* (76 *ft*) at 30th pier. The black medium clay is present below lateritic clay layer in pier 15th to 23rd and 28th to 31st. The dark-brown

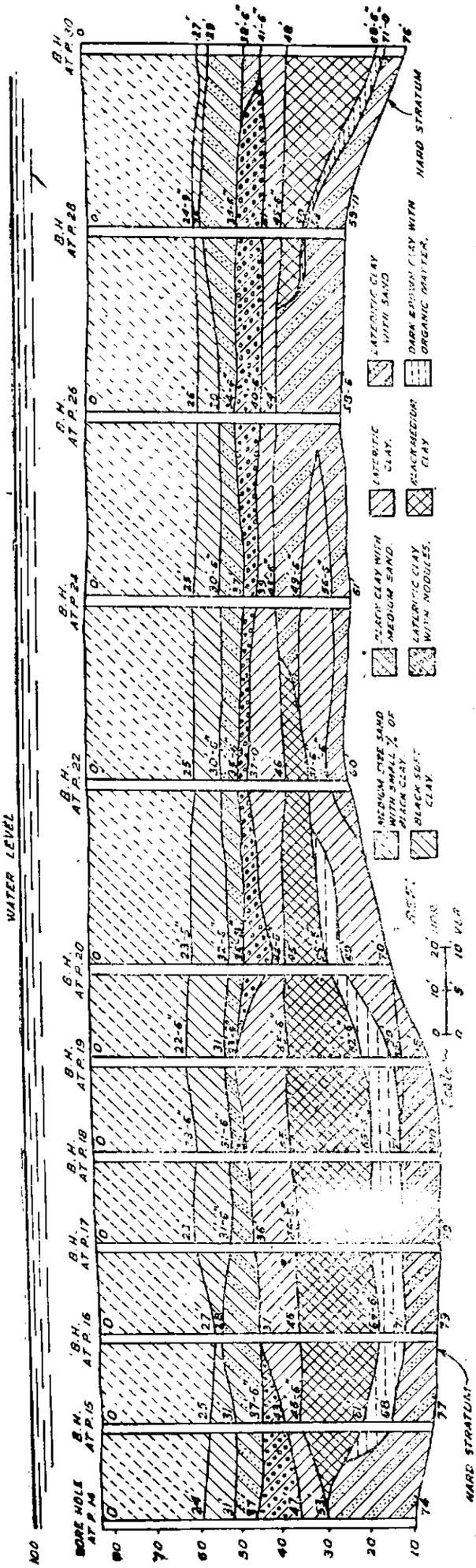

Fig 2: Sub-surface soil strata from pier 14 to 30.

clay with organic matter is present in piers 15th to 21st and 28th to 31st. A second lateritic clay layer is present in piers 19th to 25th below the black medium clay.

The depth of hard stratum as obtained by penetration tests and from the bore hole records are given in *table 1*. The results show that there

Table 1: Elevation of hard stratum with respect to *M S L* at Thanneermukkom Barrier Site

Pier No	Pier from B. H. or cone penetrometer			Pier No	Pier from B. H. or cone penetrometer		
	North end	Centre	South end		North end	Centre	South end
14 ...	-87.3	-90.0	-92.2	23 ...	-72.3	-75.2	-75.6
15 ...	-87.1	-93.4	-90.1	24 ...	-69.4	-76.7	-81.7
16 ...	-91.6	-95.7	-96.7	25 ...	-83.3	-81.3	-78.6
17 ...	-89.6	-95.5	-92.4	26 ...	-80.2	-74.5	-76.2
18 ...	-97.3	-96.4	-93.2	27 ...	-76.1	-74.9	-77.1
19 ...	-86.1	-88.7	-94.4	28 ...	-79.8	-76.0	-76.0
20 ...	-89.4	-85.5	-86.1	29 ...	-83.4	-83.8	-74.3
21 ...	-85.0	-81.7	-80.9	30 ...	-90.2	-90.7	-88.3
22 ...	-77.4	-75.4	-75.8	31 ...	-88.8	-87.8	-86.0

is a difference in the depth of hard stratum in the same pier. Though this difference is not appreciable in most of the places, at piers, 24th and 29th the difference is quite appreciable. In these places special care may be taken for proper set of the piles. The resistance offered by cone penetrometer may be due to local lenses, which should be pierced while driving the piles. It was generally noticed during boring that holes were filled with water when bore hole reached the top of hard stratum or the layer just above it. At the 16th pier the head of water was 2.13 *m* (7 *ft*) above ground level. At 17th, 18th and 19th piers the velocity of water was also appreciable. It could, therefore, be concluded that the top of hard stratum was generally pervious and water bearing.

7. Frictional resistance of piles

A summary of results on undisturbed soil samples from various strata are given in *table 2*. The value for frictional resistance between concrete and various soil types obtained by direct shear test is also incorporated in the table. The lowest value of the three tests namely triaxial, unconfined and direct shear has been taken for the estimation of skin friction on piles. The data on skin friction (*table 3*) of piles as obtained for different piers show that skin friction upto the hard stratum varies from 44 to 59 *tons*. It is thus evident that skin friction is not sufficient for the proposed load on each pile (32 *tons*) with adequate factor of safety.

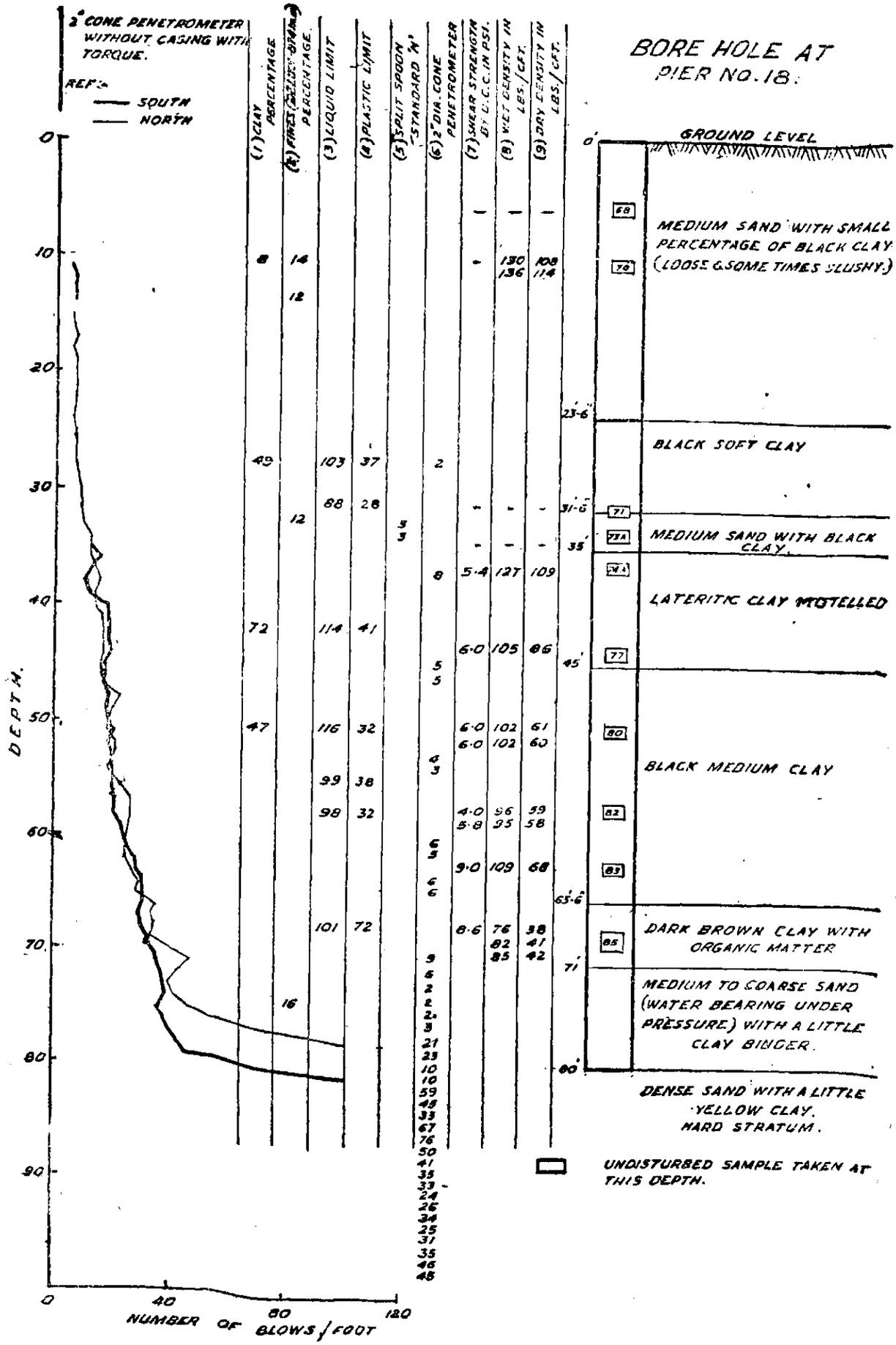

Fig 3: Bore hole and penetrometer data for pier

Table 2 : Results showing Shear Strength of Principal soil types and their frictional resistance with concrete surface

Sl. No	Soil Type	Dry Density γ_D *lbs/cft*	Average submerged density γ' *lbs/cft*	Natural moisture content W	Approx. earth pressure at rest on pile at mid depth *lbs/cft*	Unit friction between concrete and soil in Direct Shear		Average shear strength by *UCC* *lbs/sft*	Average Triaxial shear		Value taken for design
						Normal Load	Unit friction *lbs/cft*		C *lbs/sft*	ϕ in degree	
1	Medium sand with little percentage of black clay	108·5	44	19·4	265	287·5 412·5 527·5	δ between soil and concrete = 25° 98·5* *lbs/ ft²*	...	...	...	98 *lbs/sft²*
2	Black soft clay ...	58·4	35	71·3	563	563·0	162·5	305	360	1	160
3	Black clay with medium sand.	93·8	49	29·0	736	737 5	262·5	288	...	...	260
4	Lateritic clay with nodules.	101·0	47	26·5	1080	1102·0	1150·0	792	612 C + N Tan ϕ = 756	8	750
5	Lateric clay ..	81·0	46	41·6	1162	1162·0	412·5	610	1000	3·5	400
6	Black medium clay ..	62·4	38	63·6	1430	1440·0	487·0	720	1000	2	500
7	Bluish stiff clay ...	83·0	...	38·7	...	...	...	720	576 C + N Tan ϕ = 826 (min.)	8	720
8	Coarse sand with lateritic clay.	130·0	...	15·0	...	...	...	1080	...	...	1080

* $f_s = K_s \tan\delta\ \gamma' \frac{D}{2}$

$= \cdot 186 \times 12 \times 44$

Apparent Cohesion got in sand neglected.

f_s = Unit skin friction *lbs/sft*

K_s = Earth pressure coefficient at rest = ·4

$\tan\delta = \tan 25° = \cdot 465$

γ' = 44 *lbs/cft*

D = Depth of stratum

Table 3: Bearing capacity and frictional resistance of piles in various piers

	PIER *No*											
	14	15	16	17	18	19	20	22	24	26	28	30
Skin Friction in *tons*	54	50	46	59	45	59	55	44	46	53	51	58
*Terzaghi's Theory Point Bearing in *tons*.	113	104	112	117	117	115	112	98	103	94	98	119
Mayerhof's method from 'N' values Point bearing in *tons*.	388	431	282	205	149	156	226	247	253	318	142	445

*Angle of Internal friction = 35° taken same for all.
Cohesion $C = O$

Terzaghi's Theory $Q_p = A_p\ (\gamma' D_f N_q + \cdot 6 \times r \times \gamma' N\gamma)$

Where $N_q N\gamma$ are Bearing Capacity Factors ;

$\phi = 35°$; $N_q = 42$, $N\gamma = 41$

$C = O$

r = Radius of pile shoe in *ft*

γ' = Average density in *lbs/cft* (submerged)

Df = Depth of pile point from *GL*

Mayerhof's Theory $Q_p = A_p \cdot 4N$. Tons.

Where A_p = Area of Point of Pile shoe in *sq ft*

N = Terzaghis Standard penetration *blows/ft* depth

$= \frac{1}{2} N_1$ (N_1 Dynamic cone penetration *blows/ft* depth).

Table 4

Sl *No*	Sample *No*	Pier *No*	SIZE OF PARTICLE (in *mm*) %										
			.002	.002 to .02	.02 to .05	.05 to .149	.149 to .21	.21 to .59	59 to 1·49	1·49 to 2·38	2·38 to 2·58	*D* 15	*D* 10
1	1	14	9·8	2·1	·6	1·5	1·1	50·0	25·0	9·9	...	·2	·0025
2	69	18	8·2	3·8	1·5	2·4	1·9	42·7	36·0	3·7	·3	·14	·009
3	74	19	7·0	3·5	1·5	1·5	2·7	32·9	28·4	22·2	·3	·17	·013
4	102	20	7·8	3·2	1·0	2·4	6·2	43·8	31·2	4·4	...	·12	·0037
5	125	22	8·4	4·1	1·5	2·7	4·4	30·5	41·5	5·7	1·2	·054	·0043
6	143	26	7·9	14·9	4·3	2·0	2·8	42·9	22·2	3·0	...	·0063*	·0025
7	153	28	8·1	5·0	1·8	1·7	4·1	38·0	39·2	1·8	·3	·053	·008
8	171	30	6·3	2·8	1·2	0·9	1·9	40·2	43·7	2·6	·2	·230	·04

* Minimum D_{15}

It had not been possible to take any undisturbed samples of the hard stratum and even it was not possible to carry out standard penetration tests in the bore holes. To find out depth of hard stratum and its compactness, the cone penetration tests were carried out in a number of bore holes. The test data showed that the hard stratum extended more than 4.6-6.1 *m* (15-20 *ft*). The minimum cone penetration data for the hard stratum showed that the angle of internal friction could be taken above 35°. With 35° angle of internal friction, the bearing capacity of the piles had been calculated according to Terzaghi's formula. The bearing capacity of each pile was of the order of 100 *tons*. Bearing capacity had also been estimated by Mayerhof's Method (*Proc ASCE Journal*, Soil Mechanics and Foundation Division: January 1956). The bearing capacity worked out much higher than Terzaghi's equation. The results are shown in *table 2*.

8. Top Sandy Stratum

The results of mechanical analysis of this stratum from different piers are given in *table 4*.

It will be seen that the material contains appreciable amount of silt and clay. The minimum D_{15} of the material is of the order of .006 *mm*. This type of material will not be amendable to clay-cement of Bentonite grouting. Only chemical grouting may be feasible. However it may be pointed out that the layer is not pervious to any appreciable extent as observed during drilling.

9. Conclusion

As the logging of soil strata shows the presence of a highly compressible layer of dark-brown clay with organic matter, at a depth of 18.6-21.6 *m* (61 to 71 *ft*) between 15th pier to 21st pier, it is essential that the pile should penetrate this layer, otherwise settlement will be considerable. As frictional resistance is not sufficient for the proposed load with adequate factors of safety, it is necessary that the piles should be driven to hard stratum which is present below the lateritic clay layer. It has been observed that hard sand stratum and the layer just above it are some times pervious and water bearing. Great care is necessary in making *cast-in-situ* concrete pile. Use of quick setting cement or a special lining in the lower portion of the piles may be considered.

III. Right Flank, Liganamakki Dam

A 2383.54 *m* (7820 *ft*) long and about 60.96 *m* (200 *ft*) high dam is being constructed across the *river Sharavaty* at Linganamakki Site under the Sharavaty Valley Hydroelectric Project, Mysore. Granitic gneiss and hornblende schist are the main rocks found along the dam alignment. A band of dolrite dyke occurs near the right bank of the river. Due to the tropical climate with heavy rainfall, the rock in the area is covered with a deep overburden of lateritic soils except in the river bed portion.

A masonry structure was proposed for the dam. However, during the excavation and further drilling a fault zone was observed between 1844.04 to 1889.76 *m* (*Ch* 60+50 to 62+00) along the centre line of the dam. It was observed in the drill hole at 1859.28 *m* (*Ch* 61+00), 15.24 *m* (50 *ft*) downstream that the rock was not available even at *El* 470.92 *m* (1545 *ft*), So an earthen dam is being constructed between 1749.55 to 2292.10 *m* (*Ch* 57+40 to 75+20), the rest between 0+00 to 1749.55 *m* (*Ch* 00+00 to 57+40) being masonry.

Between 1889.76 to 2255.52 *m* (*Ch* 62+00 to 74+00), the excavation had been done upto the fissured rock level except between 2103.12 to 2194.56 *m* (*Ch* 69+00 to 72+00) and the trench had been filled with about 3.66 *m* (12 *ft*) layer of compacted impervious soils.

The present investigations have been carried out to find the nature of materials, in the fault zone between 2103.12 to 2194.56 *m* (*Ch* 69+00 to 72+00) and 2255.52 to 2292.10 *m* (*Ch* 74+00 to 75+20).

2. Field investigations

Five bore holes were drilled for the purpose at 2278.08, 2180.84, 2150.36, 2119.88 and 1870.56 *m* (*Ch* 74+74, 71+55, 70+55, 69+55 and 61+37). The location of the bore hole is shown in *fig 1* showing the contour plan of the earthen portion.

The overburden is sandy in nature and dry drilling was not feasible with the equipment available. Wash boring was adopted and practically no undisturbed sample was collected.

Field permeability tests were carried out by one or more methods to suit the test length in the different bore holes. Field permeability tests were also carried out in two bore holes drilled by the contractor in the fault zone at 1844.04 *m* (*Ch* 60+50) and 24.38 *m* (80 *ft*) downstream and 1828.80 *m* (*Ch* 60+00), 24.38 *m* (80 *ft*) downstream of the central line.

In addition a few undisturbed samples of different types of soil from the sides of the excavated foundation, were collected and tested for size distribution, permeability, moisture, density and shear characteristics.

3. Results and discussion

Lateritic soils and weathered rock form the foundation material for the earth dam. The re-

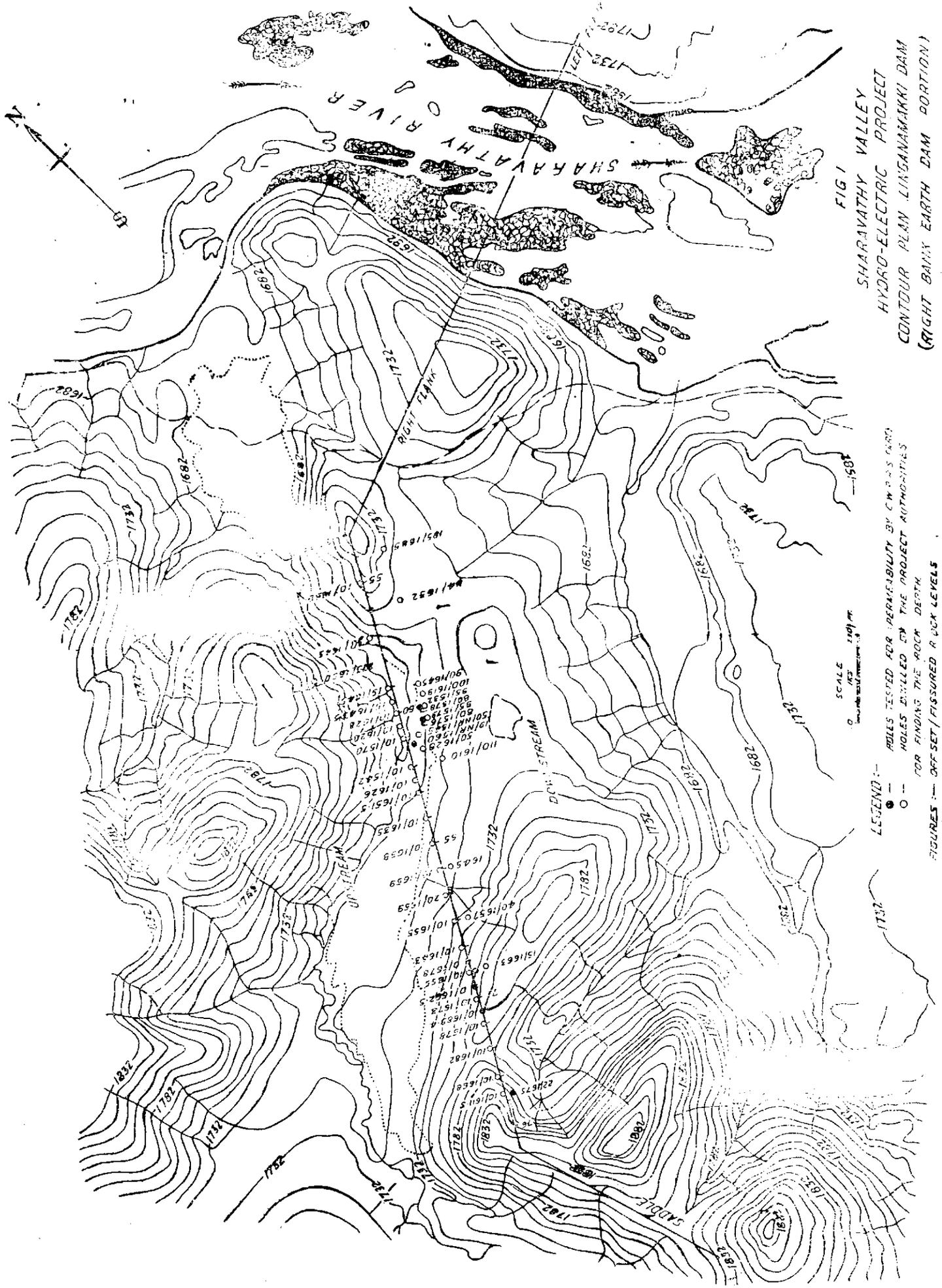

FIG 1
SHARAVATHY VALLEY
HYDRO-ELECTRIC PROJECT
CONTOUR PLAN LINGANAMAKKI DAM
(RIGHT BANK EARTH DAM PORTION)

Table 1: Results of samples collected from the sides of the excavated trench and drill holes

Lab *No*	Location			Description of Material	Mechanical Analysis					*In situ*		U. C. C.	Triaxial Shear		K
	Chainage	Off/set	Elevation		Clay .002 *mm*	Silt .002-.02 *mm*	F. S. .02-.2 *mm*	C. S. .2-2.0 *mm*	Gravel above 2.0 *mm*	M. C. *percent*	D. D. *lbs/cft*	(e) *Psi*	ϕ in degrees	C *Psi*	Permeability *cm/sec* 10^{-5}
1	2	3	4	5	6	7	8	9	10	11	12	13	14	15	16
D16	5900	68U	1662.7	Greenish Sand ...	2.7	9.3	42.8	38.6	6.6	19 6	89.9				
D17	5958	78U	1665.4	Light Grey Silty Sand ...	4.6	17.6	42.9	34.3	.6	26.9	74.5				
D18	6002	163D	1658.4	Dark-brown & Greenish sand.	6.2	7.3	36.1	50.4		25.4	91.6				
D15	6005	163D	1658.4	Whitish Silty-sand ...	3.5	19.6	47.0	29.6	.3	23.5	83.2				
D13	6095	180D	1675.4	Light-brown clayey sand.	28.8	14.7	27.0	18.9	10.6	13.4	87.7				
D14/P9	6105	165D	1669.3	Whitish yellow silty-sand.	5.2	22.0	45.6	25.6	1.6	19.1	73.5	4.0	24	4	100.7
P10	6235	153D	1671.6	Mottled grey & yellowish white silty sand.	3.4	24.0	59.2	12.1	1.3	31.4	83.5	3.2	22.5	0	22.2
D12	6245	124D	1665	Greenish silty sand ...	3.7	18.1	38.9	32.2	7.1	25.0	85.4				
D11/P5	6362	142D	1681	Reddish-brown silty sand.	4.8	17.8	45.8	31.1	.5	38.3	60.4	4.4	29.5	0	68.4
D10/P6	6577	146D	1696.4	Pinkish silty sand ...	10.1	26.0	31.0	27.9	5.0	40.1	74.3	1.5	6	6	8.2
D9/P7	6955	137D	1703.5	Mottled Yellow & Dark-brown silty sand.	5.1	20.8	50.0	23.9	.2	34.2	77.9	6.5	13	3.5	6.4
D8/P8	7075	95D	1706	Pinkish & yellowish silty sand.	7.5	29.3	39.5	22.0	1.7	34.4	78.5	3.9	7	8	7.1
D7/P3*	7075	52U	1707	Greenish yellow silty sand.	4.4	20.2	41.7	27.5	4.8	31.2	89.8	2.6	7	7.5	12.1
D6/P4	7270	65U	1713.5	Do	2.0	27.2	41.2	29.0	.6	39.0	78.3	4.2			8.0
D1/P1†	7448	61U	1736	Pinkish silty sand ...	2.4	23.0	38.4	30.5	1.6	22.1	94.3	5.9	27	0	7.2
P2	7448	62U	1736	Pinkish sand ...								2.9			10.4
D2	7457	61U	1745	Pinkish silty sand ...	6.2	23.0	48.2	20.8	1.8	23.9	79.9				
D3	7466	61U	1754	Do	8.6	24.9	44.1	22.0	.4	23.0	88.6				
D4	7475	61U	1763	Do	10.3	43.9	35.9	9.9		30.1	77.0				
D5	7484	61U	1773	Do	6.9	20.5	46.2	24.6	1.8	19.5	81.1				
AD1	6955	on *CL*	1690–1685	Reddish Brown-clay ...	44.7	30.4	13.4	10.9	.6						
AD2	6955	,,	1686–1680	Do	43.4	26.2	16.5	11.7	2.2						
AU3	6955	,,	1680–1679	Do						32.8	93.6	14.9			
BD1	7055	,,	1694.5–1689.5	Do	39.2	30.8	16.2	12.9	.9						
BU2	7055	,,	1689.5–1688.5	Do						33.4		19.6			
CD1	7158	,,	1700 –1695	Do	44.5	25.3	10.3	10.6	9.3						
CD2	7158	,,	1695–1690	Do	40.7	18.2	12.5	23.9	4.7						
DD1	7474	22D	1725–1720	Pinkish silty sand ...	12.0	21.0	19.6	35.6	11.8						
BU2	7474	22D	1719.6–1718.6	Do	5.8	27.7	32.3	33.9	.3	25.8	98.8		17	5.5	
DD3	7474	22D	1719.6–1718.25	Do	10.7	21.0	36.1	31.5	.7						
DU4	7474	22D	1715–1714	Do						27.2	96.4	9.0			
DD5	7474	22D	1715–1710	Do	8.6	31.9	39 0	20.5							
DU6	7474	22D	1710–1708.8	Do	6.5	18.3	39.0	35.4	.8	22.5	109.2	5.2			
DD7	7474	22D	1710–1705	Do	11.9	23.0	26.5	32.7	5.9						
DU8	7474	22D	1705–1704	Do	8.6	20.6	26.3	40.7	3.8				26	0	
DD9	7474	22D	1705–1700	Do	11.8	25.1	30.4	28.7	4.0						
DU10	7474	22D	1700–1699	Yellowish grey silty sand.	8.6	16.9	32.4	36.9	5.2	23.3		Sample split			
DD11	7474	22D	1700–1695	Do	5.1	20.9	41.2	30.9	2.0						

sults of the block samples collected from the sides of excavated trench (*table 1*) show that:

(i) the soils are generally sandy in texture

(ii) the density of the soils varies from 0.97 to 1.51 *gm/cc* (60.4 to 94.3 *lbs/cft*) with an average of 1.30 *gm/cc* (81.5 *lbs/cft*).

(iii) The angle of internal friction and cohesion of the samples saturated in the laboratory vary from 6 to 29.5 and 0 to .56 (0 to 8) with an average value of 17 degrees and .25 *kg/cm* (3.5 *psi*) respectively.

(iv) The permeability of the foundation materials as determined by the falling head permeameter varies from 6.4×10^{-5} to 100.7×10^{-5} with an average of 25.1×10^{-5} *cm/sec*.

The results of the investigations carried out in the year 1956 and now show that the engineering characteristics of the overburden are not quite satisfactory. The density is poor, but the soils are sandy in texture. The soils may consolidate quickly and the engineering characteristics may improve.

Fig 2 shows the logging of the bore holes and the results of the *in situ* permeability tests for different lengths tested by different methods. The logging shows that the materials found below the present ground level are classified as pinkish silty sands, yellowish grey silty sands to sand *ie* weathered gneiss and fissured rock.

A 7.62 *m* (25 *ft*) layer of pinkish lateritic soil was present only in the bore hole at 2278.08 *m* (*Ch* 74+74) below which the yellowish grey weathered gneiss extended for another 7.01 *m* (23 *ft*). Fissured gneiss and pegmatite were present in the bore holes at 2180.84 and 2119.88 *m* (*Ch* 71+55 and 69+55) respectively just below the compacted impervious fill.

Yellowish grey weathered gneiss was present in the bore holes at 2150.36 and 1870.56 *m* (*Ch* 70+55 and 61+37) for about a depth of 6.1 *m* and 28.96 *m* (20 and 95 *ft*) respectively below the impervious fill level.

It may be mentioned here that the *in situ* permeability tests carried out by different methods *viz* recuperation test, '*B*' test of the *USBR* and Thies's test have got their own limitations and as such are not expected to give identical values by different methods. However, the maximum value obtained by any one of the method has been taken as the permeability of the strata.

Table 2 : Results of *in situ* permeability tests

Depth below Gr. *L* in *ft*	Permeability ($cm/sec\times10^{-4}$)	Type of Test
B H at *ch* 74 + 74 22 *ft* downstream top *El* 1725.		
Pinkish lateritic Soil		
14.75—19.25	.79	*R*
Weathered Gniess		
26.67—32.67	5.1	*R*
26.67—35.17	5.3	*R*
27.67—40.17	5.7	*R*
27.67—40.17	2.4	*B*
B H at *ch* 70 + 58 on the centre line top *El* 1700		
Fissured Gniess		
10.5—14.8	8.6	*R*
10.5—19.25	3.3	*R*
10.5—19.25	15.0	*B*
B H at *ch* 70 + 55 on the centre line top *El* 1694.5		
Weathered Gniess		
10.3—14.8	.97	*R*
10.3—18.3	2.8	*R*
10.3—23.3	3.1	*R*
10.3—28.3	4.7	*R*
10.3—28.3	2.6	*B*
B H at *ch* 69 + 55 on the centre line top *El* 1690		
Fissured pegmatite		
16.34—22.34	61.0	*R*
16.34—28.6	31.0	*R*
16.34—28.6	28.0	*B*
16.34—28.4	12.0	*T*
B H at *ch* 61 + 37 19 *ft* downstream top *El* 1666		
Weathered Gniess		
14—16	23.0	*R*
19—22.5	7.7	*R*
24—27.	8.3	*R*
33—37.25	1.3	*R*
39.5—44.0	1.8	*R*
39.5—44.0	3.4	*B*
43.3—47.0	.58	*B*
43.3—51.8	2.7	*R*
43.3—55.0	4.1	*R*
43.3—55.0	3.0	*G*
BH at *ch* 60 + 50 80 *ft* downstream top *El* 1661.7,		
Weathered Gniess		
48—63	25.0	*R*
46—72	21.0	*R*
46—100	23.0	*B*
B H at *ch* 60 + 00 80 *ft* downstream top *El* 1660,		
Weathered Gniess		
38—41	1.5	*R*
47—72	6.2	*R*

Note:—*R* = Recuperation; *B* = B test; *T* = Thies test.

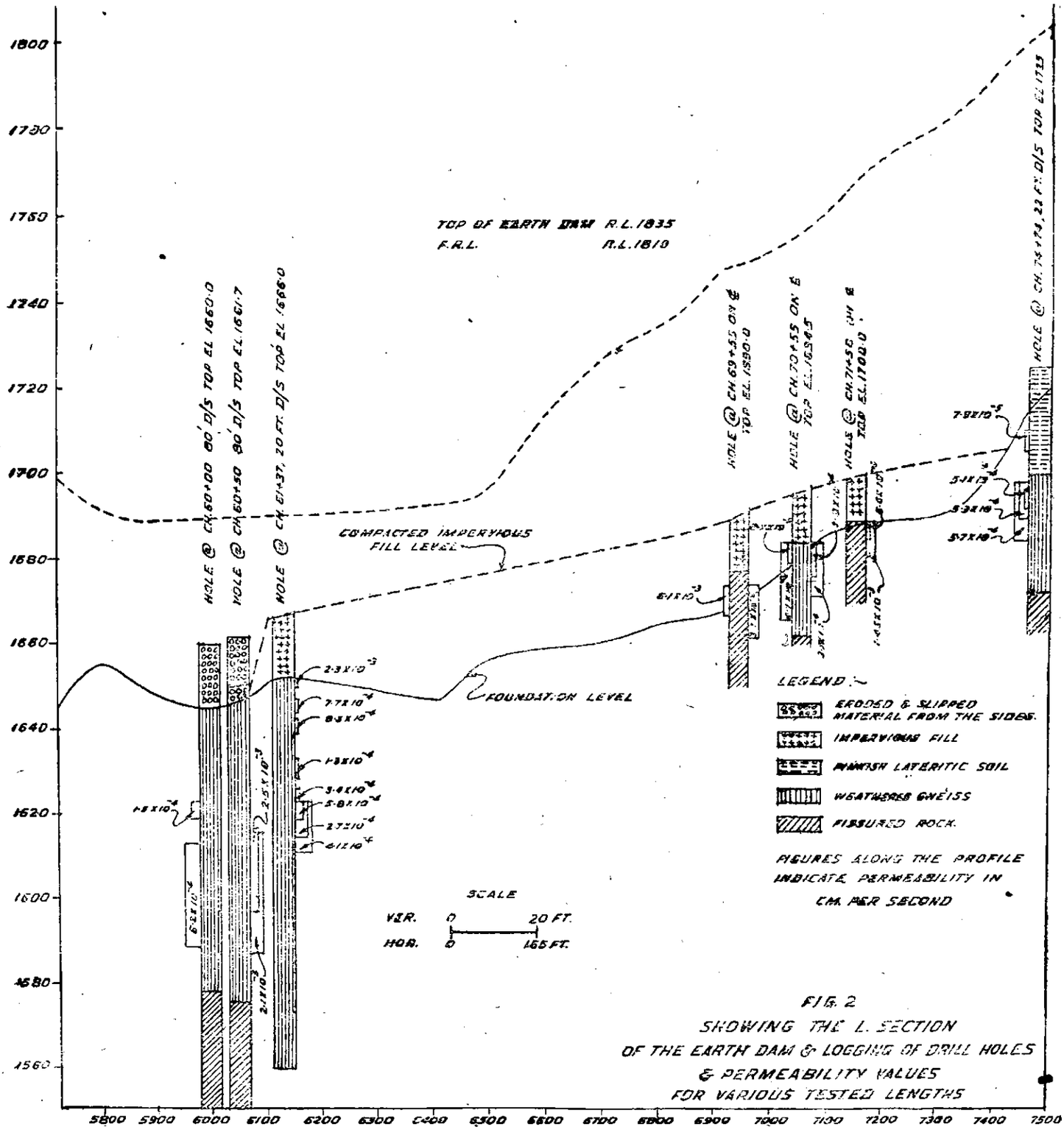

FIG. 2
SHOWING THE L. SECTION
OF THE EARTH DAM & LOGGING OF DRILL HOLES
& PERMEABILITY VALUES
FOR VARIOUS TESTED LENGTHS

The permeability results show that the pinkish lateritic soils, classified as silty sand have a permeability of 7.9×10^{-5} *cm/sec*. The value is of the same order as obtained by the block samples from similar materials. The permeability is fairly low and no treatment is necessary.

The fissured rock as tested in the bore holes at 2159.88 and 2180.84 *m* (*Ch* 69+55 and 71+55) had given a maximum permeability of 6.1×10^{-3} *cm/sec* and the figure represents the average value for 1.52 *m* (6 *ft*) tested length from which core recovery was 38 *percent*. Considering the fissured nature of the rock, the permeability is fairly high and it will be advisible to grout the fissured rock with cement.

The fault zone is mainly covered with weathered gneiss to a depth more than 30.48 *m* (100 *ft*) at places. Similar materials were also

met with in the bore holes at 2150.36 and 2278.08 *m* (*Ch* 70+55 and 74+74) as discussed earlier. The weathered material had given a maximum permeability of 2.53×10^{-3} *cm/sec*, in the bore hole at 1844.04 *m* (*Ch* 60+50), 24.38 *m* (80 *ft*) downstream of the centre line for depth 13.72 to 19.2 *m* (45 to 63 *ft*) below the ground level. The permeability of the block samples collected from the fault zone has a value of 1.0×10^{-3} *cm/sec*. The *in situ* permeability figure is slightly high.

Samples of the washed material were collected from bore holes drilled at 1870.56 *m* (*Ch* 61+37) and tested for their size distribution. The D_{15} of the washed out samples varied from .075 to .1 *mm* and the actual value will be still low. The material is fairly fine and may not be susceptible to any type of the grouting except chemical. However, considering the slightly high value of the permeability obtained by the *in situ* test a trial with bentonite cement grout can be made specially in the fault zone.

33. Earth Tremors at Mangalam Dam site

January-March 1960

REPORTS from Mangalam Dam Site, Kerala State during the last few months (Jan, Feb and Mar, 1960) suggest frequent occurrences of mild tremors, sometimes in quick succession. These are reported to be always associated with sharp sound, like those from firings of cannos at a few miles distance. This study on the tremors has been made on the basis of instrumental observations at the Mangalam Dam Site, geological reports of the dam site and other information such as questionnaires and personal reports. Similar phenomena observed sometime back at the Poringalkuthu and Sholayar Dam areas, Kerala State, were also taken into consideration.

2. Tectonics of the area

Regions along the west coast of India sometimes experience small earth tremors as a result of minor readjustments along major structural discontinuity parallel to the west coast of India. This structural discontinuity is fairly young. It originated probably in tertiary period as a result of widespread tension in earth's crust in this area and is associated with crustal upwarp of heavier simatic layer exihibiting acute positive gravity anomaly along the strike of the upwarp of faulting. It is clear from tectonics and seismicity of this and neighbouring area that no severe seismic activity is anticipated in this or other parts of west coast south of Bombay.

3. Observations

The tremors are of very small magnitude in the Richter magnitude scale affecting only areas upto several hundreds of square *km*. As such ground will have very small acceleration. During the 10 days from 1st to 10th Mar, no earth movements were registered by a sensitive Wood-Anderson seismograph of *US* Coast and Geodetic Survey Type though more than half a dozen times, peculiar sounds were heard in the area. This conclusively proved that these sounds were not associated with significant earth movements at the Mangalam Dam site. However, no immediate cause could be found for origin and nature of these sounds often heard at the Mangalam Dam Site.

Simultaneously, field inspection of possible damage to any structure and occurrence of landslides were undertaken in the adjoining areas of the Dam. Questionnaires were distributed amongst large number of people to get reliable information regarding occurrence of these tremors, their intensities and effect on structures *etc*. But, it was gathered from these questionnaires that there were one or two significant earth tremors on 19th Jan, 1960 at about 0900 *hrs* and others, mostly, were not associated with any elastic vibrations in earth. The felt area of the shock which occurred on 19th Jan, is expected to be about 200 *sq km*. Hence, the shock was a very minor one incapable of inflicting and structural damage. Such tremors might occur at depths from 5 to 20 miles inside earth. *Fig 1* shows a map of the area near the dam indicating directions of incoming vibrations on 19th Jan 1960. These prevalent directions also showed that the

Fig. 1: Direction of incoming vibrations and sound of 19-1-60 earthquake near Mangalam dam.

earthquake on 19th Jan 1960 was a local one. Assuming the felt area of 200 *sq km* to be circular, the value of the intensity (I_o) in the modified Mercalli Scale at epicentre comes out to be about 2 for depth of focus (h) 15 *km*, according to the following formula :—

$$\frac{r}{h} = \left(10^{\frac{I_o}{3} - \frac{1}{2}} - 1\right)^{\frac{1}{2}}$$

where r = radius of felt area. Also from the

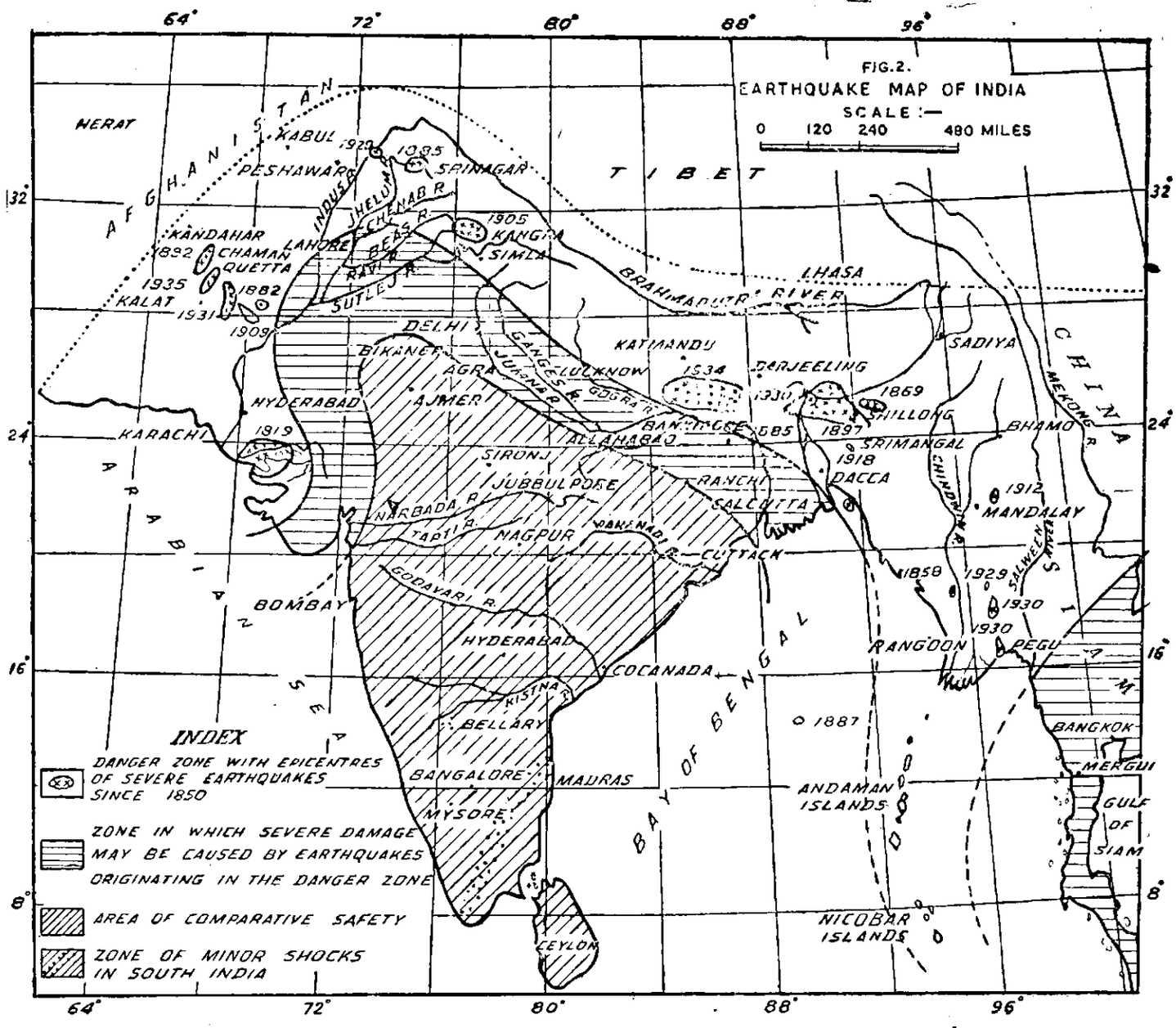

relation $M = 1.3 + 0.6I_o$, the value of magnitude M is found to be about 2.4 in the Richter Scale. This value of magnitude of 2.4 is equivalent to an energy release of about 2×10^{16} ergs when $\log E = 12 + 1.8\ M$. Acceleration a_o equivalent to I_o from the relation $M = 2.2 + 1.8 \log a_o$ (where $M = 2.4$) comes but to be 1.3 cm/sec^2. Thus, the derived value of the prevalent acceleration (a_o) at the epicentre for 19th Jan 1960 tremor confirmed the reports obtained from field questionnaires.

Fig 2 shows earthquake map of India depicting various intensity zones (after Dr West). This map also indicates a zone of minor shocks in the southern most part of India. From tectonics and geology of the area, it is improbable that this region will have earthquake of much bigger magnitudes than observed in the past. If an earthquake having area of perceptibility of 1000 *sq km* is regarded as typical of this region, then the values of I_o, M and a_o for such an earthquake as obtained from the relations mentioned in earlier para are as 2.7, 2.9 and 2.4 in their respective units.

4. Conclusions

It is thus evident that prevalent acceleration from these earthquakes even at epicentres will be very small and that, in general, no seismic factor need be incorporated in design of dams in this area. However, as a measure of precaution, seismic factor of the order of (1/30 to 1/20) *g* for both horizontal and vertical components may be incorporated specially in structures located across or near weak zones, like faults *etc* when the structure, in addition to differential movements, may also experience accentuated ground acceleration.

34. Mettur Tunnel Scheme

I. Seismic refraction on bed-rock

THE PROPOSED Mettur Tunnel Scheme comprises of a 45 feet diameter tunnel through hard country rock near the existing structures like the Mettur Dam on one side and a bridge on the other side. Seismic refraction method was employed to assess the existing rock cover along the tunnel alignment and the physical characteristics of the country rock.

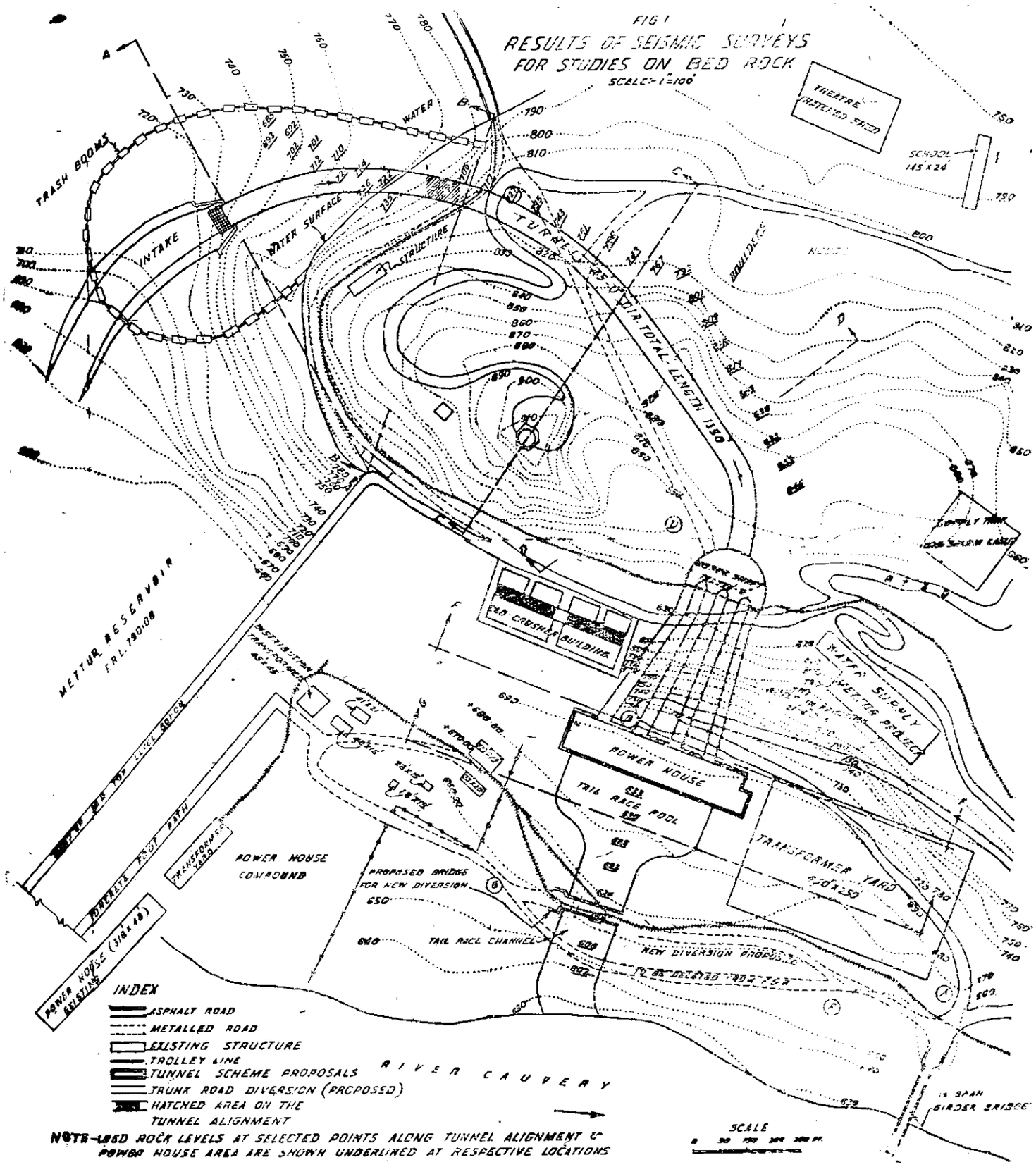

2. Geology

The country rock consists of granite-gneiss characteristic of the archaean shield of Peninsular India. At places, the rock resembles charnockite. The bedrock as usual is covered with overburden consisting of weathered country rock and boulder bed. The velocity of these beds as well as that of the bedrock and their thicknesses are favourable for application of Seismic Refraction Method for determination of depths to bedrock and characteristics of the bedrock *in situ*.

3. Field observations

The method of shallow depth Refraction Seismic Survey is well known. However, due to uneven topography of the ground surface it was not possible to utilise the analytical method for the estimation of depths to bedrock, from the refraction travel time curves. Instead, the graphical method was used, employing the principle of trial and error, in fixing depths and dip of refracting surfaces to arrive at reasonable solutions for geology of the region concerned. Bedrock levels obtained from graphical interpretation of refraction data at selected locations are shown underlined in *fig 1*, which also shows plan of the area with alignment of the tunnel and other details. These data are of particular importance for assessment of the rock cover along the tunnel alignment. At few places, bedrock levels, (*fig 1*), corroborate well with those found from boreholes, recently completed along the tunnel alignment.

Analysis of the refraction data further shows that velocity of longitudinal waves in bedrock is of the order of 19,000 to 20,000 *ft/sec*. This velocity value has been further confirmed from determinations in laboratory by passing ultrasonic waves through a few bedrock samples obtained from boreholes.

4. Conclusions

Depths to bedrock, as obtained from Seismic Refraction Measurements, have shown that rock cover is considerable over the proposed tunnel excepting near the intake and, possibly, at the hatched portion of the tunnel alignment, shown in *fig 1*. It is recommended that a borehole may be taken at the centre of the hatched area, for assessment of the condition of rock *in situ* upto about *RL* 640. Further, the rock *in situ* is highly elastic and massive as observed from propagation characteristics of longitudal waves *in situ*.

II. Maximum Allowable Charge during Blasting

THE PROPOSED tunnel for Mettur Tunnel Scheme, as shown in *fig 1*, *p* 290 is situated between the Mettur dam on one side and a bridge on the other side. The present investigation was undertaken to assess intensity of ground acceleration near blasts so that proper choice of the amount of explosive to be used in any single delay during tunnelling can be made, keeping in view the safety of the two structures. In view of the urgency expressed by the authorities, the present synopsis has been prepared to include only some tentative conclusions of the results of vibration studies. A full report on the study is under preparation. Intensities of ground acceleration from a large number of blasts available during tunneling at Kundah have been included in the study and were measured with a Phillips Acceleration Measuring Pick-up and a recording Oscillograph. Similar experiments were recently carried out at Mettur to obtain additional data.

2. Results

Though it is fairly easy to predict and systematise ground motion from any single charge, it is rather difficult in the case of resultant ground motion obtained from simultaneous multiple blasts, as is the case available in any single delay during tunneling operations. Resultant vector of ground motion from a number of simultaneous multiple blasts depths on many factors; and available literature does not reveal much information on this subject. In the present case, it is necessary for the safety of the dam and the bridge that the amount of charge in any single delay be limited. Hence the total charge may have to be divided amongst large number of delays in the pattern in order to have the necessary economic pull.

It has been found from a large number of blast records that in rocks of high elasticity as available at Mettur, 250 *millisecond* time-interval, between successive blasts (delays) in any pattern, should be sufficient for eliminating adverse effects of interference of ground motion from successive delays.

Table 1 shows values of maximum ground acceleration, measured on the circumstances of a tunnel

Table 1

S. No	Total charge (*lb*) in single delay (*c*)	No of holes, in which total charge was equally divided	Dist of tunnel face from *pt* of observation (*ft*)	Max. acceleration (cm/sec^2)	Dominant period (*sec*) of earthwaves in acceleration spectrum
1	2	3	4	5	6
1	12	8	477	1067	.0085
2	14	9	637	1330	.0023
3	16	8	257	1499	.0020
4	22	11	383	1745	.0080
5	27	14	333	1091	.0093
6	32	16	333	1394	.0093
7	28	16	300	1354	.0017
8	28	16	679	1166	.0020
9	28	16	781	965	.0020
10	28	16	827	528	.0023
11	35	20	611	1431	.0020
12	52	28	679	1622	.0020
13	52	27	781	1681	.0022
14	53	27	451	1152	.0033
15	53	27	611	1511	.0018
16	57	29	300	2045	.0017

Note:—Component of acceleration : for *S No* 1 to 6 Axial
for *S. No* 7 onwards: Redial.

at different distances, in both axial and radial directions, due to various simultaneous multiple charges equally distributed in the holes as in a single delay. This table also gives required data for period of earthwaves in acceleration spectrum. The data shows great amount of scatter which may be due to various factors. The data can be utilised for the proper choice of amount of charge to be used in any single delay to ensure safety of the dam and the bridge.

3. Discussion and conclusion

From a large number of single blasts recorded by various investigators, it is now fairly reasonable to assume a relationship of the following form for accelerations from blasts :

$$a = k \left(\frac{C^{n}}{d}\right)^{m} cm/sec^2 \qquad \ldots \quad (1)$$

where a = ground acceleration, c = amount of charge in lb, d = distance in ft and k, n and m are constants. The value of n lies between 1/2 to 1 and that of m is close to 2. However, this expression has not yet been adopted for use in the case of simultaneous multiple blasts as obtained in any single delay in tunneling operations. Limited data reveal that an expression, similar to equation (1), may also be suitable for assessing ground acceleration from simultaneous multiple blasts as in a single delay. However, it is recommended that, for the present, *table 1* may be used for assessment of accelerations at different distances due to various charges.

It is known from existing literature on the mechanics of damage due to rapidly varying forces that damage may be caused to any structure either due to :

(*a*) large response of the structure during forced oscillations and/or due to

(*b*) failure of the material due to high amplitude stress waves.

The former type of damage, *viz*, that due to large response during forced oscillations, is possible only when the existing dam or the bridge has natural period of oscillations close to the period of earth waves. From the large number of measurements undertaken by the Research Station on existing dams in India, it is reasonable to assume that the Mettur dam may have a period of natural vibration between .07 to .12 *sec*. The same may also be approximately assessed theoretically from the following formula, by assuming the dam to be a fixed-free symmetrical wedge fixed at the base:—

$$T = \frac{2\pi}{5.315} \cdot \frac{H^2}{B} \cdot \frac{\sqrt{3d}}{\sqrt{E}} \qquad \ldots \quad (2)$$

Where T = natural period of vibration, H = height of the dam, B = half-width of the dam at its base, d = density of the material of the dam, E = Young's Modulus of the dam. Thus the natural period of vibration of the dam is rather large compared to the dominant period of earth waves shown in *table 1*. Hence, the type of repetitive oscillations of the structure, due to large dynamic response during forced oscillations, is not expected from these blasts. Similar conclusions hold good for the bridge also as the bridge-piers can be approximately assumed to be dynamical analogue of fixed-free cantilevers during forced vibrations, due to blasts. As the expected dynamical response in the bridge piers is pretty small, no adverse effects are expected due to coupled or assymetric oscillations amongst the different bridge piers.

However, failure of the material due to high amplitude of stress waves is expected unless precautions are taken to delimit amplitude of stress waves by suitably reducing the amount of charge in any single delay. The acceleration waves in *table 1* have wave lengths varying from 50 to 250 *ft*. But, the dam is much longer than these wave lengths. As such full amplitude of the

stress waves will be also effective in the longitudinal direction of the dam. As the nearby structures will be repeatedly subjected to these blasts during tunneling, it is recommended that high safety factors be incorporated while evaluating stresses on the body of the dam, due to the stress waves, whose amplitudes may be proportional to accelerations, given in *table 1*, for respective charges. It is known from earthquake damage data that smaller after-shocks may, at times, cause damage to a structure which escaped the earlier main earthquake. As such, while evaluating safety of nearby structures from repeated blasts during tunneling operation, such facts have to be kept in view. It is customary in earthquake design to take design acceleration as 1/2 to 1/4 of the prevalent ground acceleration during earthquake. This is due to averaging of acceleration over the entire spectrum. Applying this principle here, it can be assumed from the data given in *table 1* that charge upto 4 *lb* in any single delay may produce ground acceleration of about .3 *g* or equivalent to .1 *g* of design acceleration, when distance of the blasted tunnel face is about 500 *ft* from the structure (assming design acceleration as 1/3 of ground acceleration). Apparantly number of delays and the total charge used in the entire pattern have not been related to safety so long as the delays are separated by time interal of at least 250 *millisecond* and each delay does not have blast load of more than 4 *lb* in this case.

4. Recommendations

As a result of the above investigations, following recommendations were made :

(*i*) Time interval between successive delays should not be less than 250 *milliseconds.*

(*ii*) Maximum blast load of 4 *lb* for each delay has been arrived at on the assumption that the dam and also the bridge will be able to withstand following accelerations :

$$\text{horizontal} = .1\ g$$
$$\text{vertical} = .08\ g$$

The Design Directorate at Central Water and Power Commission may, thus undertake the analysis of stability of Mettur Dam and that of the bridge for the above forces.

Though the distances of the dam from the proposed tunnel alignment are never less than 500 *ft*, those for the bridge are much lower for certain portion of tunnel alignment. As such safety of the bridge will demand further reduction in the value of 4 *lb* per delay. Moreover as the rock cover is low for certain portion of tunnel alignment from intake, safety of the tunnel itself will support such a reduction. The extent of further reduction in the value of 4 *lb* would depend on a number of factors, *viz* safety of the bridge the portion of the tunnel beginning from intake having low rock cover and economics of tunneling *etc.* Any decision in this respect is perhaps outside the immediate scope of a technical report as this one.

35. Electrical analogy for stratified foundations

INVESTIGATIONS [1], [2] have been made in the past, and in current work, in this country and abroad, to ascertain the distribution of uplift pressure on structures, by hydraulic models,[3] as well as electrical analogy models. [4] [5] [6] The latter depends on the analogy of the equations govering the flow of water through porous materials, involving Darcy Law and those governing the flow of electricity through conductors, involving Ohm's Law.

The work referred to above, except for a few cases, has been conducted mostly for homogeneous strata, which, however, is not the case in nature, as the permeability values may vary considerably in the horizontal, as well as in the vertical directions.

1. *Practical Design of Irrigation Works* by BLIGH, W. G. (1910).
2. *The action of water under dams*, by J B T COLMAN, *Trans Am Soc C E*, Paper *No* 1356, 1916.
   Studies on subsoil Hydraulics Investigation of observational methods for Models, by UPPAL H L and GUNN, J P, *Punjab I R I Research Publication*, Vol II, *No* 2.
4. *Hydrostatic Uplift Pressure under dams on pervious earth foundations*, by HEBERT D J, *Memorandum No* 384 *USBR*.
5. *Potential Distribution in infinite conductors and uplift pressure on dams* by GURDAS RAM, VAIDHANATHAN, V I and TAYLOR, E M.
6. *The Design of Weirs on permeable foundations*, by KHOSLA A N, BOSE N K and TAYLOR E M.

Investigators in the field of uplift pressure distribution, with the help of electrical analogy models, have used a number of techniques for simulating stratified media. They are, for example, decreasing the dimension of the structure, in the model, in the direction of greater permeability, in the ratio of the permeabilities,[7] or by varying the depth of the electrolyte in the electrolytic tray, in the inverse ratio of the permeabilities. [7 8] These methods, however, are not of a very wide application, as it will not be possible to decrease on edimension in comparison with the other, or to decrease the depth of a portion of electrolyte with respect to the other, more than certain practical limiting ratios, which in practice cannot be made very high.

As the permeability ratios of the order of 1:100 1:1000, or even more, are not infrequent in nature, in the case of several hydraulic structures, an adequate method of investigation of such cases would be highly desirable.

Use of electrolyte solution with different conductivities, to simulate layers of different permeabilities has also been adopted by some workers[9] in this field. However, the simulation of stratified layers, with such high ratios of permeability, involes some technical difficulties. These are discussed here, along with some experimental results conducted thereon.

To simulate a stratified medium, electrolyte solutions, of different electrical conductivities, representing stratified layers, have to be put in water-tight compartment in the electrolytic tray. This necessitates a method of transferring electrical potentials from one water-tight compartment to the other, to maintain continuity in the electrical potential field without the solutions in the compartments coming in contact with each other, to avoid diffusion effects, so that the conductivities of the electrolyte solutions in the various compartments remain unchanged during the investigation. The method has been investigated here in some detail regarding tolerances and accuracies which are described below.

2. Experimental set up

An electrolytic tray, with glass bottom, 120 *cm* × 90 *cm* × 5 *cm*, supported on levelling screws, was used in these investigation (*photo 87*). The same depth of electrolyte solutions, in different compartments of the tray, was used. The depth of electrolyte solution used was never less than 4 *cm* to minimise errors liable to creep in due to small variations here and there in the depth of the electrolyte solution on account of unevenness in the surface of the glass plate forming the bottom of the tray.

The potentiometer used in this investigation, has been divided in 1000 equal divisions. An electronic oscillator, frequency 1000 cycles per second, was used as source of *AC* potential. A tuning ray indicator was used an null point detector.

3. Procedure for simulating stratified layers

A two layer strata has been simulated. The layers of the strata, with different permeabilities, are to be simulated by solutions of the same electrolyte, with different conductivities (Ratio of the conductivities equal to the ratio of the permeabilities of the layers of strata simulated) in the compartments of the tray. The compartments obtained with the help of a specially constructed water-tight partition, in which suitable arrangement was made to transfer potentials from one compartment to the other.

Partition was first made from wood, .4 *cm* thick but afterwards of fibre, with copper strips, spaced at suitable intervals. Partitions, with copper strips of various widths, spaced at different intervals, have been investigated, to arrive at optimum strip width and spacing intervals, so that the results are reproduced upto the desired practical accuracies, with such a partition.

The electrolyte solutions, in the compartments, in this series of investigations for determination of tolerances consisted of the same conductivity (tap water) in both the compartments.

4. Results and discussion

(*a*) *Tolerance and accuracies with partition.—same solution on both side of partition.*—A simple floor was used for work in these determinations. The floor breadth used was 30 *cm* and the partition was placed at a depth of 30 *cm* below the floor.

7. *Photoelastic and experimental Analogue Procedures* by MOODY, W T and PHILIPS H B, *Engineering Monographs No* 23, of the *USBR*.

8. *Electrical Analogy Applied to study of Seepage into Drain Tubes in Stratified Soil, by* LUTHRA S D L, and GURDAS RAM *I & P Jour*, Vol XI, *No* 3.

9. *Some studies on Design of Relief Wells for Earth Dams on pervious Foundations, by* RAMESHWAR SARAN, *IRI, Roorkee, U P, T M No* 28 *RR* (S 8), Apr, 1958.

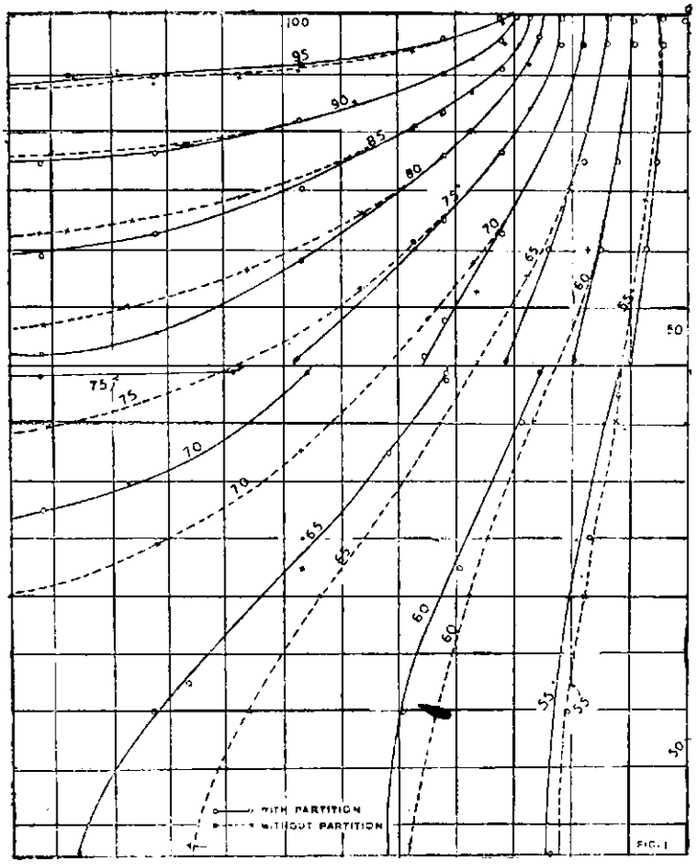

Fig 1 : Spacing of strips = b/12 *cm.*
Equipotential lines=simple floor. Floor width = 30 *cm.*
$K_1 : K_2 = 1:1$ $b/d = 1$ Thickness of partition = .4 *cm.*

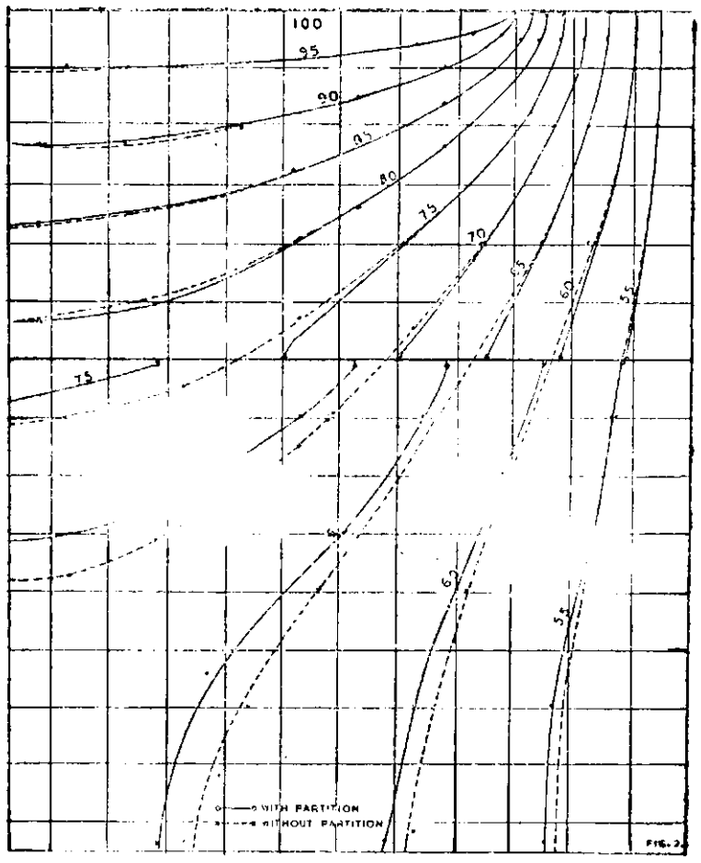

Fig 2 : Spacing of strips = b/24 cm.
Partition at d *cm* below the floor
Width of strips = .3 *cm.*

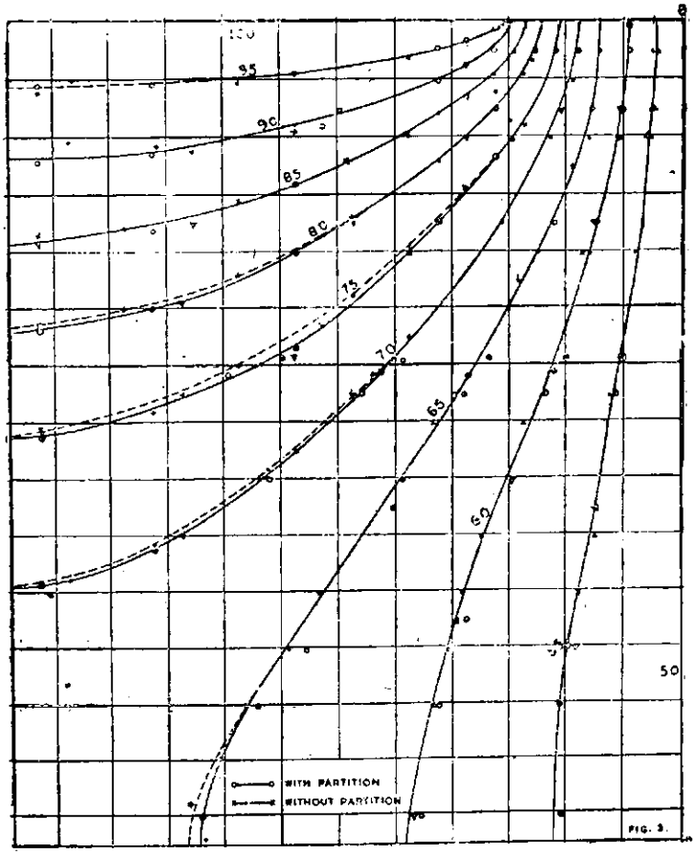

Fig 3: Spacing of strips = b/96 *cm*
$K_1 : K_2 = 1:1$ $b/d = 1$ Thickness of partition = .08 *cm.*
Equipotential lines = simple floor Floor width = 30 *cm.*

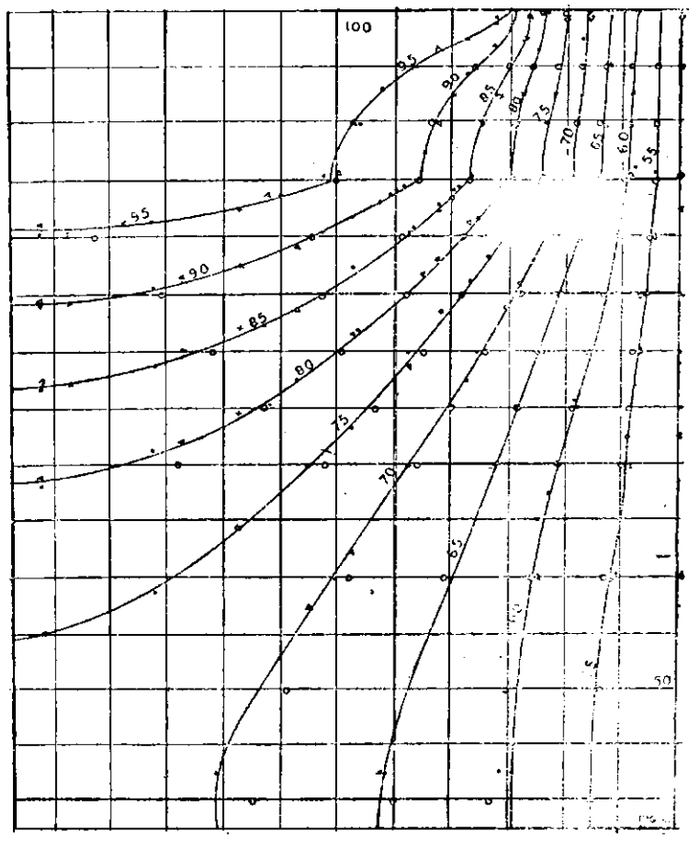

Fig 4: $K_1 : K_2 = 100 : 1$ $b/d = 1/2$.
Partition at d *cm.* below the floor width of strips = 0.3 *cm*

Partition made from wood, .4 *cm* thick with copper strips .3 *cm* wide, spaced at intervals of 2.5 *cm* was used. The results obtained with the partition are shown in *fig 1,* which give equipotential lines, at intervals of 5 *percent* potential differences. Equipotential lines without the partition are also shown in the figure. As will be seen from the figure, the partition has produced a slight shift in the potential lines. This has given rise to differences in potential values ranging from 1/2 *percent* to about 2½ *percent.*

The investigations were repeated with spacing between the strips reduced to 1.2 *cm.* Equipotential lines drawn at 5 *percent* intervals, are shown in *fig 2* along with those for the case without partition. It is seen that there is again a shift in potential lines but the amount of shift has been much reduced, thus decreasing the corresponding difference in potential values to a maximum of 1¼ *percent.*

In the next series of the tests the partition was made of a strip of fibre, .08 *cm* thick. It was provided with copper strips, of various widths, spaced at various intervals. The investigations showed that such a partition, with strips .3 *cm* wide, spaced at intervals of 0.30 *cm,* would give results of sufficient accuracy.

The equipotential lines for this investigation are shown in *fig 3.* Observations were repeated several times. Results of two independent observations, along with those for the case without partition, are given in the figure. It is seen that the difference in potential values produced by the partition is now of the order of a maximum of 1/3 *percent.*

5. Tolerances and accuracies with a stratified foundation

Weir breadth was 30 *cm* and the partition described above was placed at a depth 15 *cm* below the weir. The ratio of the permeabilities of the two strata was 100:1. The potential lines at 5 *percent* intervals thus obtained are plotted in *fig 4.*

This case was analysed also with the Relaxation Method, with permeability ratios for this strata, distance of the partition from the floor, and the floor depth same as in the experimental case. Mesh size, used in the analysis, is $b/30$, where b = breadth of the weir. These values have also been plotted in *fig 5* for comparison. The difference in potential values is of the order of 1/3 *percent.*

6. Conclusions

A suitable design of partition, for dividing the electrolytic tray into water-tight compartments, yet maintaining the continuity of potential field in the whole tray, so that electrolyte solutions of different conductivities may be used, without diffusion effects taking place, for simulating stratified layers, has been arrived at. The difference in potential values obtained has been ascertained and is of the order of a maximum of 1/3 *per cent.* This partition is being further tested for tolerances and accuracy before it is used in investigations for stratified soils.

---

36. Geophysical Investigations

I. Hathmati Reservoir Project

THE GEOLOGICAL map *fig 1* shows the locations of the two proposed earth dams, one on the river Hathmati and the other on its tributary Indrasi near Fatepur, their proposed heights being 71 and 61 *ft* respectively, and the location of the Waste Weir near Navalpur, having a discharge capacity of 1 lakh *cfs.* Micaschists belonging to Aravali System underlie river deposits of the flood planes at Hathmati dam site and granite of Erinpura series seems to underlie river deposits at Indrasi dam site. The Waste Weir alignment is situated along a band of quartzites belonging to Alwar series, near Navalpur. The purpose of this geophysical investigation was to obtain, for upstream and downstream of the alignments, a useful extension of the borehole informations already available at these sites.

2. Hathamati dam site

Twenty depth estimates have been made by seismic refraction method on the flood plane of Hathmati river at this site. Of these, four were

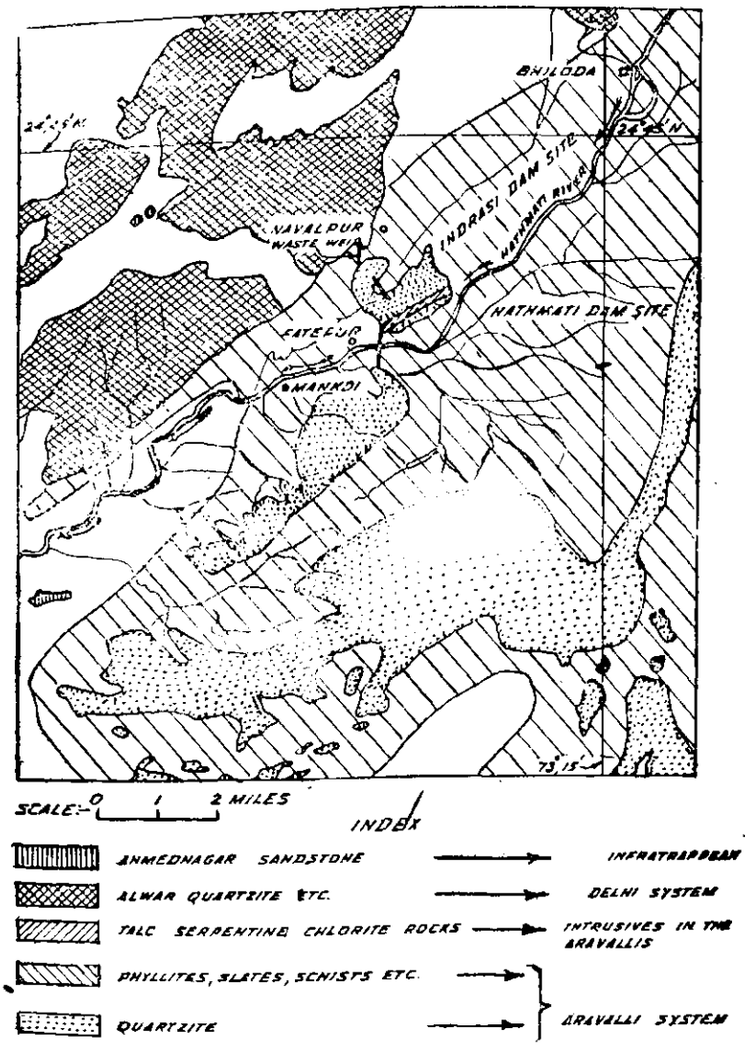

Fig 1: Geological map of the area surrounding dam sites on the rivers Hathmati and Indrasi and the waste weir site near Navalpur.

located along the alignment of the dam and the rest upstream or downstream of it. The locations of these twenty shot-points and the estimated elevations of the underlying mica-schist are given in *fig 2*. It will be seen from *fig 2* that along the dam alignment between chainage 500 and chainage 1040 mica-schist is estimated to occur at *RL* 503. The velocity with which seismic pulse is transmitted through *in situ* mica-schist here is found to be 10,000 *ft/sec* and this shows that mica-schist occurring here at this elevation, though expected to be weathered, is not at all disintegrated. Similarly between chainage 1460 and chainage 2000 mica-schist, which is likely to be much less weathered here, having an observed velocity of 12,000 *ft/sec* for transmission of seismic pulse, is expected to occur at *RL* 498. Thus the average depth of river deposits under the flood plane along the alignment here is about 45 *ft*, the average ground level being at *RL* 545, and the average rock elevation being at *RL* 500. The above geophysical findings are in general agreement with the results of three 6″ diameter, calyx drill holes recently taken at chainages 2450, 1900 and 1100, along this alignment.

Sixteen seismic depth-estimates made at places upto a distance of 1000 ft upstream and 1000 *ft* downstream of the present alignment, as shown in *fig 2*, indicate that the overall rock elevation under this flood plane is not expected to be at any shallower elevation compared to that along the present alignment, for any other parallel alignment upstream or downstream of the present one. It may be noted from *fig 2* that rock elevation is generally higher in the portion adjoining Hathmati channel immediately on its left bank than it is under the flood plane on the left bank further away from the channel portion.

From the average velocity of transmission observed in the field along the alignment namely 11,000 *ft/sec* and average density of mica-schist obtained from measurements on core samples namely 2.5 *gm/cc*, the estimated Young's Modulus of Mica-schist *in situ* comes out to be 3.0×10^6 *psi*. Laboratory determination were made for Young's Modulus from ultrasonic velocities observed on two 6 *in* diameter core samples namely of mica-schist obtained at a depth of 35 *ft* at chainage 1900 and of Talc-serpentine-chlorite rock obtained at a depth of 44 *ft* at chainage 2450. The core sample of Mica-schist from chainage 1900 has a density of 2.5 *gm/cc*, compressional wave velocity of 12,500 *ft/sec* which is consistent with the velocity of 11,500 *ft/sec* observed in the field for *in situ* rock between chainage 1460 and 2000 along the seismic profile for S_{57} and S_{58} of *fig 2*. *It has an estimated* Young's Modulus of 3.8×10^6 *psi*. The core sample of Talc-Serpentine-chlorite rock from chainage 2450 has, however, a density of 2.98 *gm/cc*, a compressional wave velocity of 14,600 *ft/sec* and an estimated Young's Modulus of 6.1×10^6 *psi*.

3. Indrasi dam site

In borehole No. II, at chainage 957 on the alignment of the dam at this site, weathered granite is met with at a depth of 61 *ft* namely at *RL* 499 and in borehole No. *III-A* located 250 *ft* upstream of chainage 660 of this alignment highly weathered granite is met with at a depth of 49 *ft* namely at *RL* 510. Two seismic profiles were taken 400 *ft* upstream of this alignment in order to assess the

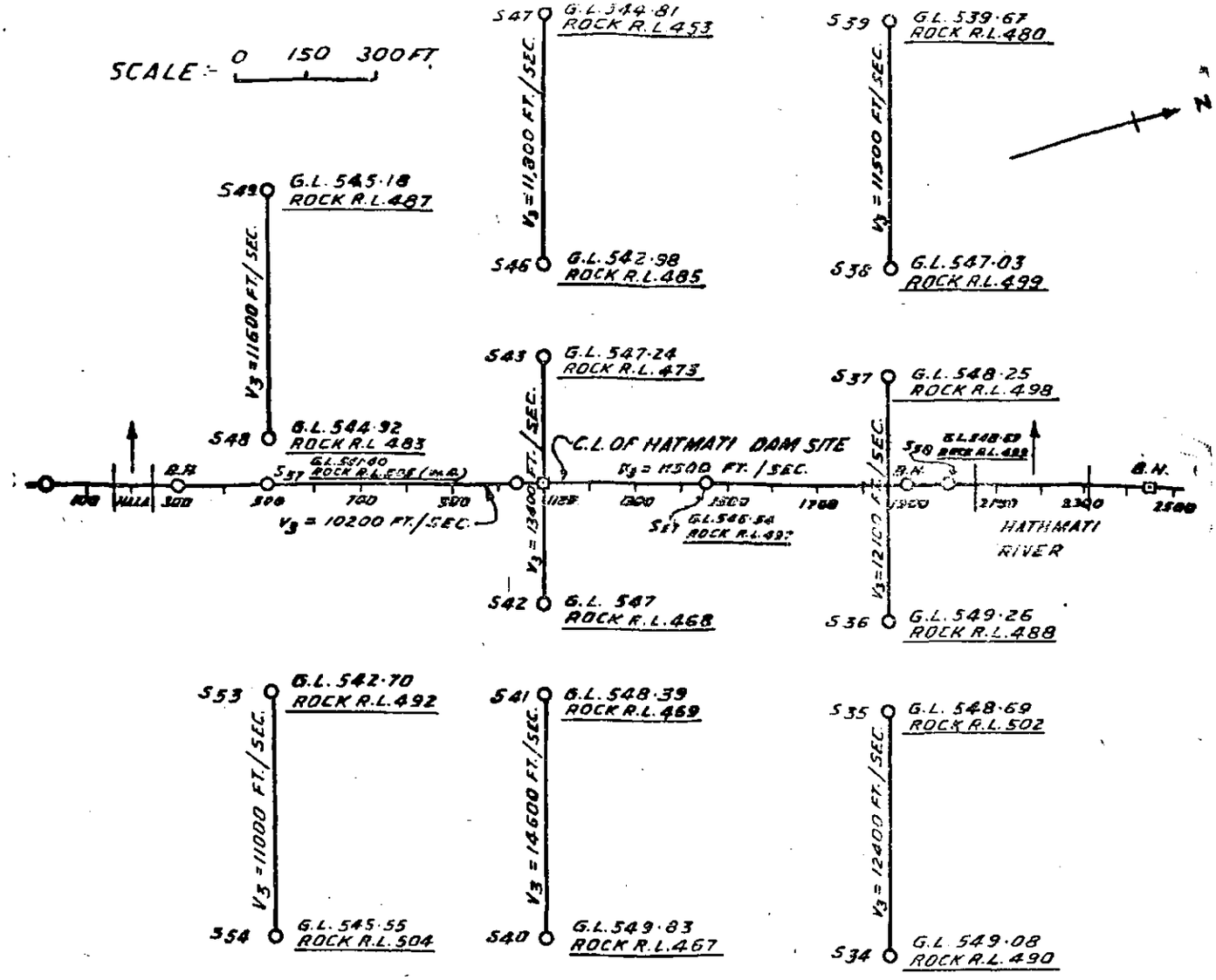

W. R. = weathered rock V_3 = rock velocity

Fig 2: Shot hole positions at Hatmati dam site and estimated rock levels underlined.

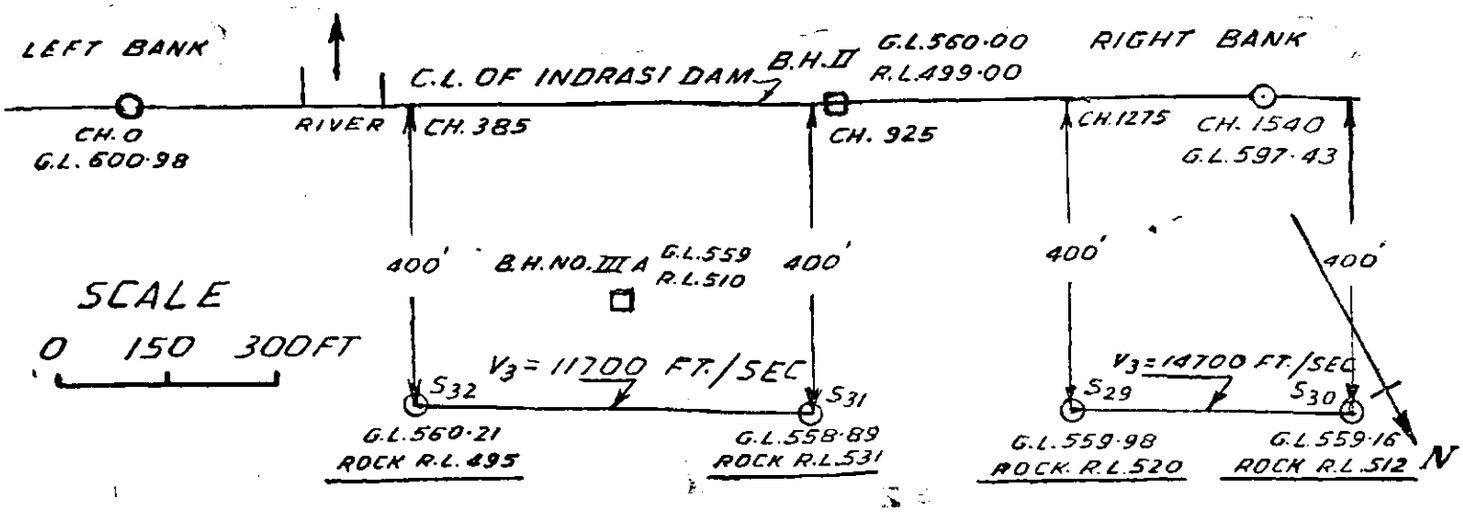

Fig 3: The shot hole positions at Indrasi dam site and estimated rock levels underlined.

rock elevation there and the results are shown in *fig 3*. It will be seen from *fig 3* that at S_{31}, 400 *ft* upstream of chainage 925 of the alignment, rock is expected to be met with at a depth of 28 *ft* namely at *RL* 531 and from there towards the left bank rock level is expected to go down at S_{32} by 36 *ft* in a distance of 540 *ft* that is to RL 495. At S_{29} and at S_{30} located 400 ft upstream of

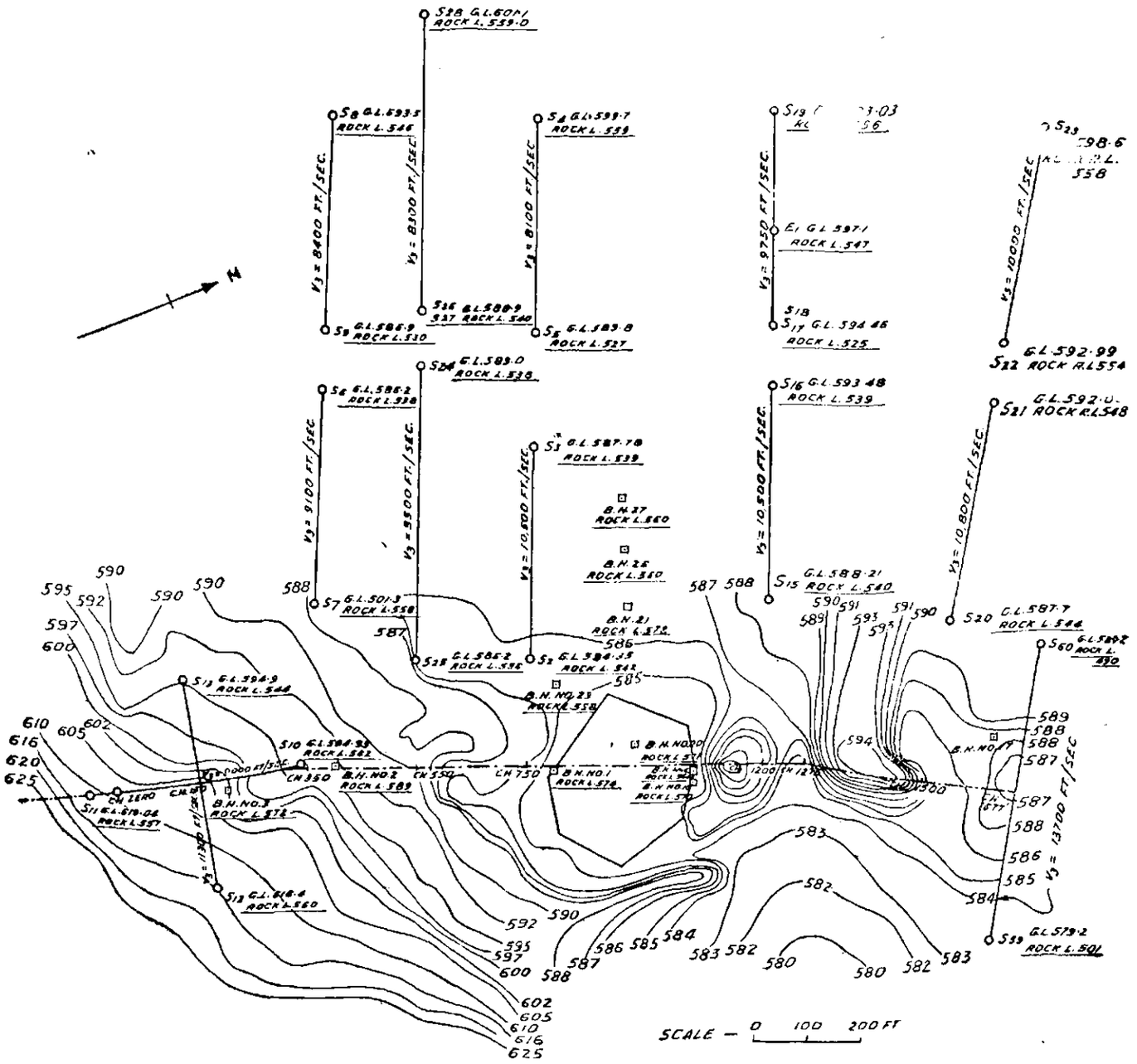

Fig 4: Shot hole positions at Navalpur waste weir site and estimated rock levels (underlined) V_s = rock velocity.

chainage 1275 and chainage 1575 of the alignment, the rock elevations are estimated to be at *RL* 520 and at *RL* 512 respectively. The velocity of transmission of seismic pulse observed between shot points S_{29} and S_{30} is 14,700 *ft/sec* suggesting that granite, which is expected to occur there at an average depth of about 45 *ft*, is not much weathered. Compared to above, the velocity of transmission of seismic pulse observed between S_{31} and S_{32} is 11,700 *ft/sec* and this would indicate that the granite that is expected to occur there, because of the proximity of this profile with the borehole *III-A* which is 150 *ft* downstream of this profile, is likely to be fairly weathered.

4. Navalpur waste weir site

26 depth estimates by Seismic Refraction Method and one by the Electrical Resistivity Method were made at this site and the locations of these, together with the estimated rock elevations, are shown underlined in *fig 4*.

Three exploratory trenches have been excavated namely *No* 1 at chainage 578 *ft*, *No* 2 at chainage 1075 *ft* and *No* 3 at chainage 1285 *ft*. In all these trenches, thinly beded quartzite alternating with some thin bands of mica-schist have been met with within a depth of about 10 *ft* of the surface, namely upto 200 *ft* downstream and 182 *ft* upstream of the alignment at trench *No* 1; upto

292 *ft* downstream and 81 *ft* upstream of the alignment at trench *No* 2, and upto 193 *ft* downstream and 150 *ft* upstream of the alignment at trench *No* 3 beyond which distances the rock surface goes down. The strike of the rock as found in the trenches varies from *N* 10° *E* — *S* 10° *W* to *N* 30° *E* — *S* 30° *W* and the dip varies from 15° to 52° towards *ESE ie,* nearly upstream of the alignment, to alignment of the Waste Weir being approximately *N* 27° *E*.

Results of ten seismic profiles taken nearly perpendicular to the alignment covering a portion from 200 *ft* downstream to 1200 *ft* downstream of the alignment between chainage 350 *ft* and 1500 ft as shown in *fig 4* indicate that except at S_7 (300 *ft* downstream of chainage 350) and S_{25} (200 *ft* downstream of chainage 550) where the estimated rock level is about *RL* 557, the average rock level is fairly constant at *RL* 540 from 200 *ft* downstream to 600 *ft* downstream of the alignment corresponding to chainage 750 to 1500 *ft*. Further downstream of it, the rock level reaches the minimum value of about RL 526 located 800 *ft* downstream of the alignment near S_5 and S_{17} and from there the rock level rises again to *RL* 560 situated 1200 *ft* downstream of the alignment near S_{23}, S_4, S_{19} and S_{21}. At chainage 1677 *ft* a seismic profile S_{59} — S_{60} was taken transverse to the alignment and it is estimated that the rock is likely to be met with under this chainage at an *RL* 496 namely at a depth of 90 *ft* and a nearby borehole *No* 17 penetrated to a depth of 41 *ft* without meeting any rock.

Between chainage —50 and 350 a seismic profile S_{11} — S_{10} was taken along the alignment and it indicates an average rock level there at *RL* 560, a nearby borehole *No* 3, 20 *ft* upstream of chainage 200 met with rock at *RL* 572. The seismic profile S_{12} — S_{13} taken transverse to the alignment at chainage 150 shows that rock level is here sloping downstream going down to *RL* 544 at S_{13} located 200 *ft* downstream of the alignment at chainage 150.

In order to be able to roughly assess the quality of rock likely to be met with at this site from the observed velocity of propagation of seismic wave through rock occurring under different seismic profiles, laboratory determinations were made for ultrasonic wave velocities on five core samples taken from this site and the results are given below in *table 1*. The actual velocity for seismic wave in the rock as observed in the field is mentioned along each seismic profile as given in *fig 4* . Nowhere was massive quartzite bedrock met with at this site and this would have a velocity 17,000 *ft/sec*, a density 2.62 *gm/cc* and Young's Modulus 7.6 × 10^6 psi as evidenced from measurements on a core sample of massive quartzite-boulder obtained at a depth of 23 *ft* 10 *in* from hole *No* 17. From above, it is reasonable to classify rock velocity obtained in the field and shown in *fig 4* along each seismic profile into two categories namely those above 10,000 *ft/sec* as likely to indicate the presence of more of quartzite bands than schist bands and those velocities falling within the range 8000 *ft/sec* to 9,000 *ft/sec* as likely to indicate the presence of more of schist bands than of quartzite bands. It is the former category of rocks which predominate at this site as is evidenced from the velocities indicated along its seismic profiles of *fig 4*.

Table 1

Bore hole No	Depth *ft in*	Rock Type	Density = ρ *gms/cc*	Velocity = *V* *ft/sec*	Elasticity = *E* in 10^6 psi (σ = ·30 assumed Poisson's ratio)
6	29 6	Shaley Quartzite	2·59	13,300	4·79
23	17 10 to 25	Shaley Quartzite (weathered)	2·57	10,300	2·71
27	43 6	Fresh shaley Quartzite	2·60	14,000	5·10
B-2	53 6	Phyllitic Schist (Soft rock)	2·62	9,200	2·13
17*	23 10 to 26 10	Massive Quartzite	2·62	17,000	7·58

* Core from boulder. No rock is met with in this borehole.

II. Alternative weir sites on Koyna

GEOPHYSICAL investigations were undertaken at the alternative Weir Sites located respectively near the villages Varunj and Chachegaon on river Koyna in order to help in comparative evalution of these sites. Seismic Refraction Method was employed in these investigations. Twenty depth

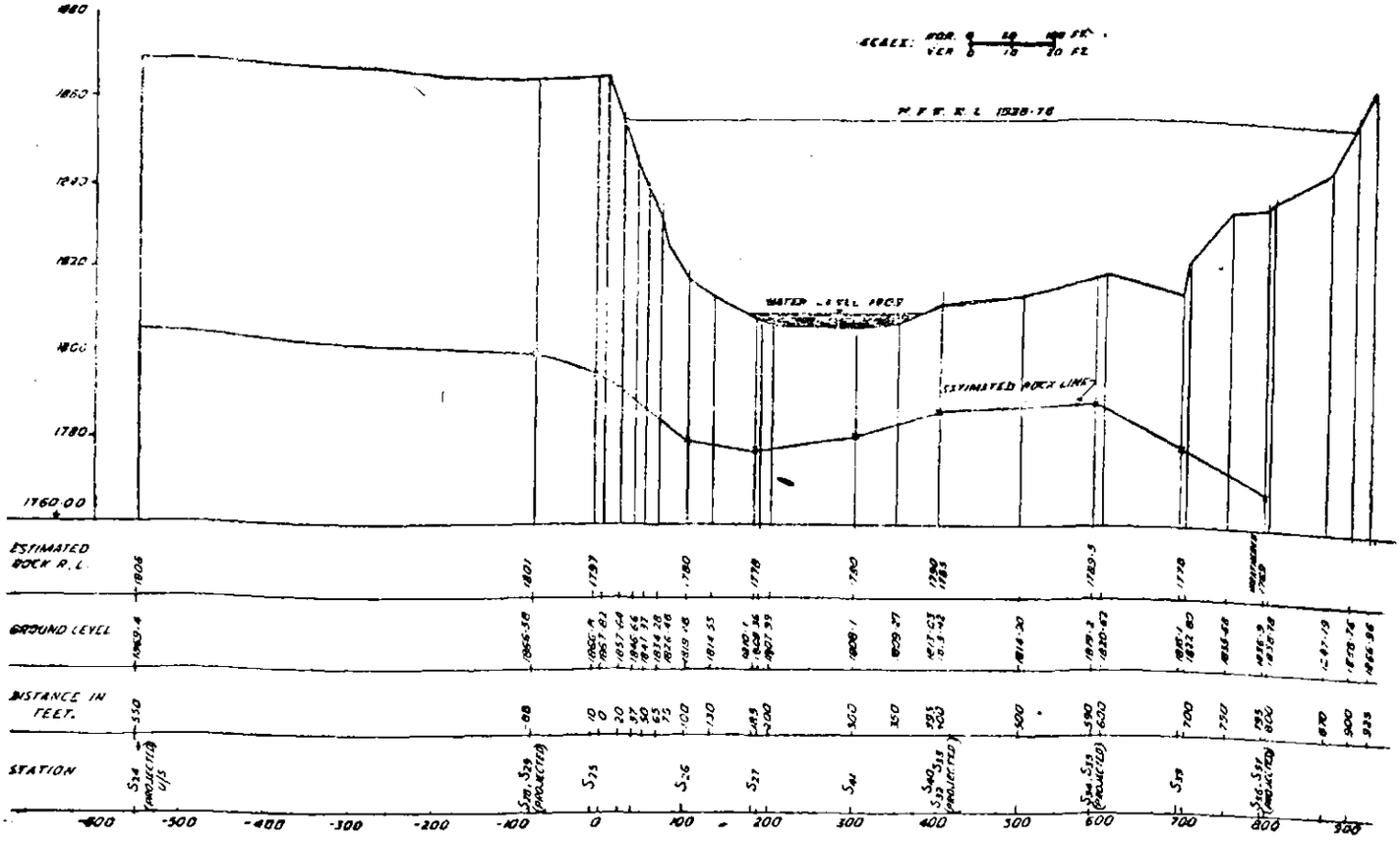

Fig 1: Cross section of river Koyna near village Varunj showing depth of bed rock estimated by seismic refraction survey.

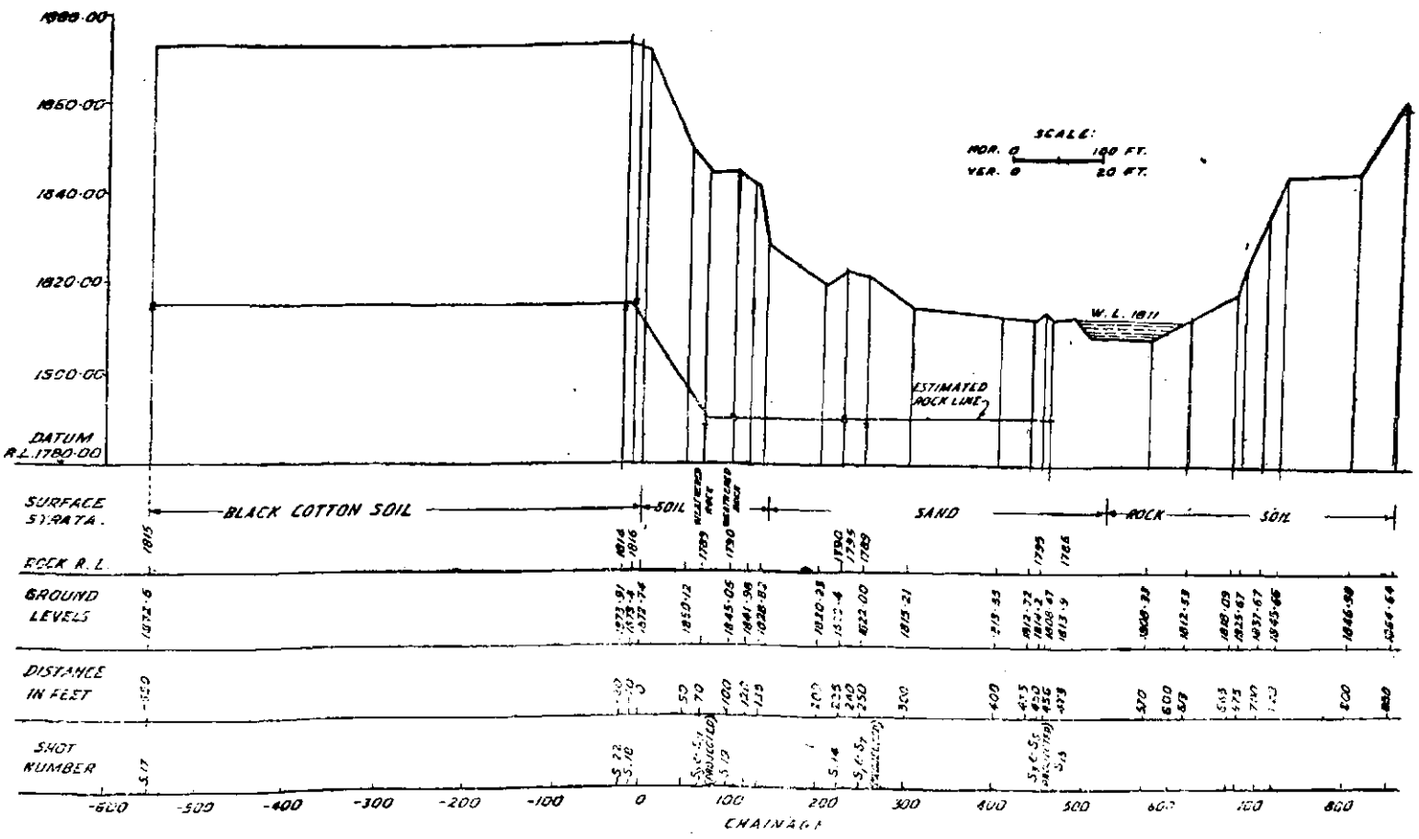

Fig 2: Cross section of river Koyna near village Chachegaon showing bed rock level as estimated from seismic refraction survey.

estimates were made at Varunj site and twenty-one at Chanchegaon site and the results given showing the locations of the different shot-points, the corresponding ground and rock elevations. The estimated sound trap-rock elevations at these shot points are shown in the cross section of *figs 1* and *2*.

2. Varunj site

It will be seen from the cross-section at Varunj site given in *fig 1* that the elevation of sound trap-rock is estimated at *RL* 1803 under the left bank. The minimum elevation of the bed rock under the river bed occurring near the chainage 185 is estimated at *RL* 1778. From there the rock level seems to rise regularly towards the right bank by about 12 *ft* upto chainage 590 and appears to go down again somewhat appreciably under the right bank upto chainage 795. The bed rock near chainage 795 also appears to be somewhat weathered as the velocity observed in this strata is about 11,000 *ft/sec* only as compared to a much higher velocity of 16,000 *ft/sec* to 22,000 *ft/sec* for the sound bed-rock occurring under the left bank as well as under the river bed.

3. Chachegaon site

From the cross section of *fig 2* given for Chachegaon site, it will be seen that the elevation of sound trap bed-rock is estimated to occur at *RL* 1815 under the left bank and at *RL* 1790 under the river bed. Rock is exposed under the shallow waters near the Right Bank at an elevation of about *RL* 1808. But this exposed rock appears to be somewhat weathered at the surface, as is also shown at the shot point S_{15}, at chainage 475, where weathered rock is estimated to occur at *RL* 1808 under a cover of 5 *ft* of overburden. The velocity in weathered rock observed at the place is 11,000 *ft/sec* compared to a much higher velocity of about 22,000 *ft/sec* for the sound trap-rock that is estimated to occur at *RL* 1786 underlying the weathered rock there. A high velocity lying between 16,000 *ft/sec* and 22,000 *ft/sec* has been consistently observed for the sound bed-rock at this site. The only exception being the somewhat weathered nature of the bed-rock which appears to occur under the terrace, on the left bank between chainage 70 and chainage 100 with a ground elevation of RL 1845, and an estimated elevation of RL 1790 for the underlying weathered bed rock as shown in *fig 2*. The weathered bed-rock there is observed to have a velocity of only about 10,000 *ft/sec*. Elsewhere at this site, estimated bed-rock elevations correspond only to the sound bed-rock having a velocity lying between 16,000 *ft/sec* and 22,000 *ft/sec* as mentioned earlier.

III. Spillway Site, Badua Project

THE LOCATION of the earth dam under construction on river Badua (Bihar), is shown in *fig 1*. The river flows here north-south, the alignment of the dam between the two hills being approximately east-west. The spillway site is located in a saddle on the right bank hill. Regional geological map of *fig 1* shows the country rock here as constituting of Archaean gneiss and schists. At the spillway site weathered sericitic schists interbeded with thin sericitic quartzitic bands are exposed in the cuttings along this spillway alignment. Approximate positions of exposed quartzitic bands are, however, marked in the contour plan of *fig 2*. These bands have a strike direction here approximately perpendicular to the spillway-channel alignment and they dip about 22° upstream with a slope 1 in 2.5. In other words, the strike direction of these bands which is parallel to topographic contours here, is nearly *E* 27° *S* and they dip about 22° towards *S* 27° *W*,

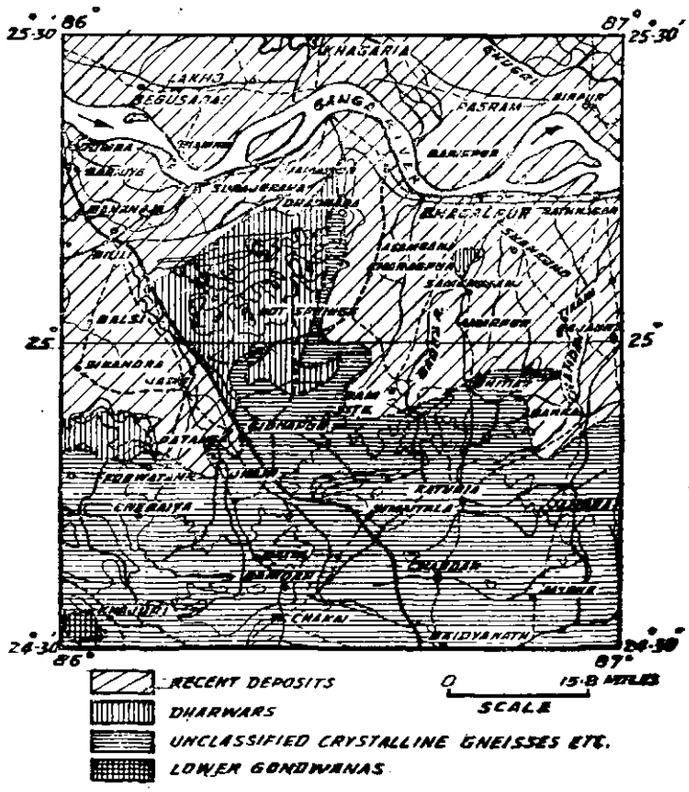

Fig 1: Regional geological map of the area around project site.

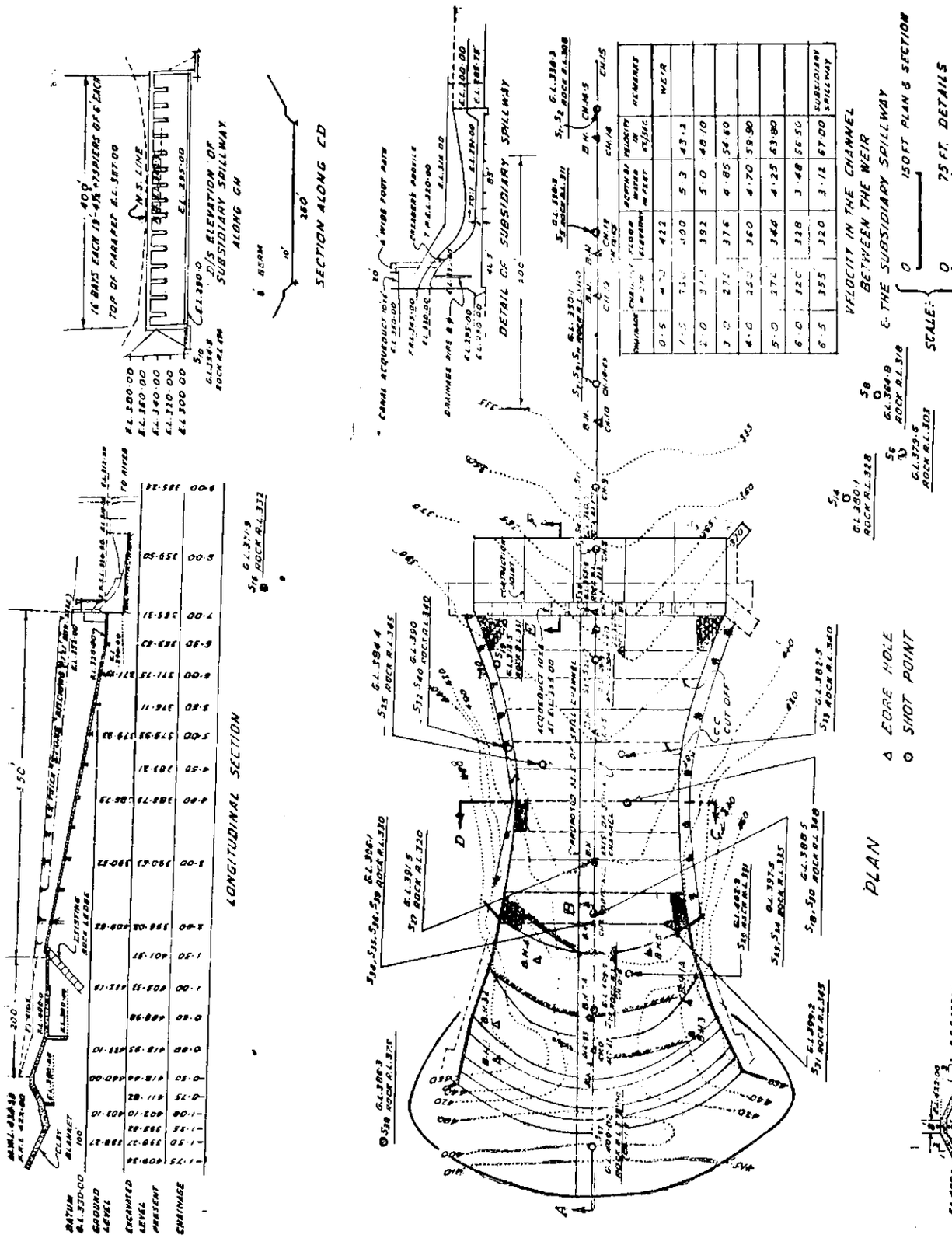

Fig 2: Plan and elevation of spillway showing locations of bore holes and seismic shotpoints with geophysically estimated rock elevations underlined.

the normal to spillway channel alignment being E 21° S. A number of bore holes have been taken at this site and their locations are shown in the contour plan of *fig 2* and the bore hole results are given in the cross-section of *fig 3* along the spillway channel alignment. Four

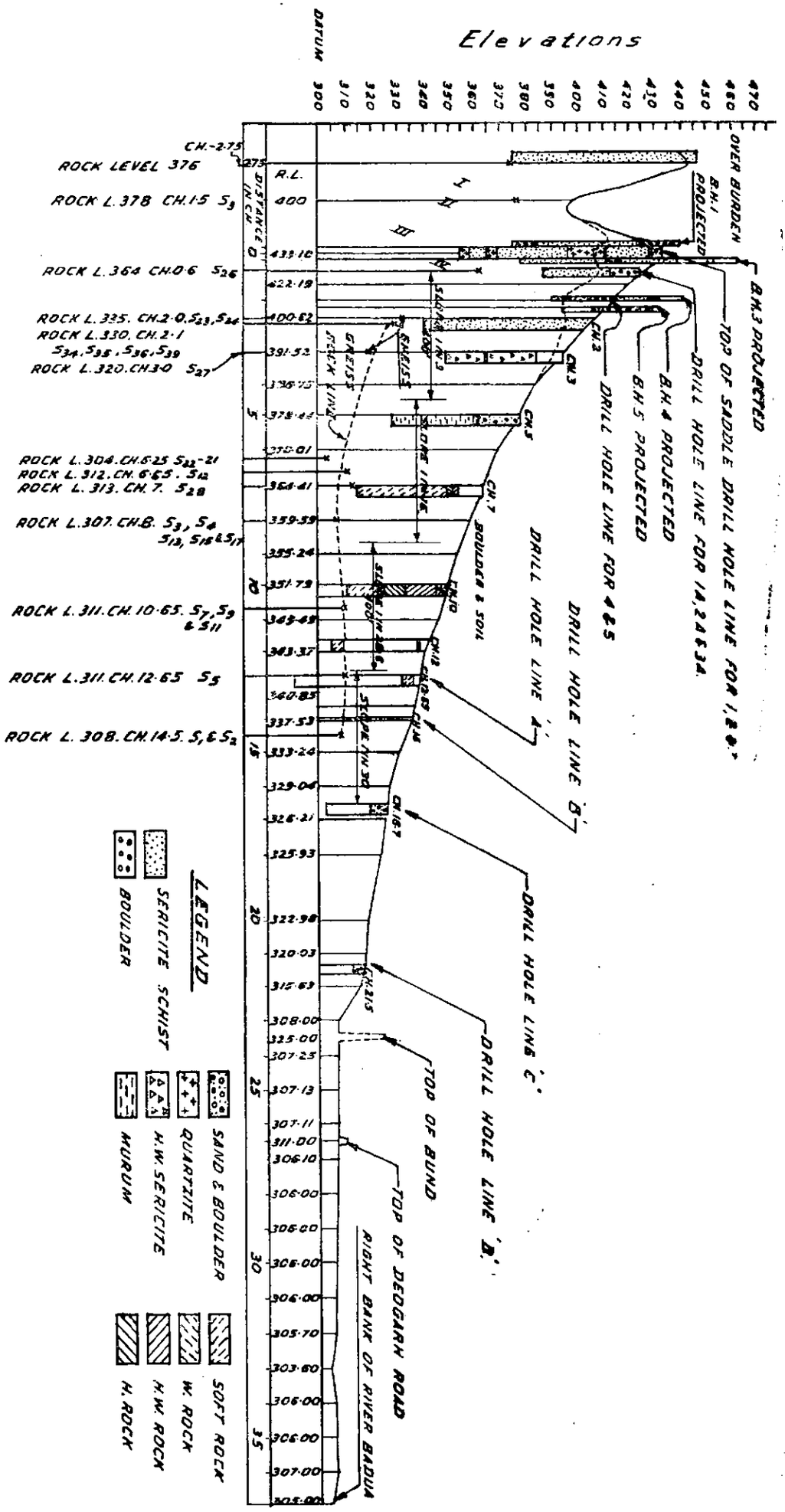

Fig 3: Longitudinal section of spill channel including log for drill holes and geophysical depth estimates.

quartzitic bands could be recognised from the results of bore holes 1 to 5 as shown in *fig 3* and from the locations and the corresponding elevations at which the surface exposures of these quartzitic bands are seen in the cuttings along the alignment as given in the contour plan of *fig 2*. These quartzitic bands are probably not very persistent in their thickness and soundness either lateraly or at depth.

Beginning from upstream in *fig 3*, there is a natural exposure of quartzitic band *No* I near chainage — 1.0, flanking the nala there, and its continuation at depth is inferred from the geophysically estimated depth of quartzite at *RL* 378 at shot point S_{37} at chainage — 1.5. The same quartzitic band would appear to correspond to the one met with between *RL* 424 — 439.4 in bore hole 1, located on the left bank abutment at a distance of 150 *ft* from chainage — .15 of the axis, and this may also correspond to a very highly weathered quartzitic band met with between *RL* 439.5 — 453.9 in bore hole 3, located 150 *ft* away from chainage .20 towards the right abutment hill.

The quartzitic band *No* II is met with in bore hole 2 at chainage 0 on the spillway axis between *RL* 397.1 — 410.6 and is actually seen exposed on the exacavated surface on the spillway axis near chainage 0 as shown in *fig 2*. This quartzitic band finds no obvious correspondence in bore hole 1 as can be seen in *fig 3*, unless these bands have a component dip of 1 in 10 normal to the spillway channel alignment which is very likely and which will make it correspond with the band just below *RL* 383.9 met with the bore hole 1. However, this band *No* II appears to have a correspondence with the quartzitic band met in bore hole 3 between *RL* 411.2 — 418.9 as shown in the cross-section of *fig 3*.

The quartzitic band No III is met with in bore hole 4, located 90 *ft* from the axis at chainage 1.4 towards the left bank abutment, between *RL* 406.4 — 416.6 and this appears to correspond with the rock exposures on the hill side cuttings on the left abutment near chainage 2 at an observed elevation of about *RL* 428 as shown in *fig 2*. This band appears to have again a correspondence with the quartzitic band met with in bore hole 2 at chainage 0 at an elevation below *RL* 369.4 and also with the quartzitic band met with between *RL* 414 — 429 in bore hole 5, located 90 *ft* towards the right bank abutment from chainage 1.6.

The fourth band is met with in bore hole 4 between *RL* 388.8 — 394.6 and is seen exposed at *RL* 400 near chainage 1.5 in the cuttings along the spillway alignment. This band finds a poor correspondence in bore hole 5 on the right abutment, there being only sand in bore hole 5 at the corresponding elevation, presumably due to complete weathering of this quatzitic band on the right bank abutment . However, this band like the band *No* I, is expected to extend at a depth along the axis as is evidenced by the geophysically estimated elevation of *RL* 364 for sound rock having a compressional wave velocity of 13,500 *ft/sec*, corresponding to sound quartzite, at shot point S_{25} at chainage .6 on the axis (*fig 3*). As a corollary, there is a likelihood of band *No* III mentioned above not being so sound at depth as otherwise the estimated rock depth at S_{26} at chainage .6 as shown in *fig 3* would have been at a higher elevation corresponding to the elevation of band No III there. Approximate positions of these four quartzitic bands as seen in the surface exposures on the cuttings are given in the contour plan of *fig 2* and their attitudes in the cross-section of *fig 3*.

In the cross-section of *fig 3*, dotted ground line shows the excavated level at the time of this investigation. The dotted rock line however shows the elevation of the gneissic rock surface from chainage 2 chainage 14.5 as obtained from bore hole results supplemented by geophysical depth estimates for sound gneissic rock, having a compressional wave velocity of about 16,000 *ft/sec*. Sound gneiss has been met with at *RL* 376 in the bore hole at chainage — 2.75, at *RL* 340 in the bore hole at chainage 2, at *RL* 313 in the deepened bore hole at chainage 7, at *RL* 312 in the bore hole at chainage 10, at *RL* 311 in the bore hole at chainage 12, at *RL* 306 in the bore hole at chainage 12.65 and at *RL* 307 in the bore hole at chainage 14. From chainage 2 to chainage 14.5, the geophysical estimated elevation of sound gneissic rock correspond very well with the observed elevations of sound gneiss obtained in these bore holes and proves a continuity of the underlying gneissic rock surface here. A similar continuity of an underlying gneissic rock surface between chainage 2 and chainage —2.75 could not, however, be definitely established. A

probability of its continuation from chainage 2 to chainage — 2.75 along the same trend as observed between chainage 2 and chainage 14.5 is indicated in the travel time curve, corresponding to a reverse profile for shot point S_{36} at chainage 2.1 and shot point S_{37} at chainage — 1.5, because of the presence of an up-dip very high apparent velocity of 40,000 *ft/sec* and an down-dip very low apparent velocity of 9,000 *ft/sec* corresponding perhaps to an underlying gneissic rock surface having here a slope downstream, in conformity with the trend of the gneissic bed-rock surface between chainage 2 and chainage 14.5.

Laboratory measurements for density and compressional wave velocity by Ultrasonic Method on samples from a sericitic quartzite band from this site shows a variation, depending on the state of weathering, of density from 2.72 to 2.13 *gm/cc*, of compressional wave velocity along the plane of the band from 15,500 to 8,000 *ft/sec*, the corresponding velocity perpendicular to the plane of the band being less by a factor of 1.8 and of Young's Modulus from 4.3×10^6 to 1.0×10^6 *psi*. In contrast very sound quartzite occuring in the band was observed to have a compressional wave velocity of 17,000 *ft/sec* paralled to the plane of the band (that perpendicular to the plane of the band being less by a factor 1.2) and an estimated Young's Modulus of 7.0×10^6 *psi*. Thus the directional variation in the physical property of sericitic quartzite band occuring here is found to be very high indeed.

Table 1

Gneiss Sample No	Location	Collected from *RL*	Compressional wave velocity in *ft/sec*	Young's Modulus (10^6 *psi*)	Density = ρ *gm/ec*
1	Ch. 7·0 (on axis)	306	15,500	6·6	2·75
2	"	307	16,700	7·7	2·76
3	"	310	13,400	4·9	2·68
4	"	312	16,300	7·2	2·71
5	"	316	11,800	3·8	2·68
6	Ch. 7·0*	312	14,300	6·0	2·75

*50 *ft* away from the axis towards right bank.

The nature of the underlying gneissic rock at chainage 7 might be of interest because of the possibility of an aqeduct being located there. The following table shows the observed variation of compressional wave velocity for samples of gneiss obtained from different depths at this chainage and the calculated Young's Modulus which is proportional to the square of the compressional velocity.

IV. Navagam Dam Site, Narmada Project

INDEX MAP of *fig 1* shows the location of the proposed dam site on *river Narmada* near the village Navagam (Gujarat), 15 *miles NNE* of Rajpipla. The river here flows North-West and the proposed alignment has a bearing *N* 41° 15′ *E*. Here the hill 451 will form the left abutment. The overall length of the dam will be 5000 *ft*. The full reservoir level will be *RL* 200, the minimum water level being *RL* 61 and the deepest portion of the river bed being *RL* 30. Deccan Trap Basalt occurs in the right abutment hill and in the river bed and Quartzites and shales interbeded with trap constitutes the left abutment hill. Results of 23 boreholes namely for *A* line along the alignment, are shown in the cross-section of *fig 2*. Similar results are available for *B, C* and *D* lines of boreholes situated 100 *ft*, 200 *ft* and 300 *ft* downstream of alignment and *E* line of bore holes situated 100 *ft* upstream of alignment. Results of percolation test in many of these boreholes are also available. Geophysical investigations employing Seismic Refraction, Electrical Resistivity, and Magnetic Methods were employed here to gain, if possible, more of subsurface information.

2. Seismic refraction method

It was employed for obtaining more of subsurface information on the left abutment hill where only 4 bore holes are available namely X_1, X_2, X_3 and X_4. The results are shown in *figs 2* and *3*. It is seen from *fig 2* that at shot point S_4 situated 90 *ft* beyond 0 chainage (namely chainage — 90) sound rock elevation is estimated at *RL* 248, under 120 *ft* of overburden. At S_{44} near chaniage 247 of bore hole X_3, estimated sound rock level at *RL* 126 nearly coincides with the top of grey vessicular basalt underlying 145 *ft* of overburden and

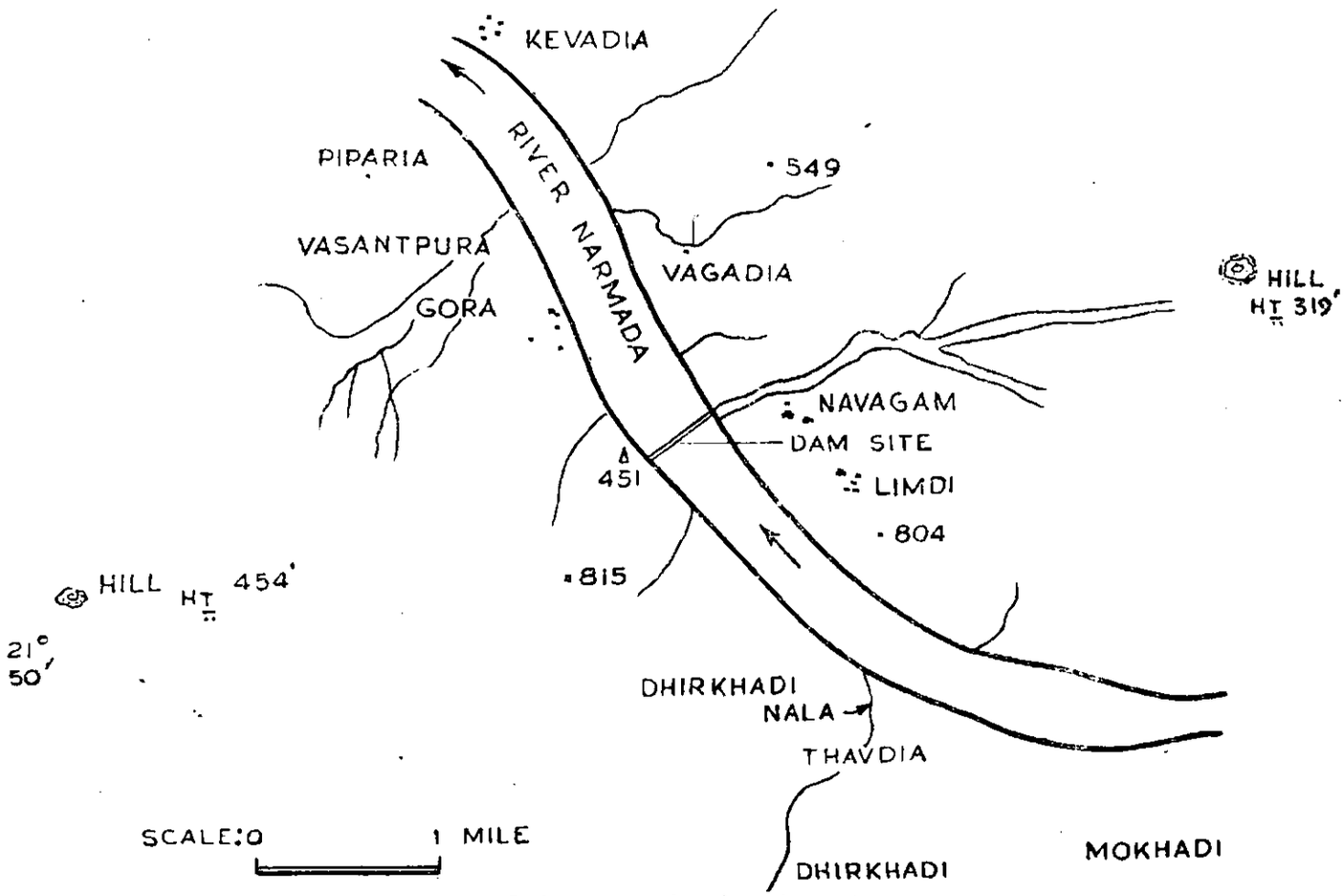

Fig 1: Index map showing dam site.

weathered trap. At S_2 and S_3 near bore hole X_1 at chainage 497 sound rock is estimated at about *RL* 10 under 110 *ft* of overburden and weathered trap. Along contour level *RL* 70 along the river bank, seismic shots at S_{30} situated 300 *ft* downstream and at S_{31}, situated 300 *ft* upstream of the alignment at *RD* 595 show that the average depth of rock here is about 15 *ft*, the rock level being about *RL* 55. The estimated depth to sound rock on the left abutment hill is generally in conformity with the few bore hole results as are available along the alignment here. Some overall information about the nature of the rock occurring under the left abutment is, however, provided by the observed velocity with which the seismic pulse is found to travel through the bed rock under each of the eleven profiles taken on this abutment. The velocities are shown in *fig 3* along each of these profiles. It will be seen that the velocity of sound in the trap rock underlying the left abutment along the alignment namely along the profile S_3 and S_4 passing through boreholes X_1 and X_4, is 15,000 *ft/sec* and that along profile S_{45} and S_{47}, and profiles S_{11} and S_{13}, situated respectively about 100 *ft* and 250 *ft* upstream of the alignment, the velocity in the underlying sound rock is about 11,000 *ft/sec* which probably indicates that trap is not likely to extend so much upstream of the alignment as to be under these two profiles. Downstream of the alignment under profile S_{43} and S_{47}, S_1, S_2 and S_{12} and S_{13}, trap is quite sound having a velocity of 15,000 *ft/sec*. In the seismic profile S_{30} and S_{31} taken nearly along the contour *RL* 70 passing through *RD* 595, it is observed that downstream of *RD* 595 the bed rock of trap has a velocity 15,000 *ft/sec* but upstream of *RD* 595 along this seismic profile bed rock has a velocity of 12,000 *ft/sec* probably indicating that sedimentary bed rock and not trap is to be expected just upstream of *RD* 595 of the alignment. A somewhat lower velocity of 10,500 *ft/sec* was observed for the bed rock along seismic profile S_5 and S_6 nearly parallel to the alignment but situated 300 *ft* downstream of it. Along the profile S_{10} and S_{11} situated on the undulating ground around *RL* 200 situated 600 *ft* upstream of alignment near boreholes Y_1 and Y_2, the bed rock velocity is only 8300 *ft/sec*. This low velocity perhaps corresponds to a bed rock

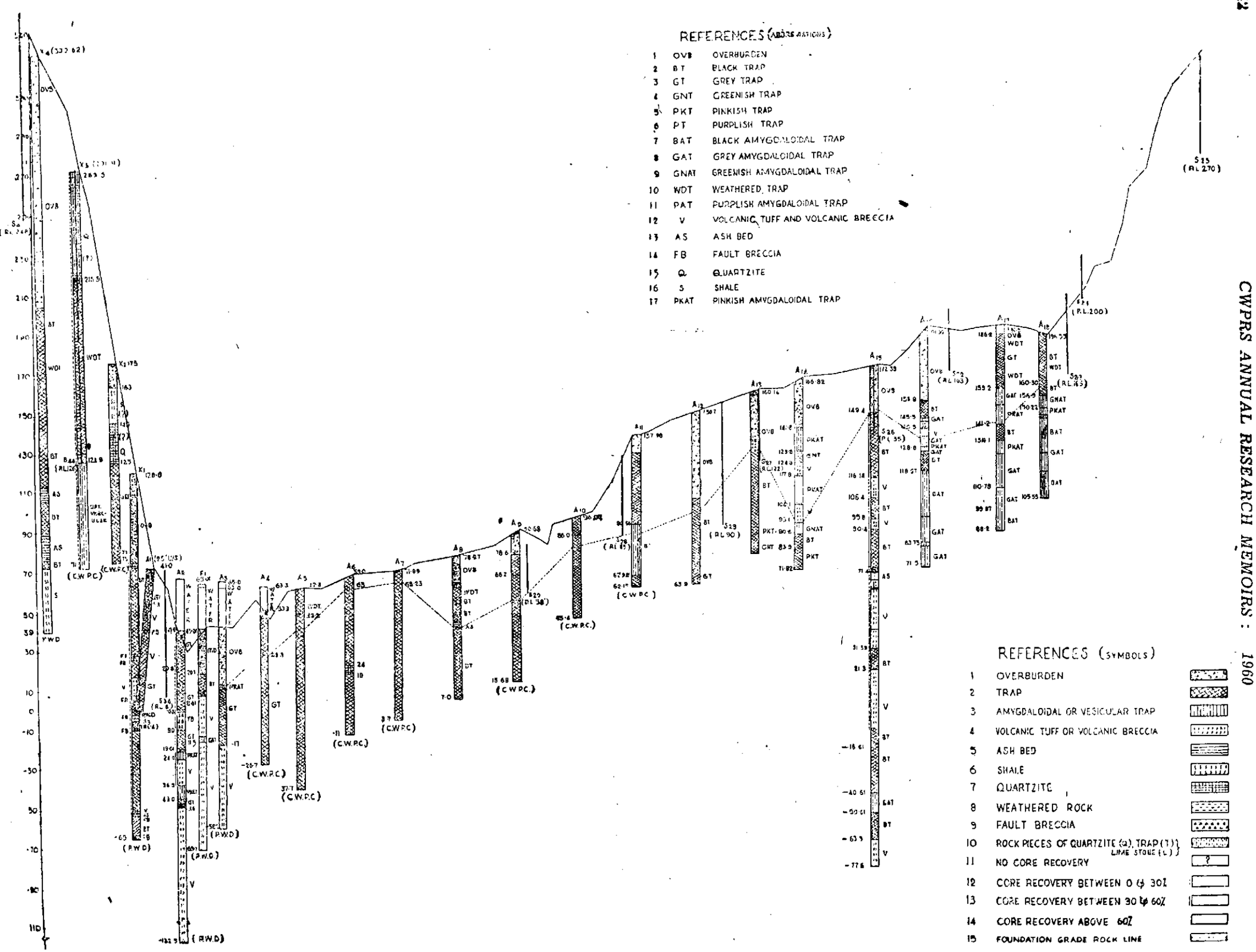
REFERENCES (ABBREVIATIONS)
1 OVB OVERBURDEN
2 BT BLACK TRAP
3 GT GREY TRAP
4 GNT GREENISH TRAP
5 PKT PINKISH TRAP
6 PT PURPLISH TRAP
7 BAT BLACK AMYGDALOIDAL TRAP
8 GAT GREY AMYGDALOIDAL TRAP
9 GNAT GREENISH AMYGDALOIDAL TRAP
10 WDT WEATHERED TRAP
11 PAT PURPLISH AMYGDALOIDAL TRAP
12 V VOLCANIC TUFF AND VOLCANIC BRECCIA
13 AS ASH BED
14 FB FAULT BRECCIA
15 Q QUARTZITE
16 S SHALE
17 PKAT PINKISH AMYGDALOIDAL TRAP
REFERENCES (SYMBOLS)
1 OVERBURDEN
2 TRAP
3 AMYGDALOIDAL OR VESICULAR TRAP
4 VOLCANIC TUFF OR VOLCANIC BRECCIA
5 ASH BED
6 SHALE
7 QUARTZITE
8 WEATHERED ROCK
9 FAULT BRECCIA
10 ROCK PIECES OF QUARTZITE (Q), TRAP (T) LIME STONE (L)
11 NO CORE RECOVERY
12 CORE RECOVERY BETWEEN 0 & 30%
13 CORE RECOVERY BETWEEN 30 & 60%
14 CORE RECOVERY ABOVE 60%
15 FOUNDATION GRADE ROCK LINE

of Volcanic Breccia and disintegrated rock met with in these two bore holes for considerable depth. It appears from above results that by shifting the alignment within 500 *ft* upstream or downstream of its present position on the left abutment hill no better bed rock condition is likely to obtain.

In the Nala at the edge of the right bank in bore hole E_5, *RL* 85, located 100 *ft* upstream of the chainage 2587, clayey material mixed with rock pieces and sand were met with at a depth of 76 to 106 *ft*. From the three seismic profiles taken there, one along and two across the nala channel sound rock was estimated at a shallow depths varying from 7 to 27 *ft* at S_{16}, S_{17}, S_{18}, S_{19}, S_{20}, S_{21} as shown in *fig 3* and the velocity of bed rock was observed to be 14,500 *ft/sec*. Seismic Method however cannot detect a weak strata of low velocity occuring below a hard strata of high velocity even if the underlying weak strata be extensive and thick enough. It cannot, therefore, be said, from the results of hard good basalt occuring at shallow depth here, whether the weak underlying strata met with in borehole E_5 between depth 76 to 106 *ft* is only localised on an extended phenomena.

Four seismic profiles were taken along the alignment on the right bank. *Fig 2* shows that along profile S_{28} and S_{29} between chainage 2950 and chainage 3450 sound rock rises from *RL* 85 at S_{28} to only *RL* 90 at S_{29} and the sound rock velocity here is 13,000 *ft/sec*. Along profile S_{27} and S_{26} between chainage 3632 and chainage 4232 sound rock rises from *RL* 122 at S_{27} to *RL* 135 at S_{26}, which is in conformity with the bore results of A_{13} and A_{15} near which they were located, the velocity in sound rock here is 13,000 *ft/sec*. From measurements of Ultrasonic velocity on cores in the laboratory, unweathered Volcanic Breccia occuring at Navagam site has usually been observed to have a fairly high velocity of transmission for sound waves which is comparable to that in moderately sound trap rock. Occurrence of Breccia can only be detected from electrical resistivity measurements to be discussed later. Occurrence of Volcanic Breccia cannot be distinguished from Basalt from seismic velocity measurements. This explains why the velocity of sound bed rock under this profile is the same as that under profile S_{28} and S_{29} discussed above though layers of Volcanic Breccia are expected to occur under profile S_{27} and S_{26} from results of borehole 14 and not under profile S_{28} and S_{29} as shown in *fig 2*. The velocity in the bed rock, which occurs at *RL* 164 under profile S_{22} and S_{23}, between

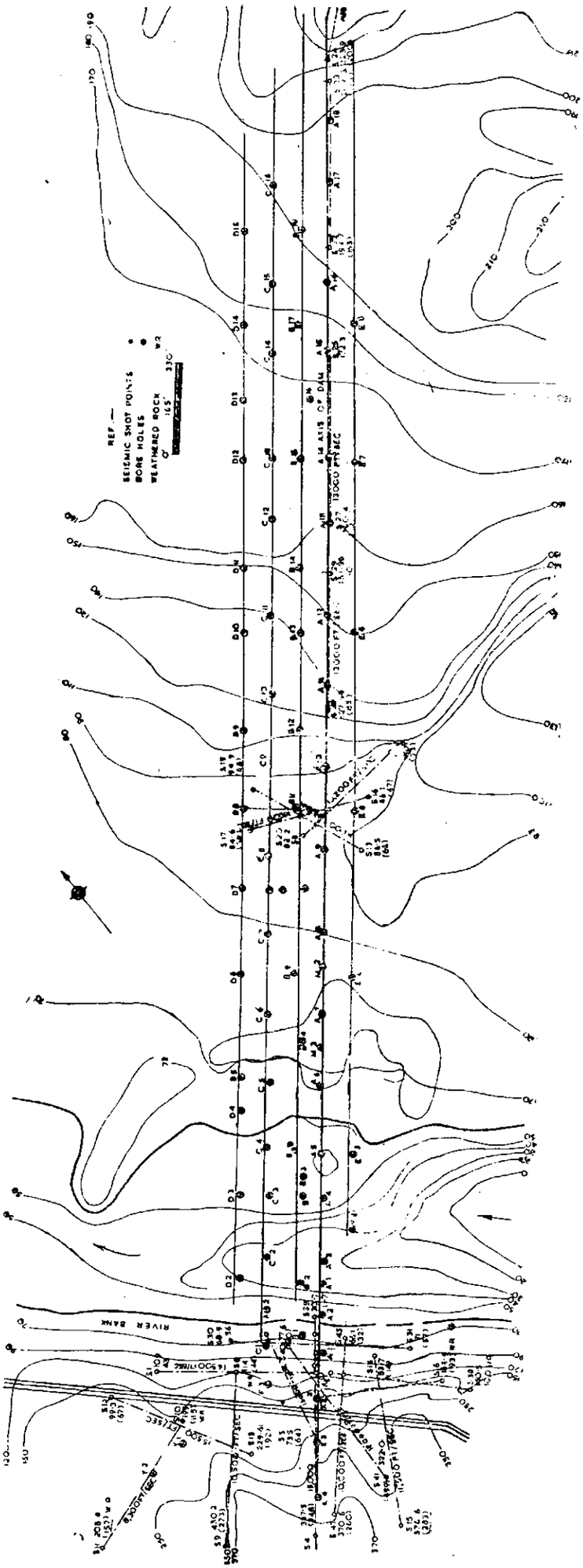

Fig 3: Locations of the bore holes and seismic shot points with the corresponding ground elevation and the estimated sound rock elevation which is underlined, The proposed axis is along the line of bore holes marked 'A'.

chainage 4598 and chainage 5198 is 12,000 *ft/sec* showing that bed rock of Basalt at that depth is somewhat weathered as is also shown by results of bore hole A_{17} and bore hole 18. In the profile S_{24} and S_{25}, along the right abutment hill, between chainage 5270 and chainage 5855, rock rises steeply from *RL* 200 at S_{24} to *RL* 270 at S_{25}, the sound bed rock velocity being observed to be 13,000 *ft/sec*. As good basalt would usually show a velocity of 15,000 to 17,000 *ft/sec*, the basalt bed rock occurring on the right bank could only be described as moderately good as the velocity observed under these four profiles taken on the right bank is only 13,000 *ft/sec*.

3. Electrical resistivity logging

Electrical resistivity logging was carried out in a few bore holes adjoining the left bank in order to help assess the *in situ* condition of rock met with there. Rock resistivities at different depths in a bore hole were measured with an equally spaced 4-electrode set-up gradually lowered in the bore hole, below the casing depth, the separation between adjacent electrodes being kept always 3 *ft*. Only 4 bore holes could be logged as they were free below their casing depth, the rest of the bore holes being all filled up. Hence only limited information could be obtained from these measurements and the results are shown in *fig 4*. At bore hole X_1 at chainage 497 at *RL* 120 on the left bank abutement hill, it is seen that rock resistivity is not very high till sound black trap is met with at *RL* 0 and that too it is very high only when the region of high water loss namely between *RL* 0 to *RL* — 10 has been passed. Values for velocity in sound rock measured on core samples taken from different depth from this bore hole are also shown in the *fig 4* togther with percentage core recovery and water loss in *gal/min* for 100 *lbs/sq in* pressure. It is seen that velocity of sound in fault breccia in borehole X_1, occurring between *RL* 27 and *RL* 30 is quite low namely 6900 *ft/sec* which is somewhat similar to that for weathered trap met at *RL* 79 in this borehole.

In bore hole F_1 situated in the river bed at chainage 837 on the alignment, it is seen that fairly high water loss occurs in Volcanic Breccia met with below *RL* 30 and this is associated with a low value for electrical restistivity, namely 400 — 200 *ohms-ft* for Volcanic Breccia met with there, though the percentage recovery of core is good. It is significant that Volcanic Breccia in borehole F_2 located at 200 *ft* downstream of chainage 729 in river bed shows very small water loss and its electrical restivity is also comaprtively quite high namely 800 to 1000 *ohms-ft*. Water loss occuring in Volcanic Breccia met with in borehole F_4 located at 110 *ft* upstream of chainage 1050 in the river bed is moderate and its electrical resistivity is also moderately high namely between 600 — 800 *ohms-ft*. It would appear from the limited data obtained for electrical resistivity logging in the 4 bore holes discussed above that Volcanic Breccia can be classified in three general categories:

(*i*) that in borehole F_1 having a high permeability corresponding to large water loss and low electrical resistivity namely below 300 *ohms-ft*

(*ii*) that occuring in borehole F_4 having intermediate values for permeability with moderate water loss and for electrical resistivity namely 600 — 800 *ohms-ft*

(*iii*) that occuring in bore hole F_2 having low values for permeability and water loss and a comparatively high electrical resistivity of above 900 *ohms-ft*.

It is observed that electrical logging could be extensively used to supplement profitably water loss test to find out localised zones of high permeability in Volcanic Breccia (perhaps because of their high porosity) as also in basalt (perhaps because of the existence of fracture). Electrical logging could be carried out very early so that all the boreholes could be covered quickly.

The following *table* shows the results of laboratory measurements on basalt and Volcanic Breccia core samples from borehole F_1 and borehole F_2, for their density and the ultrasonic velocity for compressional and shear modes of wave propagation, (from which Young's modulus and Possion's Ratio can be calculated) and the correlations obtained with apparant electrical resistivity measured from Electrical Logging and the corresponding water loss from pumping tests.

It will be seen that very good correlation is obtained both for basalt and Volcanic Breccia between their *in situ* apparant electrical resistivity as obtained by electrical logging and the degree of permeability as inferred from water loss tests in bore holes.

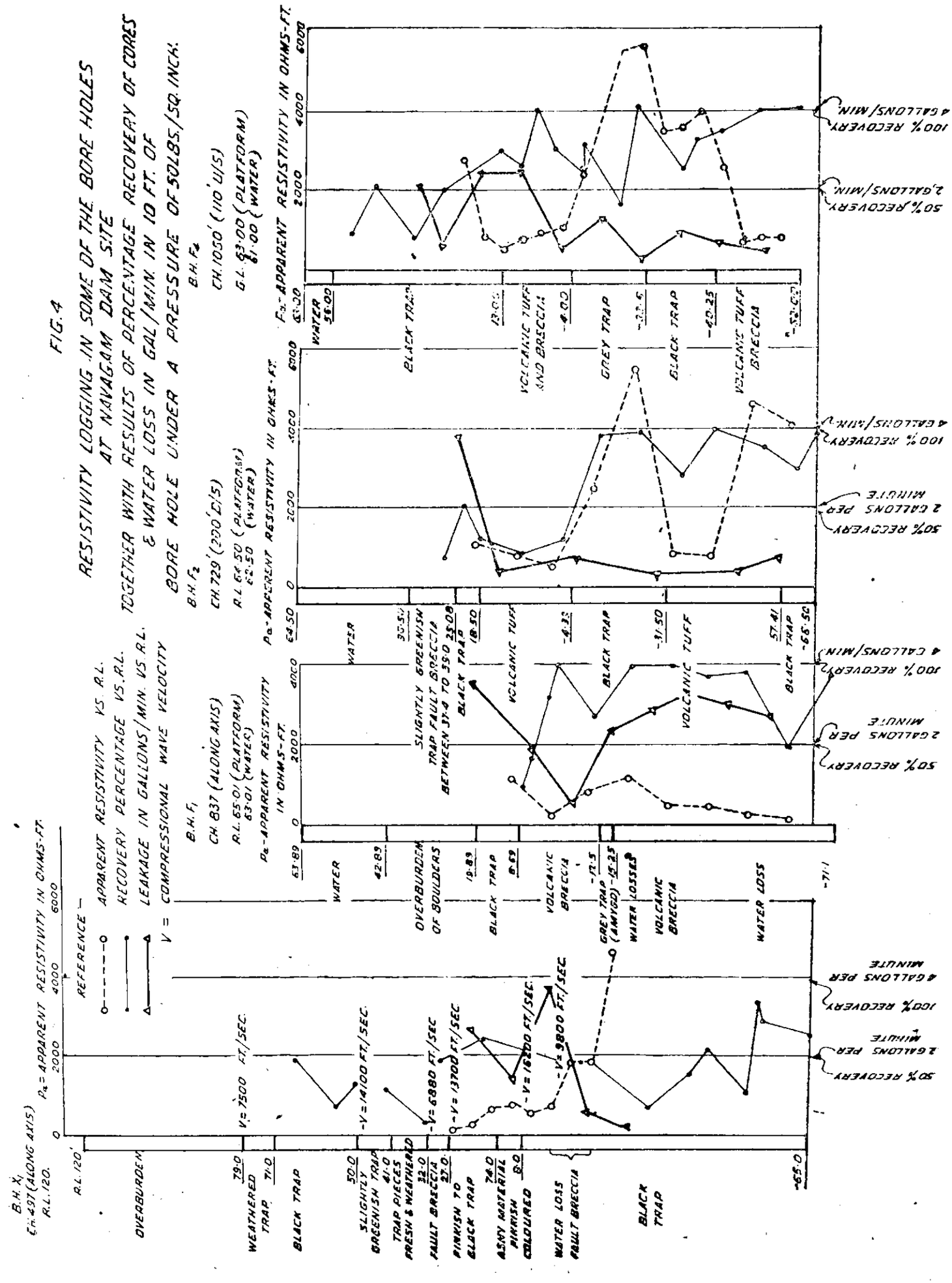

FIG. 4

RESISTIVITY LOGGING IN SOME OF THE BORE HOLES AT NAVAGAM DAM SITE TOGETHER WITH RESULTS OF PERCENTAGE RECOVERY OF CORES & WATER LOSS IN GAL/MIN. IN 10 FT. OF BORE HOLE UNDER A PRESSURE OF 50 LBS/SQ. INCH.

Table 1

	Volcanic Breccia F_1/104	F_2/99	Basalt F_2/73	F_2/83
Depth (in *ft*) ...	104	99	73	83
Density (*gm/cc* ...	2·15	2·53	2·69	...
Velocity of { Compressional wave (*ft/sec*)	13,300	11,200	17,503	...
Velocity of { Transverse wave (*ft/sec*)	...	4,800	...	...
Poisson's ratio ...	...	·34	...	...
Young's modulus in $10^6 psi$	4·5	3·0	7·9	...
*Apparent electrical resistivity. (in *ohms/ft*)	430	930	2500	5400
Water loss in 10 *ft* bore hole in *gal/min* for 100 *lb/sq in* pressure *percent.*	7·0	·4	·9	·04
Saturation by volume on keeping in water for 48 *hours* (*percent*).	4·1	8·0	...	...

* As determined from measurements on saturated core samples in laboratory, true resistivity is, however 1½. This apparent value of resistivity as obtained in Electrical Logging.

Volcanic Breccia was met with in many boreholes near the left bank namely in boreholes A_2, F_1, A_3 along the alignment in B_1, 100 *ft* downstream of alignment, in F_3, C_1 and C_2 200 *ft* downstream of alignment. A short electrical resistivity soundings profile was therefore taken with its centre 200 *ft* downstream of the alignment at *RD* 600 near the water edge on the left bank, by extending the electrode separation in steps from 2.5 *ft* upto a maximum of 50 *ft*, for a 4-electrode set-up. The results are shown in *fig* 5. Trap bed rock is estimated at a shallow depth here of about 10 — 15 *ft*. The bed rock in estimated to be at about *RL* 50, the ground level being *RL* 63. The resistivity of bed rock is about 400 *ohms-ft* as shown in *fig* 5 and this cannot be said to correspond to a good basalt bed-rock which usually shows an electrical restistivity of about 1000 *ohms-ft* or more. Only moderately weathered basalt with joints or Volcanic Breccia may be responsible for a bed rock resistivity of about 4000 *ohms-ft* as observed here.

4. Magnetic survey

Sedimentary, Quartzites and shales forming the left bank hill and also occuring upstream of the dam alignment on the river bed have been described by Datta in his Geological Report of this site as inter-trappen beds. In this area along Narmada they occur, according to him, in-between Deccan trap Basalt flows as :

(*i*) Calcareous sandstone merging into normal quartzites and sandstone over 1000 *ft* thick

(*ii*) siliceous limestone 50 — 75 *ft* thick

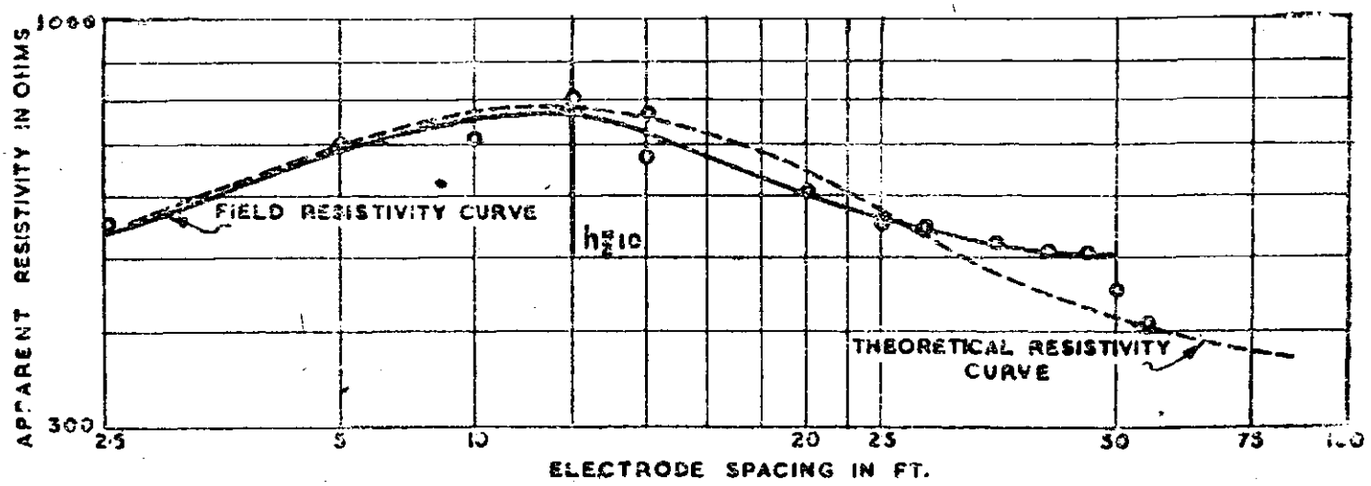

Location :—On the left bank at water-edge 200 upstream of *CH* 595 of axis traverse along the river bank on saturated sand underlain by trap rock at shallow depth.

$P_1 : P_2 : P_3 = 380 : 1140 : 380$ *ohms-ft.*
$p_1 = 380$
$p_2 = 1140$
$p_3 = 380$

$h_1 : h_2 = 1.5$
$h_2 = 10$ *ft*

Resistivity of trap bed rock = 380 *ohms-ft.*
Ground level = 63
RL of bed rock = 53

Fig 5: Electrical resistivity sounding.

(iii) Massive quartzite 400 *ft* thick and Lava flow 20 *ft* thick

(iv) Quartzites with slaty shales 160 *ft* thick

(v) Dark grey shales 60 *ft* thick

(vi) Quartzites with traps 60 *ft* thick.

According to his observations on boreholes X_1, X_2 and X_3 (results of boreholes X_4 was not available at that time) and the two drifts at *RL* 120 and *RL* 175 the following sequence of bed from top downward was found to occur on the left abutment hill 451; Massive quartzites down *RL* 245, Lava flows (weathered trap) 95 *ft* thick; Dark grey shales 60 *ft* thick, quartzite band 15 *ft* thick, and weathered trap downwards from *RL* 145. The thickness of lava flows occurring within the sedimentary beds in the left abutment is said to be very variable. The trap overlying the thick shale bed in the drift at *RL* 175 on the left abutment is found to be about 95 *ft* thick but no trap is seen overlying the thick shale bed in the exposure on the left bank only a short distance away from the alignments here. According to his observations the dip of the strata in the sedimentary rocks varies from 30° to 45°. On the left abutment hill the shales near the entrance of the upper drift at *RL* 175, dip 35° towards 195° bearing. The quartzites exposed higher up on this hill dip 45° towards 200° bearing. On the river bank the thick shale bed has some irregular dips with evidence of local slipping but the overlying quartzites show steady dips of 45° towards 145° bearing. There is thus a sharp swing according to him in the strike of the sedimentary beds from the river bank of the left abutment hill 451. The contact between the sedimentary beds and the trap rock near the base of the left bank hill, 300 *ft* upstream of the alignment, as also in the river bed is more or less in a straight line trending *E-W*, which makes a small angle with the strike direction of the sedimentary beds here. According to Saha, the nature of this contact near the base of the left abutment was not clear as there are no outcrops showing the relationships between to two. No evidence of faulting was found by him. The nature of this contact is important and has, therefore, been studied here by a vertical force magnetic survey near the base of the left abutment.

Results of these magnetic survey are shown as vertical force magnetic anomaly profiles in *fig 6* giving the variations observed in the vertical com-

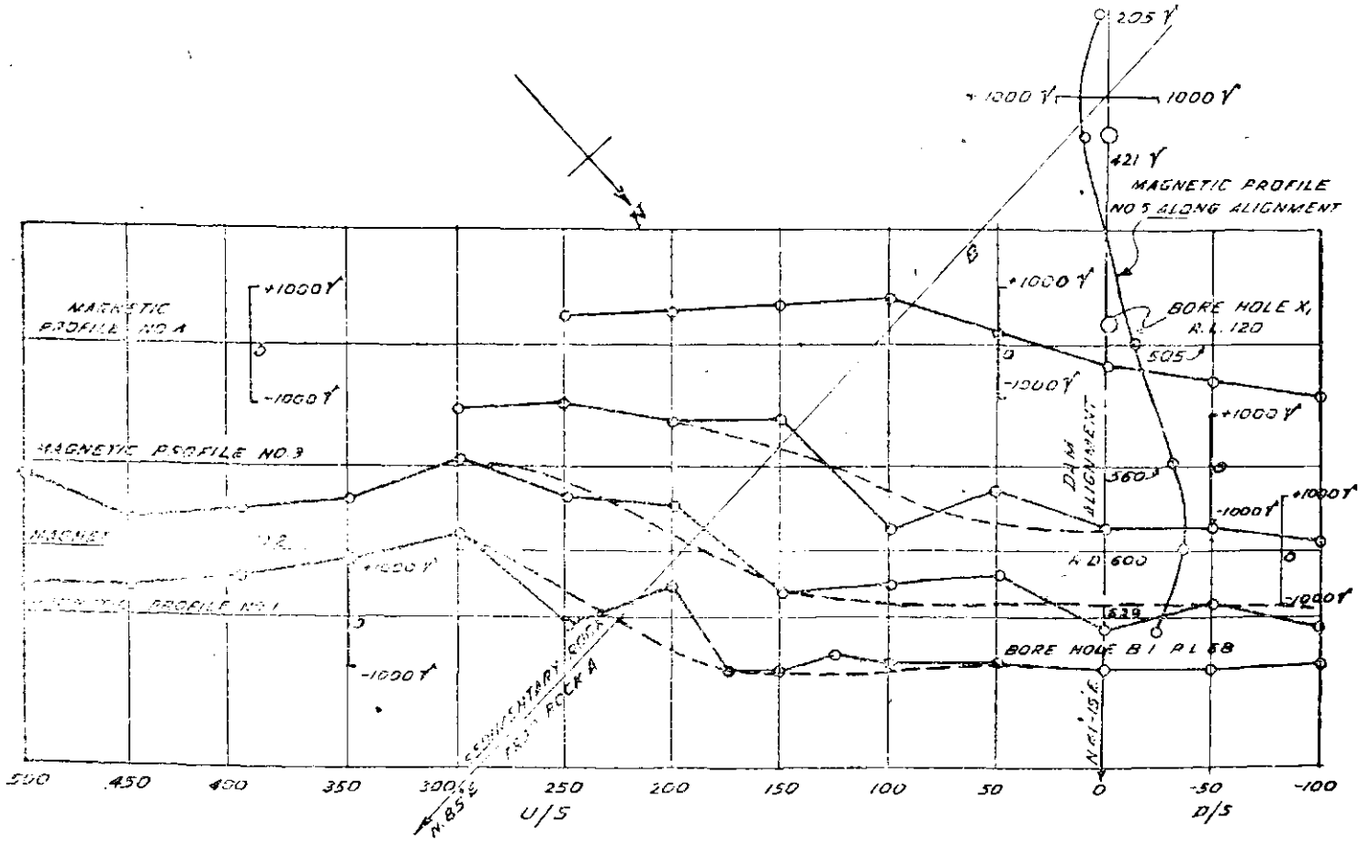

Fig 6: Vertical force magnetic anomaly profiles on left bank abutment along four traverses normal to the alignment passing through *RD* 629, 600, 560 and 505 showing the approximate location of the line of contacts *AB* between sedimentary beds and trap rock which is hidden under overburden.

ponent of the earth's magnetic field (magnetic anomaly) along five profiles, four passing nearly normal to the alignment through *RD* 629, *RD* 600, *RD* 560 and *RD* 505 on the left abutment and one along the alignment there. It is seen from *fig 6* that the estimated location of the contact between the sedimentary beds occurring on the upstream and trap rock occurring on the downstream of this contact, passes through a line approximately joining the positions of the maximum anomaly in each of the five anomaly profiles and that the bearing of this line of contact is *N* 85° *E*, corresponding approximately with the *E-W* bearing of this contact in the river bed as observed by Saha.

The difference between the maximum and minimum values for the anomaly in profile *No* 1 is 2500 ($1\ \gamma = 10^{-5}$ *gauses*), in profile *No* 2 it is 3100 γ, in profile *No.* 3 it is 2300 γ and in profile *No* 4 passing near borehole X_1, this difference is 1700 γ. It is lower in magnitude in this profile because of the fact that the overburden above trap rock is higher here than in other profiles. It would appear from this anomaly curves that trap occurring downstream of this contact and having according to Saha a dip 10° — 20° towards, in general, *S-S-E* and *S* is not likely to extend upstream of this contact under the sedimentary beds. The sedimentary trap contact surface is likely to dip downstream at a somewhat steep angle. Whether this contact is erosional or by faulting can only be decided by further geological evidences and not by the geophysical methods. It may, however, be recalled that in borehole X_4 at chainage 50, *RL* 330 on the left abutment hill shale is found to occur between *RL* 72 and *RL* 30 underlying 258 *ft* of integrated quartzite and trap rock. Lowest level in trap has, however, been reached in bore hole B_1 at *RL* 68 located 75 *ft* downstream of chainage 641 on the left bank, penetrating to *RL* — 130 in trap. This borehole is only about 300 *ft* downstream of the sedimentary-trap contact, occurring upstream of the alignment and here sedimentary-trap contact has already gone down more than 200 *ft*. Thus the sedimentary-trap contact surface is likely to dip steeply downstream as could also be inferred from the shape of the vertical force magnetic anomaly curves obtained which is similar to that to be expected over a steeply inclined contact surface separating magnetic trap and non-magnetic sedimentary bed. There is also frequent occurence of fault breccia in cores from different bore holes on this bank. A careful evaluation of implication of these evidences together with any other geological evidences that may be collected will have to be made before any fault could be definitely established here.

---

37. Base exchange reactions

Sodium and Calcium

FURTHER WORK on the study of exchange reactions has been carried out during the year. The reaction has been studied with solutions having different concentrations and on various soils. The soils include two black cotton soils with high exchange capacity, one alluvial soil with moderate exchange capacity and four lateritic, red and mattassi soils having low exchange capacity. The concentrations of the solutions used were *N*, *N*/2, *N*/5 and *N*/10 of sodium and calcium chlorides having various proportions of sodium to calcium as 97.5 : 2.5; 90 : 10; 80 : 20; 70 : 30 and 60 : 40. Higher proportions of calcium were not taken as the expected sodium adsorption is quite low and the experimental errors are comparatively large.

The soils were first changed into calcium soils and then leached with adequate volumes of the solution to reach equilibrium. The quantity of the soil taken was between 2-5 *gm* depending upon the exchange capacity. Excess of the salts were removed by washing with 80 *percent* alcohol and the adsorbed sodium and calcium ions were leached out with about 300 *cc* of *N*-ammonium acetate solution. The leachate was dried and ignited in silica dish and taken up in .2 *N*

hydrochloric acid. Calcium was estimated volumetrically and sodium by flame-spectro-photometer.

Percentage of sodium adsorption by soils under various conditions and the mean values are given in *table 1.* It is seen from the values for

Table 1.—Sodium adsorption by soils on leaching with mixtures containing various proportions of sodium and calcium chlorides:

Strength	Proportion		*Na* adsorption percentage for different soils*							
	Na	*Ca*	1	2	3	4	5	6	7	Mean
N ...	97·5	2·5	84·0	81·2	77·8	84·2	82·4	82·0	83·3	82·1
	90	10	67·1	63·5	59·4	69·4	68·0	67·4	65·3	65·7
	80	20	50·5	55·3	43·8	54·1	42·8	56·0	47·8	50·0
	70	30	38·7	38·6	36·0	35·1	42·1	40·2	41·0	39·4
	60	40	31·0	29·5	29·5	...	29·9	30·9	30·7	30·3
N/2 ...	97·5	2·5	80·9	79·2	76 6	78·1	75·7	77·6	81·1	78·5
	90	10	58·5	57·9	56·5	62·7	59·1	57·0	60·2	59·0
	80	20	43·4	43·1	42·2	44·7	44·7	43·9	43·8	43·7
	70	30	32·6	33·0	33·9	33·0	34·2	31·8	32·9	33·1
	60	40	27·3	25·3	26·6	25·7	25·4	...	24·3	25·8
N/5 ...	97·5	2·5	71·8	66·5	64·9	69·6	71·7	65·8	69·8	68·6
	90	10	45·7	45·0	42·9	46·5	46·9	44·4	44·0	45·1
	80	20	30·2	28·5	27·8	30·6	29·0	32·3	31·1	29·9
	70	30	22·5	18·2	24·4	20·3	20·6	18·1	18·4	20·3
	60	40	...	16·2	15·7	...	16·0	16·5	16·1	16·1
N/10 ...	97·5	2·5	64·8	60·9	59·7	64·0	61·1	...	...	62·1
	90	10	38·5	38 9	33 1	38·3	35·7	...	34·1	36·2
	80	20	25·7	23·6	21·1	27·7	23·0	22·1	23·3	23·8
	70	30	18·5	16·4	16·5	14·8	14·8	16·3	15·2	16·1
	60	40	12·9	10·9	10·2	...	11·1	...	...	11·3

Lab No

1	...	...	Black Cotton soil	(Local)	5	6694	...	Brown Loam (Sambalpur)
2	7636	...	Alluvial Soil	(Chinsura)	6	7208	...	Lateritic Soil (Bhagalpur)
3	...	...	Yellow Soil	(Mattassi)	7	8315	...	Black Cotton Soil (Andhra)
4	6759	...	Red Brown Loam	(Mangalore)				

all the soils that percentage of sodium adsorption is practically the same under similar treatment. Slightly lesser values for mattassi soil (*No 3*) may be due to the difficulty in working with this soil. All other values are within the experimental error and it may be said that percentage of sodium adsorption for any soil when brought in equilibrium with any leaching solution depends upon the strength of the solution and the proportion of sodium in it. It does not depend upon the nature of the soil. It is further observed from the results that the percentage of sodium adsorption goes on decreasing with decrease in the strength of the solution, proportion of sodium remaining the same. It also decreases with decrease in the proportion of sodium in the leaching solution, strength of the solution remaining same. Percentage of sodium adsorbed with normal solution having as high as 97.5 *per cent* sodium is about 82 *percent* and it falls to

about 30 *percent* when the proportion of sodium decreases to 60 *percent*. Decrease from about 78 to 26 *percent*, 69 to 16 *percent* and 62 to 11 *percent* has been found for $N/2$, $N/5$ and $N/10$ solutions respectively, when the proportion of sodium in the solution falls from 97.5 to 60 *percent*.

Fig 1 gives the relation between sodium in solution and sodium adsorbed for various strengths of the solution. Dotted lines are the extensions of the lines drawn from experimental data. It is presumed that the value of sodium adsorption will be 100 when calcium is absent in leaching solution and it will be zero when sodium is absent from leaching solution. From the curves it will be possible to find out sodium adsorption for any soil when treated with solutions of N, $N/2$, $N/5$ and $N/10$ strength, having any proportion of sodium. In *fig 2* is shown the relation between concentration of solution as normality, and percentage of sodium adsorbed for various proportion of sodium and calcium. Dotted lines are the extensions of lines drawn from experimental data. Lines for sodium proportion of 20 and 40 *percent* are from values taken from *fig 1*. The extended lines between $N/10$ and $N/1000$ strength appear to be straight lines and a line for every proportion of sodium to calcium exists there. The extended lines are subject to verification.

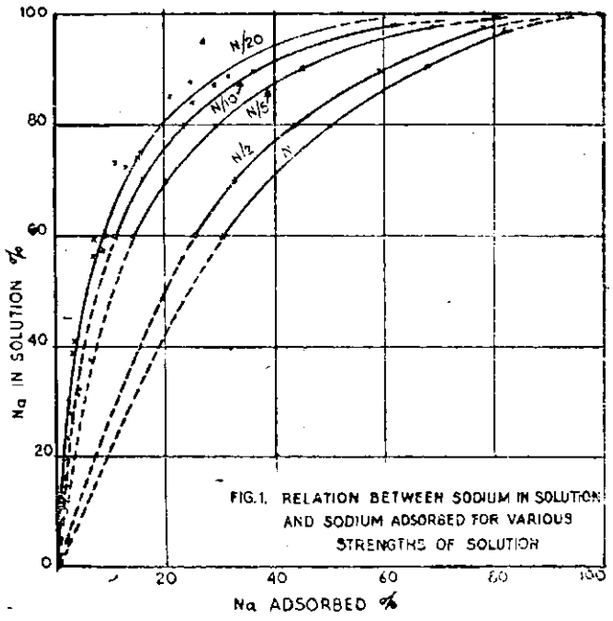

FIG.1. RELATION BETWEEN SODIUM IN SOLUTION AND SODIUM ADSORBED FOR VARIOUS STRENGTHS OF SOLUTION

The procedure followed in equilibrium reaction carried out last year and this year is different. Last year the soil was shaken with a solution of certain strength and allowed to reach equilibrium, the amount of cations in soil and in solution were estimated. In the present study, the soil has been leached with particular solution till equilibrium

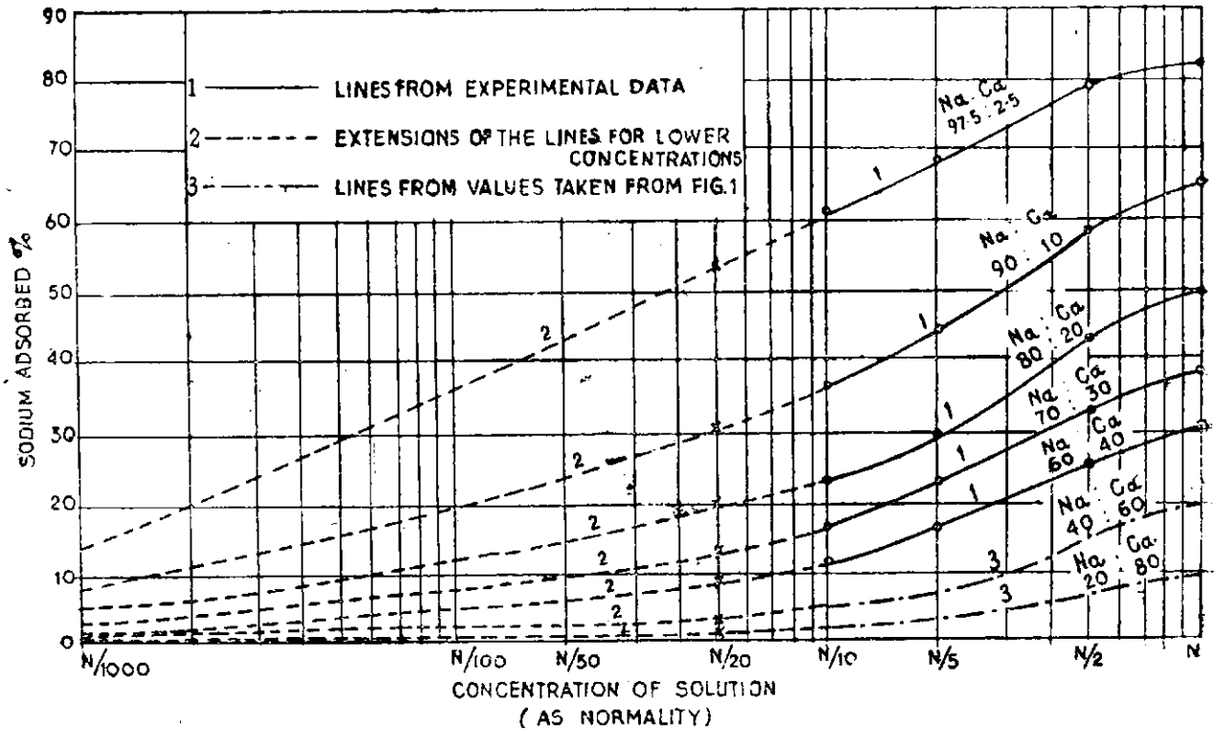

Fig 2: **Relation between concentration of solution and Sodium adsorbed for various proportions of sodium and calcium.**

Percentage of Sodium in									
Solution	Soil	Solution	Soil	Solution	Soil	Solution	Soil	Solution	Soil
84·0	25·2	87·0	28·8	89·0	31·7	85·0	21·5	88·0	24·6
72·0	13·2	74·0	15·7	75·0	16·2	69·0	12·6	73·0	15·2
55·6	7·0	59·6	8·6	44·0	4·5	51·6	7·2	37·6	6·3
38·6	3·7	41·0	3·9	31·6	4·1	35·6	5·0	32·0	4·6
25·0	2·2	28·2	3·5	23·4	2·4	28·4	3·6	26·0	3·1
15·3	1·3	19·3	1·8	15·3	1·4	21·6	2·6	...	...
...	...	...	...	...	...	15·4	1·7	...	...

is reached with leaching solution and cations estimated in the soil. It is expected that the results will be similar in both cases.

In last year's report results were presented for equilibrium reactions between black cotton soils satured with various proportions of sodium to calcium and solutions of $N/20$ strength having various proportion of sodium to calcium chlorides. Above values are calculated from the data. From the above values a curve has been drawn showing the relation between percentage of sodium adsorbed and percentage of sodium in solution in *fig 1*. The nature of this curve follows other curves and values for sodium adsorption are taken from this line for sodium content of 97.5, 90, 80, 60, 40 and 20 *percent* in solution. These values are shown in *fig 2* (as X). It is seen that the points almost lie on the extended lines, verifying to some extent the correctness of these lines which are to be further verified with values for $N/50$ solution and below.

38. "One shot" Chemical Grout

DURING the year further studies on *One Shot* Chemical grout were continued with sodium silicate as gel forming substance and ammonium-sulphate and sulphuric acid as precipitating agent. It is desirable that the mixture of sodium silicate with the precipitating agents should be fairly dilute to permit quick and easy flow into the soil, as also, economical and easy for injection purposes. Therefore, three different dilutions of sodium silicate with different concentrations of ammonium sulphate (fertilizer variety) and sulphuric acid (commerical grade) were tried for their time of gel formation, and on some suitable mixtures tests on resistivity and viscosity were also carried out.

2. Gel formation

Studies on gel forming characteristics of sodium silicate (ratio of $Na_2O/SiO_2 = 1/3$ of 1 : 2, 1 : 3 and 1 : 4 dilution having specific gravities of 1.146, 1.110 and 1.038 respectively were made with different concentrations and with different volumes of ammonium sulphate and sulphuric acid. These studies were carried out at a temperature between 25°C and 26°C and the solutions were prepared with distilled water.

To 5 *cc* lot of sodium silicate of different dilutions, a solution of ammonium sulphate of 1 to 10 *percent* ranging in volume from 1 to 10 or 15 *cc* were mixed and similarly sulphuric acid with a normality of .1 to .9 in increasing volumes upto 10 or 15 *cc* were added. After thorough mixing of the sodium silicate with the precipitating agent, the time interval between the mixing and at which the gel so formed showed no deformation or fall-out from the container, was taken as its setting time. The results are presented in *tables 1* and *2* and the data are graphically shown in *figs 1* and *2*.

Table 1 : Gel Formation with Sodium Silicate and Ammonium Sulphate

Volume of $(NH_4)_2SO_4$ added in c.	Concentration of Ammonium Sulphate (in per cent)																	
	3			4			5			6			7			8		
	A	B	C	A	B	C	A	B	C	A	B	C	A	B	C	A	B	C
1·0 ...	C	C	C	C	C	C	C	C	C	C	C	C	C	C	C	C	C	C
2·0 ...	C	C	C	C	C	C	C	C	C	C	T	T	T	T	S-60m	S-75m	S-38m	S-18m
2·5 ...	...	...	...	...	...	...	...	...	...	...	S-104m	...	...	...	S-10m	...	...	...
3·0 ...	C	C	C	C	C	C	T	T	T	S-55m	S-32m	S-14m	S-14m	S-8m	S-2m	S-3m	S-1m	S
3·5 ...	...	...	...	...	...	...	S-86m	S-62m	...	...	S-12m	...	...	...	...	...	...	...
4·0 ...	C	C	C	T	T	T	S-50m	S-26m	S-12m	S-10m	S-4m	S-2m	S-2m	S-1m	S-1m	S	S	S
4·5 ...	...	...	...	...	S-91m	...	S-26m	S-11m	...	...	...	...	...	...	...	...	...	...
5·0 ...	C	C	T	T	S-62m	S-10m	S-14m	S-6m	S-1m	S-2m	S-1m	S	S	S	S	S	S	S
5·5 ...	...	...	...	S-61m	S-34m	...	...	...	...	...	...	...	...	...	...	...	...	...
6·0 ...	C	C	T	S-38m	S-20m	S-8m	S-4m	S-4m	S	S	S	S	S	S	S	S	S	S
6·5 ...	...	...	S-80m	S-19m	...	...	...	...	...	...	...	...	...	...	...	...	...	...
7·0 ...	T	T	S-56m	S-10m	S-8m	S-6m	S-2m	S-2m	S	S	S	S	S	S	S	S	S	S
7·5 ...	...	S-90m	S-35m	...	...	...	...	...	...	...	...	...	...	...	...	...	...	...
8·0 ...	T	S-65m	S-22m	S-6m	S-4m	S-4m	S-2m	S-2m	S	S	S	S	S	S	S	S	S	S
8·5 ...		S-42m																
9·0 ...	S-110m	S-26m	S-12m	S-4m	S-3m	S-2m	S-1m	S-1m	S	S	S	S	S	S	S	S	S	S
9·5 ...		S-19m																
10·0 ...	S-66m	S-14m	S-8m	S-3m	S-2m	S-1m	S	S	S	S	S	S	S	S	S	S	S	S
11·0 ...	S-36m	S-9m	S-6m															
12·0 ...	S-18m	S-6m	S-4m															
13·0 ...	S-10m																	
14·0 ...	S-8m																	
15·0 ...	S-6m																	

Note.—

A – with $Na_2\ Sio_3$ (1 : 2) of *spgr* 1·146

B = with $Na_2\ Sio_3$ (1 : 3) of *spgr* 1·110

C = with $Na_2\ Sio_3$ (1 : 4) of *spgr* 1·088

C = clear at 90 *min.*

T = Turbid at 90 *min.*

S = Sets immediately.

S – 5*m* = sets at 5 *min.*

Results of 1, 2, 9 and 10 *percent* $(NH_4)_2\ SO_4$ with $Na_2\ Sio_3$ have not been given.

With 1 and 2 *per cent*, the mixture remained clear upto 90 *min*, but with 9 and 10 *per cent*, the set gel formed almost immediately or abruptly.

Table 2 . Gel Formation with Sodium Solicate and Sulphuric Acid

Volume of H_2SO_4 added in *cc*	Concentration of Sulpliuric Acid (in *per cent*)																	
	.3*N*			.4*N*			.5*N*			.6*N*			.7*N*			.8*N*		
	A	*B*	*C*	*A*	*B*	*C*	*A*	*B*	*C*	*A*	*B*	*C*	*A*	*B*	*C*	*A*	*B*	*C*
1·0	*C*	*C*	*C*	*C*	*C*	*C*	*C*	*C*	*C*	*C*	*C*	*C*	*C*	*C*	*C*	*C*	*C*	*C*
2·0	*C*	*C*	*C*	*C*	*C*	*C*	*C*	*C*	*C*	*C*	*C*	*C*	*C*	*C*	*C*	*C*	*T*	*C*
3·0	*C*	*C*	*C*	*C*	*C*	*C*	*C*	*C*	*C*	*C*	*C*	*C*	*C*	*T*	*T*	*T*	*T*	*T*
4·0	*C*	*C*	*C*	*C*	*C*	*C*	*C*	*C*	*C*	*C*	*T*	*T*	*T*	*S*-50*m*	*S*-15*m*	*S*-50m	*S*-5*m*	*S*-5*m*
5·0	*C*	*C*	*C*	*C*	*C*	*C*	*C*	*C*	*T*	*T*	*S*-70*m*	*S*-6*m*	*S*-30*m*	*S*-6*m*	*S*	*S*-7*m*	*S*	*S*
5·5										*S*-90*m*						*S*	*S*	
6·0	*C*	*C*	*C*	*C*	*C*	*T*	*T*	*T*	*S*-12*m*	*S*-55*m*	*S*-5*m*	*S*	*S*-6*m*	*S*	*S*	*S*	...	*S*
6·5								*S*-70*m*		*S*-30*m*								
7·0	*C*	*C*	*C*	*C*	*C*	*S*-100*m*	*T*	*S*-25*m*	*S*-5*m*	*S*-16*m*	*S*	*S*	*S*	*S*	...	*S*	...	...
7·5						*S*-40*m*	*S*-85*m*		*S*				*S*					
8·0	*C*	*C*	*C*	*C*	*T*	*S*-15*m*	*S*-60*m*	*S*-7*m*	*S*	*S*-5*m*	*S*	...	...	...	...	...	...	..
8·5					*S*-100*m*		*S*-31*m*											
9·0	*C*	*C*	*T*	*T*	*S* 55*m*	*S*-7*m*	*S*-15*m*	*S*	*S*	*S*	...	...	...	...	...	...	...	..
9·5					*S*-30*m*			*S*										
10·0	*C*	*C*	*T*	*T*	*S*-15*m*	*S*	*S*-5*m*	*S*	*S*	*S*	...	...	...	...	...	...	...	...
10·5			*S*-65*m*															
11·0			*S*-30*m*		*S*-6*m*		*S*											
12·0			*S*-16*m*		*S*													
13·0			*S*-5*m*															
14·0			*S*															

Note .—Results of .1, .2 and .9 $N-H_2SO_4$ with Na_2SiO_3 have not been given. With .1 and .2 $N\,H_2SO_4$, the setting of gel did not occur in 90 *min.*, while with .9 *N*, the formation of gel was either too rapid and or abrupt.

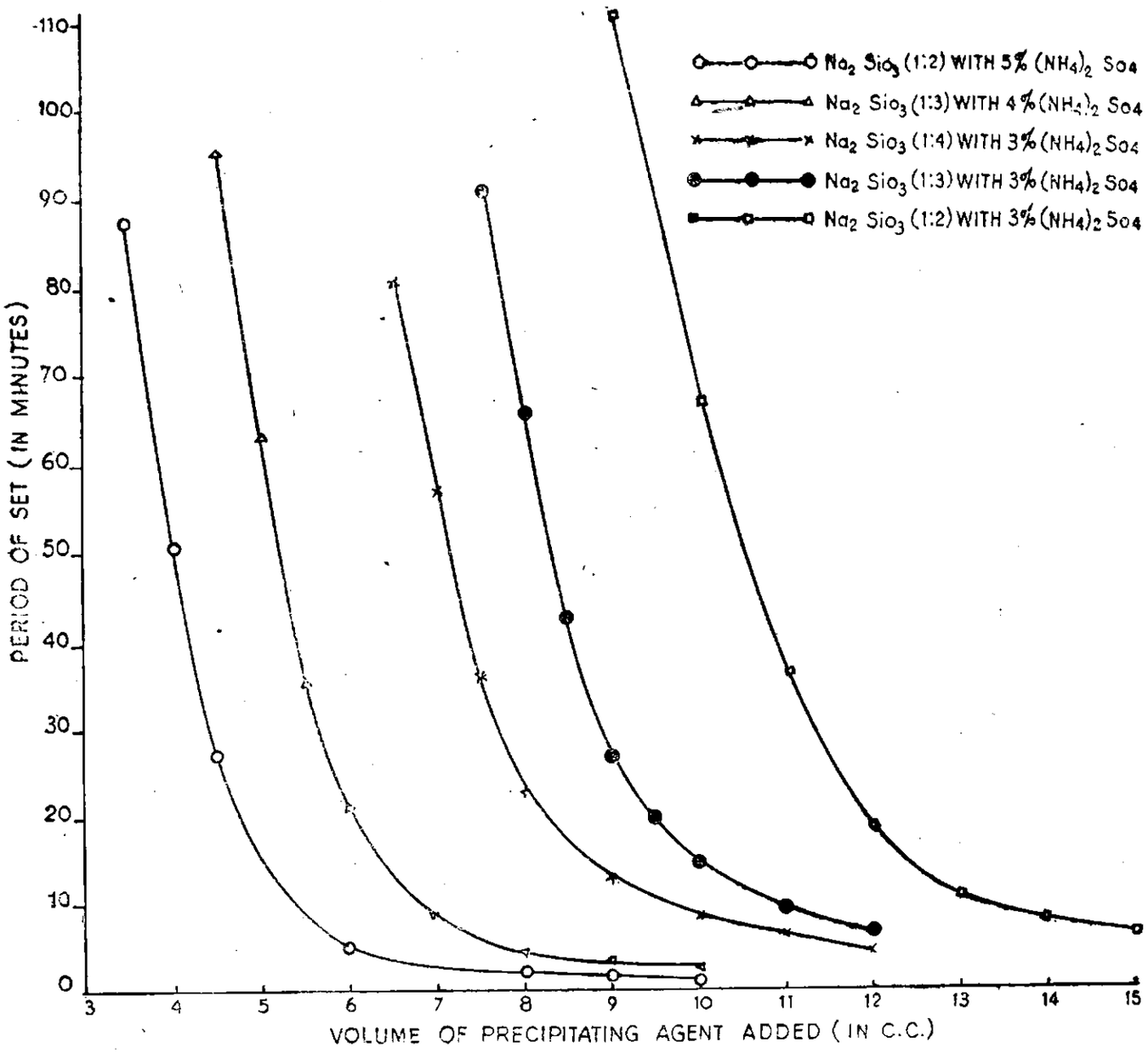

Fig 1: Time of set of 'one shot' chemical.

Following observations have been made from the *tables* :

(*i*) With 1 or 2 *percent* $(NH_4)_2\ SO_4$ and even with the addition upto 10 *cc*, the formation of gel did not occur upto 90 *min* with any of the three dilutions of Na_2SiO_3 tried. Further, the mixtures did not even develop any perceptible turbidity upto that period.

(*ii*) The gelatinisation and setting of gel occurred gradually with 3, 4 and 5 *percent* ammonium sulphate with sodium silicate of 1 : 2 and 1 : 3. Similarly 3 *percent* $(NH_4)_2SO_4$ caused setting of gel with Na_2SiO_3 of 1 : 4.

(*iii*) With higher concentrations of $(NH_4)_2SO_4$ and with increasing volume, the gelatinisation was rather too rapid or abrupt with all the three dilutions of Na_2SiO_3 tried. In general, it was indicated that with more than 6 *percent* $(NH_4)_2SO_4$, the setting of gel occurred almost immediately on mixing with any of the three dilute solutoins of Na_2SiO_2 used.

(*iv*) Sulphuric acid of concentration upto .4 *N*, even when added in increasing volumes, the gel formation did not occur upto 90 *min* with Na_2SiO_3 (1 : 2), but with .5 *N* and .6 *N*, the gelatinisation was gradual.

(*v*) With Na_2SiO_3 (1 : 3), the setting of gel did not occur upto 90 *min* with .1 *N*, 2 *N* or .3 *N* — H_2SO_4 even with increasing volumes of the precipitating agent upto 10 cc whereas gel formation occurred gradually with increasing volumes of .4 *N* and .5 *N* — H_2SO_4.

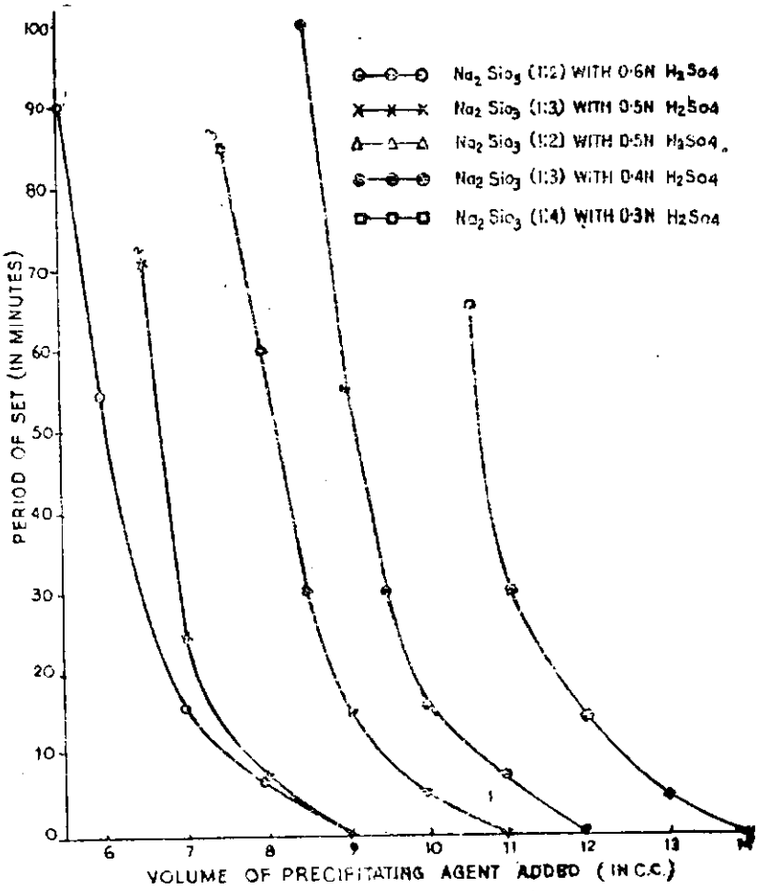

Fig 2: Time of set of 'one shot' chemical.

(*vi*) With .1 N or .2 N — H_2SO_4 the setting of did not occur even with increasing volumes upto 10 *cc* with Na_2SiO_3 (1 : 4). But with .3 N to .4 N — H_2SO_4, the gel formation occurred gradually.

(*vii*) With higher concentrations and with increasing volume of H_2SO_4 the formation of gel was too rapid and abrupt with all the three dilutions of Na_2SiO_3 tried. However, with 1 of 2 cc of H_2SO_4 the setting of gel did not occur even upto 90 *min*.

It is considered from practical point of view that the grout mixtures should be relatively clear for a fairly considerable length of time (about 30-40 *min*) for purposes of injection and to facilitate easy percolation into the soil medium and after penetration the mixture should form a set gel with enough resistivity.

A few suitable mixtures were selected for further study on resistivity and viscosity from the above results.

3. Resistivity

This test is intended to obtain the relative strengths of various set gels. The resistance of the set gel at different period of intervals has been estimated by using a wooden plunger having a sectional area of 3.33 *sq cm* which penetrated to a depth of 2.5 *cm* in set gel. The penetration of the plunger was effected by the addition of load at the rate of one *lb* in four minutes and the resistivity is expressed in terms of *gm* per *sq cm*.

The resistivity tests were carried out on the set gel at 30 *min*, 1, 2, 3, 4, 5, 6 and 24 *hours*. The results are given in *tables 3* and *4* and the values are graphically shown in *figs 3* and *4*.

Tables 3 and 4: **Resistivity (*gm/sq cm*) of set gel of Sodium Silicate**

	$Na_2 Sio_3$			Density of Mixture	Period after hours of set							
		$(NH_4)_2So_4$ %	Proportion by volume		1/2	1	2	3	4	5	6	21
Table 3	1:2	3	1:2	1.052	99	145	180	202	221	235	248	292
	1:2	5	5:4	1.085	123	170	231	276	327	354	368	444
	1:3	3	5:8	1.044	80	119	135	151	167	182	198	222
	1:3	4	1:1	1.058	108	146	193	228	252	265	277	306
	1:4	3	5:7	1.040	74	99	122	134	144	151	158	220
Table 4		H_2SO Strength										
	1:2	.5N	5:8	1.058	156	208	259	288	306	319	340	401
	1:2	.6N	5:6	1.072	167	246	334	399	423	440	460	553
	1:3	.5N	5:6·5	1.052	87	113	160	189	213	235	252	335
	1:3	.4N	5:9	1.044	75	110	134	149	159	171	178	210
	1:4	.3N	1:2	1.029	20	30	35	38	43	47	55	90

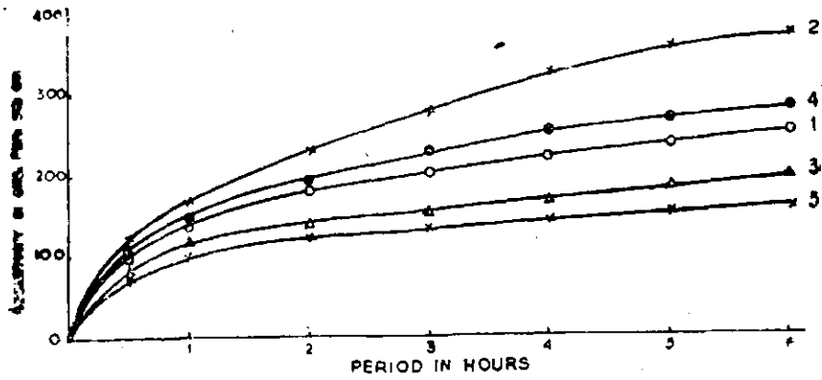

Fig 3: Resistivity of set gel of Sodium Silicate with Ammonium Sulphate.

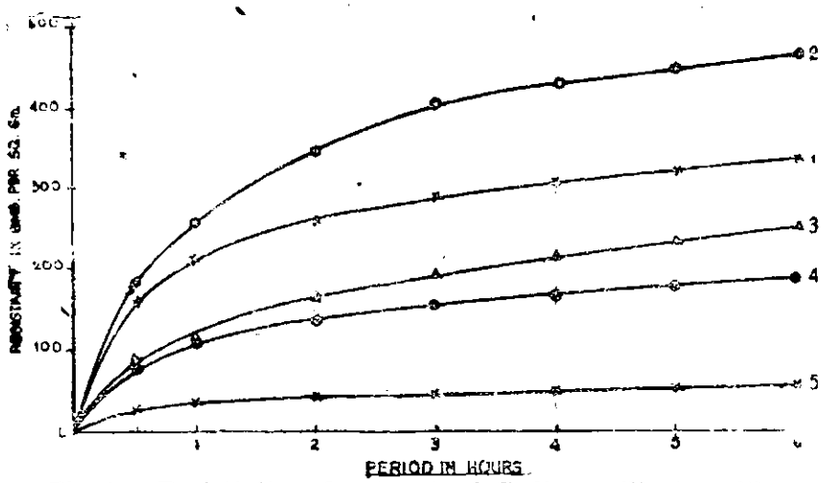

Fig 4: Resistivity of set gel of Sodium silicate with Sulphuric acid.

It is observed from the tables, that the resistivity of the set gel depends on the ultimate density of the chemical grout mixture as well as the nature of the precipitating agent. Sodium silicate of same density gave higher strength with more concentrated precipitating agent.

Na_2SiO_3 (1 : 2) with 5 *percent* $(NH_4)_2SO_4$ in the proportion of 5 : 4 by volume had yielded the maximum resistivity of 444 *gm per sq cm* in 24 *hours* while Na_2SiO_3 (1 : 4) with 3 *percent* $(NH_4)_2SO_4$ in the proportion of 5 : 7 by volume had a very low resistivity and was only 50 *percent* of the former. However, Na_2SiO_3 (1 : 2) with 4 *percent* $(NH_4)_2SO_4$ in the proportion of 1 : 1 by volume had also a fairly high resistivity *ie* 306 *gm per sq cm*.

The maximum resistivity of 553 *gm per sq cm* was obtained with Na_2SiO_3 (1 : 2 and .6 $N-H_2SO_4$ in the proportion of 5 : 6 by volume while with Na_2SiO_3 (1 : 4) and .3 N H_2SO_4 in the proportion of 1 : 2 by volume had yielded the least resistivity of 90 *gm per sq cm* in 24 *hours*. Na_2SiO_3 (1 : 2) with .5 N H_2SO_4 in the proportion of 5 : 8 by volume the set gel had given a fairly high resistivity value *ie* 401 *gm per sq cm* in 24 *hours*.

In general, the set gel developed about 60 to 70 *percent* of the one day resistivity within about 3 *hours* with either of the precipitating agents and in about 6 *hours* nearly 85 to 90 *percent* of the 24 *hours* resistivity was attained. However, with increased dilutions of the mixture the set gel developed rigidity very gradually. It was observed that the gel formed of Na_2SiO_3 (1 : 4) and .3 $N - H_2SO_3$ in the proportion of 1 : 2 by volume was too labile and had a very poor resistivity.

Table 5 : Viscosity of "one shot" Chemical grout mixtures (in milli-poises)$_n$

Particulars of Mixtures	Time in *minutes*			
	0	10	20	30
5 *cc* of Na_2SiO_3 (1:2) + 10 *cc* of 3% $(NH_4)_2SO_4$	10.3	11.2	12.2	13.5
5 *cc* of Na_2SiO_3 (1:2) + 4 *cc* of 5% $(NH_4)_2SO_4$	13.5	14.4	14.9	17.0
5 *cc* of Na_2SiO_3 (1:3) + 8 *cc* of 3% $(NH_4)_2SO_4$	10.8	11.6	12.5	13.1
5 *cc* of Na_2SiO_3 (1:3) + 5 *cc* of 4% $(NH_4)_2SO_4$	12.0	13.0	14.2	15.3
5 *cc* of Na_2SiO_3 (1:4) + 7 *cc* of 3% $(NH_4)_2SO_4$	12.2	13.0	14.4	16.3
5 *cc* of Na_2SiO_3 (1:2) + 8 *cc* of 0·5 N-H_2SO_4	9.1	12.6	23.1	...
5 *cc* of Na_2SiO_3 (1:2) + 6 *cc* of 0·6 N-H_2SO_4	9.1	12.6	19.4	...
5 *cc* of Na_2SiO_3 (1:3) + 9 *cc* of 0·4 N-H_2SO_4	9.3	10.7	19.4	...
5 *cc* of Na_2SiO_3 (1:3) + 6·5 *cc* of 0·5 N-H_2SO_4	9.3	10.7	20.4	...
5 *cc* of Na_2SiO_3 (1:4) + 11 *cc* of 0·3 N-H_2SO_4	8.9	10.0	13.2	...

4. Viscosity

It is necessary that the mixture of Na_2SiO_3 with any of the precipitating agent should be relatively thin and the gelatinisation of such mixture should not attain a high degree before it is injected into the soil medium. Viscosity of 5 mixtures with $(NH_4)_2SO_4$, and 5 mixtures with H_2SO_4 as the precipitating agents had been determined and the results are given in *table 5*. It can be seen from the results that the viscosity of the mixture with $(NH_4)_2SO_4$ did not appreciably change upto 30 *min* while that with H_2SO_4 the mixture became fairly viscous in about 20 *min*. Thus, it was indicated that $(NH_4)_2SO_4$ as the precipitating agent with Na_2SiO_3 afforded a longer time for completion of injection of the material while the same will have to be completed a little quicker when H_2SO_4 is used as the precipitating agent.

39. Physico-chemical properties of Indian bentonites

THE TERM bentonite was first used for a particular type of highly plastic, colloidal and swelling clay found near Fort Benton. It was found later that such clays are mainly composed of montmorillonitic clay minerals. The term as now used by many mineralogists has no reference to the physical properties of the clay. Because of various commercial uses of bentonites, such as, in decolourising oils, in bonding moulding sand, in drilling muds for oil wells, in canal lining and in grouting alluvium, search for locating bentonite has been made throughout the world. Bentonite has been located in a number of States in India and some firms are now supplying bentonites of Indian origin for commercial use. However, detailed physico-chemical and mineralogical studies of Indian bentonites have not been made. In the present studies, a few bentonite samples have been studied for their physico-chemical and mineralogical characteristics. The bentonite samples studied are:

Bentonite			
1	B_1	Supplied by Industrial mineral Company.	Non-swelling type bentonite
2	B_2	„	Swelling type bentonite
3	B_3	„	Thoroseal, a treated bentonite
4	B_4	Rajasthan	Barmer
5	B_5	„	Karauli

Following properties have been studied:

(i) Mechanical Composition
(ii) pH
(iii) Soluble salts
(iv) Carbon, nitrogen
(v) Base-exchange capacity
(vi) Exchangeable bases
(vii) Chemical composition of clay fraction
(viii) Electro-viscous properties
(ix) Differential Thermal Analysis.

2. Results and discussion

The physical properties of bentonites are presented in *table 1*:

Table 1

	B_1	B_2	B_3	B_4	B_5
Clay ...	61·9	81·8	82·2	81·6	48·1
Silt ...	30·6	14·0	12·4	15·2	36·4
Fine Sand ...	6·9	4·0	5·3	2·8	14·5
Coarse Sand ...	·2	·1	·1	·4	·6
H ...	7·7	9·3	9·5	9·6	9·4
TSS *percent* ...	3·00	1·37	1·75	2·80	·43
Nitrogen ...	·06	·01	·01	·04	·03
Carbon ...	·17	·1	·14	·21	·13
Base exchange capacity *me*/100 *gms*	28·3	78·0	65·4	50·4	29·8
Exchangeable *Ca* ...	13·7	36·4	17·2	25·7	18·9
Exchangeable *Mg* ...	11·2	21·5	15·1	9·9	8·6
Exchangeable *Na* ...	1·2	19·0	31·6	22·4	1·6
Exchangeable *K* ...	1·4	·5	·9	2·2	·6
egree of *Na* saturation	4·4	24·3	48·3	37·1	5·3

It will be seen that B_2, B_3 and B_4 contain more than 80 *percent* of clay of .002 *mm* and clay and silt are of the order of 95-97 *percent*. The other two samples contain only 48 and 60 *percent* clay. The *pH* values show that all the bentonites are alkaline and contain some soluble salts varying from .4 *percent* to 3 *percent*. Only small amount of nitrogen and carbon are present in all the samples. The base exchange capacity of B_2, B_3 and B_4 are quite high varying from 60 *me* to 78 *me*/100 *gms*, whereas the base exchange capacity of other two bentonites are of the order of 30 *me*/100 *gms*. The data on base exchange capacity show that predominant mineral in B_2, B_3 and B_4 may be montmorillonitic but the predominant mineral in B_1 and B_5 is probably illite or halloysite. The data on exchangeable bases show that B_3 contains 48 *percent* sodium as exchangeable cation, whereas B_2 contains 24 *percent*, B_4 contains 37 *percent*. In all these bentonites, the effect of sodium on despersion, swelling and plasticity will be quite marked. Bentonites B_1 and B_5 have very low sodium saturation.

The chemical analysis of clay fractions of different bentonite samples are presented in *table 2*.

Table 2

	B_1	B_2	B_3	B_4	B_5
Adsorbed water ...	5·0	13·53	11·05	9·25	4·95
Combined water ...	13·17	9·6	10·2	7·69	5·15
SiO_2 ...	45·99	44·64	42·82	49·05	53·66
R_2O_3 ...	33·0	29·65	33·4	31·75	29·75
$_2O_3$ ...	18·05	15·47	13·75	16·33	6·88
Al_2O_3 ...	14·95	14·18	19·65	15·42	22·87
CaO ...	·37	·75	·75	·53	·37
MgO ...	1·66	1·07	·94	1·34	3·47
Na_2O ...	·17	·14	·07	·34	·59
K_2O ...	·88	·38	·22	·48	1·85
Base Exchange capacity *me/gms*	37·80	71·2	63·0	70·0	40·0

It will be seen from the table that the adsorbed water in case of B_2, B_3 and B_4 is about 10-13 *percent*, whereas for bentonites B_1 and B_5 is only about 5 *percent*. This indicates that though montmorillonite may be predominant mineral in the former group, the latter group does not contain much of montmorillonitic minerals. Appreciable amount of iron oxide is present in all the samples showing that they are quite different in composition than the Wyoming bentonite. The nontronite may be the predominant minerals in place of montmorillonite in B_2, B_3 and B_4. The presence of about 1.85 *percent* of K_2O in B_5 indicates illitic mineral. High combined water and low exchange capacity in B_1 indicates that halloysite may be the predominant mineral in this sample.

The potentiometric titration curves and viscosity curves with addition of caustic soda, for the clay are presented in *figs 1* and *2*. It will be seen from the figures that B_2, B_3 and B_4 show

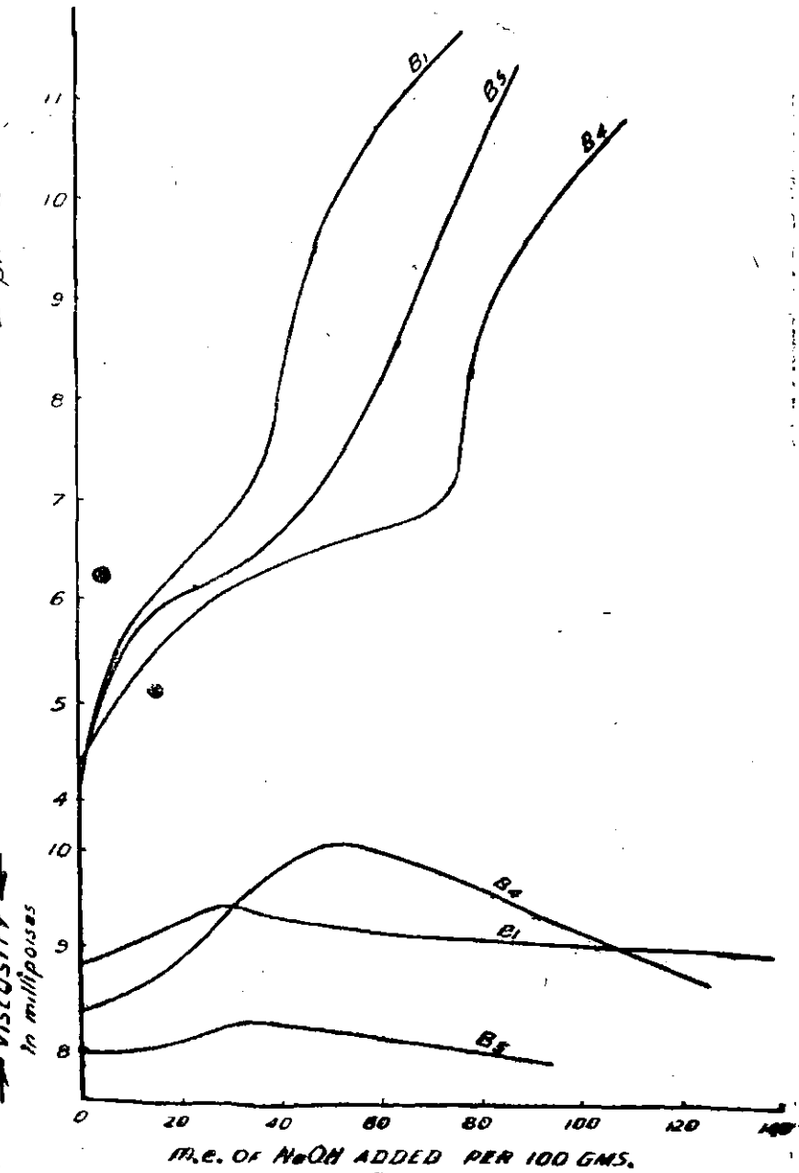

Fig 1: **Electrometric titration and viscosity curves of H-clays.**

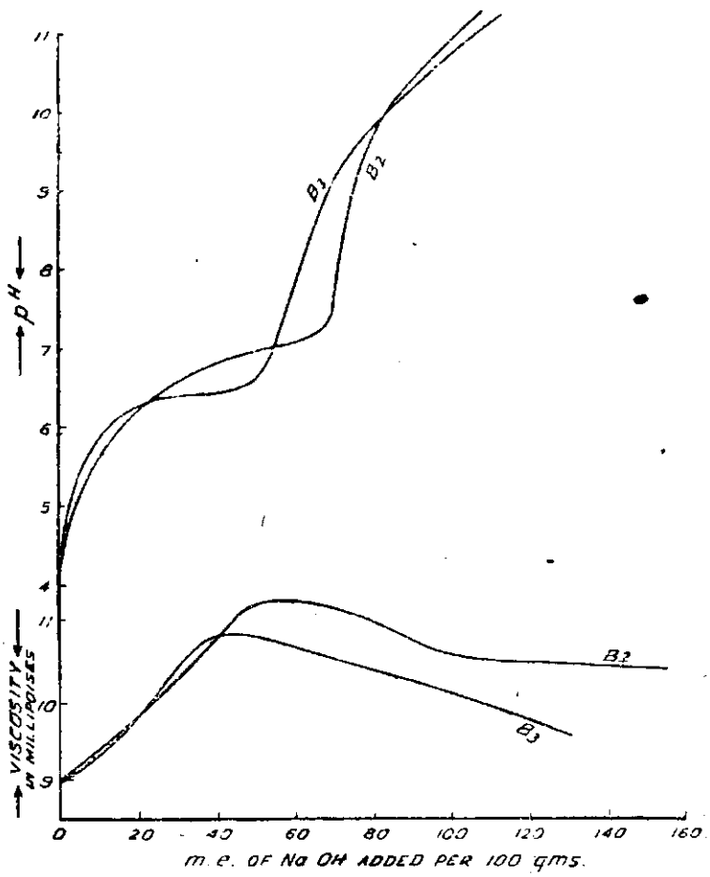

Fig 2: Electrometric titration and viscosity curves of *H*-clay.

high buffering capacity, whereas B_1 and B_5 show no such buffering. The viscosity curves for B_2, B_3 and B_4 show a gradual increase in the value with addition of caustic soda reaching a maximum at about 70 to 80 *percent* saturation, showing that montmorillonitic mineral is present in, these clays. The other two curves do not show any such pronounced characteristics, the viscosity does not change appreciably with the addition of caustic soda.

In *fig. 3* the curves for differential thermal analysis of clays are presented. The curve for B_3 shows that there are three endothermic reactions at temperatures 140°, 660° and 860°*C* indicating that illite with some montmorillonite are the minerals present in the sample. The curves for

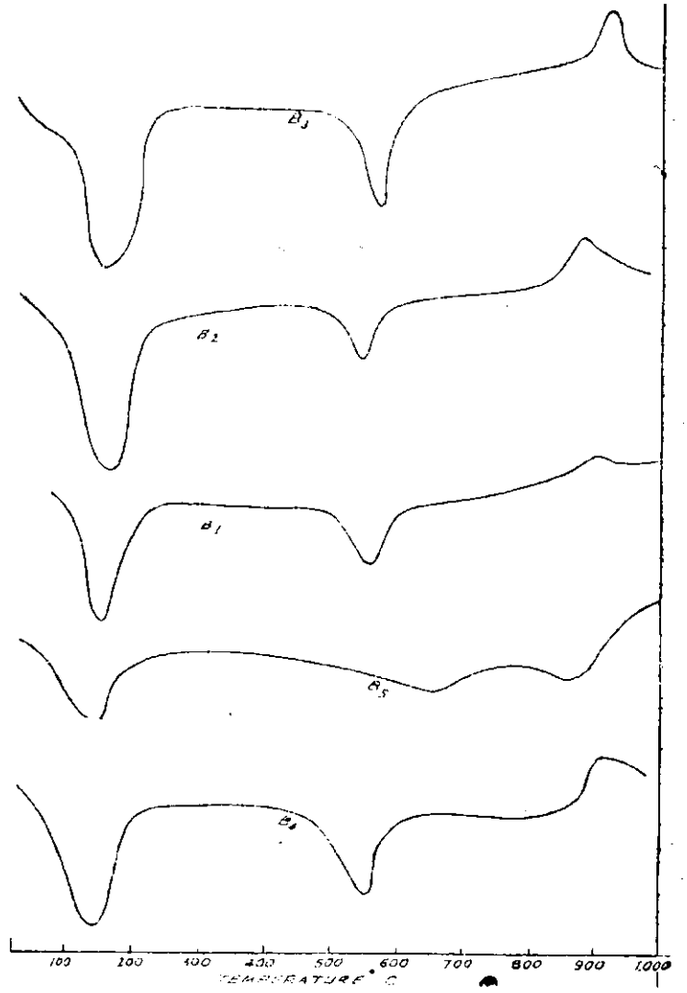

Fig 3: Differential thermal curves of *H*-clays.

B_2, B_3 and B_4 show endothermic peaks at about 140-170°*C*, 500-600°*C* and exothermic peak at about 900°*C* showing that nontronite is the predominant mineral present.

The studies thus show that out of five samples of bentonite tested three samples contain mainly nontronite minerals with clay content of more than 80 *percent*. The exchangeable sodium varies from 24 *percent* to 48 *percent* for these three samples. The other two samples contain appreciable amount of silt and sand with low base exchange capacity and low sodium saturation. One sample contains illitic mineral and other halloysitic mineral.

40. Swelling Pressure of Black Cotton Soil

Effect of various chemical treatments

THE BLACK cotton soil of South India is generally a very heavy clay with predominantly montmorillonitic clay mineral. It exhibits pronounced swelling on coming in contact with water and shrinkage on drying up. The structures founded on black cotton soils crack due to the unequal settlement caused by swelling and shrinkage. In the previous work carried out at

the *CWPRS* on the stabilization of black cotton soils it was observed that when calcium hydroxide was mixed with black cotton soil, both swelling pressure and amount of swell became negligible. In order to find out whether the reduction of swelling pressure was of a permanent nature and whether other chemicals could also reduce the swelling pressure, the present investigations were taken up.

2. Experiments

The black cotton soil was thoroughly mixed with different chemicals in a moist state and then allowed to dry. Liquid limit, plastic limit and maximum dry density and optimum moisture were found out for all the treated soils. For determining swelling pressure the soil was compacted in a direct shear box at optimum moisture and maximum dry density. The shear box was then loaded with a vertical load and a dial gauge was fixed above the sample. The soil was then allowed to saturate and the expansion was measured. Similar tests were carried out under 4-5 vertical loads. A curve was drawn showing expansion or contraction under different loads. The swelling pressure was taken as that load where there was no expansion or contraction.

3. Results and discussion

Table 1 shows that the liquid limit generally decreased on treatment with various chemicals. However sodium carbonate treatment increased the liquid limit considerably. There was no appreciable change in maximum density and optimum moisture content except for potassium salt treated soils. The most interesting data were those of swelling pressure. Calcium hydroxide treatment, as observed previously, reduced the swelling pressure almost to nil. Other salts of calcium had practically no effect on swelling pressure. Sodium chloride treatment had no effect on swelling pressure. Ammonium hydroxide, sodium hydroxide, megnesium hydroxide and potassium hydroxide treatment reduced swelling pressure in the order mentioned but even potassium hydroxide treated soil developed appreciable swelling pressure. Sodium carbonate treatment increased swelling pressure by three times. The most interesting fact, however, was that swelling pressure was regained almost completely of calcium hydroxide treated soil and potassium hydroxide treated soil when carbon dioxide was passed through the treated soils, converting probably the calcium hydroxide and potassium hydroxide to carbonates. It was thus evident that permanent benefit was not likely to occur in swelling

Table 1 : Limit values, maximum dry density and swelling pressure of black cotton soil

	Atterberg's limit		Compaction Test		Swelling pressure
	LL percen	*PL* percent	*OMC* percent	*MDD* lbs/cft	*Tons/ sq. ft*
	92	45	32.5	85.8	1.15
Ca Salts :					
+5 percent $Ca(OH)_2$	64	42	33.8	85.5	.08
+5 percent $Ca(OH)_2$ treated with CO_2	67	41	33.5	86.5	.94
+5 percent $CaCl_2$	72	40	30.3	91.3	1.14
Na Salts :					
+5 percent $NaOH$	65	45	34.0	87.0	.7
+5 percent $NaCl$	83	42	32.8	87.8	1.15
+2.5 percent Na_2CO_3	113	46	30.5	89.5	2 18
+5 percent Na_2CO_3	155	44	33.6	85.6	3.42
K Salts :					
+2.5 percent KOH	76	42	32.8	87.8	.44
+5 percent KOH	49	34	29.0	90.8	.23
+5 percent KOH treated with CO_2	51	35	21.2	95.2	1.11
+5 percent KCl	53	38	26.0	95.5	.56
+5 percent K_2CO_3	59	47	27.8	95.2	1.25
Mg Salts :					
+5 percent MgO	62	40	32.3	87.5	.45
NH_4 *Salts :*					
+5 percent NH_4OH	77	47	34.8	84.3	.95

pressure by lime treatment. Present study has showed that practical application of treating soil with lime or other chemicals to prevent swelling was limited; but it may be feasible to develop some treatment which may be of permanent nature. Further work is under progress.

41. Bentonite as a grouting material

IN a clay grouting operation, the cost of the drilling and injecting amounts to nearly 90 *per-cent* and the cost of the material is only 10 *per-cent* of the total cost. Preliminary studies carried out last year with bentonite showed that the cost of grouting operations with bentonite may be compared favourably, with the cost of a similar operation carried out with the local clays, because the quantity of bentonite required was about one sixth to one seventh of the clay. Further the operations like processing and dispersion required for the local clays are avoided, which make the entire process of grouting with bentonites much simpler.

Thus bentonites offer a good material for grouting operations. The present study was undertaken to determine the physical properties of bentonites available in India and to find out their suitability as a grouting material. The problem is still under investigation and only the work carried out during the current year is reported. Four samples were selected for the present study.

Table 1

Sample *No*	Mechanical Analysis percent			
	Clay .002 *mm*	Silt .002 to .02 *mm*	Fine Sand .02 to .2 *mm*	Liquid Limit
2401 ...	77.2	17.3	5.5	299
2656(Thoroseal) ...	77.4	12.1	10.5	375
2666(Bentonite I) ...	76.0	15.0	9.0	368
2667(Bentonite II) ...	77.2	17.2	5.6	250

*Sample *No* 2401 was supplied by the Executive Engineer, Ukai and others by I. M. Co., Bombay.

2. Effect of chemical on liquid limit of bentonites

The results in *table 1* show that though Indian bentonites have high clay content and fairly high liquid limit, the liquid limit values of some of the bentonites are not sufficiently high to be used for grouting or lining purpose. The plasticity of clays is generally improved by the addition of chemicals especially those used as dispersing agents. The effect of different amount of sodium hydroxide, sodium carbonate, sodium silicate, sodium hexametaphosphate and calcium hydroxide was studied on four samples (*table 1*) of bentonite. The required quantity of chemical was dissolved in 200 *cc* of water and the solution was thoroughly mixed with 100 *gm* of bentonite. The liquid limit of the paste was estimated after 24 hours. The results are given in *table 2*.

Table 2

Sample *No*	Percentage of Chemical.			
	Sodium Carbonate Na2 Co3			
2401 ...	285	263	242	171
2656 ...	326	296	280	245
2666 ...	372	340	328	264
2667 ...	269	254	213	158
	Sodium Hexametaphosphate $(NaPo_3)_6$			
2401 ...	238	230	223	201
2656 ...	279	262	239	224
2666 ...	282	280	259	246
2667 ...	215	213	212	192
	Sodium Hydroxide NaoH			
2401 ...	370	277	167	134
2656 ...	431	327	217	114
2666 ...	448	339	191	121
2667 ...	347	249	132	104
	Calcium Hydroxide $Ca(OH)_2$			
2401 ...	266	234	151	126
2656 ...	361	278	224	180
2666 ...	348	256	163	137
2667 ...	238	179	147	130
	Sodium silicate Na_2Sio_3			
2401 ...	242	220	211	193
2656 ...	348	291	265	244
2666 ...	296	277	248	242
2667 ...	222	205	185	175

	Original liquit limit	plastic limit
2401 ...	299	50
2656 ...	392	54
2666 ...	368	...
2667 ..	250	52

It is seen from the results that one *percent* of sodium hydroxide increased the liquid limit quite appreciably for all the samples, the increase being 15-40 *percent* of the original value of the liquid limit. With higher percentage of sodium hydroxide the liquid limit decreased considerably. Liquid limit was not increased by other chemicals; on the contrary there was a decrease when more chemical was added.

3. Effect of cement on bentonite slurries

Clay grouts are generally mixed with cement to give rigidity. Experiments were carried out to find the properties of bentonite-cement grouts. Grout slurries (Sample *No* 2401 and *table 1*) with water-bentonite ratio 12.5 : 1, 15.0 : 1, 17.5 : 1 and 20.0 : 1 were prepared with different proportions of cement (expressed as a percentage of bentonite). Required quantities of cement and bentonite were mixed separately in 500 and 1500 *cc* of water respectively by high speed immersion type stirrers for five minutes. Then the cement slurry was added to the bentonite slurry and the mixing was continued for another five minutes.

The time of efflux (a measure of viscosity), rigidity and bleeding were measured by the methods explained in the *ARM 1959*.

The results in *table 3*, on the effect of mixing different percentages of cement to bentonite slurries, showed that:

(i) bleeding of all the samples was within limit
(ii) for 20 : 1 water-bentonite slurry about 30 *percent* cement was required to give reasonable rigidity in 48 hours whereas for more concentrated slurries 20 *percent* was sufficient.

It will be seen from *table 3* and *fig 1* that the time of efflux increased with a small percentage of cement and had a maximum value when cement added was 5 *percent* in all the mixes. Further increase in the percentage of cement decreased the time of efflux and there was practically no variation in the time of efflux when cement was more than 30 *percent*.

The variation was comparatively more pronounced in richer mixes of bentonites. This variation in the time of efflux is probably due to the presence of free alkali in the cement. To verify the same following study was made:

Table 3

Cement as percentage of bentonite	Time of Efflux in *sec*	Bleeding after 48 *hours*	Remarks.
	Water : *Bentonite* : 12.5 : 1		
0	48	...	A
5	Very thick	...	A
10	83	1.1	A
20	53	.3	B
30	42	.6	B
50	40	.5	B
	Water : *Bentonite* : 15.0 : 1		
0	35.2	...	A
5	60	1.1	A
10	51	1.2	A
20	40	.4	B
30	38.5	.8	B
50	37	1.2	B
	Water : *Bentonite* : 17.5 : 1		
0	33	...	A
5	41.6	3	A
10	36.5	3	A
20	34.4	1.6	B
30	33.8	2	B
60	34	1.7	B
	Water : *Bentonite* : 20 : 1		
0	33	...	A
5	36	3.5	A
10	36	4.5	A
20	35	2.3	A
30	34.6	2.3	B
50	33.2	2.6	B

Notes :—A = Not set in 48 hours
B – Sets in 48 hours.

4. Effect of chemicals on the time of efflux

Effect of four chemicals *viz* sodium hydroxide, sodium carbonate, sodium hexametaphosphate and calcium hydroxide was studied on bentonite sample *No* 2401 (*table 1*) with water-bentonite ratio of 15 : 1. It was carried out firstly by adding bentonite to chemical solution of desired strength and stirring vigorously for ten minutes and secondly by adding the required amount of chemical solution to the bentonite slurry already mixed for five minutes and continuing the mixing for another five minutes. Calcium hydroxide being sparingly soluble, the procedure followed was similar as in the case of cement, described earlier.

The results, plotted in *fig 2*, show that when bentonite is added to the chemical solution the time of efflux does not vary much, but when the chemical solution is added to the bentonite slurry the trend of the curves obtained with hydroxides

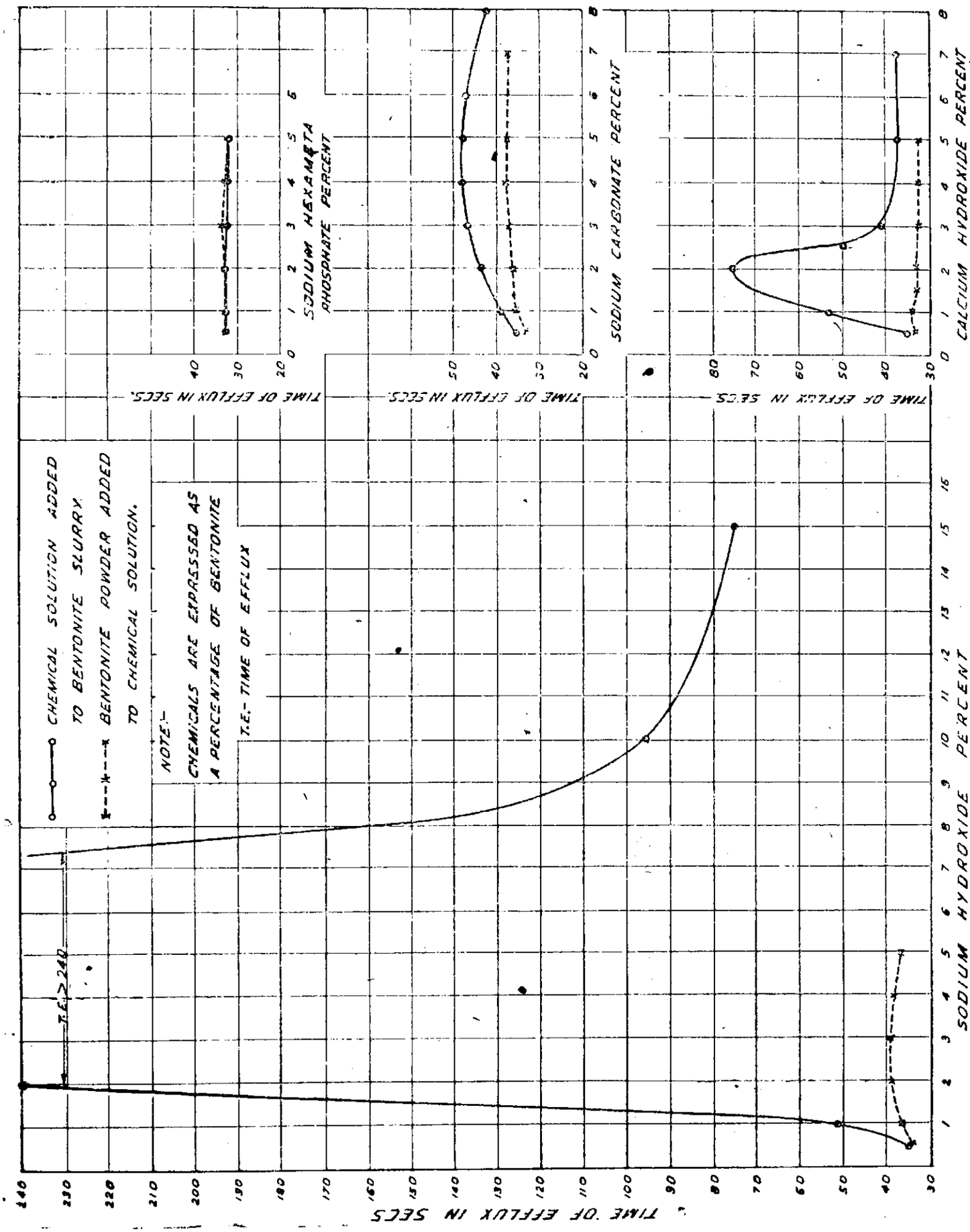

Fig 2: Relation between time of efflux ie viscosity and mixing different percentages of chemicals to Bentonite.

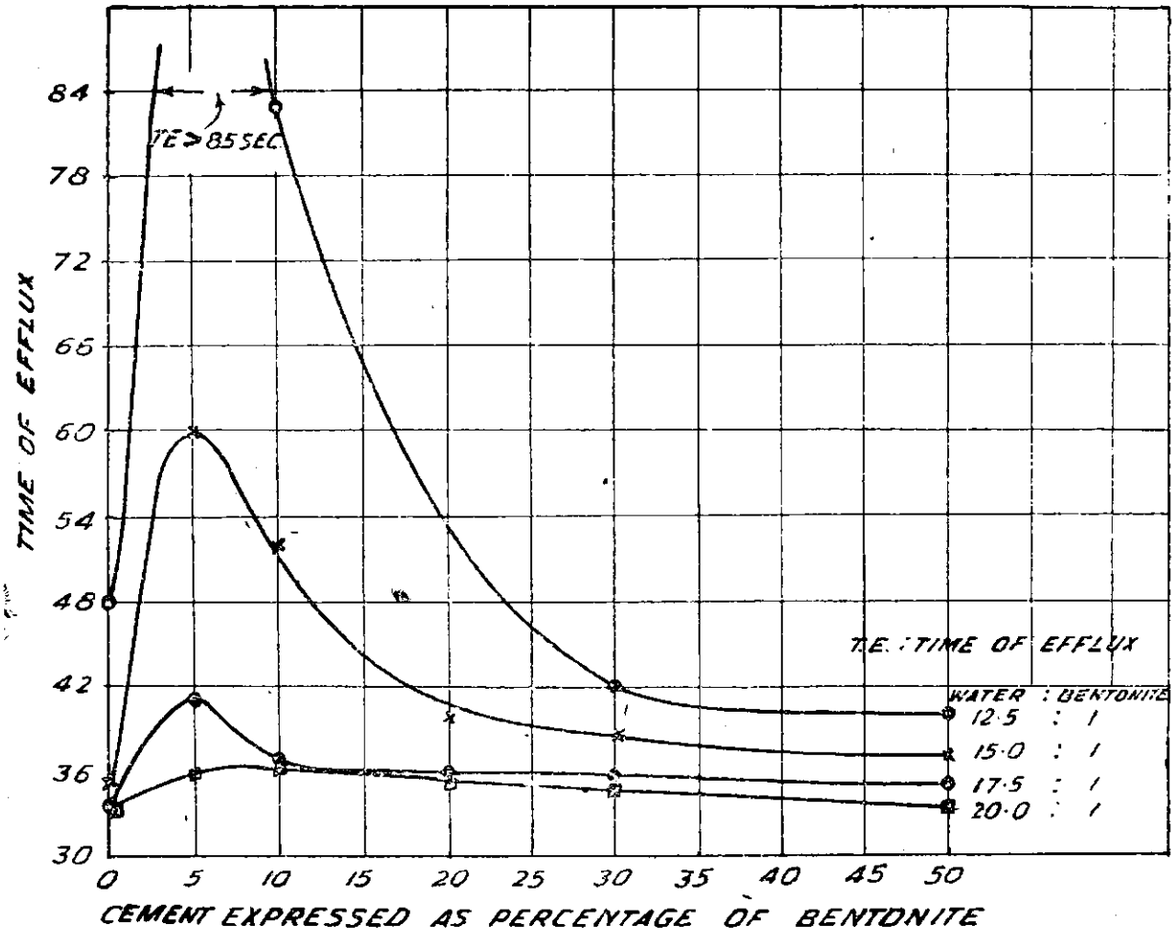

Fig 1: Relation between time of efflux *ie* viscosity and mixing different percentages of cement to Bentonite.

of sodium and calcium is similar to that obtained with the cement which supports the previous assumption. With sodium carbonate the time of efflux increased gradually and then decreased whereas sodium hexametaphosphate did not change it materially.

It is not possible to offer any explanation at this stage for different behaviour of the bentonite slurries when bentonite is added to chemical solution and when the chemical is added to the bentonite slurries. This point is under further investigation.

---

42. Modulus of Elasticity of Rock Cores

SOME of the rock samples received from Koyna Project were of weaker types and heterogeneous material (Tuff-breccia). The project authorities wanted determination of compressive and tensile strengths of this type of weak rock and the modulus of elasticity, both under compression and tension.

For finding out modulus of elasticity both under tension and compression, the following equipment was used. The mechanical extensometer was the one manufactured by M/s. A Macklow Smith Ltd., London, and the electrical resistance strain gauges and strain recording equipment was that manufactured by M/s Tinsley, England. Both the methods of measuring strains, by mechanical extensometer and electrical strain gauge were adopted for measuring strains under compressive loads. As the mechanical extensometer was not used due to risk of damage to the extensometer due to sudden failure of a

sample in tension, the strains under tensile loading were measured by electrical strain-gauges. For finding out modulus of elasticity under tensile load and also tensile strength special grips were manufactured for holding the sample at the College of Engineering, Poona.

Strain recording equipment was calibrated for both mechanical electrical strain gauges for a homogeneous basaltic rock core sample before conducting tests on tuff breccia samples. The results of tests are shown in *table 1* and *figs 1* and *2*.

Table 1: *Results of tests for Young's Modulus E on rock cores (Koyna Project)*

Location of Sample				Modulus of Elasticity in million *psi*		
Bore Hole *No*	Depth			Under compressive Stress using		Under tensile stress using electrical strain gauge
				Mirror Extensometer	Electrical strain gauge	
Homogeneous Basalt from Navgaon Site.				6·72	7·0	
Tuff-Breccia Samples						
	ft *in*		*ft* *in*			
39	106 5	to	107 7½	·9	1·5	1·4
33A	40 8	to	41 11½	1·3		1·3
33A	37 2½	to	38 6½	1·4	1·3	
9B	42 4½	to	43 9	1·4		
33A	38 7	to	39 9	1·0	·5	
44	204 1	to	205 2	·7	·8	
8	...			·9	1·3	

From *fig 1*, it will be seen that both the methods of measuring strains gave similar results of modulus of elasticity. A good basaltic rock showed 6.7×10^6 *psi* as value of *E by* using mirror extensometer, while a value of 7.0×10^6 *psi* is shown by using electrical resistance strain gauges.

Tuff breccia is comparatively a weak type of rock having compressive strength ranging from 1800 to 2440 *psi* and tensile strength of about 80 *psi*. Within such a short range, it was not possible to obtain sufficient strain measurements for finding out the stress-strain relationship under tensile loads by means of extensometer and hence electrical resistance strain gauge method alone was adopted for these measurements.

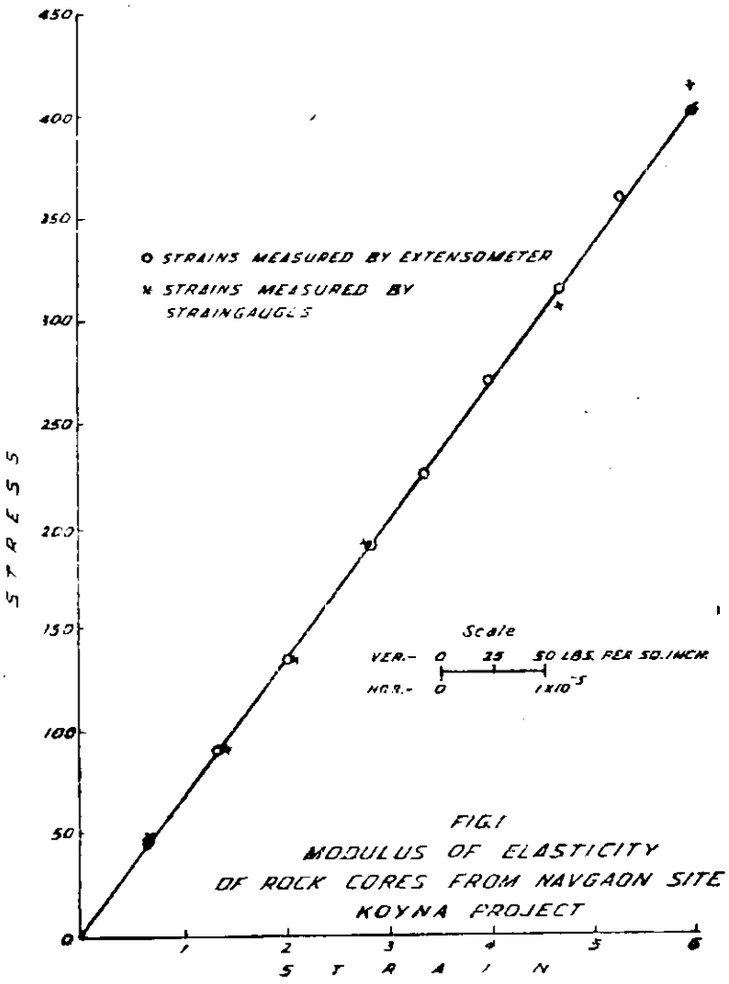

FIG. 1
MODULUS OF ELASTICITY OF ROCK CORES FROM NAVGAON SITE KOYNA PROJECT

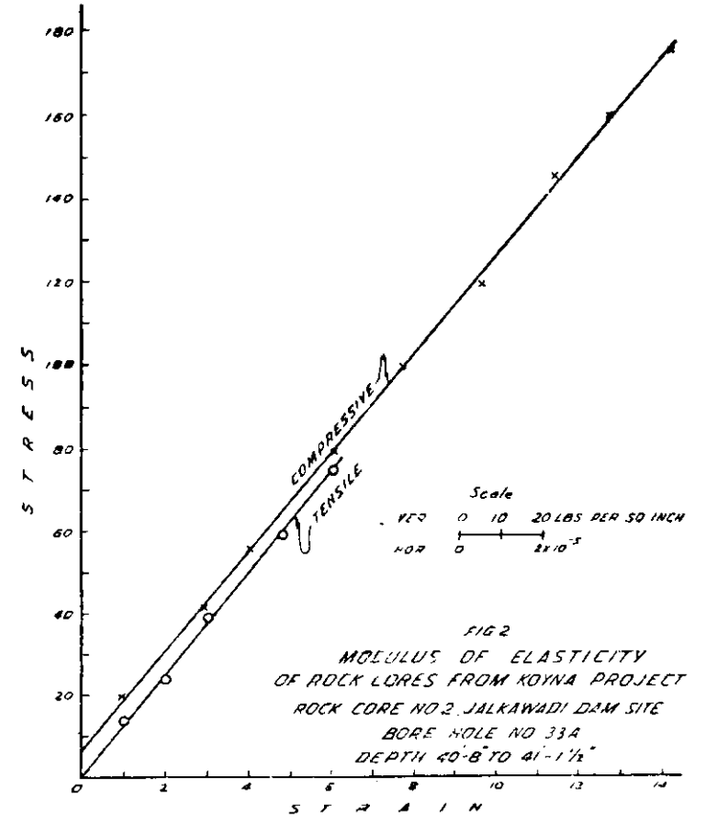

FIG 2
MODULUS OF ELASTICITY OF ROCK CORES FROM KOYNA PROJECT
ROCK CORE NO 2 JALKAWADI DAM SITE
BORE HOLE NO 33A
DEPTH 40'-8" TO 41'-1½"

The modulus of elasticity ranges from 0.7 to 1.5 × 10^6 *psi* under compression. Due to heterogeneous character of the core sample the values of *E* as obtained by extensometer method slightly differ from those of electrical strain gauge method. The stress range adopted for the measurement of strains for all the tuff breccia samples was from 0 to 200 *psi* for compressive loads and 0 to 80 *psi* for tensile loads. From the curve of stress versus strain, it was found that the strains within the selected range of stress followed the Hooke's Law.

With regard to Young's modulus under compression and tension, the results were of the same order of magnitude and did not differ appreciably even in the case of weak tuff breccia type of rock and the average value obtained for tuff breccia is about 1.3 × 10^6 *psi*.

43. Typical Sands from Deccan Trap

THE SANDS derived from Deccan Trap contain appreciable amount of zeolites and lime in addition to reactive minerals such as opal and chalcedony. A study has been made on the effect of zeolite and lime on the soundness of aggregate and also alkaliaggregate reactivity. Typical sands from Koyna Project, Ukai Project and Wainganga Project were taken up for the study.

Different fractions of the sands were tested for their soundness characteristic by magnesium sulphate test and for the weathering qualities by subjecting them to weathering cycles consisting of alternate heating and wetting. The sands were petrologically examined for the zeolite content and chemically tested for lime content before and after magnesium sulphate treatment and weathering cycles.

A quick chemical test consisting of determination of silica release and reduction in alkalinity together with a mortar bar test for finding out the deleterious expansion if any for a period of one year were also done to study the role of zeolites and reactive aggregates in causing alkali-aggregate reaction.

2. Results and discussion

Table 1 gives a summary and data obtained on soundness test, petrological test, chemical reactivity test and mortar bar expansion test. The soundness test of Koyna and Wainganga samples showed considerable loss, Ukai samples however showed only 8-9 *percent* loss. Though chalcedony a reactive mineral was present to the extent of 3 *percent* neither chemical reactivity test nor mortar bar expansion test showed any deleterious effect with any of the samples of sand.

Last year a detailed study of Koyna sand samples had been made with respect to zeolite and lime. This year similar study had been made with Ukai sand and the results are presented in *table 2*.

Table 1 :

Sand Sample from Project	Weighted loss in soundness test percent	Chemical Test Silica Release	Petrographic Test*		Mortar bar expansion for 1 year percent	
		Reduction in alkalinity	Chalcedony percent	Zeolites percent	Low alkali cement	Low alkali cement +1 percent *NaOH*
Koyna...	25·8 to 36·0	·04 to ·13	1·2 to 2·0	7·0 to 8·4	--·013	--·075
Ukai ...	8·1 to 9·0	·12	·89 to 3·2	5·9 to 8·3	--·20	--·12
Wainganga.	18 to 22	·08	1·20 to 3·6	3·2 to 8·5	Under	Progress

*Only traces of opal were present

It will be seen from the table that zeolite was fairly distributed in all the fractions upto 52 *mesh*. The finest fraction (*ie* + 100) contained proportionally less amount of zeolite than the other fractions. The zeolite content after magnesium sulphate test showed that zeolite in all the fractions had been affected by the treatment. The total weighted loss of materials was

Table 2

Size (*in*) of *Mesh No*	Percentage retained	Loss in $MgSO_4$ test Percent	Loss in Weathering test Percent	Zeolite Content				Lime Content			
				Untreated		After $MgSO_4$ test	After Weathering test	Untreated		After $MgSO_4$ test	After Weathering test
					Percent of individual fraction				Percent of individual fraticon		
3/16 ...	28·0	6·5	2·0	2·90	10·4	2·40	2·74	·98	3·5	·40	·92
No 7 ...	42·8	4·5	2·5	3·24	7·6	3·00	2·78	2·42	5·7	1·82	1·42
14 ..	20·5	3·7	1·8	1·60	7·8	1·45	1·42	1·12	5·5	·95	1·02
25 ...	6·5	5·5	2·6	·44	6·8	·37	·33	·41	6·3	·37	·36
52 ...	1·4	6·8	1·5	·11	8·1	·10	·10	·03	5·7	·07	·05
100 ...	0·8	8·5	1·2	·02	...	·02	...	·04	...	·03	...
Total ...	100·0	...	...	8·31	...	7·34	7·37	5·05	...	3·64	3·77
Weighted loss.	—	5·02	2·2	...	...	0·97	0·94	...	...	1·41	1·28

5.02 *percent* of which loss of zeolite was .97 *percent*. Thus nearly 20 *percent* of the total loss was of zeolite. Weathering test showed that though total weighted loss was only 2.2 *percent*, the loss of zeolite was .94 *percent*, thus accounting for more than 40 *percent* loss. Lime content of sand in different fractions showed that it was also well distributed in different fractions. They were affected by both magnesium sulphate test and weathering test. In magnesium sulphate test loss of lime accounted for 27 *percent* of total loss and in weathering test loss of lime accounted for more than 55 *percent* of total loss. The study indicated that both zeolite and lime present in Ukai sand were not very sound materials; however as the amount was not large, it may not on the whole have any deleterious effect on the concrete made with this type of sand.

44. Studies on Puzzolona

IN continuation of the last year's work, studies on puzzolonic materials such as coal ash, and fly ash including their behaviour in concrete have been carried out. A few soil samples from Tawa Project and Upper Wainganga Project have been tested for their suitability as surkhi. A comparative study of Lime reactivity and *ASTM* tests for evaluation of a puzzolonic material have also been made.

The results of lime reactivity and *ASTM* tests are presented in *table 1*. The strength of concrete made with a few puzzolonas are also presented for comparison. It will be seen from the results that the lime reactivity test shows that sample *Nos* 1, 4, 7 and 7 have fair to moderate activity whereas other samples are of poor activity. The *ASTM* test shows that sample *Nos.* 1, 4, 5, 6 and 8 are of good activity. The strength of concrete with 10 *percent* replacement of cement by puzzolona (samples 1, 2, 3, and 4) show that good strength is given by samples 1, 2 and 4 and sample 3 gives moderate strength. It is thus seen that both the methods namely lime reactivity test and *ASTM* test have their limitations in evaluation of puzzolonic activity.

To determine the puzzolonic activity, the loco-shed coal ash and the fly ash from Chola Power House have been used in concrete with cement to aggregate ratio of 1 : 6, 1 : 9 and 1 : 12. The chemical composition of loco-shed coal ash has already been given in last year's report. The chemical composition of fly ash is given in *table 2*

Table 3

Sieve Analysis of the total aggregates (combined grading)

B. S. Sieve Size	*Inches*				Mesh *No*				
	1½	3/4	3/8	3/16	7	14	25	52	100
Cumulative Percentage retained	2	29	46	59	66	75	85	94	99

Pozzolona (−100 size)	Replacement Percent	C : A = 1 : 6, *w/c* = .7 to .8					C : A = 1 : 9, *w/c* = .8.5					C : A = 1 : 12, *w/c* = 1·2				
		7 days.	28	90	180	360	7 days	28	90	180	360	7 days	28	90	180	360
Locoshed Coal Ash.	5	96	95	92	93	118	67	95	96	96	90	71	95	78	73	80
	7·5	88	87	90	94	100	54	80	83	83	74	66	67	65	63	65
	10	65	79	88	93	113	53	73	75	74	73	62	63	66	62	68
	15	56	64	70	94	86	43	67	68	76	66	54	60	66	55	64
	20	54	54	52	90	80	42	62	67	68	62	54	60	63	54	58
Chola Power House Fly Ash Sample *No* 1.	5	83	105	138	Under progress		55	75	90	under progress						
	7·5	94	105	135	,,		52	78	80	,,						
	10	117	113	134	,,		80	80	82	,,						
	15	88	95	118	,,		61	75	85	,,						
	20	78	87	105	,,		40	53	60	,,						

Table 4 : Physical properties of soils and lime reactivity strengths on calcined soils

Project	Lab Sample *No.*	Mechanical Analysis percent					Atterberg's Limits			Lime Reactivity Strengths in *psi*		
		Clay	Silt	Fine Sand	Coarse Sand	Gravel	Liquid Limit	Plastic Limit	Plasticity Index	600° *C*	800° *C*	900° *C*
Upper ...	1977	30·1	31·1	27·8	9·4	...	63	33	29	230	440	307
Wainganga ...	1932	35·3	45·0	16·8	2·9	...	70	35	35	257	653	400
Project ...	1990	51·2	30·5	16·1	2·2	...	71	28	43	235	385	335
Tawa ..	2300	25·1	21·8	37·5	14·2	1·4	38	24	13	346	500	284
Project ..	2301	19·5	32·2	35·9	11·2	1·3	34	23	11	237	425	246
	2266	60·0	34·1	2·7	3·2	...	31	23	23	908	711	...
	2267	56·7	36·2	3·8	3·3	..	50	25	25	470	570	...
	2268	27·2	17·6	38·1	11·0	6·1	34	21	13	420	410	...

Table 1 : Lime reactivity *ASTM* Test for Puzzolona and concrete cube strength.

Sl. No.	Puzzolonic material	Lime reactivity test strength (*psi*)	A.S.T.M. Test*		1 year strength of (10% replacement) puzzolona mix expressed as % of control mix C:A=1:6
			7 days	28 days	
1	Underburnt Surkhi.	960	2.10	2.22	84
2	Overburnt Surkhi.	312	0.38	0.42	91
3	Rice Husk Ash.	434	0.47	0.44	65
4	Loco-shed Coal ash	880	1.26	1.12	113
5	Chola Power House Fly ash Sample 1	250	2.10	1.70	under progress
6	Chola Power House Fly ash Sample 2.	270	1.64	1.25	...
7	Bombay Port Trust Coal ash Sample 1.	740	0.44	0.72	...
8	Bombay Port Trust Coal ash Sample 2.	530	0.40	0.78	...
9	Chola Power House coal ash.	240	1.40	1.20	...

*Figure indicates the ratio of strength of puzzolonic mix to control mix.

and the relative strength of concrete with various replacement of puzzolona is given in *table 3*.

It will be seen from *table 3* that locoshed coal ash gives fairly good strength after one year in richer mixes. In leaner mixes and with 20 *percent* replacement of cement the strength development is about 60 *percent* only. Similar study with fly ash though not completed shows that very high strength is obtained even at 90 days. Fly ash is thus expected to be a good puzzolona with reference to strength development in concrete.

Table 2 : Chemical composition of fly ash.

		Percent
Ignition Loss	=	16.2
SiO_2	=	46.2
R_2O_3	=	29.1
CaO	=	5.6
MgO	=	2.9

The authorities from Tawa Project and Upper Wainganga Projects wanted the *CWPRS* to carry out some experiments to find out the suitability of local soils for preparation of surkhi. Some clayey soils were selected for the same. The results of mechanical analysis, limit values, lime reactivity test values on the samples calcined at 600°, 800° and 900° *C* are given in *table 4*.

It will be seen from the table that the soils from Upper Wainganga were more plastic with the liquid limit varying between 62 to 71 than the soils from Tawa having a liquid limit between 34 to 51. None of the soils from Upper Wainganga showed any appreciable activity except sample *No* 1982 calcined at 800°*C*. The sample *No* 2266 from Tawa showed good reactivity when calcined at 600°*C*. Calcination at higher temperatures did not improve the reactivity of the surkhi. The results showed that it was not possible to predict the behaviour of a soil after calcination as a surkhi from mechanical composition and limit values.

45. Admixtures in Mortars and Concrete

VARIOUS admixtures are used in mortars and concrete to improve some of their specific properties. These admixtures are accelerators, rapid hardeners and antifreeze agents, water proofing agents, surface hardners, surface active agents or wetting agents and air entraining agents. The properties of mortars and concrete as affected by the use of few of these admixtures have been studied.

2. Accelerators

Materials which accelerate the hardening and promote early strength development of mortars and concrete are called accelerators.

(*a*) *Calcium Chloride*.—The effect of addition of calcium chloride from 1 *percent* to 4 *percent* on setting time, soundness and compressive strength have been studied in mortars. Calcium chloride

was dissolved in water prior to its mixing with cement. *Table 1* shows the results of the test.

Table 1

Tests	Addition of $CaCl_2$ in *percent*				
	0	1	2	3	4
1. Setting time (Minutes)					
Initial ...	45	43	35	10	5
Final ...	365	260	237	115	84
2. Soundness percent expansion (Auto clave)	·089	·003	·006	·119	·116
3. Compressive strength in *psi* of 1 : 3 *cm.*					
3 days ...	2000	2400	2480	2530	2540
7 days ...	2430	3180	3260	3460	4000
28 days ...	3700	4100	4260	4400	4500

The results showed that both the initial and final setting times was accelerated with the increased proportion of calcium chloride. Addition of 3 to 4 *percent* calcium chloride decreased the initial setting time considerably from 45 minutes to 10 and 5 minutes respectively.

Soundness test showed that the addition of 1 to 2 *percent* of the calcium chloride reduced the expansion, while 3 *percent* or more increased it beyond specification limits.

The strength development under normal curing conditions showed that with increasing proportions of calcium chloride, the compressive strength upto 28 days increased. The amount of calcium chloride to be used may, however, be restricted to 2 *percent* as greater addition of calcium chloride accelerated the initial time of set to such an extent that placing and finishing operations were likely to prove difficult.

The addition of upto 2 *percent* calcium chloride in mortars used for preparation of rigid beds in hydraulic models would reduce the time between placing of mortar beds and starting of experiments.

(*b*) *Green Hydrol.*—This is a product of "Hydrol" Cement Water Proofers Ltd London and is supplied by M/s Dialdas & Sons, Bombay. It is a patented product for use in concrete as an accelerator and anti-freeze agent. It is supplied in liquid form. According to the supplier it does not affect the initial set so that the mix could be made and placed in usual manner. Thus it could be effectively used for mixes to be placed under water or in waterlogged areas or in flooded conditions. The effect of "Green Hydrol" on 1 : 2 : 4 and 1 : 3 : 6 concrete have been studied. The results are given in *table 2*.

Table 2

Test		Normal cement	Mix *A**	Mix *B**
Setting time (Minutes)	Initial ...	45	33	34
	Final ...	365	295	304

Age (days)	Compressive Strength in *psi*					
	C:A = 1:6			C:A = 1:9		
	W/C = 0.50	Mix *A**	Mix *B**	W/C = 0.65	Mix *A**	Mix *B**
1 ...	555	1555	1530	514	883	622
2 ...	1090	2640	2320	920	1570	1215
3 ...	1375	3472	2880	1300	1920	1545
7 ...	3240	4150	3570	1760	2400	2380
28 ...	4500	6220	4867	2815	3750	3600
90 ...	5325	6670	6220	3990	4720	4400

*Mix *A*—1 part of hydrol to 16 parts of water

*Mix *B*—1 part of hydrol to 24 parts of water

The increase in early strength is more pronuonced in richer mix of 1 : 6 than the leaner mix of 1 : 9. In early ages at one and two days the increase in strength is 180 *percent* and 107 *percent* in 1 : 6 mix and 72 and 21 *percent* in 1 : 9 mix for mixes *A* and *B* which gradually decreases to 23 *percent* and 17 *percent* for 1 : 6 mix and 18 *percent* and 10 *percent* for 1 : 9 mix at 90 days. From the results it is seen that 1 part of hydrol to 16 parts of water gives better results in both richer and leaner mixes.

3. Waterproofing agents

Waterproofing agents are used for two separate and distinct purposes in concrete namely :

(1) to resist the absorption of water.

(2) to make concrete impervious to water under pressure

Various firms in India are now producing waterproofing compounds for use in concrete. Some of these products have been tested and the results are given in *table 3.*

Table 3

Proportion of cement to sand used was 1 : 3, the specimen were cured in water for 21 days.

Admixture	Setting time (minutes)		Soundness (autoclave) per cent expansion	Permeability in *cc* under 7 *ft* head	Per cent Absorption in hours			Compressive Strength of 1 : 3 *cm*	
	Initial	Final			24	48	72	7 days	28 days
Nil ...	45	365	.089	3.7	4.9	4.9	4.9	2060	3600
A ...	50	390	.118	1.0	3.8	3.9	3.9	2120	3870
B ...	50	350	.133	1.0	3.0	3.0	3.2	1910	4050
C ...	39	410	.069	Nil	6.1	8.8	8.8	2608	4090
D ...	36	413	.036	0.4	4.1	4.1	4.1	1714	3430
E ...	48	322	.109	1.0	4.1	4.1	4.3	1930	2080
F ...	46	318	.112	Nil	3.9	3.9	4.6	2500	4340

Almost all admixtures are effective in reducing the rate of percolation of water, compounds *C* and *F* being most effective. None of these are effective in reducing absorption to any appreciable extent. Compound *C* rather shows an increase in absorption.

Compound *E*, though shows good waterproofing characteristics, reduces the compressive strength of mortar from 3600 to 2080 at 28 days. Other compounds have not affected compressive strengths appreciably. It may, however, be mentioned that better concrete can be produced with regard to impermeability by using higher cement content.

4. Concrete surface hardeners

Few integral concrete hardeners produced in India were tested for their abrasion characteristic. The abrasion test was carried out in Dorry's abrasion testing machine. Specimen were prepared with and without the use of surface hardeners, using quartzite chips as aggregates. *Table 4* shows the results of test.

All the surface hardeners received were essentially ferrous admixtures. The results show that the resistance to abrasion of concrete is increased by the use of these ferrous surface hardeners. But admixture Z reduced the compressive strength of concrete from 4675 to 2795 *psi* at 28 days, while compound Y decreased the initial setting time making it difficult to work with. It was also observed that the abrasion resistance of mixes with the ferrous admixtures could easily be attained by using the same amount of cement by weight instead of admixture if the mix is properly handled, placed and cured. It was also observed that the ferrous particles got rusted under water and flaked off when subjected to further abrasion.

5. Surface active agent

In the design of concrete mixes, it is often required to restrict the water-cement ratio from the point of view of strength development. At the same time the desired degree of workability has also to be attained for the same water-cement ratio. Increase in w/c ratio increases the workability, but reduces the strength. In the hardening

Table 4

Hardener.	Setting time (minutes)		Soundness (Autoclave) percent expansion.	Percent Loss in Dorry's abrasion machine	Compressive strength of 1 : 3 C. M. *psi*	
	Initial	Final			7 days	28 days.
Nil ...	30	500	.194	8.4	2750	4675
X ...	26	390	.112	5.7 to 7.8	...	...
Y ...	8	466	.180	5.4 to 6.8	2750	4620
Z ..	14	477	.066	4.7	914	2795

Table 5

FM of Sand = 3·1 $C : A = 1 : 10{\cdot}6$

Sieve Analysis of the total aggregate (Combined Grading)

	Inches				*Mesh No*				
BS Sieve Size	1½	¾	3/8	3/16	7	14	25	52	100
Cumulative per cent passing ...	0	73	53	36	28	22	17	10	2

Lissapol *N* in *ozs per wt* of cement	W/*C*	Slump (*inches*)	Per cent Flow	*CF*	Per cent Air content	Unit *wt*	Compressive Strength (psi)	
							7 days	28 days
0	·80	Nil	60	·85	2	153	1200	1575
1	·75	Nil	56	·87	1·6	158	1390	2400
1½	·75	1/8	58	·88	1·5	158	1360	2200
2	·75	1/4	53	·885	1·7	153	995	1670
2½	·75	1/2	60	·88	1·6	157	950	1500
3	·75	3/4	60	·84	1·4	157	775	1460

Table 6

Sieve analysis of combined aggregates (cumulative per cent retained.

Mix	BS Sieve Size–*Inches*						*Mesh No*				
	6	3	1½	3/4	3/8	3/16	7	14	25	52	100
6 *in* maximum size aggregate	0	19	36	55	65	72	77	84	94	99	100
3 *in* maximum size aggregate	0	0	25	43	56	65	70	80	93	98	100

No air entraining agent was used in mixes with 3 *in* maximum size aggregate. "FEBCRETE" air entraining agent was used in mixes with 6 *in* maximum size aggregate.

Cement content in bags (100 *cft*)	Maximum size of aggregate. (*inches*)	in C : A C = 1. value of A	*W/C*	Per cent Air entrained.	Compressive Strength (*psi*)	
					7 days	28 days
9	3	13·5	·88	...	965	1000
	6		·75	4·5	980	1575
10	3	12·0	·83	...	990	1200
	6		·70	4·5	1230	2220
11	3	10·6	·76	...	1000	1400
	6		·60	4·0	1430	2920
13	3	8·85	·70	...	1345	2110
	6		·55	4·5	1680	2960
15	3	7·26	·63	...	2180	3500
	6		·50	4·0	2630	4300
16	3	6·9	·60	...	2400	4040
	6		·48	4·0	2680	4450
18	3	5·93	·55	...	2600	4480
	6		·45	4·2	3100	5200

of concrete hydration of cement particles requires large solid-liquid interface. The use of surface active agent in concrete reduces the surface or interfacial tension producing a more fluid mix. Thus incorporation of such agents in concrete improve the workability and will enable a lower *w/c* ratio to be used without affecting the strength.

"Lissapol *N*" supplied by Imperial Chemical Industries was tried as a Surface Active Agent in concrete and *table 5* gives the results of the tests.

From the test results it is observed that incorporation of "Lissapol *N*" in leaner mix such as 1 : 10.6 (*C* : *A*) increases the plasticity of the mix by preventing the segregation of water and improves the finish. In mixes where two or more fluid ounces of "Lissapol *N*" per *cwt* of cement are used 7 days strengths are, affected, showing that the development of strength is slow in such mixes. It may also be pointed out that "Lissapol *N*" does not entrain air to any appreciable extent.

6. Air entraining agent

In previous work done at the *CWPRS* on the design of mixes for Barapani Project, it was observed that strength of concrete with 3 *in* maximum size aggregate, was quite low for the respective cement to aggregate ratios than the normal concrete. The aggregates from Barapani were essentially flaky and elongated. Hence it required higher cement content to attain the required strength and workability than the rounded aggregates. In order to improve the strength characteristics, the mixes were redesigned for 6 *in* size maximum aggregate concrete using air entraining agent. The air entraining agent used was "FEBCRETE" supplied by M/s M Dialdas & Sons, Bombay. Two fluid *ounces* of "FEBCRETE" air entraining agent per *cwt* of cement were required to incorporate 4 *percent* air in the mix.

The results of test with and without the use of air entraining agent are given in *table 6.*

From the results, it is evident that for getting a particular strength, amount of cement can be reduced considerably, when 6 *in* maximum size aggregate and air entraining agent is used in place of 3 *in* maximum size aggregate without air entraining agent, keeping workability of both the mixes constant.

Thus for mixes with 2 *in* slump it required 9.6 bags per 100 *cft* using 6 *in* maximum size aggregate concrete and air entraining agent as against 12.7 bags per 100 *cft* with 3 *in* maximum size aggregate without air entraining agent, to develop 2000 *psi* at 28 days. 3000 *psi* strength can be attained at 28 days with 12 bags per 100 *cft* in redesigned mixes instead of 14.1 bags per 100 *cft* in previous mixes. A mix of 14.4 bags per 100 *cft* for 6 *in* maximum size aggregate and 4 *percent* entrained air develops 4000 *psi* at 28 days which otherwise required 16.4 bags per 100 *cft* for 3 *in* maximum size aggregate concrete.

---

46. Activities in Instrumentation

I. Automatic Tide Generator

To GENERATE tidal cycles automatically in a model, an electro-mechanical device was designed and built which was described earlier.[1] This system has a motor driven master cam and a float operated by the water level in the model to detect an error. This error directs the radial gates to open or close so as to reduce the error. The block scheme is shown in *fig 1.*

2. Modifications in design

The previous design of the interruptor consisting of revolving drum was modified considerably.

The present interruptor for varying the active time, *ie* when the gates operate and idle time *ie* when these remain stationary, consists of two cams each driven by a d-c motor. These cams operate relays through microswitches which finally control the electromagnets operating the gates. The proportion of active and idle time is different for each and gives an optimum gate speed suited for different portions of the tidal cycle. One of the two cams is selected at the proper position of the tidal level by another cam mounted side by side of the Master Cam.

3. Results

The optimum values of incoming discharge, length of gates and sill level of weir are determined from the tidal cycle to be reproduced. The magnitude of the error in reproducing the tidal

(1) CWPRS Annual Research Memoirs 1958 pp 380-382.

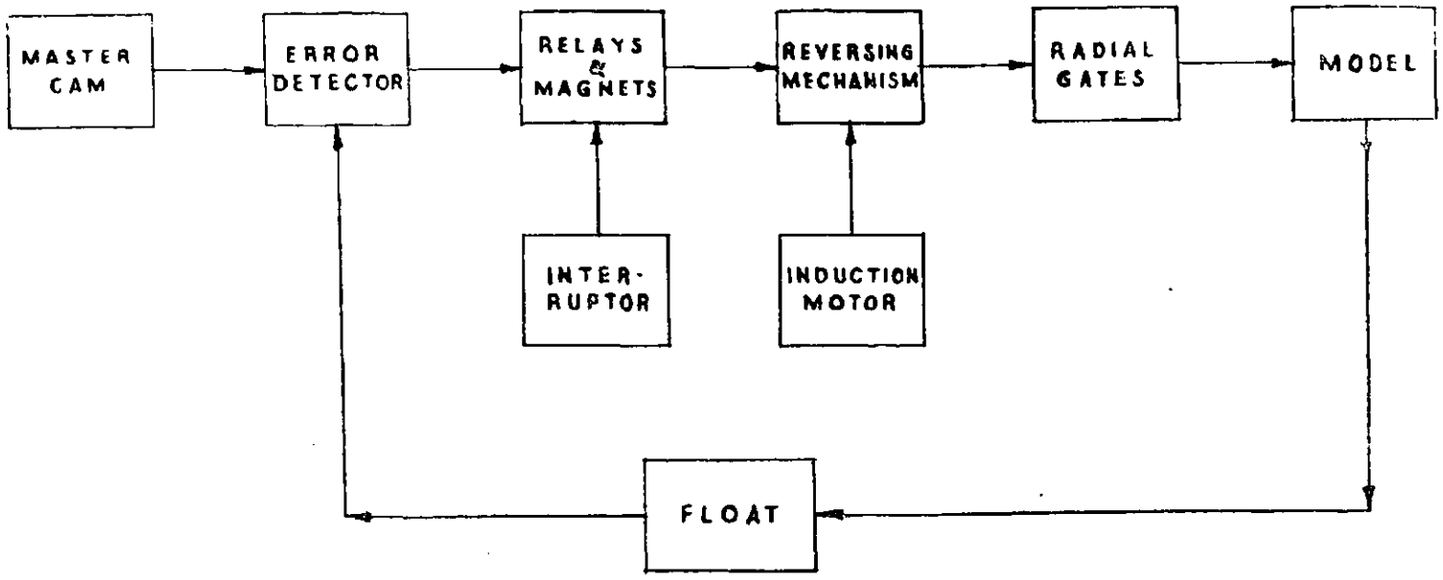

Fig 1: Block scheme of Automatic Tide generator.

cycle depends on the length and the rate of gate opening. These are therefore important parameters which have to be adjusted by trial and error so as to reduce the error. Several combinations of the gate length, active period and idle period were tried in the model to minimise the final error in tidal reproduction. Some typical curves are given below :

Curve shown in *photo 88* was obtained by operating Six gates (3.66 *m* total length) and keeping the idle time 3.5 *sec* and active time 1.5 *secs*. The maximum error was ± 6.0 *mm*. From this curve it was concluded that the number of gates was too high.

The curve in *photo 88* was obtained by operating three gates (total length 1.83 *m*) and keeping the idle time 3 *secs* and active time 1 *sec*. The error was reduced to ± 3 *mm*.

Results with a better combination are shown in *photo 88*. A single gate of .61 *m* length controlled the discharge. Two combinations for interruption were employed in this case so as to suit the different portions of the tidal curve. The maximum error was ± 2 *mm* and the portion in which this occurred was very limited.

4. Further refinements

With a view to further minimise the magnitude of error in tidal reproduction, the following changes will be incorporated in the design :

(b) Error magnification for detecting small changes in model water level.

(b) Variable interruption dependant on magnitude of error.

(c) Selection of interruption suitable for reproducing different parts of the tidal cycle.

II. Miniature Currentmeter

THE MINIATURE current meter reported earlier[1] was made particularly suitable for observation of velocities in tidal model by counting every pulse as each vane of the propeller passed a fixed electrode. Velocities can be measured in short intervals of 10 or 15 *secs* as pulses can be counted fast by the binary counters. This, however, necessitates complicated circuits and a costly counter.

In a one-way river model, where velocity at a point is steady, observation can be continued for a longer period, say 60 *secs* and a pulse counted for every revolution of the propeller instead of for each vane. Considerable simplification and economy can be effected in the counter by adopting a slower rate of counting. Such a unit in now developed.

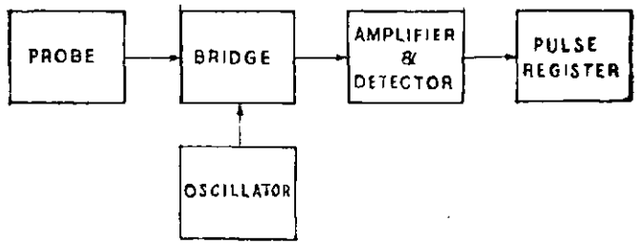

Fig 1: Block diagram of Simple Currentmeter.

(1) *CWPRS* Annual Research Memoirs 1959 *pp* 377-380.

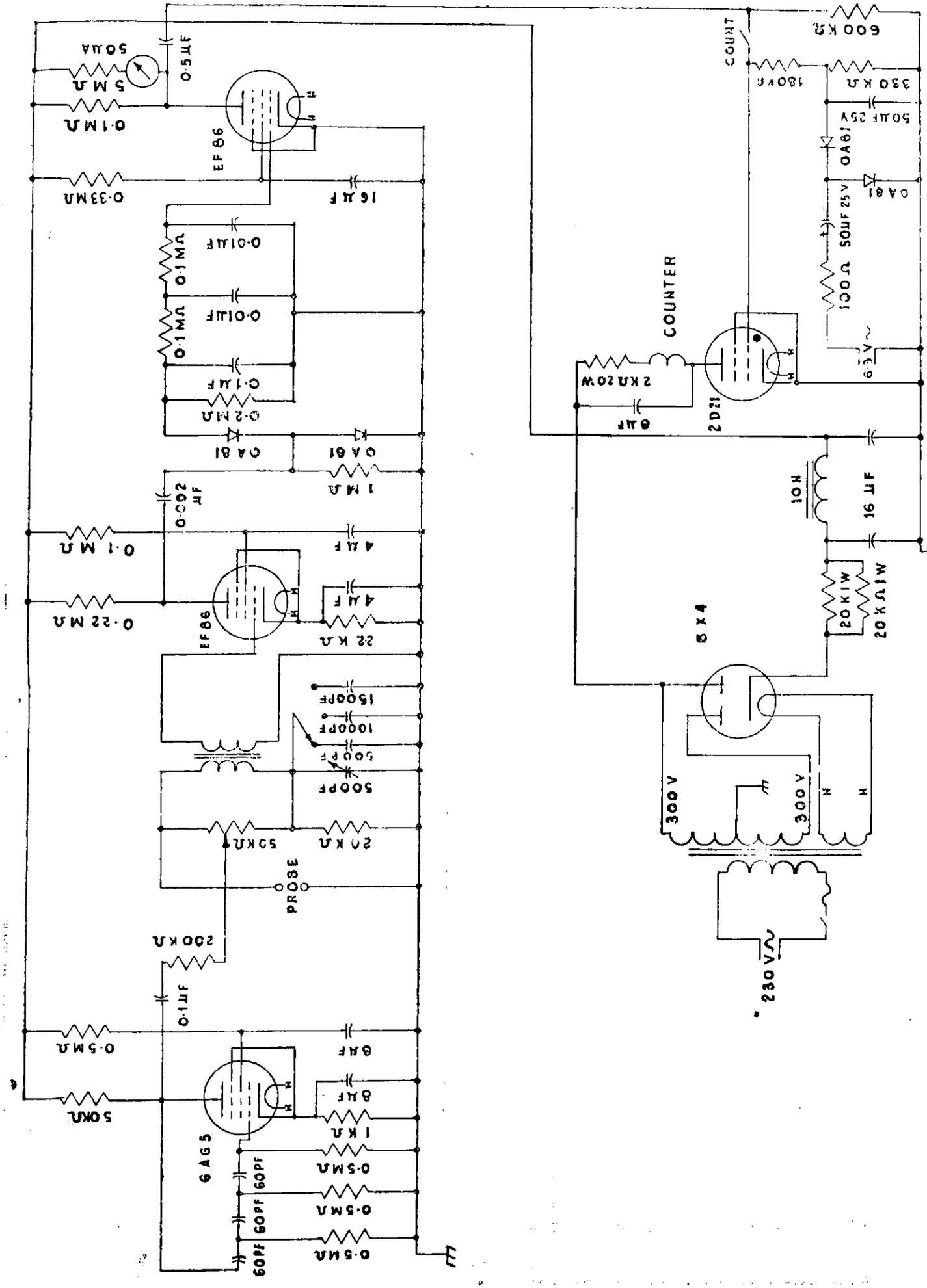

Fig 2: Simplified counter for miniature Currentmeter.

2. Simplified counter for currentmeter

(*a*) *Block diagram* (*fig 1*).—Initially balanced bridge becomes unbalanced due to a change in conductance caused by the passage of the vane near the fixed probe. The resultant pulse modulated output, after necessary amplification and detection, is fed to the thyratron circuit which operates a relay counter. Details of the system are described below and shown in *fig 2*.

(*b*) *Bridge*.—Since the currentmeter, alongwith the connecting cable is electrically equivalent to a parallel *R-C* combination, one of the bridge arms is an *R-C* in parallel. Other two arms are resistive. The advantage of this bridge is that the null point is insensitive to frequency. High bridge sensitivity has been achieved by choosing nearly equal impedances for different bridge arms.

Oscillator.—A phase shift oscillator has been used since it requires a single tube only, and gives high and reasonably pure output. This feeds a 2.5 *kcs*, 10 *V* signal to the bridge.

(*c*) *Amplifier-Detector*.—The pulse modulated output of the bridge is amplified, detected and fed to the thyratron circuit. The Amplifier tube after detector stage derives its grid bias from the detector output. Hence a voltmeter across its plate load indicates balance position.

(*d*) *Pulse Register*.—An electromagnetic relay counter type *No* 100 *A B* 59/2 (*Mfr M/S ITI Ltd*) has been used to register the number of pulses. It is operated by a thyratron which derives its grid bias from 6.3 *V* filament supply through Cockcroft-Walton Voltage doubler.

3. Results and discussion

This counter can record at a maximum rate of 7 pulses per *sec*. With a propeller of suitable pitch, velocities upto 2.5 *ft/sec* can be measured.

The upper limit of the counting rate of the present circuit is set by two factors :

(i) Operating time of the relay counter
(ii) Frequency of the Thyratron power supply.

The latter effect, however, is not significant in the present case. A fast operating relay counter will further improve the counting rate.

III. Bed profile recorder for model

THIS instrument is being developed with a view to plot a cross-section in a model automatically. At present this is done by manual observations, which limits the accuracy of measurement, consumes much more time and gives a plot from measurements at a discreet number of points which further reduces the accuracy.

2. Principle

The bed level is detected by means of a probe which, by electronic means, is made to maintain itself within a fixed, small distance from the bed. If such a probe is given a transverse motion across a section, it will follow the profile at that section; the vertical and horizontal movements of the probe can be recorded on rectangular coordinates by direct mechanical linkage to produce a plot of the section to known scales.

3. Probe and electronic circuit

The probe consists of two copper conductors embedded in an insulating tubing such that only their lower ends are exposed and conducting. When this probe is immersed in water and an alternating voltage applied, a current flows from one conductor tip to the other. The electrical resistance between the two conductors remains constant for any position in water as long as the distance of either tip from the bed is more than about one *millimeter*. If the probe further approaches the bed, there is a sharp increase in the electrical resistance due to the restriction of the conducting path through water. This proximity effect, which detects the presence of the bed close to the probe, is used to control automatically the probe position.

The probe is connected (*fig 1*) in a bridge circuit fed at 2 *kcs* from an oscillator. The bridge output is amplified, detected and used to actuate a relay with a change-over contact. A split field, *d-c* series motor is fed through the change-over contact and used to give a reversible vertical drive to the probe.

Initially, the bridge is balanced with the probe much more than a *millimeter* away from the bed; there is thus no bridge output and the motor is wired to run in such a direction as to take the probe downwards. As soon as the probe ap-

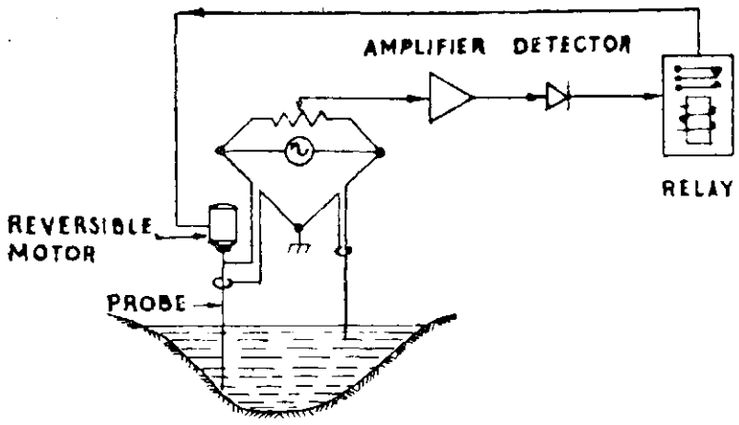

Fig 1: Bed profile recorder for model (schematic).

proaches close to the bed, the probe resistance rises and the bridge output due to this unbalance actuates the relay, thus reversing the probe drive motor. When the probe is raised just enough from the bed so that the bridge again becomes balanced, the motor resumes the downward motion of the probe. This process causes an oscillation or hunting of the probe close to the bed. With proper circuit constants, the amplitude of oscillations can be limited to less than one *millimeter*. In effect the probe maintains itself automatically just off the bed by about a *millimeter*.

4. Recording *(photo 89)*

The horizontal motion provided by another motor is converted as a rotational motion of the recording drum through a chain and sprocket wheel drive and the vertical movement of the probe is transferred as a horizontal motion of a pen through gears, a screw and nut arrangement. The probe movement along the section is thus plotted on a graph paper wrapped round the drum to scales of 1 in 12 horizontal and 1 in 1 vertical. These scales can be changed if required.

5. Results

An experimental set-up is made as described above. The maximum gradient that the system can negotiate depends firstly on the relative speeds of horizontal and vertical traverses and secondly on the edge sensitivity of the probe itself. Both these factors are found to limit, in the present design, the maximum gradient to 1 in 7.

6. Further improvements

Improvements have to be made by increasing the motor speed for vertical drive and by modifying the probe design so that at least a 1 in 1 slope is followed by the probe. The electronic circuit will also need a few modifications to achieve a stable operation after these changes.

IV. Wave height recorder for prototype

THE GENERAL requirements of the problem and the system proposed has been described earlier[1]. During implementation of the Scheme, however, a number of difficulties were encountered, which necessitated modifications.

2. Defects in old design

(*a*) There was considerable difficulty due to a continuous water film remaining on the gauge after recession of a wave. Sea water being a good conductor of electricity, this film causes an effective shunt across the contact points resulting in incorrect indication of wave height. This tendency is further accentuated in the lower portion of the gauge where heavy barnacle growth occurs after sometime.

(*b*) The gauge construction and the method of installation was found to be somewhat delicate to withstand the tidal current and wave impact.

(*c*) The gauge proposed to be installed in a pipe to eliminate the effect of tidal variations was found to be undesirable in many respects. The constricted opening at the bottom was also liable to get choked due to marine growth, thus putting the whole gauge out of operation.

(*d*) The unit has to work on a 12V battery. As all electronic valve circuits need much higher voltages, a vibrator type of supply has to be used. This proved to be a stumbling block due to the non-availability of proper components in the country. Valve circuits, in addition, consume considerable power and thus increase the battery drain to inconvenient magnitudes.

These difficulties were serious enough to necessitate major changes in the design. Salient features of the modified design are described below.

(1) CWPRS Annual Research Memoirs 1958 pp 286-7

3. New design (*photo 90*)

(*a*) The stainless steel rod fixed to the gauge along its length is eliminated. The stainless steel contact strips have been replaced by 6 *mm* rods properly secured inside. For ease of transport and handling, the gauge is made in 1 *m* length pieces and the interconnections are made with a flexible cable in the laboratory. This eliminates the necessity of making waterproof electrical connections at site while retaining the flexibility of construction. It is also proposed to fix the separate gauge pieces on a full length mild steel flat which could be quickly attached to or removed from the joist at the site without removing any individual gauge piece.

(*b*) To reduce the shunt paths due to the water film and the barnacle growth, a number of measures have been taken. The location of the contact points have been staggered to increase the length of leakage path and their shape so chosen as to hasten dripping of water. Secondly, the whole gauge is coated with "Araldite", a cold setting epoxy resin, which produces a protective, glassy surface impervious to water. The gauge is then painted with an antifouling paint used on ship hulls to retard barnacle growth. Even then, the gauge may have to be cleaned and repainted every few months.

(*c*) Gauge in the pipe is eliminated by changes in the electronic circuit (*fig 1*). Use is made of the fact that the wave to be recorded has a small period of some seconds as campared to the tidal period of twelve hours. The time constant of

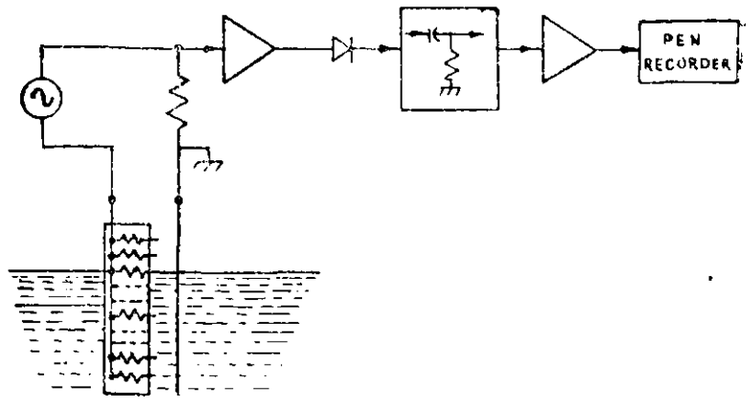

Fig 1: Wave height recorder for prototype (schematic).

response of the cricuit it adjusted to respond to wave variations and not to the tidal ones.

(*d*) The recorder (*photo 91*) described before[1] is modified in some respects. The chart speed is reduced from 40 to 20 *mm/min* to increase the period of possible unattended operation, consistent with obtaining a clear record. The specifications of the pen motor are also changed to suit the modified electronic circuitry.

(*e*) With a view to reduce the power consumption to a minimum, the whole electronic circuit is worked with Transistors instead of with valves. The present consumption of 1.4 *watts* may be compared to about 75 *watts* needed by a valve circuit. Transistor circuits are also inherently more stable and relaible. The main problems in the design are in respect of constancy of gain for all input levels, drift in the output voltage and the temperature stability. All these have been solved satisfactorily.

V. Capacitive wave height recorder

THIS instrument is developed for automatic recording of wave heights in harbour models for a range of 2-75 *mm* and periods from .5 *sec* and above. A unit using resistance type wave height probe was reported earlier.[2] It uses the change in resistance of water between two conducting wires with variation in water level. However, the conductivity of water changes with dissolved chemicals and also with temperature. These factors which affect the stability of calibration in the case of resistance probe have no effect on the capacitive probe developed.

2. Capacitive probe (*photo 92*)

The probe designed to transform water level variations into linear capacitance variations consists of one super enamel coated copper wire of *SWG No* 31 and a 3 *mm* stainless steel rod separated from it by a distance of 10 *mm*. The enamelled copper wire is run twice in order to increase the change in capacitance per *mm* of water level variation. When immersed in water, this system is electrically equivalent to a series combination of a capacitor formed by the insulated wire and water and is proportional to the depth of submergence of the probe and the resistance of water. The resistive part is made negligible by making

(1) *CWPRS* Annual Research Memoirs 1951, pp. 286-87 (2) *CWPRS* Annual Report (Tech) 1954, p. 10.

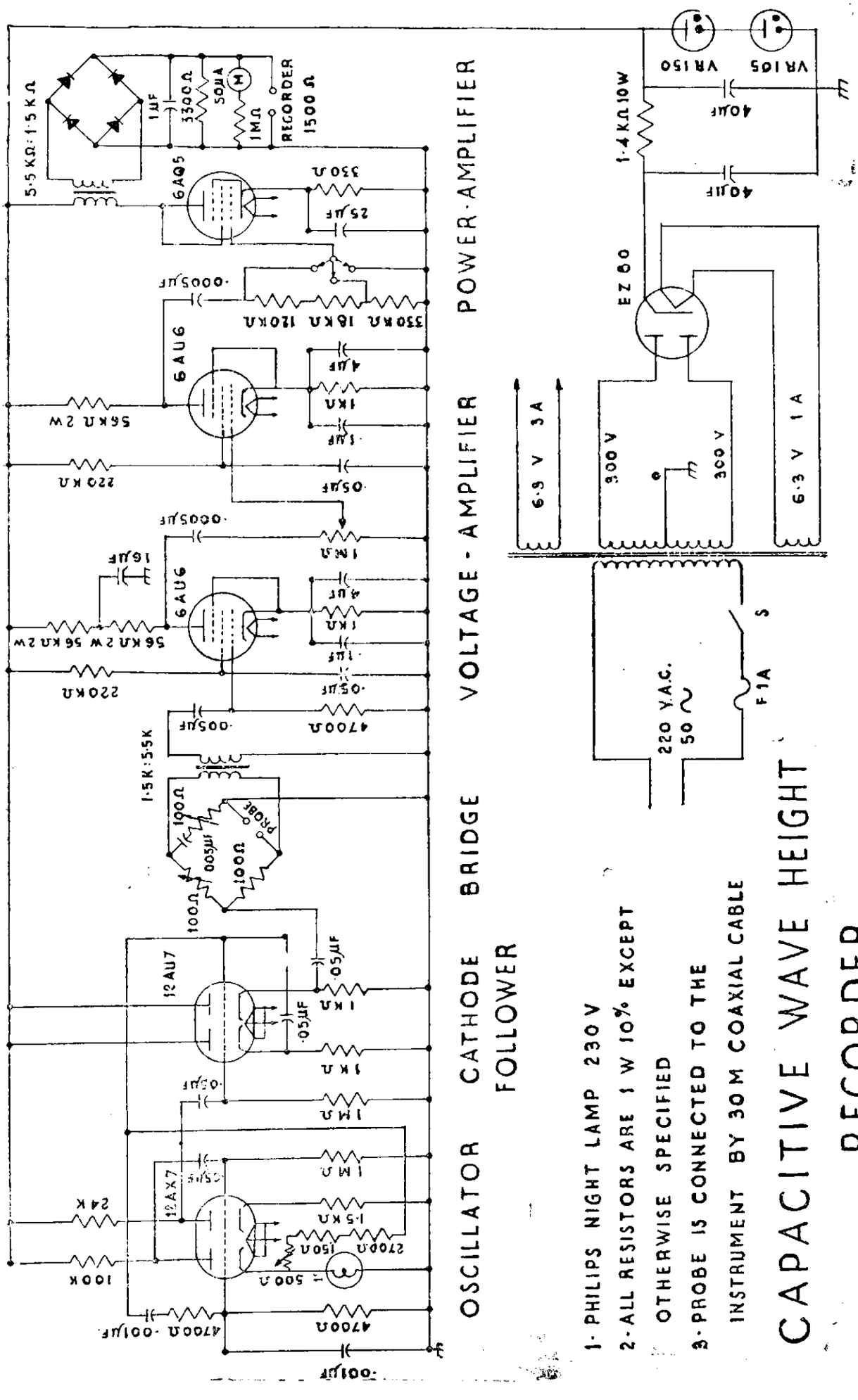
OSCILLATOR CATHODE FOLLOWER
BRIDGE VOLTAGE-AMPLIFIER
POWER-AMPLIFIER
CAPACITIVE WAVE HEIGHT RECORDER
1. PHILIPS NIGHT LAMP 230 V
2. ALL RESISTORS ARE 1 W 10% EXCEPT OTHERWISE SPECIFIED
3. PROBE IS CONNECTED TO THE INSTRUMENT BY 30 M COAXIAL CABLE
220 V A.C. 50
F1A
S
EZ 80
VR 105
VR 150
6·3 V 3A
300 V
6·3 V 1A
6AQ5
6AU6
12AU7
12AX7
PROBE
REGORDER 1500 Ω

Fig 2:

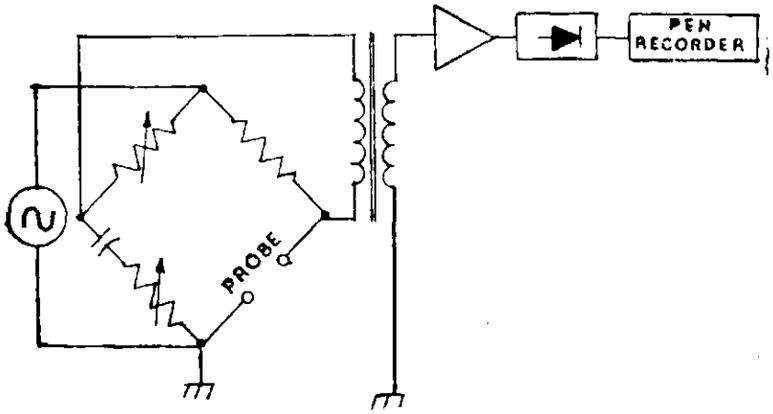

Fig 1: Block diagram of the electronic circuit.

the capacitive reactance quite high comparted to it. The electric impedance of the probe is, therefore, entirely capacitive, thus eliminating the errors due to conductivity and temperature changes of water. The capacitance of this probe is 5 *pf/mm*.

Due to level variations with waves, water wets the enameled copper wire. This affects the wave frequency response of the probe.[1] To have a flat frequency response upto 3 *cps*, the oscillator frequency is kept at 40 *kcs*.

3. Electronic circuit

The block diagram of the circuit is shown in *fig 1* and the details in *fig 2*. The probe is connected to the bridge by a 30 *m* long coaxial cable. The oscillator supplies 4 *volts* at 40 *kcs* to the bridge. The bridge can be balanced for any depth of submergence of the probe to eliminate the mean water level effect. The output is converted to single ended condition by the transformer. The output of the transformer is amplified, rectified and fed to a recorder with an impedance of 1500 *ohms*.

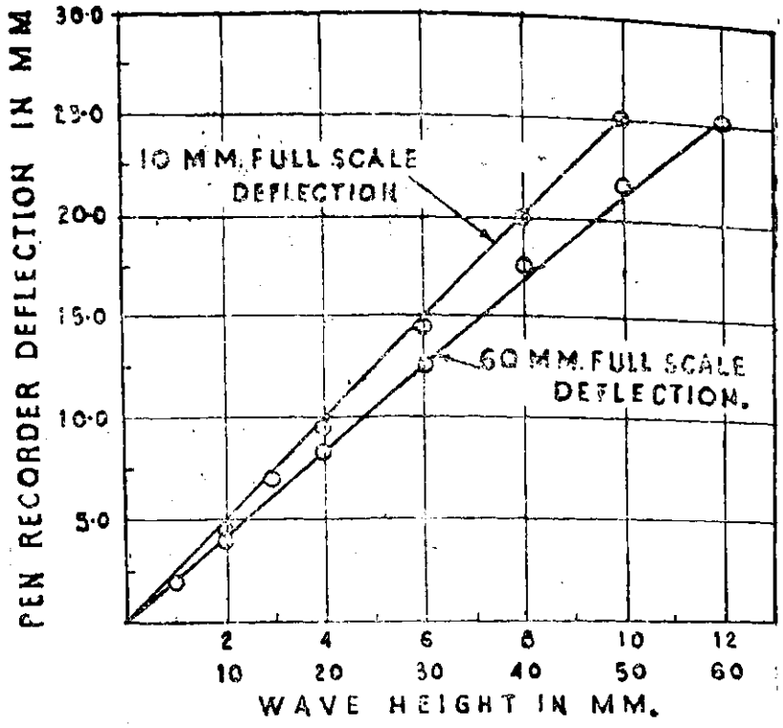

Fig 3: Calibration curves.

4. Sensitivity and accuracy

For reducing recording inaccuracies, amplification is desirable while recording wave heights smaller than 10 *mm*. A range is, therefore, so chosen that 1 *mm* of wave height is recorded as 2.5 *mm* by the pen recorder, thus giving a full scale deflection of 25 *mm* for 10 *mm* wave height while recording waves upto 75 *mm* this sensitivity can be suitably reduced, so as to limit full scale deflection to 30 *mm*. The instrument gives a linear calibration in all the ranges and the frequency response is flat upto a wave frequency of 3 *cps* (*fig 3*).

VI. Velocity tables and temperature corrections for liquids in manometers

SUITABLE indicating liquids of varying specific gravities for use in *U* tube manometers were reported[2] earlier wherein velocity tables based on values of specific gravities at different temperatures were given. It was, however, realized that these liquids have significant coefficients of cubical expansion in the normal temperature range of 10° to 40°*C* and though changes in absolute values of specific gravities look small, the relative variation in difference between liquid and water specific gravity cannot be ignored.

Table 1: Specific gravity of water and indicating liquids at different temperatures

S. *No*	Temp *oC*	Water	Dibutyl Phthalate	Methyl salicylate	Carbon tetrachloride	Bromoform
1	2	3	4	5	6	7
1	10	·99965	1·0520	1·193	1·6130	2·9033
2	15	·99905	1·0480	1·188	1·6036	
3	20	·99820	1·0446	1·183	1·5942	2·8904
4	25	·99705	1·0418	1·178		
5	30	·99570	1·0390	1·173	1·5747	2·8631
6	35	·99400	1·0366	1·168		
7	40	·99220	1·0345	1·163	1·5556	2·8273

(1) 'An instrument for Measuring liquid level and slosh in the Tanks of a liquid Propellant Rocket' L. B. WILNER, W. L. MORRISON, A. E. BROWN. Proceedings of the Institute of Radio Engineers, April, 1960, pp. 786-788.

(2) *Annual Research Memoirs 1958*, Central Water and Power Research Station, Poona, *Velocity tables for different chemicals for Pitot tubes'*, pp. 278-283.

It was, therefore, considered desirable to recalculate the velocity tables basing these on specific gravities at a common temperature and establish magnitudes of errors at other temperatures.

2. Temperature effect

Specific gravities of water and four selected indicating liquids, [1] [2] for the above temperature variation, are given in *table 1* and shown in *photo 93*.

The effect of change in specific gravity of water and indicating liquid on measured velocity is worked out as below :

$$V = C\sqrt{2gh'} \quad \ldots (1)$$

where V = velocity of water stream in mm/sec
C = Pitot tube coefficient, assumed as unity
g = Acceleration due to gravity 981 mm/sec^2
h' = Equivalent deflection of water column in manometer in mm
h = Total deflection of indicating liquid Col. in manometer in mm

Now $h' = h\left\{\begin{matrix}\text{Sp. gr. of indicating}\\ \text{liquid at } T°C\end{matrix}\right\} - \left\{\begin{matrix}\text{Sp. gr. of water at}\\ T°C\end{matrix}\right\}$

Designating $\left\{\begin{matrix}\text{Sp. gr. of indicating}\\ \text{liquid at } T°C\end{matrix}\right\} - \left\{\begin{matrix}\text{Sp. gr. of water at}\\ T°C\end{matrix}\right\} = P$

$$V = \sqrt{2ghP} \quad \ldots (2)$$

Taking value of P at 15°C $= P'$

$$V = \sqrt{2ghP'} = K\sqrt{h} \quad \ldots (3)$$

Where K at 15°C $= \sqrt{2gP'}$ ... (4)

The value of K does not remain the same at other temperatures. The percentage increase in h, indicating liquid total column height, at any other temperature as compared to 15° C is given by:

$$\text{Percentage increase in } h \text{ at } T°C \text{ with respect to } 15° C = \left(\frac{P'}{P} - 1\right) 100 \quad \ldots (5)$$

The corresponding percentage error in indicating velocity at higher temperature is:

$$\text{Percentage error in indicated velocity at Temp. } T°C \text{ with respect to } 15°C = \left(\sqrt{\frac{P'}{P}} - 1\right) 100 \quad \ldots (6)$$

3. Temperature corrections

Considering specific gravities at 15°C as standard, the percentage errors at 40°C, in estimated velocities are given in *table 2, col* (3).

The indicating liquid column in a manometer is small and isolated and can be considered to be at the same temperature as the surrounding air. Estimation of water column temperature is rather uncertain but the variations in water specific gravity are much smaller as compared to indicating liquids. If specific gravity of water is assumed as 1.0 (at 15°C it is 0.99) throughout the temperature range of 15°-40°C and specific gravities of indicating liquids at 15°C are taken as standard, then the percentage error in velocity measurement encountered at higher temperatures are given in *table 2, Cols* 4, 5 and 6.

Table 2: Percentage errors in velocity measurement due to change in specific gravity with temperature.

Indicating liquid	Percentage error in velocity taking sp. gravity of liquid at 15°C as standard and taking sp. gr. of water as 1·0			
	at 40°C	25°C	30°C	40°C
1	2	3	4	5
Dibutyl Phthalate.	13	3·8	11·0	13·0
Methyl Salicylate ..	5·2	1·3	4·2	7·4
Carbon Tetra chloride.	3·6	0·7	2·5	4·2
Bromoform ..	1·6	0·25	1·05	1·8

Note.—All percentage errors in *table 2* have a positive sign *i. e.* at temperature above 15°C, deflection 'h' of indicating liquid is more and hence velocity as read from standard table will be higher by given percentage.

In hydraulic model experiments, the velocities are generally low enough to require the lightest liquid, methyl salicilate in this case. It will be observed that the error in estimated velocity is of the order of 4 *percent* at 30°C. The errors become much smaller for heavier liquids.

4. Velocity tables

The total deflection of liquid column and corresponding velocity for three indicating liquids based on specific gravities of water and liquids at 15°C and Pitot tube coefficient of unity are given in *table 3* for a range of h equal to 1-600 mm.

If the magnitude of error due to temperature variation, as indicated in *table 2*, is considered large for a particular investigation, then correction can be applied by allowing for changes in specific gravities from *fig 1*.

For measuring velocities below 300 mm/sec more accurately, a lighter liquid DIBUTYL PHTHALATE is considered suitable as it has a specific gravity of 1.048 at 15°C. The relative change in specific gravity with temperature is, however, appreciable (*table 1, Col.* 4) and the percentage error in velocity measurement becomes quite large; the error at 30°C being 11 *percent*. Temperature correction is considered essential for this liquid and hence velocity table at 15°C standard temperature is not given.

(1) *International Critical Tables*, Vol III, *Density* by McGraw Hill Co.

(2) *Physico chemical constants of pure organic compounds* by J. Timmermann. Publishers Eisvier.

Table 3-A: Velocity table for pitot tube. Indicating liquid - METHYL SALICYLATE Sp Gravity at 15°C - 1.118.
Velocity of water stream = $C\ K\sqrt{h}$ where C - Pitot tube coefficient - assumed as unity
K - 60.895 at 15°C h - Total deflection of indicating liquid column in manometer, *mm*

VELOCITY IN *mm/Sec.* at 15°C

h	0	1	2	3	4	5	6	7	8	9
0 ...	0	60.9	86.1	105.5	121.8	136.2	149.2	161.1	172.2	182.7
10 ...	192.6	202.0	210.9	219.6	227.8	235.8	243.6	251.1	258.4	265.4
20 ...	272.3	279.1	285.6	292.0	298.3	304.5	310.5	316.4	322.2	327.9
30 ...	333.5	339.0	344.5	349.8	355.1	360.3	365.4	370.4	375.4	380.3
40 ...	385.1	389.9	394.6	399.3	403.9	408.5	413.0	417.5	421.9	426.3
50 ...	430.6	434.9	439.1	443.3	447.5	451.6	455.7	459.7	463.8	467.7
60 ...	471.7	475.6	479.5	483.3	487.2	491.0	494.7	498.4	502.2	505.8
70	509.5	513.1	516.7	520.3	523.8	527.4	530.9	534.4	537.8	541.2
80 ...	544.7	548.1	551.4	554.8	558.1	561.4	564.7	568.0	571.2	574.5
90 ...	577.7	580.9	584.1	587.3	590.4	593.5	596.6	599.7	602.8	605.9
100 ...	609.0	612.0	615.0	618.0	621.0	624.0	627.0	629.9	632.8	635.8
110 ...	638.7	641.6	644.5	647.3	650.2	653.0	655.9	658.7	661.5	664.3
120 ...	667.1	669.8	672.6	675.4	678.1	680.8	683.5	686.3	688.9	691.6
130 ...	694.3	697.0	699.6	702.3	704.9	707.5	710.2	712.8	715.4	717.9
140 ...	720.5	723.1	725.6	728.2	730.7	733.3	735.8	738.3	740.8	743.3
150 ...	745.8	748.3	750.8	753.2	755.7	758.1	760.6	763.0	765.4	767.9
160 ...	770.3	772.7	775.1	777.5	779.8	782.2	784.6	786.9	789.3	791.6
170 ...	794.0	796.3	798.6	800.9	803.3	805.6	807.9	810.2	812.4	814.7
180 ...	817.0	819.3	821.5	823.8	826.0	828.3	830.5	832.7	834.9	837.2
190 ...	839.4	841.6	843.8	846.0	848.2	850.3	852.5	854.7	856.9	859.0
200 ...	861.2	863.3	865.5	867.6	869.8	871.9	874.0	876.1	878.2	880.3
210 ...	882.5	884.5	886.6	888.7	890.8	892.9	895.0	897.0	899.1	901.2
220 ...	903.2	905.3	907.3	909.4	911.4	913.4	915.5	917.5	919.5	921.5
230 ...	923.5	925.5	927.5	929.5	931.5	933.5	935.5	937.5	939.4	941.4
240 ...	943.4	945.3	947.3	949.3	951.2	953.2	955.1	957.0	959.0	960.9
250 ...	962.8	964.8	966.7	968.6	970.5	972.4	974.3	976.2	978.1	980.0
260 ...	981.9	983.8	985.7	987.6	989.4	991.3	993.2	995.0	996.9	998.8
270 ...	1000.6	1002.5	1004.3	1006.1	1008.0	1009.8	1011.7	1013.5	1015.3	1017.1
280 ...	1019.0	1020.8	1022.6	1024.4	1026.2	1028.0	1029.8	1031.6	1033.4	1035.2
290 ...	1037.0	1038.8	1040.6	1042.4	1044.1	1045.9	1047.7	1049.4	1051.2	1053.0
300 ...	1054.7	1056.5	1058.2	1060.0	1061.7	1063.5	1065.2	1067.0	1068.7	1070.4
310 ...	1072.2	1073.9	1075.6	1077.3	1079.1	1080.8	1082.5	1084.2	1085.9	1087.6
320 ...	1089.3	1091.0	1092.7	1094.4	1096.1	1097.8	1099.5	1101.2	1102.9	1104.5
330 ...	1106.2	1107.9	1109.6	1111.2	1112.9	1114.6	1116.2	1117.9	1119.5	1121.2
340 ...	1122.8	1124.5	1126.1	1127.8	1129.4	1131.1	1132.7	1134.3	1136.0	1137.6
350 ...	1139.2	1140.9	1142.5	1144.1	1145.7	1147.3	1149.0	1150.6	1152.2	1153.8
360 ...	1155.4	1157.0	1158.6	1160.2	1161.8	1163.4	1165.0	1166.6	1168.2	1169.8
370 ...	1171.3	1172.9	1174.5	1176.1	1177.7	1179.2	1180.8	1182.4	1183.9	1185.5
380 ...	1187.1	1188.6	1190.2	1191.7	1193.3	1194.8	1196.4	1197.9	1199.5	1201.0
390 ...	1202.6	1204.1	1205.7	1207.2	1208.7	1210.3	1211.8	1213.3	1214.8	1216.4
400 ...	1217.9	1219.4	1220.9	1222.5	1224.0	1225.5	1227.0	1228.5	1230.0	1231.5
410 ...	1233.0	1234.5	1236.0	1237.5	1239.0	1240.5	1242.0	1243.5	1245.0	1246.5
420 ...	1248.0	1249.5	1250.9	1252.4	1253.9	1255.4	1256.9	1258.3	1259.8	1261.3
430 ...	1262.7	1264.2	1265.7	1267.1	1268.6	1270.1	1271.5	1273.0	1274.4	1275.9
440 ...	1277.3	1278.8	1280.2	1281.7	1283.1	1284.6	1286.0	1287.5	1288.9	1290.3
450 ...	1291.8	1293.2	1294.6	1296.1	1297.5	1298.9	1300.4	1301.8	1303.2	1304.6
460 ...	1306.1	1307.5	1308.9	1310.3	1311.7	1313.1	1314.5	1316.0	1317.4	1318.8
470 ...	1320.2	1321.6	1323.0	1324.4	1325.8	1327.2	1328.6	1330.0	1331.4	1332.8
480 ...	1334.1	1335.5	1336.9	1338.3	1339.7	1341.1	1342.5	1343.8	1345.2	1346.6
490 ...	1348.0	1349.3	1350.7	1352.1	1353.5	1354.8	1356.2	1357.6	1358.9	1360.3
500 ...	1361.7	1363.0	1364.4	1365.7	1367.1	1368.4	1369.8	1371.2	1372.5	1373.9
510 ...	1375.2	1376.5	1377.9	1379.2	1380.6	1381.9	1383.3	1384.6	1385.9	1387.3
520 ...	1388.6	1390.0	1391.3	1392.6	1393.9	1395.3	1396.6	1397.9	1399.3	1400.6
530 ...	1401.9	1403.2	1404.5	1405.9	1407.2	1408.5	1409.8	1411.1	1412.4	1413.8
540 ...	1415.1	1416.4	1417.7	1419.0	1420.3	1421.6	1422.9	1424.2	1425.5	1426.8
550 ...	1428.1	1429.4	1430.7	1432.0	1433.3	1434.6	1435.9	1437.2	1438.5	1439.8
560 ...	1441.0	1442.3	1443.6	1444.9	1446.2	1447.5	1448.7	1450.0	1451.3	1452.6
570 ...	1453.8	1455.1	1456.4	1457.7	1458.9	1460.2	1461.5	1462.7	1464.0	1465.3
580 ...	1466.5	1467.8	1469.1	1470.3	1471.6	1472.8	1474.1	1475.4	1476.6	1477.9
590 ...	1479.1	1480.4	1481.6	1482.9	1484.1	1485.4	1486.6	1487.9	1489.1	1490.4
600 ...	1491.6									

Table 3-B: Velocity table for pitot tube Indicating liquid - CARBON TETRACHLORIDE Sp. Gravity at 15°C - 1.6036

Velocity of water stream $= CK\sqrt{h}$ where C - Pitot tube coefficient - assumed as unity

K - 108.914 at 15°C h - Total deflection of indicating liquid column in manometer, *mm*

VELOCITY IN *mm/Sec.* at 15°C

h	0	1	2	3	4	5	6	7	8	9
0 ...	0.0	108.9	154.0	188.6	217.8	243.5	266.8	288.2	308.1	326.7
10 ...	344.4	361.2	377.3	392.7	407.5	421.8	435.7	449.1	462.1	474.7
20 ...	487.1	499.1	510.9	522.3	533.6	544.6	555.4	565.9	576.3	586.5
30 ...	596.5	606.4	616.1	625.7	635.1	644.3	653.5	662.5	671.4	680.2
40 ...	688.8	697.4	705.8	714.2	722.4	730.6	738.7	746.7	754.6	762.4
50 ...	770.1	777.8	785.4	792.9	800.4	807.7	815.0	822.3	829.5	836.6
60 ...	843.6	850.6	857.6	864.5	871.3	878.1	884.8	891.5	898.1	904.7
70 ...	911.2	917.7	924.2	930.6	936.9	943.2	949.5	955.7	961.9	968.0
80 ...	974.2	980.2	986.3	992.3	998.2	1004.1	1010.0	1015.9	1021.7	1027.5
90 ...	1033.2	1039.0	1044.7	1050.3	1056.0	1061.6	1067.1	1072.7	1078.2	1083.7
100 ...	1089.1	1094.6	1100.0	1105.4	1110.7	1116.0	1121.3	1126.6	1131.9	1137.1
110 ...	1142.3	1147.5	1152.6	1157.8	1162.9	1168.0	1173.0	1178.1	1183.1	1188.1
120 ...	1193.1	1198.1	1203.0	1207.9	1212.8	1217.7	1222.6	1227.4	1232.2	1237.0
130 ...	1241.8	1246.6	1251.3	1256.1	1260.8	1265.5	1270.1	1274.8	1279.4	1284.1
140 ...	1288.7	1293.3	1297.9	1302.4	1307.0	1311.5	1316.0	1320.5	1325.0	1329.5
150 ...	1333.9	1338.4	1342.8	1347.2	1351.6	1356.0	1360.3	1364.7	1369.0	1373.4
160 ...	1377.7	1382.0	1386.2	1390.5	1394.8	1399.0	1403.3	1407.5	1411.7	1415.9
170 ...	1420.1	1424.2	1428.4	1432.5	1436.7	1440.8	1444.9	1449.0	1453.1	1457.2
180 ...	1461.2	1465.3	1469.3	1473.4	1477.4	1481.4	1485.4	1489.4	1493.4	1497.3
190 ...	1501.3	1505.2	1509.2	1513.1	1517.0	1520.9	1524.8	1528.7	1532.6	1536.4
200 ...	1540.3	1544.1	1548.0	1551.8	1555.6	1559.4	1563.2	1567.0	1570.8	1574.5
210 ...	1578.3	1582.1	1585.8	1589.5	1593.3	1597.0	1600.7	1604.4	1608.1	1611.8
220 ...	1615.5	1619.1	1622.8	1626.4	1630.1	1633.7	1637.3	1641.0	1644.6	1648.2
230 ...	1651.8	1655.4	1658.9	1662.5	1666.1	1669.6	1673.2	1676.7	1680.2	1683.8
240 ...	1687.3	1690.8	1694.3	1697.8	1701.3	1704.8	1708.3	1711.7	1715.2	1718.6
250 ...	1722.1	1725.5	1729.0	1732.4	1735.8	1739.2	1742.6	1746.0	1749.4	1752.8
260 ...	1756.2	1759.6	1762.9	1766.3	1769.6	1773.0	1776.3	1779.7	1783.0	1786.3
270 ...	1789.6	1793.0	1796.3	1799.6	1802.8	1806.1	1809.4	1812.7	1816.0	1819.2
280 ...	1822.5	1825.7	1829.0	1832.2	1835.5	1838.7	1841.9	1845.1	1848.3	1851.5
290 ...	1854.7	1857.9	1861.1	1864.3	1867.5	1870.7	1873.8	1877.0	1880.1	1883.3
300 ...	1886.4	1889.6	1892.7	1895.9	1899.0	1902.1	1905.2	1908.3	1911.4	1914.5
310 ...	1917.6	1920.7	1923.8	1926.9	1930.0	1933.0	1936.1	1939.2	1942.2	1945.3
320 ...	1948.3	1951.4	1954.4	1957.4	1960.5	1963.5	1966.5	1969.5	1972.5	1975.5
330 ...	1978.5	1981.5	1984.5	1987.5	1990.5	1993.5	1996.4	1999.4	2002.4	2005.3
340 ...	2008.3	2011.2	2014.2	2017.1	2020.0	2023.0	2025.9	2028.8	2031.8	2034.7
350 ...	2037.6	2040.5	2043.4	2046.3	2049.2	2052.1	2055.0	2057.9	2060.7	2063.6
360 ...	2066.5	2069.4	2072.2	2075.1	2077.9	2080.8	2083.6	2086.5	2089.3	2092.2
370 ...	2095.0	2097.8	2100.7	2103.5	2106.3	2109.1	2111.9	2114.7	2117.5	2120.3
380 ...	2123.1	2125.9	2128.7	2131.5	2134.3	2137.0	2139.8	2142.6	2145.4	2148.1
390 ...	2150.9	2153.6	2156.4	2159.1	2161.9	2164.6	2167.4	2170.1	2172.8	2175.6
400 ...	2178.3	2181.0	2183.7	2186.4	2189.1	2191.9	2194.6	2197.3	2200.0	2202.6
410 ...	2205.3	2208.0	2210.7	2213.4	2216.1	2218.7	2221.4	2224.1	2226.7	2229.4
420 ...	2232.1	2234.7	2237.4	2240.0	2242.7	2245.3	2248.0	2250.6	2253.2	2255.9
430 ...	2258.5	2261.1	2263.7	2266.4	2269.0	2271.6	2274.2	2276.8	2279.4	2282.0
440 ...	2284.6	2287.2	2289.8	2292.4	2295.0	2297.5	2300.1	2302.7	2305.3	2307.8
450 ...	2310.4	2313.0	2315.5	2318.1	2320.7	2323.2	2325.8	2328.3	2330.9	2333.4
460 ...	2335.9	2338.5	2341.0	2343.5	2346.1	2348.6	2351.1	2353.7	2356.2	2358.7
470 ...	2361.2	2363.7	2366.2	2368.7	2371.2	2373.7	2376.2	2378.7	2381.2	2383.7
480 ...	2386.2	2388.7	2391.2	2393.6	2396.1	2398.2	2401.1	2403.5	2406.0	2408.4
490 ...	2410.9	2413.4	2415.8	2418.3	2420.7	2423.2	2425.6	2428.1	2430.5	2433.0
500 ...	2435.4	2437.8	2440.3	2442.7	2445.1	2447.5	2450.0	2452.4	2454.8	2457.2
510 ...	2459.6	2462.0	2464.4	2466.8	2469.3	2471.7	2474.0	2476.4	2478.8	2481.2
520 ...	2483.6	2486.0	2488.4	2490.8	2493.2	2495.5	2497.9	2500.3	2502.7	2505.0
530 ...	2507.4	2509.7	2512.7	2514.5	2516.8	2519.2	2521.5	2523.9	2526.2	2528.6
540 ...	2530.9	2533.3	2535.6	2538.0	2540.3	2542.6	2544.9	2547.3	2549.6	2551.9
550 ...	2554.3	2556.6	2558.9	2561.2	2563.5	2565.8	2568.2	2570.5	2572.8	2575.1
560 ...	2577.4	2579.7	2582.0	2584.3	2586.6	2588.9	2591.1	2593.4	2595.7	2598.0
570 ...	2600.3	2602.6	2604.8	2607.1	2609.4	2611.7	2613.9	2616.2	2618.5	2620.7
580 ...	2623.0	2625.3	2627.5	2629.8	2632.0	2634.3	2636.5	2638.8	2641.0	2643.3
590 ...	2645.5	2647.8	2650.0	2652.2	2654.5	2656.7	2658.9	2661.2	2663.4	2665.6
600 ...	2667.8									

Table 3-C : Velocity table for pitot tube Indicating liquid BROMOFORM Sp gravity at 15°C - 2.9033
Velocity of water stream = $CK\sqrt{h}$ where C - Pitot tube coefficient - assumed as unity
K - 193.2935 h - Total deflection of indicating liquid column in manometer, *mm*

	VELOCITY IN *mm/Sec.* at 15°C									
h	0	1	2	3	4	5	6	7	8	9
0	...	193.3	273.4	334.8	386.6	432.2	473.5	511.4	546.7	579.9
10	... 611.3	641.1	669.6	696.9	723.2	748.6	773.2	797.0	820.1	842.5
20	... 864.4	885.8	906.6	927.0	946.9	966.5	985.6	1004.4	1022.8	1040.9
30	... 1058.7	1076.2	1093.4	1110.4	1127.1	1143.5	1159.8	1175.8	1191.5	1207.1
40	... 1222.5	1237.7	1252.7	1267.5	1282.2	1296.7	1311.0	1325.2	1339.2	1353.1
50	... 1366.8	1380.4	1393.9	1407.2	1420.4	1433.5	1446.5	1459.3	1472.1	1484.7
60	... 1497.3	1509.7	1522.0	1534.2	1546.3	1558.4	1570.3	1582.2	1593.9	1605.6
70	... 1617.2	1628.7	1640.2	1651.5	1662.8	1674.0	1685.1	1696.2	1707.1	1718.0
80	... 1728.9	1739.6	1750.3	1761.0	1771.6	1782.1	1792.5	1802.9	1813.2	1823.0
90	... 1833.7	1843.9	1854.0	1864.1	1874.1	1884.0	1893.9	1903.7	1913.5	1923.3
100	... 1932.9	1942.6	1952.2	1961.7	1971.2	1980.7	1990.1	1999.4	2008.8	2018.0
110	... 2027.3	2036.5	2045.6	2054.7	2063.8	2072.8	2081.8	2090.8	2099.7	2108.6
120	... 2117.4	2126.2	2135.0	2143.7	2152.4	2161.1	2169.7	2178.3	2186.9	2195.4
130	... 2203.9	2212.3	2220.8	2229.2	2237.5	2245.9	2254.2	2262.4	2270.7	2278.9
140	... 2287.1	2295.2	2303.4	2311.5	2319.5	2327.6	2335.6	2343.6	2351.5	2359.5
150	... 2367.3	2375.2	2383.1	2390.9	2398.7	2406.5	2414.2	2422.0	2429.7	2437.3
160	... 2445.0	2452.6	2460.2	2467.8	2475.4	2482.9	2490.4	2497.9	2505.4	2512.8
170	... 2520.2	2527.6	2535.0	2542.4	2549.7	2557.0	2564.3	2571.6	2578.9	2586.1
180	... 2593.3	2600.5	2607.7	2614.8	2622.0	2629.1	2636.2	2643.2	2650.3	2657.3
190	... 2664.4	2671.4	2678.4	2685.3	2692.3	2699.2	2706.1	2713.0	2719.9	2726.7
200	... 2733.6	2740.4	2747.2	2754.0	2760.8	2767.5	2774.3	2781.0	2787.7	2794.4
210	... 2801.1	2807.7	2814.4	2821.0	2827.6	2834.2	2840.8	2847.4	2853.9	2860.5
220	... 2867.0	2873.5	2880.0	2886.5	2892.9	2899.4	2905.8	2912.3	2918.7	2925.1
230	... 2931.5	2937.8	2944.1	2950.5	2956.8	2963.1	2969.4	2975.7	2982.0	2988.2
240	... 2994.5	3000.7	3006.9	3013.2	3019.3	3025.5	3031.7	3037.8	3044.0	3050.1
250	... 3056.2	3062.3	3068.4	3074.5	3080.6	3086.6	3092.7	3098.7	3104.8	3110.8
260	... 3116.8	3122.8	3128.7	3134.7	3140.7	3146.6	3152.5	3158.4	3164.3	3170.2
270	... 3176.1	3182.0	3187.9	3193.7	3199.6	3205.4	3211.2	3217.0	3222.8	3228.6
280	... 3234.4	3240.2	3246.0	3251.7	3257.4	3263.2	3268.9	3274.6	3280.3	3286.0
290	... 3291.7	3297.3	3303.0	3308.6	3314.3	3319.9	3325.5	3331.1	3336.8	3342.4
300	... 3347.9	3353.5	3359.1	3364.6	3370.2	3375.7	3381.3	3386.8	3392.3	3397.8
310	... 3403.3	3408.8	3414.2	3419.7	3425.2	3430.6	3436.1	3441.5	3446.9	3452.3
320	... 3457.7	3463.1	3468.5	3473.9	3479.3	3484.7	3490.0	3495.3	3500.7	3506.0
330	... 3511.4	3516.7	3522.0	3527.3	3532.6	3537.9	3543.1	3548.4	3553.7	3558.9
340	... 3564.2	3569.4	3574.6	3579.9	3585.1	3590.3	3595.5	3600.7	3605.9	3611.0
350	...3616.2	3621.4	3626.5	3631.7	3636.8	3641.9	3647.1	3652.2	3657.3	3662.4
360	... 3667.5	3672.6	3677.7	3682.7	3687.8	3692.9	3697.9	3703.0	3708.0	3713.1
370	... 3718.1	3723.1	3728.1	3733.1	3738.1	3743.1	3748.1	3753.1	3758.1	3763.0
380	... 3768.0	3772.9	3777.9	3782.8	3787.8	3792.7	3797.6	3802.5	3807.4	3812.3
390	... 2817.2	3822.1	3827.0	3831.9	3836.8	3841.6	3846.5	3851.4	3856.2	3861.0
400	... 3865.9	3870.7	3875.5	3880.3	3885.2	3890.0	3894.7	3899.5	3904.3	3909.1
410	... 3913.9	3918.7	3923.4	3928.2	3932.9	3937.7	3942.4	3947.2	3951.9	3956.6
420	... 3961.3	3966.1	3970.8	3975.5	3980.2	3984.8	3989.5	3994.2	3998.9	4003.6
430	... 4008.2	4012.9	4017.5	4022.2	4026.8	4031.5	4036.1	4040.7	4045.3	4049.9
440	... 4054.6	4059.2	4063.8	4068.4	4072.9	4077.5	4082.1	4086.7	4091.3	4095.8
450	... 4100.4	4104.9	4109.5	4114.0	4118.6	4123.1	4127.6	4132.2	4136.7	4141.2
460	... 4145.7	4150.2	4154.7	4159.2	4163.6	4168.2	4172.6	4177.1	4181.6	4186.0
470	... 4190.5	4195.0	4199.4	4203.9	4208.3	4212.7	4217.2	4221.6	4226.0	4230.4
480	... 4234.8	4239.3	4243.7	4248.1	4252.5	4256.8	4261.2	4265.6	4270.0	4274.4
490	... 4278.7	4283.1	4287.5	4291.8	4296.2	4300.5	4304.9	4309.2	4313.5	4317.8
500	... 4322.2	4326.5	4330.8	4335.1	4339.4	4343.7	4348.0	4352.3	4356.6	4360.9
510	... 4365.2	4369.5	4373.7	4378.0	4382.3	4386.5	4390.8	4395.0	4399.3	4403.5
520	... 4407.8	4412.0	4416.2	4420.5	4424.7	4428.9	4433.1	4437.3	4441.6	4445.8
530	... 4449.9	4454.1	4458.3	4462.5	4466.7	4470.9	4475.1	4479.2	4483.4	4487.6
540	... 4491.7	4495.9	4500.0	4504.2	4508.3	4512.5	4516.6	4520.7	4524.9	4529.0
550	... 4533.1	4537.3	4541.4	4545.5	4549.6	4553.7	4557.8	4561.9	4566.0	4570.1
560	... 4574.2	4578.2	4582.3	4586.4	4590.5	4594.5	4598.6	4602.7	4606.7	4610.8
570	... 4614.8	4618.9	4622.9	4626.9	4631.0	4635.0	4639.0	4643.1	4647.1	4651.1
580	... 4655.1	4659.1	4663.1	4667.1	4671.2	4675.2	4679.1	4683.1	4687.1	4691.1
590	... 4695.1	4699.1	4703.0	4707.0	4711.0	4714.9	4718.9	4722.9	4726.8	4730.8
600	... 4734.7									

5. Conclusions

(*i*) Four indicating liquids of varying specific gravity are selected for use in monometer so as to cover a range of velocities from 100 *mm/sec* to 4000 *mm/sec*. These are :

(a) DIBUTYL PHTHALATE,
(b) METHYL SALICYLATE,
(c) CARBON TETRACHLORIDE,
(d) BROMOFORM.

These chemicals should be of extra pure quality only to obtain given specific gravities.

(*ii*) All these liquids are colourless and a minute quantity of waxolin dye should be added to give the indicating liquid a pale Yellow colour.

(*iii*) These are immiscible with water and give good meniscus with water especially if couple of drops of a wetting agent such as turkey red oil are added to water column in manometer.

(*iv*) The coefficient of expansion and its effect on specific gravity in the range 10°*C* to 40°*C* cannot be neglected especially for the first two lighter liquids. It is desirable to apply temperature correction to specific gravity for investigations of more accurate nature.

---

47. Activities in Ship Model Testing Tank

1. Model suspension system on the trolley

The model suspension arrangement originally supplied by *M/s* Kempf and Remmers (*photo 94*) consists of horizontal and vertical arms mounted on ball bearings. The vertical arm at its lower end has a small steel plate mounted on self-aligning ball bearing which is screwed to the model to be towed by the carriage.

An ideal suspension system is that which offers least resistance to the longitudinal movement of the model. With this in view, the horizontal and vertical arms of the above system were brought to neutral equilibrium by adjusting the balancing weights. It was observed that the vertical arm remained stationary at any position and could be moved with a force of .2 *gm*.

There was, however, one drawback in this arrangement. Longitudinal displacement of a model required relative movement of the inner race of the bearing in its outer race which offered considerably high resistance.

It was, therefore, decided to replace the bottom ball bearing by another system consisting of two rigid ball bearings for allowing free longitudinal movement and a self-aligning ball bearing for the rolling action of the model (*photo 95*) with the above modifications, the model of Mariner ship to 1/80 *scale* could be moved from its position of rest with a force of 2.88 *gm*.

In spite of the above refinements in the Kempf and Remmer system, it was felt that this left much to be desired. The physical connection between the arms and the model was not found to be a good feature as it transmitted every disturbance on the trolley to the model.

2. Rigid rod and slot system

The above suspension system was, therefore, replaced by a rigid rod and slot system. This consists of two, one inch diameter, mild steel rods rigidly fixed on the trolley and two slotted plates mounted on ball bearings. The fixture for plate is screwed on to the model. The rods are quite free to move in the slot (*photo 96*). This gives following advantages over the previous system.

(i) Friction is practically eliminated
(ii) There is no rigid physical contact between the model and the trolley
(iii) Greater freedom exists for the model to move longitudinally, without retstraint.

It is decided to use rigid rod and slot system in all future experimental work.

3. Resistance dynamometer

For measuring towing resistance of a ship model, two arrangements, (1) Pendulum dynamometer and (2) spring dynamometer, were supplied. Both were thoroughly tested for their accuracy and suitable range. It was observed that pendulum dynamometer could never give steady readings especially when measuring small resistances. The pointer fluctuated in a wide range and it was impossible to take a mean value.

Several methods were employed to damp the oscillations (*photo 97*), but these could hardly improve the performance. This dynamometer was thus found unsuitable for accurate measurement of small resistances.

In the spring dynamometer, the resistance of a model is measured as the sum of added weight and spring tension. One small plate, carrying the spring, moves on ball bearings between supporting and guide rails. With best possible adjustment, the friction between the rails and the ball bearing could be reduced to 7-8 *gms* (originally it was 21 *gms*). This friction, adversly affects the experimental accuracy, especially on small models, in the low speed region.

The spring was, therefore, removed and replaced by a bar and a sliding weight arrangement. This system worked satisfactorily for low speeds upto .5 *m/sec* when testing Mariner Ship Model (*scale* 1/80) ; however, at high speeds, the large surging of the model made it impossible to get steady readings with the system.

Surging being the chief source of the above trouble, several damping devices were tried on the model (*photos 98* and *99*). The damping could slightly improve the stability of the model and readings upto .7 *m/sec* speed could be taken satisfactorily; but for higher speeds the same difficulty persisted.

Accepting that surging of a model is an evil that could not be satisfactorily remedied, it was thought that its effect of dynamometer could be minimised by changing the ratio of model and weight movement. A double pulley with 5 : 1 ratio was mounted at the lower end of the arm (*photo 98*). The model was connected to the larger pulley and the weights to the smaller one. Thereby, the effect of model surging on the dynamometer was reduced to 1/5.

Very satisfactory readings were obtained at low speeds but the full possibilities of the arrangements remain to be examined.

With the composite pulley, it is also possible to go back to the weight and spring arrangement as the effect of friction in the spring carriage on the actual resistance of the model is reduced by a ratio 5 to 1. In this case the resistance of model = 1/5 (weight + spring tension + frictional resistance)

The uncertain factor due to friction is thus reduced to ± 1.6 *gm* instead of ± 8 *gm*. This system would be adopted for routine testing in future.

4. Turbulence stimulation in ship models

Turbulence stimulation on ship models, especially small, is a subject still far from satisfactorily resolved. Trip wire which is put as a routine is not an entirely satisfactory stimulator. Several other types of stimulators were tested on Mariner Ship Model (*Scale* 1/80). Pertinent details of the model are :—

Length at load water line	=	1.98 *m*
Displacement	=	36.15 dm^3
Draught at even keel	=	.1028 *m*
Block coefficient	=	.6125

The various combinations of stimulators tried were :—

(i) Trip wire .5 *mm* dia fixed at 5 *percent* length from the bow

(ii) Triangular strips, 38 *mm* from front edge at *LWL of* model and trip wire as before—*fig 1* (*a*)

(iii) Triangles with gap of 2 *mm* in between at 38 *mm* from front edge and trip wire—*fig 1* (*b*)

(iv) Triangles with gap and small booster triangle 5 *mm* and a trip wire—*fig 1* (*c*).

(v) Two rotating rods each 3 *mm* diameter and 10 *mm* centre to centre. Rods were rougheved by 40 *mesh* coal powder. The rods were held vertical in front of model at 150 *mm* from bow and were driven by a variable speed motor (*photo 100*).

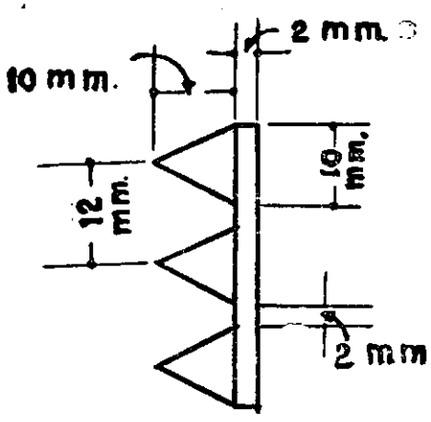

FIG - 1 (a)

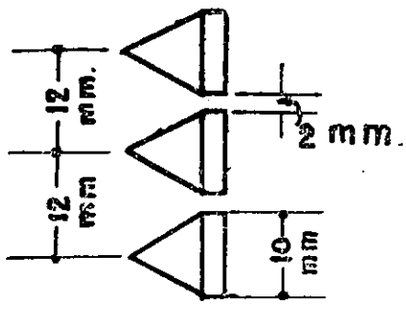

FIG - 1 (b)

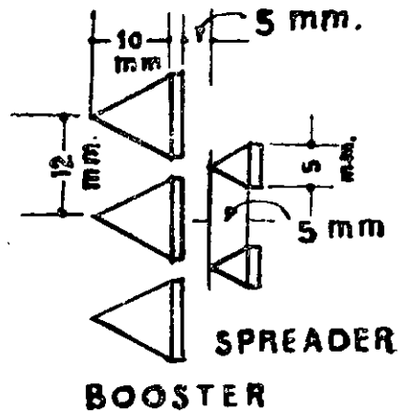

FIG - 1 (c)

TURBULENCE STIMULATOR

For the above experiments, the model was painted white. Hypodermic needles with .6 *mm* capillary tube were fixed at five locations. A strong solution of potassium permangnate in water was injected through the needles. The flow conditions could be vividly seen with the eye.

It was observed that with trip wire and triangular strip, the flow remained essentially laminar for speeds upto .35 *m/sec Photo* 101 shows the laminar flow lines on the model fitted with trip wire and traingular strips.

The results with the rotating rods were very encouraging. At .15 *m/sec* speed, when the rods were not rotating, clear laminar streaks formed behind all injection points. Immediately after the rods started rotating, the turbulence travelled aft dispersing each laminar tube. Stopping of rod rotation re-established the laminar flow.

The transition from laminar to turbulent flow by rotating rods has to be further established by observing increase in model frictional resistance with and without stimulation. These experiments are being planned.

5. Current meters

One hundred and twenty-five current meters were rated during the year 1960.

---

48. Bed Material for Hydraulic Models

I. Physical properties

IN CONTINUATION of last year's work, further work has been carried out to find out a suitable bed material for hydraulic models. Following types of material have been investigated.

(i) Lac and lac products
(ii) Wood products
(iii) Coal and lignite

2. Lac and lac products

The lac as obtained in nature is called *Stick Lac*. This lac is washed to remove dye, sugars, insect debries and other impurities. The washed product is called *Seed Lac*. This lac is further refined by heat treatment. The refined lac obtained by heat treatment is known as *Button Lac*. The *molamma* and *kiri* are varieties of lac which are obtained as by-products during preparation of *seed lac* and shellac. These two varieties contain in addition to lac, other impurities such as sand, insect debries and fibrous materials. The percentage of lac in *molamma* varies from 50 to 70. *Garnet Lac* is prepared from *molamma* and *kiri* lacs by treating them with alcohol. Lac is dissolved in alcohol and the impurities are filtered away. Lac obtained after distilling alcohol is called garnet lac. *molamma* and *kiri* are the cheapest varieties whereas button lac and shellac are the costliest varieties of lac. As reported last year, it was observed from preliminary studies that there were two drawbacks in using lac as bed material. The lac particles formed lumps when placed in the sun at a temperature of about 35°-38°*C* and some varieties showed swelling when placed in water. To improve the performance of lac, it was thought that partial polymerisation of lac would avoid softening and formation of lumps. The partial polymerisation is possible by mixing with 2 to 3 *percent* urea. The swelling can also be prevented by impregnation of calcium stearate. The cost of lac can also be reduced by mixing with barytes, saw dust, china clay and coal powder. The mixing of lac and other ingredients is done by placing the material in powder form between hot rollers of rubber mixing type. The material comes out in form of a sheet which is then powdered in crushing machine. Different varieties of lac with various treatments, obtained from Central Lac Research Institute were studied for their suitability as bed material. In addition to the determination of density and swelling, other observations such as behaviour under water and action of sun-rays were also taken and the results are presented in *table 1*.

The *molamma* and *kiri* varieties of lac did not give any encouraging results. The samples showed high swelling and in addition gave deep coloured solution and very bad smell in a few days when kept under water. Fungus growth was also noticed

Table 1

Sl. No	Materials	Density	Swelling approximately in *percent*	Action under water	Action under sun
1	*Molamma* ...	1.12	70	Deep coloured solution, bad smell, fungus growth and considerable swelling.	Formed lumps at 38°C
2	*Molamma* + Urea 3 percent	1.17	40	,,	No effect upto 38°C
3	*Molamma* + Urea + Calcium stearate.	1.15	45	,,	,,
4	*Kiri* ...	1.14	60	,,	,, 35°C
5	*Kiri* + 3 *percent* Calcium stearate	1.18	40	,,	,,
6	Shellac + Jute sticks ...	1.12	40	Coloured solution, considerable swelling and formed lumps.	Formed lumps at 36°C
7	*Garnet lac* ...	1.16	7.0	Colour of lac changed to brownish, slight swelling, no smell.	No effect upto 35°C
8	*Garnet* + Stearic acid 3 *percent*	1.15	3.7	,,	Formed lumps at 35°C
9	*Garnet* + Calcium Stearate 3 *percent* + Urea 2% + Baryte.	1.44	5.8	,,	No effect upto 35°C
10	Seedlac + Stearic acid 3 *percent*	1.13	1.3	Colour faded, reddish yellow to yellow, no smell.	Formed lumps at 35°C
11	Shellac + Baryte ...	1.47	...	No change in colour, no smell, no marked swelling.	No effect upto 35°C
12	Shellac + Calcium stearate 3 *percent* + Urea 2 *percent* + Baryte	1.43	2.8	,,	,,

in a few days time. Thus both *molamma* and *kiri* will not be a suitable bed material. Untreated garnet lac showed about 7 *percent* swelling. *Garnet lac* treated with stearate showed about 3 to 7 *percent* swelling. Shellac-baryte mixtures showed very little swelling from nil to 3 *percent*. Both *garnet lac* and *seed lac* with 3 *percent* strearic acid softened and formed lumps even at a temperature of 35°C under the sun. Urea treated samples however did not form lumps even at 38°C under the sun.

Test to find out the uniformity of particles with regard to density was carried out with potassium iodide solution of different densities. (It was found difficult to get the correct results without adding wetting agent to remove air from the particle.) The results are given in *table 2*. It will be seen that the particles lie between two density ranges. This shows that lac and other impregnated materials have been well distributed.

From the results of experiments so far carried out it seems that shellac or *garnet lac* with urea and baryte will be a suitable bed material. Further experiments are necessary to determine whether baryte can be replaced by coal powder or lignite powder. The cost of production can be reduced considerably, since proportion of coal can be increased to a greater extent than baryte without increasing density.

3. Wood products

In the previous study with sawdust it was found that lime-coppersulphate treatment improved the performance of saw dust with regard to flock formation for considerable length of time. Another defect of sawdust was that once it dried up in the model, it floated when coming in contact with water. The present study was taken up to find

Table 2

Material	Average density	Percentage of lac having density					
		< 1.1	1.1–1.2	1.2–1.3	1.3–1.4	1.4–1.5	> 1.5
Garnet lac ...	1.16	4.0	96.0	...	...	...	...
Garnet lac + Stearic acid 3 *percent* ...	1.15	6.0	94.0	...	...	...	...
Garnet lac + calcium stearate 3 *per cent* + urea 2 *percent* + Barytes.	1.44	...	...	...	5.8	93.5	...
Seedlac + Sreatic acid 3 *per cent* ...	1.13	9.2	90.8	...	...	...	...
Shellac + calcium stearate 3 *percent* + Urea 2 *percent* + Barytes.	1.43	...	...	...	3.2	96.3	...
Shellac + Barytes ...	1.47	...	...	...	1.7	93.9	4.0

out the behaviour of some heavy wood products. The following materials have been tried:

(i) Kindle wood sawdust
(ii) Jamba wood sawdust
(iii) Walnut Shell
(iv) Almond shell

Wood products are porous materials and the pores get filled up when placed in water. The movement of wood particles in models will, therefore, depend on the density of saturated material. It is, however, difficult to determine the saturated density of sawdust since intersticial water between particles cannot be removed without removing at least partially the pore-water. To find out the bulk density, density of solid matter and saturated density blocks of respective wood were taken. Dry bulk density and saturated density were found out before and after complete saturation respectively. Solid density was determined by deducting the amount of water adsorbed on saturation. As the particles of almond shell and walnut are fairly big and rounded in shape, it was found possible to remove intersticial water without removing pore water. It was possible to estimate saturated density and solid density in the ordinary way. However, in these cases, the bulk density of the particles could not be determined. The bulk density was calculated by assuming that there was no swelling of particles on saturation. The bulk density thus obtained would be slightly less than the actual value depending upon the amount of swelling. The results are presented in *table 3*.

Table 3

	Kindle wood sawdust	Jamba wood sawdust	Walnut shell	Almond shell
Dry Bulk density ...	0.95	0.75	1.00	1.03
Saturated density ...	1.28	1.21	1.31	1.34
Solid density ...	1.47	1.43	1.46	1.50
Volume expansion on saturation (swelling).	8.8%	7.6%	...	...

It will be seen that dry bulk density of kindle wood sawdust is .95 and of Jamba wood sawdust .75. The sawdust of both the varieties being elongated in shape does not sink immediately and floats when in contact with water. The dry bulk density of walnut and almond shell particles is just above one and the particles being cubical in shape sink and do not float even in dry state when in cotact with water. The saturated density lies between 1.3 to 1.4. Walnut shells are not easily attacked by fungus. A field trial with walnut shell as bed material will be made shortly.

4. Coal and lignite

In continuation of last year's work, the ash content of different density fractions of coal have been estimated for a few coal samples. The results are given in *table 4*. It will be observed that percentage of ash increases with increase in the density of the fractions for all the samples. Thus mean ash content is 2.5 *percent* for 1.3 density fraction and 62 *percent* for 1.93-2.33 fraction.

Table 4 : Analysis of coal samples collected from different collieries

Lab No	Description	Moisture content	Ash content	Average density	Density						
					<1·3	1·3-1·4	1·4-1·5	1·5-1·6	1·6-1·7	1·7-1·93	1·93-2·33
10128	Slack Coal (below 1") from Basta-colla Colliery	·67	18·7	1·19	3·95	48·0	28·3	5·9	1·63	1·15	11·0*
					1·60	9·9	18·4	28·5	33·3	50·0	62·4†
10129	Slack Coal (below 1") from Pera Colliery.	·87	14·7	1·45	4·45	39·1	34·3	10·1	2·58	1·18	8·17*
					1·80	9·9	18·2	28·1	35·1	51·2	72·5†
10130	Slack Coal (below 1") from E. Basuria	·74	25·2	1·51	8·10	27·2	22·8	13·8	7·3	9·65	11·10*
					1·40	9·4	18·7	28·5	58 6	47·6	56·3†
10131	Middlings (below 1/2") from Lodna Washery	1·00	38·0	1·65	3·90	10·1	15·3	14·5	12·8	25·4	17·4*
					4·3	13·0	21·4	30·0	35·8	52·2	64·4†
10132	Washed slacks (below 1/2") from Lodna Washery.	1·41	21·0	1·46	13·8	30·4	26·2	14·7	2·95	4·95	4·3*
					3·6	12·4	20·4	29·8	40·0	49·7	53·0†

*Percentage fraction. †Ash percentage of the fraction.

The ash content of same density fractions of coal from different sources are of the same order. From the above results, it can be inferred that the density of organic constituents of coal is of the same order but due to the presence of inorganic matter to varying extent, the density of coal particles differs widely. The chemical composition of ash from different density fractions of coal from Basta-Colla has been found out and the results are presented in *table 5*.

Table 5

Density fraction	Silica *percent*	Fe_2O_3 *percent*	Al_2O_3 *percent*	*CaO percent*	*MgO percent*
< 1·3	56·9	11·0	27·5	·66	2·4
1·3-1·4	57·3	8·2	31·6	·66	·94
1·4-1·5	71·5	6·0	20·3	·54	·99
1·5-1·6	68·9	6·0	22·3	·60	1·07
1·6-1·7	60·4	4·5	33·0	·66	1·07
1·7-1·8	64·2	4·0	30·5	·42	1·03
1·8-1·93	73·8	3·0	21·8	·42	·64
> 1·93	72·9	6·0	16·3	1·85	2·36

It will be seen from the results that though silica is the main constituent of the ash, alumina, iron oxide, calcium and magnesium oxide are also present in appreciable amount. The composition of ash indicates that the ash is mainly an integral part of the plant material deposited during its growth and later mineralisation and it will be difficult to remove the ash from coal particles. It may not be ruled out that some portion of ash especially in higher density-fractions may also be derived from the mechanical adherence of clay particles to the coal.

5. Lignite

Raw lignite and carbonised lignite briquettes obtained from Neyvali Lignite Corporation were tested for their suitability as bed material. The samples were powdered to different size fractions and separated for different density fractions. Average density and ash content were also estimated. The lignite particles are water repellent and do not sink in water or in potassium iodide solution used for separation. Wetting agent was used to remove this repellency. The results are presented in *table 6*.

It is seen from the table that raw lignite gives an average density of 1.43 whereas carbonised lignite gives a density of 1.55. The raw lignite particles are more of uniform density than carbonised lignite. In raw lignite 90 *percent* of the particles have density between 1.3-1.4. About 6 *percent* particles are below 1.4 and 3 *percent* between 1.5-1.6. Raw lignite thus seems a suitable bed material as regards density. One defect as already pointed out has, however, to be overcome

Table 6 : Density and Ash Content of Lignite

Dia. range in *mm*	Raw Lignite					Carbonised Lignite						
	Densities			Average density	Ash content percent	Density					Average density	Ash content percent
	<1·4	1·4–1·5	1·5–1·6			<1·4	1·4–1·5	1·5–1·6	1·6–1·7	>1·7		
·1—0·6 ...	6·7	89·3	3·3	1·44	12·0	·5	20·7	45·8	26·2	4·8	1·56	16·5
·6—1·0 ..	3·4	95·0	1·3	1·43	10·3	·3	23·6	48·2	21·7	6·2	1·54	15·5
1·0—2·0 ...	5·0	92·0	2·3	1·43	9·8	·2	5·8	60·8	29·1	4·0	1·53	15·5

before it can be used as a bed material in models. The lignite particles being water repellent do not sink easily and also float when they come in contact with water in dry state. The particles sink easily when a wetting agent is added to water. They can also be prevented from floating if wetting agent is sprayed over them before water is allowed to come in contact with the particles. In big models this process may not be very successful and some treatment which will permanently remove the water repellency of lignite particles appears necessary. The experiments in this connection have been taken up in co-operation with National Chemical Laboratory.

II. Biological studies

EXPERIENCE has shown that bed materials otherwise quite suitable, cease to behave satisfactorily due to biological growth like fungus, algae *etc.* Laboratory studies have been carried out on different varieties of lac, bakelite and other materials to see whether these are likely to grow fungus and algae and if so to what extent and whether this growth could be controlled by the lime-copper treatment developed in the *CWPRS* for treating sawdust. Results of observations are shown in *Statement I.*

(*i*) *Button Lac.*—Button lac showed the growth of flocks in traces only in four months and this growth could be prevented by the L-C treatment.

(*ii*) *Shellac.*—Shellac Barytes 3 : 1 and 2 : 1 were free from flocks for two months and produced only traces of flocks in four months but 3 : 2 and 1 : 1 mixtures though free from flocks for 2 months, produced good amount of flocks by six months. Shellac-calcium stearate was free from flocks for a month but produced only traces of flocks by six months. In all these cases flock formation was completely prevented for six months by L-C treatment. Shellac impregnated in jute stick dust was also free from flocks for a month, but produced good flocks in six months and it produced fair amount of flocks in six months even after L-C treatment.

(*iii*) *Molamma Lac.*—Molamma and molamma treated with urea was free from flocks for a month but produced only fair amount of flocks by six months; but molamma treated with 3 *percent* calcium stearate and 3 *percent* urea produced traces of flocks in one month and produced excellent flocks in two months. L-C treatment improved the first two but could not improve the 3rd. Another undesirable characteristic of the molamma was that it gave out a lot of orgnanic substances into solution which later on produced foul smell and also a lot of fungus on the surface of water.

(*iv*) *Kiri Lac.*—Kiri and Kiri treated with calcium stearate produced traces of flock in the first month and excellent flocks by two months. Kiri seemed to be much improved by the L-C treatment. L-C treated Kiri produced only traces of flocks by two months and the L-C treated Kiri-calcium stearate showed traces of flock by four months.

Garnet Lac.—Garnet lac produced good amount of flocks even in a month and it could not be much improved by the L-C treatment, as it produced fair amount of flocks in the first month after L-C treatment.

(*vi*) *Saw-dusts.*—Country teak wood sawdust (untreated) produced plenty of flocks but it was much benefited by the L-C treatment. This confirmed the previous findings. It produced good

Statement I

Bed material	Treatment	Intensity of the growth of flocks after				Remarks
		1 month	2 months	4 months	6 months	
Button Lac ...	B*	*n*	*n*	*t*	*t*	Water clear and colourless.
	LC†	*n*	*n*	*n*	*n*	,,
Shellac barytes 3 : 1 ...	*B*	*n*	*n*	*t*	*t*	,,
	LC	*n*	*n*	*n*	*n*	,,
Shellac barytes 2 : 1 ...	*B*	*n*	*n*	*t*	*t*	,,
	LC	*n*	*n*	*n*	*n*	,,
Shellac barytes 3 : 2 ...	*B*	*n*	*n*	*f*	*g*	,,
	LC	*n*	*n*	*n*	*n*	,,
Shellac barytes 1 : 1 ...	*B*	*n*	*n*	*t*	*g*	,,
	LC	*n*	*n*	*n*	*n*	,,
Shellac + calcium stearate	*B*	*n*	*t*	*t*	*t*	,,
	LC	*n*	*n*	*n*	*n*	,,
Shellac 2.5 parts + jute stick dust.	*B*	*n*	*t*	*f*	*g*	,,
	LC	*t*	*f*	*f*	*f*	,,
Molamma ...	*B*	*n*	*t*	*f*	*f*	Layer of scum on the surface of water. Colour of water red.
	LC	*n*	*n*	*t*	*t*	Fine reddish deposition on the surface of bed, water turbid. White membrane on the surface of water.
Molamma + Urea ...	*B*	*n*	*f*	*f*	*f*	Layer of scum on the surface of water and colour of water red.
	LC	*n*	*n*	*t*	*t*	Water slightly turbid and reddish. White membrane on the surface of water.
Molamma treated with calcium stearate 3 *per-cent* and urea 3 *per-cent.*	*B*	*t*	*e*	*e*	...	Thick membrane on the water and water pinkish.
	LC	*n*	*t*	*g*	...	Water milky. Sediment on bed and membrane on water.
Kiri ...	*B*	*t*	*e*	*e*	...	Sediment on bed and membrane on water.
	LC	*n*	*t*	*g*	...	Water milky. Colour of bed material turned blackish from brownish.
Kiri treated with calcium stearate	*B*	*t*	*e*	*e*	...	Sediment on bed and membrane on water.
	LC	*n*	*n*	*t*	...	Water less milky than the untreated. Bed material turned blackish from brownish.
Garnet lac ...	*B*	*g*	*g*	*g*	...	Sediment on bed.
	LC	*f*	*g*	*g*	...	Top part of the bed attacked. Colour of bed turned brownish from greyish.
C. T. W ...	*B*	*g*	*g*	*e*	*e*	Water pinkish.
	LC	*t*	*t*	*t*	*t*	Water clear.
S. D. 1 ...	*B*	...	*g*	*e*	*e*	Colour of the sawdust brownish grey.
	LC	*n*	*n*	*n*	*n*	Colour of sawdust is black.
S. D. 3 ...	*B*	...	*f*	*g*	*g*	Water pinkish, colour of the sawdust brown.
	LC	*t*	*t*	*f*	*f*	Water colourless and colour of sawdust blackish brown.
S. D. 4 ...	*B*	*e*	*e*	*e*	*e*	Colour of water yellowish brown. Colour of sawdust yellowish brown.
	LC	*f*	*f*	*g*	*g*	Water clear and colour of sawdust blackish brown.
Kindal wood ...	*B*	*t*	*g*	*g*	*e*	Water dark pink, upper layer blackish, lower layer greyish.
	LC	*t*	*g*	*f*	*f*	Water clear and colourless.
Jamba wood ...	*B*	*t*	*f*	*f*	*f*	Water deep pink.

Statement I : contd.

Bed material	Treatment	Intensity of the growth of flocks after				Remarks
		1 month	2 months	4 months	6 months	
Jamba wood ...	*LC*	*t*	*t*	*t*	*t*	Water pinkish
Bakelite ...	*B*	*n*	*t*	*t*	...	Water clear
	LC	*n*	*n*	*n*	...	Water more clear than that on the untreated.
Raw lignite ...	*B*	*n*	*n*	...	...	Water clear and transparent
	LC	*n*	*n*	...	...	,,
Corbonised lignite ...	*B*	*n*	*n*	...	...	,,
	LC	*n*	*n*	...	...	,,
Walnut shell ...	*B*	*t*	*t*	*t*	...	Water clear but coloured faint yellow
	LC	*n*	*t*	*t*	—	Water clear and colourless; bed material turned blackish brown from brown.
Almond shell ...	*B*	*f*	*g*	...	...	Water clear but coloured faint yellow.
	LC	*n*	*n*	...	...	Water clear and colourless; bed material turned blackish brown from brownish.

* Blank i. e. without lime water and copper treatment.
† L-C i. e. Lime Water and copper treated.

Note.—*n* = nil *f* = fair
t = trace *e* = excellent
g = good

amount of flocks in even a month but only traces of it in six months after L-C treatment. Sawdust *No* 1 received from the Forest Research Institute produced good amount of flocks in 2 months and excellent flocks in four months, but if L-C treated, it did not produce any flocks even in six months. Sawdust *No* 3 produced good amount of flocks by four months and was not much improved by the L-C treatment. Sawdust *No* 4 produced excellent flocks in one month but produced good flocks only in four months after L-C treatment. Kindal wood sawdust produced good amount of flocks in two months and it seemed, it was not much improved by the L-C treatment. Jamba wood sawdust produced fair amount of flocks in two months and this flock did not increase noticeably in six months. L-C treatment improved it but could not keep it free from flocks as traces of flocks were found in the L-C treated Jamba wood sawdust.

(*vii*) *Other Materials.*—Bakelite did not favour the growth of flocks. It produced only traces of flocks in two months and these traces of flocks did not increase with time. But it was perfectly clean of flocks even for the experimental period of four months after L-C treatment. Raw lignite as well as carbonised lignite did not produce any flocks for the experimental period of two months. Walnut shell seemed to be quite resistant to fungus attack. It produced only traces of flocks by four months and was not found to be further improved by the L-C treatment. Almond shell was quite susceptible to the growth of fungus, but was much improved by the L-C treatment. It produced fair and good amounts of flocks by one and two months respectively but was compltely free from flocks for the experimental period of two months by the lime-coppersulphate treatment.

(*viii*) *Observations on algae.*—Observations showed that the growth of algae was not a big problem with the bed materials studied here. Traces of algae were observed in the untreated shellac barytes 3 : 2 in six months. In the untreated shellac barytes 1 : 1, algae was observed in traces in four months and good amount of algae was observed in six months. Other samples of bed materials did not show conspicuously the growth of algae under experimental conditions.

5. Conclusion

These studies showed that most of the bed materials studied developed flocks to more or less extent with time and flock formation in most of the bed materials studied was controlled to some extent by the lime-coppersulhphate treatment developed at the Research Station.

49. Fluorescent material as sediment transport tracer

THE PROBLEM of study of sediment movement on sea bed, in rivers and harbours has been engaging the attention of engineers and research workers for a long time. During the last few years various methods, such as coloured tracers, radio-isotopes, fluorescent materials, *etc*, have been used to study sediment transport.

The technique of using radio-isotopes was applied in India by the *CWPRS* while studying the suitability of dumping grounds off Bombay harbour. The use of radio-isotopes sometimes poses problems of health hazards. In some cases, therefore, it is advantageous to use fluorescent materials for the laboratory and field experiments. Inquiries showed that fluorescent material was not available in this country and could only be obtained from abroad at a probable cost of *Rs.* 6000 per ton. It was, therefore, decided to investigate the possibility of developing fluorescent material indigenously. The Project was referred to the National Chemical Laboratory and the studies carried out in collaboration with the *CWPRS*. Results of preliminary studies carried out, the technique of using fluorescent materials, merits and demerits of radio-isotopes and fluorescent materials are discussed below.

2. The technique and specific requirements

The technique consists of coating dry sand from the area under study with a fluorescent dye. The coated sand is then dried and deposited on the sea or river bed at selected places. The sand samples are collected at frequent intervals ranging from few hours to few days at various distances from the place of deposition and are examined under a spectrum of ultra-violet rays with the aid of a luminoscope. The property of fluorescent material glowing under a beam of ultra-violet rays is being made use of in this technique of detection of sediment transport. The fluorescent grains are clearly distinguishable from the ordinary ones and even a single marked grain can be readily detected among 10 million untreated grains. Before dumping fluorescent material, however, it is necessary to ascertain that the original river or sea bed does not consist of any fluorescent material. If it does, it is necessary to select a particular dye which is different from the one existing on the river or sea bed. This technique provides a convenient means of ascertaining how far sand has been transported. In order that the selected fluorescent compound effectively succeeds as a tracter it should

(i) not get dissolved under water and the dye should not get decomposed under the action of weathering, sunlight and bacterial attack

(ii) be harmless to human beings

(iii) resist abrasion,

(vi) be cheap in cost and be readily available in large quantities

3. Methods of preparation and experiments

There are three methods of preparation of fluorescent sand

(i) to coat the grains with a layer of fluorescent dye carried in a hydrophilic colloid

(ii) to coat the grains with a solution of suspension of dye in a resin

(iii) to incorporate the dye in the mass of artificial particles

of which any one can be used depending upon the availability of materials and prevailing conditions.

Agar, bone glue, gum, starch, polystyrene, methyl-methacrylate and cellulose-acetate are used as binding media. According to the experiments carried out in Russia the mixture of agar and bone glue retains the dye under water for a period of 3 months and upwards. If a mixture of gum and starch is used the dye disappears in about 2 weeks and this period further reduces if sugar is added.

Experiments were first carried out by the National Chemical Laboratory, Poona, at the request of the *CWPRS* with anthracene, which is readily available in the country. Experiments showed that with agar as binding material there was a possibility of its decomposition by weathering, sunlight and bacterial attacks. Preliminary trials with plastic material like cellulose, acetate, poly-styrene, *etc*, in suitable solvents like benzene, acetone, were therefore, carried out by the National Chemical Laboratory to obtain a stable film. Satisfactory results have been obtained with these media on sand, on a small scale. Sand coated by anthracene, with polystyrene and with methyl-methacrylate as binding media showed blue fluorescence, whereas sand coated with anthracene, with cellulose-acetate as binding media showed green fluorescence under ultra-violet rays. It is also

found that it is possible to prepare fluorescent sand in this country at a comparatively low cost.

For treating one ton of sand about 2 *lbs* of anthracene, 7 *lbs* of cellulose-acetate and 330 *litres* of acetone would be required. It may not be possible to take out samples of material from the sea bed due to long spell of rough weather. In such cases, even if this spell is interposed by calm periods, the latter may not be long enough to allow collection of samples all over the area, where the material is dispersed. The main question which arises, in such a case, is the life of fluorescent material. It is, therefore, proposed to carry out further tests to study this aspect in particular.

In some of the hydraulic models at the *CWPRS* coal is being used as a bed material. It is proposed to carry out some tests to see whether it would be possible to coat bituminous coal with fluorescent material for use as a tracer in the model.

4. Merits and demerits of fluorescent materials and radioactive-isotopes

(*a*) With the use of radio-isotopes it is possible to select the material having a half-life varying from few hours to many years. This is not possible in case of fluorescent material.

(*b*) With fluorescent materials it is necessary to take samples from many places and subject them to microscopic examination. It is likely that sometimes one may miss the place where the fluorescent material has actually travelled.

Thus the procedure involved is laborious, and sometimes interpretation of results is difficult. With radio-isotopes large areas can be covered within a short time.

(*c*) Health hazard aspects have to be carefully considered while using radio-isotopes. It may not be possible to carry out such studies in rivers where people bathe all along the banks, where water is pumped from rivers for industrial and domestic use and where fishing on large scale exists.

(*d*) Generally tracer study is required to determine the effect of tidal currents, storms and waves on littoral transport. If the sea remains rough for a long time and is interposed by short periods of calm spells, the period available for observation may not be sufficient to ensure a complete exploration of the region under study. This is possible with radio-isotopes as large areas can be scanned within a short period. This may not be possible with a fluorescent tracer.

(*e*) Fl[illegible]t technique requires large quantities of sand to be dumped, and a considerable sampling which may be difficult in a wide estuary.

(*f*) The radio-isotope study requires skilled personnel, intricate equipment and facilities for activating the material, whereas adoption of fluorescent tracer, requires hardly any special equipment and skilled establishment.

---

50. Studies on aquatic weed Ceratophyllum Demersum

EXPERIMENTS carried out to study the effect of various weedicides on different aquatic weeds have shown that the aquatic plant, ceratophyllum demersum is very sensitive to traces of ionic copper. Copper at a concentration as low as .005 *ppm* damaged the weed and the disintegration of the weed was quicker as the concentration increased from .005 *ppm* to .25 *ppm*. It disintegrated completely in about 25 *hours* in .05 *ppm* solution, in about 10 to 14 hours in .1 *ppm* solution and in about 6 to 8 hours in concentration ranging from .25 to 5 *ppm*. This suggested the possibility that traces of ionic copper acted through some enzyme system. If so, the disintegration of the weed in presence of traces of ionic copper was likely to be dependent on the *pH* and temperature of water or the solution in which the weed was submerged. It also indicated the possibility of an optimum *pH* and temperature at which the weed was likely to disintegrate in the shortest period of time, other conditions remaining the same.

2. Experimental set-up

(*i*) *Sources of the weed studied.*—The aquatic weed ceratophyllum demersum grows in plenty

in ponds and canals of India, specially in the Deccan Irrigation Canals. The weeds used in experiments were collected from the Mula river near the Poona Engineering College and from a nearby well.

(*ii*) *Chemicals used.*—As the present study describes the effect of traces of copper on the aquatic weed, chemicals of very high grade were used in these studies. Pyrexglass distilled water was used instead of ordinary distilled water which disintegrates the weed.

(*iii*) *Apparatus.*—The disintegration of the weed at different constant temperatures was studied in the constant temperature bath of the newly received Warburg Apparatus.

3. Experiments

About 3 *cm* long twigs of the aquatic weed ceratophyllum demersum were treated in copper-sulphate solution containing 2.5 *ppm* of copper, for one hour, after which they were washed three times very carefully in tap water and then were taken, one in each of 100 *cc* glass beakers containing 50 *cc* of .001 *M* buffers of different *pH* ranging from 5.2 to 10.0. They were kept in the bath of Warburg apparatus at desired constant temperatures ranging from 15°*C* to 40°*C* and the disintegration of the weed was observed every hour as usual.

4. Observations

Observations showed that the disintegration of the aquatic weed ceratophyllum demersum

Table 1 : Effect of *pH* and temperature on the disintegration of the weed collected from the Mula River

Temp.	Period in *Hours*	Tris Malaic acid *NaOH* Buffer ·001 *M*					Boric acid Borax Buffer .001 *M*	Carbonate bi-carbonate buffer .001 *M*
		pH value						
		5·2	6·0	7·0	8·0	8·6	9·2	10·0
23°.4 *C*	5	0	0	0	0	0	0	0
	6	0	5	2	40	5	20	0
	7	0	50	50	97	98	90	30
	8	10	95	90	99	99	100	70
	9	30	97	95	99	100	100	97
	10	50	99	96	99	100	100	93
	27	97	99	99	100	100	100	100
31°.9 *C*	3	0	0	0	0	0	0	0
	4	0	0	0	30	30	30	2
	5	10	30	50	90	90	70	30
	6	20	80	90	97	95	95	95
	7	30	90	95	97	98	98	97
	8	30	99	97	98	99	98	98
	9	30	99	97	98	99	99	93
	26	97	99	97	99	100	99	99
35°.0 *C*	2	0	0	0	0	0	0	0
	3	0	30	70	60	80	70	20
	4	95	95	97	100	98	99	95
	5	99	98	93	100	98	99	99
	6	99	98	98	100	98	99	99
	7	99	98	98	100	98	99	99
	24	100	99	99	100	98	99	99
38°.0 *C*	6	0	0	0	0	0	0*	0
	7	0	10	0	10	0	10	0
	8	5	20	5	20	10	10	0
	9	5	30	20	25	20	10	0
	10	20	30	30	30	30	10	2
	27	40†	99	99	97	40†	99	99
	28	40	99	99	97	50	99	99

* Carbonate bi-carbonate buffer of ·001 *M* was used at this temperature and *pH*.

† Weed lost fresh appearance.

by traces of ionic copper was sensitive to both *pH* and temperature of the water or solution in which it was submerged. The optimum temperature for its disintegration seemed to lie between 31°C and 35°C. Other conditions remaining same, the period for disintegration to start decreased as the temperature increased upto about 31°C; it remained approximately constant upto a temperature of about 35°C and then increased as the temperature went up. The disintegration was prevented at a temperature of 39°C and above. *Table 1* shows that weeds collected from the Mula river started disintegrating in 6, 4, 3 and 7 hours at temperatures of 23°.4C, 31°.9C, 35°.0C and 38°.0C respectivelv. The experiments were repeated with weeds collected from a different source *viz* a nearby well. Observations showed a similar trend, though not exactly the same results. This may be due to the fact that weeds from the two different sources were not identical physiologically. Disintegration of the weeds collected from the well by traces of ionic copper was completely prevented for the experimental period of thirteen hours at 20°C and less. *Fig 1* shows that its disintegration started in 7 *hours* at 29°.0C, in 6 *hours* at 30°C, in 5 *hours* at 31°C, in 4 *hours* at 32°C, 33°C, 34°C and 35°C in 5 *hours* at 36°C and 37°C and in 7 *hours* at 38°C. There was no disintegration at 39°C and 40°C and the weeds lost the fresh appearance at these temperatures.

Observations also showed that the disintegration of the weed by traces of ionic copper was also sensitive to *pH* of the aqueous medium in which it was submerged. Though it is difficult at this stage to pin point the optimum *pH* of disintegration, it has been observed that other conditions remaining same, the disintegration took place first at *pH* ranging approximately from 6 to 9.2. It seemed to be delayed at *pH* lower than 6 and higher than 9.2 as shown in *table 1.*

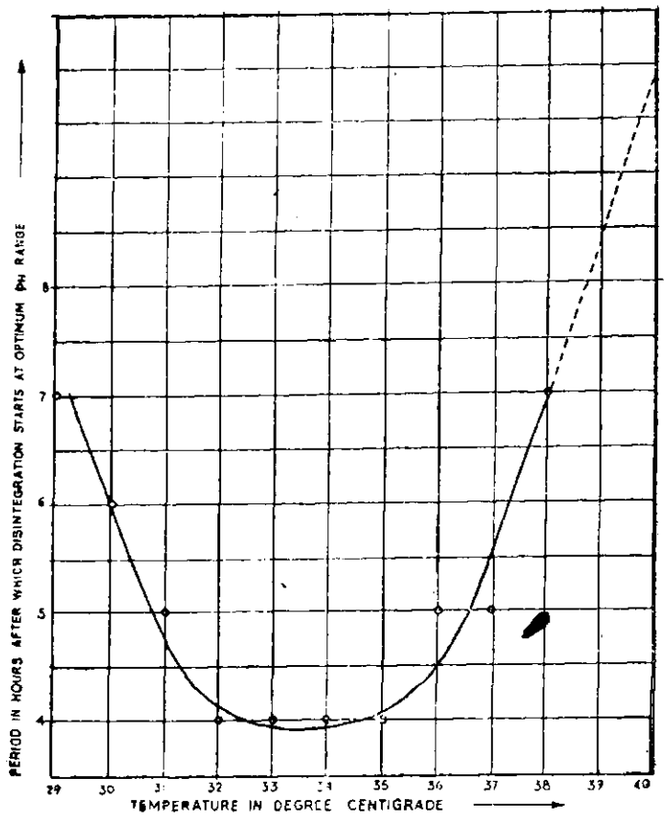

Fig 1: Effect of temperature on the disintegration of the weed.

5. Conclusion

That the disintegration of the aquatic weed ceratophyllum demersum by traces of ionic copper was sensitive to temperature and *pH* suggests the possibility that it was brought about through some enzyme system. This may help in planning its control. It has been found that the weed disintegrated early at *pH* between 6 and 9.2 and at temperatures between 31°C and 35°C. As the *pH* of water of irrigation canals *etc*, is within that range, *pH* requires no consideration in controlling this weed by copper treatment. To have the maximum effect of the copper treatment, it should be done when the temperature of the irrigation waters is in the range of 31°C to 35°C.

---

51. Khadakwasla Weather Summary : 1960

A DAILYWISE summary extracted from the continuous autorecords of weather data observed at Khadakwasla (latitude 18° 25′ 30″ *N*, longitude 73° 15′*E*, and elevation above mean sea level 574.548 *m* or 1885 *ft*) during 1960 is presented in *fig 1.* It presents a complete record of the daily

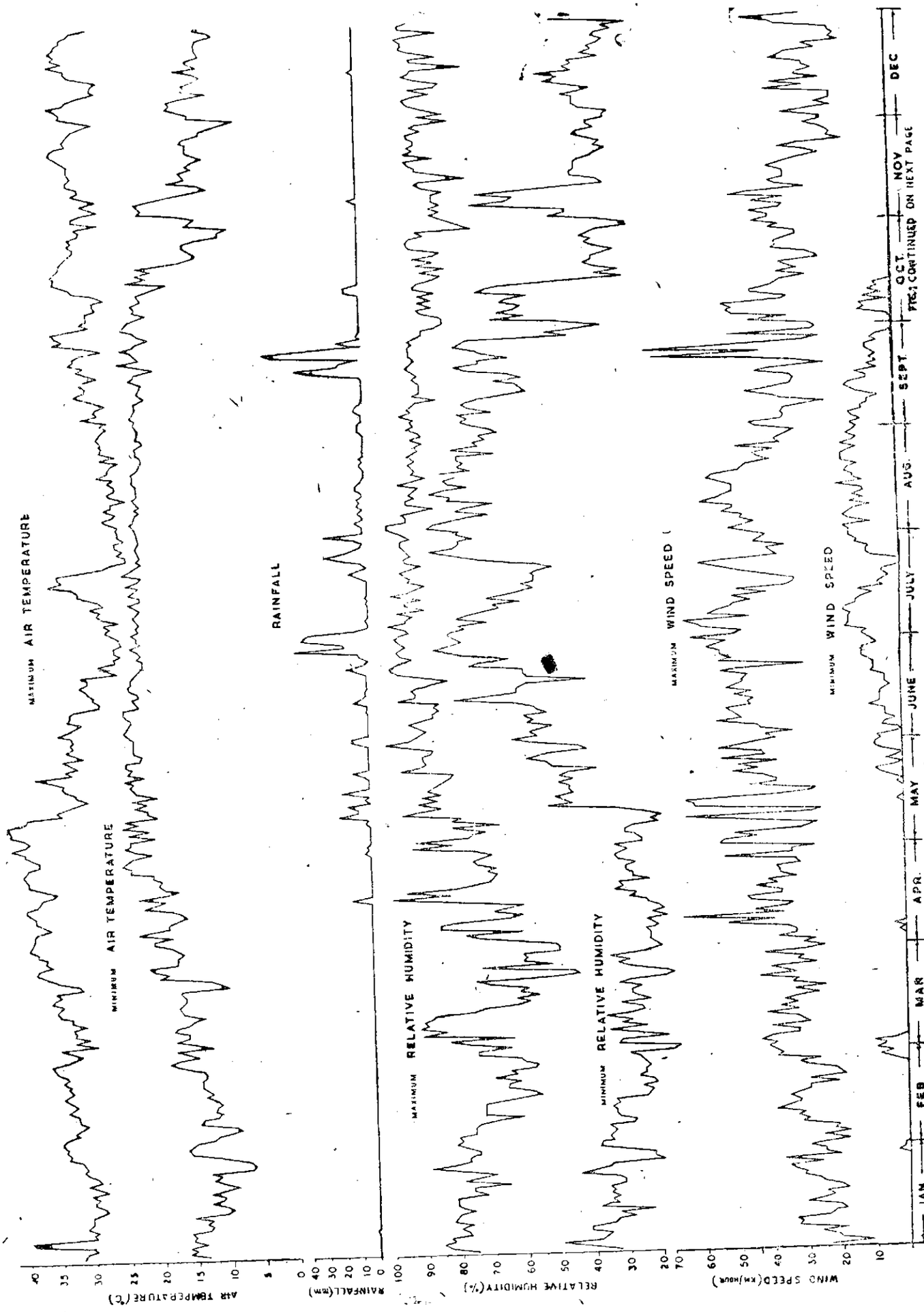
MAXIMUM AIR TEMPERATURE
MINIMUM AIR TEMPERATURE
AIR TEMPERATURE (°C)
RAINFALL
RAINFALL (mm)
MAXIMUM RELATIVE HUMIDITY
MINIMUM RELATIVE HUMIDITY
RELATIVE HUMIDITY (%)
MAXIMUM WIND SPEED
MINIMUM WIND SPEED
WIND SPEED (km/hour)
JAN
FEB
MAR
APR.
MAY
JUNE
JULY
AUG.
SEPT
OCT.
NOV
DEC
PTO; CONTINUED ON NEXT PAGE

Fig 1

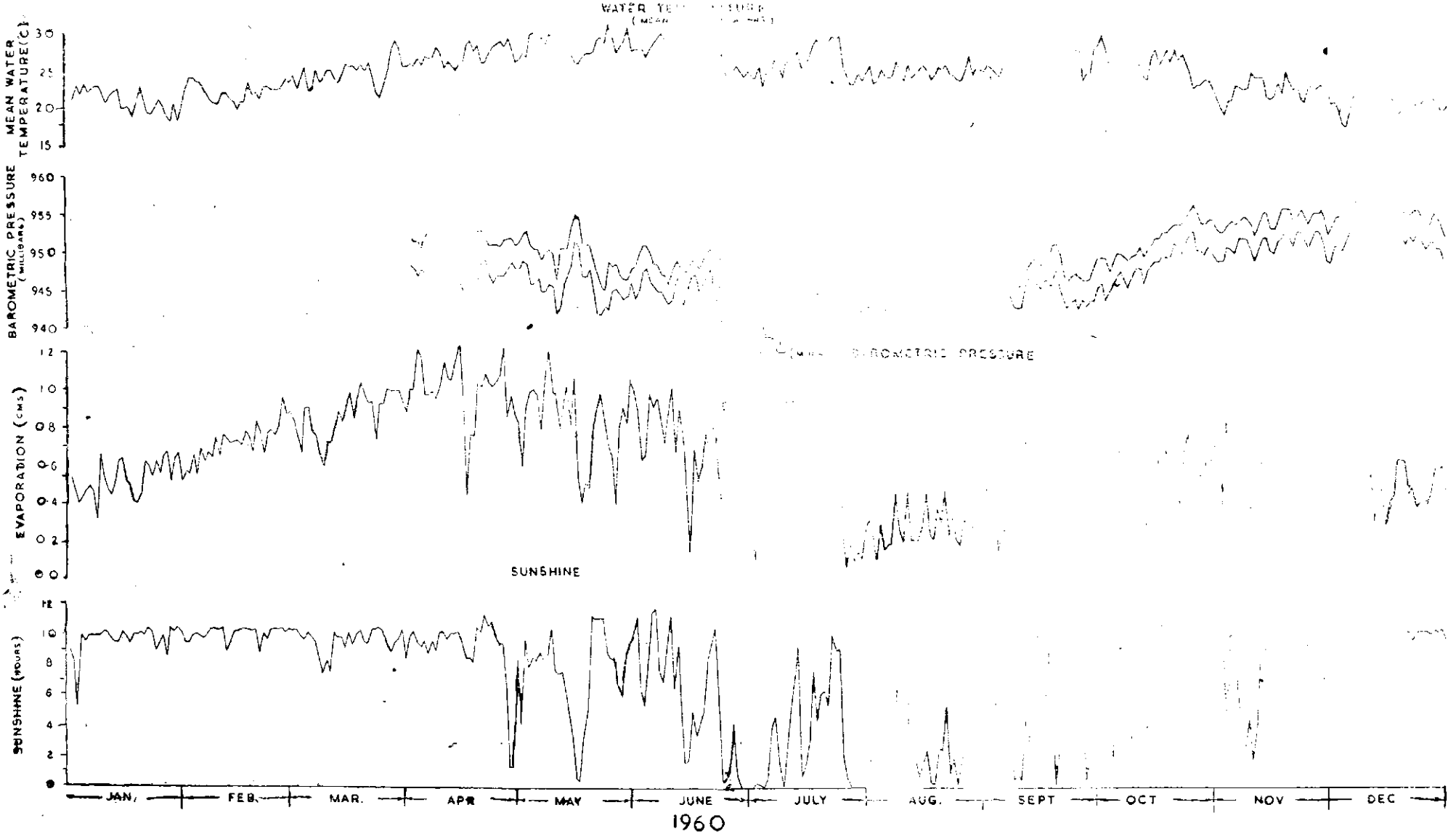

Fig 1: Khadakwasla Weather Summary for 1960. Lat. 18° 25 30″ N, Long. 73° 15′ 0″ E. Elevation above *MSL*-574.548 *m* (1885 *ft*).

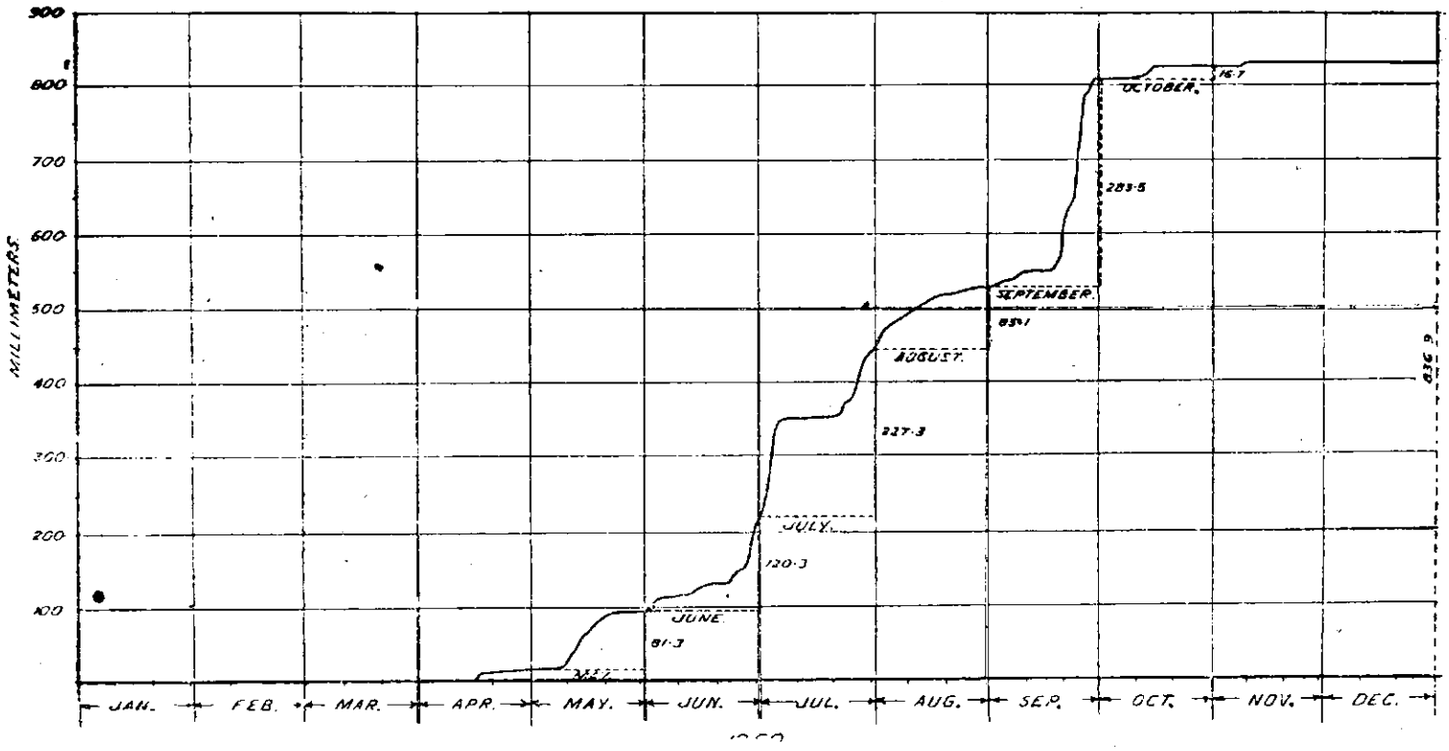

Fig 2: Cumulated precipitation depth, Khadakwasla, 1960.

Table 1

Character		Year's Lowest		Year's Highest		
Minimum air temperature	...	Dec 3	5.8	Apr 28	25.0	°c
Maximum air temperature	...	Aug 14	23.1	May 9, 10	41.7	°c
Mean water temperature	...	Dec 4, 13	17.9	May 24	31.1	°c
Minimum humidity	...	Mar 2	14.0	Jul 28; Aug 4	86.0	percent
Maximum humidity	...	Mar 24	43.0	Jun 1	99.0	percent
Minimum wind speed	...		0	Aug 14	17.7	*km/hr*
Maximum wind speed	...	Jan 2	11.0	Sep 24	72.4	*km/hr*
Minimum barometric pressure	...	Jul 3	937.0	Dec 9	955.5	*mb*
Maximum barometric pressure	...	Jul 3	939.5	Dec 10	959.2	*mb*
Evaporation in 24 hours	...	Sep 24	.07	Apr 14	1.24	*cm*
Rainfall in 24 hours	...		0	Sep 25	57.4	*mm*
Sunshine	...		0	Jun 6	11.85	*hrs*

exact values of the 12 principal weather characters. Their highest and lowest values touched by the autorecords during the year are shown in *table 1.*

Barring very negligible precipitation depths which occurred casually on four days only through all the dry months, the season's earliest rainfall precipitated on 16th April. A graph prepared for the year's cumulated daily precipitations is presented in *fig 2.* A cumulated depth of 733 *mm* or 75.6 *percent* of the year's total depth of 837 *mm* precipitated during the 5 monsoon months June-October. The maximum intensity of 26.5 *per hour* observed on 23rd September lasted for about 30 *minutes.* The highest monthly depth of 283.5 *mm* also precipitated during September.

PRINTED AT THE YERAVDA PRISON PRESS, POONA

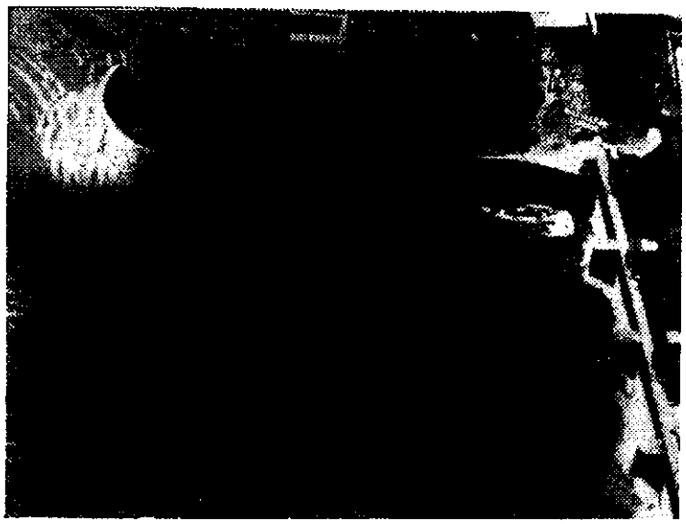

Photo 1 (*Chap 1, II*) : **Flow conditions with 1300 *ft* guide bank normal to the barrage.** $Q = 45{,}000$ *cfs*.

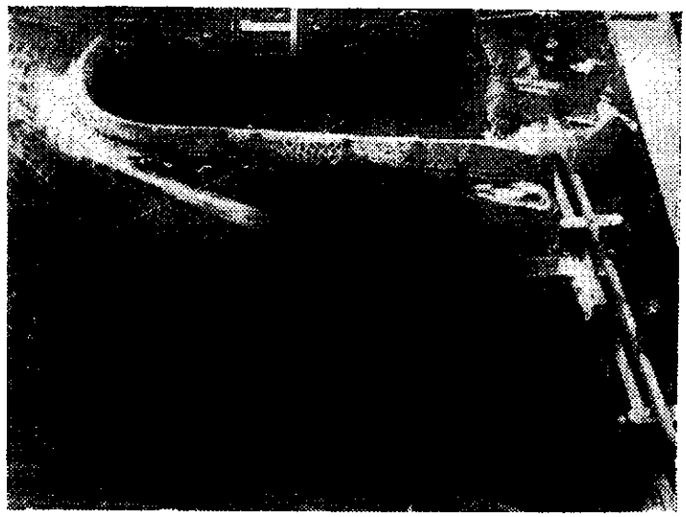

Photo 2 (*Chap 1. II*) : **Flow conditions with 1300 *ft* left guide bank inclined at 13^0 to the normal.** $Q = 45{,}000$ *cfs*

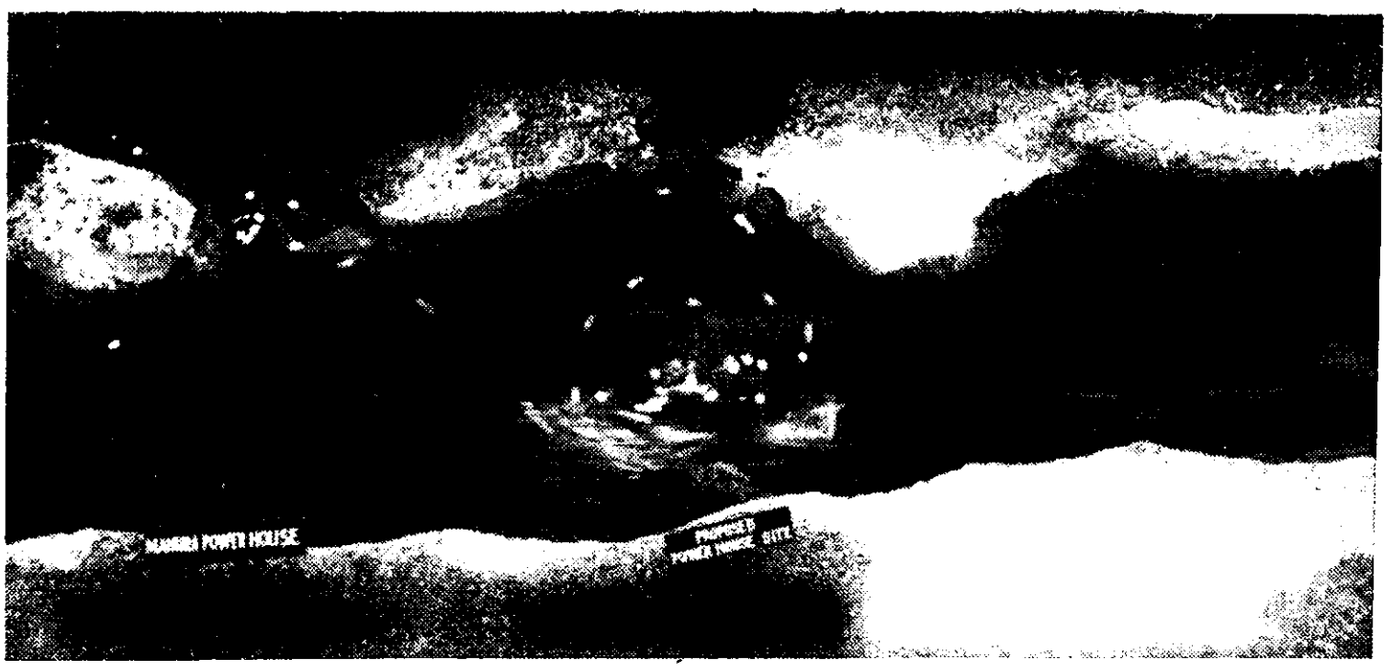

Photo 3 (*Chap 2*) : Flow conditions with $Q = 2661.8$ m^3 / *sec.* (94,000 *cfs*) at the existing and proposed power house sites Water impinges on the left bank at the proposed site and flow is very turbulent.

Photo 4 (*Chap 2*) : Flow conditions with Q=2661 8 m^3/sec (94, 000 *cfs*) when the projection opposite the proposed power house site is cut off as described in Para 5 (ii). Flow is less turbulent and high velocities have shifted to the right.

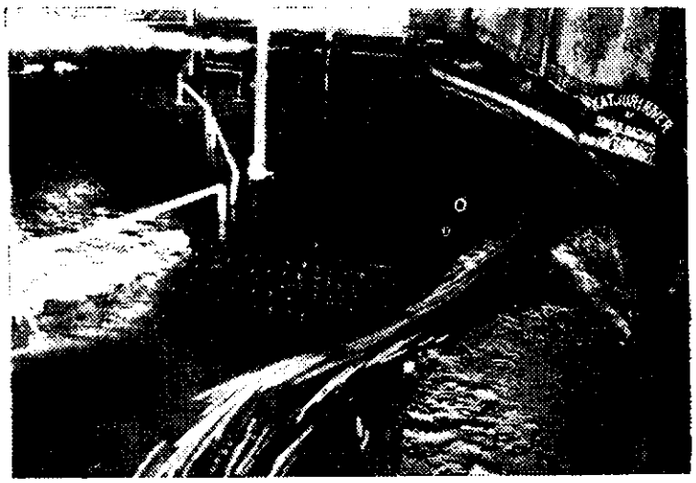

Photo 5 (Chap 3) : Flow conditions at simuldaghai with spurs (Expt 1) at 1.5 lakh *cfs* flood stage looking downstream.

Photo 6 (Chap 3) : Flow conditions at simuldaghai with spurs (Expt 1) at 3.9 lakh *cfs* flood stage looking downstream.

Photo 7 (Chap 5) : Looking upstream from the second Ovara along the right bank. The clayey ledge at about the top level is clearly seen.

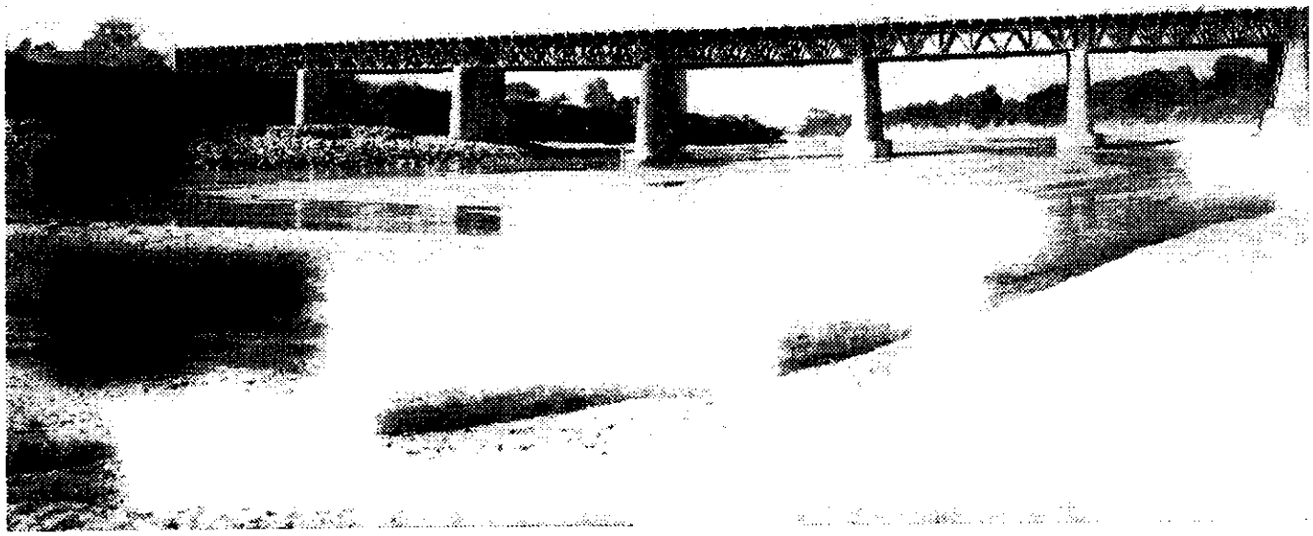

Photo 8 (Chap 6): **sand berm covered with stones washed down from the breached spur covering the top end spans on the left.**

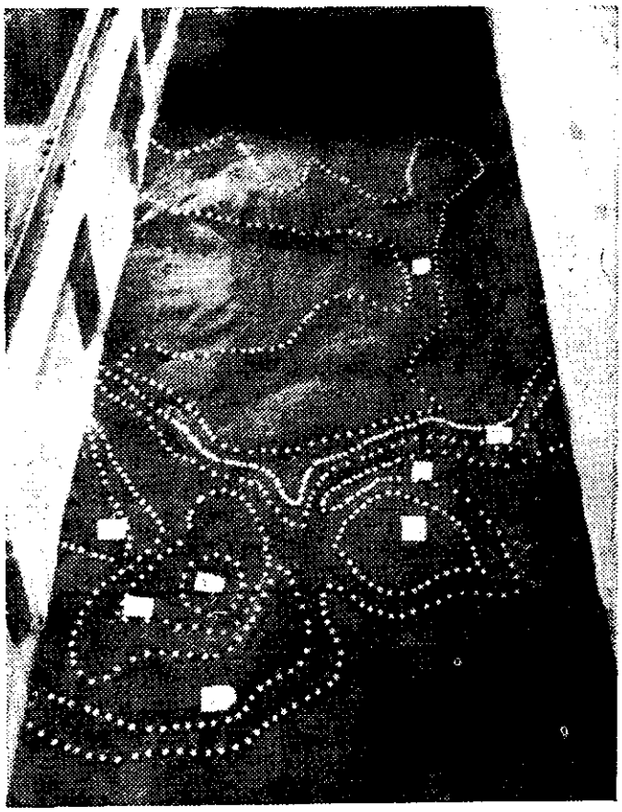

Photo 9 (Chap 11): **Scour contour under Experiment 1.**

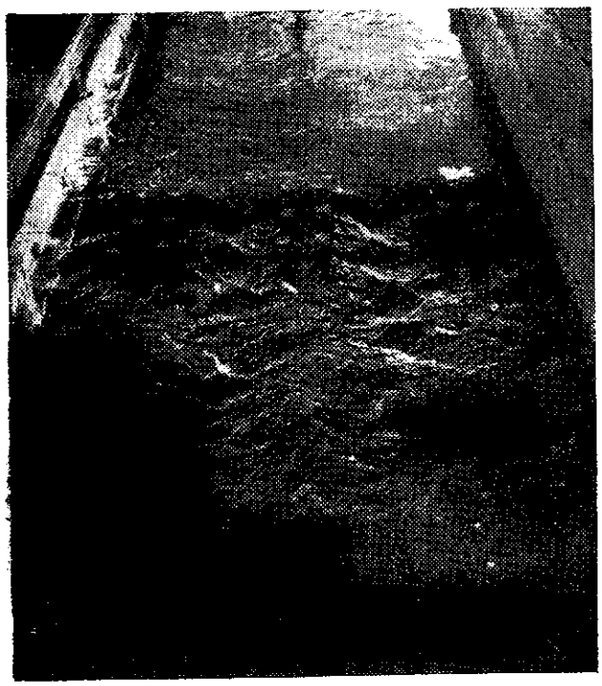

Photo 10 (Chap 11) : **Flow conditions under Experiment 2. The turbulence caused by the bridge piers can be seen.**

Photo 11 (*Chap 11*) : **Scour under Experiment 2. The pitching is exposed.**

Photo 12 (*Chap 11*) : **Scour under Exprriment 3. The exposed barrel tops can be seen.**

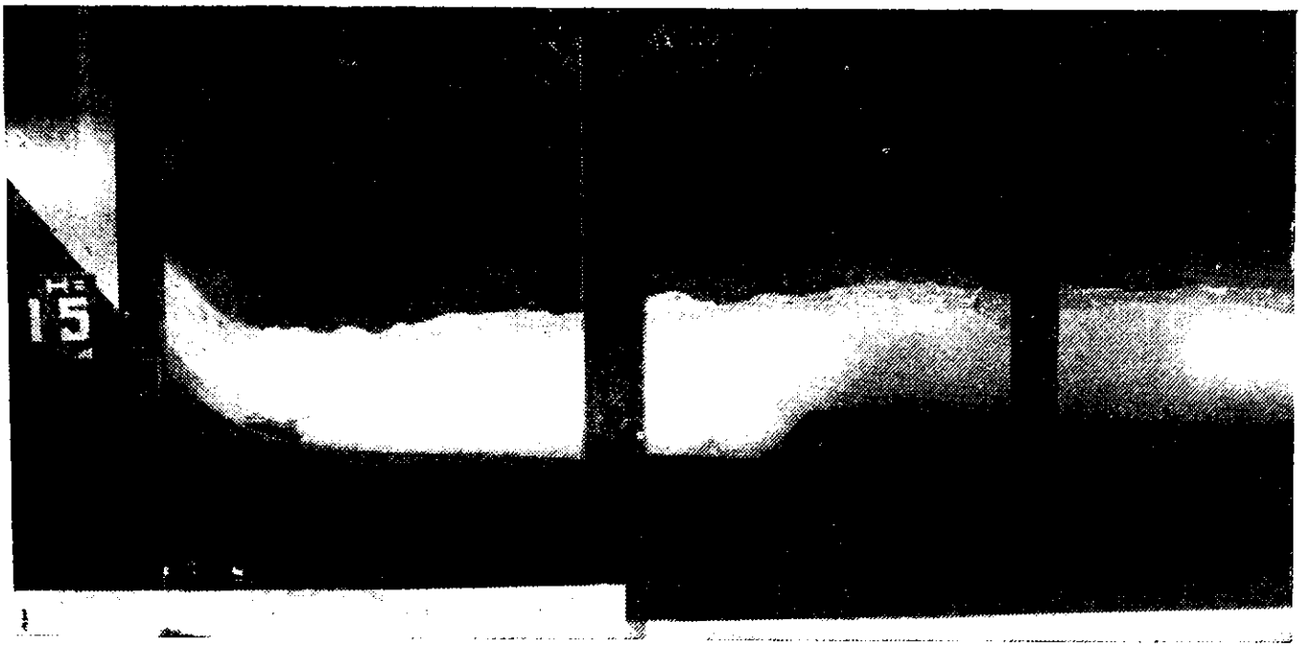

Photo 13 (*Chap 12. I*) : **Apron sloping at 1 in 16 ending in a plain end sill, 3.05 *m* (10 *ft*) high. Conditions :** $L = 36\ 57\ m$ (120 *ft*), $H = 4.57\ m$ (15 *ft*)

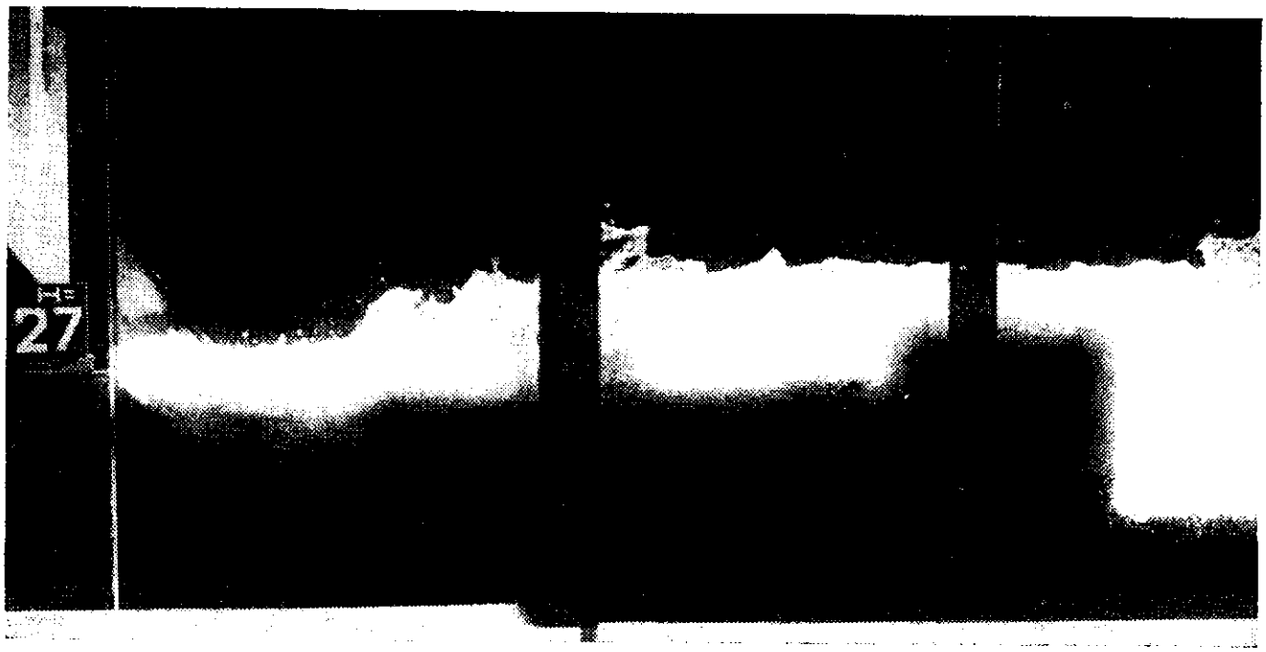

Photo 14 (Chap 12.I) : **Apron sloping at 1 in 16 ending in a plain end sill, 10 *ft* high. Conditions : $L = 120$ *ft*, $H =$ 27 *ft*.**

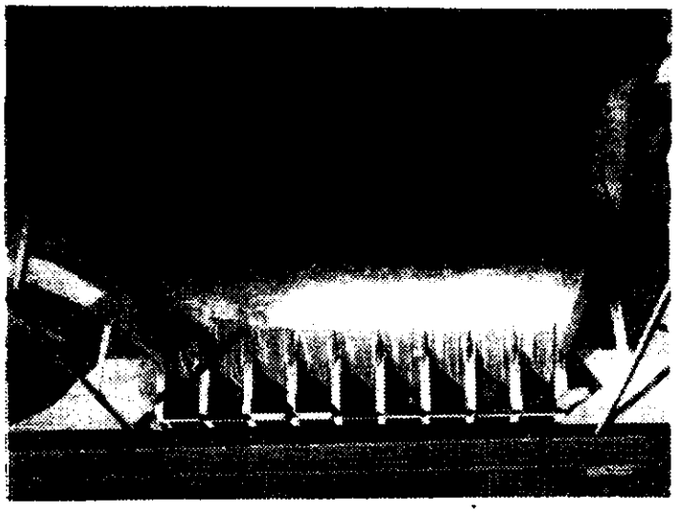

Photo 15 (Chap 12.I) : **Flow Conditions along right guide wall straight and curved for 86 *ft* with 150 *ft* radius shows water splash along embankment of Nira Right Bank Canal. Conditions : $L = 120$ *ft*, $H = 27$ *ft*.**

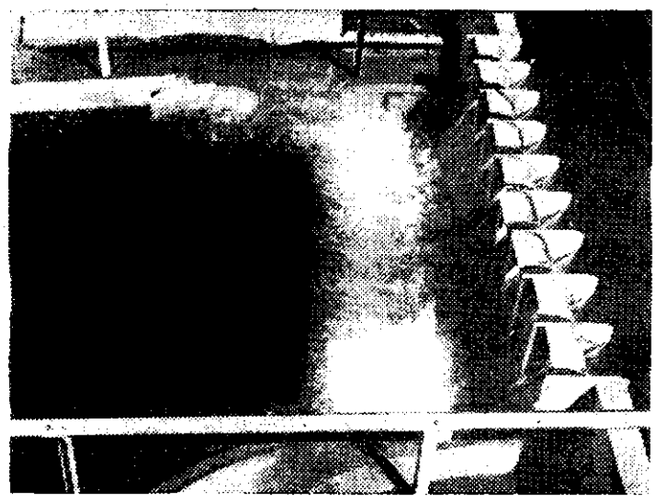

Photo 16 (Chap 12.I) : **Action of right guide wall as recommended. Conditions : $L =$ 120 *ft*, $H = 27$ *ft*.**

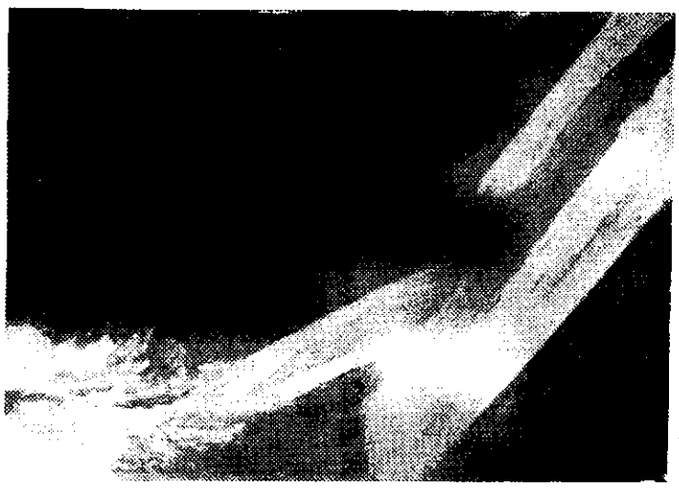

Photo 17 (Chap 12. II) : **Performance of the sluice constructed by Project authorities $H =$ 35 *ft*.**

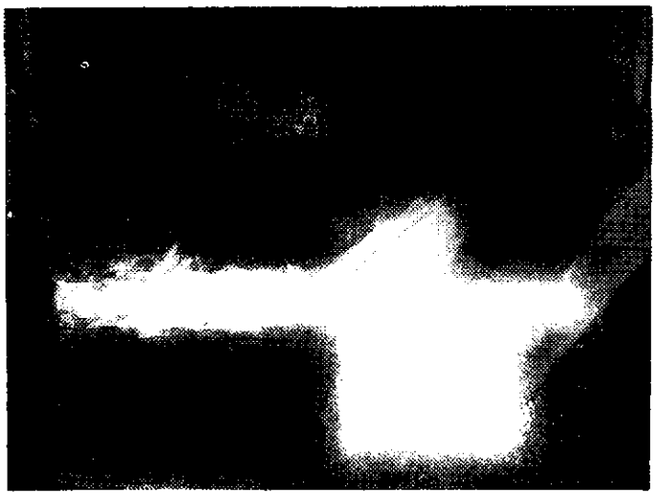

Photo 18 (Chap 12.II) : **Performance of sluice of original design. $H = 35$ *ft*.**

Photo 19 (Chap 12. III) : **Performance of roller bucket. Conditions** H= 5. 02m (16. 5 ft), R=11. 27 m (37 ft), θ=53°, **Bucket invert** EL = 135. 33 m (RL 444. 25) .

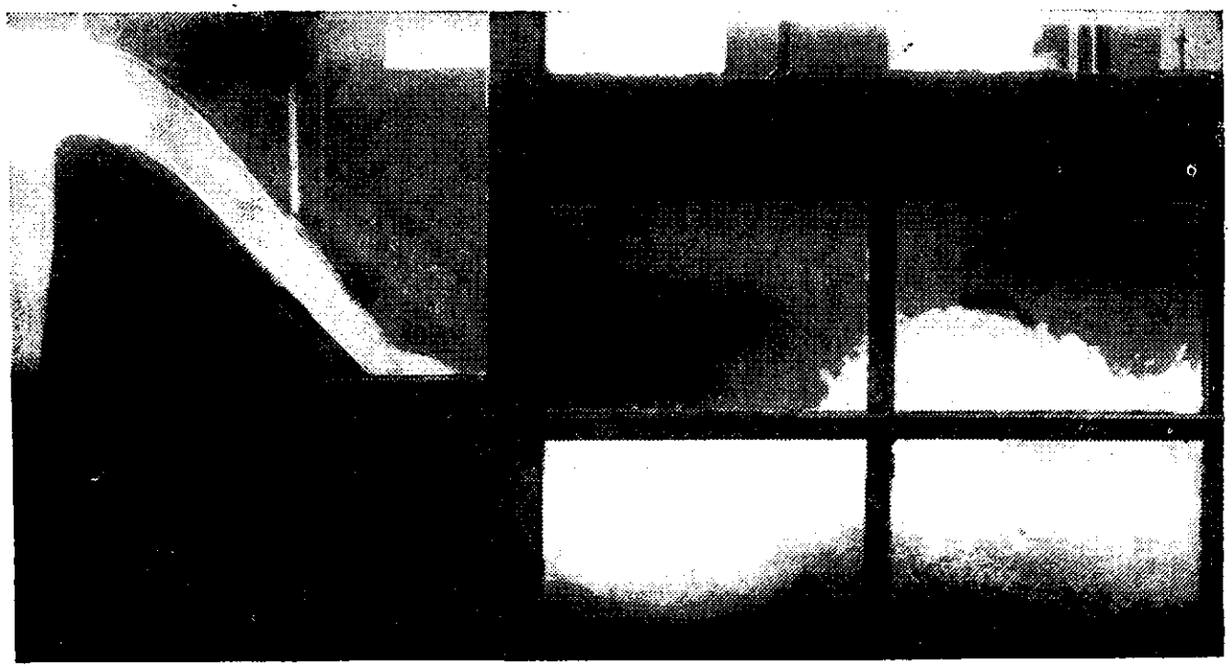

***Photo** 20 (Chap 12 IV) H*=8. 229 m (27 ft), Q=6916 m^3/ sec (2,44,000 cfs). Action of bucket R= 15. 24 m (50 ft). θ =35° invert EL =140,208 n. The hurdling action was quite unsatisfactory.

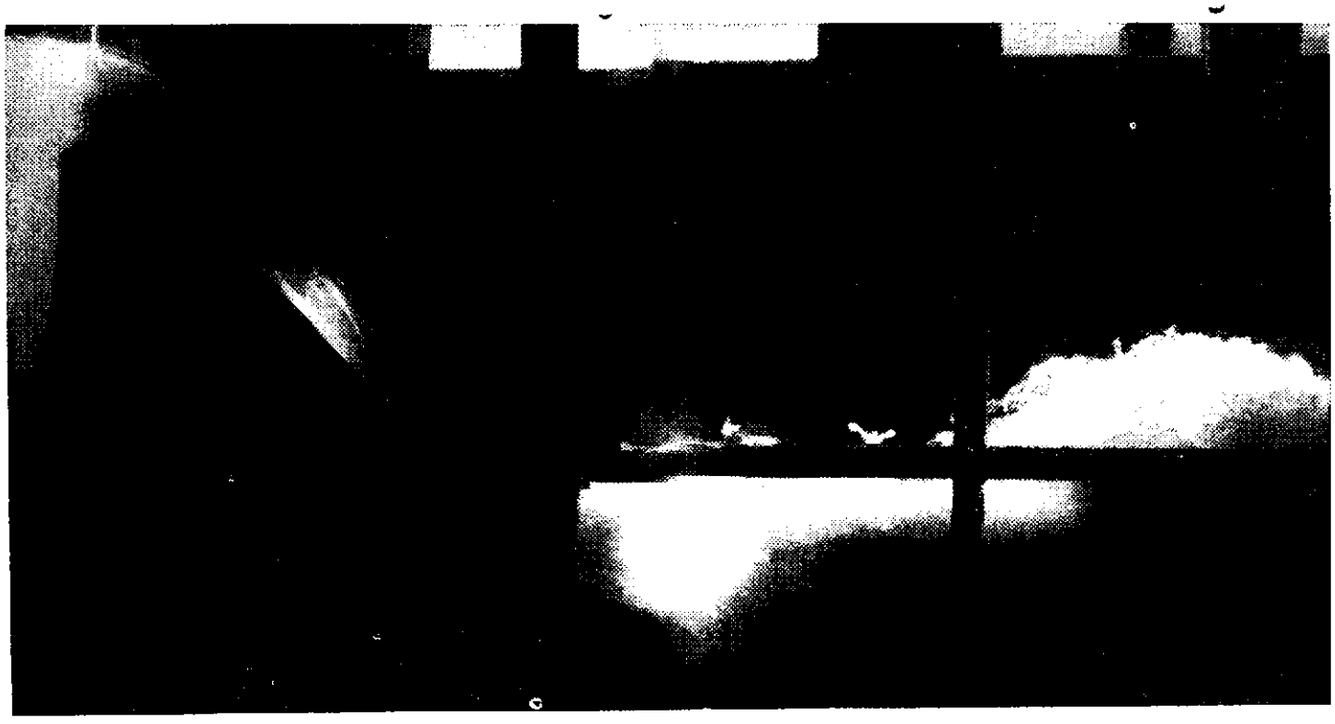

Photo 21 (*Chap 12 IV*) : H=8. 229m (27 *ft*), Q=6916 m^3/sec (2, 44,000 *cfs*). Action of bucket R = 18. 288m (60 *ft*), θ = 35^{0}invert EL = 140. 208m Note the satisfactory flow conditions and roller action.

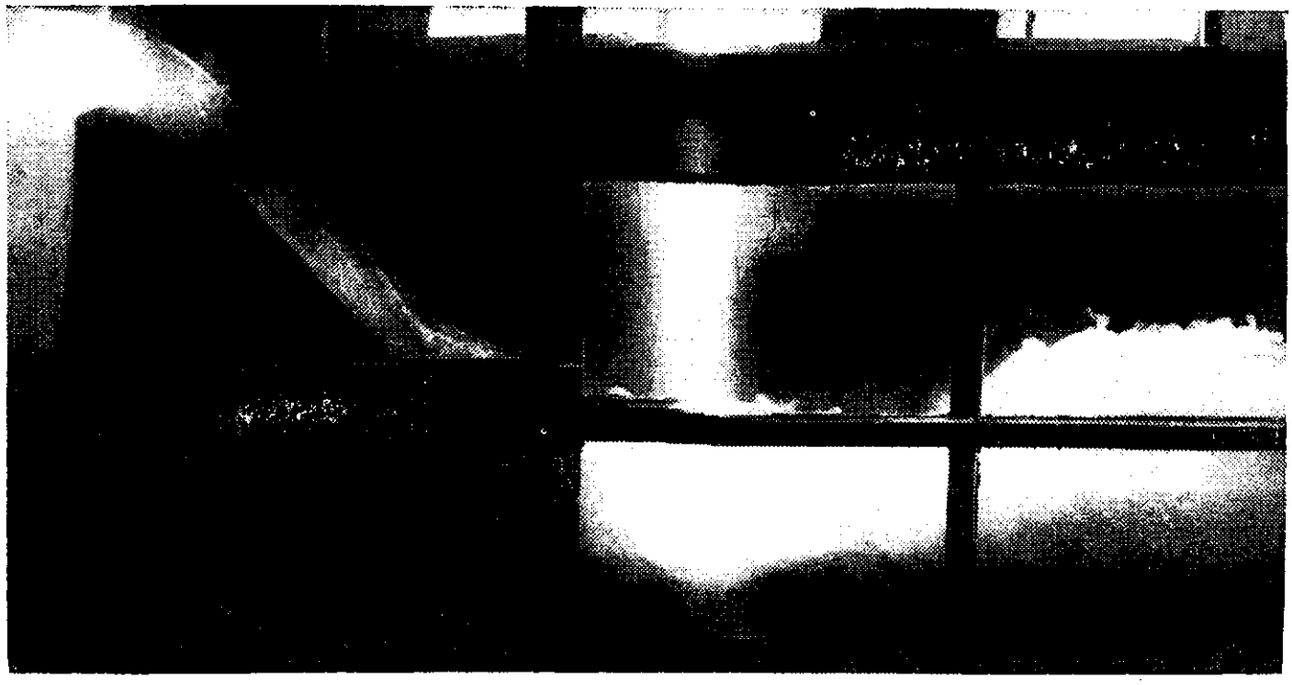

Photo 22 (*Chap 12 IV*) : H = 8. 229m (27 *ft*), Q = 6916 m^3/sec (2, 44, 000 cfs). Action of bucket R = 21. 945m (72 *ft*), θ = 35^0 invert EL 144. 122m The dissipating roller and stabilizing roller were well defined and rigorous.

Photo 23 (Chap 12.IV) : $H = (8\ 229m)\ (27\ ft)$, $Q = 6916\ m^3/sec$ (2,44,000 *cfs*) Action of bucket $R = 21\ 945m$ (72 *ft*), $\theta = 35^0$ invert $El = 141.122\ m$ with boulder outcrops reproduced downstream. Note the haphazard flow conditions downstream.

Photo 24 (Chap 12.IV): $H = 8.229m$ $Q = 6916\ m^3/sec$ (2, 44, 000 *cfs*) Combination of high level ski-jump and low level roller bucket in action with the boulder outcrops and high ground levels downstream reproduced. Note the haphazard flow conditions downstream and submergence in the high level ski-jump bucket.

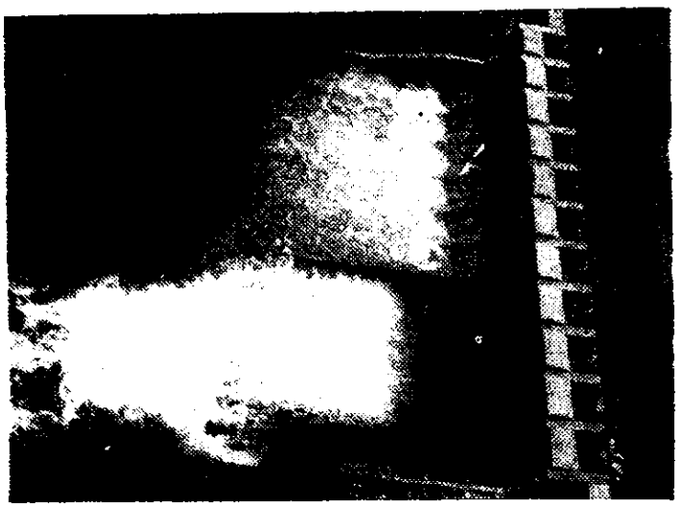

Photo 25 (Chap 12.IV) : $H = 8\ 229\ m$ (27 *ft*), $Q = 6916\ m^3/sec$ (2,44,000 *cfs*) Combination of high level ski-jump bucket and low level roller bucket in action. Flow conditions were satisfactory.

Photo 26 (*Chap 12.IV*) : $H = 6{,}086\ m$ (20 *ft*). $Q = 4185\ m^3/sec$ (1,47,900 *cfs*). Combination of low level roller bucket and high level ski-jump bucket for normal high flood.

Photo 27 (Chap 12.V) : Action of spillway (original design) for maximum discharge 2122.5 m^3/ *sec* (75,000 *cfs*). Note the unsymmetrical flow and the jump hurdling over the piers of the spillway.

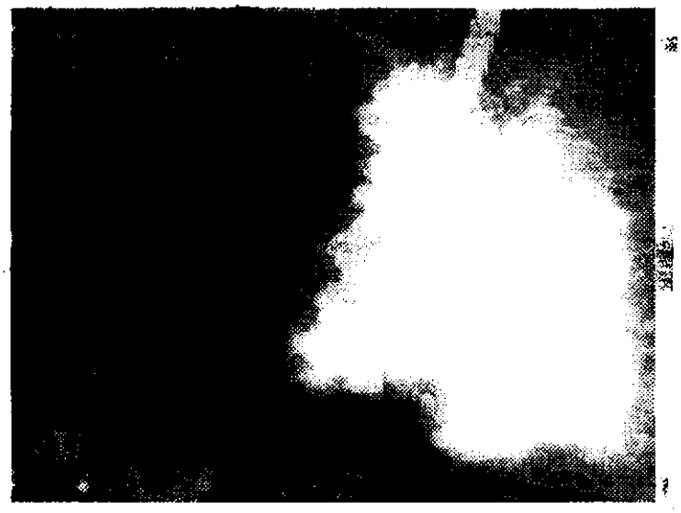

Photo 28 (Chap 12.V): Side view of *Photo* 27 showing the jet hurdling over the spillway.

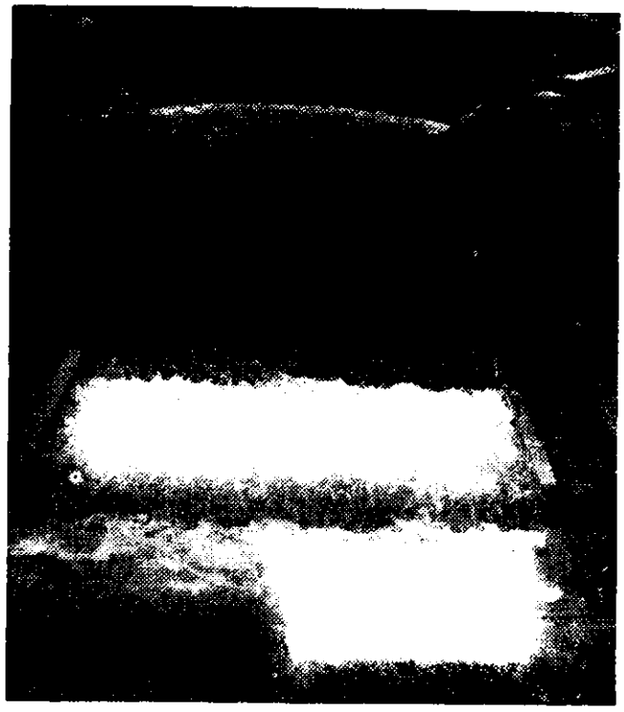

Photo 29 (Chap 12. V) : Action of spillway (recommended) for maximum discharge. Note satisfactory flow conditions.

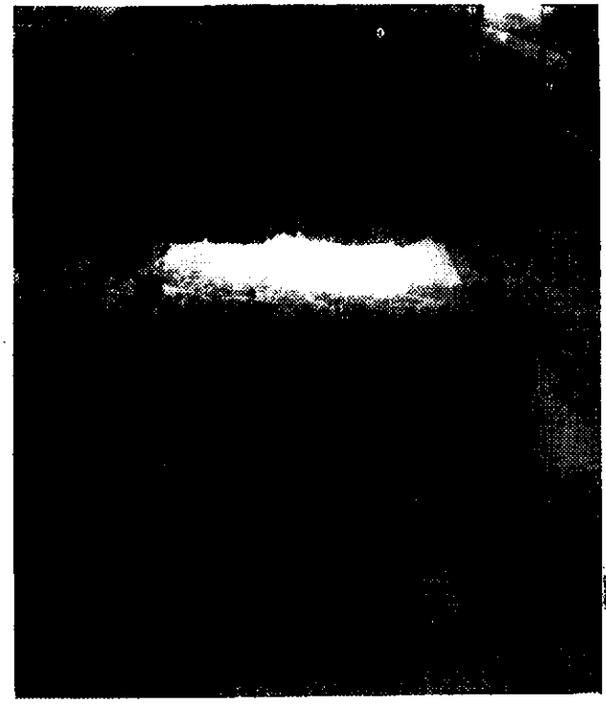

Photo 30 (Chap 12. V) : $Q = 2122.5\ m^3$/ *sec* (75, 000 *cfs*). Action of spillway with the downstream pilot channel 30.48*m* (100 *ft*) wide. Note the slight spill over the channel.

Photo 31 (Chap 12.V) : Q=1132.40 m^3/ *sec* (40,000 *cfs*). Flow conditions with downstream channel 50 *ft* wide. Limiting flow conditions are seen.

Photo 32 (Chap 12.V) : Q = 2122 5 m^3/ *sec* (75,000 *cfs*). Flow conditions with 50 *ft* wide channel. Note the tailwater affecting the hydraulic jump on the chute, eddies on the sides and the overtopping of the side walls.

Photo 34 (Chap 12 VI) : Development of scour for 40 *ft* depth of overflow and *TWL* 1447 for 70 *ft* radius bucket at invert *RL* 1388 and exit angle 30°.

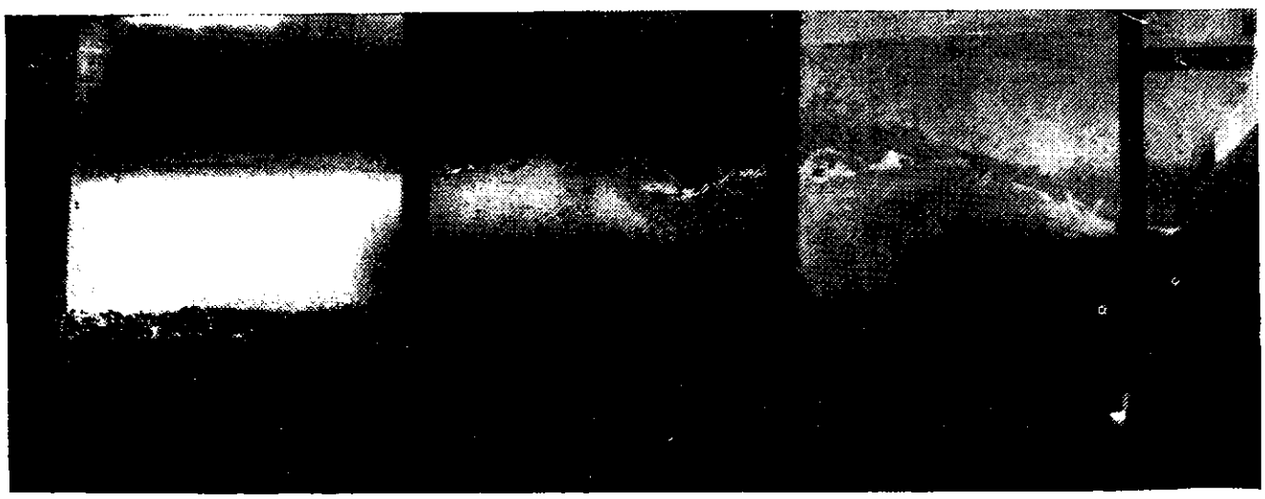

Photo 33 (Chap 12 VI) : Spillway in action for 40 *ft* overflow depth and *TWL* 1447, 70 *ft* radius upturned bucket at invert *RL* 1388 and exit angle of 30°.

Photo 35 (Chap 12, VI) : Spillway in action for 40 *ft* overflow depth and *TWL* 1447 with 70 *ft* radius bucket at invert *RL* and exit angle 30°.

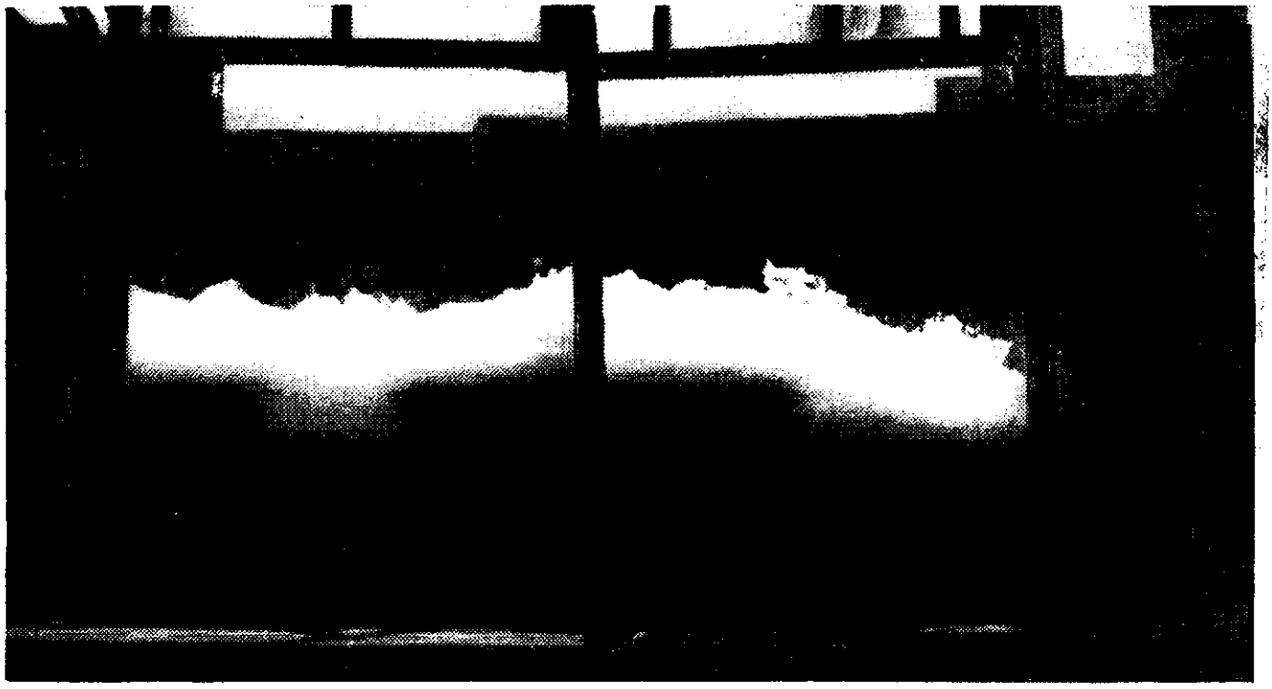

Photo 36 (Chap 12, VI) : Spillway in action for 40 *ft* depth of overflow and *TWL* 1443 for 70 ft radius bucket at invert *RL* 1384 and exit angle 30°.

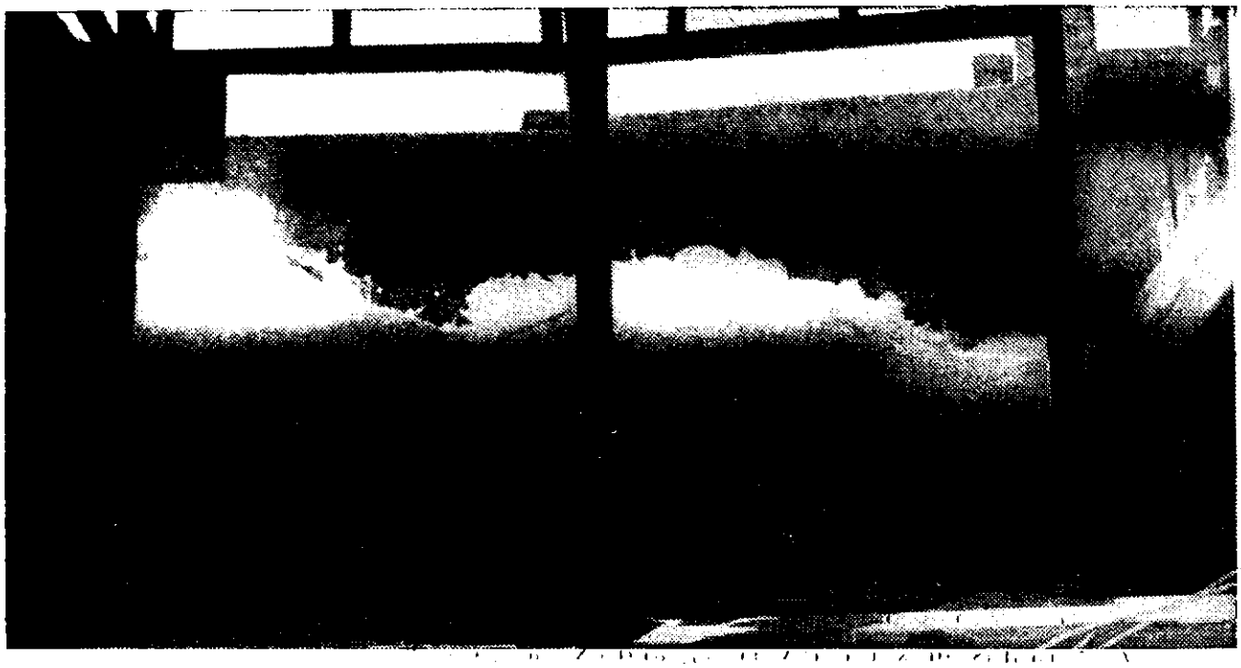

Photo 37 (Chap 12. VI) : **Spillway in action for 40 *ft* overflow depth and *TWL* 1447 for 70 *ft* radius upturned bucket at invert *RL* 1384 and exit angle 35^0**

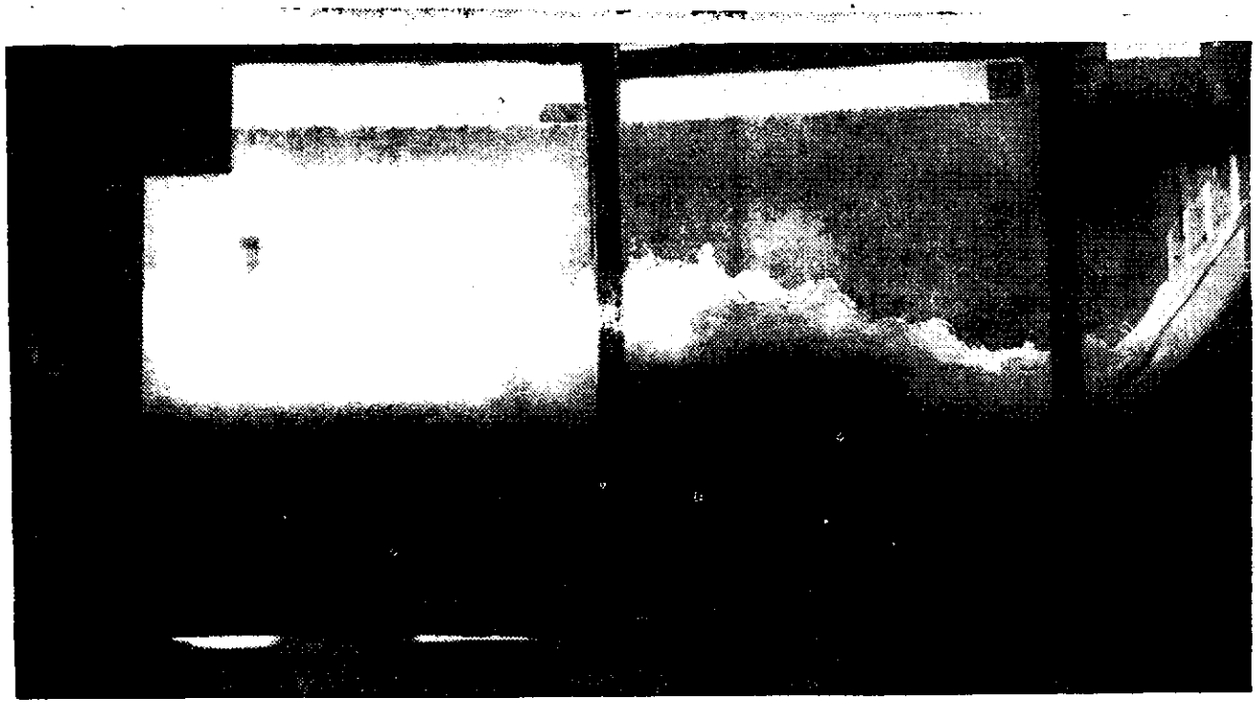

Photo 38 (Chap 12. VI) : **Spillway in action for 35 *ft* overflow depth and *TWL* 1445 for the above bucket**

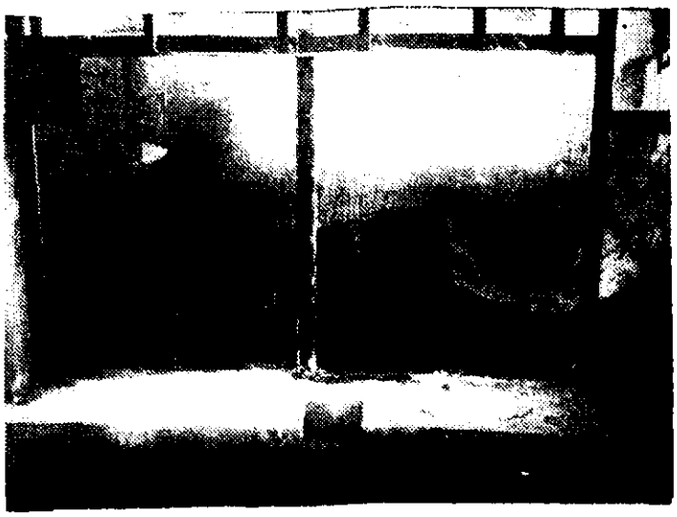

Photo 39 (Chap 12.VI): Development of scour for 40 *ft* overflow depth and *TWL* 1447, for the 70 *ft* radius upturned bucket at invert *RL* 1384 and exit angle 35°.

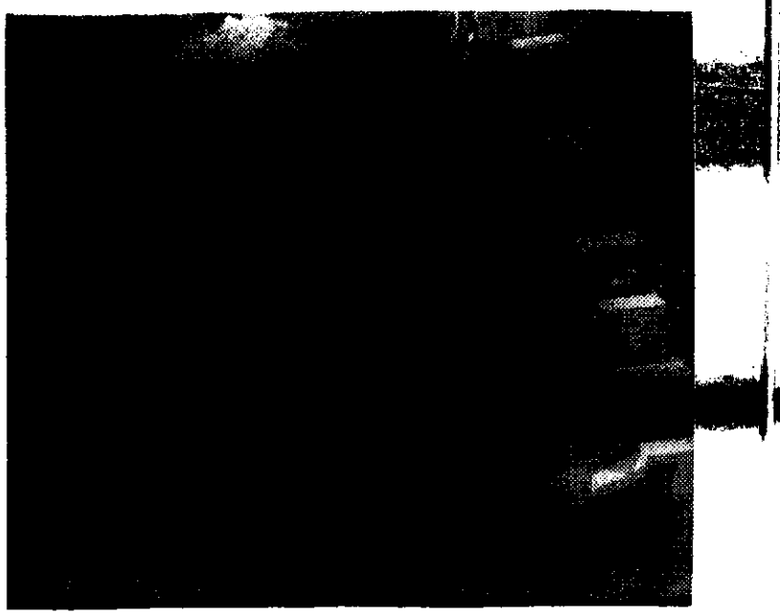

Photo 41 (Chap 13.I): Ski-jump action of the 70 *ft R* bucket at invert *RL* 1388 and 30° exit angle for 40 *ft* overflow depth *TWL* 1445.

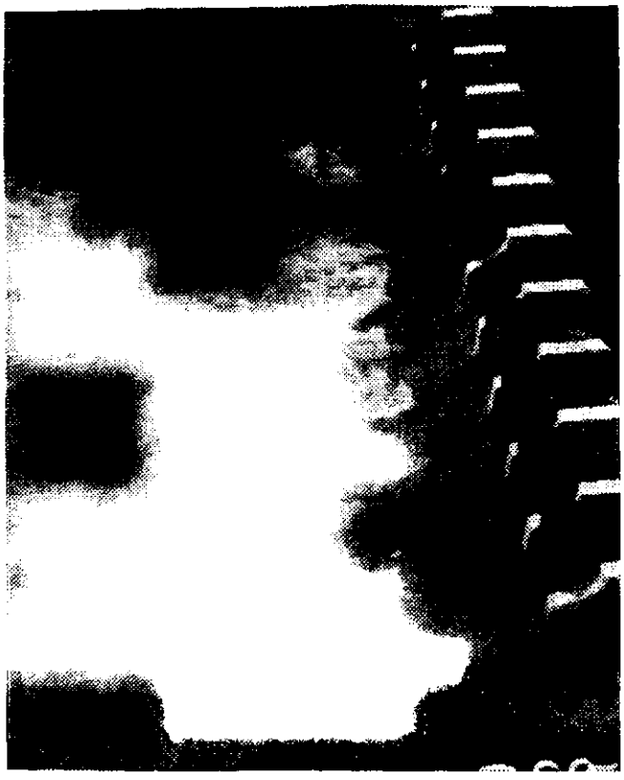

Photo 40 (Chap 13.I): Action of the 70 *ft R* bucket at invert *RL* 1388 and exit angle 30° 40 ft depth of overflow and *TWL* 1447, With very little lowering of *TWL* the action changes to ski-jump.

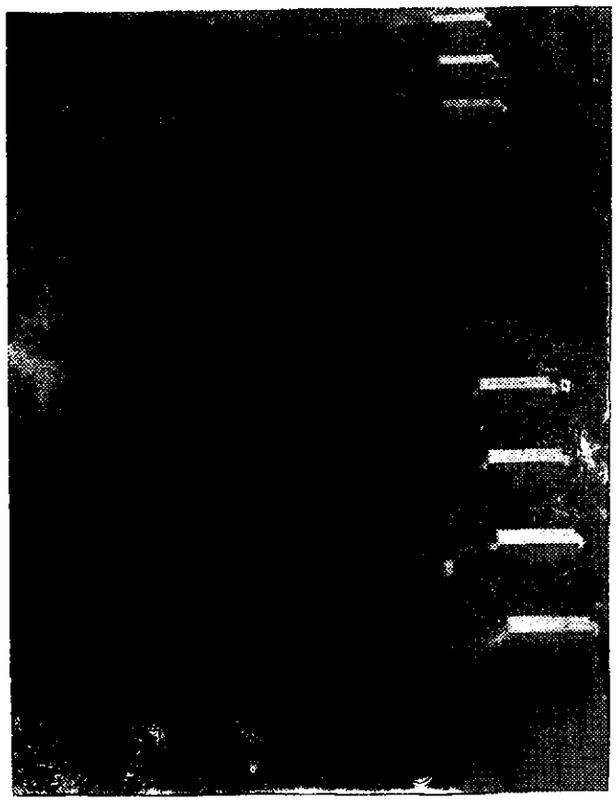

Photo 42 (Chap 13.I): 70 *ft R* bucket at invert *RL* 1384 and exit angle of 30° in action for 35 *ft* depth of overflow and *TWL* 1445. The jet from the bucket is seen suppressed in foreground.

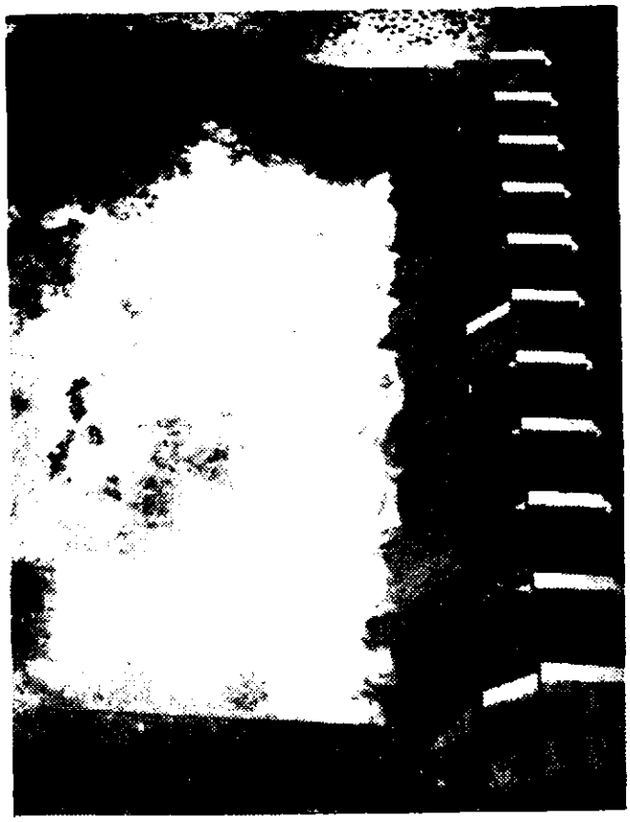

Photo 43 (Chap 13.I): Spillway in action for 40 *ft* depth of overflow and *TWL* 1447, end sill exit angle 35°, invert *RL* 1384.

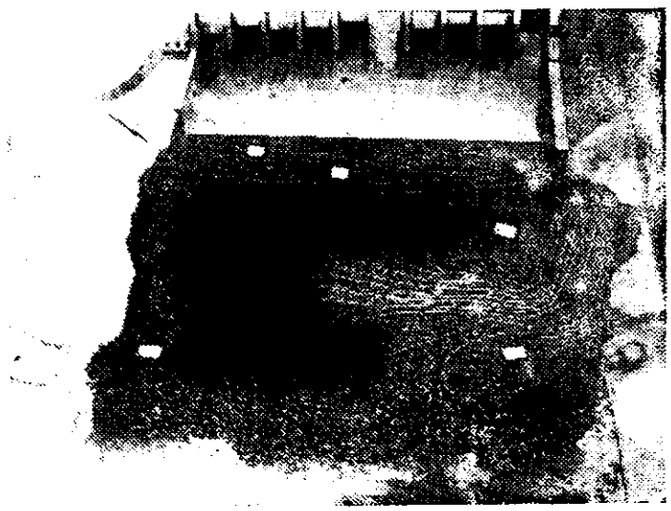

Photo 45 (Chap 13.I): Scour for 40 *ft* overflow depth and *TWL* 1447 for 70 *ft R* bucket at invert *RL* 1384, exit angle 35°.

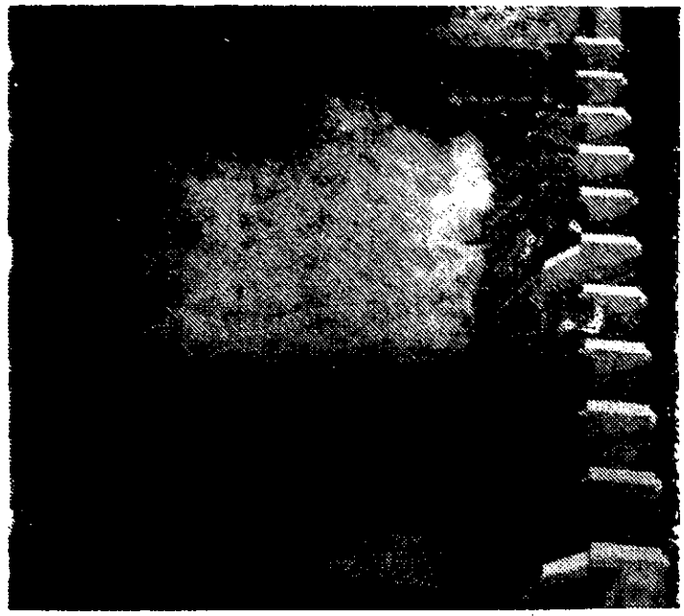

Photo 44 (Chap 13.I): Spillway in action for 40 *ft* depth of overflow and *TWL* 1443, end sill exit angle 35°, invert *RL* 1384.

Photo 46 (Chap 13.I): Cross flow in tail race channel and water spillway over the divide wall at left constructed according to *CDO* design.

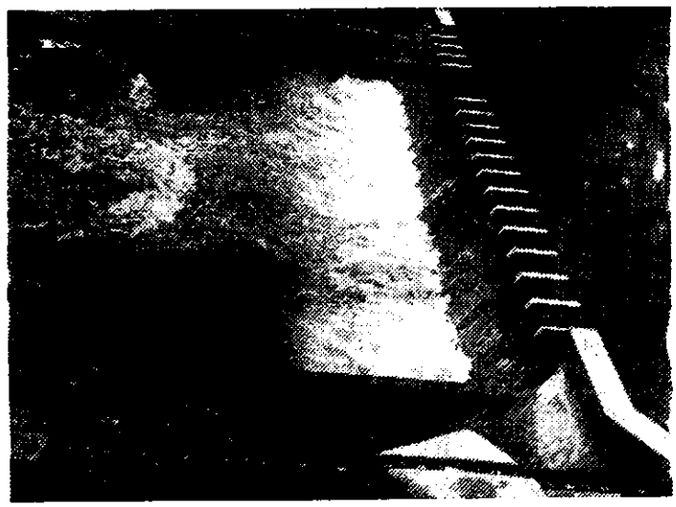

Photo 49 (Chap 13.II): Spillway in action for 40 *ft* depth of overflow and *TWL* 338 exit angle of bucket 35°.

Photo 47 (Chap 13.I): Improved flow conditions in the tail race channel due to the extension of divide wall and raising its top to RL 1365.

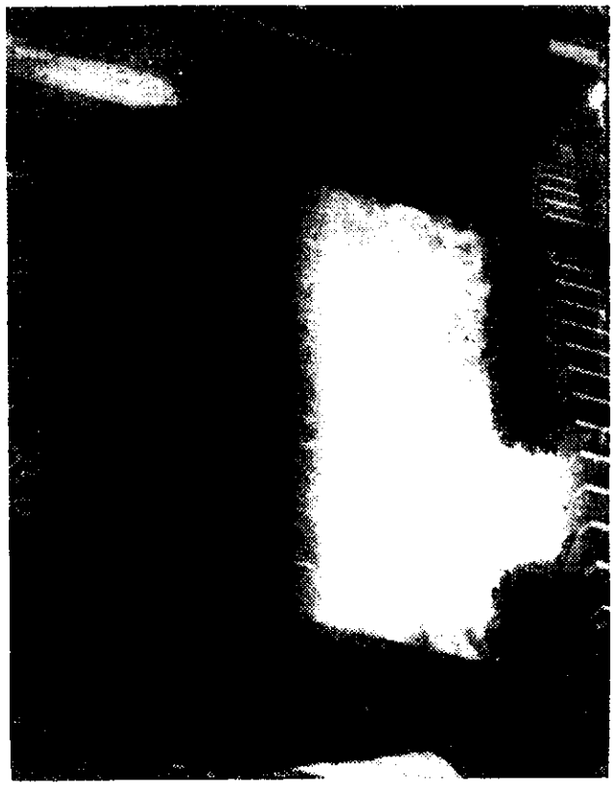

Photo 48 (Chap 13.II): Spillway in action for 40 *ft* depth of overflow, *TWL* 338, exit angle of the bucket 30°.

Photo 51 (Chap 13.III): Spillway in action for 14 *ft* overflow depth and *TWL* 313 with 110 *ft* straight (Horizontal) apron at *RL* 283.

Photo 50 (Chap 13.III): Spillway in action for 10 *ft* overflow depth and *TWL* 305.5 with 110 *ft* straight (Horizontal) apron at *RL* 283.

Photo 52 (Chap 13.III): Spillway in action for 14 *ft* overflow depth *TWL* 313.0 with 110 *ft* straight (Horizontal) apron at *RL* 283 (side view).

Photo 53 (Chap 13.III): Spillway in action for 14 *ft* overflow depth *TWL* 305.5 with 110 *ft* straight (Horizontal) apron at *RL* 283 (side view).

Photo 54 (Chap 13.III): Spillway in action for 14 *ft* overflow depth and *TWL* 313 with 40 *ft R* upturned bucket and 30° exit angle, invert at *RL* 283.

Photo 55 (Chap 13.III): Spillway in action for 10 *ft* depth and TWL 305.5 with 40.*ft* radius upturned bucket and 30° exit angle, invert at *RL* 283.

Photo 56 (Chap 13.IV): General layout of model The entrance bellmouth, the emergency and the service gate and the sluice conduit system fabricated in perspex is seen.

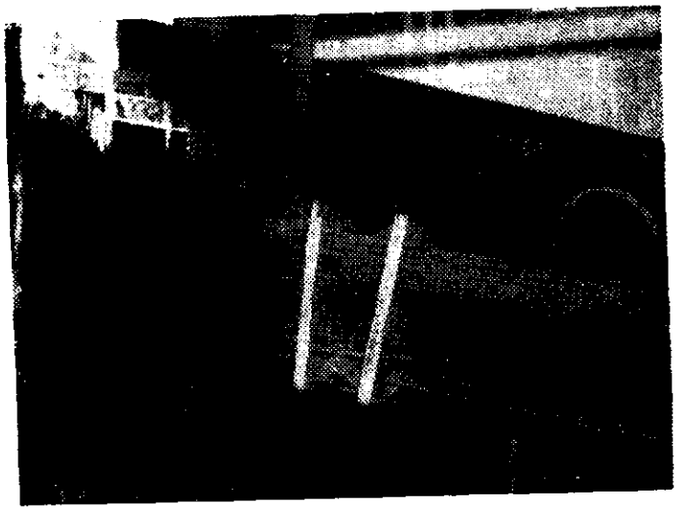

Photo 57(Chap 13.IV): Service gate air vent position, and perspex conduit system downstream of service gate.

Photo 58 (Chap 14): View of Talkalale Balancing Reservoir looking downstream.

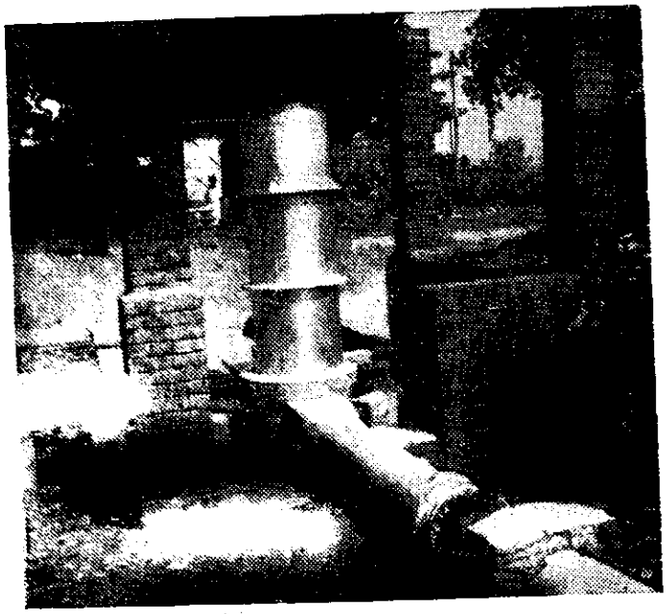

Photo 61 (Chap 14): View of surge tank looking downstream showing entry of tunnel and friction disc.

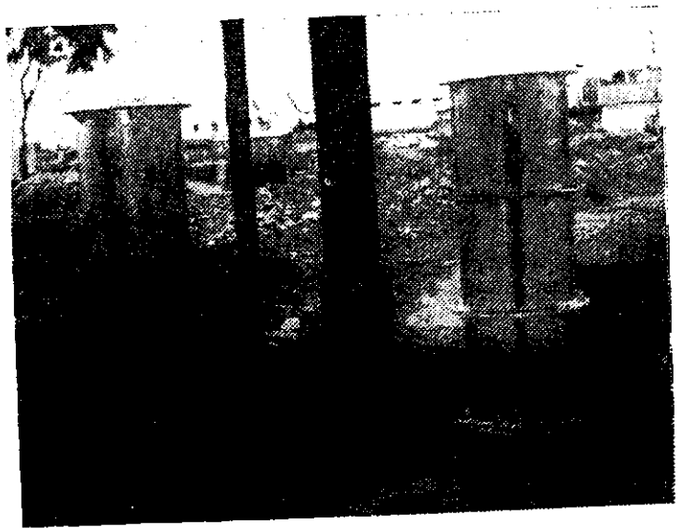

Photo 60 (Chap 14): Twin surge tanks of masonry and steel, looking upstream.

Photo 59 (Chap 14): View of the twin hume pipes representing tunnels.

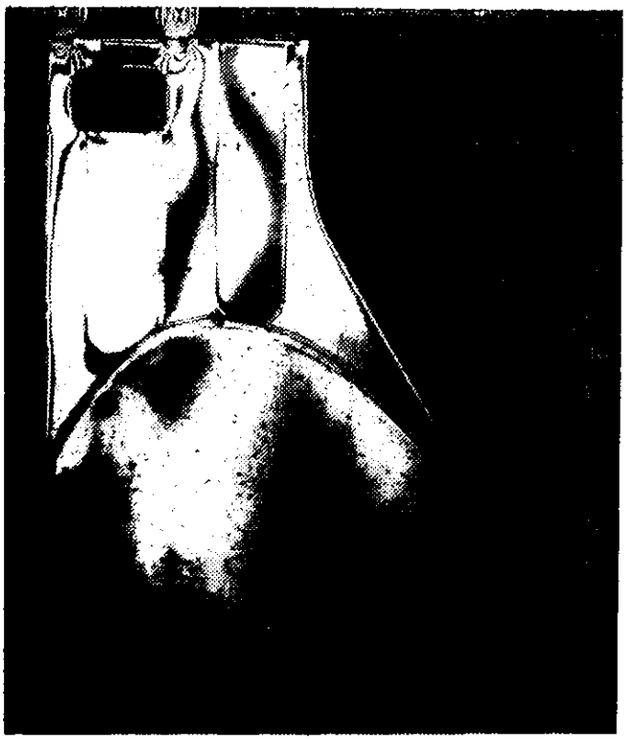

Photo 64 (Chap 18.I): Isochromatic Fringe Pattern for Vertical load.

Photo 62 (Chap 15): Flow near the existing right divide wall for low floods.

Photo 63 (Chap 17): Model of Hirakud Reservoir in operation for the reservoir *WL* at *RL* 630 and discharge corresponding to 6 lakh *cfs*.

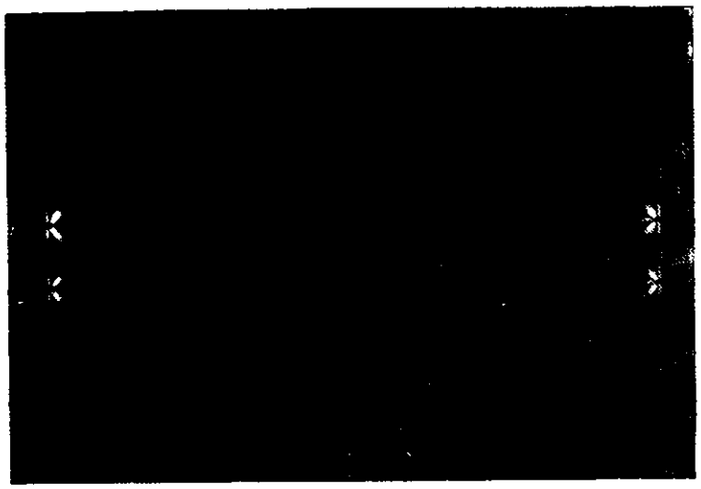

Photo 65 (Chap 18.II): Dark field Isochromatics, $d/r = 0.25$.

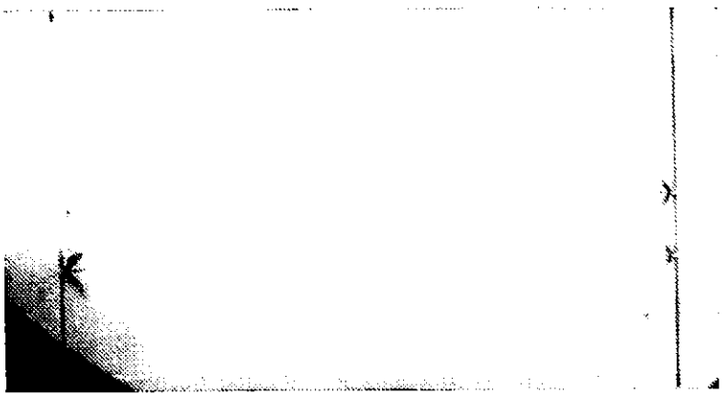

Photo 66 (Chap 18.II): Light field Isochromatics, $d/r = 0.25$.

Photo 67 (Chap 18.II): Dark field Isochromatics, $d/r = 0.50$.

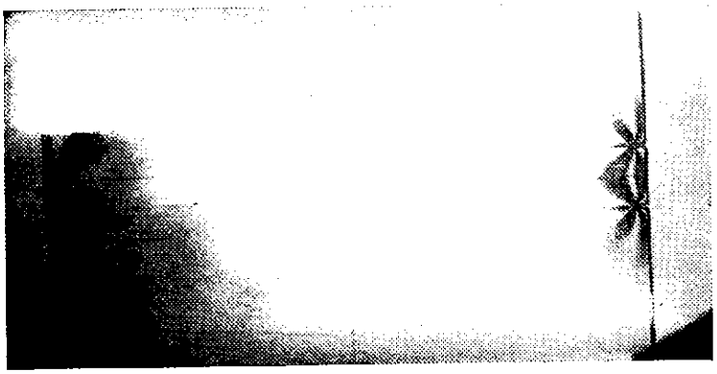

Photo 68 (Chap 18.II): Light field Isochromatics, $d/r = 0.50$.

Photo 69 (Chap 18.II): Dark field Isochromatics, $d/r = 1.0$.

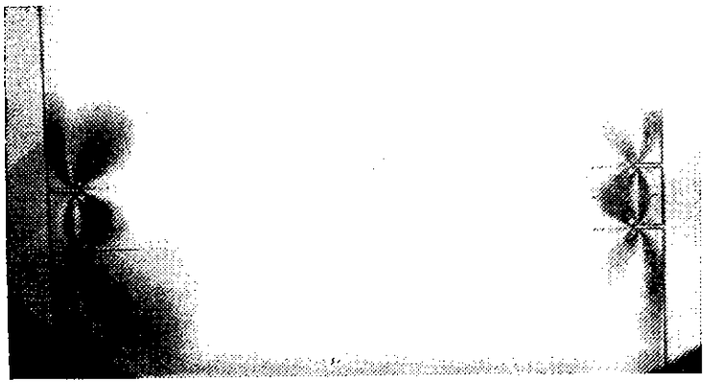

Photo 70 (Chap 18.II): Light field Isochromatics, $d/r = 1.0$.

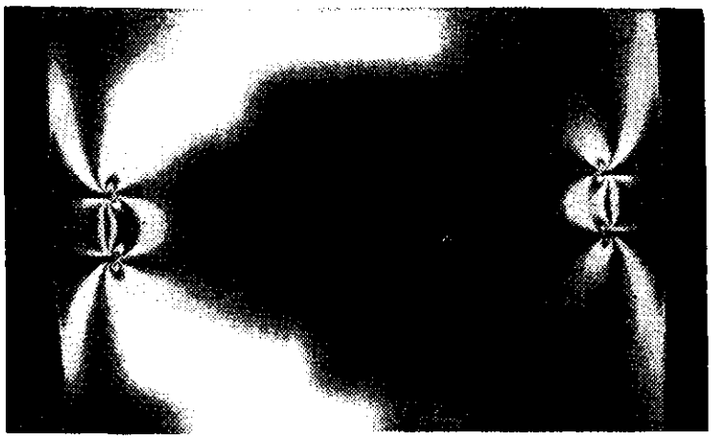

Photo 71 (Chap 18.II): Dark field Isochromatics, $d/r = 2.0$.

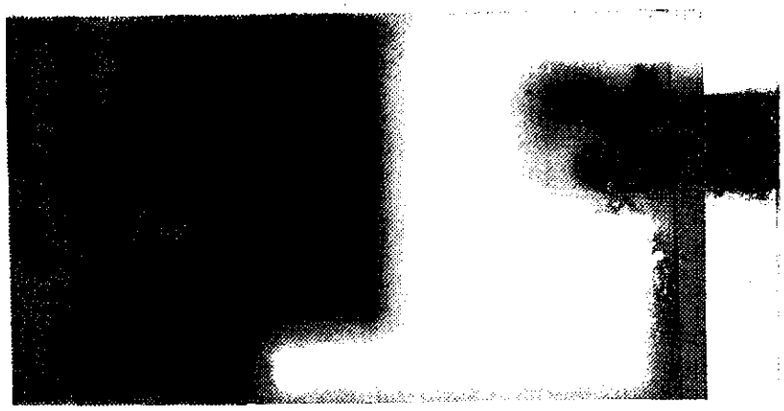

Photo 72 (Chap 18.II): Light field Isochromatics, $d/r = 2.0$.

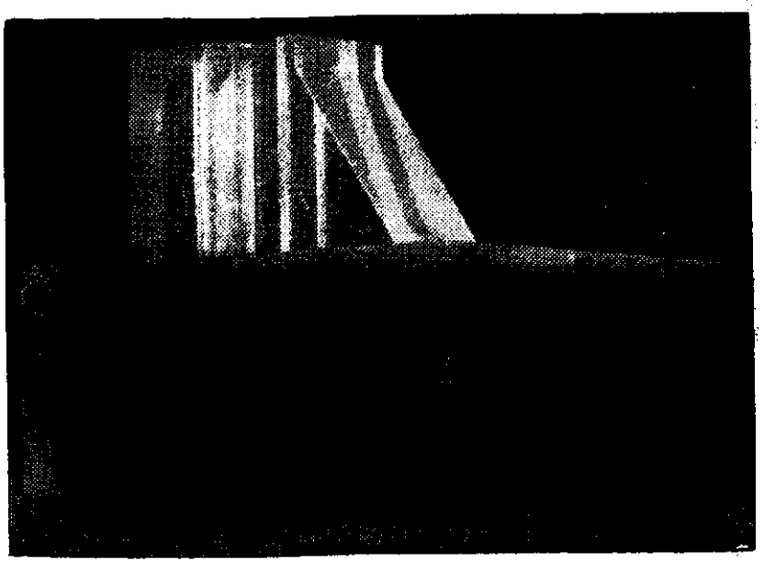

Photo 73 (Chap 19): Oblique view of the model

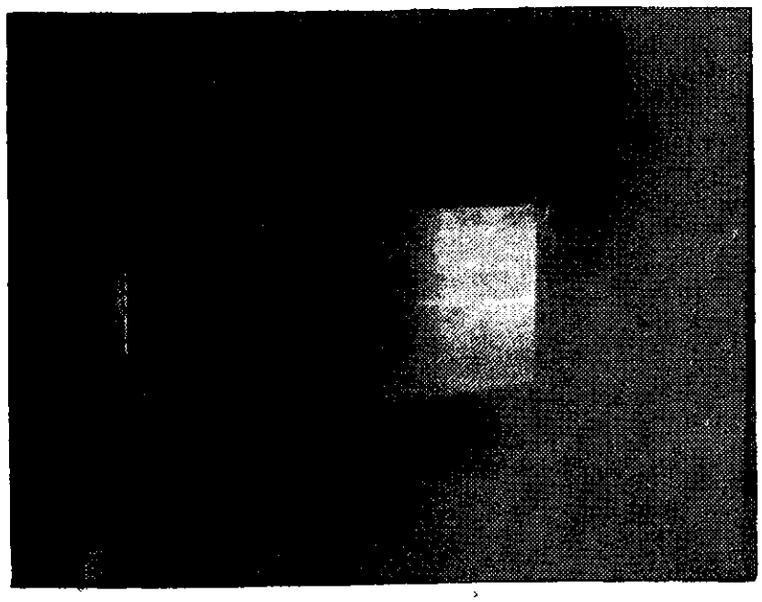

Photo 74 (Chap 19): Top view of the Model.

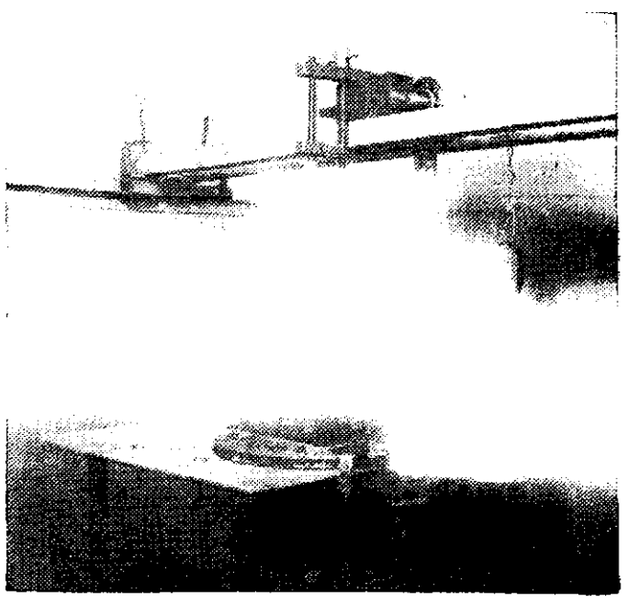

Photo 75 (Chap 19): Model and loading arrangement.

Photo 76 (Chap 19): Stress pattern for vertical cantilever slice (isochromatics—Dark field).

Photo 77 (Chap 19): Stress pattern for Horizontal portal slice (Isochromatics—Dark field).

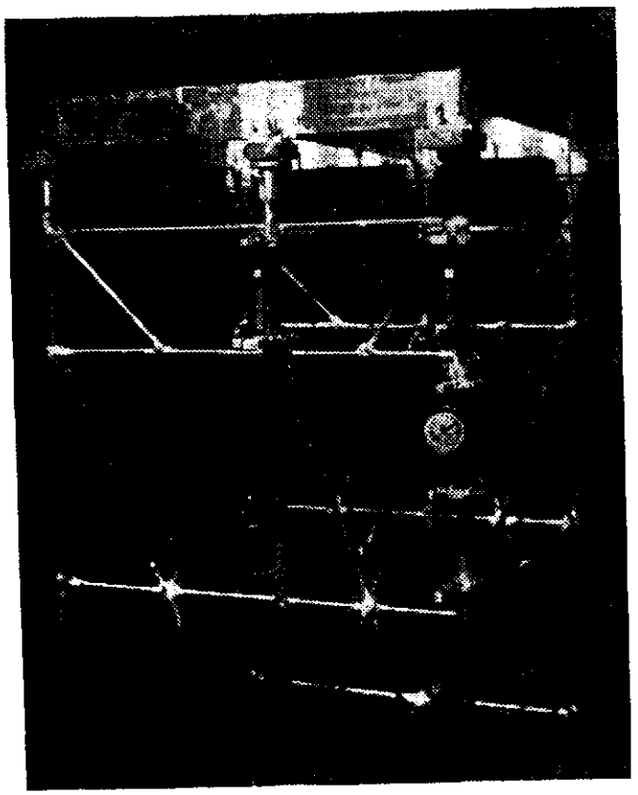

Photo 80 (Chap 20.II): Moment indicator.

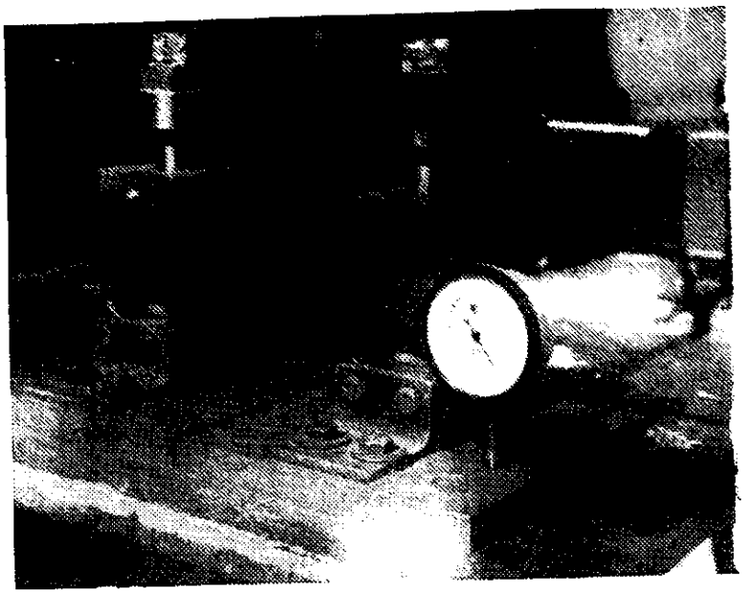

Photo 78 (Chap 20.II): Movement device.

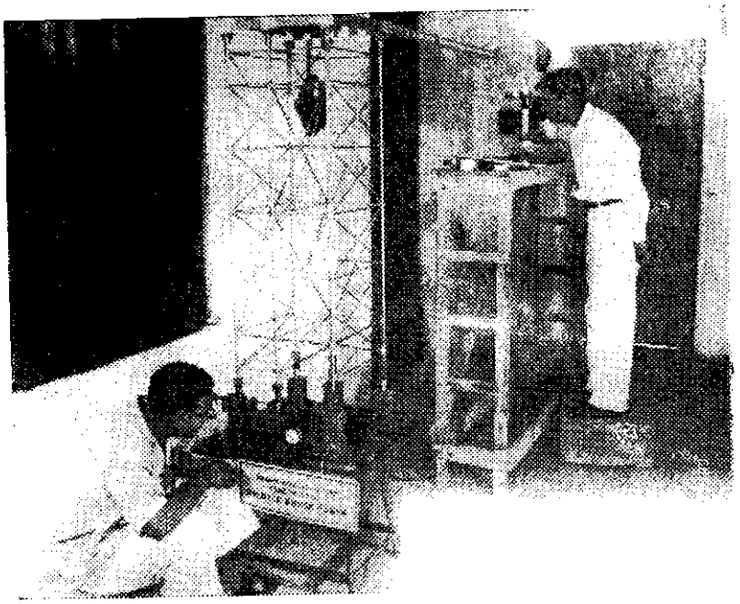

Photo 79 (Chap 20.II): Model and method of observations.

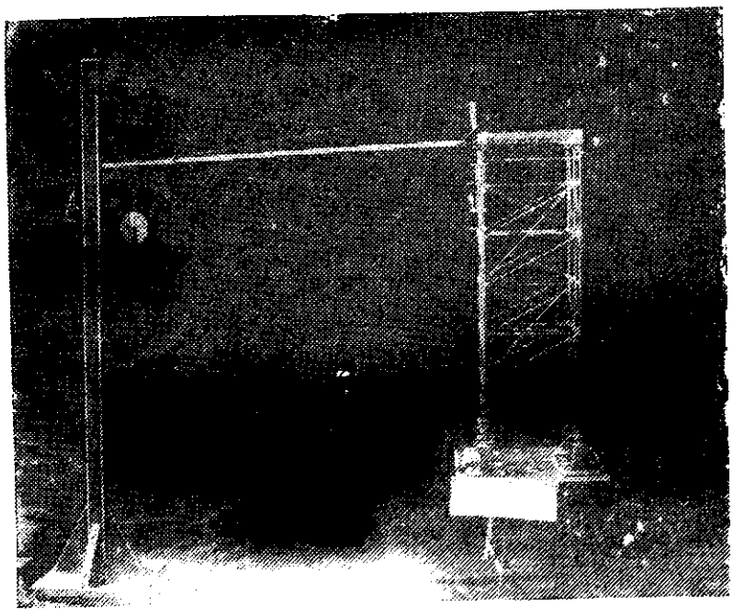

Photo 81 (Chap 20.II): Method of measuring moments in columns.

Photo 82 (Chap 22): Ship Testing tank, towing carriage and other equipment.

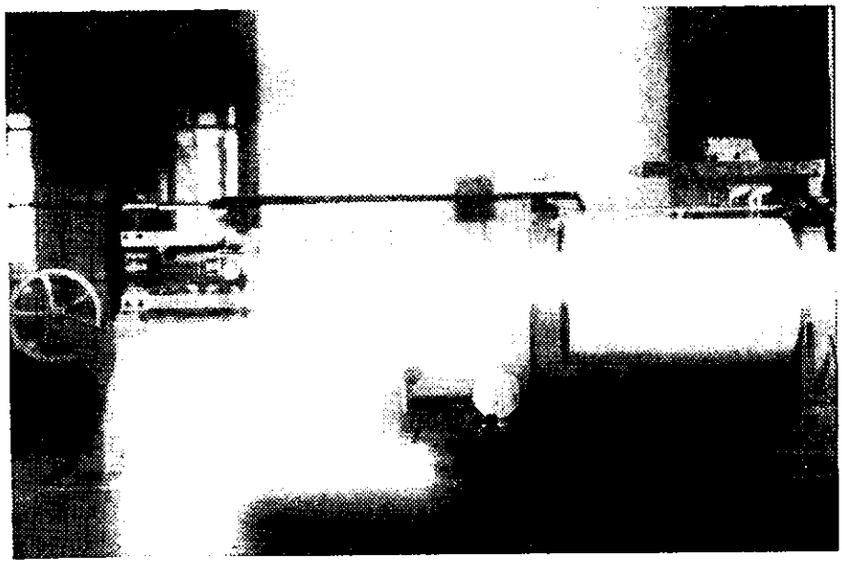

Photo 83 (Chap 22): Automatic recording is shown at the right.

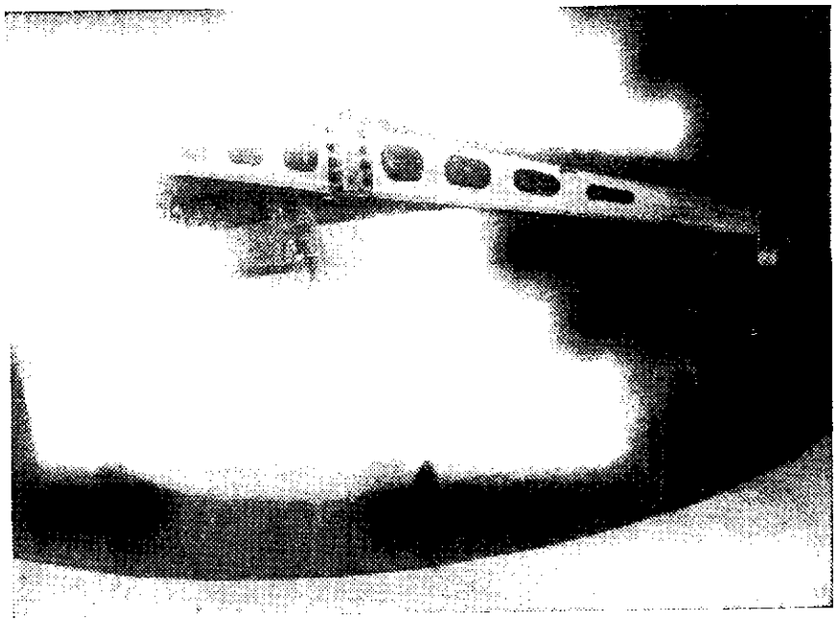

Photo 84 (Chap 22): Circular rating tank.

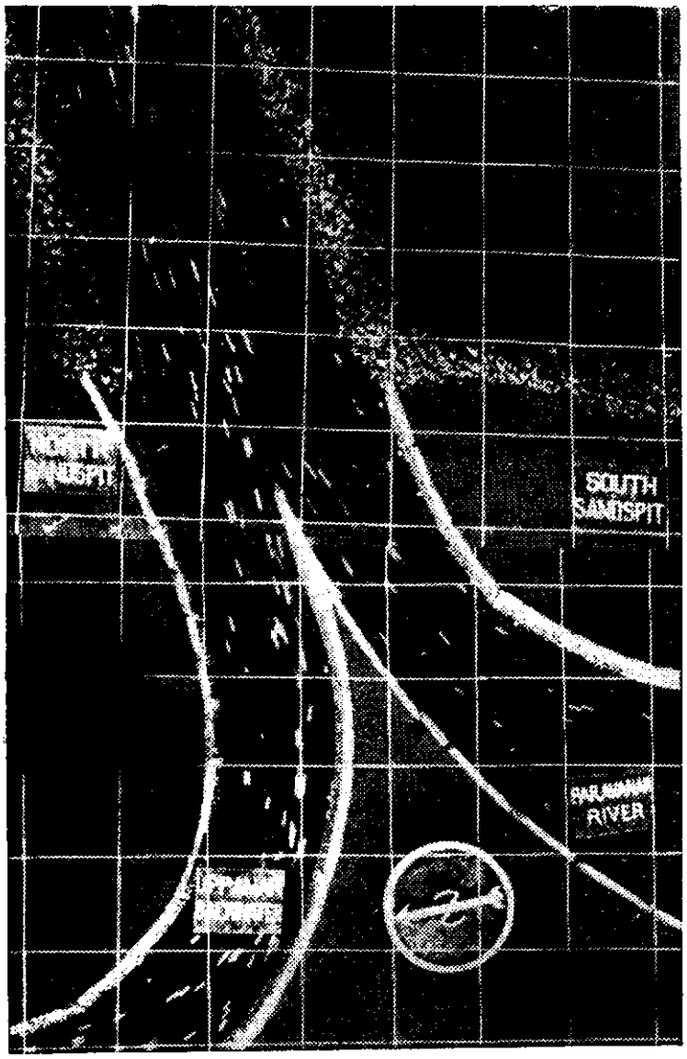

Photo 85 (Chap 25): **Flow pattern in Paravanar** and Uppanar channels and in entrance formed by breakwater (1st stage proposal C).

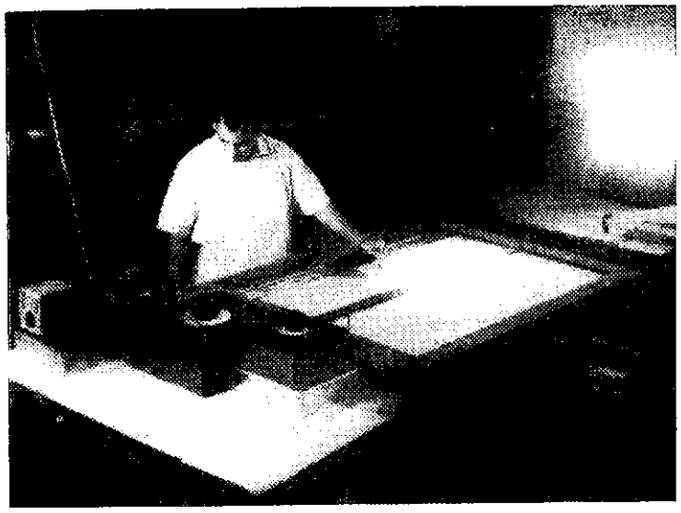

Photo 87 (Chap 35): Electrical analogy ; Experimental set-up.

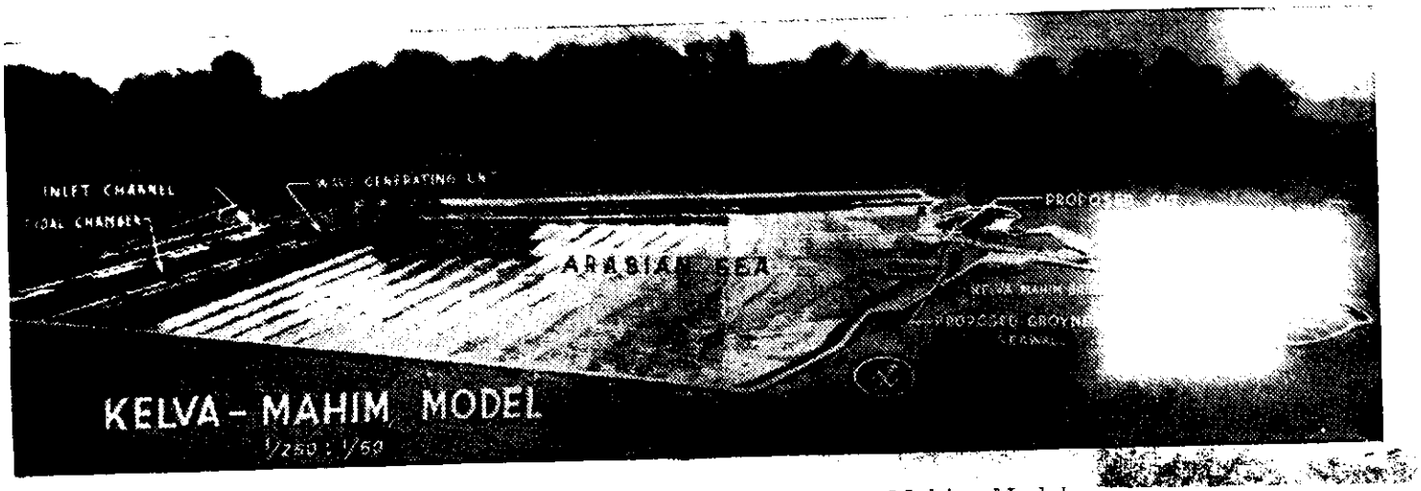

Photo 86 (Chap 26): General view of the Kelva- Mahim Model.

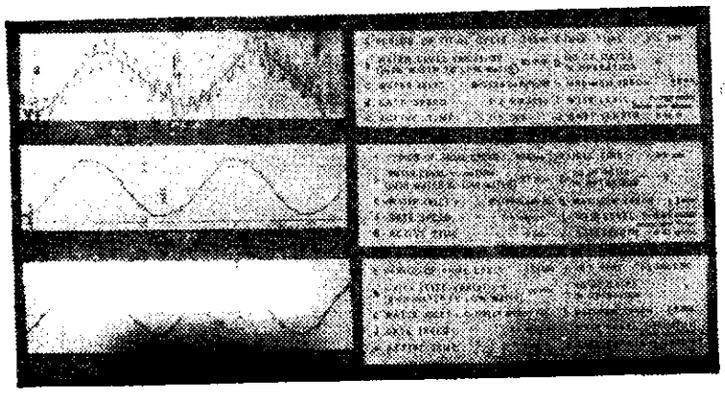

Photo 88 (Chap 46)

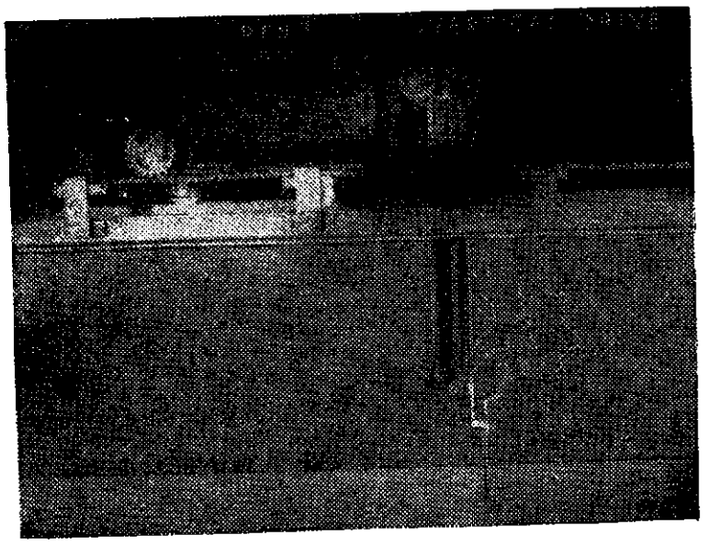

Photo 89 (Chap 46): Bed profile recorder for model.

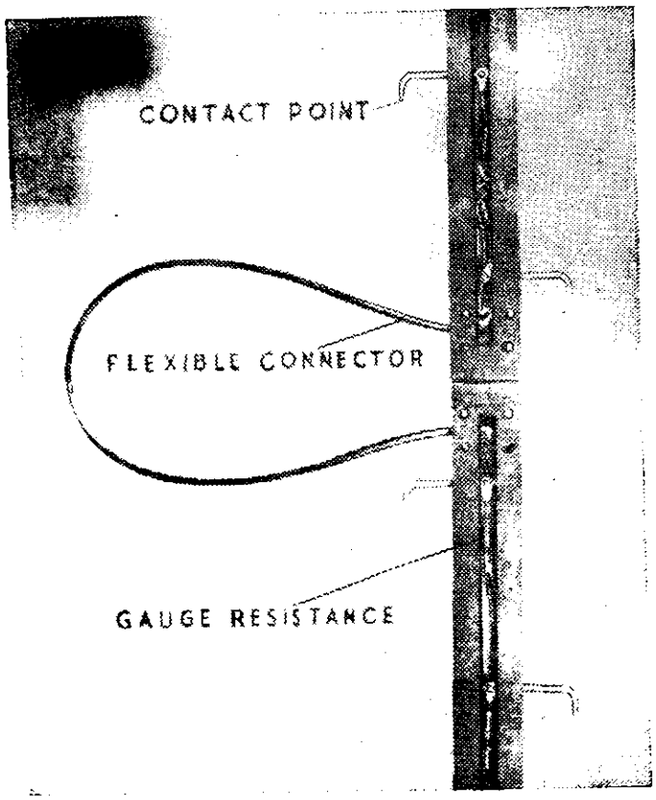

Photo 90 (Chap 46): Gauge for wave height observation.

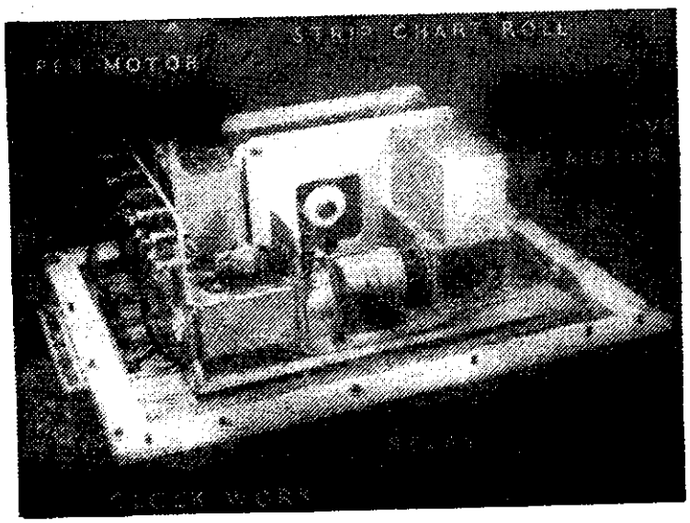

Photo 91 (Chap 46): Recorder.

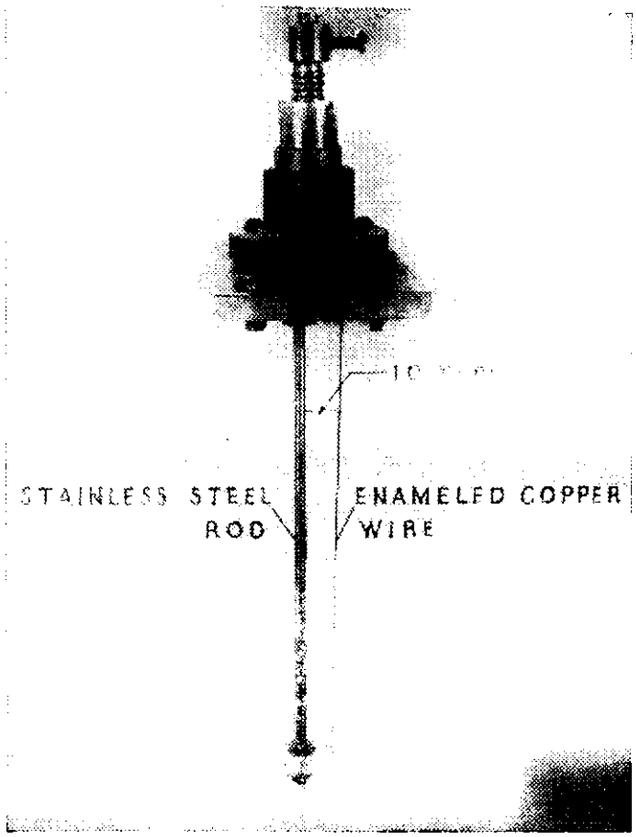

Photo 92 (Chap 46): Capacitive probe.

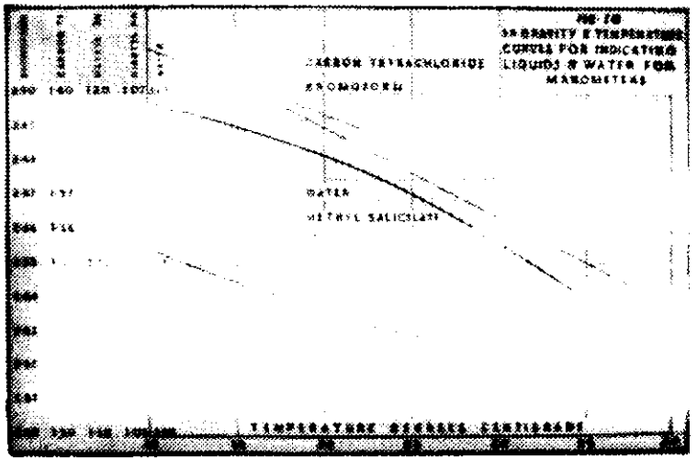

Photo 93 (Chap 46)

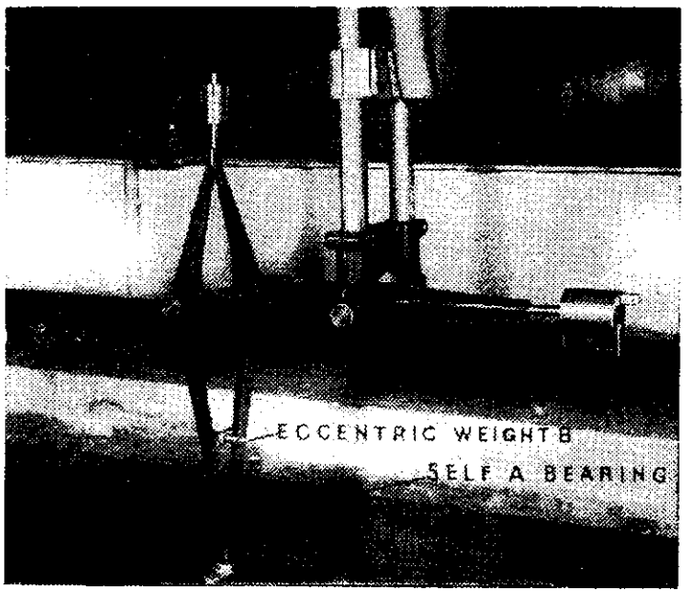

Photo 94 (Chap 47)

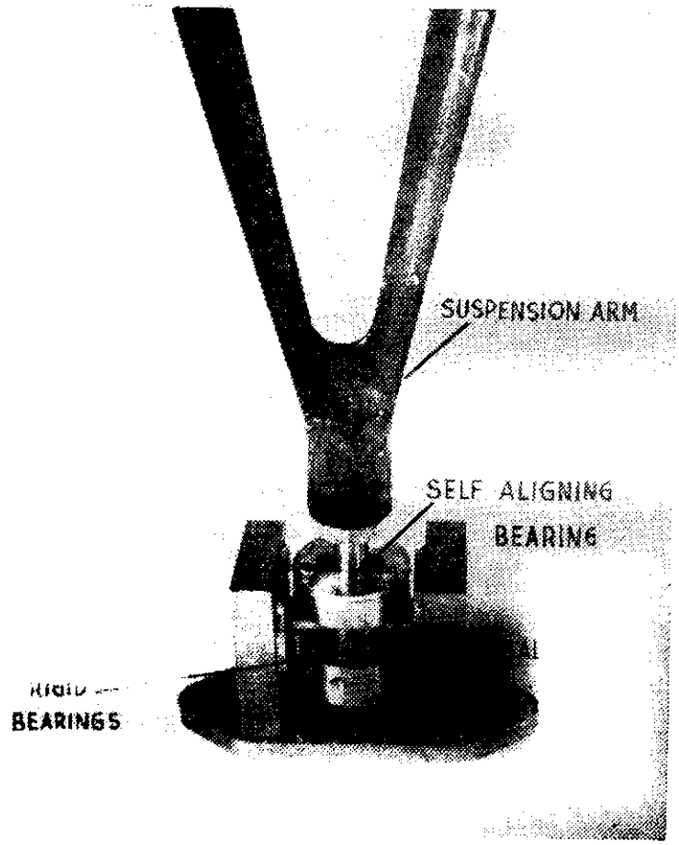

Photo 95 (Chap 47)

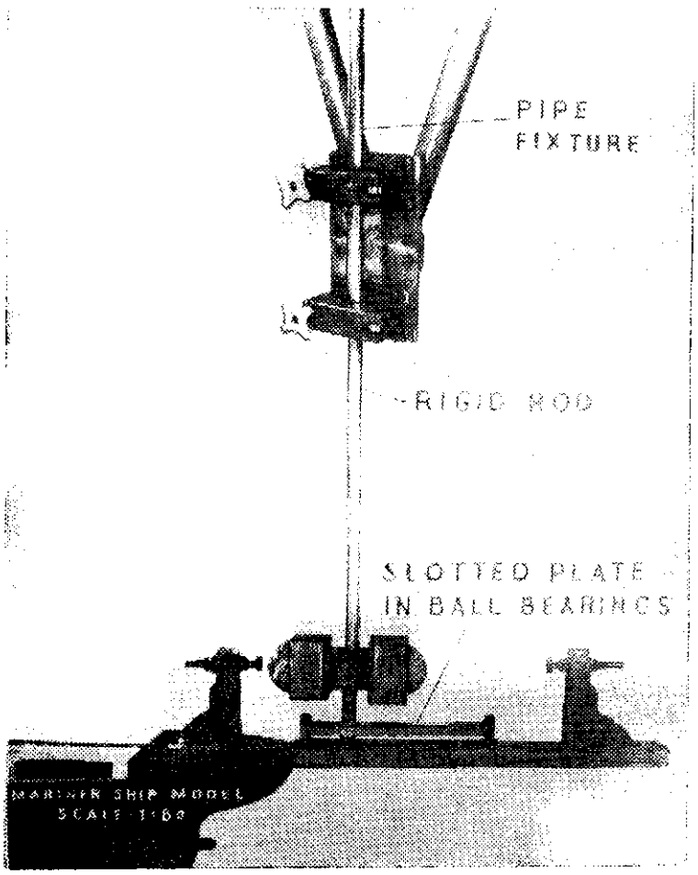

Photo 96 (Chap 47)

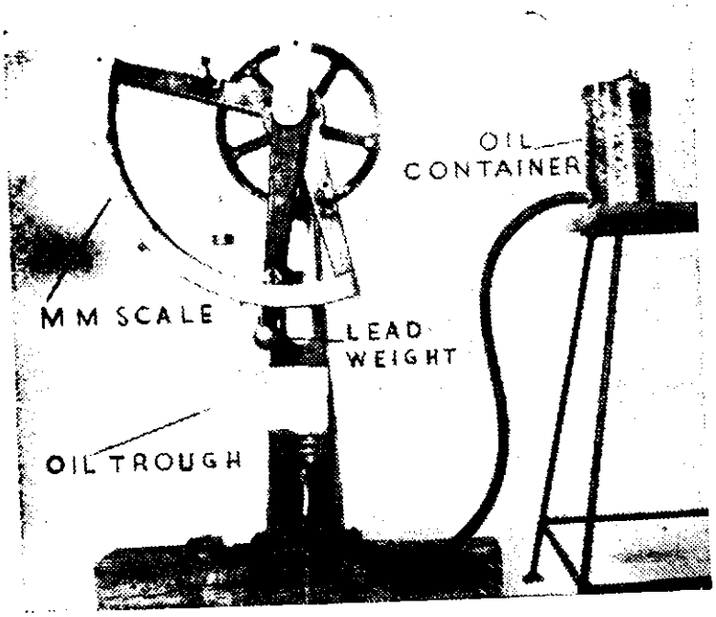

Photo 97 (Chap 47)

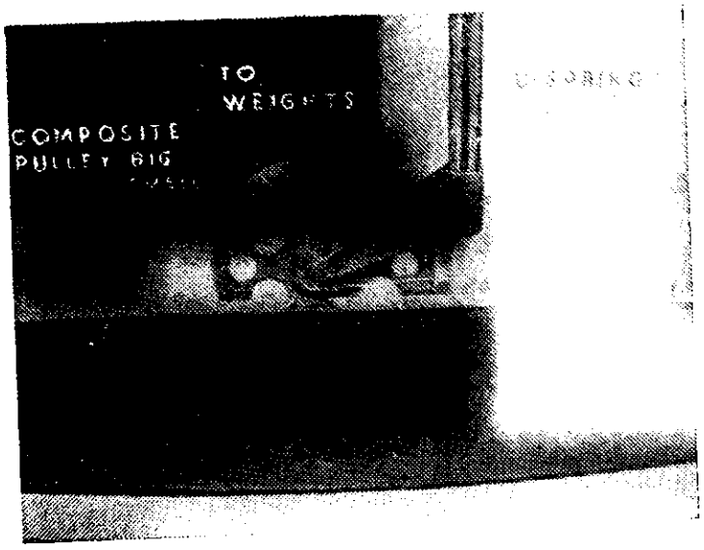

Photo 98 (Chap 47)

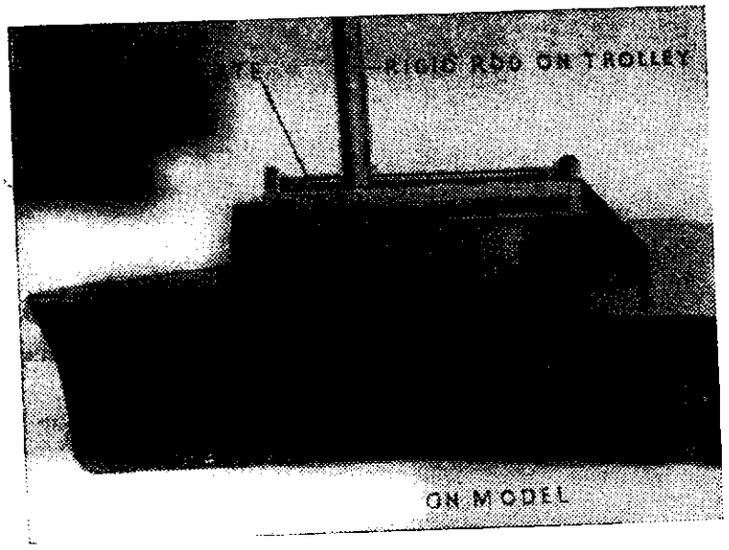

Photo 99 (Chap 47)

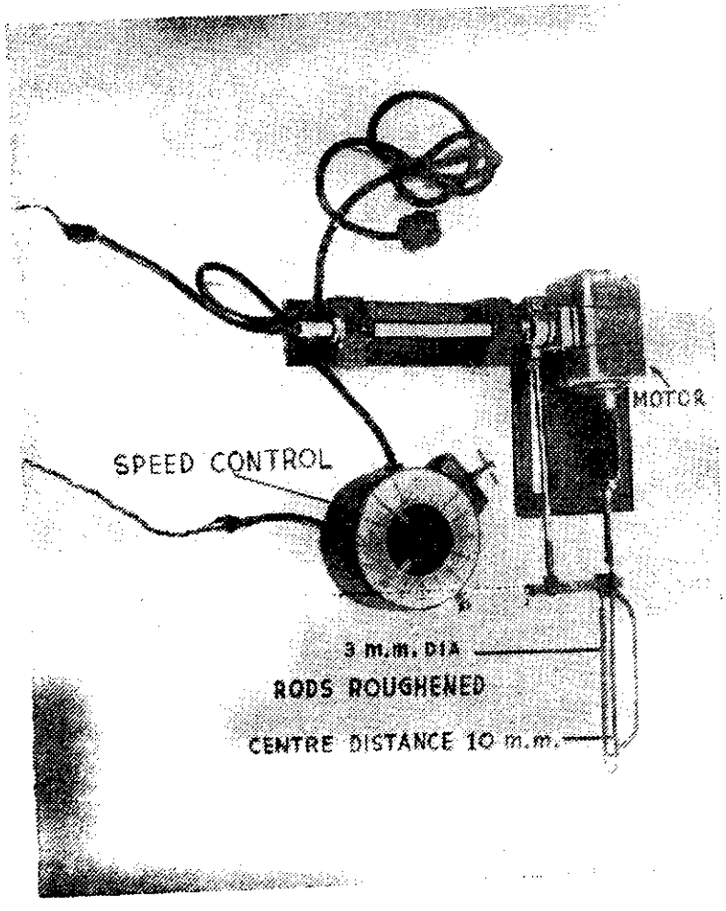

Photo 100 (Chap 47)

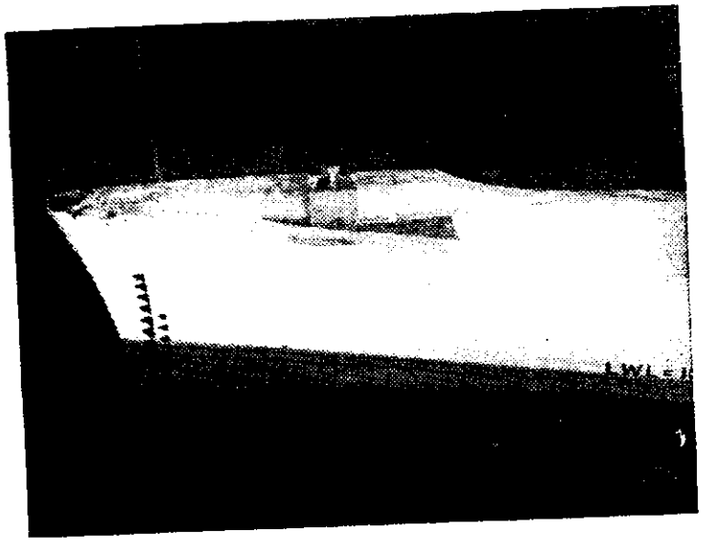

Photo 101 (Chap 47)

PERSONNEL

Chairman ... M Hayath, B E (Mech), B S E E, M I E (Ind)

Member (Designs & Research) ... K L Rao, M Sc, Ph D, M Inst C E, M I Struct E, M I E (Ind), M I E (Lond)

Director ... M G Hiranandani, B A, B Sc (Engg) (Lond)

Deputy Directors and Chief Research Officers

S L Banerjee, M Sc, D Sc
S V Chitale, B E, A M I E
B C Deb, M Sc, D Sc, Ph D (Lond)
S C Desai, B E, A M I E
S T Ghotankar, M Sc
C V Gole, B E
P K Kulkarni, B Sc (E and M)
G M Panchang, B A (Hons), M Sc (Lond)
B Pant, M Sc, A Inst P, A M I E
S D Phansalkar, B E, A M I E
Gurdas Ram, M Sc, Ph D
S K Roy, M Sc, D Phil, A R I C (Lond)
G T Wadekar, B E, Ph D (Lond)

Research Officers

V P Aggarwal, M A
A S Apte, M A, Ph D, D Sc (Grenoble)
S C Barai, M Sc
S K Guha, M Sc, Dr Rer Nat (Germany)
J R Khanna, B Sc, A M I E
A Krishnachar, B E
V D Kulkarni, B E
Kumari K Padmavally, M A, M Sc, Ph D
B G Pattegar, B E
Y D Pendse, B E
S Y Phatak, M Sc Engg, A M I R E
N S Rangachar, B E
P C Saxena, M Sc, D I I Sc, A M I R E
R V Surya Narayan, B E

Assistant Research Officers

P M Advani, B E
O P Anand, B E
K S Ayodhyanathan, B Sc, B E
Y D Barve, B E
V P Bhatt, B E
A N Biswas, B E
S P Chadha, B Sc (Hons), M Sc
S T Chaudhari, B E
P M Damle, B Sc
S S Dass, B Sc, A M I E T
P R Deobhankar, B E
B Garudachar, B E
V G Ghanekar, B E
M B Gidwani, B Sc (Hons)
P D Gosavi, M Sc
P R Govindan, M Sc
D R Goyal, B E
J P Gupta, M Sc
V N Kanhere, B E
J T Karira, B Sc (Hons)
Y S Kelkar, B E
B D Kolhe, B E
R Krishnamurthy, B E
B M Lalwani, B Sc, B E
S L Mokashi, B E
T V Pratinidhi, B E
G V Rao, M Sc
N Sen Roy, M Sc (Tech)
H N Shahani, B E
U P Shenoy, M Tech
C Sudhindra, B E, M E (I I Sc)
V S Thakar, M Sc
D K Vaid, B Sc (Hons), M Sc
P P Vaidyaraman, B Tech (Hons)
C P Venkataraman, B E

Superintendent : G D Vaswani

PUBLICATIONS

of Central Water and Power Research Station Poona

		Price Rs.
	Stream Gauging : A Manual (1960)	6.75
1	Annual Report for 1937-38	7.50
2	Annual Report for 1938-39	7.50
3	Note on Gibb Modules, 1941	1.50
‡4	Annual Report for 1939-40	7.50
‡5	Annual Report (Technical) for 1940-41 with INDEX for 1937-41 ...	7.50
‡6	Annual Report (Technical) for 1941-42	7.50
‡7	Annual Report (Technical) for 1942-43	7.50
‡8	Annual Report (Technical) for 1943	7.50
‡9	Annual Report (Technical) for 1944 with INDEX for 1940-44 ...	7.50
10	Annual Report (Technical) for 1945 with INDEX for 1937-45 ...	25.00
11	Annual Report (Technical) for 1946	7.50
12	Annual Report (Technical) for 1947 with INDEX for 1943-47 ...	25.00
†*13	The Behaviour and Control of Rivers and Canals (Parts I and II), 1949 by Sir Claude C. Inglis	8.00
14	Annual Report (Technical) for 1948 with INDEX for 1944-48 ...	10.00
15	Annual Report (Technical) for 1949 with INDEX for 1945-49 ...	21.25
16	Annual Report (Technical) for 1950	22.50
17	Annual Report (Technical) for 1951	30.00
18	Annual Report (Technical) for 1952	15.00
19	Annual Report (Technical) for 1953	15.00
‡20	Annual Report (Technical) for 1954	32.50
†*21	Annual Report (Technical) for 1955	32.00
†*22	Annual Report (Technical) for 1956	35.50
†*23	Annual Report 1957	27.50
†24	Annual Research Memoirs 1958	41.00
†25	Annual Research Memoirs 1959	47.50
†26	Annual Research Memoirs 1960	

All publications are normally available for sale from the Director, Central Water and Power Research Station, Poona 3. The prices are exclusive of packing and postage charges etc.

* Available from the Manager of Publications, Civil Lines, Delhi-8.

† Available from the High Commission of India, India House, Aldwych, London WC 2 for sale in Europe and America at conversion rate of Rs. 2 = 3 shillings.

‡ Copies out of [illegible]